Your file   Votre référence

Our file   Notre référence

NOTICE

The quality of this microform is heavily dependent upon the quality of the original thesis submitted for microfilming. Every effort has been made to ensure the highest quality of reproduction possible.

If pages are missing, contact the university which granted the degree.

Some pages may have indistinct print especially if the original pages were typed with a poor typewriter ribbon or if the university sent us an inferior photocopy.

Reproduction in full or in part of this microform is governed by the Canadian Copyright Act, R.S.C. 1970, c. C-30, and subsequent amendments.

AVIS

La qualité de cette microforme dépend grandement de la qualité de la thèse soumise au microfilmage. Nous avons tout fait pour assurer une qualité supérieure de reproduction.

S'il manque des pages, veuillez communiquer avec l'université qui a conféré le grade.

La qualité d'impression de certaines pages peut laisser à désirer, surtout si les pages originales ont été dactylographiées à l'aide d'un ruban usé ou si l'université nous a fait parvenir une photocopie de qualité inférieure.

La reproduction, même partielle, de cette microforme est soumise à la Loi canadienne sur le droit d'auteur, SRC 1970, c. C-30, et ses amendements subséquents.

Canada

MONOCLONAL ANTIBODY-BASED DETECTION AND TREATMENT OF HUMAN B-CELL CHRONIC LYMPHOCYTIC LEUKEMIA / LYMPHOMA AND RENAL CELL CARCINOMA IN EXPERIMENTAL MODELS

BY

ZHENPING ZHU

Submitted In partial fulfillment of the requirements for the degree of

Doctor of Philosophy

at

Dalhousie University

Halifax, Nova Scotia

June, 1993

The author has granted an irrevocable non-exclusive licence allowing the National Library of Canada to reproduce, loan, distribute or sell copies of his/her thesis by any means and in any form or format, making this thesis available to interested persons.

L'auteur a accordé une licence irrévocable et non exclusive permettant à la Bibliothèque nationale du Canada de reproduire, prêter, distribuer ou vendre des copies de sa thèse de quelque manière et sous quelque forme que ce soit pour mettre des exemplaires de cette thèse à la disposition des personnes intéressées.

The author retains ownership of the copyright in his/her thesis. Neither the thesis nor substantial extracts from it may be printed or otherwise reproduced without his/her permission.

L'auteur conserve la propriété du droit d'auteur qui protège sa thèse. Ni la thèse ni des extraits substantiels de celle-ci ne doivent être imprimés ou autrement reproduits sans son autorisation.

Canada

Name **Zhenping Zhu**

Dissertation Abstracts International is arranged by broad, general subject categories. Please select the one subject which most nearly describes the content of your dissertation. Enter the corresponding four-digit code in the spaces provided.

Immunology

SUBJECT TERM

| 0 | 9 | 8 | 2 |

U·M·I

SUBJECT CODE

Subject Categories

THE HUMANITIES AND SOCIAL SCIENCES

COMMUNICATIONS AND THE ARTS
Architecture	0729
Art History	0377
Cinema	0900
Dance	0378
Fine Arts	0357
Information Science	0723
Journalism	0391
Library Science	0399
Mass Communications	0708
Music	0413
Speech Communication	0459
Theater	0465

EDUCATION
General	0515
Administration	0514
Adult and Continuing	0516
Agricultural	0517
Art	0273
Bilingual and Multicultural	0282
Business	0688
Community College	0275
Curriculum and Instruction	0727
Early Childhood	0518
Elementary	0524
Finance	0277
Guidance and Counseling	0519
Health	0680
Higher	0745
History of	0520
Home Economics	0278
Industrial	0521
Language and Literature	0279
Mathematics	0280
Music	0522
Philosophy of	0998
Physical	0523

Psychology	0525
Reading	0535
Religious	0527
Sciences	0714
Secondary	0533
Social Sciences	0534
Sociology of	0340
Special	0529
Teacher Training	0530
Technology	0710
Tests and Measurements	0288
Vocational	0747

LANGUAGE, LITERATURE AND LINGUISTICS
Language	
General	0679
Ancient	0289
Linguistics	0290
Modern	0291
Literature	
General	0401
Classical	0294
Comparative	0295
Medieval	0297
Modern	0298
African	0316
American	0591
Asian	0305
Canadian (English)	0352
Canadian (French)	0355
English	0593
Germanic	0311
Latin American	0312
Middle Eastern	0315
Romance	0313
Slavic and East European	0314

PHILOSOPHY, RELIGION AND THEOLOGY
Philosophy	0422
Religion	
General	0318
Biblical Studies	0321
Clergy	0319
History of	0320
Philosophy of	0322
Theology	0469

SOCIAL SCIENCES
American Studies	0323
Anthropology	
Archaeology	0324
Cultural	0326
Physical	0327
Business Administration	
General	0310
Accounting	0272
Banking	0770
Management	0454
Marketing	0338
Canadian Studies	0385
Economics	
General	0501
Agricultural	0503
Commerce Business	0505
Finance	0508
History	0509
Labor	0510
Theory	0511
Folklore	0358
Geography	0366
Gerontology	0351
History	
General	0578

Ancient	0579
Medieval	0581
Modern	0582
Black	0328
African	0331
Asia, Australia and Oceania	0332
Canadian	0334
European	0335
Latin American	0336
Middle Eastern	0333
United States	0337
History of Science	0585
Law	0398
Political Science	
General	0615
International Law and Relations	0616
Public Administration	0617
Recreation	0814
Social Work	0452
Sociology	
General	0626
Criminology and Penology	0627
Demography	0938
Ethnic and Racial Studies	0631
Individual and Family Studies	0628
Industrial and Labor Relations	0629
Public and Social Welfare	0630
Social Structure and Development	0700
Theory and Methods	0344
Transportation	0709
Urban and Regional Planning	0999
Women's Studies	0453

THE SCIENCES AND ENGINEERING

BIOLOGICAL SCIENCES
Agriculture	
General	0473
Agronomy	0285
Animal Culture and Nutrition	0475
Animal Pathology	0476
Food Science and Technology	0359
Forestry and Wildlife	0478
Plant Culture	0479
Plant Pathology	0480
Plant Physiology	0817
Range Management	0777
Wood Technology	0746
Biology	
General	0306
Anatomy	0287
Biostatistics	0308
Botany	0309
Cell	0379
Ecology	0329
Entomology	0353
Genetics	0369
Limnology	0793
Microbiology	0410
Molecular	0307
Neuroscience	0317
Oceanography	0416
Physiology	0433
Radiation	0821
Veterinary Science	0778
Zoology	0472
Biophysics	
General	0786
Medical	0760

EARTH SCIENCES
Biogeochemistry	0425
Geochemistry	0996

Geodesy	0370
Geology	0372
Geophysics	0373
Hydrology	0388
Mineralogy	0411
Paleobotany	0345
Paleoecology	0426
Paleontology	0418
Paleozoology	0985
Palynology	0427
Physical Geography	0368
Physical Oceanography	0415

HEALTH AND ENVIRONMENTAL SCIENCES
Environmental Sciences	0768
Health Sciences	
General	0566
Audiology	0300
Chemotherapy	0992
Dentistry	0567
Education	0350
Hospital Management	0769
Human Development	0758
Immunology	0982
Medicine and Surgery	0564
Mental Health	0347
Nursing	0569
Nutrition	0570
Obstetrics and Gynecology	0380
Occupational Health and Therapy	0354
Ophthalmology	0381
Pathology	0571
Pharmacology	0419
Pharmacy	0572
Physical Therapy	0782
Public Health	0573
Radiology	0574
Recreation	0575

Speech Pathology	0460
Toxicology	0383
Home Economics	0386

PHYSICAL SCIENCES

Pure Sciences
Chemistry	
General	0485
Agricultural	0749
Analytical	0486
Biochemistry	0487
Inorganic	0488
Nuclear	0738
Organic	0490
Pharmaceutical	0491
Physical	0494
Polymer	0495
Radiation	0754
Mathematics	0405
Physics	
General	0605
Acoustics	0986
Astronomy and Astrophysics	0606
Atmospheric Science	0608
Atomic	0748
Electronics and Electricity	0607
Elementary Particles and High Energy	0798
Fluid and Plasma	0759
Molecular	0609
Nuclear	0610
Optics	0752
Radiation	0756
Solid State	0611
Statistics	0463

Applied Sciences
Applied Mechanics	0346
Computer Science	0984

Engineering
General	0537
Aerospace	0538
Agricultural	0539
Automotive	0540
Biomedical	0541
Chemical	0542
Civil	0543
Electronics and Electrical	0544
Heat and Thermodynamics	0348
Hydraulic	0545
Industrial	0546
Marine	0547
Materials Science	0794
Mechanical	0548
Metallurgy	0743
Mining	0551
Nuclear	0552
Packaging	0549
Petroleum	0765
Sanitary and Municipal	0554
System Science	0790
Geotechnology	0428
Operations Research	0796
Plastics Technology	0795
Textile Technology	0994

PSYCHOLOGY
General	0621
Behavioral	0384
Clinical	0622
Developmental	0620
Experimental	0623
Industrial	0624
Personality	0625
Physiological	0989
Psychobiology	0349
Psychometrics	0632
Social	0451

To my parents and grandparents
for their never ending
encouragement and support

Table of Contents

Materials and Methods

Section 2 Pharmacokinetics, Biodistribution and Tumor Localization of Radioiodinated Dal B01, Dal B02 and Their F(ab)'2 Fragments after Injection into Human B-Cell Chronic Lymphocytic Leukemia Xenograft bearing Nude Mice

Section 3 Comparison of the Reactivity, Stability, Pharmacokinetics and Biodistribution of Dal B02 after Radioiodination by Three Different Iodination Methods

List of Figures

xiv

List of Tables

xix

ABSTRACT

Two monoclonal antibodies (MoAbs) directed against human B-cell chronic lymphocytic leukemia (CLL), i.e., Dal B01 (an IgG2a) and Dal B02 (an IgG1), reacted specifically with D10-1 cells, a subclone of the Epstien-Barr virus (EBV) transformed human B-cell CLL line EBV-CLL-1. After intravenous (i.v.) injection into subcutaneous (s.c.) D10-1 xenograft bearing nude mice, there was selective localization of radiolabeled Dal B01, Dal B02 or their F(ab)'2 fragments in the xenografted tumors. Excellent tumor images were obtained in mice given ^{131}I-Dal B02, as well as in mice given ^{131}I-Dal B02 F(ab)'2 fragment. Two chemotherapeutic agents, i.e., methotrexate (MTX) and adriamycin (ADR), were covalently linked to Dal B01 as well as Dal B02 using several different linkages. Both Dal B01-MTX and Dal B02-MTX conjugates demonstrated selective cytotoxicity towards target D10-1 cells. In vitro uptake studies showed that D10-1 cells took up much more Dal B01 or Dal B02 conjugated MTX than non-target MOLT-3 cells did, although MOLT-3 cells took up more MTX than D10-1 cells did when incubated with free MTX. Four different types of Dal B01-ADR or Dal B02-ADR conjugates were prepared and their cytotoxicity was evaluated in vitro. One of these conjugates, i.e., Dal B02-Dex-ADR (ss), was found to be not only selectively cytotoxic to D10-1 cells, but also was more potent than free ADR. Therapy in s.c. D10-1 xenograft bearing nude mice with this conjugate demonstrated that at approximately equal toxic dose level, the antitumor activity of this conjugate was superior to that of free ADR, non-specific IgG1-Dex-ADR (ss) conjugate, Dex-ADR binary conjugate or a mixture of Dex-ADR and Dal B02.

To evaluate the antitumor activity of ^{131}I labeled Dal B02, I developed two clinically relevant models of human B-cell CLL in SCID or irradiated nude mice by inoculating these mice i.p. or i.v. with D10-1 cells. Hundred percent of tumor inoculated mice developed either ascites or solid tumors with metastases in lymph nodes and a number of internal organs and died within 5 to 7 weeks after tumor inoculation. Using these models, as well as a s.c. D10-1 model described above, the antitumor activity of Dal B02, either alone or lableled with ^{131}I, was investigated. Results revealed that, although Dal B02 itself had some antitumor effect, ^{131}I labeled Dal B02 was the most potent tumor inhibitor. Treatment with 50 μg of Dal B02 linked to 300 μCi of ^{131}I resulted in significant tumor inhibition as well as complete cure in a proportion of mice in all the three models.

Studies with an anti-human renal cell carcinoma (RCC) MoAb Dal K29-OKT3 heteroconjugate showed that after i.v. injection, this heteroconjugate selectively localized in xenografted s.c. Nu-caki-1 tumors in nude mice. In an ascites model of human RCC, treatment with this heteroconjugate along with human peripheral blood lymphocytes (PBLs) significantly prolonged the survival of tumor inoculated nude mice.

List of Abbreviations

% ID / g	percentage of the injected dose localized in per gram tissue
(A)BMT	(autologous) bone marrow transplantation
[^{3}H]	tritium
ADCC	antibody-dependent cellular cytotoxicity
ADR	adriamycin
AE	active ester
AFP	alpha fetoprotein
ALL	acute lymphocytic leukemia
AML	acute myelogenous leukemia
ATCC	American type culture collection
ATL	adult T-cell leukemia
Au	colloidal gold particle (s)
AUC	area under curve
BSA	bovine serum albumin
CAA	cis-aconityl anhydride
CD	cluster of differentiation
CDC	complement-dependent cytotoxicity
CDR	complmentarity-determining region (s)
CEA	carcinoembryonic antigen
CL	clearance rate
CLL	chronic lymphocytic leukemia
cpm	count per minute
CR	complete remission
CTL	cytotoxic T lymphocyte (s)

CTLL	cutaneous T-cell leukemia
Dal B01-C13-ADR	ADR was linked to Dal B01 via its C13 moiety using a hydrazone bone
Dal B01-CAA-ADR	ADR was linked to Dal B01 via a CAA spacer using an amide bond
Dal B01-MTXAE	MTX was linked to Dal B01 via an active ester
Dal B01-MTXH	MTX was linked to Dal B01 site-specifcally via the carbohydrate residues of the IgG using a hydrazone bond
Dal B02-C13-ADR	ADR was linked to Dal B02 via its C13 moiety using a hydrazone bond
Dal B02-CAA-ADR	ADR was linked to Dal B02 via a CAA spacer using an amide bond
Dal B02-Dex-ADR (nss)	ADR was linked to Dex via its amino sugar group, the Dex-ADR binary conjugate was then linked to Dal B02 randomly using a Schiff's base bond
Dal B02-Dex-ADR (ss)	Dex was first linked to Dal B02 site-specifically via the carbohydrate residues of the IgG, and then loaded with ADR via the C13 moiety of the drug using a hydrazone bond
Dal B02-MTXAE	MTX was linked to Dal B02 via an active ester
Dal B02-MTXH	MTX was linked to Dal B02 site-specifcally via the carbohydrate residues of the IgG using a hydrazone bond
DCC	dicyclohexylcarbodiimide
Dex	dextran (T-40)
Dex-ADR	ADR was linked to Dex via its C13 moiety using a hydrazone bond
dgA	deglycosylated ricin A chain
DHFA	dihydrofolic acid

DHFR	dihydrofolate reductase
DMF	dimethylformamide
DPBS	Dulbecco's phosphate buffered saline
DT	diphtheria toxin
DTNB	5, 5' - dithiobis- 2 -nitrobenzoic acid
DTPA	Diethylenetriaminepentaacetic acid
DTT	dithiothreitol
EBV	Epstein-Barr virus
EDCI	1-(3-dimethylaminopropyl)-3-ethylcarbodiimide
EDTA	ethylenediaminetetraacetic acid
EGF	epidermal growth factor
ELISA	enzyme-linked immunosorbent assay
EM	electron microscope
FACS	fluorescence activated cell sorter
FCS	fetal calf serum
Fig	figure
FITC	fluorescinisothiocyanate
FPGS	folylpolyglutamyl synthetase
FPLC	fast protein liquid chromatography
GAM	goat anti-mouse
GD	ganglioside (s)
GVHD	graft-versus-host disease
H & E	hematoxylin and eosin
HAMA	human anti-mouse antibody
HAT	hypoxanthine aminopterine thymidine
hCG	human chorionic gonadotropin
HGPRT	hypoxantine-guanine-phosphoribosyl transferase

HPDP	3-(2-pyridyldithio) propionic acid
HPDP	SPDP-hydrazide
HPLC	high performance liquid chromatography
hr	hour (s)
HRP	horseradish peroxidase
HTLV	human T-cell lymphotropic virus
I	iodine
i.p.	intraperitoneal
i.v.	intravenous
IC50	concentration that inhibits cell growth by 50%
ICAM	intercellular adhesion molecule
IFN	interferon
Ig	immunoglobulin
IgG1-Dex-ADR (ss)	Dex was first linked to IgG1 site-specifically via the carbohydrate residues of the IgG, and then loaded with ADR via the C13 moiety of the drug using a hydrazone
bond IL-2	interleukin 2
IRF	immunoreactive fraction
IT (s)	immunotoxin (s)
ITES	insulin-transferrin-ethanolamine-selenium containing serum free medium
Ka	association or affinity constant
kD	kilo dalton
L	liter
LAK	lymphokine activated killer cells
LI	localization index
M	molar

m.w.	molecular weight
mCi	millicurie
MEM	minimum essential medium
mg	milligram
min	minute (s)
ml	milliliter
mM	millimolar
MoAb	monoclonal antibody
MTD	maximum tolerant dose
MTX	methotrexate
MTXAE	MTX-active ester derivative
MTXH	MTX-hydrazide derivative
N-CAM	neural cell adhesion molecule
NADPH	nicotinamide adenine dinucleotide phosphate
NCS	N-chlorosuccinimide
NHL	non-Hodgkin's lymphoma
NHS	N-hydroxysuccinimide
NK	natural killer cells
nm	nanometer
NMG	normal mouse immunoglobulin
o-PDM	o-phenylenedimaleimide
O.D.	optical density
OPD	ortho-phenyldiamine
PAP	pokeweed antiviral protein (s)
PB	phosphate buffer
PBL	peripheral blood lymphocyte (s)
PBS	phosphate buffered saline

PDGF	platelet derived growth factor
PE	pseudomonas exotoxin
PIB	N-succinimidyl-para-iodobenzoate
pmol	picomolar
PR	partial remission
Pristane	2, 6, 10, 14-tetramethyl pentadecaine
RAM	rabbit anti-mouse
RAT	ricin A chain toxin
RCC	renal cell carcinoma
RES	reticulo-endothelial system
RIP	ribosomal inhibitory polypeptide (s)
RPMI	Roswell Park Memorial Institute
s.c.	subcutaneous
SCID	severe combined immune deficiency
SD	standard deviation
SDS-PAGE	sodium dodecyl sulphate polyacrylamide gel electrophoresis
SPDP	N-succinimidyl-3-(2-pyridyldithio)-propionate
T/NT	tumor / normal tissue ratio
T1/2α	half-life of distribution
T1/2β	half-life of clearance
TAA	tumor associated antigen (s)
TACA	tumor associated carbohydrate antigen (s)
TBI	total body irradiation
TCA	trichloracetic acid
TCR	T cell receptor
TEM	transmission electron microscopy
TEMED	N, N, N', N' - tetramethyl ethylenediamine

TIL	tumor infiltrating lymphocyte (s)
TK	thymidine kinase
TLC	thin layer chromatography
TNF	tumor necrosis factor
TRF	transferrin
TRITC	tetramethylrhodamine isothiocyanate
TS	thymidine synthetase
TSTA	tumor specific transplantation antigen (s)
v / v	volume / volume
Vd	volume of apparent distribution
w / v	weight / volume
WBC	white blood cells
x g	gravity
μCi	microcurie
μg	microgram
μl	microliter
μM	micromolar
μm	micrometer

Acknowledgments

INTRODUCTION

1   Concept of Targeted Therapy of Cancer

1.1   Statement of the Problem

The lack of specificity of currently available chemo- and radiotherapeutic agents constitutes the major obstacle to the treatment of cancer (Holland, 1983). The difference between malignant and normal cells as regards to their sensitivity to chemo- and radiotherapeutic agents is not sufficient to allow potentially curative doses of drugs or radiation to be administered without unacceptable toxicity to normal cells. The administration of therapeutic doses of chemo- or radiotherapeutic agents during the treatment of cancer also kill or damage normal rapidly proliferating cells (Baserga, 1981). It is widely accepted that the usefulness of many chemo- and radiotherapeutic agents would be enhanced if these agents or radiation were rendered tumor selective (Ghose et al., 1983a; Ghose and Blair, 1987).

The targeted therapy of cancer is based on the use of specific carriers to deliver cytotoxic agents, including chemotherapeutic drugs, radioisotopes and toxins, to their site of action (i.e., tumor). For targeted delivery of cytotoxic agents, it is important to select a carrier that can be recognized by target cells only. The drug or radioisotope is then attached to this carrier to form a conjugate. Administration of such a conjugate should lead to the accumulation of drug or radioisotope in target tumor followed by selective damage to the tumor cells. Several specific carriers have been evaluated for the selective delivery of drugs or radioisotopes to tumors. Such tumor specific carriers include antibodies (Ghose and Blair, 1978; Dillman, 1989b), hormones (Varga et al., 1977), growth factors (May and Cuatrecasas, 1985) and cytokines (Waldmann et al., 1992). Because of their unique specificity and high affinity for tumor antigens, antibodies are particularly attractive, and in

fact, are the most widely studied specific carriers of cytotoxic agents (Oldham, 1983; Dillman, 1984b; Pietersz and McKenzie, 1992).

1.2   Antibody-Based Drug Targeting

At the beginning of this century, Paul Ehrlich reported on the discovery of antibodies and pointed out the possible use of antitumor antibody-bound diphtheria toxin as a " magic bullet " against malignant cells (Ehrlich, 1956). Antibodies are glycoproteins, consisting of four polypeptide chains that contain a variety of reactive chemical groups, such as amino, carboxyl, hydroxyl and sulfhydryl groups. Functionally, antibodies possess a molecular polarity based on the joining of antigen-binding fragments (Fab) to a complement-fixing fragment (Fc). The Fab fragment is responsible for specific antigen binding whereas the Fc fragment binds to effector cells, fixes complement, and elicits other in vivo biological responses. It is presumed that when cytotoxic agents are delivered as antibody conjugates, the agents will reach and accumulate in the target tumor in greater amounts without significant accumulation in normal tissues because of the specific binding of the antibody to target cells. This reduces the detrimental side effects associated with free cytotoxic agents.

Before the hybridoma technique for producing virtually unlimited amounts of homogenous monoclonal antibodies (MoAbs) of defined specificity became available, the major difficulty in the use of polyclonal antibodies for targeted delivery was their heterogeneity with respect to size, charge, antigen specificity, affinity, low IRF and the contamination of unwanted (potentially harmful) antibodies. The production of highly specific polyclonal antitumor antisera / antibodies is difficult and unreliable because it requires purified tumor antigens. Different lots of antisera have different specificities and affinities towards the antigen, and the quantity is usually limited (Tyle and Ram, 1990). Despite the above limitations, many investigators used these polyclonal antitumor antibodies as specific

carriers for drugs in cancer therapy, especially before the development of MoAbs (Ghose and Blair, 1978). Early work using experimental animals and polyclonal antibodies involved the use of those few clinically used anti-cancer drugs which appeared to lend themselves to covalent coupling to antibodies by simple methods (Ghose et al., 1972a; Hurwitz et al., 1975; Ghose et al., 1976). The first report on the use of antibody-drug conjugate was published in 1958, when Mathe et al. linked MTX by diazotization to antibodies raised against murine L1210 leukemia cells and used the conjugate in the successful treatment of L1210-bearing DBA/2 mice (Mathe et al., 1958). Although this result appeared to be promising, no serious efforts to extend this therapeutic modality to clinical patients were made until 1972, when Ghose and colleagues coupled chlorambucil to antitumor antibodies raised in rabbits and goats (Ghose et al., 1972b; Ghose and Nigam, 1972a), and used this chlorambucil-antibody preparation to treat patients with melanoma (Ghose et al., 1975; Ghose et al., 1977). Early studies from Dr. Ghose's laboratory, along with those from others, have suggested that antibody-linked cytotoxic agents might find their use in the eradication of small numbers of circulating tumor cells and micrometastases remaining after removal of primary tumors. The factors that influence the production of polyclonal antitumor antibodies, the methods of linkage of various cytotoxic agents to these antibodies, and the problems associated with the use of antibody-cytotoxic agent conjugates have been reviewed extensively by Ghose and Blair (1978).

In 1976, Kolher and Milstein, by employing a method of somatic cell hybridization, successfully generated " hybridoma " cell lines producing MoAbs of defined specificities (Kolher and Milstein, 1975). The principal advantages of MoAbs over conventional polyclonal antibodies include: the defined specificity, homogeneity, and the availability of MoAbs in practical unlimited quantities. Furthermore, because the hybridomas are immortalized, the same MoAb can be obtained whenever required. These properties of MoAb render them as the most attractive carriers for the delivery of therapeutic agents to

specific sites, e.g., malignant tumors (Ghose and Blair, 1987). To date, numerous antitumor MoAbs have been produced. These MoAbs react with a wide range of human cancers including carcinomas of colon, rectum, breast, ovary, lung, pancreas and bladder, as well as malignant melanomas, bone and soft tissue sarcomas and leukemias. Many of these MoAbs have been evaluated as tumor-specific carriers of cytotoxic agents, i.e., chemotherapeutic agents, radioisotopes and toxins, in either animal models or patients (Mellstedt, 1990; Mach et al., 1991; Reithmuller and Johnson, 1992) (see appropriate sections for detailed discussion).

2   Tumor Associated Antigens

Antibody-based delivery of cytotoxic agents to tumors presupposes the existence of distinctive tumor associated antigens (TAA) and the feasibility of the production of antibodies against these TAA. In early studies, antigens that had preferential distribution or enhanced expression in tumors were regarded as TAA (Schwartz, 1990). Some of these TAAs were defined by antitumor antibodies generated in xenogeneic systems (Srivastava, 1991). Recent studies have clearly demonstrated that neoplastic transformation is usually accompanied by the acquisition of new and specific antigenic components not detected in normal untransformed cells (Urban and Schreiber, 1992). These tumor specific antigens may result from the structural mutations of oncogenes and/or tumor suppressor genes, and are recognized as novel proteins or aberrantly glycosylated self-molecules. Several MoAbs directed against some of these tumor specific antigens (e.g., p53 and gp 95/97 antigen of human melanoma) have been obtained and used in the diagnosis and treatment of human cancers (see following sections for detailed discussion).

2.1 Characterization of Tumor Associated Antigens

The fact that tumor cells express antigens that can stimulate immune response in the host has been clearly demonstrated in both experimental animal models and in cancer patients. Two main approaches have been used to identify TAA. Firstly, antibodies can be produced by immunizing an animal with appropriate tumor cells, and these antibodies can then be used as probes for different molecules expressed on the tumor cell surface. Secondly, tumor antigens can be operationally defined as molecules that stimulate T cell-mediated rejection of tumor transplants in syngeneic animals previously immunized with the tumor (Thurin, 1990).

2.1.1 Antibody defined tumor-associated antigens

Antitumor antibodies have been described in tumor-bearing or tumor-immunized hosts (Deleo et al., 1977; Srivastava and Das, 1984). Although the tumor specificity of these antibodies are questionable (i.e., these antibodies are not specific to tumors and react with one or more normal tissues as well in most of cases), several recent studies have clearly demonstrated the existence of antibodies specific for TAA. I shall briefly discuss here several examples of antibody defined tumor specific antigens, i.e., gp95/97, p53 molecules and mucins.

The gp95/97 antigen of the human melanoma provides an excellent example of TAA detected by autologous antibody. A 95kD molecule was detected by autologous antibody (in the serum of the patient) only in the patient's melanoma cells but not in melanoma cells from other patients (Real et al., 1984). However, murine MoAbs to gp95/97 react with most human melanoma cells. The patient's antibody apparently detects a specific epitope on the common gp95/97 molecule (Furukawa et al., 1989).

Another example of serologically defined TAA is the p53 tumor suppressor molecules. Antibodies to p53 were found in sera of mice immunized with MCA-induced sarcomas and p53 molecules were precipitated from a number of transformed but not normal cells (Deleo et al., 1979). It has been observed that p53 molecules derived from virally transformed cells were very similar, whereas p53 molecules obtained from antigenically distinct MCA-induced sarcomas were unique for individual tumor (Srivastava, 1991).

Highly glycosylated proteins (i.e., mucins) have been found to express unique antigenic moiety in many types of human cancer. One of the tumor-associated mucins characterized so far is the polymorphic epithelial mucin (PEM) detected in human carcinomas by MoAb SM3 (Swallow et al., 1987). The PEM epitopes recognized by MoAb to mucins map to the multiple tandem repeat region of the mucin. The difference between the reactivity of normal and tumor tissues seems to be due to polymorphism of the mucin genes and difference in glycosylation of the core peptides of these mucins (Gendler et al., 1988).

2.1.2   T-cell defined tumor-associated antigens

The existence of tumor rejection antigens, i.e., tumor specific transplantation antigen (TSTA) in chemically or UV induced tumors in mice, was established 40 years ago (Foley, 1953). Two of these antigens in MCA-induced mouse sarcomas were identified independently as the cell surface glycoprotein gp96 (Srivastava et al., 1986) and an intracellular antigen p84/86 (Ullrich et al., 1986), both antigens share considerable homology with each other and belong to the heat shock protein (hsp) family (Maki et al., 1990). Despite their individual distinctiveness, i.e., a tumor elicits immunity against itself but not against another tumor even when both the tumors are induced by the same carcinogen in the same animal (Srivastava and Old, 1988). Both the gp96 and the p84/86

antigens do not show any tumor-specific DNA sequence polymorphism (Srivastava et al., 1987; Moore et al., 1990). It has been suggested that gp 96 and p84/86 are not antigenic *per se*, but are carriers of immunogenic peptides and the specificity of immunogenicity resides in the peptides rather than in the carrier (Srivastava and Maki, 1991).

Tum⁻ antigens of P815 mastocytoma were the first T-cell recognized antigen to be defined structurally. Stable highly immunogenic mutants (Tum⁻ variants) that are rejected in syngeneic mice were generated in vitro by mutagenesis of the P815 cell line (Boon, 1983). The antigens responsible for rejection are unique and each clone elicits transplantation immunity to itself and the parent tumor but not to others. CTL generated against the variants show the same specificity (Boon, 1983). CTL-defined antigens in variant P91A was characterized by transfection of P91A DNA into P815 cells and then evaluating the susceptibility of the transfected clones to CTL against P91A (Lurquin et al., 1989). A 800-base pair restriction fragment was found to express the antigen responsible for recognition by CTL. This antigen was a 60 kD protein that differs from its normal counterpart by a single amino acid, indicating a single point mutation in the gene sequence (Srivastava, 1991; Thurin, 1990). Thus a single amino acid difference resulting from a single point mutation in the 60 kD protein enables the protein to bind to MHC molecule and stimulate the CTL response.

Among the T-cell recognized human tumor antigens, mucins of pancreatic, breast and colon carcinomas are the best characterized (Gendler et al., 1988). The tandem repeat structure of mucins can stimulate CTL in a MHC-unrestricted fashion (Barnd et al., 1989). Anti-mucin CTL can be obtained from cancer patients with a relatively high efficiency. However, it is not clear why these CTL do not eliminate cancer cells in vivo (Finn, 1991). Several other human tumor antigens recognized by CTL have also been described, e.g., MZ2-E antigen encoded by a novel gene MAGE-1 in human melanoma cell line MZ2 (van der Bruggen et

al., 1991), and a single chain 92kD glycoprotein expressed by human breast carcinoma cells but not by gastrointestinal carcinoma cells (Okubo et al., 1989). CTL clones against these antigens have been found to kill autologous tumors in a MHC-restricted fashion (Okubo et al., 1989).

2.2   Structure and Function of Tumor Associated Antigens as Defined by MoAbs

Few TAA have been found that are expressed only by tumor cells but not by any normal cells of the same or other lineages. However, the expression of a tumor antigen by malignant cells may be much higher than its expression by normal cells. To date, several hundred MoAbs defining different human tumor antigens have been described (Herlyn et al., 1990). With MoAbs as a tool, many types of human tumors have been studied for the quantitative or qualitative expression of antigens either on the cell surface or intracellularly. These TAA have been categorized into several groups based on their functions.

(A) Tumor antigens that have signalling and/or transport functions: This type of tumor antigens includes (i) growth factor receptors such as receptors for epidermal growth factor (EGF), transferrin (TRF), platelet-derived growth factor (PDGF), fibroblast growth factor and insulin-like growth factor; (ii) cation binding and transport proteins such as melanoma-associated antigen p97 (melanotransferrin) (Rose et al., 1986) and common acute lymphoblastic leukemia antigen (CALLA, CD10), a zinc-containing metallo-peptidase identical to neutral endopeptidase (Letarte et al., 1989); and (iii) toxin-binding proteins such as P-glycoprotein (p-170) associated with multiple drug resistance (Juranka et al., 1989).

(B) Tumor antigens that are involved in cell-cell and cell-matrix interactions: Many tumors express large amounts of glycoproteins and glycolipids that physiologically involved in

cell-cell and cell-matrix interaction (Herlyn and Koprowski, 1988). For example, carcinoembryonic antigens (CEA), a member of the Ig gene superfamily, was found to be a TAA with potential function in tumor progress as a Ca^{2+} independent homotypic adhesion molecule (Benchimol et al., 1989). Other members of the CEA family include neural cell adhesion molecule (N-CAM) (Cunningham et al., 1987), myelin-associated glycoprotein (Salzer et al., 1987) and the melanoma-associated antigen MUC-18 (Lehmann et al., 1989).

Two families of cell surface antigens that participate in cell-matrix interactions and cell migration are the integrins and disialogangliosides such as GD2 and GD3. Integrin receptors span the plasma membrane of cells and link the internal cytoskeletal network of a cell with the extracellular matrix (Albelda and Buck, 1990) and include receptors for laminin, fibronectin, vitronectin and collagen. Disialogangliosides GD2 and GD3 are expressed on melanoma cells in situ and in culture (Herlyn and Koprowski, 1988). Antibodies to these molecules can inhibit the attachment of tumor cells to their substrates and may also prevent invasion of tumor cells through basement membrane (Iliopoulos et al., 1989).

(C) Blood group and blood group-related tumor antigens: Tumor cells express a variety of blood group and blood group-related antigens with carbohydrate antigenic determinants. Sialylated forms of Lewis[a] and Lewis[x] antigens and dimeric and trimeric forms of Lewis[x] and Lewis[y] are the main carbohydrate tumor antigens on cancer cells (Hakomori et al., 1984; Itzkowitz et al., 1986). The specific functions of these tumor-associated carbohydrate antigens (TACAs) is difficult to determine because they may be present on different carriers, i.e., on mucins circulating in serum (Herlyn et al., 1987), or on proteins or lipids within the cytoplasm or on the cell surface (Basu et al., 1987). It seems that aberrant cell-surface glycosylation provides a basis for aberrant tumor cell behavior.

Some of these TACAs are now recognized as adhesion molecules of tumor cells essential for their adhesion to target cells (Hakomori, 1991). Monoclonal antibodies to TACAs may serve not only as classic immunological reagents but also as anti-adhesion reagents for the prevention of tumor spread (Hakomori, 1991).

2.3 Molecular Basis of Tumor Antigens

2.3.1 Tumor-specific antigens derived from structural mutation of oncogenes or tumor suppressor genes

Evidences have been obtained from recent studies that human tumors harbor a variety of tumor specific mutant proteins that may be recognized as tumor specific antigens (Urban and Schreiber, 1992). These proteins are encoded by oncogenes (e.g., *ras*) or tumor suppressor genes (e.g., p53) that have undergone structural mutations resulting from point mutations, chromosomal translocations, internal deletions and viral insertional mutagenesis. Several of these changes may result in the production of fusion proteins (e.g., ABL-BCR fusion protein).

Proto-oncogenes and tumor suppressor genes play an important role in the proliferation and differentiation of normal cells. The alteration in the structural and/or the level of expression of these genes often contributes critically to the formation of a variety of animal and human cancers. For example, *ras* genes, proto-oncogenes encoding a highly conserved family of inner membrane-bound proteins (p21 *ras*) that are thought to play a role in signal transduction across the cell membrane and in the control of cell cycle, could undergo point mutation as a result of single nucleotide substitution. Mutant p21 proteins may acquire oncogenic potential because of a single amino acid substitution, usually at residue 12, or 61, or (less commonly) 13 (Taparowski et al., 1982; Seeburg et al., 1984)). The sites of

mutation in *ras* gene is limited and the same mutation can be found among many different types of tumors. Mutations of *ras* gene have been detected in a substantial proportion of many types of malignant lesions (Urban and Schreiber, 1992), however, there is as yet no evidence that the mutant p21 proteins can be a rejection antigen and thus the target for immunotherapy of human cancers. Another common genetic abnormality in human tumors is the mutation of the p53 suppressor gene (Srivastava, 1991). The sites of mutation in p53 gene are much more diverse than those involving the *ras* gene and tend to be different in different tumors. Recent discovery has shown that the p53 gene is a hot spot for mutation in a broad spectrum of human cancers (Levine et al., 1991). The mutation in different regions of p53 structural gene may generate extensive polymorphism of the p53 products. The mutation may also cause conformational changes in the proteins that can be readily identified by antibodies (Gannon et al., 1990). Such antibodies may be useful in the diagnosis of malignancy.

Chromosomal translocations or internal deletions are common in human cancer and may result in the formation of fusion proteins. For example, the Philadelphia (Ph) chromosome seen in the leukemic cells of patients with chronic myelogenous leukemia (CML) results from the translocation of the BCR gene from chromosome 22 to the 5' end of the c-ABL proto-oncogene on chromosome 9 (De Klein et al., 1982). Expression of the chimeric BCR-ABL gene results in the production of an aberrant fusion protein, a tyrosine kinase with tumorigenic properties (Hariharan et al., 1989). An example of genetic abnormality that results from internal deletion is observed in malignant glioblastoma, where the gene for EGF receptor is often structurally rearranged and undergo a deletion mutation, which results in the expression of variant forms of the EGF receptor on the cell surface (Humphrey et al., 1991).

It is known that the integration of a retroviral gene in normal cellular genes can produce a variety of structural mutations that may lead to the expression of tumor specific antigens (Weinstein et al., 1986). In addition, the expression of TAA can also result from the integration of retroviral sequences that serve as a promotor or activator for the transcription of normal cellular proto-oncogenes. The integration causes aberrant expression or over-expression of proto-oncogenes (Fung et al., 1983).

Tumor-associated protein antigens (including mutant proteins, fusion proteins and truncated proteins that might result from gene mutations) expressed on tumor cell surface may present new antigenic determinants that can be specifically recognized by antibodies because of the change in the amino acid sequence in the mutant protein. The change in the amino acid sequence will not only cause structural changes of the protein, but may also cause alteration of the conformation of the existing structure and/or exposure of previously hidden regions of the molecule. For those tumor antigens that are expressed intracellularly and are therefore not accessible to antibodies, new T-cell recognized epitopes may be created from these mutant proteins. These epitopes may bind to MHC class I molecules and be presented on the surface of tumor cells leading to the recognition by T cells. For example, both structural and conformational changes may produce new patterns of proteolytic cleavage to create novel peptide fragments prior to binding to MHC molecules. Alternatively, the novel fragments may have markedly altered affinity for MHC and TCR molecules (Reddehase et al., 1989).

2.3.2 Tumor-associated antigens derived from aberrant glycosylation of self molecules

In addition to structural gene mutations which result in the expression of novel proteins in tumor cells as tumor specific antigens, aberrant glycosylation of self-molecules by tumor cells may also give rise to new antigenic moieties in tumor cells (Hakomori, 1989; Lloyd,

1990). Cell surface associated glycoproteins or glycolipids of the majority of experimental and human tumors display abnormalities in their carbohydrate moieties (Hakomori, 1990). These tumor-associated carbohydrate antigens (TACAs) may result from (i) blocked synthesis of a particular carbohydrate chain with or without the accumulation of the precursor; (ii) enhanced synthesis of certain chemical moieties that are not detectable or only minimally expressed in the normal homologous tissue ('neosynthesis'); and (iii) changes in membrane organization (Hakomori, 1991). Although none of these TACAs appear to be tumor-specific and they can be found in small amounts on certain normal tissues, some of them are useful in the diagnosis and treatment of cancer.

2.3.3 Tumor-associated antigens derived from the over-expression of self molecules

Some normal self molecules have been found to be over-expressed in certain tumors. These molecules include growth factors (e.g., EGF and TRF) and their receptors, cytokines (e.g., IL-2) and their receptors, hormones (e.g., hCG) and their receptors, cell adhesion molecules (e.g.. ICAM-1 and CEA) and embryonic antigens such as alpha-fetoprotein (AFP). The usefulness of these shared antigens depends on the level of their expression and the spectrum of distribution of these antigens in normal cells and tissues. Most of these TAA may be shared by cells of the same differentiation lineage and amplified by cancer cells (Van den Eynde, 1991).

2.4 Potential Clinical Application of Tumor Associated Antigens

MoAbs to TAA have been used in a variety of ways for cancer diagnosis and therapy. The cellular location of a tumor antigen may determine its use as a target for MoAbs in diagnostic or therapeutic approaches. TAA can be expressed on tumor cell surface and/or in the cytoplasm of tumor cells. They can also be secreted or shedded by the tumor and

eventually gain entrance into the blood and other body fluids. TAA in body fluids, particularly in blood, are clinically useful in the screening, diagnosis and therapeutic management of cancer patients (Schwartz, 1989). Several examples of these circulating TAA that are used clinically include CEA in colorectal carcinoma, AFP in hepatocellular carcinoma and CA-125 in ovarian cancer (Schwartz, 1990). For radioimmunoimaging, target antigens should be expressed on the cell surface at high density or secreted into the intercellular space at high concentrations. For use in immunotherapy, the tumor antigens should also be adequately expressed on the cell surface. When unmodified antibody is used to activate the host's effector cells and/or complement, the antigen should not be rapidly endocytosed or shedded because the stable location of the antigen-antibody complex on the cell surface enables the antibody to recruit the effectors and kill the tumor cell. On the other hand, when antibody is used as a carrier of toxins or chemotherapeutic agents, the binding of the antibody to tumor antigen on the cell surface should induce a rapid and efficient internalization of the immunoconjugates since the targets of most toxins and chemotherapeutic agents are intracellularly distributed. Alternatively, when a radioisotope such as ^{131}I is used as cytotoxic agent, the internalization of the radiolabeled MoAb after binding to target cell surface antigen is not required for cell killing.

Several other potential applications of TAA in the therapy of cancer have been explored. For example, some TAA function as adhesion molecules, MoAbs to these molecules can be used to block the interaction between tumor and adhesive proteins to inhibit tumor metastasis (anti-adhesion therapy) (Iliopoulos et al., 1989). Furthermore, some TAA function as growth factor receptors, MoAbs may down-regulate the rapid growth of the tumor cells and enable host's immune system to eradicate the tumor cells (Drebin et al., 1986; Hadziak et al., 1989). When a single malignant cell expresses multiple independent tumor-associated antigenic molecules (Wortzel et al., 1983; Ioannides et al., 1991), a multi-pronged immune attack may substantially decrease the chance of tumor escape. Finally,

several tumor specific mutant proteins encoded by mutant oncogenes or suppressor genes are essential for the malignant phenotype. These proteins could be excellent targets for therapy since cancer cell could not survive in the absence of these proteins.

TAA may also be used to construct tumor vaccines and then used in active immunotherapy of cancer. Once relevant tumor antigens defined by antibodies or CTLs as target structures for immune intervention become available, it is possible to use these tumor antigens to construct tumor vaccines by either of the following approaches: (i) covalent attachment (i.e., conjugation) of the antigen to immunogenic carrier proteins; or (ii) expression of the gene encoding tumor associated antigens (protein or peptide) in cellular vectors. It is also possible to transfect the gene encoding a TAA into a cellular vector that has been modified to express certain adjuvant proteins, costimulatory factors and/or cytokines that are essential for efficient antigen presentation (Blankenstein et al., 1991). This might provide a potent tumor vaccine that can be used to treat either genetically susceptible individuals prophylactically or therapeutically in patients with cancer.

3   Human B-Cell Chronic Lymphocytic Leukemia

Human B-cell chronic lymphocytic leukemia (CLL) is usually characterized by a monoclonal proliferation and accumulation of lymphocytes of the B phenotype, though in 5% of patients, T cells comprise the clone (Gale and Foon, 1985). These leukemic B cells appear to be morphologically mature but are biologically immature (Foon et al., 1990). Two working groups, the International Workshop on Chronic Lymphocytic Leukemia (International Workshop on Chronic Lymphocytic Leukemia, 1989) and the National Cancer Institute-Sponsored Working Group (Cheson et al., 1988), have recently put forward comparable guidelines for the diagnosis of CLL. The criteria for the diagnosis of CLL according to these guildlines are lymphocytosis (> 5 x 10^9 / L) sustained for at least 4

weeks; monoclonal proliferation of B cells with either kappa or lambda light chain; low-density cell surface Ig; the presence of CD5 antigen; mature lymphocytes with no more than 55% atypical or immature lymphoid cells; and bone marrow contains more than 30% leukemic B lymphocytes.

3.1 Epidemiology and Etiology

CLL is the most common type of leukemia and accounts for 30% of all leukemia cases in Western countries (Foon et al.,1990). It typically occurs in persons over 50 years of age. Concordance in genetically identical twins is rare. The cause of the disease is unknown. Unlike other leukemias, the incidence of CLL is not increased by exposure to alkylating drugs, radiation, or chemicals (Bizzozero et al., 1967). The possible role of either retroviruses (e.g., HTLV-1 or HTLV-2) or DNA viruses (e g., Epstein-Barr virus or cytomegalovirus) in CLL is unknown, although it is believed that retroviruses are implicated in the etiology of some lymphoid leukemias, e.g., HTLV-1 in adult T-cell leukemia (Gallo, et al., 1983). Direct involvement of the EBV seems unlikely. CLL cells can be infected by EBV, as indicated by the expression of the EBV nuclear antigen, and these cell lines can be grown in nude mice (Ghose et al., 1988b).

3.2 Immunology and Cytogenetics

CLL cells display low-density surface membrane Ig, typically mu or mu and delta heavy chain and either kappa or lambda light chain. The cells have receptors for mouse erythrocytes, a marker of immature B cells. In addition, they express B-cell associated antigens such as CD19, CD20, CD21, CD23, and CD24. The cells also express the nominal T-cell associated antigen, CD5, which is also seen in a subpopulation of normal B cells (Gadol and Ault, 1986). Leukemic cells from about 50% patients also express the

CD25 activation antigen (Freeman et al., 1987). The expression of common acute lymphocytic leukemia antigen (CALLA, CD10) and other T-cell associated antigens, such as CD3, have not been observed in leukemic CLL B cells (Foon and Todd, 1986a).

There is usually inversion of the normal T helper cell (CD4) to T suppressor cells (CD8) ratio in the blood of CLL patients (Kay, 1981). Most studies suggest decreased T helper cell function. Some data suggest that CLL cells secrete an inhibitory factor of low molecular weight that suppresses T cell as well as natural killer cell activity (Burton et al., 1989). Almost all patients with CLL eventually develop hypogammaglobulinemia. Consistent with hypogammaglobulinemia and T cell abnormality, patients have impaired antibody and cell-mediated immunity to recall antigens (Cone and Uhr, 1964). Infections, particularly with encapsulated organism₋ are common (Chapel and Bunch, 1987).

The frequency of autoantibodies and autoimmune disorders in CLL patients is high. Most of these antibodies are to mature hematopoietic cells: erythrocytes, platelets, and granulocytes. The mechanisms of these autoimmune abnormalities are unknown. Recent data suggest that the involvement of a specific subset of CD5 positive B cells may be especially important in autoimmunity as well as in the development of CLL. There is also evidence that a few specific subsets of CD5 positive B cells may be more likely to be transformed in CLL (Kipps et al., 1987).

In approximately 50% of patients with CLL, chromosomal abnormalities are detected. The most common abnormality is trisomy of chromosome 12 (Autio et al., 1979), followed by $14q^+$, $13q^+$ and $11q^+$. Most of theses abnormalities involve translocations with unknown donor chromosomes. Karyotypic complexity correlates with the likelihood of progressive disease and even simple cytogenetic abnormalities portend a poorer prognosis (Juliusson and Gahrton, 1990).

3.3 Staging

Several staging systems that reflect groupings of prognostic variables have been proposed. The systems proposed by Rai and colleagues (stage 0, I, II,III, and IV) (Rai et al, 1975) and Binet and colleagues (stage A, B, and C) (Binet et al., 1981) have received wide international acceptance and usage. Because actuarial survival statistics suggested three rather than five patterns of survival, Rai recently simplified his system from 5 stages into three risk categories, i.e., low- (stage 0), intermediate- (stages I and II), and high- (stages III and IV) risk categories (Rai, 1987).

3.4 Therapy

3.4.1 Initiation of therapy

CLL has well defined pattern of stability and progression (Gupta and Good, 1980). In the initial phase, the counts of leukemic cells increase slowly, doubling at six monthly or yearly intervals. Then usually the counts level off and stay at that level for variable periods during which the patient remains asymptomatic and does not require any treatment. Finally the counts of leukemic cells increase again with clinical deterioration necessitating initiation of treatment. Therapy is usually instituted if any of the following indications are present: disease-related symptoms, such as fever, night sweats, and greater than 10% loss of body weight; progressive bone marrow failure (anemia, thrombocytopenia); autoimmune hemolytic anemia or thrombocytopenia; massive splenomegaly; " bulky " disease in the lymph nodes or other organs; disease-related recurrent bacterial infections; or progressive lymphocytosis (Foon et al., 1990).

3.4.2 Response criteria

Evaluation of therapy has been difficult in CLL because of the lack of uniform response criteria. Recently, the International Workshop (International Workshop on Chronic Lymphocytic Leukemia, 1989) and the National Cancer Institute-Sponsored Working Group (Cheson et al., 1988) defined complete remission (CR) as the resolution of lymphadenopathy and organomegaly, a lymphocyte count of less than 4×10^9 / L; a granulocyte count of more than 1.5×10^9 / L, and a platelet count of more than 100×10^9 / L. The International Workshop also includes the resolution of constitutional symptoms and a normal bone marrow biopsy specimen, while the National Cancer Institute - Sponsored Working Group requires fulfillment of the above for longer than 2 month, after which a bone marrow aspiration and biopsy shows less than 30% leukemic B lymphocytes.

Partial response (PR), as defined by the International Workshop, is a change from Binet stage C disease to stage A or B or from stage B to stage A. The National Cancer Institute-Sponsored Working Group defines a PR as a greater than 50% decrease in the peripheral blood lymphocyte count; a 50% decrease in the size of enlarged lymph nodes, the spleen, and the liver; a hemoglobin count of more than 110 g/L, a platelet count of more than 100×10^9 / L; and a granulocyte count of more than 1.5×10^9 / L; or an improvement of 50% in these values from baseline values obtained before the initiation of therapy (Foon et al., 1990).

3.4.3 Chemotherapy of CLL

The median survival of patients with low-risk CLL is longer than 10 years. Recent data have shown that low-risk patients receiving chlorambucil showed no benefit of therapy, as compared with control (untreated) patients under observation only (French Cooperation

group on Chronic Lymphocytic Leukemia, 1990a). For intermediate-risk patients and those low-risk patients who require therapy, single-agent chemotherapy with chlorambucil is the standard mode of initial treatment. At least 60% of patients responded in most reported studies. However, the majority of the response were partial (Knospe et al., 1974; French Cooperation group on Chronic Lymphocytic Leukemia, 1990b). Survival of patients in the high-risk group is poor; the median duration of survival is less than 2 years. Several regimens of combination chemotherapy have been investigated in randomized clinical trials. The regimens that were evaluated include chlorambucil plus prednisone (Han et al., 1973), cyclophosphamide plus vincristine and prednisone (COP) (Montserral et al., 1985), and COP plus doxorubicin (CHOP) (French Cooperation group on Chronic Lymphocytic Leukemia, 1989; Bennett et al., 1990). The results of these trials are not conclusive to date.

There are no established chemotherapy regimens for patients with CLL after the failure of the initial therapy. Three new drugs have recently been used as second-line therapy. All of these drugs are currently under phase II and III investigations. Perhaps the most promising is fludarabine monophosphate (2-fluoro, 5' phosphate derivative of 9-beta-D-arabinofuranosyl-adenine) (Keating et al., 1989). The other two compounds are pentostatin (2-deoxycoformycin) (Dillman et al., 1989) and 2-chlorodeoxyadenosine (Piro et al., 1988).

3.4.4 Treatment with radiation, splenectomy and/or bone marrow transplantation

Total body radiation (TBI) is not recommended for patients with CLL because it causes excessive myelosuppression. Local radiation has been used to treat bulky lymph nodes or an enlarged spleen when the enlargement of these organs cause symptoms. Splenectomy is beneficial when hypersplenism has not responded to radiation or chemotherapy (Adler et al., 1975).

Patients with advanced CLL have been treated with HLA-matched bone marrow transplants following high dose chemotherapy and radiation. Preliminary results have been promising. However, this approach only applies to less than 5% of cases of CLL.

3.4.5   Treatment with interferon and/or monoclonal antibodies

Interferon has been shown to induce the differentiation and proliferation of CLL cells in vitro (Ostlund et al., 1986). Whether this phenomenon is clinically useful is unknown. Alpha-interferon is not active in patients with intermediate- and high-risk CLL (Roth and Foon, 1986). This contrasts with the 50% rate of response in patients with non-Hodgkin's lymphoma (Foon et al., 1984b) or cutaneous T-cell lymphoma (Bunn et al., 1984), and the 90% rate of response in patients with hairy-cell leukemia (Foon et al., 1986b). Recent studies have reported greater than 50% responses in patients with previously untreated low-risk CLL when treated with low-dose $(2 \times 10^6 \text{ U} / \text{m}^2$, three times per week) of recombinant alpha-interferon (Rozman et al., 1988). However, more studies are needed to determine whether this treatment would be beneficially affect survival of CLL patients.

MoAbs have been used to treat CLL and other lymphoid malignancies (Foon . al. 1984a; Dillman, 1989b). Treatment with anti-CD5 MoAb transiently reduced levels o. c. r. ating leukemic cells, but there was no effect on the leukemic infiltrations in bone marrow, lymph nodes, or other organs (Dillman et al., 1984a). The use of antibodies conjugated with chemotherapeutic agents, radioisotopes or toxins may prove to be more effective (see the following section for a detailed discussion).

4 Potential Applications of MoAbs in the Treatment of Leukemias and Lymphomas

4.1 MoAb Alone in the Treatment of Leukemias and Lymphomas

4.1.1 Antitumor effects of unmodified MoAbs in experimental and clinical studies

There are several reports on the use of unmodified murine MoAbs in the treatment of human tumors xenografted in immuno-incompetent mice (Herlyn et al., 1980; Herlyn and Koprowski, 1982; Hellstrom et al., 1986; Gil et al., 1990; Kasprzyk et al., 1992; Ohta et al., 1993). Treatment with unmodified MoAbs usually resulted in delayed tumor growth and in a few cases, complete remission (CR). Most of CR, however, were achieved by initiating the antibody treatment within 24 hr of tumor inoculation, i.e., when the tumors were not established. Thus, these " remissions " should be considered as the prevention of tumor engraftment.

Since the first report of serotherapy with MoAbs in cancer patients in 1980 (Nadler et al., 1980), several phase I trials enrolling hundreds of patients with hematological malignancies have been carried out (Jansen et al., 1989). Murine MoAbs have been used alone in patients with acute myelogenous leukemia (AML) (Ball et al., 1983; Scheinberg et al., 1991), acute lymphocytic leukemia (ALL) (Ritz et al., 1981), CLL (Foon et al., 1984a; Dillman et al., 1986), and B-cell and T cell lymphomas (Press et al., 1987a; Hale et al., 1988; Miller et al., 1983). These clinical studies have rarely demonstrated durable antitumor effects except for the use of anti-idiotype MoAb in B cell lymphoma patients (Levy and Miller, 1990), and in a few cases, T cell lymphomas (Miller and Levy, 1981). CR has been rare. The responses have generally been brief and resistance emerges rapidly from idiotype variants when anti-idiotype MoAbs are used (Meeker et al., 1985; Raffeld et

al., 1985). In leukemias, most antitumor effects have appeared to be limited to the removal of circulating cells that were opsonized by MoAbs and then sequestrated in the reticulo-endothelial system (RES), and resulted in the transient decrease of circulating tumor cells (Nadler et al., 1980; Dillman et al., 1982). According to Jansen (1989), who reviewed 25 clinical trials of over 135 patients, passive serotherapy have resulted in overall response rates of 5% CR, 16% partial remission (PR) and 17% minor response. Recently, more promising results have been reported by several investigators (Scheinberg, 1991b; Matthews et al., 1992). Dyer et al. (1989) treated 18 patients with B-NHL with a IgG2b MoAb CAMPATH-1, which has been shown to be good at fixing human complement and mediating ADCC. There was CR in one patient and consistent reduction in the number of circulating malignant lymphocytes in all other patients. In the study reported by Brown et al. (1989), fourteen patients received anti-idiotypic MoAbs (including IgG1, IgG2a and IgG2b subclasses). Two patients had a sustained CR lasting several years and 7 others experienced PR of shorter durations. An interesting observation in this study was that tumor regression often continued for several months after the completion of treatment. The authors suggest that the anti-idiotypic MoAbs may have an antitumor effect by altering the idiotype/anti-idiotype network in the patients. Some clinical success have been achieved with the use of MoAbs that interfere with vital functions of cell surface molecules (e.g., growth factor receptors) of malignant cells. For example, IL-2 receptors (p55) are constitutively expressed on human T-cell leukemia virus (HTLV-1) induced adult T cell-leukemia cells but are only expressed sparsely on normal cells. Waldmann et al. (1988) reported the use of a MoAb directed against the IL-2 receptor, i.e., anti-Tac (p55) MoAb, in T-cell leukemia / lymphoma, with 1 CR, 2 PR and 4 minor responses in 9 patients studied.

In recent years, MoAbs have also been used in conjunction with complement, magnetic beads, or chemotherapeutic drugs to deplete malignant cells from harvested bone marrow before its reinfusion in patients undergoing autologous bone marrow transplantation (ABMT) (Kvalheim et al., 1988). Three to 6 log depletion of malignant cells from tumor cell contaminated bone marrow have been achieved by these approaches (Gribben et al., 1991). Alternatively, MoAbs directed against T cells have been used to purge bone marrow from allogeneic donors before transplantation to reduce the risk and severity of graft-versus-host disease (GVHD) (Champlin et al., 1990).

4.1.2   Toxicity and side effects of unmodified MoAbs

Minor adverse reactions have been noted in about one-third of patients (Dillman et al., 1986b). About 10-20% patients have exhibited various degrees of hypersensitivity reactions, including urticaria, pruritus and bronchospasm. Other patients have experienced fever, sweating, chill, diarrhea, nausea, vomiting and abdominal pain. Anaphylaxis has occurred rarely (less than 1%). In some more severe cases, systemic toxicity such as elevation in the level of serum transaminases was observed. However, the majority of patients have tolerated repeated infusions of murine MoAbs without severe complications. With the exception of patients with CLL and perhaps some patients with B cell lymphoma, virtually all patients exposed to murine MoAbs developed an anti-mouse Ig immune response (human anti-mouse antibody, HAMA) (Dillman et al., 1984a; Schroff et al., 1987), which can greatly reduce the efficacy of repeated MoAb therapy. Formation of antibody-antigen complexes not only neutralizes the antitumor effects of MoAbs but also enhances their clearance from circulation. Furthermore, the deposition of immunocomplexes may cause end organ damage (see Introduction section 5 for detailed discussion).

4.1.3 Effector mechanisms of unmodified MoAbs

(A)   Complement-dependent cytotoxicity (CDC) and antibody-dependent cellular cytotoxicity (ADCC)

Antitumor antibodies can fix complement or interact with cytolytic and phagocytic cells to eliminate tumor cells that are recognized by distinct surface antigens. Complement-dependent cytotoxicity (CDC) involves the fixation of complement to the Fc portion of the Ig molecule followed by activation of the complement cascade which results in puncturing of the tumor cell membrane and cell death (Frank, 1987). Different classes and subclasses of murine antibodies have different affinities for human complement because of the differences in the Fc portion of the heavy chain. Usually, murine IgM is most efficient in CDC, followed by IgG3, whereas IgG2a, IgG1 and IgG2b are generally ineffective (Herlyn and Koprowski, 1981). For human antibodies, the order of effectiveness in mediating CDC is IgM > IgG1 >IgG3 > IgG2 > IgG4 (Steplewski et al.; 1988; Shakib, 1986).

Certain effector cells such as monocytes, macrophages, NK cells and granulocytes have Fc receptors that bind to Fc portion of Ig molecules. Cell killing via this process is called antibody dependent cellular cytotoxicity (ADCC). The best results for ADCC with murine antibodies and human effector cells are obtained with IgG2a and IgG3 (Ortaldo et al., 1987), whereas for human MoAbs and human effector cells, effective ADCC is obtained with IgG1 and IgG3 subclasses (Seplewski et al., 1988; Shakib, 1986). The efficacy in mediating ADCC directly correlates with the binding affinities of the Fc receptors on effector cells for Ig molecules (Lubeck et al., 1985) and the number of antigen binding sites on tumor cells (Thurin et al., 1987). Different antibodies of the same subclass or antibodies of different subclasses directed against the same antigen display different extent of Fc binding (Dillman et al., 1986c). Because CDC and ADCC both involve binding of the Fc

portion of the antibody molecule to effector cells, only intact antibodies can be used for this approach.

(B)   Anti-receptor antibodies

Tumor cells may express on their surface increased number of various molecules which are important for cell proliferation and differentiation (Goustin et al., 1986). Such molecules can be receptors for growth stimulating factors, e.g., IL-2 (Waldmann, 1986), EGF (Singletary et al., 1987) and TRF (Hopkins and Trowbridge, 1983) receptors, or receptor associated molecules that transmit signals essential for growth regulation, e.g., *ras* p21 (Urban and Schreiber, 1992) and ABL-BCR protein (De Klein et al., 1982). Many of these molecules are the products of oncogenes. MoAbs directed against these receptors may successfully compete with the growth factors and / or down-regulate the expression of these receptors, so that the effect of growth factors on cell proliferation is lost. Many investigations in this field have been carried out with MoAbs directed against receptors for TRF (Sauvage et al., 1987), IL-2 (Waldmann et al., 1988) and EGF (Rodeck et al., 1987). Furthermore, antibodies specific for oncogene products may be able to inhibit tumor growth if the oncogene products are essential for the transformed phenotype. For example, MoAbs against cell surface proteins encoded by *erb* B-2 and *neu* oncogenes have been shown to be capable of inhibiting tumor growth in vivo (Kasprzyk et al., 1992; Drebin et al., 1988). Special attention must be paid when choosing an anti-receptor MoAb as a means for the treatment of a defined cancer. In some situations, the use of anti-receptor MoAb has been observed to stimulate tumor cell proliferation and eventually accelerate the growth of the tumor.

(C)   Regulatory antibodies

B lymphocytes express the idiotype of their secretory Ig molecule on their surface and these proteins are important in B cell activation and regulation. According to the " network hypothesis " of Neil Jerne (1974), an anti-idiotype MoAb could inhibit proliferation of an aberrant B cell clone (Sikorska, 1988). Theoretically, anti-idiotype antibodies based treatment might be effective in malignancies involving B lymphocytes, e.g., B-cell lymphomas and CLL (Levy and Miller, 1990).

(D)   Immunizing effects of antibodies

An additional indirect effector mechanism might be operating when an idiotypic cascade is generated by MoAbs. According to Jerne's network hypothesis, the injection of MoAb (Ab1) may elicit in patient an antibody response (Ab2) against an epitope on the V region of the heavy chain of Ab1. The V region of a low pencentage of Ab2 may express an " internal image " of the Ab1 defined antigen and may induce an anti-antiidiotypic antibody (Ab3) response. Some of these Ab3 have the same binding specificity as Ab1. These Ab3 might thus have a direct antitumor effect (DeFreitas et al., 1985). Although this phenomenon has not been observed consistently in the clinical setting, another approach based on the same rationale may be possible. In this approach, one immunizes the patient directly with Ab2 which is an anti-idiotype for an antibody Ab1 that reacts with tumor-associated antigen. In this case, the human anti-idiotype response would result in an antibody (Ab3) that would react with the desired tumor antigen with the reactivity of Ab1 (i.e. , murine Ab), except it would be a human antibody produced endogenously (Herlyn et al., 1987).

(E)   Catalytic antibodies

MoAbs can be raised against molecules whose structures resemble the transition state of certain bonds (Tramontano et al., 1986). Antibody binding in that setting can function as catalyst to induce hydrolysis of the cell membrane, cell proteins or nucleic acids. If appropriate specificity can be defined, these catalytic antibodies could be used for treating cancer (Shokat and Schultz, 1990; Lerner et al., 1991).

(F)   Other mechanisms

In addition to the mechanisms described above, other not well elucidated mechanisms may also play a role in the antitumor activity of unmodified MoAbs. For example, T cell activation by anti-T cell receptor MoAbs, as well as the nonspecific activation of certain cells, may result in the release of different kinds of cytokines which may augment the tumor inhibitory effect of MoAbs (i) by the direct toxicity to tumor cells (e.g., TNF), and (ii) by indirect effects, e.g., stimulation of various tumor killer cell functions, such as the lytic activity of CTLs, NK cells and macrophages.

4.2   MoAbs as Carriers in Targeted Therapy of Leukemias and Lymphomas

4.2.1   MoAbs as carriers for cytotoxic agents

As stated, only very limited antitumor efficacy has been obtained in clinical studies when antitumor MoAbs were used alone. The major limitation of this approach is its dependence upon the efficient recruitment of effector cells which may not be present in sufficient numbers in the tumor host or may lack accessibility to tumors, especially those in

immunologically privileged sites in the body, e.g., brain. Furthermore, the general immunological status of cancer patients, including effector cells, complement and immune regulation function are usually suppressed. Many investigators have tried to use MoAbs as carriers of cytotoxic agents which can exert cytotoxic effects that are independent of the immune system of the host. In this approach, agents that have inherent cytotoxic activity but no intrinsic selectivity for target cells, such as chemotherapeutic drugs, radioisotopes and natural toxins are chemically linked or conjugated to MoAb to form conjugates, i.e., chemo-immunoconjugates (Ghose et al., 1983b), radio-immunoconjugates (Sfakianakis et al., 1990) and immunotoxins (Ramakrishnan et al., 1992). Biodistribution studies with radiolabeled antitumor MoAbs in xenografted tumors in animal models have clearly demonstrated the specific localization of the MoAbs in the tumors (Pimm, 1988). Therefore, it is expected that the administration of MoAb-cytotoxic agent conjugates should lead to specific localization, accumulation and action of those cytotoxic agents in the targeted tumor only.

4.2.2 Selection of MoAbs

One important aspect of MoAb-based targeted cancer diagnosis and therapy is the selection of an appropriate MoAb to be used as the carrier of the diagnostic or cytotoxic agents. The choice of an ideal MoAb may vary with different requirements in different situations. The most important factor for the selection of carrier MoAb is the intended use of the conjugate, i.e., diagnosis versus treatment. For example, for radioimmunoimaging, the radiolabeled antibody should localize in the tumor specifically and rapidly to create an early high T/NT ratio that is required for a good image soon after the administration of the conjugate. Ideally, the radiolabeled antibody should also be cleared from the body (including the tumor) rapidly once the tumor images have been obtained. For targeted immunotherapy, in addition to its specific localization, the conjugate should remain in the tumor for an

adequate period of time to allow the MoAb-linked cytotoxic agent (i.e., drug or radioisotope) to exert its cytotoxic effect. The nature of the cytotoxic moiety to be linked and its mode of action also need consideration. A radioisotope decaying by beta emitter can kill cells within an area of several diameters of a tumor cell, while most chemotherapeutic drugs and toxins require internalization to exert their cytotoxic effect. Thus, an MoAb that is ideal for using as a carrier for targeting radioisotope may not be a good carrier for targeting drug or toxin (see detailed discussion in appropriate sections). There are many other factors that are likely to affect the effectiveness of the intended targeted therapy. These factors are briefly described below.

Class of the MoAb   Different classes of MoAbs, e.g., IgG and IgM, have been used in the preparation of different kinds of conjugates (Ghose et al., 1988a; Ballou et al., 1992). These molecules are very large (150, 000 dalton of IgG and 900, 000 dalton of IgM) compared to the molecular weight of several hundred dalton of most of the classical drugs. Most investigators prefer IgG antibodies to IgM because that IgG molecule is easier to handle in the preparation of conjugates and their localization in targeted tumors is facilitated by their smaller size.

Intact MoAb and its fragment   Whether whole antibodies or their fragments are preferable for tumor targeting is difficult to predict. There will probably be different requirements in different situations. Whole intact MoAb may accumulate in large quantities in the liver and other organs (e.g., spleen) that are rich in reticular-endothelial cells (Sands, 1990). The metabolism of antibody fragments, i.e., F(ab)'2, Fab' and single chain Fv, differs from that of the intact molecule. These smaller fragments are excreted quickly in the urine (the clearance rate, Fv > Fab' > F(ab)'2). It is believed that the fragments, in general, are more useful than the intact MoAb for tumor imaging because they penetrate tumors faster and more homogeneously, accumulate less in organs of RES and clear faster from the

circulation (Colapinto et al., 1988). Another advantage of the use of fragments is that they are less immunogenic than the intact antibodies due to the lack of the Fc portion. However, for the purpose of immunotherapy, some investigators prefer the intact MoAb because higher percentage of injected dose (i.e., % ID) of intact MoAb, as well as MoAb-linked radioisotope or drug localizes in the target tumor compared to their fragments (Holton et al., 1987). Also, the longer residence time of the intact MoAb in tumors may be beneficial for targeted drug or radioisotope to exert their cytotoxic effects (Dykes et al., 1987).

Specificity and binding affinity of the MoAb High specificity of MoAb are universally recognized as an advantage attribute for MoAb-based drug targeting. The importance of specificity of antitumor MoAb is obvious because it allows the antibody or its immunoconjugate to anchor on the target selectively. The importance of antibody affinity remains controversial. In order to accomplish effective targeting, the affinity of a MoAb need to be of 10^8 M^{-1} or better (Cannon and Hui, 1990). Most investigators presume that high antibody affinity is desirable (Schlom et al., 1992), but others suggest that MoAbs with moderate affinity may percolate more homogeneously into tumor masses than high affinity MoAbs that may be trapped by binding to perivascular tumor cells, and therefore, retarded in their movement to distal locations in the interstitium (Fujimori et al., 1990).

Species Most of the MoAbs currently used in targeted therapy are of murine origin and elicit HAMA response when used in patients (Schroff et al., 1987). The generation of humanized and chimeric antibodies for clinical application has been viewed as a potential advantage over the use of murine antibodies because the formers elicit less HAMA formation, are more effective in recruiting human effector cells, and have prolonged serum half-life (see Introduction section 5 for detailed discussion of humanization of MoAbs). It is pertinent to mention that the use of humanized MoAb may still trigger immune response after repeated injections into patients because they retain both idiotypic and allotypic

antigenic determinants. However, idiotypic responses are likely to be weaker and need longer period of exposure than those against xenogeneic MoAbs (Goodman et al., 1993).

Antigen density on tumor cells and antigen internalization As stated, for MoAb-based diagnosis and therapy of cancer, an ideal target antigen should be expressed on the surface of tumor cells at high density. The usefulness for targeting of an entirely tumor-specific antigen would be compromised if the antigen were expressed at the cell surface at a very low level that would not permit the binding of adequate amounts of conjugates needed to achieve the therapeutic response. Furthermore, for MoAbs directed against cell surface associated tumor antigen(' cytotoxic agents that are active at the cell surface would be more effective when delivered to surface of the target cells as immunoconjugates. However, only a few cell surface active chemical entities, e.g., phospholipases (Flickinger, 1976) and probably in some extent, ADR (Awasthi et al., 1992), have been evaluated for antibody based targeting. Most toxins (e.g., ricin and abrin) and currently used chemotherapeutic drugs (e.g., MTX and vinca alkaloids) are active intracellularly. Some of them exert their effect on DNA or protein synthesis, while others alter the function of the spindle apparatus. If the target of the cytotoxic moiety is intracellular, the ideal immunoconjugate should be endocytosed by the tumor cells and release active forms of the cytotoxic agent intracellularly. Thus, antibodies that are specific to those antigens that lead to maximum degree of endocytosis may be more effective for intracellular drug or toxin delivery (Mariani et al., 1990). However, antibodies with a high rate of internalization may be poorly retained by tumor cells after initial binding because of rapid endocytosis, intracellular degradation and efflux of low molecular weight metabolites. This has been shown to be a disadvantage for radioimmunotherapy. For ^{131}I labeled MoAbs, the rapid degradation of radioiodinated antibody and efflux of the catabolic small fragments may result in the rapid loss of radioactivity from the tumor (Press et al., 1988). Novel protein radioiodination techniques may overcome this problem (Ali et al., 1990). Alternatively,

radiometal isotopes, such as ^{111}In and ^{90}Y, may prove beneficial for targeting rapidly modulating antigens because these isotopes appear to be selectively retained intracellularly after degradation of the carrier MoAb (Naruki et al., 1990). In fact, for radioimmunotherapy, endocytosis is not required for the cytotoxic effect of the radiolabeled MoAbs.

4.2.3 Factors that influence the accumulation of MoAbs or their immunoconjugates in tumors and normal tissues

A key problem with MoAb-based targeted therapy is the inability of conjugate to reach all regions of a tumor in vivo in adequate quantities. In most clinical trials, very little of the injected dose of MoAbs or their conjugates, usually between 0.001% to 0.01% ID / g tissue, accumulates in the tumor (Epenetos et al., 1986; Sands and Jone, 1990). There are numerous factors that can affect the localization of MoAbs or their conjugates in tumors in vivo (Cobb, 1989; Thomas et al., 1989; Jain, 1990; Schlom et al., 1990a).

(A) Physiological factors

Several tumor-related physiological factors that can adversely affect the tumor localization of circulating MoAbs or their conjugates have been identified. These factors include the heterogeneity of blood supply, the elevated intratumoral interstitial pressure and the large transport distance (i.e., from the site of antibody transvasation to tumor cells in the peripheral region) in the interstitium.

The tumor vasculature is highly heterogeneous and may be completely different from host's normal vasculature depending on the tumor type, its growth rate and its location. It consists of vessels recruited from the preexisting network of the host vasculature and vessels

resulted from the angiogenic response of the host vessels to cancer cells (Folkman, 1985). A key difference between normal and tumor vessels is that the latter are dilated, saccular, and tortuous and may contain tumor cells within the endothelial lining of the vessel wall (Jain, 1988). The tumor vasculature is highly heterogeneous and does not conform to the standard normal vascular organization. Also, the organization of vessels in tumors may be different from one location to another and from one time to the next. It is known that a antibody must first be distributed to tumor through the vasculature and then transported across the microvascular wall and the interstitial space to reach the tumor cells. The heterogeneity of blood supply would reduce the chance of delivery of MoAbs or their conjugates to some area of tumor due to the poor blood supply. In addition, an increase in the intercapillary distance would require the MoAbs or their conjugates to traverse longer distance in the interstitium to reach tumor cells in peripheral regions. Tumor necrosis has a similar adverse effect on antibody localization in the tumor since necrosis destroys or narrows intratumoral vessels by thrombosis.

Once the MoAbs or their conjugates have reached an exchange vessel in tumor, its extravasation occurs by diffusion (i.e., solute movement resulting from solute concentration gradients) and convection (i.e., solute movement associated with bulk solvent movement), and to some extent, transcytosis. The rate of extravasation of MoAbs or their conjugates is dependent on (i) surface area of exchange; (ii) the transvascular concentration and pressure gradients; and (iii) other transport parameters, such as vascular permeability and hydraulic conductivity (a constant related to fluid leakage to pressure gradient). Studies of animal and human tumors have shown that the vascular permeability of tumor vessels was higher than that in normal tissues (Jain, 1987a). Two factors are believed to be responsible for the poor extravasation of circulating MoAbs or their conjugates. Firstly, tumors contain regions of high interstitial pressure due to (i) rapid tumor growth; (ii) necrosis and/or infiltration; (iii) increased concentration of plasma

protein in tumor interstitium because of the higher vascular permeability; and (iv) lack of lymphatic drainage. This high intratumoral interstitial pressure impedes the fluid extravasation. Since the transvascular passage of macromolecules under normal conditions occurs primarily by convection, a decrease in fluid extravasation would lead to a decrease in extravasation of the MoAbs or their conjugates (Baxter and Jain, 1989). Secondly, the average area of vascular surface per gram of tumor tissue decreases with tumor growth due to rapid proliferation of tumor cells, hence lead to a reduction in the transvascular exchange (Jain and Baxter, 1988).

Extravasated MoAbs or their conjugates could move through the interstitial space by diffusion and convection to reach the target tumor cells (Swabb et al., 1974). The interstitial space in tumors is usually larger than that in normal tissue (Jain, 1987b). This means that the MoAbs or their conjugates have to transverse longer distance in the tumor interstitium to reach tumor cells in the peripheral regions of vascular supply. This may increase the probability of catabolism of MoAbs or their conjugates in tumor interstitium before the MoAbs or their conjugates could bind to target cells. Tumor catabolism of MoAbs or their conjugates may adversely affect the amount of accumulation as well as the residence time of MoAbs or their conjugates within the tumor, because the products of the catabolism are usually smaller in molecular weight and hence may be cleared relatively rapidly (Press et al., 1988). Furthermore, the MoAbs or their conjugates may also bind nonspecifically to proteins or other tissue components, as well as specifically to the target cells during its transportation in tumor interstitium (Jain et al., 1980). It is known that the binding reaction lowers the diffusion rate of molecules (Astarita, 1967). The binding of MoAb to antigens proximal to the vessels may retard its movement to peripheral regions in the tumor interstitium, especially when a MoAb with high affinity was used (Dedrick and Flessner, 1989; Fujimori et al., 1990).

(B) Pharmacokinetic factors

A number of pharmacokinetic factors influence the accumulation of antibodies in target tumors. These factors include: the classes (e.g., IgG versus IgM) and the forms (e.g., intact molecule versus its fragment) of antibody (which have been discussed above), the dose, the route of administration (e.g., i.v. versus i.p.), and the metabolism and clearance of antibodies or their conjugates from the blood.

The effect of the administered dose of an antibody on the percentage of the injected dose of antibody localized in the tumor (i,. e., % ID / g tumor) is difficult to predict. Increase of the dose of radiolabeled MoAbs given to xenograft bearing mice has produced conflicting results, with increased, decreased, and unchanged tumor uptake reported (as regard to % ID / g tumor tissue) (Carrasquillo, 1988; Fenwick et al., 1989; Boerman et al., 1992). Studies conducted to date in patients have used a wide range of antibody doses varying from less than 1.0 mg to more than 1.0 g (Grossbard et al., 1992). The optimal antibody dose for either diagnostic or therapeutic uses may vary depending on many factors, such as the quality of antibody (e.g., specificity, affinity and immunoreactivity), the quantity of antigen (e.g., the level of antigen expression and the tumor burden), antibody internalization rate, and different tumor types and tumor hosts (Grossbard et al., 1992). It must be born in mind that for a tumor of defined type and size, the number of antigenic sites is limited and may be saturated with appropriate amount of MoAb. Once saturated, increase the dose of MoAb given to the tumor-bearing host will not increase the absolute amount of MoAb that localized in the tumor. Under this situation, the value of % ID / g tumor tissue will decrease although the absolute amount of MoAb that localized in the tumor remains the same.

For intracavitary cancers (e.g., ovarian and colon cancers), the administration of MoAbs or their conjugates via the relevant intracavitary route may provide several theoretical advantages, including increased concentration of antibody at the tumor site and decreased toxicity to those normal organs that are involved in the metabolism of antibody, such as the liver. Some studies either in animal models or patients have shown that the i.p. route of injection was better than the i.v. route for targeting of peritoneal tumors (Rowlinson et al., 1987).

Uptake and catabolism of antibodies by organs of RES (e.g., liver and spleen) and clearance of the antibody fragments through kidney appear to be the major routes of elimination of circulating MoAbs or their conjugates (Jones et al., 1990). It has been suggested that liver cells have receptors for a component of the Fc portion of the antibody which is responsible for the non-antigen specific uptake of radiolabeled antibody (Sands, 1990). However, it is not know yet whether these receptors are for the protein component of Fc, or the carbohydrates which are found predominantly on the Fc portion.

(C) Immunological factors

As discussed above, the quality, the forms and the species of antibodies may significantly affect the localization of MoAbs or their conjugates in tumors as well as in normal tissues. Additional immunological factors are the following:

Antigenic heterogeneity Antigen heterogeneity of the tumor cells includes the difference in (i) the proportion of cells within the tumor expressing the antigen; (ii) the levels of antigen expression in different tumor cells within the tumor; (iii) the exact location of the antigen (cell surface or intracellular), their accessibility and their availability in the environment of the cells.

Antigen modulation and secretion   Antigen modulation, e.g., antigen internalization or shedding, and the level of circulating reactive antigen in the blood or in other body fluid may significantly affect the effectiveness of MoAb-based targeted therapy. If the internalized or shedded antigens are not re-expressed, subsequent administration of MoAbs or their conjugates will not produce significant amount of binding to tumor cells. Furthermore, shedding of tumor antigen from surface of tumor cells or secreting of tumor antigen by tumor cells into body fluids, especially into blood, constitute an additional problem that may impede delivery of MoAbs or their conjugates to tumor. There is a concern that the injected MoAbs or their conjugates may be trapped by the circulating antigen to form immune complex and may never reach the tumor. This may also result in the rapid clearance of MoAbs or their conjugates from the circulation. Despite all above concern, clinical observation to date have shown that the problem did not have practical significance.

HAMA response   The development of host antibodies against the foreign antibodies may not only neutralize the antitumor effect of the MoAbs or their conjugates, but also accelerate the clearance of the antibody form the circulation, reduce antibody localization in the tumor, and induce hypersensitivity reaction (Schroff et al., 1985; Shawler et al., 1985; Courtney-Luck et al., 1986).

(D) Physical and technical factors

In the preparation of an immunoconjugate, the biological properties of the antibody must correlate with the physical properties of the cytotoxic agents chosen for conjugation. For example, an antibody with a high rate of internalization upon binding to target antigen on tumor cell surface is desirable for immunotoxin, because internalization is required for

cytotoxic effect of most toxins. While in radioimmunotherapy, a long half-life radioisotope should be used when a long time is required for the antibody to accumulate in the tumor, or vice versa. Chemical modification of antibody or drug, and / or the subsequent coupling process may damage the antibody binding ability and / or the drug activity. In radioimmunoimaging or radioimmunotherapy, there are additional limitations such as the availability of suitable radioisotopes, the choice of appropriate methods of radiolabeling and the availability of instrumentation for the handling of radionuclides. Furthermore, the doses, physical half-life and the type of the emitted radiation(s) of the radionuclide, as well as the time of imaging may determine to a great extent the quality of the image and the effectiveness of treatment (see appropriate sections for detailed discussion).

4.3 MoAb-Drug Conjugates (Chemoimmunoconjugates)

Targeting of conventional chemotherapeutic drugs to tumors using MoAbs is being developed as a method to improve their therapeutic index. This may result either from increased localization and / or longer retention of antibody-linked drugs in tumors compared to their localization and / or retention in normal tissues, or by reducing normal tissue toxicity. Because the majority of available MoAbs react to some degree with normal tissues, it is important to develop immunoconjugates that will not produce unacceptable levels of toxicity towards vital normal tissues. Due to the extreme potency of toxins, i.e., one molecule of toxin can kill one cell when delivered to the cytosol of the cell, immunoconjugates produced with conventional chemotherapeutic drugs offer a significant safety advantage. Several additional advantages of using chemotherapeutic drug for the preparation of immunoconjugates include: (i) the clinically used anti-cancer drugs have established profiles of antitumor activity; (ii) the dose-limiting toxicities of the drugs have been well characterized; (iii) method to monitor drug level in body fluid, e.g., serum, are readily available; and (iv) control and / or reversal of toxic manifestations may also be

possible. Therefore, these immunoconjugates are likely to be accepted more readily by clinical oncologists.

4.3.1 Selection of chemotherapeutic drugs for the preparation of MoAb-drug immunoconjugates

The selection of cytotoxic agents for the preparation of immunoconjugates usually depends upon (i) mechanism(s) of action and pharmacokinetic profiles of the chemotherapeutic agents; and (ii) the nature of the MoAb available for the construction of immunoconjugate (Ghose et al., 1985). Since the targets of most of currently used chemotherapeutic agents are intracellularly distributed and some drugs are active only when they are in free form, an ideal conjugate should be endocytosed once bound to the surface antigen of target cells, and to release active drug molecules in free form or associated with small catabolic fragments intracellularly. In contrast, if the MoAb dose not undergo significant internalization after binding to target cell surface antigen, only those agents that exert their cytotoxic effect via plasma membrane (e.g., phospholipase and ADR) or agents that emit ionizing radiations (e.g., ^{131}I and ^{90}Y) are likely to yield effective conjugates.

To date, many chemotherapeutic drugs with different mechanisms of action including alkylating agents (e.g., chlorambucil, melphalan), DNA intercalators (e.g., daunomycin, adriamycin), mitotic inhibitors (e.g., vinblastine, vindesine), and antimetabolites (e.g., methotrexate, 5-fluorouracil) have been chemically conjugated to a number of antitumor MoAbs with the use of different coupling methods (Ghose et al., 1983b; Ghose and Blair, 1987). A selective cytotoxicity against target tumor cells either in vitro or in vivo in animal models has been observed in most studies (Pimm, 1988).

In this study, two drugs with different mechanisms of action, i.e., MTX and ADR were covalently coupled to two MoAbs, Dal B01 and Dal B02, via different types of linkage. Both drugs are in clinical use for the treatment of a wide range of cancers. The detailed characteristics of these two drugs, e.g., the spectra of antitumor activity, mechanisms of action, clinical pharmacology , will be discussed later (see Fig. 1 for the chemical structure of MTX and ADR).

4.3.2 Linkage of drugs to MoAbs

Methods for the coupling of chemotherapeutic agents to MoAbs must ensure the retention of activity of both MoAbs and drugs (Blair and Ghose, 1983; Ghose and Blair, 1987). Optimal coupling methods should allow controlled drug incorporation, avoid formation of homopolymers of MoAbs or drugs and aggregates of the conjugate. The method should also be technically straightforward and reproducible. Furthermore, the drug must be delivered to the target site in a form that is active or can be activated *per se*. Since most antitumor drugs have certain functional groups that are essential for binding to target molecules, chemical groups used for linkage to MoAb should be the one that is not required for drug action, or as an alternative, the one that become available following endocytosis and intracellular catabolism of the conjugate. Chemo-immunoconjugates have been produced by linking drugs to antibodies using a number of functional groups such as an amino-, carboxyl-, hydroxyl-, or sulphydryl- residues. In some instance, these functional groups exist in drug or MoAb molecules, while in other cases, they are introduced in drug or MoAb molecules by initial modification (Blair and Ghose, 1983; Ghose and Blair, 1987).

(A) The use of carrier

Conjugates prepared by coupling drugs directly to MoAbs have been successfully synthesized. However, this type of conjugates has a limited potential because only a small number of functional groups are available per antibody molecule for chemical linkage without significant loss .-i .- 'igen binding activity (Blair and Ghose, 1983). For the delivery of adequate amounts of chemotherapeutic agents to target tumor cells, it may be necessary to a 'ch a relatively large number of drug molecules per antibody molecule while preserving antibody activity. Retention of antigen binding activity in carrier antibody molecule is influenced by a number of factors which include the size and charge of the drug, the molar incorporation, the site of linkage and the nature of the antibody. Unfortunately, most of studies using direct linkage have shown that the substitution of more than 10 drug residues per antibody molecule usually produces unacceptable loss of antibody activity (Kulkarni et al., 1985). Furthermore, the attachment of a high payload of certain hydrophobic drug molecules to antibody may result in the loss of solubility of the conjugate (Mitra and Ghosh, 1990). This has led to the use of intermediate carriers where high levels of drug substitution is possible and then one or two molecules of the drug-loaded carrier are linked to one antibody molecule. The conjugates constructed in this manner contain a large number of drug molecules per antibody molecule. The use of an intermediate carrier can also overcome, to some extent, the steric hindrance of drug or antibody activity resulted from the direct linkage of the agents. The criteria for the selection of intermediate carrier include the molecule size and shape (e.g., globular or linear chain), charge, number of available functional groups, homogeneity, ease r·f handling, ease of coupling stability, ιoxicity and biodegradability (Mitra and Ghosh, 1990).

An alternative approach to increase the amount of drug that can be loaded on MoAb is the use of liposome (Ghose et al., 1988c). Use of liposome as drug carrier has attracted considerable interest in recent years because of their ability to load with large amount of drug molecules without the requirement of any chemical modification, i.e., the drug packed

inside the liposome remains in their natural free form (Singh, 1989). Also, intravenously administered liposome-entrapped drug does not come in contact with blood directly, and the tissue distribution is controlled by their carrier (McDougall et al., 1974). Thus by linking the liposome with MoAbs directed against tumor associated antigens, the drug can be specifically targeted to tumors (Singh et al., 1991).

(B) The use of spacer

As stated, when a drug molecule was coupled directly to an antibody molecule, its cytotoxic effect might be significantly affected by (i) steric hindrance; and (ii) the use of those chemical groups for conjugation that are essential for the cytotoxicity of the drug. Some drug molecules linked directly to antibodies have been observed to be poorly released from the carrier antibody by lysosomal enzymes. Such slow release might be due to either a steric effect, i.e., the inaccessibility of the lysosomal enzyme to the chemical bond of linkage between the drug and the MoAb, or the insusceptibility of the linkage to the lysosomal enzymes (Trouet et al., 1982). The introduction of a spacer either in drug or antibody molecule may be of help of overcoming the above problems.

In one approach, spacers are designed in such a way that conjugates remain stable in circulation as well as in other extracellular compartment, but release the free drug in the lysosomal milieu after endocytosis. One of the example of such spacer is the Ala-Leu-Ala-Leu tetrapeptide which has been demonstrated to release the free drug in the presence of lysosomal enzymes (Trouet et al., 1982). An alternative approach is based on the acid pH within the lysosomal compartment. An acid-labile spacer, e.g., cis-aconityl spacer, has been used to link drugs, such as DNR and ADR, to antibody molecules (Shen and Ryser, 1981; Dillman et al., 1988).

(C) Site-specific linkage

Most "conventional" conjugation methods of coupling drugs to antibodies lack specificity because the incorporated drug molecules are randomly distributed in antibody molecules. This may result in linkage of drugs at antigen-binding sites of the antibody. This is believed to be mainly responsible for the partial or complete loss of antibody activity after conjugation, especially when large amounts of drugs are linked to an antibody molecule. When drugs are loaded on antibody via intermediate carriers, one may still confront the problem of loss of antibody activity if the intermediate carriers are incorporated in the antigen binding site of antibodies. It is well known that oligosaccharide residues are infrequent in the antigen binding site (i.e., Fab portion of antibody), and are restricted mainly to the Fc portion of antibody (Beale and Feinstein, 1976). The linkage of drug or drug-loaded carriers to the oligosaccharide residues may provide a method to avoid drug loading in antigen binding site of antibodies. Most coupling reactions for the linkage of drug to oligosaccharide residues on antibody are based on oxidation of the oligosaccharide residues followed by formation of Schiff's base or hydrazone bond with the drug or drug-loaded carrier molecules (Rodwell et al., 1986; Kralovec et al., 1989a). This method has been successfully used in the preparation of immunoconjugates of MTX (Kralovec et al., 1989b), ADR (Dillman et al., 1988) and vinca alkaloid derivatives (Johnson et al., 1987).

4.3.3 Methotrexate (MTX)

(A) Spectrum of antitumor activity and mechanism of action

The folic acids are an attractive target for antitumor chemotherapy because of their critical role in the synthesis of the precursors of DNA. The clinical effectiveness of antifolate

compounds, e.g., MTX, has been proven in the treatment of leukemias, breast cancer, head and neck cancer, choriocarcinoma and lymphomas (DeVita et al., 1985)

The critical structure feature associated with the antitumor activity of folate analogues is the substitution of an amino group for the hydroxyl at 4 position of pterdine ring and the presence of a methyl group at the N^{10} position (Figs. 1A and 1B). These changes transform the molecule from a substrate to a tight-binding inhibitor of DHFR, a key enzyme in intracellular folate metabolism. The importance of DHFR stems from the fact that folates are active as coenzymes only in their fully reduced forms as tetrahydrofolates. In actively proliferating tumor cells, inhibition of DHFR by MTX leads to accumulation of folates in the inactive dihydrofolate form, with partial depletion of reduced folates (Baram et al., 1987). There are additional factors that contribute to the cytotoxicity of MTX. These include metabolism of the parent compound to polyglutamate derivatives and the accumulation of dihydrofolate and formyldihydrofolate as a consequence of DHFR inhibition (Allegra et al., 1987). All these metabolites directly inhibit folate-requiring enzymes of thymidylate and purine synthesis (Allegra et al., 1985). Thus, the inhibition of synthesis of DNA precursor by MTX is multifactorial and includes both partial substrate depletion and direct inhibition of folate-dependent enzymes.

(B) Cellular pharmacology

(a) Transmembrane transport

MTX enters cells mainly by a single high-affinity influx mechanism, an energy-dependent, temperature-sensitive and concentrative process that probably depends on the function of specific intramembrane proteins (Anthony et al., 1985).The mechanism is anion-dependent and glucose-insensitive and account for all MTX influx at extracellular drug concentration up to 50 μM (Henderson et al., 1987). The affinity of the influx carrier for MTX has been

estimated to be 0.7 to 6.0 μM for various tumor cell lines (Goldman et al., 1968; Warren et al., 1978). It is well known that the physiologic folates compete with MTX for entering cells. When high concentration of extracellular reduced folate cross the cell membrane, it also lead to efflux of intracellular MTX from cytoplasm through a process known as heteroexchange (Goldman et al., 1971). In addition to the high affinity transport mechanism, a second relatively less efficient transport mechanism has been described at high drug concentrations (i.e., in excess of 20 μM) (Warren et al., 1978; Hill et al., 1979). This second mechanism may represent passive diffusion and this transport mechanism is not subjected to competition between folate and MTX, and does not lead to heteroexchange.

The efflux of MTX from cells takes place through multiple mechanisms. In one of mechanism, the carrier appears to be identical with the influx carrier (Henderson et al., 1984; Dembo et al., 1984). This mechanism accounts for the majority of the efflux of MTX from tumor cells in the absence of glucose. In the glucose-replete conditions, most efflux occurs by two other glucose and ATP-dependent mechanisms (Henderson et al., 1986). The cell cycle status of tumor cells strongly influence the rate of folate and MTX transport. In general, more rapidly dividing cells have a greater rate of MTX uptake and a decreased rate of drug efflux, as compared to its transport in stationary phase or slowly growth cells (Chello et al., 1980).

(b) Intracellular metabolism

Like naturally occurring folates, MTX undergoes polyglutamation through the action of an enzyme, folylpolyglutamyl synthetase (FPGS) that is present in the cytoplasm of many types of normal as well as tumor cells (Whitehead, 1977; Joliver et al., 1982). Polyglutamation of MTX increases its retention in the cells because the polyglutamates of MTX is not subjected to efflux (Balinska et al., 1981). It has a slower dissociation rate

from DHFR than that of MTX (Whitehead, 1987), and has markedly enhanced inhibitory potency for TS. Several parameters influence a cell's ability to polyglutamate MTX. Important factors are: the level of intracellular FPGS, the rate of cell growth (Kennedy et al., 1985) and the level of intracellular folates (Joliver et al., 1987). Growth factor induced cell proliferation increases polyglutamation of MTX. On the other hand, increase in the intracellular folate pools decreases polyglutamation of MTX.

(c) Binding of MTX to DHFR and inhibition of the enzyme

Optimal binding of MTX to DHFR is dependent on the concentration of NADPH (Kamen et al., 1983). Binding of MTX to DHFR from bacterial and mammalian sources generates a solely formed ternary complex. The overall process has been termed slow, tight-binding inhibition and involves an initial rapid but weak enzyme-inhibitor interaction followed by a slow but extremely tight-binding isomerization to the final complex (Williams et al., 1980). The polyglutamates of MTX are at least equally as potent in their tight-binding inhibition of mammalian DHFR, and the metabolites seem to possess a slower rate of dissociation from the enzyme compared to the parent compound (Galivan, 1980).

(d) Mechanisms of development of MTX resistance

Several mechanisms have been described to be responsible for the resistance of tumor cells to MTX. These mechanisms include: (i) reduced transport of MTX cross the membrane (Schuetz et al., 1988); (ii) decreased ability to form MTX polyglutamates (Pizzorno et al., 1988); (iii) increased level of intracellular DHFR activity and/or reduced affinity of binding of the enzyme to MTX (Kaufman et al, 1978).

(C) MTX and immunoconjugates

Since the early study in 1958 in which Mathe coupled MTX to an antibody directed against L1210 leukemia cells and observed an improved antitun.or activity of the conjugate in tumor-bearing mice (Mathe et al., 1958), the drug has been extensively used to prepare immunoconjugates (Baldwin and Byers, 1987; Umemoto et al., 1989). Specific cytotoxic effects of these immunoconjugates have been demonstrated both in vitro and in vivo in animal models (Ghose et al., 1988a; Shih and Goldenberg, 1990). Biodistribution studies in tumor bearing mice showed that after i.v. administration, the MoAb-MTX conjugates selectively localized in the xenografted tumors (Pimm et al., 1988a; Ballou et al., 1992). Several studies have also demonstrated an enhanced sensitivity to antitumor MoAb linked MTX of some tumor cell lines that are highly resistant to free MTX (Embleton and Ho, 1986). From studies on the mechanism of action of MTX immunoconjugates, it appears that the conjugate first binds to the tumor cell surface via tumor-associated antigens and is then internalized by endocytosis and degraded by lysosomal enzymes, providing active forms of the drug (see appropriate sections in Discussion for detailed discussion).

4.3.4   Adriamycin (ADR, or Doxorubicin, DOX)

(A) Spectrum of antitumor activity and mechanisms of action

ADR (Fig. 1C) has a spectrum of antitumor activity that is second only to the alkylating agents and is currently one of the most widely used antitumor drug. It is highly active against epithelial tumors such as carcinoma of breast, lung, thyroid and stomach and against mesenchymal malignancies such as sarcomas, Hodgkin's and non-Hodgkin's lymphoma, multiple myeloma, and acute lymphocytic and myelogenous leukemias (Myers and Chabner, 1990).

The transmembrane movement of ADR is by free diffusion of the non-ionized drug (Dalmark and Strom, 1981; Gianni et al., 1983). In some cells, ADR can undergo active efflux which is mediated by the p170-glycoprotein, a membrane protein capable of pumping out of the cell a wide range of drugs (Kartner et al., 1983). Although the general processes by which ADR crosses cell membrane have been established, the kinetics of this process are far from adequately studied. Once inside cells, free ADR tend to bind to many intracellular proteins, DNA and perhaps, glycosaminoglycans. It has been suggested that ADR kills cells by several different mechanisms, these include: (i) Binding to topoisomerase II and cause DNA breakage (Ross et al., 1978; Waring, 1981; Tewey et al., 1984). ADR appears to stabilize topoisomerase-DNA complex leading to both single and double-strand DNA breakage. Correlation was observed between cellular DNA cleavage and cytotoxicity. (ii) Binding to membrane lipids and cause extensive disruption of membrane functions (Tritton and Dorshow, 1986). It is believed that ADR-membrane interaction occurs primarily through high affinity binding of ADR to specific membrane lipids (Goormaghtigh et al., 1980; Goormaghtigh et al., 1984). The binding causes membrane changes which include an altered liquid crystal structure of membrane lipids (Tritton et al., 1978; Dupou-Cezanne et al., 1985), inhibition of membrane ion transport proteins (Hasmann et al., 1989), disruption of mitochondrial membrane integrity and electron transport (Mailer and Petering, 1976; Gosalvez et al., 1974) and tyrosine kinase mediated signal transduction (Donello-Deana et al., 1989; Zhao et al., 1989). The observation that ADR can be cytocidal without entering the cells strongly indicate that ADR may exert its cytotoxic effect through its interaction with cell membrane (Triton and Yee, 1982). It has also been suggested that the cumulative injury in cell membrane is extensive enough to inhibit the proliferation of neoplastic cells at concentrations lower than those required to interfere with nucleic acid synthesis (Murphree et al., 1976). (iii) Generation of free radical (Bachur et al., 1977; Keizer et al., 1990). ADR can be converted into a semiquinone free radical which may further transfer its free electron to molecule oxygen,

leading to the formation of superoxide radical (O2-). The O2- radical can react with two protons (H+) to form hydrogen peroxide (H2O2) which may be reduced to form hydroxy! radical (OH-). Both O2- and OH- radicals can damage cells by initiating lipid peroxidation (Cummings et al., 1991). Certain types of cells like cardiac and some tumor cells with a relatively deficiency in their anti-oxidant defense capacity are more susceptible to the effect of free radicals, thus are more sensitive to the cytotoxicity of ADR. (iv) Direct binding of ADR to DNA by intercalation. ADR inserts between the base pairs of DNA by intercalation. This may cause inhibition of DNA replication and RNA transcription by inhibition of DNA-polymerase and RNA-polymerase (Cummings et al., 1991).

(B) Clinical pharmacology and pharmacokinetics

ADR have no documented antagonistic interaction with any of the other widely used antitumor drugs. In addition, clinicians have a wide latitude as regard the dose and schedule of administration of this drug. At present, there is little evidence that changes in the schedule of administration of ADR have any significant effect on its antitumor activity. The drug has essentially an equivalent antitumor activity when an identical dose is administered as a single large bolus once a month, or weekly doses or as a prolonged infusion. The antitumor activity of ADR is proportional to the area under curve (AUC) and not to the serum peak drug level. Variation in the schedule of administration do, however, significantly change the pattern of normal tissue injury (Legha et al., 1982). Because the serum peak level correlates with the cardiac toxicity, administration of ADR by prolonged infusion has reduced its cardiac toxicity, and has also dramatically decreased the nausea and vomiting associated with bolus administration.

After i.v. administration of ADR, there is an early distribution phase during which the serum level of drug falls rapidly ($t1/2\alpha$ = 10 min) as the drug gain access to all tissues of

the body except the brain. In this phase, the bulk of the drug binds to DNA throughout the body (Terasaki et al., 1989). Plasr. a protein-bound drug accounts for approximately 75% of the drug in the plasma (Greene et al., 1983). However, tissue / plasma ratios of ADR range from 10 to 1 to 500 to 1, because of the higher affinity of the drug for DNA compared to its affinity for plasma. The short $t1/2\alpha$ is followed by a secondary half-life of 1 to 3 hr. The terminal half-life of 30 to 50 hr accounts for over 70% of the total drug AUC. These results suggest that drug level sufficient for tumor cell kill may persist for prolonged periods even after a single dose injection (Greene et al., 1983).

The major toxicities of ADR in clinical application include myelosuppression, mucositis, hair loss, severe local injury after extravasation, and most importantly, cardiac toxicity.

(C) ADR and immunoconjugates

ADR has been covalently conjugated to MoAbs via either direct linkage or through an intermediate carrier (e.g., dextran) (Hurwitz et al., 1975; Pimm et al., 1982). Biodistribution study carried out by rang and Reisfeld (1988) showed that administration of a MoAb-ADR conjugate to tumor bearing mice resulted in a 4.5-fold more ADR localized in xenografts compared to the amount ADR localized in xenograft after administration of free ADR. Selective cytotoxicity has been demonstrated with MoAb-ADR conjugates both in vitro and in animal models (Greenfield et al., 1990; Dillman et al., 1988). In several reports, MoAb-ADR conjugates retarded subcutaneous tumor growth more efficiently than free drug (Braslawsky et al., 1990; Trail et al., 1992). ADR similarly conjugated to a control IgG had no significant antitumor effect. There were also reports demonstrating that the toxicity of ADR was significantly reduced after conjugation with macromolecular carriers (e.g., antibody and dextran). For example, in one recent study, all mice given i.p. 5 injections (q2d) of 20 mg MoAb-linked ADR/kg or 3 injections (q4d)

of up to 35 mg MoAb-linked ADR/kg survived without showing evidence of systemic toxicity, while 3 injections of 8 mg free ADR/kg killed one third of the treated mice (Trail et al., 1992).

4.3.5 Clinical studies with antibody-drug immunoconjugates

Although promising results have been achieved with a number of antibody-drug immunoconjugates in human xenograft bearing animals, few clinical studies have been performed. According to Pietersz and McKenzie (1992), only approximately 160 patients have been treated with antibody-drug immunoconjugates since 1975, when Ghose et al. reported the first clinical trial in melanoma patients using polyclonal anti-melanoma antibody-chlorambucil conjugate (Ghose et al., 1975). These trials involved patients with different types of cancer, e.g., carcinomas of colorectal (Takahashi et al., 1988), ovarian (Ford et al., 1983) and lung (Schneck et al., 1989), melanoma (Ghose et al., 1975) and neuroblastoma (Melino et al., 1984). Various drugs have been linked to antitumor antibody and used in these clinical studies, including: chlorambucl (Ghose et al., 1975), vindesine (Ford et al., 1983), daunomycin (Melino et al., 1984), adriamycin (Oldham et al., 1988), neocarzinostatin (Takahashi et al., 1988), melphalan (Tjandra et al., 1989), vinca alkaloid (Schneck et al., 1989), mitomycin (Oldham et al., 1989; Orr et al., 1989) and methotrexate (Elias et al., 1990). PR or minor response have been obtained in only a small proportion of treated patients, and CR was not seen. Treatment related toxicity has been minor, including fever, rash, chills, vomiting, diarrhea and abdominal pain. In more severe case, serum sickness, marrow depression, or leukocytosis have been observed.

Fig. 1

Chemical structures of MTX, folic acid and ADR.
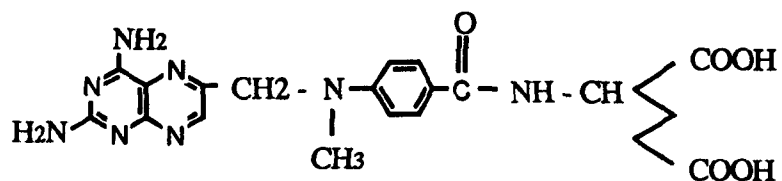
(A) MTX
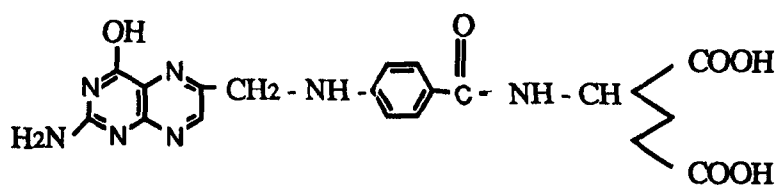
(B) Folic Acid
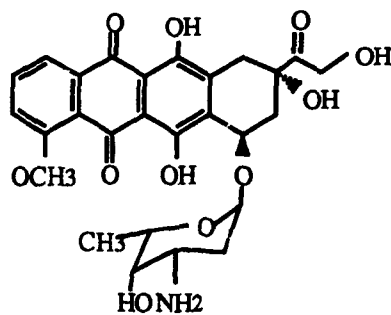
(C) ADR

4.4 MoAb-Radioisotope Conjugates (Radioimmunoconjugates)

4.4.1 Radiolabeled MoAbs for treatment of cancer: radioimmunotherapy

MoAbs can be also used to specifically deliver radionuclides emitting ionizing radiation to tumor cells (Goldenberg, 1988; 1992). The use of radiolabeled MoAbs for the treatment of cancer offers several theoretical advantages compared with the use of chemo-immunoconjugates and immunotoxins. Treatment with radiolabeled antibody does not require that every malignant cell be bound by the carrier antibody to be killed or rendered sterile, as the radiation from a radionuclide attached to an antibody molecule is emitted in all direction within an area defined by the path length of the radionuclide and the composition of the tissue (Goldenberg, 1990). This may allow the killing (or render sterile) of antigen-negative tumor cell variants, or of malignant cells whether antigen-positive or negative which are inaccessible to the radiolabeled antibody by radioactivity emitted from nearby antibody-coated cells (Nourigat et al., 1990). Furthermore, as stated, internalization of the conjugate, which is necessary for the cytotoxicity of most toxin or drug conjugates, is generally not necessary for radiolabeled antibody.

4.4.2 Selection of radioisotopes

(A) Radioimmunoimaging

It is generally accepted that an ideal isotope for tumor imaging should satisfy the following criteria: (i) decay by pure gamma emission; (ii) energy f the emitted gamma ray should be between 100 to 200 KeV; (iii) have a physical half-life (t1/2) between 1 to 3 days; (iv) be easily linked to antibody without affecting the biological properties of the protein; (v) ease of availability; and (v) inexpensive It is obvious that no currently available radionuclide

satisfies all these criteria (Goldenberg, 1991a; Goldenberg and Larson, 1992). Some of the radionuclides that are most commonly used for tumor imaging are listed in Table 1.

For many years, ^{131}I has been the most commonly used radioisotope because of its availability and well-defined radiochemistry (Sfakianakis, et al., 1990). This isotope, however, has a relatively long half-life of 8.05 days with a suboptimal gamma energy level of approximately 364 KeV and also emits beta radiation. In vivo dehalogenation constitutes another limitation for the use of radioiodinated antibody. [123]I, with a pure gamma emission of energy level of 159 KeV, has a half-life of 13 hr, which makes it suitable for obtaining images up to 24 hr after administration. However, its short half-life renders it unsuitable for intact carrier antibodies which take much longer time to achieve high T/NT ratios of localization. In addition, ^{123}I is not widely available and relatively expensive. With the use of F(ab)'2 or Fab fragments, ^{123}I may demonstrate some advantages over the more commonly used [131]I. [111]In, with a half-life of 67 hr and gamma energy level of 171 and 245 KeV, is also a very attractive isotope for tumor imaging. The major disadvantages of ^{111}In include problem associated with chemical li kage to antibodies, relatively high cost and localization of released radionuclide in RES. [99m]Tc has superior imaging qualities but again, its short half-life (t1/2 = 6 hr) is a disadvantage for linkage to intact antibodies. Several other radioisotopes that are being currently investigated include ^{67}Ga, [201]Tr, [97]Ru and [203]Pb. All these isotopes decay by pure gamma emission and possess appropriate energy spectra (135 to 279 KeV) and physic half-life (52 to 79 hr) suitable for gamma camera imaging. However, studies with these isotopes are limited because of the difficulty in availability.

Table 1 Radionuclides currently in use for radioimmunoimaging of cancer

Nuclide	Half life	Energy (keV)	Mode of decay	Remarks
^{131}I	8.05 days	364, 608	β, γ	Easily available, Inexpensive, Ease of protein labeling, T $1/2$ too long for imaging, β emission, Dehalogenation.
^{123}I	13.3 hr	159	EC	Good energy for imaging, No β emission, Expensive, Low availability, Dehalogenation.
^{111}In	67.4 hr	171, 247	EC	Good energy and t $1/2$ for radioimmunoimaging. Easily available, Expensive, Affinity for RES.
^{99m}Tc	6 hr	141, 322	isomeric transition (IT)	Easily available, Inexpensive, Pure γ emission, T $1/2$ too short for imaging.

(B) Radioimmunotherapy

Controversy still exists regarding the advantages and disadvantages of the various alpha, beta and gamma emitters for radioimmunotherapy (Goldenberg, 1991b). Isotopes such as ^{131}I, ^{90}Y and ^{188}Re have the advantage of releasing beta particles that penetrate several millimeters and therefore could be of value for antigen-negative tumor variants and those nearby tumor cells which are inaccessible to the antibody. This will clearly reduce the chance of escape of antigen-negative tumor cells. However, it compromises the selectivity of targeted radioimmunotherapy by damaging nearby normal tissues. Among these radionuclides, ^{131}I has been the one used most often because of its availability and ease of manipulation for protein labeling, favorable emission characteristic and successful therapeutic use in the therapy of carcinoma of thyroid (Grossbard et al., 1992). There has been a recent increase in interest for the use of ^{90}Y because of its pure energetic beta emission and its virtual absence of gamma emission. Alpha emitters, such as ^{211}At and ^{212}Bt are more effective in inducing cell damage once delivered to the vicinity of the cell, but because their energy dissipates over such a short range, damage is likely to be limited to a single cell. Some isotopes decay by electron capture and subsequent Auger cascade. It has been postulated that the Auger cascade may be highly efficient in producing lethal effects if initiate in the cell nucleus (Chan et al., 1976). Therefore, the antitumor potential of Auger emitters (such as ^{125}I) may be considerably greater than hitherto expected, when linked to antibodies that undergo active internalization (Kassis et al., 1987). However, result obtained so far failed to support this postulation (Aronsson et al., 1993). Some of the radionuclides that are being used or that are believed to have potential use in tumor radioimmunotherapy are listed in Table 2.

Table 2   Radionuclides for radioimmunotherapy of cancer

Nuclide	Half life	Mode of decay	Path Length (mm)	Particulate energy (MeV)
^{131}I	8.05 days	β, γ	0.8	0.6
^{90}Y	2.66 days	β	5.3	2.28
^{188}Re	16.7 hr	β	4.4	2.1
^{186}Re	3.68 days	β	1.8	1.07
^{67}Cu	2.44 days	β	0.6	0.577
^{212}Bt	1.01 hr	α	0.04 - 0.08	6.09
^{211}At	7.2 hr	α	0.04 - 0.08	5.8
^{125}I	60.2 days	EC	0.01 - 0.02	0.35

4.4. Radiolabeling of antibodies

For both radioimaging and radioimmunotherapy, it is necessary to link a radioisotope to the antibody molecule so that the resultant product is stable and yet retains its ability to bind to the target antigen. Until recently, iodination was the most common method for radiolabeling of antibodies (Powe, 1986). Most of the current clinical trials are still using ^{131}I labeled antibody preparations (Sfakianakis et al., 1990). Alternative procedures for radiolabeling of antibodies are being investigated during the past years (Hnatowich, 1990). The availability of metallic isotopes, such as ^{111}In and ^{90}Y, and the rapid development of bifunctional chelating agents have provided new approaches for radiolabeling of antibodies.

(A) Radiolabeling of antibodies with radioisotopes of iodine

The labeling of antibodies and other proteins with radioisotopes of iodine predate all other approaches to label proteins for imaging purpose (Wilbur, 1992). Of the currently used protein iodination methods, all but one (i.e., the Bolton-Hunter method) involves the covalent attachment of radioiodine to tyrosine residues in proteins (Reogoeczi, 1984). Thus, Chloramine-T, Iodogen and the enzymatic methods all oxidise iodine to a cationic species capable of replacing a hydrogen atom in the phenolic group of tyrosine in the ortho position (Saha, 1983). Chloramine-T is a very reactive substance and end to easily damage antibodies by both chlorination and the production of aggregates. However, by the proper adjustment of concentration of reactants and the duration of reactions, most antibodies can be efficiently labeled to a high specific activity without significant loss of immunoreactivity. Iodogen and Iodobead are useful alternatives to Chloramine-T. The former is chloramide 1, 3, 4, 6 - tetrachloro - 3a,6a - diphenylglycouril, while in the latter, the oxidant N - chloro - bezensulfonamide is attached to solid beads. The most common enzymatic method of oxidizing iodide is the use of lactoperoxidase in association with low concentrations of

hydrogen peroxide. Hydrogen peroxide oxidizes iodide to elemental iodine and the lactoperoxidase acts as a catalyst. The reaction proceeds efficiently with little damage to the antibody. However, sometimes self iodination of lactoperoxidase becomes a problem. With all of these oxidative methods, the conditions of iodination need to be individualized for each antibody in order to obtain the highest yield of radiolabeled antibody with the minimal damage to antibody activity. Factors that influence the retention of antibody activity and the incorporation of iodine include concentrations of the reactants, pH, temperature and time.

One non-oxidative method for the radioiodination of proteins is the Bolton-Hunter method (Bolton and Hunter, 1973). The reagent used is N - hydroxysuccinimide ester of iodinated p - hydroxyphenyl propionic acid. This reagent reacts with the lysine groups on antibody and is especially useful to iodinate antibodies that are easily denatured by oxidative methods. However, the reagent is expensive and yields are relatively low.

The major problems associated with existing methods of protein iodination include (i) the loss of antibody activity during radiolabeling; (ii) the denaturation of antibody which results in altered biodistribution and catabolism; and (iii) the relative instability of the label, i.e., in vivo dehalogenation, which occurs at many sites in the body, including the tumor. All the above not only decrease the absolute amount of radioactivity that accumulates in target tumors, but also lead to unwanted concentration of radioactivity in the thyroid and the stomach. Clinically, up to 50% of the injected radioactivity appears in patient's urine within 24 hr after administration (Sullivan et al., 1982), as free iodines or as low molecular weight antibody fragments (DeNardo et al., 1986). It has been suggested that dehalogenation of radiolabeled antibodies occurs via deiodinases which cannot distinguish labeled tyrosine residues from thyroxine (Zalutsky and Narula, 1987a and 1987b). It is possible that the extent of dehalogenation in vivo may decrease if the iodine is linked to proteins in a way that does not render it susceptible to deiodinases. There is an ongoing search for

developing methods for iodination of antibodies that are not susceptible to dehalogenation. Recently, several methods have been developed for the iodination of proteins via non-phenolic aromatic rings. All these approaches employ an intermediate, such as N - succinimidyl (tri - n - butylstannyl) benzoate (Zalutsky and Narula, 1988; Wilbur et al., 1989), N - succinimidyl 2, 4 - dimethoxy - 3 - (trialkylstannyl) benzoate (Vaidyanathan and Zalutsky, 1990) and N - [m - [125/131I] idiophenyl) bromoacetamide (Khawli et al., 1991). A radiolabeled intermediate is first prepared and then covalently conjugated to protein. Animal studies with these reagents have shown significantly decreased accumulation of free radioiodine in the thyroid and the stomach, indicating the increased stability of radioiodinated antibodies prepared by these approaches.

(B) Radiolabeling antibodies with other radioisotopes

Although radioiodine has been the of choice for radiolabeling antibodies, a number of metallic isotopes, such as ^{111}In and ^{90}Y, are also being investigated in recent years for using in radiolabeling antibodies. The principal method of the linkage of metallic isotopes to antibodies involves the use of bifunctional or heterobifunctional chelating agents (with the exception of ^{99m}Tc which can also be attached to antibodies ' directly ' via endogenous groups). A relatively large number of such agents are currently available. However, the basic principle is the same for all these methods. A chelator which has the ability to bind metallic isotopes (e.g., ^{111}In, ^{90}Y and ^{67}Ga, etc.) is first labeled with an appropriate radioisotope and is then attached to the antibody by a reactive functional group (Wensel and Meares, 1983). A popular method for conjugation has been the cyclic anhydride method (Hnatowich et al., 1983). Chelators in common use are diethylenetriaminepentaacetic acid (DTPA), EDTA and deferoxamine. While bifunctional chelators can be designed for linkage to different functional groups in the antibody molecule (e.g., amino group, free

sulfhydryls, tyrosines, etc.), most of these bifunctional chaletors are designed to bind to lysine residues that are readily available in the antibody molecule (Powe, 1986).

The major drawback associated with the use of metallic isotope labeled antibodies is their observed accumulation of radioactivity in the liver and bone. It is known that the liver is the major organ that uptake and catabolism of antibodies, particularly xenogeneic antibodies (Jone et al., 1990). When ^{111}In is carried to the liver by antibody or its fragment, after endocytosed by Kupfer cells, the radiolabel may be stripped from the chelate and subsequently strongly bound by intracellular proteins that have a very high affinity for metallic ions (Powe, 1986). Furthermore, there is usually a small but significant transchelation of metallic isotopes like ^{111}In to circulating transferrin which may finally localize in the liver (Hnatowich et al., 1987). Finally, the possible intra- or intermolecular cross-link which occurs during antibody radiolabeling process may denature the protein in a manner which increase clearance into the liver (Carney et al., 1989). Several approaches have been studied to circumvent this problem, which include: (i) development of chelate with stronger affinity for the isotopes (Esteban et al., 1987); (ii) development of new method of conjugation such as " site-specific " linkage in which the chelate is attached to the carbohydrate side chain which are mostly restricted to the Fc portion of antibody (Alvarez et al., 1988).

4.4.4 Clinical studies with radiolabeled antibodies

Leukemias and lymphomas are particularly attractive targets for radioimmunotherapy because of their radiosensitivity, the well-defined profile of cell surface associated antigens, the availability of MoAbs directed against a variety of antigens, the well developed vascularization of lymphomas and the relative accessibility of malignant cells to circulating antibodies (Badger et al., 1986; Houghton and Scheiberg, 1988). Furthermore, HAMA

formation are relatively infrequent among these patients compared to patients with other types of solid tumors (Kaminski et al., 1992). Preclinical evaluations in animal models have shown the feasibility and efficacy of this approach (Ghose and Cerini, 1969; Ghose and Guclu, 1974; Wessels, 1990; Buchsbaum et al., 1992). Earlier clinical trials involved the use of ^{131}I labeled polyclonal anti-ferritin antibodies to treat hepatomas and Hodgkin's lymphomas. There was tumor regression in approximately 40% of the patients (Order et al., 1980). In last decade, over several hundreds of cancer patients have been treated with radiolabeled antitumor antibodies. For the reasons discussed above, the majority of these clinical trials are performed on patients with malignancies of lymphoid or myeloid lineages (especially B-cell malignancies) (Press et al., 1989a; DeNardo et al., 1990; Bernstein et al., 1990; Parker et al., 1990), and only a few case, ovarian (Stewart et al., 1989; Stewart et al., 1990) and colorectal carcinomas (Brady et al., 1988; Mellstadt et al., 1991). Most of these studies have demonstrated significant clinical responses. Recently, several groups have evaluated ^{131}I-labeled anti-B cell antibody preparations in the treatment of B-cell malignancies. The most promising result came from studies carried out by Eary et al. (1990) and Press et al. (1992). Both studies treated the NHL patients with MoAb MB-1 (anti-CD37) labeled with high doses of radioiodine (from 232 mCi to 628 mCi per patient) followed by autologous bone marrow transplantation (ABMT). In Eary's study, four out of five patients experienced CR, the other patient had a PR, while in study reported by Press, 13 of 15 NHL patients had CR or PR. Goldenberg et al. (1991c), treated seven NHL patients using ^{131}I labeled MoAb LL2. Two died of advanced disease before the completion of treatment, two experienced a PR, two had a minor or mixed response, and one had no response. In two more recent reports, Kaminski et al. (1992) treated 12 NHL patients using ^{131}I labeled MB-1. Response was observed in 6 patients. Four of them had tumor response that last 2 to 6 month, which included one CR, one PR, one minor response and one mixed response. Gobuty et al. (1992) treated 20 B-cell leukemia/lymphoma patients using ^{131}I labeled MoAb Lym-1 (anti-HLA-DR). CR was

observed in 10% of the treated patients, and PR in 85% of treated patients. To date, objective tumor regression has been reported with the use of antibodies against (i) idiotypic Ig (Parker et al., 1990), HLA-DR (DeNardo et al., 1990), CD37 (Press et al., 1989a), CD20 and CD21 (Czuczman et al., 1990) in patients with B-cell lymphomas; (ii) CD5 antigen in patients with cutaneous T-cell lymphomas (CTLL) (Rosen et al., 1989) and CLL (Zimmer et al., 1988); (iii) IL-2 receptor in patients with adult T-cell leukemias (ATL) (Waldmann, 1992); and (iv) CD33 in patients with AML (Scheinberg et al., 1991a).

Clinically, wide variations have been observed in the doses of ^{131}I required to achieve remission, i.e., from as low as 50 mCi (Goldenberg et al., 1991c) to 600 mCi or more (Eary et al., 1990) . Because bone marrow suppression tends to be a dose-limiting factor, some investigators rely on ABMT as a rescue after the administration of high doses of radiolabeled antibodies (Eary et al., 1990; Press et al., 1992). To date, the best clinical responses (CR and PR in 13 out of 15 patients) have been reported by Press et al. (1992). They used 232 mCi to 628 mCi of radioiodine linked to antitumor MoAb followed by ABMT. Apart from myelosuppression, other side effects of radioimmunotherapy in clinical trials have been minor, e.g., transient fever, nausea, pruritus and occasional thyroid dysfunction (from ^{131}I therapy).

The amount of antibodies used in these clinical trials also varied, i.e., from less than 1.0 mg per patient to more than 1000 mg per patient. It has been postulated that the optimal dose of antibodies may vary depending on antibody specificity, antigen expression on target tumor cells, tumor burden and antibody internalization. Most studies have used small doses of MoAbs (from 1.0 mg to 50.0 mg). In most studies, little effect of antibody dose on its biodistribution has been observed after the administration of MoAb within this small dose range (Scheinberg et al., 1990).

The potential advantage of administration of multiple fractionated doses of radiolabeled antibodies in contrast to a single, massive marrow-ablative dose followed by BMT remains controversial. The steep dose-response curve observed for hematologic malignancies treated with external beam radiation therapy follow $\sim$ $_\vee$ onventional BMT suggests that a single massive dose of $_\iota$ oimmunotherap may be more efficacious than the same dose of radiation administered in multiple small fractions (Appelbaum, 1991). In fact, several clinical trials using this approach have yielded the most impressive rate of response and durations of remission. In one study, 16 out of 17 patients (including 14 CR) showed objective response lasting as long as 42+ month (Press et al., 1989a). In another study, 11 out of 17 patients achieved objective response (including 7 CR). The longest remission lasted for 26+ month. Two patients died of marrow aplasia (Vriesendorp et al., 1991). Other trials have used repetitive multiple courses of nonmyeloablative radioimmunotherapy because of the minimal toxicity of this approach and thus do not need BMT (DeNardo et al., 1990; Schlom et al., 1990). This schedule has been justified by the assumption that fractionated doses will allow successive layers of tumor cells to be stripped away, and that such a progressive approach may yield therapeutic results superior to those observed with a single massive dose, while leaving the patients avoided from otherwise required BMT. However, clinical data are not available to date with this fractionated low-dose therapy to compare with the clinical responses obtained with the use of massive dose therapy (Grossbard, 1992).

4.5   MoAb-Toxin Conjugates (Immunotoxins, ITs)

4.5.1 Selection of toxin molecules and production of ITs

Three types of toxin polypeptides are used in the preparation of immunotoxins (ITs) : (i) bacterial toxins such as pseudomonas exotoxin A (PE) and diphtheria toxin (DT); (ii) plant

toxins such as ricin and abrin; and (iii) fungal toxins such as alpha sarcin. All the three groups of toxins catalytically inhibit protein synthesis in eukaryotes but each at a distinct step during translation. Based on their biochemical characteristics, plant toxins can be grouped as type I, single chain ribosomal inhibitory polypeptides (RIPs) such as pokeweed antiviral proteins (PAP) and saporin, and type II such as ricin and abrin which are heterodimers. The A chains of type II toxins are the toxic moieties, whereas the B chains contain binding sites for carbohydrates through which the A chain gains access to the interior of the cell. Bacterial toxins differ from plant toxins as regard their binding to cells, enzymatic specificity, and mechanism of entering cytosol. Fungal toxins such as alpha sarcin are also single chain proteins but are functionally different from type I polypeptides. For example, alpha sarcin is a phosphodiesterase while type I toxins are N-glycosidases.

Many ITs using intact toxins (e.g., ricin, PE and DT) and antitumor MoAbs or growth factors have been produced. They are extremely cytotoxic to relevant target cells, but the specificities are suboptimal since B chains of the intact ricin or DT (or uomain Ia of PE) may bind to surface via the carbohydrate residues on non-target cells (Press,1991; Pai et al., 1991; Cumber et al., 1985). To circumvent this problem, ITs that contain only the toxic A chain have been made. The specificities of these ITs are excellent because of the absence of nonspecific binding via the B chain (Krolick et al., 1980; Chang et al., 1977). However, the potency of these ITs are relatively lower than that of intact ricin ITs due to the loss of translocation function of the B chain (Vallera et al., 1984). To potentiate ricin A chain ITs, the B chain can be either delivered directly to cell-bound A chain ITs or indirectly via a second antibody homing onto the same target cell (Wawrzynczak et al., 1991). Alternatively, intact toxins can either be chemical modified (e.g., blocked ricin) or genetically truncated so that the translocation properties of the B chain is retained but the sugar binding sites is blocked (Wawrzynczak et al., 1991). As alternative, single chain ribosomal inhibitory proteins (RIPs) such as pokeweed antiviral proteins (PAP) and

saporin are widely used in IT preparation. Since these single chain polypeptides do not contain any cell binding components, ITs prepared with them have been highly specific in their cytotoxicity to target cells. For example, PAP-IT directed to CD40 was selectively cytotoxic to clonogenic acute lymphoblastic leukemia cells and non-Hodgkin's lymphoma cells but not to normal progenitor cells (Uckun et al., 1990).

4.5.2 "Second generation" ITs

Ideal ITs should have potent cytotoxicity and high specificity. Based on the fact that the binding and the translocation functions of toxin B chain can be separated, several truncated forms of toxins, in which the cell binding domain of the toxin was mutated, deleted or replaced, have been constructed with the use of genetic engineering techniques (Batra et al., 1989; Madhus e al., 1991). These toxin derivatives contain the toxic A chain and the truncated B chain that retains the translocation function but not cell binding ability. ITs prepared with these truncated toxins have been shown to retain its full cytotoxicity. The selectivity of these ITs was increased several orders of magnitude compared to original untruncated MoAb-toxin ITs (Frankel, 1988).

ITs made by chemically coupling protein toxins to specific antibodies usually have low yields, and contain various heteromers. There are also difficulties in the large-scale production of ITs chemically. To circumvent some of these problems, various chimeric toxins have been prepared by genetically fusing the coding sequences of toxin moieties to carrier proteins (Batra et al., 1990b). For example, Chaudhary et al. (1988) constructed a single chain antibody toxin fusion protein by ligating the DNA fragment of anti-Tac (Fv) with the gene of PE40. The fusion protein anti-Tac(Fv)-PE40 was highly cytotoxic to two IL-2 receptor-bearing human cell lines but was not cytotoxic to receptor-negative cells. In addition, many receptor-specific chimeric toxins have been constructed by the fusion of

cDNA encoding cytokines (TGFα, IL-2,, IL-6) to the gene of PE40 (Batra et al., 1990a). Each chimeric protein was specifically cytotoxic to the appropriate receptor-bearing cells (Siegall et al., 1988; 1989) (see Introduction section 5 for a detailed discussion).

4.5.3 Studies with ITs in animal models and in patients

Most ITs constructed from various toxins and antitumor antibodies have been effective in vitro in inhibiting the proliferation of tumor cells (Ramakrishnan, 1990). However, only a few ITs were effective in vivo and inhibited tumor growth in experimental tumor models. In general, injection of IT at the time or immediately following tumor inoculation has led to decreased tumor incidence and / or slower growth of grafted tumors. A delay in the onset of treatment has resulted in only limited arrest in the growth of tumors. The difference between in vitro and in vivo effects of ITs is attributed to the pharmacological and toxicological properties of the ITs. Specifically, the biological half life, stability of the bond between toxin and antibody, sequestration by sensitive organs such as liver, inability to penetrate the interior of the tumor, and side effects like capillary leakage syndrome limit the clinical application of ITs.

Several investigators have developed animal models of human leukemias by implanting human leukemia cells in various strains of nude and SCID mice, with or without the use of additional immunosuppression. Ghetie et al. (1991), treated SCID mice bearing xenograft of human Daudi B-cell lymphoma with two deglycosylated ricin A chain (dgA) ITs, i.e., anti-CD22 antibody IgG-dgA and anti-CD22 antibody IgG Fab'-dgA. A 4-5 log cell kill with the IgG-dgA IT and a 2 log cell kill with Fab'-dgA IT were achieved, compared to 1 log cell kill with unconjugated IgG alone and no cell kill with the unconjugated Fab'. Fishwild et al. (1992), used anti-CD7-ricin A chain IT to treat CEM T-cell leukemia cell line in NIH-III mice and demonstrated a 100 to 200-fold depletion of leukemia cells by IT

compared to a 3-fold depletion using antibody alone. Uckun et al. (1992), constructed anti-CD19 antibody B43-PAP IT. The administration i.p. of three daily doses of the IT after i.v. injection of human pre-B-cell ALL line NALM-6 in SCID mice, reduced the death rate from 100% to 36%. In SCID mice inoculated with human t (4;11) leukemia cell line i.v. or i.p., the same treatment resulted in no discernible tumor in the liver and spleen 33-34 days after i.v. tumor cell inoculation, and a 60% survival rate of mice that received tumor cells i.p., compared to 100% death of control mice.

Phase I clinical trials are underway in many medical centers using ITs made from different toxin moieties and tumor specific carrier molecules. Vitetta et al. (1991) treated 15 refractory B-cell lymphoma patients with IT consisting of anti-CD22 antibody RFB4 linked to dgA chain, 38% of the patients demonstrated a greater than 50% reduction in tumor size. LeMaistre et al. (1991) have used anti-CD5 antibody H65-RTA IT in 14 patients with cutaneous T-cell lymphoma. There was partial response persisted for 3-8 months in 4 patients. Grossbard et al. (1992) constructed an IT consisting of anti-CD19 antibody B4 and "blocked" ricin. Treatment of 23 refractory B-cell NHL patients with this IT resulted in one CR, two PR and eight with transient or mixed responses.

Other clinical trials that completed or still continuing include: T101-RTA IT in refractory chronic lymphocytic leukemia (Hertler et al., 1988); WT1-RTA in T cell leukemia (Preijers et al., 1989); 260F9-RTA (recombinant) IT in breast cancer (Gould et al., 1989); 454A12-RTA (recombinant) IT and OVB3-PE in ovarian cancer (Pastan et al., 1990); genetically engineered DAB486 IL-2-DT fusion protein in Hodgkin's lymphoma (LeMaistre et al., 1990).

4.5.4 Limitations of IT therapy

In addition to the general limitations of MoAb-based immunotherapy which I shall discuss later, there are several disadvantages specifically associated with IT therapy. Firstly, because of the potency of toxins, there should be no or minimal non-specific binding of MoAb, as well as of toxins, to non-target tissues. Also, the linkage between the MoAb and the toxin must be stable enough to prevent release of the intact toxin in the circulation, but be able to release active toxin in the cytoplasm of the targeted cells. Secondly, due to the high molecular weight of IT, the penetration of tumor by these molecules may be somewhat difficult. Thirdly, both components of ITs are immunogenic. Repeated uses of ITs in patients may cause the development of immune response to both the MoAb and the toxin (Godal et al., 1983). The tissue damage caused by precipitation of immune complexes in end organs may be enhanced if there is endocytosis of ITs and/or release of free toxin in the tissue. Finally, the systemic toxicity of ITs is another limiting factor in their clinical use and dose escalation. The most common dose-limiting toxicity in clinical trials is the capillary leakage syndrome which is likely to result from non-specific endothelial damage (Spitler et al., 1987). The symptoms of this syndrome range from weight gain and mild peripheral edema to hypertension and pleural effusions. In addition, low grade fever, anorexia, and myalgias are also frequently observed.

4.6 Bispecific Antibody

4.6.1 Bispecific antibodies: a new tool for diagnosis and treatment of cancer

Another way of specifically linking diagnostic or therapeutic agents (including cytotoxic agents and effector cells) to target tumor cells is the use of bispecific antibodies (Songsivilai and Lachmann, 1990). Bispecific antibodies have two different antigen-specific binding

sites, by one site the antibody binds to tumor-associated antigen (target binding arm), and by the other to diagnostic or cytotoxic agents, including effector cells (effector binding arm). A specifically designed bispecific antibody is firstly targeted to the tumor site. After allowing a suitable period of time for the non-specifically bound antibody to be cleared, the imaging or cytotoxic agents, which is recognized by the second arm of the tumor cell bound antibody, is then injected to bind to the second arm of the bispecific antibody. By achieving high T/NT ratios, this system may minimize the toxicity in therapy and maximize the quality of tumor imaging. The advantages of using bispecific antibody over conventional immunoconjugates is obvious. The chemical damage to antibody and toxic agent during the coupling process is avoided and the agent is released to specific targets without the necessity of splitting of covalent bonds. Since the middle of 1980's, bispecific antibodies have been extensively studied and used in areas ranging from immunodiagnosis to targeted delivery of effector cells or cytotoxic compounds to tumors. Promising results have been obtained.

4.6.2 Methods of production of bispecific antibodies

Bispecific antibodies are produced mainly by two methods, i.e., fusion of two different hybridoma cell lines, or chemical linkage of two antibody molecules or their derivatives. Recently, bispecific antibodies have also been produced by genetic engineering.

(A)   Fusion of hybridomas

Fusion of two myeloma clones, each secreting different Igs, results in the co-dominant expression of both parental Ig genes. Two sets of heavy and light chains have been found to be secreted (Cotton and Milstein,1973). The assembly of Ig molecules thus allows the formation of both parental Igs, and also the hybrid molecules. This approach has been used

to produce a number of bispecific antibodies (Suresh et al., 1986a). Fusions have been carried out between pairs of hybridoma cells secreting two defined monoclonal antibodies to form a "quadromas" (Tiebout et al., 1987), or between hybridoma cell and immune spleen cell to form a "triomas" (Milstein and Cuello, 1983). The main advantage of this fusion technique is that the resulting bispecific antibodies are synthesized, assembled and secreted by the same process as that of the native Ig. Their stability, both in vitro and in vivo, and pharmacokinetics are theoretically comparable to those of normal antibodies. Once the hybrid hybridoma cell lines are obtained, they will serve as machines to produce therapeutic amounts of antibody in the same way as normal hybridomas. However, some disadvantages exist. which include: (i) difficulty of fusion and selection of hybrid hybridoma cells. Cell fusion is labour-intensive, time consuming and may not always succeed with the hybridoma pairs of choice. The lack of an easy method for selecting appropriate hybrid hybridoma cells results from the fact that most parental hybridomas are derived from the fusion of HAT-sensitive myeloma fusion partners and immune spleen cells, and are thus HAT-resistant. Several approaches have been developed to overcome this problem. Parental hybridoma cell lines were rendered HAT-sensitive by selecting mutants that lack the HGPRT marker in the medium containing 8-azaguanine or 6-thioguanine, and then fused with immune spleen cells (Milstein and Cuello, 1983). Alternatively, hybridoma cells lacking markers such as thymidine kinase (TK) or adenosine phosphoribosyltransferase may also be selected in the medium containing bromodeoxyuridine or 6-chloropurine, respectively. Two HAT-sensitive hybridoma cell lines, one deficient in HGPRT and the other in TK, have also been fused and the resulting hybridoma cells selected in simple HAT-containing medium (Urnovitz et al., 1988). Other selectable markers, such as the resistance to neomycin, methotrexate or actinomycin D, have also been used to select hybridomas (De Lau et al., 1989; Chervonsky et al., 1988) . Another approach which does not involve mutants is the use of two different irreversible biochemical inhibitors of protein synthesis, such as emetine, actinomycin D or

iodoacetamide, to inhibit two independent metabolic pathways of each of the two parental cell lines. Fused cells apparently survive by complementing each other (Suresh et al., 1986b). Finally, the use of two different vital fluorescence dyes (e.g., FITC and TRITC) and the subsequent sorting of double labeled cells by a fluorescent-activated cell sorter (FACS) has also been used to select fused hybridoma cells (Karawajew et al., 1987); (ii) instability of resulting hybrid hybridoma cells. Hybrid hybridoma cells are polyploid, and contain approximately the sum of the chromosomes of both parental hybridomas, and are therefore unstable (Koolwijk et al., 1988). For the continuing production of bispecific antibodies, hybrid hybridoma cells may require frequent cloning to maintain the presence of both sets of heavy and light chains; and (iii) low yield and difficulty in purification of resulting bispecific antibodies. Hybrid hybridoma cell may produce ten different combinations of Ig molecules. Only one of them has the desired bispecific activity. If the rate of production of two pairs of heavy and light chains is the same and the association of heavy and light chain is totally random, the yield of desired bispecific antibody is 2 of 16, or 12.5% (Staerz and Bevan, 1986). In fact, the yield can range from 0 to 50% since preferential association may occur (Corvalan and Smith, 1987a). Isolation of the resulting bispecific antibody is also difficult since a total of ten species of molecules are formed. Purification has been achieved by isoelectric focusing (Wong and Colvin, 1987), hydroxylapatite chromatography (Staerz and Bevan, 1986), ion-exchange chromatography (Suresh et al., 1986b), or double affinity chromatography (Corvalan and Smith, 1987a).

(B)   Chemical linkage of antibody molecules or their derivatives

The technique for producing bispecific antibodies by chemical manipulation was pioneered by Nisonoff and Rivers (1961). It can be achieved by two methods. The first is direct coupling of the whole antibody molecules or their immunoreactive fragments (i.e., F(ab)'2 or Fab fragments) (Karpovsky et al., 1984; Glennie et al., 1987). The second method

involves dissociation and reassociation of heterologous Igs. The latter requires chemical manipulation to dissociate Igs into half molecules without damaging the antigen binding sites, and then to reform the disulfide bonds to link the heavy chains without allowing any interfering side reactions such as the formation of intrachain or mismatched disulfide bonds. The most common method currently employed to link two antibody molecules together involves the use of heterobifunctional cross-linking agents, such as SPDP (Gravelle et al.,1989), DTNB (Nitta et al., 1989) and o- PDM (Glennie et al., 1987). Chemical linkage does not require cell fusion, the desired bispecific antibodies can be made more quickly and the products are also comparatively easy to purify. However, the heteroconjugates may differ in their physical and biological properties from those of the native Ig molecules. The chemical manipulations frequently disturb the biological activity of antibody by alteration of the antigen binding sites (Webb et al., 1985). The heteroconjugates derived by direct coupling of two antibody molecules may have short half-life and difficulty in penetrating into the target sites due to their large size. The stability in vitro and in vivo, and their pharmacokinetics. have yet to be investigated.

(C)   Genetic engineering of bispecific antibodies

Bispecific antibodies have been produced using genetic engineering method, i.e., by introduction of two sets of Ig heavy and light chain genes into myeloma cells, by transfection of a set of heavy and light chain genes into secreting hybridoma or transfectoma cell lines, or by generation of single chain bispecific antibodies constructed with peptide linkers between the variable domains of two distinct MoAbs (Songsivilai et al., 1989; Bird et al., 1988). The latter construct allows a 100% yield of bispecific antibodies. These techniques are important for the production of tailor-made bispecific antibodies.

4.6.3 Applications of bispecific antibodies

(A) Immunoassay

The effector binding arm of a bispecific antibody can be designed to have specificity for marker enzymes or other indicator systems. The anti-target-anti-peroxidase bispecific antibodies have been investigated in several assay systems, and have led to improvements in the sensitivity and signal-to-noise ratios (Tadu et al., 1989; Takahashi et al., 1988). It also simplified the staining procedure for assays such as single-step immunoassay (Suresh et al., 1986b). Bispecific antibodies to both HRP and FITC which can be used as an universal binding agents between the FITC-labeled protein and the marker enzyme have been developed (Karawajew et al., 1988).

(B) Targeting of cytotoxic agents to tumors

Targeting of cytotoxic agents to tumors has been investigated by using bispecific antibodies with specificities for tumor cell surface associated antigens and chemotherapeutic drugs or toxins. Bispecific antibodies with one arm to CEA, and the other to vinca alkaloid or bleomycin, have shown good tumor localization and low uptake by liver, spleen and bone marrow (Corvalan et al., 1987b). Results of treatment of xenografted models have indicated that this method is more effective in suppressing tumor growth than free drugs (Corvalan et al., 1988). Bispecific antibodies directed against tumor antigens and toxins, e.g., ricin or saporin, have also shown encouraging antitumor efficacy in vitro and in vivo (Raso et al., 1981; Glennie et al., 1988).

(C) Tumor radioimmunoimaging and radioimmunotherapy

Bispecific antibodies have been used to reduce background radioactivity during radioimmunoimaging by preadministration of an unlabeled bispecific antibody in which one binding site recognizes a tumor-associated antigen and the other a chelate. After a interval to allow maximum T/N ratios of antibody localization, a radiolabeled chelate is administered for imaging (Stickney et al., 1989). With this approach, some short-lived radionuclides with good imaging properties, such as ^{99m}Tc and ^{123}I, can be used for tumor-imaging. This method may be also useful for radioimmunotherapy because there would be rapid elimination of those small radiolabeled chelate that are not bound to tumor-localized bispecific antibody. This may significantly reduce the non-specific radiation delivered to normal organs by circulating radiolabeled antibodies as in the case of single-step radioimmunotherapy.

(D) Cross-linking of cellular antigens and focusing of effector cells

Many efforts have been made to use bispecific antibodies to focus effector cells to target tumors. This system has been studied both in vitro as well as in vivo in animal models (de Palazzo et al., 1992). Several effector cells have been used. These included effector cells with Fc receptor (Hsieh-Ma et al., 1992), T cell receptor/CD3 complexes (van Dijk et al., 1989), CD2 (Goedegebuure et al., 1989) and CD16 molecules (de Palazzo et al., 1992). Bispecific antibodies that cross-link the target to effector cells can activate effector cells into functional effectors bypassing normal, MHC and antigen specific restriction. The use of bispecific antibodies does not simply link the targets and effector cells together, but may also trigger the cytolytic process (Karpovsky et al., 1984). Cytotoxicity has been shown not to be due to bystander lysis, since direct contact between effector and target cells is required (Lanzavecchia and Scheidegger, 1987). To date, human effector cells have been

targeted using bispecific antibodies to various kind of tumors, which including B-cell lymphoma (Gravelle et al., 1989), T-cell lymphoma (Staerz and Baven, 1986), melanoma (Jung et al., 1987), carcinomas of colon (Titus et al., 1987), ovarian (Pupa et al., 1988) and kidney (van Dijk et al., 1989). Results from most of these reports are promising.

5 Problems and Future Directions of MoAb-Based Cancer Immunotherapy

Although MoAbs and their immunoconjugates have shown considerable promise in tumor therapy, their use as a therapeutic agent has been hampered by several problems.

1. Most of currently available MoAb directed against human tumor associated antigens are of murine origin. They are recognized by patients as foreign antigens and a second antibody (i.e., HAMA formation) response is elicited (Schroff et al., 1985; Shawler et al., 1985; Courtney-Luck et al., 1986). The unique idiotypic determinants of any type of antibody may also induce a anti-idiotype immune response. These second antibodies can react with therapeutic MoAb and neutralize its antitumor effect, which makes repeated courses of treatment with the same antibody ineffective, and may prevent patients from receiving future injection of murine MoAb preparations. Several approaches have been attempted to overcome this problem, which include:

(1) The use of F(ab)'2 or Fab fragments that lack the Fc portion, which is mainly responsible for the immunogenicity of antibody molecule;

(2) Chemical modification of antibody, such as covalent linkage of polyethylene glycol (PEG) (Wilkinson et al., 1987) or oxidized dextran (Fagnani et al., 1990) to IgG;

(3) The use of immunosuppressive agents such as cyclosporin A , cyclophosphamide and steroids (Lederman et al., 1988; LoBuglio et al., 1988);

(4) Human MoAbs. The ideal solution of immunogenicity of murine MoAbs is the production of MoAbs of human origin. However, human MoAbs of appropriate specificity and affinity have been difficult to produce (Jones and Bell, 1987). There are two major obstacles to this approach. Firstly, there are few adequate, genetically marked human myeloma cell lines that can be used to fuse with sensitized human B cells. The use of mouse myeloma cells as fusion partners for human B cells often leads to preferential loss of human chromosomes and instability of the resulting hybridoma cells. Secondly, obtaining of appropriate human sensitized B cells has proved to be difficult, since one cannot ethically immunize a human being with tumor antigens. As an alternative to fusion, the immortalization of human cells by EBV leads to production of B cell lines that are often low producer of IgM type antibody (Sikora et al., 1983). The development in recent year of the SCID-hu mice may provide a solution to these problems (Bosma and Carroll, 1991). In this mouse model, SCID mice are reconstituted with human peripheral blood or human thymus, bone marrow and fetal lymph nodes. When peripheral blood is used, a specific antibody may be produced if the donor has already been primed with that antigen.

(5) The rapid advance in genetic engineering techniques provides an alternative approach for the production of human or human/mouse chimeric MoAbs that bypasses currently used hybridoma technique (Morrison, 1992). Genetic engineering techniques may facilitates the production of antibodies tailor-made for an intended use. The relevant genes encoding the variable regions of MoAb can be obtained by genomic or cDNA cloning and then expressed in either bacterial or mammalian expression systems to produce MoAbs (e.g., chimeric MoAbs and humanized MoAbs) or MoAb-like molecules, such as single chain MoAbs and fusion proteins.

(A) Mouse/human chimeric antibodies. Chimeric antibodies can be produced by combining the rodent genetic elements encoding variable or hypervariable regions with the human genetic element encoding constant region (Morrison et al., 1984; Boulianne et al., 1984). This may provide antibodies of appropriate specificity that are less immunogenic than the parent murine antibodies. Chimeric antitumor MoAbs have been produced with specificities directed against antigens expressed by colorectal, mammary, and pancreatic carcinomas and by B-cell and T-cell leukemia/lymphoma cells (Morrison, 1992). Among the most extensively characterized chimeric antibodies are those made using the variable regions from a murine MoAb 17-1A, a antibody recognizing a TAA expressed on the surface of colorectal carcinoma cells. Chimeric 17-1A antibodies of all four IgG isotypes and IgM have been produced (Steplewski, et al., 1988; Fogler et al., 1989). These chimeric antibodies mediated ADCC in vitro with human effector cells. When injected into patients, these antibodies had longer half-lives in circulation and were less immunogenic than their murine counterparts. For example, in one study, only one of ten patients given human/mouse chimeric MoAb had a modest HAMA response, and none had allergic and toxic reactions (Lobuglio et al., 1989). Samilar results were also reported by Goodman et al. (1993).

(B) Antibody humanization or CDR grafting. This method takes advantage of the conserved structure of the Ab domains (Jones et al., 1986). It is known that the framework residues in a IgG serve as a scaffold to support the CDR loops which are the regions that bind to antigen. Recognizing the importance of the frameworks in determining the proper function of the CDRs, appropriate choice and modification of the framework residues is critical for the retention of immunoreactivity of the resulting humanized antibody (Carter et al., 1992). Two approaches have been employed to ensue a successful humanization: (i) to choose a human framework that is as close as possible to that of the original murine

antibody; (ii) to identify framework amino acids that might directly interact with antigen or critically affect the conformation of particular CDRs, and then transfer these amino acids to the human framework along with the CDRs. In addition, unusual amino acids within the chosen human framework were changed to the consensus human sequence. Experience in a number of systems have demonstrated the feasibility of transferring the CDRs from murine MoAbs to human frameworks to produce humanized antibodies (Reichman et al., 1988; Queen et al., 1989; Gorman et al., 1991). An example of humanized MoAb constructed by CDR grafting is anti-Tac-H, an anti-T cell receptor (p55) antibody. The anti-Tac-H exhibited ADCC not seen with the murine antibody and showed increased half-life and decreased immunogenecity in cynomegalous monkeys (Brown et al., 1991).

(C) Single chain MoAbs and MoAb-like molecules. Single chain MoAbs are usually composed of an antibody VL tethered to a VH by a peptide linker. In general these antibodies have the same specificities and affinities for their antigens as the parent MoAbs. In addition to the reduced immunogenicity (due to the lack of Fc portion), another advantage of these single chain McAbs is their rapid clearance in vivo. It has been shown that the tumor uptake of single chain MoAbs was comparable to that of Fab fragment (Colcher et al., 1990). One of the potential application of ... se single chain antibodies is the construction of immunotoxins, in which the toxin is linked to either the amino terminus or carboxyl terminus of the single chain Fv. For example, anti-Tac(Fv)-PE40 (Batra et al., 1990b) and anti-Tac(Fv)-DT (Chaudhary et al., 1990a) chimeric single chain ITs have been constructed, and these ITs are extremely cytotoxic to IL-2 (p55) receptor-bearing cells. The construction of other single chain ITs such as anti-TRF(Fv)-PE40 (Batra et al., 1991) and anti-TRF(Fv)-DT (Chaudhary et al., 1990b) have also been reported. Both of these ITs kill cells bearing human transferrin receptors.

(D) Fusion proteins. In this approach, a part of the Ig molecule is replaced by a non-Ig sequence to create a protein with novel properties. The fusion can occur either in the constant region of the antibody leaving the variable region (i.e., antigen binding region) free or in the variable region (i.e., to block the antigen binding site of the antibody) but leaving the constant region intact. An excellent example of this approach is the construction of antibody-growth factor fusion proteins, which provide a way to deliver antibody to cells expressing growth factor receptors. When IL-2 was used to replace the variable region of a IgG1 antibody, the fusion antibody secreted by the transfectant was able to mediate the specific lysis of IL-2 receptor-bearing cells in the presence of complement (Landolfi, 1990). On the other hand, when IL-2 was used to replace the constant region of the MoAb, the fusion protein bound to antigen site on tumor cells as well as to IL-2 receptors on activated human T cells. Tumor cells coated with this fusion protein caused T cell proliferation, which resulted in enhanced cell-mediated destruction of the tumor cells (Fell et al., 1991). Similarly, another fusion protein, OKT3-EGF, made by fusing EGF with OKT3 antibody in the CH3 domain, was found to be able to mediate the lysis of EGF receptor-bearing tumor cells by TIL and CTL (Gillies et al., 1991).

Despite the remarkable advances in approaches described above, several unresolved issues still remain. Firstly, it is not confirmed whether these manipulations will produce tumor specific MoAb or MoAb-like molecules with sufficiently reduced immunogenicity to be used clinically. The neutralizing antibodies produced by patients can be anti-framework as well as anti-idiotypic, therefore, the treatment with human and humanized antibodies may still elicit host immune response (LoBuglio et al., 1989; Goodman et al., 1993). Secondly, the presumed effectiveness of these human or humanized MoAbs or MoAb-like molecules (e.g., recruitment and/or activation human effector cells, receptor blockage, etc.) still remains to be clinically demonstrated.

Genetic engineering techniques have also been used to modify recombinant/chimeric antibodies to produce molecules with novel properties (Schlom et al., 1990a). These include: (i) production of antibodies of different isotypes with a variety of human constant regions to improve pharmacokinetics, effector cell interactions, and complement mediated cytotoxicity: (ii) production of antibodies with Ig domain deletion or alterations in glycosylation to obtain optimal clearance kinetics; (iii) alteration in the hypervariable region to produce antibodies with higher affinity; and (iv) insertion of sequences coding for specified amino acid sequences that may function as binding site for specific chelates, drugs or effector cells.

2. For therapeutic purpose, MoAbs have to cross anatomical and physiological barriers to gain assess to tumor cells (Jain, 1990). This limits the amount of MoAbs or their conjugates that could reach tumor cells. Studies with radiolabeled MoAbs in patients have shown that the amount of antibody that localizes in tumors range from 0.005% to 0.01% of the injected dose per gram of tumor tissue (Sands and Jones, 1990). Several efforts have been made to increase antibody localization and penetration in tumor tissue. This include: (1) to increase the blood supply of the tumor by pre-treatment of tumors with external radiation (Kalofonos et al., 1990), local hyperthermia (Cope et al., 1990), or vasoactive agents (Jain, 1987); (2) to increase the expression of tumor antigen and/or facilitate antibody extravasation by co-injection of biological response modifiers (BRM) such as IFN-α (Greiner et al., 1987) and IL-2 (LeBerthon et al., 1991). IFN-γ may induce the expression of target antigen, whereas IL-2 may increase vascular permeability at the tumor site. Both the effects may enhance the antitumor activity of MoAbs or their immunoconjugates as a result of the increased tumor uptake of these agents ; (3) to increase the interstitial transport rate of the antibody molecule by the use of lower molecular weight F(ab)'2 or Fab fragments; or lower the tumor interstitial pressure by the use of osmotic agents (e.g., mannitol) (Neuwelt et al., 1987) and hence increase antibody penetration.

Alternatively, antibodies directed against tumor endothelial cells have been used to deliver cytotoxic agents to tumors (Burrows et al., 1992). The extravasation and intratumor penetration of antibodies would be unnecessary under these situations. Finally, it is pertinent to state that no of above problems are involved when the MoAbs or their conjugates are given to patients by local injection (i.e., intracavitary injection such as intraperitoneal, intraarterial and interstitial). This method may be proved to have some advantage in some situations, e.g., intraperitoneal ovarian (Hnatowich et al., 1988) and colorectal carcinomas (Hyams et al., 1987).

3. Binding of an antibody molecule to a target cell sometimes leads to antigen modulation where shedding or internalization of the antigen may occur. Internalization is necessary for the action of most MoAb-drug or toxin conjugates, i.e., when the targets of these drug or toxins are intracellularly distributed. However, if the antigens are not re-expressed, subsequently administrated MoAbs or their conjugates will not bind avidly to tumor cells. Also, the presence of circulating antigen may lead to the formation of antibody-antigen complexes which may not only neutralize the antitumor effect and cause rapid clearance of the antibodies or their immunoconjugates, but also may cause damage to those organs where these complexes are deposited. Efforts have been made to overcome this problem by plasmapheresis or by pre-infusion of an excess amount of unlabeled antibodies to saturate the free circulating antigens before infusion of immunoconjugates (Parker et al., 1990).

4. The MoAbs or their immunoconjugates must be able to recognize a tumor specific antigen that clearly distinguishes tumor cells from normal cells. However, with the exception of idiotypes on B or T cells, no such tumor specific antigen has yet been defined. As stated, this constitutes a serious limitation for the clinical application of ITs.

5. Heterogeneity of tumor cells as regards antigen expression is another serious problem in MoAb-mediated cancer therapy (Douillard et al., 1986). The use of a single MoAb or its immunoconjugate may allow the escape of antigen-negative tumor cells. This problem can possibly be overcome by (1) the use of a " cocktail " of antibodies that recognize different tumor associated antigens (Krizan et al., 1985; Munz et al., 1986); (2) Co-injection of biological response modifiers such as IFN that both increase the amount of tumor antigen expressed by a given tumor cell and increase the percentage of cells within the tumor cell population that express the antigen, i.e., it may induce the expression of tumor antigen in antigen-negative tumor cells (Rosenblum et al., 1988). As an alternative, the use of radiolabeled MoAb may allow the killing of antigen-negative tumor variants within an area defined by the path length of the radionuclide. Finally, as described above, the use of antibodies directed against tumor endothelial cells or components of the subendothelial matrix may prove to be a way to overcome the problem associated with heterogeneity of tumor antigen expression. Antibodies directed against tumor vascular or matrix may result in the destruction of tumor vessels leading to necrotic changes in the tumor tissue (Burrows et al., 1992).

6. Many antitumor MoAbs are not specific for a given type of tumors, therefore, it may be sometimes necessary to raise MoAb against tumor from individual patient to produce an effective immunoconjugate.

7. The linkage of various cytotoxic agents to a MoAb to form an immunoconjugate may introduce additional complications, such as partial inactivation of the antibody or the agent itself, increased immunogenecity, and altered pharmacokinetic properties as result of increasing in size or altered charge. Definitive pharmacology and pharmacokinetics of immunoconjugates in patients remain to be established.

8. Although in many animal models, immunoconjugates (i.e., antitumor MoAb linked to drug, or toxin, or radionuclide) have been shown to be therapeutically more effective than the agent alone or the agent linked to non-specific carriers, there is no evidence that such immunoconjugates can eradicate large tumor masses containing more than 1 to 5 x 10^7 tumor cells (i.e., a tumor larger than 1 to 5 gram). Thus, this method of treatment is likely to be useful in the treatment of cancer micrometastases and residual diseases, after the bulky tumor mass have been removed by surgical excision, or the majority of tumor cells have been eradicated by conventional radiotherapy or chemotherapy. In fact, micrometastases and residual disease are the major causes of relapse of cancer, and it constitutes the real problem in the treatment of cancer.

MATERIALS AND METHODS

Materials

1. Chemicals

Chemicals purchased from Sigma Chemical Company, St. Louis, Missouri :

BSA, DHFR, DHFA, NADPH, DTT, MTX, SDS, TEMED, poly IC, cholorauric acid (AuCl4), coomassie brilliant blue, caprylic acid, pepsin, protein solution of standard concentration (used for the determination of antibody concentration by Lowry's method), transferrin, insulin, glycine, RPMI 1640 medium powder, MEM medium powder, dextran T-40, Trizma Base, Trizma HCl, 2,6,10,14-tetramethyl-pentadecane (Pristane), goat anti-mouse IgG-gold complex, FiTC labeled goat anti-mouse IgG, ammonium persulfate, selenium ($Na_2SeO_3 \cdot 5H_2O$), penicillin, streptomycin, incomplete Frenud's adjuvant.

Chemicals purchased from BDH Chemicals, Toronto, Ontario:

Chloramine T, Folin phenol reagent and all solvents used in this study.

Chemicals purchased from Pharmacia Fine Chemicals, Uppsala, Sweden:

Sephadex G-25, Sephacryl S-200, Sephadex G-25 NAP^{TM}-10 column and PD-10 column.

Chemicals purchased from J. T. Baker Chemical Co., Phillipsburg, New Jersey:

Sodium meta-bisulfate ($Na_2S_2O_5$), Ethylenedinitrilo tetraacetic acid (EDTA), Trichloracetic acid (TCA)

Chemicals purchased from Fisher Scientific, Nepean, Ontario

Ammonium sulfate, sodium iodide, sodium citrate

Chemicals purchased from Aldrich Chemical Co., Milwaukee, Wisconsin

N-Chlorosuccinimide (NCS)

Chemicals purchased from Bio-Rad Laboratory, Richmond, California

ABTS peroxidase EIA substrate kit, mouse Typer (mouse sub-isotyping panel), AFFi-Gel Hz Hydrazide gel, Econo-Pac P6 Sephadex G-25 column.

Chemicals purchased from ICN Biomedicals Inc. Costa Mesa, California

Fetal calf serum (FCS)

Chemicals provided by Adria Laboratories Inc. Columbus, Ohio

Adriamycin™ (doxorubicin·HCl)

Radiochemicals

$Na^{125}I$ (specific activity: 13.5 to 17 mCi/μg of I) : two sources of $Na^{125}I$ have been used in this study, they are ICN Biochemicals Canada Ltd. Mississauga, Ontario and Amersham Canada Ltd, Oakville, Ontario.

$Na^{131}I$ was purchased from Merck Frosst Canada MC, Kirkland, Quebec, and ICN Biochemicals Canada Ltd. Mississauga, Ontario .

[3',5',7 - ^3H]-MTX was purchased from Amersham Canada Ltd., Oakville, Ontario.

$Na^{51}Cr$ was purchased from ICN Biochemicals Canada Ltd. Mississauga, Ontario.

Liquid scintilation cocktail (Ready Safe™) was purchased from Beckman, Fullerton, California.

Kodak X-Omat AR film-pelicula, nuclear track emulsion (Type NTB3) and Dektol film developer and fixer were purchased from Kodak, Rochester, New York.

2. Equipments and Instruments:

Biogard Hood : The Baker Company, Inc., Sanford, Maine.

CO_2 *incubator* : Johns, Scientific Inc., Canada.

Microscopes : Inverted microscope: Olympus, Tokyo, Japan. Immunofluorescence microscope: Nikon, Model AFX 11A, Tokyo, Japan. Electron microscope: EM-200, Phillips, Eindhoven, Netherland.

Coulter Counter : Model Zf, Coulter Electronics, Inc., Hialeah, Florida.

Centrifuges : Model CL, Model B-35 and Model PR-6, International Equipment Co., Needham Heights, Massachusetts. Sero-fuge centrifuge, Clay Adams, Division of Becton,

Dickinson and Company, Parsippany, New Jersey. Microfuge (Type 152), Beckman Instruments Inc., Fullerton, California.

Spectrophotometer : Model 24, Beckman Instruments Inc., Fullerton, California.

Balances : Mettler PL 300 and Type H15, Mettler Instrument AG, Zurich, Swiss.

Water bath : Model B-1, Messgerate-Werk Lauda, Germany.

Micro-shaker II : Dynatech Laboratories Inc., Alexandria, Virginia.

Deluve mixer : Model S-8820, Scientific Products, Division of American Hospital Supply corporation, Evanston, Illinois.

Ultra-Microtome : Huxley, LKB, Bromma, Sweden.

Magnetic stirrer : Thermix^R Stirrer, Model 220T, Fisher Scientific, Nepean, Ontario.

Homogenizer : Polytron, Kinematica Gmbh, Luzern, Schweiz.

ELISA Reader : Model MR 580 Micro-ELISA Auto-Reader, Dynatech, Laboratories Inc., Alexandria, Virginia.

Fraction collector : Model FC-80K, Gilson Medical Electronics, Inc., Meddleton, Wisconsin.

Electrophoresis apparatus : Model PS-1200, Hoefer Scientific instruments, San Francisco, California.

pH Meter : Accumet Model 210, Fisher Scientific, Nepean, Ontario.

Radiation survey meter : Ludlum Measurement Inc., Sweetwater, Texas.

Thermo-incubator : Fisher isotemp incubator, Senior Model, Fisher Scientific, Nepean, Ontario.

Gamma Dose Calibrator : Mediac dose calibrator, Nuclear-Chicago Co¬poration, DesPlaines, Illinois.

Gamma counter : Beckman Gamma 4000, Beckman Instrument Inc., Fullerton, California.

Liquid Scintillation System : Beckman LS-7000, Beckman instruments Inc., Fullerton, California.

Cell culture plates : 24 well plate: Costar [R], Cambridge, Massachusetts. 96 well sterile cell culture plate and 96 non-sterile ELISA plates: Nunclon [R], Gibco, Burlington, Ontario.

Eppendorf tube : micro test tube (400 µl polypropylene) and premium flex-tubes™ (1.5 ml polypropylene), Brinkmann Instruments Co. Westbury, New York.

Tips: 5 to 200 µl and 100 to 1000 µl tips for pipetman, Fisher Scientific Ltd., Nepean, Ontario.

Equipments used with the consent of other Department and individuals

Computer-linked General Electric Maxicam Gamma Camera (for scanning tumor bearing mice injected with ^{131}I labeled MoAb), Courtesy of Department of Nuclear Medicine (Director: Dr. J. Aquino), Halifax Infirmary Hospital, and Courtesy of Department of Radiology (Director: Dr. S. Iles), Victoria General Hospital, Halifax, NS.

Theratron 80 (T-80) and 1000 (T-1000), Cobalt-60 radiation source (for total body irradiation of nude mice), Theratronic International Ltd, Kanata, Ontario. Courtesy of Department of Radiology (Director: Dr. J. Andrew), Victorial General Hospital, Halifax, NS.

3. Animals

The inbred female BALB/c mice (retired breeders) were purchased from Charles River Canada Inc., Lasalle, St. Constant, Quebec. Nude mice were obtained from Harlan Sprague Dawley Inc., Indianapolis, IN. The C.B-17 SCID mice were produced by specific pathogen-free (SPF) C.B-17 scid/scid breeders maintained in the Animal Care Center (ACC) of Dalhousie University, Halifax, NS. All mice were housed in specific pathogen-free (SPF) conditions. The food were purchased from Agway Inc. (Rat, Mouse and Hamster 3500, Agway Laboratory Diets, Agway Inc., Country Foods Division, Syracuse, NY). Both food and tap water were sterilized by autoclaving at 121°C for 30 min.

4. Tumor Cell Lines

The Epstein-Barr virus transformed human leukemic B cell line EBV-CLL-1 from a CLL Rai stage II patient (Lee et al., 1986) and of its sunclone D10-1 with partial duplication of chromosome 1q, i.e., 46, XY, dup (1) (q11--q32) (Lee et al., 1988), was established in Dr. Ghose's laboratory, Department of Pathology, Dalhousie University, Halifax, NS. The human T leukemic cell line MOLT-3, human erythroleukemic cell line K562, human promyelocytic leukemic cell line HL60, human renal cell carcinoma cell line Caki-1, NK-sensitive mouse lymphoma cell line Yac, mouse myeloma cell line SP-2, and nonspecific IgG1 producing mouse myeloma cell line TIB9 were purchased from American Type Culture Collection (ATCC, Rockvills, MD). Nu-caki-1 is a cell line obtained in our laboratory from Caki-1 tumors after several passages in nude mice as s.c. xenografts.

5. Antibodies

The two monoclonal antibodies (Dal B01 and Dal B02) were produced by hybridomas which were constructed in Dr. Ghose's laboratory by immunization of BALB/c mice with EBV-CLL-1 cells derived from Epstein-Barr virus transformed B lymphocytes from a chronic lymphocytic leukemia (CLL) patient and then fusing the splenic cells from the immunized mice with mouse myeloma cell line SP-2 with the use of polyethylene glycol. Both antibodies precipitated M.W. 22,000 and 33,000 bands from surface labeled RAJI or EBV-CLL-1 cells. Subclass typing revealed that Dal B01 belongs to the IgG2a subclass, while Dal B02 belongs to the IgG1 subclass. Immunofluorescence revealed strong reactivity of the antibodies with EBV-CLL-1 cells and with most lymphocytes in tonsil follicles, in the intestine wall, around splenic arterioles and near Hassall's corpuscles in the neonatal thymus as well as with small proportions of lymphocytes in some large reactive lymph mode follicles. These two MoAbs also reacted weakly with 20% of peripheral blood

B lymphocytes (PBL), but did not react with platelets, granulocytes and non-lymphoid tissues. These two MoAbs reacted strongly with all the non-Hodgkin's lymphomas of various histological types and with all Burkitt's lymphoma lines examined, but not with the 3 T lymphoblastoid and 12 nonlymphoid tumor lines examined (Guha et al., 1990). HI98, a IgM MoAb directed against surface associated antigens on human myelogenous leukemic cells, was kindly provided by Dr. C. Yang, Institute of Hematology, Chinese Academy of Medical Sciences, Tianjin, China.

Normal mouse IgG (NMG) was isolated from mouse serum by precipitation with 33% saturated ammonium sulfate. Anti-BSA polyclonal antibody was obtained by immunizing rabbits with BSA. The IgG fraction in the antisera of the rabbits was precipitated by ammonium sulfate and further purified by Protein-A chromatography. Mouse myeloma derived monoclonal IgG1 and IgG2a were purified from the ascites fluid from mouse inoculated with appropriate myeloma cells in the same way as described for Dal B01 or Dal B02.

Before purification, all ascites or antisera were incubated at 56°C for 30 min to inactivate complement components.

6. Buffers and Solutions

0.01 M Phosphate buffered saline (PBS, pH 7.2)

$NaH_2PO_4 \cdot H_2O$		3.45 g
Na_2HPO_4		10.7 g
NaCl		85.0 g
Distilled water	q.s.	10,000 ml

Dulbeccos PBS (DPBS, 20 X)

NaCl		160.0 g
KCl		4.0 g
Na2HPO4		23.0 g
KH2PO4		4.0 g
Distilled water	q.s.	1000 ml

Hank's balanced saline solution (HBSS)

KCl		0.4 g
KH2PO4		0.06 g
NaCl		8.0 g
Na2HPO4		0.0475 g
Dextrose		1.0 g
Distilled water	q.s.	1000 ml

1.0 M Acetic acid

Glacial acetic acid		57.5 ml
Distilled water	q.s.	1000 ml

Acetic buffer (pH 5.0)

1M Acetic acid		21 ml
Andydrous sodium acetate		4.3 g
(or NaAc·3H2O)		6.8 g
Distilled water	q.s.	1000 ml

0.5 M Boric acid-borax buffer (pH 9.1)

Boric acid		3.1 g
Sodium tetraborate·10H2O		42.9 g
Distilled water	q.s.	1000 ml

0.5 M Sodium bicarbonate-sodium carbonate buffer (pH 9.2)

NaHCO3		28.4 g
Na2CO3		5.7 g
Distilled water	q.s.	1000 ml

Lugol's iodine solution

KI		1.95 g
Iodine		1.3 g
Distilled water	q.s.	30 ml

0.1 M Sodium Cacodylate buffer (pH 7.3)

Sodium cacodylate		21.4 g
(Na(CH3)2AsO4·3H2O)2		
0.2 M HCl		22 ml
Distilled water	q.s.	500 ml

0.25% Trypsin solution

Trypsin		1.25 g
NaCl		0.4 g
KCl		0.1 g
Na2HPO4		0.75 g
KH2PO4		0.1 g
Dextran		0.25 g
Phenol red		0.0025 g
Distilled water	q.s.	500 ml

EDTA solution

EDTA (sodium salt)	0.2 g
KCl	0.4 g
NaCl	0.8 g
NaHCO3	0.35 g

Dextran		1.0 g
Phenol red		0.005 g
Distilled water	q.s.	1000 ml

TBS buffer (pH 8.2)

Tris		2.42 g
BSA		10.0 g
NaCl		8.8 g
Distilled water	q.s.	1000 ml

Substrate buffer for ELISA

0.1 M Citric acid		2.4 ml
0.2 M Phosphate		2.6 ml
Distilled water	q.s.	10.0 ml
Orthophenyldiamine (OPD)		4.0 mg (in ethanol)
30% H_2O_2		5.0 µl

Cell lysing buffer

Tris·HCl		0.79 g
NaCl		2.85 g
EDTA		0.186 g
10% SDS		2.5 ml
Distilled water	q.s.	500 ml

Buffers for SDS-PAGE

Separation gel buffer (1.5 M Tris-HCl, pH 8.8)

HCl		48 ml
Tris		36.3 g
Distilled water	q.s.	100 ml

Stacking gel buffer (0.5 M Tris-HCl, pH 6.8)

Tris		5.98 g
1 N HCl adjust pH to 6.8		
Distilled water	q.s.	100 ml

7.5% Separation acrylamide gel

Distilled water	15-17 ml
30% Acrylamide	7.5 ml
Separation gel buffer	7.5 ml
Ammonium persulfate (0.1%)	0.15 ml
10% SDS	0.3 ml
Deaerate under vacuum suction	
TEMED	15.0 µl

3.75% Stacking acrylamide gel

Distilled water	6.0-7.0 ml
30% Acrylamide	1.88 ml
Stacking gel buffer	3.75 ml
10% SDS	0.15 ml
Ammonium persulfate (0.1%)	75.0 µl
Deaerate under vacuum suction	
TEMED	7.0 µl

Electrode buffer (10 X concentrated pH 8.3)

Tris		6.0 g
Glycine		28.8 g
10% SDS		10.0 ml
1 N HCl or 1 N NaOH	q.s.	pH 8.3
Distilled water	q.s.	1000 ml

Sample buffer (2X concentrated)

Glycerol		2.0 ml
Bromophenol blue dye		40.0 μl
10% SDS		2.0 ml
Stacking gel buffer		2.5 ml
Distilled water	q.s.	10 ml

For reducing sample buffer, add in 20μl β-mercaptoethanol

Staining solution

Coomassie brilliant blue	100 mg
Methanol	40 ml
10% Acetic acid	60 ml

Destaining solution

Glacial acetic acid		100 ml
Distilled water	q.s.	1000 ml

Reagents for protein estimation by Lowry's method

(1) Alkaline copper reagent

(a) 2% sodium carbonate in 0.1 N NaOH

(b) 1% cupric sulfate in H_2O

(c) 2% potassium tartrate in H_2O

Mix equal volumes of (b) and (c) and add 1.0 ml to 50 ml of (a) before use.

(2) Folin phenol reagent : Dilute 1 volume of the reagent (BDH Chemicals,

Toronto) with 2 volumes of distiled water before use.

Cell culture media

RPMI 1640 medium

RPMI 1640 medium powder (Sigma)		10.4 g
Sodium bicarbonate		2.0 g
Distilled water	q.s.	1000 ml

MEM medium

MEM medium powder (sigma)		9.5 g
Sodium carbonate		2.2 g
distilled water	q.s.	1000 ml

The pH of the media was adjusted to 7.2 with 1N NaOH or 1N HCl and sterilized by membrane (0.22 μM) filtration and supplemented with 10% (for PRMI 1640) or 15% (for MEM) fetal calf serum, 100 units/ml of penicillin, 100 μg/ml of streptomycin and 0.11% sodium pyruvate (for MEM only) before use.

ITES serum free medium

Insulin (dissolved in 50mM HCl)		5.0 mg
Transferrin		33 mg
Ethanolamine		1.2 mg
selenium ($Na_2SeO_3 \cdot 5H_2O$)		6.6 μg
$NaHCO_3$		1.2 g
DE-F12 medium powder	for	1000 ml
Distilled water	q.s.	1000 ml

Methods

1. Production of Dal B01 and Dal B02 and Their F(ab)'₂ Fragments

1.1 Production of Dal B01 and Dal B02

The hybridoma clones (Dal B01 and Dal B02) were grown in culture in a serum free medium (ITES). Cells were harvested and washed twice with HBSS. Each BALB/c mouse received 1.5×10^7 cells (in 0.5 ml HBSS) by i.p. injection 7 days after i.p. injection of 0.5 ml pristane or 0.1 ml incomplete Frenud's adjuvant. Ascites fluid was collected from the ascites tumor bearing mice (10 to 14 days after i.p. injection of hybridoma cells) by a sterile 18-gauge needle and were centrifuged at 300 x g for 15 to 20 min to get rid of tumor cells and the contaminating red blood cells. The supernatant was collected and stored at -20°C.

(2) Purification of Dal B01 and Dal B02 from mouse ascites

Two different methods were used for the purification of Dal B01 or Dal B02 from mouse ascites in this study.

(A) Caprylic acid method

This method was used to purify Dal B02, an IgG1 McAb. The method reported by (McKinney and Parkinson, 1987) was followed. Briefly, the ascites were dialysed against acetate buffer (60 mM, pH 4.5) overnight or directly diluted with 4 volumes of acetate buffer (60 mM, pH 4.0) and the pH was adjusted to 4.5 with 0.1 N NaOH. Caprylic acid (25 µl per ml of diluted ascites) was slowly added dropwise with thorough mixing and the solution was stirred for an additional 30 min at room temperature. The ascites were

centrifuged at 12, 000 x g for 30 min to remove the insoluble materials (e.g. lipoprotein, etc.) and the supernatant was filtered through a #4 filter paper. 1/100 volume of 1.0 M PBS (pH 7.4) was added to the supernatant and the pH of the supernatant was adjusted to 7.4 by 1 N NaOH. The supernatant was then fractionated with ammonium sulfate (0.277 g/ml of supernatant) at 4°C overnight and the precipitated IgG was collected by centrifugation at 12, 000 x g for 20 min. The IgG pellet was dissolved in a small amount of PBS (0.01 M, pH 7.2) and dialysed against PBS for 48 to 72 hr. The antibody was sterilized by membrane (0.22 μm) filtration and characterized by SDS-PAGE .

(B) Protein-A chromatography

This method was used to purify Dal B01, an IgG2a subclass MoAb. Briefly, the mouse ascites were first dialysed against 60 mM acetate buffer (pH 4.5) overnight to remove the lipoprotein as described above. The ascites were then dialysed against 0.01 M PBS to reach a neutral pH and loaded on a Protein-A column (1.5 x 50 cm) which was equilibrated with PBS (0.01 M, pH 7.2). The column was eluted with PBS to wash away the unbound component , and the bound component, which is IgG2a, was eluted out with 0.58% acetate buffer (pH 2.8). The antibody fractions were pooled and immediately dialysed against PBS to get back to neutral pH.

1.3 Determination of protein concentration

The method reported by Lowry et al. (1951) was followed. Briefly, the samples, as well as the standard protein solution (1.0 mg/ml), were mixed with 2.5 ml alkaline copper reagent and placed at room temperature for 10 min after which 0.25 ml Folin phenol reagent was added in and mixed thoroughly. The absorbance at 700 nm of the samples was measured after an additional 30 min. The protein concentration of the samples can be calculated as following :

Protein concentration (mg/ml) =

$$\frac{O.D_{700}nm \text{ of sample} - O.D_{700}nm \text{ of background}}{O.D_{700}nm \text{ of standard} - O.D_{700}nm \text{ of background}} \times \text{ dilution factor of the sample}$$

1.4 Sodium dodecyl sulfate polyacrylamide gel electrophoresis (SDS-PAGE)

SDS-PAGE was carried out with a Hoefer Scientific Instrument apparatus model PS 1200. The gel consisted of a stacking gel of 3.5% acrylamide (height about 2.5 cm) and a separating gel of 7.5% acrylamide (height about 7.5 cm) and approximately 1.5 mm in thickness. A constant current of 20 mA was applied through out the process which lasts about 45 min. The gel was then stained with Coomassie brilliant blue for about 30 min and destained with 10% acetic acid.

1.5 Preparation of F(ab)'2 fragments from Dal B01 and Dal B02

A series of preliminary experiments were carried out to determine the optimal pH and the time required at 37°C for pepsin digestion. A ratio of 1/40 (w/w) of pepsin to antibody was used. Aliquots of antibodies (1.0 mg/ml) were dialysed against acetic acid buffers at different pH (i.e., pH 3.7, 3.8 or 4.0) overnight. Precipitates if formed were removed by centrifugation. Pepsin was added and the mixture was incubated at 37°C for different time intervals. The digestion process was monitored by SDS-PAGE.

In my final protocol for the preparation of Dal B01 F(ab)'2 and Dal B02 F(ab)'2 fragments, the intact MoAbs (15 - 20 mg/ml) were dialysed against acetic acid buffer (pH 3.7) overnight and digested with pepsin at 37°C for 3 hr (Dal B01) or 6 hr (Dal B02),

respectively. The oH of the mixture was adjusted to 8.6 to terminate the digestion process by adding equal amount of 0.6 M Tris after which the mixture was loaded on a Sephacryl S-200 column (1.5 x 90 cm) pre-equilibrated with 0.01 M PBS (pH 7.2). The column was eluted with 0.01 M PBS, and 80 fractions of 3 ml each were collected. The absorbance of each of the fractions was measured at 280 nm using a UV spectrophotometer and was plotted against the fraction number. SDS-PAGE was run on peak fractions and the fractions representing F(ab)'2 fragment were pooled. The concentration of F(ab)'2 was determined by Lowry's method.

1.6 Determination of antibody activity by membrane immunofluorescence

This method was used to determine the antibody activity of Dal B01, Dal B02 and their F(ab)'2 fragments, either in free form or as drug conjugates, using D10-1 cells. Aliquots of 5×10^5 D10-1 cells (in 50 µl PBS) were mixed with different concentrations of MoAbs or their F(ab)'2 fragments, either in free form or as drug conjugates (from 10 µg/ml to 0.03 µg/ml, usually in a double-dilution pattern) and incubated at 4°C for 60 min. After washing twice with cold PBS, the cells were incubated with 35 µl FITC labeled rabbit anti-mouse IgG (1:12 dilution) at 4°C for additional 30 min and washed another 2 times with cold PBS. The cells were then mixed with 10 µl glycerol and the cell smears were observed under fluorescence microscope. The maximum MoAb dilution that gave staining of 50% of cells was defined as the titer of the antibody.

2. Growth of Tumor Cell Lines

2.1 Cell culture

D10-1, MOLT-3, K562 and HL60 cells were grown in RPMI 1640 medium supplemented with 10% fetal calf serum, 100 units/ml penicillin and 100 µg/ml streptomycin at 37°C in a 95% air / 5% CO_2 incubator. The cells were subcultured every 3 to 4 days.

Caki-1 and Nu-caki-1 cells were grown in MEM medium supplemented with 15% fetal calf serum, 100 units/ml penicillin, 100 µg/ml streptomycin and 0.11% sodium pyruvate at 37°C in a 95% air / 5% CO_2 incubator. Cells were harvested using sterile EDTA solution (0.2%) and washed 3 times with 0.01 M PBS before subculture or experimental use.

2.2 Doubling time determination and growth curve

Constant number of cells were plated in each well of a 24 well culture plate with fresh medium and incubated at 37°C in a 95% air / 5% CO_2 incubator. At intervals of 0, 1, 2, 3, 4, 5, 6 days, the number of cells in each well was counted with a Coulter Counter. Growth curves were constructed by plotting the number of cells versus time in hours, and the doubling time was calculated by the following formula:

$$\text{Cell doubling time (hr)} = \frac{T_2 - T_1}{\dfrac{\log N_2 - \log N_1}{\log 2}}$$

whereas ($T_2 - T_1$) is the period of time (hr) during which cell grew exponentially, and N_1 and N_2 are the number of cells at time T_1 and T_2, respectively.

3. Studies on Dal B01, Dal B02 or Their F(ab)'2 Fragment Induced Capping on D10-1 Cells

The method reported by Guclu et al. (1975) was followed. Briefly, the antibodies or their fragments (10 μg/ml) were incubated with D10-1 cells at 4°C for 30 min after which the cells were washed 3 times with cold PBS. The washed cells were incubated at 37°C for a period of 6 hr. Aliquots of cells were collected at different intervals of 0, 0.5, 1, 2, 4, and 6 hr and were immediately transferred to cold PBS containing 0.02% sodium azide. The cells were then stained for membrane immunofluorescence by incubation with FITC-labeled rabbit anti-mouse IgG for 30 min at 4°C. After another 3 washes with cold PBS, the cells were assayed for:

(a) viability of cells by trypan-blue exclusion assay;

(b) immunofluorescence membrane staining;

(c) number of cells that formed caps.

At least 200 consecutive cells were counted to estimate the proportion of cells showing membrane staining and /or capping.

4. Cytotoxicity of Dal B01 and Dal B02 to D10-1 Cells

4.1 Cytotoxicity of Dal B01 or Dal B02 alone

D10-1 cells (3 x 10^4 / 100 μl medium) were plated in each well of a 96 well plate and incubated at 37°C in a 95% air / 5% CO_2 incubator overnight. Different amounts of sterile Dal B01 or Dal B02 in 100 μl medium were added in triplicate wells to achieve final concentrations of 1 to 500 μg/ml. The cells were cultured for an additional 72 h and the number of cells in each well was counted with a Coulter Counter.

4.2 Antibody-dependent cell-mediated cytotoxicity (ADCC)

(A) Target cells: D10-1 cells were washed 3 times with fresh RPMI 1640 medium containing 5% FCS. The cell pellet (about one million cells) was incubated with 100 μCi Na^{51}Cr in 0.2 to 0.3 ml medium at 37°C for 60 min. The cells were then washed 4 times, resuspended in 1.0 ml medium containing 5.0 μg/ ml of MoAbs and incubated at 4°C for 30 min. The cells were washed twice again, resuspended in 1.0 ml medium and counted using a hematocytometer.

(B) Effector cells: The nude or SCID mice were primed i. p with 100 units of poly IC (for splenic cells) or 0.1 ml incomplete Frenud's adjuvant (for peritoneal macrophages) 24 hr before harvesting the effector cells. To obtain splenic cells, the spleen was removed from the mouse and single cell suspensions were made by mechanic teasing. For peritoneal macrophages, 2.0 ml of PBS was injected into the mouse peritoneal cavity. The peritoneal cells were washed out with an additional 3.0 ml of PBS. The cell concentration was determined using a hematocytometer.

(C) Cytotoxicity assay : 5 x 10^3 of labeled target cells were mixed with various numbers (from 1.25 x 10^4 to 1 x 10^6, i.e., E/T ratios varied from 25 to 1 to 200 to 1) of effector cells, i.e., splenic cells or peritoneal macrophages, in 200 μl medium in triplicate of a 96 well culture plate. The plate was incubated at 37°C for 4 hr after which the cells were centrifuged down and 100 μl of supernatant was taken out. Radioactivity in the supernatant was determined by a gamma counter. The spontaneous release of radioactivity was determined by incubation of the labled cells in the absence of effector cells, and the maximum release was determined by lysis of cells using 10% SDS. NK-sensitive cell line Yac was used as a positive control. The percentage of specific lysis was calculated as following:

$$\text{Cell lysis (\%)} = \frac{\text{cpm (experimental group)} - \text{cpm (spontaneous release)}}{\text{cpm (maximum release)} - \text{cpm (spontaneous release)}} \times 100$$

4.3 Complement-dependent cytotoxicity (CDC)

(A) Target cells: D$_{10-1}$ cells were labeled with ^{51}Cr as described above.

(B) Complement: Lyophilized rabbit complement was reconstituted in 1.0 ml distilled water.

(C) Cytotoxicity assay: 5×10^3 of labeled D$_{10-1}$ cells were mixed with different amount of MoAb (5.0, 2.5 and 1.25 µg/ml) and complement (final dilution 1 to 10). The mixture was incubated at 37°C for 1.0 hr after which the cells were centrifuged down. One hundred µl aliquots of supernatant was taken out and counted. The spontaneous release of radioactivity was determined by incubation of labeled cells in the absence of complement, and maximum release was determined by lysis of cells using 10% SDS. The percentage of specific lysis was calculated using the formula described above.

5. Radioiodination and Characterization of Dal B01 and Dal B02 and Their F(ab)'₂ Fragments

5.1 Radioiodination of Dal B01, Dal B02 and their F(ab)'₂ fragments

Chloramine-T method (Ghose and Guclu, 1974) was initially chosen to radioiodinate Dal B01, Dal B02 and their F(ab)'₂ fragments. In order to achieve the best iodine recovery (i.

e., high radiolabeling efficiency) and also to retain the best antibody activity, a series of preliminary experiments were carried out to determine the optimal reaction conditions. The reaction conditions that were investigated include: (a) the duration of exposure of radioiodine and antibody to chloramine T ; (b) the amount of chloramine T used in the reaction; (c) the effect of the level of iodine incorporation on antibody activity.

(A) The effect of variation in the duration of exposure of radioiodine and Dal B02 to chloramine T on iodine incorporation and antibody immunoreactivity

Dal B02 (250 µg in 0.5 M phosphate buffer, pH 7.2) was mixed with 50 µl chloramine T (2.0 mg/ml) and 500 µCi of $Na^{125}I$. At different intervals of 1, 2, 3, 5, and 10 min, the reactions were stopped by adding 50 µl sodium metabisulfate (5.0 mg/ml) and 50 µl sodium iodide (5.0 mg/ml).

(B) The effect of variation in the amount of chloramine T used in the reaction mixture on iodine incorporation and antibody immunoreactivity

Dal B02 (250 µg in 0.5 M phosphate buffer, pH 7.2) was mixed with 500 µCi of $Na^{125}I$. Different amounts of chloramine T were added (chloramine T concentrations varied from 25 to 200 µg/ml). The mixtures were stirred for 2 min and the reactions were stopped as described in (A).

(C) The effect of the level of iodine incorporation on antibody immunoreactivity

Constant amount of Dal B02 (50 µg in 0.5 M phosphate buffer, pH 7.2) and chloramine T (final concentration, 100 µg/ml) were mixed with different amounts of $Na^{125}I$ (from 100 µCi to 1000 µCi). The mixtures were stirred for 2 min and the reactions were stopped as described in (A).

The mixtures were then loaded on NAP-10 columns (pre-equilibrated with 1% BSA in 0.01 M PBS). The columns were eluted with 0.01 M PBS and 0.5 ml fractions were collected. The radioactivity of fractions were counted with a gamma counter and the fractions which contained the labeled protein were pooled (usually from fraction No.3 to No.5). The level of iodine incorporation and the retention of antibody activity of each radiolabeled antibody preparation was then compared.

For in vivo localization studies, Dal B01 and Dal B02 or their F(ab)'2 fragments were labeled with ^{131}I while the control nonspecific IgG1 or IgG2a and their F(ab)'2 fragments were labeled with ^{125}I. Specific activities of the labeled proteins ranged from 0.5 μCi to 1.0 μCi/μg protein. For in vivo radiotherapy, the Dal B02 or its F(ab)'2 fragment were labeled with ^{131}I and the specific activity ranged from 6 to 10 μCi/μg.

5.2 Determination of the levels of iodine incorporation in radiolabeled Dal B01, Dal B02 and their F(ab)2 fragments

(A) Determination of the specific activity of radiolabeled IgG (μCi/μg of IgG)

The cpm of a known amount of ^{125}I or ^{131}I (usually 0.025 μCi was used) was counted and used as a standard for the calculation of the specific activity of labeled IgG. The specific activity of the labeled antibodies was then calculated by the following formula:

Specific activity of labeled protein (μCi/μg) =

$$\frac{\text{sample cpm}}{\text{standard iodine cpm}} \times 0.025 \text{ mCi} \times \frac{1}{\text{volume of sample counted(ml)}} \text{ / sample IgG concentration (μg/ml)}$$

(B) Determination of radioiodine incorporation (atom I /molecule IgG)

(a) μCi/atom of iodine

$$\frac{\text{specific activity of iodine } (\mu Ci/\mu g \text{ of iodine}) \times 10^6 \times \text{atomic weight of iodine}}{6.023 \times 10^{23}}$$

(b) μCi/molecule of IgG

$$\frac{\text{specific activity of IgG } (\mu Ci/\mu g) \times 10^6 \times \text{molecule weight of IgG}}{6.023 \times 10^{23}}$$

(c) level of radioiodination (atom I/molecule IgG)

$$\text{Ratio of (b)/(a)} = \frac{\mu Ci/\text{molecule of IgG}}{\mu Ci/\text{atom of iodine}}$$

5.3 Determination of immunoreactive fraction (IRF) of radiolabeled Dal B01, Dal B02 and their F(ab)'₂ fragments

The method described by Lindmo et al (1984; 1986) was followed. Briefly, D10-1 or MOLT-3 cells (the number of cells varied from 0.5×10^6 to 8×10^6) were incubated with a constant amount of radioiodine labeled Dal B01 or Dal B02 or their F(ab)'2 fragments (typically about 30 to 50 ng) in a total volume of 100 μl. Incubation was carried out at 4°C for 90 min in 1% BSA coated glass test tube (12 x 75 mm). Cells were then washed 4

times with cold PBS (0.1% BSA, pH 7.2) and the cell pellets were counted for cell-associated radioactivity.

To determine the IRF, the ratio of the total amount of radiolabeled MoAbs or F(ab)'2 fragments added to the amount of MoAbs or F(ab)'2 fragments bound to the cells (T/B ratio) was plotted against the inverse of the cell concentration (ml/million cells). Linear regression of the data to determine the Y-axis intercept of the plot yields a value that equals the inverse of the IRF.

5.4 Determination of the number of binding sites on D_{10-1} cells and Ka of binding of radiolabeled Dal B01, Dal B02 and their F(ab)'2 fragments

The number of D_{10-1} cells was kept constant (5×10^5) and the amount of iodinated MoAbs or their F(ab)'2 fragments were varied. Incubation of D_{10-1} cells with labeled antibodies was carried out at 4°C in glass test tubes (precoated with 1.0% BSA in PBS) for 90 min after which the cells were washed four times with cold PBS containing 0.1% BSA. The cell pellets were counted for cell associated radioactivity.

To calculate the binding site per cell, Scatchard analysis was carried out (Frankel and Gerhard, 1979). The ratio of bound MoAb to free MoAb (total MoAb added minus what was bound) was plotted against specifically bound MoAb. The slope of the plot gives Ka. The X intercept yields maximum specific bound antibody from which the number of binding sites can be calculated:

$$\text{number of binding sites per cell} = \frac{\text{maximum specific bound antibody}(\mu g) \times 10^{-6} \times 6.023 \times 10^{23}}{\text{molecular weight of IgG or F(ab)'2} \times \text{number of cells used}}$$

5.5 Kinetics of binding of radiolabeled Dal B01, Dal B02 or their F(ab)'2 fragments to D10-1 cells in vitro

D10-1 cells (1 x 10^7) were incubated with labeled MoAbs or their F(ab)'2 fragments (10 μg/ml) in a total volume of 1.0 ml up to 6 hr at either 37°C or 4°C. At different intervals, aliquots of cells were taken out and washed 4 times with cold PBS containing 0.1% BSA. The cell bound radioactivity was determined and plotted against time in min.

5.6 The fate of radiolabeled Dal B02 bound to the surface of D10-1 cells in vitro

D10-1 cells (1 x 10^7) were incubated with ^{125}I labeled Dal B02 (10 μg/ml) in a total volume of 1.0 ml at 4°C for 90 min. After washing with cold PBS to remove unbound ^{125}I-Dal B02, the cells were reincubated at 37°C with or without the presence of a large excess of unlabeled Dal B02 for various periods from 0 to 6 hr. The concentration of unlabeled Dal B02 was 50-fold higher than that of radiolabeled counterparts. At each point of time, an aliquot of cells was taken out and centrifuged down. Half of the supernatant was collected and the radioactivity in the supernatant was counted. The other half of the supernatant was treated with cold TCA (final concentration 10%). After centrifugation at 12,000 x g for 30 min, the cpm in the precipitate was determined. The cell pellet from the same sample was also counted to determine the cell-associated cpm. So, at each time point, we determined the percentage of retained cpm in the cells and the percentage of released cpm. The released cpm were determined in the TCA precipitable and TCA soluble fractions.

6. Studies Using Gold Particle Complexed Dal B01 or Dal B02

6.1 Preparation of Dal B01-Au and Dal B02-Au complexes

(A) Production of colloidal gold particles

Colloidal gold particles with a mean diameter of 15 nm was prepared by controlled reduction of a boiling solution of 0.01% chloroauric acid (100 ml) with 1% sodium citrate (4.0 ml) (Frens, 1973). The sodium citrate was added dropwise to a boiling chloroauric acid solution. Boiling was continued till the color of the solution turned from dark blue to golden brown (it usually takes about 10 to 15 min). The size of the gold particles was confirmed by electron microscopy.

(B) Determination of the optimal coupling pH and the minimal amount of Dal B01 or Dal B02 required to stabilize a given amount of colloidal gold

An antibody concentration variable absorption isotherm (Roth, 1983; De Meij, 1983) was carried out under two different pH conditions (i. e., pH 7.1 and pH 9.2). Briefly, to 1.0 ml of colloidal gold solution (pH 7.1 or 9.2), different amounts of antibodies (Dal B01, Dal B02 or Dal K29) were added in (varied from 0 to 100 μg). The mixtures were placed at room temperature for 2 to 3 min before 0.1 ml of 10% sodium chloride was added. After an additional 5 min, the absorbance at 580 nm of each sample was measured and the minimal amount of antibody that could stabilize the colloidal gold solution was determined (The color of a stabilized colloidal gold solution stays golden brown. It turns to purple blue on destabilization). In the same way, the optimal pH that stabilizes the antibody-Au complexes was also determined.

(C) Preparation of Dal B01-Au, Dal B02-Au and Dal K29-Au complexes

For the preparation of Dal B01-Au complex, both the antibody and the colloidal gold solution were dialysed against 20 mM borax buffer (pH 9.2) to adjust the pH to 9.2.

Iodine-125 labeled Dal B01 (550 μg, specific activity: 0.271 μCi/μg) was mixed with 10 ml colloidal gold solution and the mixture was placed at room temperature for 2 to 3 min before 10% BSA solution (pH 9.2) was added to a final concentration of 1%. The reaction mixture was centrifuged at 27,000 x g for 45 min. The supernatant was discarded and the pellet was resuspended in 10 ml TBS buffer (pH 8.2). This washing procedure was repeated 4 times and the final pellet was dissolved in 3.0 ml PBS (pH 7.2).

For the preparation of Dal B02-Au and Dal K29-Au complexes, the coupling reaction was carried out at pH 7.1. Iodine-125 labeled B02 (440 μg, specific activity : 0.234 μCi/μg) or ^{125}I labeled Dal K29 (660 μg, specific activity: 0.2 μCi/μg)) was mixed with 10 ml colloidal gold solution. BSA (pH 7.1) was added to a final concentration of 1% after 2 to 3 min at room temperature. The washing procedure was carried out as described above.

To determine the amount of antibody adsorbed to gold particle, the radioactivity in the complexes was counted and the amount of antibody that bound to the gold particles was calculated as described in Method 5.2. The number of gold particles was determined by measuring the absorbance of the solution of antibody-Au complexes at 520 nm (for 15 nm gold particle solution, 1 x 10^{12} particle / ml gives the absorbance of 1.0). The number of IgG molecules per gold particle was then calculated.

6.2 Characterization of Dal B01-Au, Dal B02-Au and Dal K29-Au complexes

(A) Immunoreactive fraction (IRF) of the complexes

The IRF of ^{125}I labeled Dal B01, Dal B02 and Dal K29, either free or complexed to gold particles, were determined using D10-1 cells as described in Method 5.3.

(B) Stability

(a) Stability at 37°C

MoAb-Au complexes were diluted with RPMI 1640 medium and incubated at 37°C for up to 6 hr. At different intervals, aliquots were taken out and centrifuged at 27,000 x g for 45 min. The radioactivity in the pellet and in the supernatant was determined.

(b) Stability after repeated freezing and thawing

Diluted MoAb-Au complexes were frozen at -80°C for 5 min and then thawed at 37°C in a minute. The procedure was repeated 5 times and an aliquot was taken out at each time. Aliquots were centrifuged at 27,000 x g for 45 min and the radioactivity in the pellet and in the supernatant was determined.

(c) Stability at low pH

Diluted MoAb-Au complexes were incubated in RPMI 1640 medium (buffered with HCl) at pH 4.5 at 37°C for up to 6 hr. At different intervals, aliquots were taken out and centrifuged. The radioactivity in pellet and supernatant was determined.

(C) Cytotoxicity

D_{10-1} or Caki-1 cells (5×10^5) in 50 µl RPMI 1640 medium were mixed with 50 µl of ^{125}I labeled MoAbs, ^{125}I labeled MoAb-Au complexes or medium only. The cells were incubated at 37°C for up to 6 hr. At different intervals, aliquots of cells were taken out and cell viability was examined by trypan blue exclusion assay.

6.3 Electron microscopy studies on D_{10-1} cells exposed to Dal B01-Au or Dal B02-Au complexes

D_{10-1} cells (6×10^6) in 0.5 ml RPMI 1640 medium were mixed with ^{125}I labeled B01-Au or B02-Au complexes to a final concentration of MoAbs of about 12 to 20 μg/ml. The cells were incubated at 4°C for 90 min before washing 4 times with cold PBS containing 0.1% BSA. The cell pellets were resuspended in plain RPMI medium and incubated at 37°C for up to 6 hr. At intervals of 0, 0.5, 1, 2, 4, 6 hr, aliquots of cells were taken out and centrifuged down. The cells were then fixed with 5% glutaraldehyde (in PBS) overnight and sent for electron microscopic studies.

Several control groups were set up. These included incubation of : (1) D_{10-1} cells with non-specific anti-BSA IgG-Au complex; (2) D_{10-1} cells with ^{125}I labeled B01 followed by non-specific anti-BSA IgG-Au conjugate; (3) D_{10-1} cells with non-specific rabbit anti-mouse IgG-Au conjugate; (4) D_{10-1} cell with gold particles; (5) non-target MOLT-3 cells with gold particles; (6) non-target MOLT-3 cells ^{125}I labeled B02-Au complex; (7) non-target M_{21} cells with ^{125}I labeled B01-Au complex.

For electron microscopic studies, D_{10-1} cells that have exposed to Dal B01-Au or Dal B02-Au complex, as well as all the control samples were collected at each time point indicated. Cells were fixed in 5% glutaraldehyde in 0.01 M PBS overnight and then washed 3 times with cacodylate buffer (pH 7.3) and covered with 1% OsO_4 for 2 hr and subsequently rinsed with distilled water twice for 5 min each. Cells were then treated with 0.025% uranyl acetate overnight, rinsed in distilled water and dehydrated with increasing concentrations of acetone (i. e., 50%, 70%, 95%) and then 100% of acetone twice for 10 minutes each. Infiltration was carried out in a combination of resin (TAAB : DDSA : MNA, 10 : 7 : 3 (v/v), with one drop of DMP-30 for each ml of complete resin made) and acetone (4 : 1, 1 : 1, 1 : 5) for 2 hr each. Cells were then transferred to a beam capsule containing complete resin which was then subsequently allowed to mature in a oven maintained at 65-70°C. Thin sections were cut with a LKB Huxley ultramicrotome and picked up on 300

mesh nickle coated grids and stained with 2% uranyl acetone and lead citrate. The cellular localization of Dal B01-Au or Dal B02-Au complex (i. e., whether particles remained on cell surface or internalized inside cells) were determined (this part of work was done by Dr. G. Faulkner, Department of Microbiology and Immunology, Dalhousie University, Halifax, NS).

7. In Vivo Tumor Localization of Radiolabeled Dal B01, Dal B02 and Their F(ab)'2 Fragments

7.1 Establishment of s.c. D_{10-1} xenograft in nude mice

Nude mice (female, 6 to 8 weeks old, 20 to 22 g) were exposed to 400 rad total body irradiation (TBI) 48 hr before inoculation with D10-1 cells. D10-1 cells were harvested and washed twice with PBS, and 5 to 10 x 10^6 cells were injected subcutaneously into the flank of each mouse. The mice were observed daily for the appearance of tumor. Usually, 100% mice developed a subcutaneous tumor within about 10 days. Biodistribution studies were carried out at 10 to 14 days post tumor cell inoculation when the tumors weighed approximately of 0.5 to 0.8 g.

7.2 Injection of D10-1 xenograft bearing mice with radiolabeled Dal B01, Dal B02 or their F(ab)'2 fragments

To block the uptake of radioactive iodine by thyroid, nude mice were given Lugol's iodine containing water (0.2 ml of Lugol's iodine solution in 100 ml of sterile tap water) starting 48 hr prior to the administration of radioiodinated antibodies or their F(ab)'2 fragments. Usually, 40 to 50 μCi of ^{131}I labeled Dal B01, Dal B02 or their F(ab)'2 fragments were

mixed with 10 to 15 μCi of ^{125}I labeled isotype-matched non-specific control IgGs or their F(ab)'2 fragments and injected i.v. into each mouse via a tail vein.

7.3 Pharmacokinetic studies

Serial blood samples were obtained from a tail vein at indicated times after the administration of radiolabeled antibody, i. e., at 0, 0.25, 0.5, 1.0, 2.0, 3.0, 4.0, 6.0, 8.0, 16.0, 24.0 hr and day 2, 3, 4, 5, 6, and 7. The ^{131}I and ^{125}I activities of each sample were counted with a dual-window gamma counter (Beckman Gamma 4000, Beckman, CA). The total body ^{131}I activity was determined using a Mediac Dose Calibrator (Nuclear-Chicago, IL).

The pharmacokinetics of radiolabeled Dal B01, Dal B02 or their F(ab)'2 fragments were analyzed by a computerized nonlinear least-square regression logarithm (Jennrich and Sampon, 1968). The experimental data were most consistent with a two compartment open pharmacokinetic model described by bi-exponential equation : $Ct = Ae^{\alpha t} + Be^{\beta t}$, where Ct is the concentration at time t and A, B, and α and β are the concentration and rate constants, respectively. The α and β - phase half-lives were calculated as $t_{1/2} = 0.693 / \alpha$ or β. The area under the serum concentration versus time curve at definite times after injection (AUC) was calculated as the intergral of the curve using the formula $AUC = A / \alpha + B / \beta$. The apparent volume of distribution (V) and the clearance in the circulation (CL) were also calculated (The calculation of all the pharmacokinetic parameters described in this study were done by of Dr. C. Yang, Institute of Hematology, Chinese Academy of Medical Sciences, Tianjin, China).

7.4 Biodistribution of radiolabeled Dal B01, Dal B02 and their F(ab)'2 fragments in D10-1 xenograft bearing mice

At days 1, 2, 3, 5 (for F(ab)'2 fragments) and days 2, 4, 7 (for intact MoAbs) post i.v.injection of radiolabeled antibody preparations, three mice in each group were sacrificed. After sacrifice. organs were flushed with PBS via the inferior vena cava, right and left ventricles, until they were free of blood. The internal organs, i. e., brain, heart, lung, liver, spleen, kidney, stomach, intestine, femur, muscle, skin, tail, neck soft tissue (thyroid), as well as blood samples and tumors were removed and weighed. Organ-associated ^{131}I and ^{125}I activities were determined with a dual-window gamma counter. The cpm of the ^{125}I window was corrected by subtraction of the contribution of cpm of the ^{131}I window (this contribution usually amounted to about 30-31% of cpm of ^{131}I window). Organ associated radioactivity was calculated as μCi ^{125}I or ^{131}I / g tissue according to the ^{125}I or ^{131}I standard. From these data, the percentage of injected dose % ID / g tissue and tumor/normal tissue ratio (T / NT), as well as the localization index (LI) were determined. Corrections were made for radioisotope decay using a ^{131}I standard in all analysis.

$$\text{The percentage of injected dose per g tissue (\% ID / g)} = \frac{^{125}\text{I or }^{131}\text{I } \mu\text{Ci / g tissue}}{^{125}\text{I or }^{125}\text{I } \mu\text{Ci injected}}$$

$$\text{Tumor : Non-tumor ratio (T / NT)} = \frac{\text{ID \% / g in tumor tissue}}{\text{ID \% / g in non-tumor tissue}} \quad \text{or}$$

$$\text{(T / NT)} = \frac{\mu\text{Ci / g tissue in tumor tissue}}{\mu\text{Ci / g tissue in non-tumor tissue}}$$

$$
\text{Localization index (LI)} = \frac{\dfrac{\text{ID\%/g tissue of specific MoAb in the organ}}{\text{ID\%/g tissue of non-specific MoAb in the organ}}}{\dfrac{\text{ID\%/g tissue of specific MoAb in the blood}}{\text{ID\%/g tissue of non-specific MoAb in the blood}}}
$$

7.5 Gamma camera imaging

Whole mouse body images were obtained with a computer-linked gamma camera (Maxicam, General Electric) at indicated intervals, i.e., 24, 48 and 72 hr after i.v. administration of ^{131}I lableled F(ab)'$_2$ fragments and 24, 48, 72, 96 and 192 hr after i.v. administration of ^{131}I labeled intact MoAbs. Animals were anaesthetized with phentobarbitol (100 µg, i.p.) during the imaging procedure.

7.6 Stability and reactivity of Dal B01, Dal B02 and their F(ab)'$_2$ fragments recovered from the serum of tumor-bearing mice

Two methods were used to test the stability of radiolabeled antibody in the circulation of tumor-bearing mice: (1) 0.1 ml mouse serum was treated with 10% cold TCA (final concentration) and centrifuged at 12, 000 x g for 30 min, the radioactivity in the precipitated pellet and in the supernatant was counted. The precipitated activity represented the protein-associated radioiodine. (2) 0.2 ml serum was passed through a Sephadex G-25 NAP-10 column. Twenty fractions of 0.5 ml each were collected and the radioactivity of each fraction was counted. The first peak represented the radioactivity associated with intact IgG or its large catabolic fragments while the second peak represented free iodine or iodine

associated with degraded small molecules (if any). The ability to bind to D_{10-1} cells of the MoAbs or their fragments in the serum was determined as described in Method 5.3 and 5.4.

7.7 Autoradiography of tumor tissues after the i.v.administration of ^{131}I labeled Dal B01, Dal B02 or their F(ab)'$_2$ fragments

Tumor tissues were obtained at 48 hr (for F(ab)'2 fragments) or 96 hr (for intact MoAbs) after i.v.administration of radiolabeled antibody preparations and stored at -70°C. Five μm frozen sections were cut, air-dried and fixed on glass slides with formaldehyde vapour at 37°C overnight. All subsequent steps were done in the dark room. Kodak nuclear track emulsion (Type NTB3, Kodak, NY) was warmed to 45°C in a water bath. The liquefied emulsion was mixed with an equal volume of pre-warmed distilled water. The slides were coated with the diluted emulsion and left to dry. The slides were then transferred to light-proof black boxes and stored at 4°C for 2 to 4 weeks. Slides were developed and fixed using Kodak Dektol developer and fixer. The slides were then stained using H & E and examined using an optical microscope.

8. Comparison of Reactivity, Stability, Pharmacokinetcs and in vivo Distribution of Dal B02 after Radioiodination by Three Different Protein Iodination Methods

Three different protein iodination methods, i.e., Chloramine-T, Bolton-Hunter reagent and N-succinimidyl-para-iodobenzoate (PIB) based methods were compared using Dal B02, as regards to the retention of antibody activity, stability in vitro and pharmacokinetics and biodistribution after injection into D_{10-1} xenograft bearing mice.

8.1 Radioiodination of Dal B02 using PIB, Chloramine-T and Bolton-Hunter reagent based methods

(A) PIB method

The method reported by Wilbur et al (1989) was followed with some minor modifications.

(a) The synthesis of PIB reagent

This part of work was done in association with Dr. J. Kralovec, Department of Pathology, Dalhousie University, Halifax, NS. Briefly, Methyl-4-bromobenzoate (compound 1) was reacted with hexabutylditin and tetrakis (triphenylphosphine) palladium. The product 4-tri-n-butylstannylbenzoate (compound 2) was purified and converted to 4-tri-n-butylstannylbenzoic acid (compound 3).The compound 3 was then reacted with N,N'-dicyclohexylcarbodiimide followed by N-hydroxysuccinimide to give the final product, N-succinimidyl, 4-tri-n-butylstanylbenzoate (compound 4).

(b) Radioiodination of compound 4 and antibody labeling (Fig. 2A)

Into a reaction vial was placed 50 μl of 0.25 mg/ml solution of compound 4 in 1.0% HOAc/MeOH (0.025 μmol), 10 μl of a 1.0 mg/ml solution of N-chlorosuccinimide in MeOH (0.075 μmol), and 10 μl of PBS. The desired quantity of $Na^{131}I$ was added (from 1.0 to 2.0 mCi). After 5 min at room temperature the reaction was quenched by the addition of 10 μl of a 0.72 mg/ml aqueous solution of $NaHSO_3$ (10 μl, 0.075 μmol). The MeOH was evaporated by passing a stream of N_2 gas through the reaction vial. After the MeOH has been evaporated (about 10 to 15 min), A solution of the protein in 0.5 M sodium borate buffer, pH 9.2 (or 0.5 M sodium carbonate buffer, pH 9.2), was added. The conjugation reaction was allowed to proceed for 5 min at room temperature, and the labeled protein (compound 6) was purified by gel filtration using Sephadex G-25 NAP-10 column pre-

equilibrated with 0.01 M PBS containing 0.1% BSA. The scheme for the synthesis of compound 4 and for radioiodinating proteins are shown in Fig. 2A.

(B) Bolton-Hunter method (Fig. 2B)

The procedure described by Bolton and Hunter was followed (Bolton and Hunter, 1973). Briefly, a 10 µl (0.4 mg) aliquot of NSHPP solution (in toluene:ethyl acetate 1:1,v/v) was pipetted into a glass tube and the solvent was evaporated in a gentle stream of dry N2. A small magnetic stirrer was placed in the tube and agitation commenced. Two mCi of ^{125}I was added and followed immediately and rapidly by : 50 µg chloramine T (in 10 µl 0.25 M PB, pH 7.5), 120 µg sodium iodine (in 10 µl PB), 2 µl dimethyformamide and 250 µl benzene. The tube was stoppered and the contents vortexed gently to extract the labeled NSHPP into benzene. The benzene was transferred to a fine pointed, conical glass tube and the aqueous layer was extracted with two further 250 µl aliquots of benzene and the benzene extracts were pooled. The benzene was then evaporated with N2 stream and Dal B02 (1.0 mg in 0.1 M borate buffer, pH 8.5) was added to the dried residue and the reaction was allowed to proceed for 15 to 30 min in an ice bath. To obviate subsequent conjugation to carrier protein, 0.5 ml of 0.2 M glycine solution was next added to react with excess iodinated NSHPP. After a further 5 min at 0°C, the radiolabeled protein was separated from small molecules by a NAP-10 column pre-equilibrated with 0.01 M PBS containing 0.25% gelatin.

(C) Chloramine-T method (Fig. 2C)

Antibody iodination was carried out as described before. Briefly, 1.0 mg Dal B02 was mixed with 1.0 mCi of ^{125}I and 100 µg chloramine T. After stirring at room temperature for 2 min, the reaction was quenched by the addition of 50 µl of sodium metabisulfate (5.0 mg/ml) and 50 µl of sodium iodine (5.0 mg/ml). The radiolabeled protein was separated

from free iodine using a NAP-10 column pre-equilibrated with 0.01 M PBS containing 1% BSA.

8.2 Radiochemical purity of labeled Dal B02 preparations

The radiochemical purity of radiolabeled Dal B02 preparations was assessed by two methods. In the first method, i. e., thin layer chromatography (TLC), samples were spotted on silica gel impregenated glass fiber strips (ITLC-Gelman) and eluted with 80% MeOH in H_2O. After elution, the plates were cut into small pieces and the radioactivity that was protein-bound (stayed at the point of origin) or free iodine (migrated to the front edge of elution) were determined using a gamma counter. In the second method (TCA precipitation), TCA was added to each sample to a final concentration of 10%. After 10 min at room temperature, samples were centrifuged at 12, 000 x g for 30 min and the radioactivity in precipitate and supernatant was counted by a gamma counter.

8.3 Specific activity of radioiodinated Dal B02 and iodine incorporation

The specific activity of radioiodinated Dal B02 was determined as described before (see Method 5.2). The iodine incorporation, i.e., labeling efficiency, was calculated for each iodination method.

8.4 Determination of IRF and immunoreactivity of radiolabeled Dal B02 preparations

The IRF and immunoreactivity of Dal B02 preparations labeled by the three different methods, i.e., Dal B02 (PIB), Dal B02 (B-H) and Dal B02 (Chl. T), were determined using D10-1 cells as described in Methods 5.3 and 5.4.

8.5 In vitro stability assay

The stability of incorporation of iodine as well as the IRF of Dal B02 (PIB), Dal B02 (B-H) and Dal B02 (Chl. T) preparations were determined after their incubation with human serum, mouse liver homogenate and human thyroid homogenate.

(A) Stability in human serum

Fresh human serum was filtered through a 0.22 μm sterile filter and placed in sterile, capped tubes. Given amounts of radioiodinated Dal B02 were added into 1.5 ml serum and incubated at 37°C for up to 7 days.

(B) Stability in mouse liver homogenate

Fresh mouse liver was obtained from newly sacrificed BALB/c mice and homogenized in 10 ml of 0.1 M acetate buffer (pH 4.5) with a Polytron Homogenizer (Kinematica Gmbh, Luzern, Schweiz). The homogenate was centrifuged at 600 x g for 15 min and the supernatant was taken out. The protein in supernatant was determined by Lowry's method. Given amounts of radiolabeled Dal B02 were added to 1.5 ml of homogenate supernatant and incubated at 37°C for up to 7 days.

(C) Stability in human thyroid homogenate

Fresh human thyroid was obtained during autopsy of a young male victim of traffic accident. The homogenate supernatant was obtained as described in (B) in pH 7.2, 0.01 M PBS. Given amounts of radiolabeled Dal B02 were added into 1.5 ml of homogenate supernatant containing 5 mM DTT and 1 mM NADPH and incubated at 37°C for up to 3 days.

At indicated intervals, aliquots were taken out from each incubated preparation. Protein bound and free radioactivity were determined by TLC or 10% TCA precipitation. The IRF of Dal B02 in each sample was also determined.

8.6 Biodistribution of radioiodinated Dal B02 preparations

Investigations on the biodistribution of Dal B02 (PIB), Dal B02 (B-H) and Dal B02 (Chl. T) preparations were carried out in D_{10-1} tumor bearing nude mice as described before (Method 7.4). One group of mice received i.v. injection of ^{131}I-Dal B02 (PIB) mixed with an equal amount of ^{125}I-Dal B02 (Chl. T). The other group similarly received ^{131}I-Dal B02 (PIB) mixed with an equal amount of ^{125}I-Dal B02 (B-H). Each mouse was given a total of 80 μg of protein. To detect possible differences in the uptake of radioiodine by thyroid tissue, the mice were not given Lugol's iodine prior to and during the experiment. Serial blood samples were obtained from the tail vein at indicated times. The pharmacokinetic analysis of the three Dal B02 preparations was carried out using a two compartment open model as described before. At 48, 96 and 168 hr post i.v. administration of radiolabeled Dal B02 preparations, three mice in each group were sacrificed. The tumor, blood a l other internal organs were removed and weighed. The tissue-associated ^{131}I and ^{125}I activities were determined with a dual window gamma counter. The cpm in ^{125}I window was corrected by subtracting the contribution from ^{131}I window. The radioactivity that accumulated in tumor or normal organs was determined as the percentage of injected dose per gram of wet tissue (% ID / g). From these data the tumor to normal tissue ratios (T / NT) were determined. Corrections were made for radioisotope decay in all analysis.

Fig. 2

Synthetic schemes showing radioiodination of Dal B02 by different methods.

Fig. 2A Synthesis of PIB reagent and use of this reagent to radioiodinate Dal B02.

Fig. 2B Radioiodination of Dal B02 by Bolton-Hunter method.

Fig. 2C Radioiodination of Dal B02 by Chloramine T method.

Fig. 2A
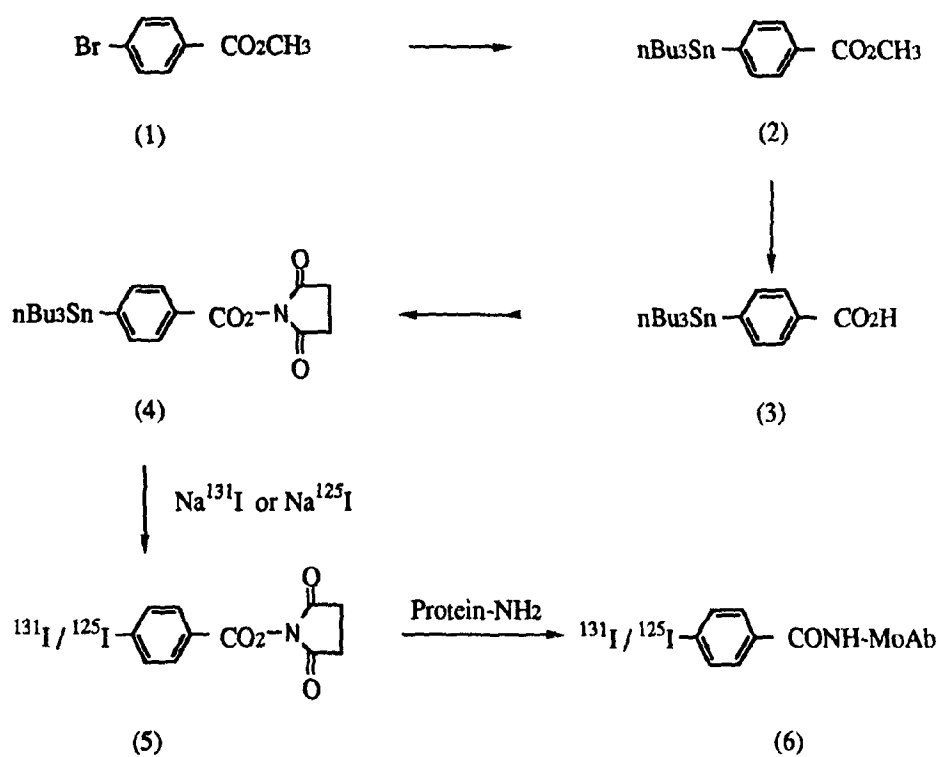
(1) Methy 4-bromobenzoate   (2) 4-tri-n-butylstannylbenzoate

(3) 4-tri-n-butylstannylbenzoic acid   (4)N-succinimidyl 4-tri-n-butylstannybenzoate

(5) Radioiodinated N-succinimidyl para-iodobenzoate   (6) Radioiodinated protein

Fig. 2B

(1)   (2)

+

(4)   (3)

(1) N-succinimidyl 3 (4-hydroxypheny) propionate   (2) Radioiodinated propionate

(3) ε - amino group of lysine or terminus in protein   (4) Radioiodinate protein

Fig. 2C

(1)   (2)

(1) Tyrosine residue in protein   (2) Radioiodinated protein
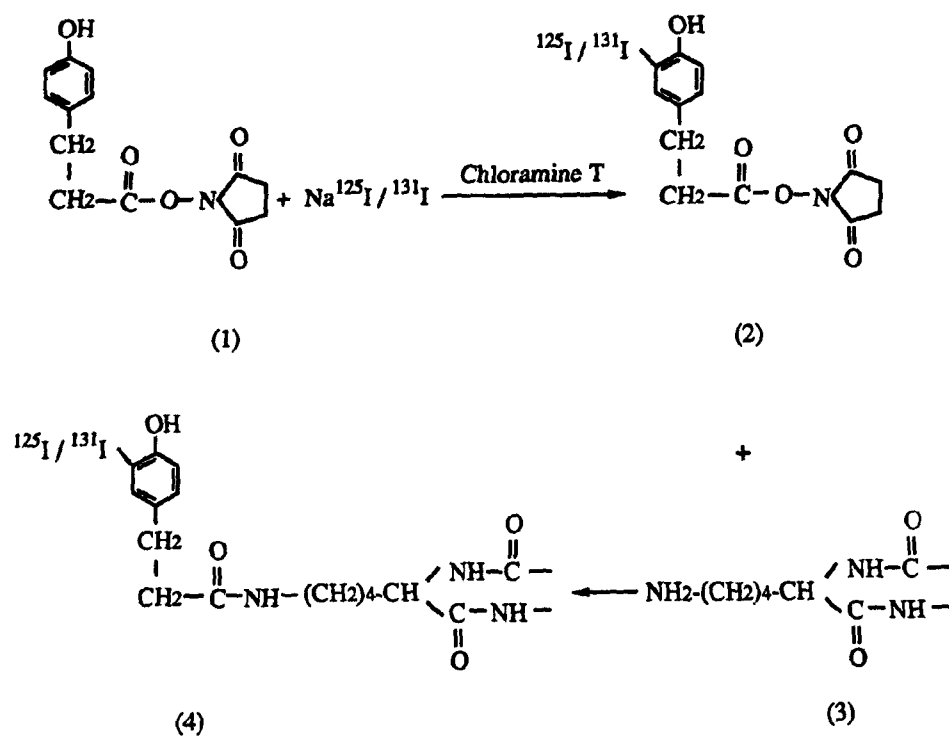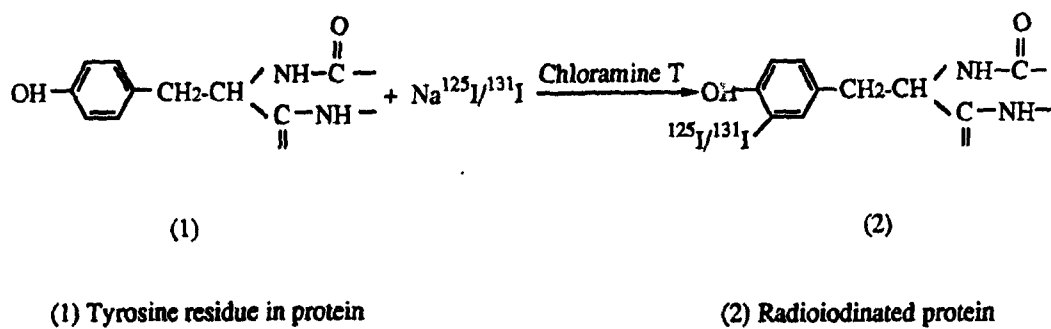
8.7 The stability, IRF and antigen binding ability of Dal B02 recovered from the serum of tumor-bearing mice

Sera from tumor-bearing mice were obtained at 48, 96 and 168 hr post the administration of radiolabeled Dal B02 preparations . Sera were passed through a NAP-10 column and the radioactivity in protein fraction (first peak) or in free iodine fraction (second peak) , if any, were determined by a gamma counter. The IRF and D_{10-1} cell binding ability of Dal B02 in the serum were determined using D_{10-1} cells as described before (Method 7.6).

9. Preparation of Dal B01-MTX and Dal B02-MTX Immunoconjugates, Their Cytotoxicity and Uptake of Conjugated MTX by Tumor Cells in vitro

All conjugates used in this study were prepared by Dr. J. Kralovec, Department of Pathology, Dalhousie University, Halifax, NS.

9.1 Preparation of Dal B01-MTX and Dal B02-MTX conjugates

The synthetic pathways used in the preparation of different types of Dal B01-MTX and Dal B02-MTX conjugates are shown in Fig. 3.

(A) Preparation of Dal B01-MTX and Dal B02-MTX conjugates via active ester linkage

MTX was dried over phosphorus pentoxide before use and its purity was checked by TLC and DHFR inhibitic assay. TLC was performed on silica gel sheets (Kiesel gel 60-F 254). Spots were visualized with ultraviolet viewing lamp at 254 nm. For the preparation of the conjugate, the method reported by Kulkarni et al.(1981) was followed with minor modifications. Briefly, a mixture of MTX (0.76 mg), NHS (0.21 mg) and DCC (0.38 mg)

were dissolved in dimethyformaniide (0.2 ml) at 4°C and then stirred for 18 hr at room

temperature. After removal of precipitates, the mixture (MTX-AE, 0.001 mmol, 20 µl) was

added dropwise to a stirred solution of Dal B01 or Dal B02 (5.0 mg, 3.3 x 10 $^{-5}$ mmol) in

1.2 ml of PBS / DMF (5:1). The reaction was carried out for about 4 hr after which the

solution was centrifuged at 20,000 x g for 10 min. The supernatant v. :s passed through an

Econo-Pac P6 Sephadex G-25 column (Bio-Rad, CA) and the protein fractions were

collected and pooled. The protein concentration in the conjugate was estimated by Lowry's

method and the MTX content was calculated by using ε 373nm (1 cm) = 7100 M^{-1}. The molar

incorporation of MTX into MoAbs (molar ratio of MTX and MoAbs) can thus be

determined.

(B) Preparation of Dal B01-MTX and Dal B02-MTX conjugates via hydrazide linkage

(site-specific linkage)

(a) synthesis of MTXH

To a stirred DMF solution of MTX-AE, freshly prepared from MTX (9.2 mg, 0.02 mmol),

hydrazine (0.1 ml) was added and the reaction was continued for 24 hr. The reaction

mixture was then diluted with 0.5% NH4HCO3 (0.5 ml) ,the resulting precipitate was

removed by centrifugation and the supernatant was passed through a DEAE-52 cellulose

column using a linear NH4HCO3 gradient (0.05-0.4 M). MTXH accompanied with small

amounts of unreacted MTX and MTX dihydrazide eluted in a single peak.

(b) Oxidation of Dal B01 and Dal B02

To a solution of Dal B01 or Dal B02 (5.0 mg) in 750 µl acetate buffer (0.1 M, pH 5.5),

sodium periodate (14 mg in 250 µl of acetate buffer) was added and incubated at 4°C for

30 min after which 7 µl of ethyleneglycol was added. The mixture was then passed through

a Econo-Pac P6 Sephadex G-25 column pre-equilibrated with 0.1 M acetate buffer containing 0.1 M NaCl (pH 4.5).

(c) Coupling of MTXH with oxidized Dal B01 or Dal B02

MTXH (2.0 mg, 0.033 mmol) was dissolved in 200 μl of DMSO and added to the solution of oxidized Dal B01 or Dal B02 in 2.0 ml 0.1 M acetate buffer containing 0.1 M NaCl and 10% DMF (pH 4.5). The mixture was stirred at 4°C overnight and then dialyzed against 0.1 M PBS to yield the conjugate. The molar ratio of MTX to MoAbs in conjugates was calculated as described above.

9.2 Retention of antibody activity in Dal B01-MTX and Dal B02-MTX conjugates

Membrane immunofluorescence staining was routinely used to determine the retention of antibody activity after conjugation to drugs. The procedure was carried out as described before (see Method 1.6).

9.3 Retention of drug activity in Dal B01-MTX and Dal B02-MTX conjugates

Assay of DHFR inhibition activity of Dal B01-MTX and Dal B02-MTX conjugates was carried out according to the method reported by Peterson et al. (1975). Briefly, to a 5 ml cuvette, reagents and test samples were added to a required volume of distilled water in the order as given: 1.0 ml of 1.5 M sodium acetate buffer (pH 6.0), 1.0 ml of 1.8 M KCl, 150 μl of 10 mM NADPH, 0 to 100 μl of MTX or its MoAb conjugates in 0.01 M PBS (2 x 10^{-5} to 2 x 10^{-6} M with respect to MTX), 10 μl (0.01 unit) of bovine liver DHFR (diluted with distilled water just before use). The DHFR was introduced and mixed gently with a teflon adder-mixer and incubated at 22°C for 1 to 3 min. The reaction was initiated by the addition of DHFA (100 μl, 1.0 mM). The change in the absorbance at 340 nm per min was

calculated from the recorder tracing during a 3 min period. At least four concentrations of each test sample were assayed. The IC50 values were obtained from semi-logarithmic plots of percent of DHFR activity as a function of MTX (free or conjugated) concentration.

9.4 Determination of cytotoxicity of Dal B01-MTX and Dal B02-MTX conjugates

For the determination of IC50 values of each conjugate, the effects of continuous exposure for 72 hr and pulse exposure for 6 hr of target or non-target cells to the conjugates were investigated.

(A) Continuous exposure for 72 hr

Aliquots of 3×10^4 D10-1 cells (antibody-reactive cell line) or MOLT-3 cells (a control cell line that does not bind to Dal B01 and Dal B02) in 100 µl medium were plated in each well of a 96 well culture plate and incubated in a 37°C 95% air / 5% CO_2 incubator overnight. Different amounts of free MTX or its conjugates in 100 µl medium were added (triplicate wells for each concentration of test agent) and the cells were incubated for an additional 72 hr after which the total number of cells in each well were counted with a Coulter Counter. The inhibition of proliferation was determined on the basis of proliferation of cells in control preparation that contained plain medium only.

(B) Pulse exposure for 6 hr

The procedure was carried out as described above except that the cells were incubated with drugs or their conjugates for only 6 hr after which the cells were washed 3 times with plain medium. The cells were then incubated in 200 µl fresh medium for an additional 72 hr and the total cell numbers were counted.

Fig. 3

Synthetic schemes showing the synthesis of different types of MoAb-MTX conjugates via either the active ester (non-site-specific) or hydrazone (site-specific) linkage (see text for a detailed description of the synthetic procedures).

Fig. 3
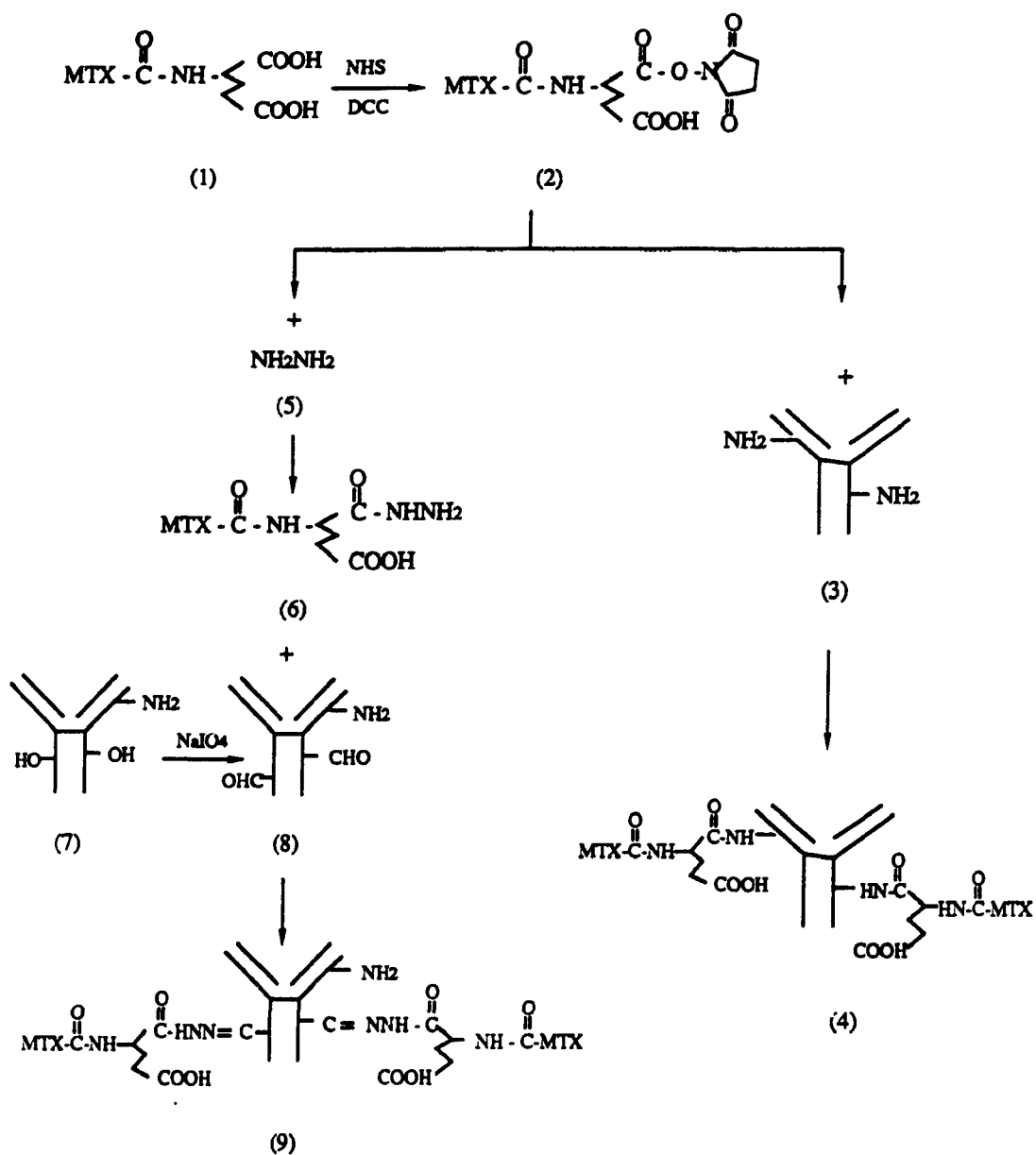
(1) MTX   (2) MTX-AE   (3) IgG   (4) IgG-MTXAE

(5) Hydrazide   (6) MTXH   (7) IgG   (8) Oxidised IgG

(9) IgG-MTXH

9.5 Uptake of [^{3}H]-MTX and Its conjugates by D10-1 and MOLT-3 cells

(A) Preparation of Dal B01-[^{3}H]-MTX and Dal B02-[^{3}H]-MTX conjugates

[^{3}H]-MTX was linked to Dal B01 or Dal B02 via active ester method (see Method 9.1 (A)). The MTX to IgG molar ratios were 4.3 to 1 (Dal B01-MTX) and 4.2 to 1 (Dal B02-MTX), respectively.

(B) Uptake of free [^{3}H]-MTX, [^{3}H]-MTX conjugated to Dal B01 or Dal B02 at different extracellular concentrations by D10-1 and MOLT-3 cells

One to 2 x 10^6 D10-1 or MLOT-3 cells in separate test tubes containing 100 μl plain RPMl 1640 medium were incubated at 37°C or 4°C for 3 min with different extracellular concentrations of free [^{3}H]-MTX varying from 80 to 0.078 μM after which the cells were washed 6 times with cold PBS containing 0.1% BSA and 0.01% sodium azide. The cell pellet was dissolved in 1.0 ml SDS cell lysing buffer (Johnson et al, 1978). Half of the cell lysate was used for protein estimation by Lowry's method while the other half was mixed with 3 ml of liquid scintillation cocktail (Ready Safe™). [^{3}H] activity was counted with a liquid scintillation system. From the protein content and the [^{3}H] activity, the amount and rate of [^{3}H]-MTX uptake by the cells were determined and Eadie-Hofstee plots were generated, i.e. the Vmax and Km were determined.

For the uptake of [^{3}H]-MTX conjugated to Dal B01 or Dal B02, D10-1 or MOLT-3 cells were incubated with different concentrations of conjugates for 90 min at either 4°C or 37°C. For comparison, the cells were also incubated with free [^{3}H]-MTX at the same concentrations of [^{3}H]-MTX as in conjugates under the same conditions. The cells were washed and processed for the determination of cell-associated radioactivity as described above.

(C) Time-course of uptake of free [^{3}H]-MTX, [^{3}H]-MTX conjugated to Dal B01 or Dal B02 by D10-1 or MOLT-3 cells

Twenty millions of D10-1 or MOLT-3 cells were incubated with 5 μM of either free [^{3}H]-MTX or [^{3}H]-MTX conjugated to Dal B01 or Dal B02 in 1.5 ml RPMI medium at either 37°C or 4°C. At intervals of 0, 1, 3, 5, 7, 10, 15, 30, 45, 60, 90, 120 and 180 min (for free MTX) or intervals of 0, 5, 15, 30, 45, 90, 180 min (for conjugated MTX), aliquots of cells were taken out and washed 6 times with cold PBS. The cells were then processed for determination of cell associated [^{3}H] activity as described above.

(D) Efflux of [^{3}H]-MTX from D10-1 or MOLT-3 cells incubated with free [^{3}H]-MTX

Twenty million D10-1 or MOLT-3 cells were incubated with 10 μM of free [^{3}H]-MTX in 1.5 ml medium at 37°C for 90 min after which the cells were washed with cold PBS containing 0.1% BSA. The cells were then incubated at 37°C in 1.5 ml fresh medium devoid of free MTX for up to 120 min. At various time intervals of 0, 1, 3, 5, 7, 10, 15, 30, 45, 60, 90, 120 min, aliquots of cells were taken out and washed 3 times with cold PBS containing 0.1% BSA and 0.02% sodium azide. Cell-associated [^{3}H] activity was then determined as described above.

(E) Determination of the amount of free [^{3}H]-MTX or [^{3}H]-MTX conjugated to Dal B01 or Dal B02 remained associated with tumor cells after pulse exposure for 6 hr

One million D10-1 or MOLT-3 cells were incubated with different concentrations of free [^{3}H]-MTX or [^{3}H]-MTX conjugated to Dal B01 or Dal B02 at 37°C for 6 hr after which the cells were washed for 4 times with PBS. The cell associated [^{3}H] activity was determined.

(F) Release of [^{3}H]-MTX from D10-1 cells incubated with [^{3}H]-MTX conjugated to Dal B01 or Dal B02

Ten millions of D10-1 cells were incubated with 10 µM of [³H]-MTX conjugated to Dal B01 or Dal B02 either at 4°C or 37°C for 90 min after which the cells were washed 4 times with PBS. The cells were reincubated at 37°C in the presence or absence of 50-fold higher concentration of unmodified Dal B01 or Dal B02. At intervals of 0, 5, 10, 15, 30, 60 min, aliquots of cells were taken out and centrifuged down. The [³H] activity in cell pellets was determined as described.

10. Preparation, Cytotoxicity, in vivo Tumor Localization and Anti-tumor Activity of Dal B01-ADR and Dal B02-ADR Immunoconjugates

10.1 Preparation of Dal B01-ADR and Dal B02-ADR conjugates

The synthetic pathways used in the preparation of different types of Dal B01-ADR and Dal B02-ADR conjugates are shown in Fig. 4.

(A) Preparation of Dal B01-ADR and Dal B02-ADR conjugates via CAA spacer (Fig. 4A)

(a) Preparation of ADR-CAA. Ten mg CAA (in 1.0 ml dioxane) was added dropwise to a ADR solution (7.9 mg ADR in 300 µl pyridine) and the mixture was stirred at 4°C overnight. The product was then purified by distributing between chloroform and 5% NaHCO3. The chloroform phase was removed and the extraction was repeated 2 times. The pH of the aqueous phase was lowered down to 2.5 and ADR was further extracted with ethyl acetate. The organic phase was washed with brine, dried with Na2SO4. Finally, the solvent was evaporated to yield ADR-CAA.

(b) Coupling of ADR-CAA to MoAbs. Ten mg of MoAb dissolved in 0.2 M phosphate buffer (pH 8.0) was mixed with 100 µl of DMF. 3.0 mg ADR-CAA in 100 µl of DMF

and 13 mg EDCI in 200 μl of 0.01 M acetate buffer (pH 5.0) were added and the mixture was stirred at 4°C overnight. The conjugate was purified by using an Econo-Pac P6 Sephadex G-25 column. To calculate the molar ratio of ADR to MoAb, the content of ADR in the conjugate was determined by ε 480nm (1 cm) =12100 M^{-1} and the protein content estimated by Lowry's method.

(B) Preparation of Dal B01-ADR and Dal B02-ADR conjugates via C13 linkage (Fig. 4B)

(a) Preparation of ADR-hydrazide. ADR (5.45 mg, 0.01 mmol) along with 2.3 mg HPDP (0.01 mmol) was dissolved in 0.5 ml methanol and 2 drops of trifluormethanesulfonic acid were added. The reaction mixture was stirred at room temperature overnight after which the pH was adjusted to 7. Methanol was removed and the residue was chromatographed on a C-18 RP silica gel column using 3% NH_4CHO in aqueous 50% methanol. After lyophilization, the preparation (TLC homogeneous, red powder) was used for coupling with Dal B01 or Dal B02.

(b) Introducing a spacer into Dal B01 and Dal B02. Five mg (3.3 x 10 $^{-5}$ mmol) of MoAbs in 1.0 ml PBS was reacted with 20-fold molar excess of SPDP in 100 μl of DMF. Desalting of SPDP by using a Econo-Pac P6 column yielded 4.1 mg of modified protein with an average content of 4 mol of spacer per mol of IgG. One hundred μl of DTT solution (15%) was added and the mixture was incubated at room temperature for 30 min after which it was passed through a Econo-Pac P6 column pre-equilibrated and eluted with 0.1 M phosphate buffer (pH 7.2) containing 1 mM EDTA.

(c) Coupling of ADR-hydrazide to Dal B01 or Dal B02. Fifty-fold molar excess of ADR-hydrazide in 100 μl of DMF was mixed with freshly modified MoAbs described above. The reaction was continued at 4°C overnight and the precipitate formed was removed by

centrifugation. The mixture was then passed through a Econo-Pac P6 column eluted with 0.1 M phosphate buffer. The protein fractions were collected. The content of ADR and protein in the conjugate was determined as described.

(C) Preparation of Dal B02-ADR conjugates using dextran T-40 as an intermediate carrier

ADR was covalently linked to Dal B02 via dextran T-40 by two different methods, i.e., using either the ι mino sugar group or the C13 moiety of ADR molecule as the coupling site, via either site-specific (hydrazone bond) or non site-specific linkage (Schiff's base bond).

(a) ADR-Dex-B02 (ss), a conjugate with site specific linkage via the C13 moiety of ADR (Fig. 4C)

(i) Oxidation of dextran and loading with glutaric acid dihydrazide. Dextran T- 40 was dissolved in distilled water (200 ml) and NaIO4 (0.47 g) was added. The solution was stirred at 25°C for 2 hr and then concentrated (Amicon YM-30). The concentrated product was dialysed exhaustively against distilled water and lyophilized to obtain 542 mg of the desired product. One half of the amount was dissolved in acetate buffer pH 4.5 (50 ml), glutaric acid dihydrazide (230 mg) was added and stirred overnight at room temperature. The formed hydrazone bond was stabilized with 0.05 M sodium cyanoborohydride and the small compounds were dialysed off against PBS.

(ii) Coupling to IgG and loading the carrier with ADR. A four-fold molar excess of modified dextran was reacted with oxidized IgG, which was prepared as described in Method 9.1, at 4°C in 0.1 M acetate buffer (pH 4.5) overnight. The formed bond was then stabilized with 0.05 M sodium cyanoborohydride, and the material was dialysed

exhaustively using Spectropor 6 tubing (cut-off level: 40,000). ADR · HCl (2.9 mg) was added to Dex -IgG (5.0 mg/ml) and stirred overnight. The pH was adjusted to 7.8 and the conjugate was dialysed (Spectropor 6 tubing) against 0.01 M PBS (pH 7.2). The final molar incorporation was 25: 1.2 : 1 (ADR /Dex/ IgG, mol/mol / mol).

(b) ADR-Dex-B02 (nss), a conjugate with non site-specific linkage via the amino sugar group of ADR (Fig. 4D)

ADR · HCl (10 mg) was added to the oxidized dextran (10 mg) dissolved in PBS and the mixture was stirred overnight. The pH was adjusted to 7.8 and the conjugate was desalted on a Sephadex G-25 column . Coupling with Dal B02 (10 mg/ml) in PBS was carried out at 4°C overnight and the bonds formed were stabilized by incubation for 4 h with sodium cyanoborohydride (0.05 M) in acetate buffer (pH 4.5). The pH was then adjusted to 7.8 and the conjugate was dialysed against PBS (Spectropor 6). The final molar incorporation was 41: 1.8 : 1 (ADR /Dex/ IgG, mol/mol/mol).

10.2 Retention of antibody activity in Dal B01-ADR and Dal B02-ADR conjugates

(A) Indirect immunofluorescence

Membrane immunofluorescence staining was routinely used to determine the retention of antibody activity after conjugation to drugs. The procedure was carried out as described before (see Method 1.6).

(B) Radioimmunoassay (RIA)

For Dal B02-Dex-ADR conjugates, a competition assay was used to determine the retention of antibody activity. To a test tube containing 5×10^5 D10-1 cells and 0.5 µg/ml ^{125}I-labeled Dal B02, various concentrations of cold unmodified Dal B02 or Dal B02-Dex-ADR

conjugates (either site-specific or non-site specific one) were added. The incubation was carried out at 4°C for 90 min after which the cells were washed 4 times with cold PBS. The cell-associated radioactivity was determined using a gamma counter. The inhibition of binding of ^{125}I-labeled Dal B02 to D10-1 cells by conjugates or the unmodified Dal B02 was compared.

10.3 Determination of cytotoxicity of Dal B01-ADR and Dal B02-ADR conjugates

The cytotoxicity of Dal B01-ADR and Dal B02-ADR conjugates was determined following the method described in Method 9.4 with the following modifications: (i) in continuous exposure assay, the cells were incubated with ADR, either free or conjugated to MoAbs, for 48 hr before the cells were counted; and (ii) in pulse exposure assay, the cells were pulse exposed to ADR, either free or conjugated to MoAbs, for 6 or 3 hr, and then incubated in fresh medium for an additional 48 hr.

10.3 The pharmacokinetics and biodistribution of Dal B02-Dex-ADR (ss) conjugate in D10-1 xenograft bearing nude mice

Both Dal B02 and Dal B02-Dex-ADR (ss) conjugate were labeled with ^{131}I using chloramine T. To ascertain that there was no release of free ADR from Dal B02-Dex-ADR (ss) conjugate during the iodination process, the reaction was monitored by TLC assay. Aliquot of samples was obtained before the addition of chloramine T, after 2 min incubation with chloramine T (before the purification of radioiodinated Dal B02-Dex-ADR (ss) conjugate) and after purification using a NAP-10 column to remove free iodine and chemicals of small molecule. The samples were spotted on a silica gel TLC plate and eluted with CHCl$_3$/MeOH/AcOH (7/3/1.5, v/v). Free ADR and the mixture of free ADR and Dal B02 were used as positive control preparations. The IRF and immunoreactivity of the Dal

B02-Dex-ADR (ss) conjugate after radioiodination were determined using D10-1 cells as described in Methods 5.3 and 5.4.

D10-1 xenograft bearing nude mice (see Method 7.1 for the production of the tumor model) were given either ^{131}I-Dal B02-Dex-ADR (ss) conjugate or ^{131}I-Dal B02, mixed with ^{125}I labeled non-specific IgG1. The pharmacokinetic and biodistribution studies of the conjugate was carried out as described in Methods 7.2, 7.3 and 7.4).

10.4 Treatment of D10-1 xenograft bearing nude mice with Dal B02-Dex-ADR (ss) conjugate

Before the initiation of treatment of D10-1 xenograft bearing nude mice, a series of experiments were carried out to determine the optimal dose, optimal schedule and route of administration of either free ADR or Dal B02-Dex-ADR (ss) conjugate (see Results section 5.5 for detailed description of the experiments).

Treatment started at about 10 days after D10-1 cell inoculation in nude mice when the tumor volume reached approximately of 60 to 200 mm^3. Each treatment group consisted of 4 to 5 tumor bearing nude mice. All injections were given via the i.v. route. The tumors were measured twice a week, and the tumor volume was calculated according to the equation:

$$V = L \times W^2 \times 1/2$$

where V = tumor volume (mm^3), L = measurement of the longest axis (mm), and W = measurement of axis perpendicular to L (mm).

Fig. 4

Synthetic schemes showing the synthesis of different types of MoAb-ADR conjugates.

Fig. 4A Synthesis of Dal B01-CAA-ADR and Dal B02-CAA-ADR conjugates. ADR was linked to Dal B01 or Dal B02 via its amino sugar group using an amide bond.

Fig. 4B Synthesis of Dal B01-C13-ADR and Dal B02-C13-ADR conjugates. ADR was linked to Dal B01 or Dal B02 via its C13 moiety using a hydrazone bond.

Fig. 4C Synthesis of Dal B02-Dex-ADR (ss) conjugate using Dextran T-40 as an intermediate carrier. Dex was first linked to Dal B02 site-specifically via the carbohydrate residues of IgG using a hydrazone bond. After reduction by sodium cyanoborohydride, the Dal B02-Dex binary conjugate was loaded with ADR via the C13 moiety of the drug using a hydrazone bond.

Fig. 4D Synthesis of Dal B02-Dex-ADR (nss) conjugate using Dextran T-40 as an intermediate carrier. ADR was first linked to Dex via its amino sugar group. The Dex-ADR binary conjugate was then linked to Dal B02 randomly using a Schiff's base bond. The Schiff's bases formed were reduced with sodium cyanoborohydride.

Fig. 4A

(1) ADR   (2) CAA   (3) ADR-CAA

(4) IgG   (5) IgG-CAA-ADR

Fig. 4B

(1)

(2)

(3)

(4)

(5)

(6)

DTT

(7)

(8)

(1) ADR   (2) HPDP

(3) ADR-hydrazide   (4) IgG

(5) SPDP   (6) IgG-SPDP

(7) IgG-SH   (8) IgG-C13-ADR

Fig. 4C

(1) Dextran T-40

(2) Oxidised T-40

(3) Glutaric acid dihydrazide

(4) Dextran T-40 dihydrazide

(5) IgG

(6) Oxidised IgG

(7) ADR

(8) IgG-Dex binary conjugate

(9) IgG-Dex-ADR (ss) conjugate

Fig. 4D

(1)

NaIO4

(2)

+

ADR - NH2

(3)

(4)

+

OR

(5)

(6)

(1) Dextran T-40   (2) Oxidised dextran T-40   (3) Dextran - ADR binary conjugate

(5) IgG   (6) IgG-Dex-ADR (nss) conjugate

11. Establishment of Human B-cell CLL in Immunodeficient Nude and SCID Mice

11.1 Growth of D10-1 cells in nude o. SCID mice after i.p. or i.v.inoculation

For the i.p. model, all the nude and SCID mice were primed i.p. with 0.5 ml/mouse of pristane followed after two weeks by a second i.p. injection of 0.3 ml of pristane. One week after the second pristane injection, mice were given 5 x 10^6 D10-1 cells i.p.. For the i.v.model, mice were given the same number of D10-1 cells via a lateral tail veir All nude mice received 400 rad TBI 48 to 72 hr before tumor inoculation.

11.2 Autopsy and histological examination of tissues from tumor-bearing mice

All mice were observed daily for the appearance of ascites or solid tumors. Mice with advanced tumors were sacrificed at the terminal stage. Autopsy was performed on every mouse. Peripheral blood leukocytes were counted with a hematocytometer. The smears of peripheral blood were stained with Wright's stain and differential counts were performed. Ascites tumor cells were collected under sterile conditions. Solid tumors were excised under sterile conditions and single cell suspensions were obtained by mechanic teasing without the use of any enzyme. Tumor cells harvested from either ascites or solid tumors were grown in RPMI 1640 medium and used for cytogenetic study, immunofluorescence assay and evaluation of chemosensitivity. Organs and tumors were fixed in 10 volumes of 10% formaldehyde. The tissues were dehydrated through graded alcohol and xylene and embedded in paraffin. Five μm sections were cut and stained with H & E and examined under an optical microscope (All sections were cut and stained by Ms. Dean Shirley, Department of Pathology, Dalhousie University).

11.3 Cytogenetic study of tumor cells obtained from the ascites or solid tumors in D10-1 inoculated nude mice

This part of work was done by Dr. C.L.Y. Lee, Department of Pathology, Dalhousie University, Halifax, NS.

Chromosomal analysis of tumor cells harvested from ascites and solid tumors, as well as their parental D10-1 cells, was carried out following the method described by Ghose et al. (1988b). Briefly, for harvesting metaphases, aliquots of dissociated cells were first exposed to Colcemind (0.05 μg/ml) for approximately 2 hr and then to a 0.075 M KCl solution for 20 min. The cells were fixed in 3 changes of a 3:1 mixture of absolute methanol and acetic acid, air dried and stained with a G banding procedure described by Lee et al. (1972). Well spread metaphases (a minimum of 30 cells/specimen) were located on slides under low power (x 16) and analyzed at a magnification of x 100.

11.4 In vitro characterization of tumor cells harvested from ascites or solid tumors in D10-1 cell inoculated nude or SCID mice

(A) Membrane staining with MoAbs against D10-1 cell surface associated antigen and FITC labeled goat anti-human Ig λ light chain antibodies

Immunofluorescence assay using two MoAbs directed against D10-1 surface antigens, i.e., Dal B01 and Dal B02, was performed on parent D10-1 cells, tumor cells harvested from ascites and solid tumors of D10-1 cell inoculated nude or SCID mice. These tumor cells, as well as bone marrow and splenic cells from tumor-bearing mice were also stained directly with FITC-labeled goat anti-human Ig λ light chain antibodies for the detection of D10-1 cells that are known to express cell surface Ig λ light chain.

[

(B) In vitro doubling time and chemosensitivity of tumor cells obtained from ascites or solid tumors in D_{10-1} cell inoculated nude mice

The population doubling times of parent D_{10-1} cells, tumor cells recovered from ascites and solid tumors were derived from the semi-log plot of cells growing in the exponential phase as described in Method 2.2. The chemosensitivity of tumor cells to MTX and ADR were determined as described in Methods 9.4.

12. Targeted Radioimmunotherapy of D_{10-1} Xenografts by ^{131}I-labeled Dal B02 or Its F(ab)'2 Fragment

Nude mice or SCID mice that had received D_{10-1} cells via i.p. injection were treated using the i.p. route, and mice that had received tumor cells s.c. or i.v.were treated using the i.v.route.

12.1 Targeted radioimmunotherapy of human B-cell CLL s.c. xenograft in nude mice with ^{131}I labeled intact Dal B02 and ^{131}I labeled Dal B02 F(ab)'2 fragment

In this study, nude mice were inoculated s.c. with 5×10^6 D_{10-1} cells. The treatment was given at about 10 days after D_{10-1} cell inoculation when the tumor reached a volume of approximately 60 to 200 mm^3. Groups of 4 mice were given two injections of either ^{131}I labeled intact Dal B02 (15 days apart) or ^{131}I labeled Dal B02 F(ab)'2 fragment (4 days apart). Each injection consisted of 50 μg of Dal B02 labeled with 300 μCi of ^{131}I or 100 μg of Dal B02 F(ab)'2 fragment labeled with 500 μCi of ^{131}I. Controls included groups of mice given PBS, or unlabeled Dal B02, or ^{131}I labeled non-specific IgG_1, or unlabeled Dal B02 mixed with ^{131}I labeled non-specific IgG_1. The total body radioactivity of each mouse

was monitored at defined intervals. The tumors were measured twice a week and the tumor volume was calculated as described in Method 10.4.

12.2 Targeted radioimmunotherapy of human B-cell CLL i.p. and i.v. models in nude or SCID mice with ^{131}I labeled intact Dal B02

In the first experiment, nude or SCID mice that had received 5×10^6 D$_{10\text{-}1}$ cells, i.p or i.v., were treated with one injection of 50 μg of Dal B02 or a nonspecific IgG$_1$, either alone or radiolabeled with 300 μCi ^{131}I, 48 to 72 hr after tumor cell inoculation.

In the second experiment, nude mice were injected i.p. with 15×10^6 D$_{10\text{-}1}$ cells and treated with one injection of either different amounts of non-labeled Dal B02, i.e., 50 μg, 150 μg and 500 μg, or 50 μg of ^{131}I-labeled Dal B02 (300 μCi), 48 to 72 hr after tumor cell inoculation.

In the third experiment, nude mice were injected i.v. with 5×10^6 D$_{10\text{-}1}$ cells. The treatment was given 7 days after tumor cell inoculation and consisted of one injection of 50 μg of Dal B02, either alone or labeled with 300 μCi ^{131}I.

12.3 Targeted immunotherapy of human B-cell CLL i.p. and i.v. models in nude mice with ^{131}I labeled Dal B02 F(ab)'$_2$ fragment

Nude mice were given 5×10^6 D$_{10\text{-}1}$ cells via either i.p. or i.v. injection. In one study, the treatment was given at 48 to 72 hr after tumor cell inoculation with one injection of 100 μg of Dal B02 F(ab)'$_2$ fragment, either alone or labeled with 500 μCi ^{131}I. In another study, all the mice were given a second injection of 100 μg of Dal B02 F(ab)'$_2$ fragment, alone or labeled with 500 μCi ^{131}I, 4 or 7 days after the first treatment.

12.3 Experimental observation and statistical studies

In all studies described above, control groups were treated with PBS alone. All the mice were given Lugol's iodine containing water starting from 72 hr prior to the administration of radioiodinated MoAbs. The sawdust in the cages which housed the treated mice were changed twice during the first 24 hr and every day thereafter. The mice were kept isolated and monitored for total body radioactivity, the appearance of ascites or solid tumors and survival. Estimates of survival were calculated by the Kaplan-Meier product limit method and difference were tested by the logrank test (Kaplan P and Meier, 1958).

13. Inhibition of Intraperitoneal Human Renal Cell Carcinoma Xenograft in Nude Mice with A Heteroconjugate (K29-OKT3) Reacting with Human Renal Cell Carcinoma and T-Cell Receptor Complex CD3

13.1 Construction of K29-OKT3 heteroconjugate

The heteroconjugate was prepared by Dr. L. Kerr et al. in the Department of Immunology, Mayo Clinic, Rochester, MN. Briefly, both Dal K29 (a MoAb directed against human renal cell carcinoma, produced in Dr. Ghose's laboratory, Department of Pathology, Dalhousie University, Halifax, NS) (Luner et al., 1986) and OKT3 were dialyzed against 0.1 M potassium phosphate containing 0.1 M NaCl (pH 7.5), and incubated separately for 2 hr at room temperature with four-fold molar excess of SPDP. The Dal K29 was dialyzed against the coupling buffer and OKT3 was dialyzed against 0.1 M sodium acetate, 0.1 M NaCl, pH 4.5. DTT was then added to OKT3 to a final concentration of 0.02 M. After 30 min at room temperature, the OKT3 was passed through a Sephadex G-25 PD-10 column equilibrated with coupling buffer, and immediately added to Dal K29 antibody. After 4 hr

incubation at room temperature, 1.0 mg of iodoacetamide was added and the antibody dimers (m.w. 300, 000) and larger heteroconjugates (m.w. 600, 000 to one million) were separated from monomeric IgG on a Sephacryl HR-300 gel filtration column (2 x 100 cm). Purity and m.w. of pooled peaks were evaluated by analyzing fractions on SDS-PAGE. In vitro studies had demonstrated that the heteroconjugate was capable of mediating a high level of killing of tumor cells in the presence of PBL or tumor infiltrating lymphocytes (TIL) from renal cell carcinoma patients (Kerr et al., 1990).

13.2 Assay for dual specificities of heteroconjugate K29-OKT3

(A) Immunofluorescence assay

The membrane staining of target or non-target cells by Dal K29, OKT3 and K29-OKT3 heteroconjugate was determined using Nu-caki-1, MOLT-3, D10-1 cell lines and fresh human T lymphocytes. The experimental procedure was described in Methods 1.6.

(B) FACS assay

One million cells (Nu-caki-1, MOLT-3, D10-1 or human T cells) in 100 µl PBS were put in each test tube and incubated at 4°C for 60 min with different concentrations of either Dal K29 or K29-OKT3 heteroconjugate (from 0.32 to 80 µg/ml). The cells were washed 3 times with cold PBS and then incubated with 35 µl FITC labeled rabbit anti-mouse IgG for an additional 30 min. The cells were washed another 3 times and resuspended in 1.0 ml cold PBS and analyzed with a fluorescence activated cell sorter (FACS III). The percentage of fluorescence-positive cells was then determined (This work was done with the help of Dr.S.H.S.Lee, Department of Microbiology and Immunology, Dalhousie University, Halifax, NS).

(C) Rosette formation assay

One million Nu-caki-1 cells were incubated with K29-OKT3 heteroconjugate (20 µg/ml) for 60 min at 4°C. After washing 3 times with cold PBS, either human T cells or D10-1 cells were added and the cell mixtures were incubated at 4°C for an additional 60 min. Smears of cell suspensions were examined under an optical microscope.

13.3 Determination of reactivity of Dal K29 and K29-OKT3 heteroconjugate by ELISA

Nu-caki-1 cells (3×10^5) in 200 µl MEN medium were grown in a 96 well cell culture plate for 3 days after which the cells were washed 3 times with DPBS and fixed with 0.5% glutaraldehyde for 3 min at room temperature. The cells were washed another 3 times with DPBS and incubated with different concentrations (from 0.04 to 10 µg / ml) of either Dal K29 or K29-OKT3 heteroconjugate for 90 min. After washing away the unbound antibodies with PBS containing 0.05% Tween-20 , 100 µl of goat anti-mouse IgG-HRP conjugate (Sigma, 1:3000 dilution) was added and incubated with the cells for an additional 90 min. The cells were then washed another 3 times and 100 µl substrate solution (OPD along with hydrogen peroxide in substrate buffer) was added. The reaction was stopped by 2.5 M H_2SO_4 and the absorption at 493 nm was measured with a Micro ELISA auto reader.

13.4 Subclass determination

The procedure was basically the same as described above for ELISA except that after the cells were incubated with either Dal K29 or K29-OKT3 heteroconjugate (20 µg / ml) and washed 4 times with PBS, the cells were then incubated with GAM Ig subclass antibody-HRP conjugates (i.e. IgG1, IgG2a, IgG2b, IgG3, IgA, IgE, IgM, and κ and λ light chains, respectively). The latter procedure was carried out as described above.

13.5 Biodistribution of Dal K29 or K29-OKT3 heteroconjugate in Nu-caki-1 tumor-bearing nude mice

(A) S.c xenograft of Nu-caki-1 tumor in nude mice

Nu-caki-1 cells were grown in MEN medium and harvested using 0.02% trypsin solution and then washed 2 times with HBSS. Each nude mouse received 10 x 10^6 Nu-caki-1 cells (in 0.2 ml HBSS) s.c.. Usually, 100% of mice grew s.c.tumor within 2 weeks.

(B) Radioiodination of Dal K29 or K29-OKT3 heteroconjugate

K29 or K29-OKT3 heteroconjugate was iodinated with ^{131}I using the Chloramine-T . The specific activity for the antibodies ranged from 2.0 to 2.5 µCi /µg protein. The IRF and target cell binding ability of radioiodinated antibodies were determined as described before in Methods 5.3 to 5.5.

(C) Injection of Nu-caki-1 xenograft bearing nude mice with radioiodinated antibodies

The pharmacokinetic and biodistribution study of radiolabeled Dal K29 or K29-OKT3 in tumor-bearing mice were carried out as described before (Methods 7.2 to 7.4.). Ten µg protein (about 20 to 25 µCi of ^{131}I) of either Dal K29 or K29-OKT3 heteroconjugate was injected into each mouse via tail vein. Ten µl of blood samples were taken out from each mouse at different intervals and the radioactivity was determined. At 24, 48, 96 and 168 hr after antibody administration, three mice from each group were sacrificed. Tumors and mouse organs were taken out and the organ or tumor-associated radioactivity was determined. The % ID / g tissue and T / NT ratios were then calculated (the decay of ^{131}I was corrected using a ^{131}I standard).

To examine the possible breakdown of the Dal K29 or K29-OKT3 heteroconjugate in circulation and mouse tissues, samples of mouse organs (including tumor, liver, spleen, kidney and thyroid) were taken out, homogenized and centrifuged at 600 x g for 15 min. The supernatants were precipitated with 10% TCA and centrifuged at 12,000 x g for 30 min. The radioactivity in precipitates or supernatants was then determined.

(D) The stability and IRF of Dal K29 or K29-OKT3 heteroconjugate recovered from the serum of tumor-bearing mice

The serum from tumor-bearing mice injected with radiolabled Dal K29 or K29-OKT3 were obtained at 24, 48, 96 and 168 hr after antibody administration. The stability and IRF of antibodies in the serum were determined as described in Method 7.6.

(E) Autoradiography of Nu-caki-1 tumor tissues after i.v. administration of ^{131}I labeled Dal K29 or K29-OKT3 heteroconjugate

The Nu-caki-1 tumors in nude mice were taken out at 48 and 96 hr after administration of radiolabeled Dal K29 or K29-OKT3 heteroconjugate. Autoradiography of tumor tissues was carried out as described in Method 7.7.

13.6 Therapy of intraperitoneal Nu-caki-1 xenograft in nude mice with K29-OKT3 heteroconjugate and human PBL cells

(A) Nu-caki-1 ascites tumors in nude mice

Nude mice were primed with two injections of pristane i.p. (two weeks apart). One week after the second pristane injection, each mouse received 3 to 5 x 10^6 Nu-caki-1 cells i.p.. Usually, 100% of nude mice developed ascites tumor within 2 to 3 weeks.

(B) Immunotherapy with K29-OKT3 heteroconjugate and human PBL

Treatment started 24 hr after tumor cell inoculation. Each mouse was given 30 μg of heteroconjugate mixed with different numbers of freshly isolated human PBL. Two different ratios of effector cells to tumor cells (E/T ratio) were used, i.e., 3 to 1 or 10 to 1. The mice in control groups received PBS, equal amount of K29-OKT3 heteroconjugate alone, or equal amount of mixture of Dal K29 and OKT3 plus PBL (E/T ratio, 10 to 1). The mice were monitored daily for the development of ascites and survival. Estimates of survival were calculated by the Kaplan-Meier product limit method and difference were tested by the logrank test (Kaplan and Meier, 1958).

RESULTS

Section 1 Production and Characterization of Dal B01, Dal B02 and Their F(ab)'₂ Fragments

1.1 Production and Purification of Dal B01 and Dal B02

All BALB/c mice developed ascites 10 to 15 days after i. p. inoculation of hybridoma cells. A mean of 2.5 ml (range from 1 to 5 ml) of ascites fluid was obtained from each mouse at the time of tapping. The two MoAbs were isolated from other contaminating proteins in the ascites fluid, using Protein A chromatography for Dal B01, an IgG2a, and caprylic acid precipitation for Dal B02, an IgG1. The yield of purified MoAb per ml of Dal B01 ascites fluid ranged from 0.5 to 1.0 mg/ml, whereas for Dal B02 ascites fluid the range was from 5.0 to 7.0 mg/ml. After purification, SDS-PAGE analysis under non-reducing conditions of both MoAbs yielded a single band with a molecular weight of approximately 150, 000 kD (Fig. 5).

1.2 Preparation of F(ab)'₂ Fragments of Dal B01 and Dal B02

F(ab)'₂ fragments of Dal B01 and Dal B02 were obtained by peptic digestion. Preliminary experiments were carried out to determine the time needed for complete digestion of Dal B01 or Dal B02 at different pH conditions. A ratio of pepsin : protein of 1 : 40 (w/w) was used in all the digestion mixtures. The digestion process was terminated by raising the pH of the mixtures to 8.6 by the addition of an equal volume of 0.6 M Tris buffer. SDS-PAGE analysis of aliquots taken at different intervals during peptic digestion showed that the time needed for complete digestion were different for the two MoAbs, and varied with the pH of the digestion mixture. For example, Dal B01 was fully digested after incubation for 3 hr at pH 3.7, or 4 hr at pH 3.8, or 6 hr at pH 4.0 (Fig. 6), but the complete digestion of Dal B02 took 6 hr at pH 3.7 (Fig. 7). The F(ab)'₂ fragments were purified from the digestion

mixture by chromatography using a Sephacryl S-200 column. Two peaks were eluted out from the column (Figs. 8A and 8B). The first peak represented the F(ab)'2 fragments while the second peak represented the breakdown low molecular weight fragments. The fractions containing the F(ab)'2 fragment were pooled and the protein concentration was determined. SDS-P/\GE analysis of the fractions containing F(ab)'2 fragments showed a single protein band with molecular weight of approximately 110, 000 kD, indicating the success of separation (Fig. 9). The yields of F(ab)'2 fragments from Dal B01 and Dal B02 in this experiment were about 54.3% and 60.8% of the starting amount of intact MoAbs, respectively. This is approximately 74.1% (for Dal B01) and 82.9% (for Dal B02) of the theoretical maximum yield.

1.3   Interaction of Dal B01, Dal B02 and Their F(ab)'2 Fragments with D10-1 cells

1.3.1   Membrane immunofluorescence

Both Dal B01, Dal B02 and their respective F(ab)'2 fragments bound to 100% of viable D10-1 cells. The titers were 0.3 μg/ml for Dal B01, 0.4 μg/ml for Dal B01 F(ab)'2 fragment, 0.1 μg/ml for Dal B02 and 0.3 μg/ml for Dal B02 F(ab)'2 fragment. The two MoAbs and their F(ab)'2 fragments did not bind to MOLT-3, K562 and M21 cells.

1.3.2   Binding of Dal B01 and Dal B02 to D10-1 cells and the induction of caps

After D10-1 cells were incubated with either Dal B01 or Dal B02 at 5 μg antibody / ml at 4°C for 30 min, staining with FITC-labeled GAM-IgG showed that fluorescence was evenly distributed on the cell surface. When the antibody-coated cells were incubated at 37°C, the distribution of membrane fluorescence became increasingly uneven. "Patching"

was observed in a large proportion of cells after 60 min incubation at 37°C. However, only a small proportion of cells showed "capping" (Fig. 10). Table 3 presents the percentage of cells that formed caps at various times after incubation with Dal B01 or Dal B02 at 37°C. There was no difference in the proportion of D10-1 cells that showed caps or the time needed to induce caps after exposure of D10-1 cells at 37°C to either Dal B01 or Dal B02 antibody.

1.4 Radioiodination of Dal B01, Dal B02 and Their F(ab)'2 Fragments

Dal B01, Dal B02 and their F(ab)'2 fragments were radiolabeled with ^{125}I for the determination of specificity and Ka of binding of the MoAbs to target D10-1 cells, the number of binding sites available per cell and the immunoreactive fraction (IRF) of the radioiodinated MoAb preparations. Studies were first carried out to determine the optimal conditions for radioiodination of the Dal B01, Dal B02 and their F(ab)'2 fragments using the chloramine T method.

1.4.1 The effect of the length of exposure of Dal B02 to chloramine T on the iodine incorporation and the IRF of the radioiodinated Dal B02

In this experiment, a given amount of Dal B02 was incubated with a constant amount of radioactive ^{125}I and chloramine T at room temperature. At different intervals, the reaction was stopped by the addition of sodium metabisulfate, and the radiolabeled protein was purified using a NAP-10 column. The iodine incorporation and the IRF of labeled Dal B02 were then determined. Results showed that after 2 min, the IRF of labeled Dal B02 decreased with the duration of exposure to chloramine T (Table 4). For example, the IRF of Dal B02 decreased from 66% to 33% when the duration of exposure of the antibody to

Fig. 5

Photograph of SDS PAGE of Dal B01 or Dal B02-containing ascites fluids, Dal B01 purified by protein-A chromatography, Dal B02 purified by caprylic acid precipitation, non-specific myeloma derived IgG1. See Materials and Methods for detailed descriptions of the purification procedures.

Lane 1 Ascites fluid of Dal B01

Lane 2 Purified Dal B01 under non-reducing condition

Lane 3 Purified Dal B01 under reducing condition

(picture shows the band of heave chain only)

Lane 4 Ascites fluid of Dal B02

Lane 5 Purified Dal B02 under non-reducing condition

Lane 6 Purified Dal B02 under reducing condition

(picture shows the band of heave chain only)

Lane 7 Ascites fluid of non-specific IgG1

Lane 8 Purified non-specific IgG1 under non-reducing condition

Lane 9 Purified non-specific IgG1 under reducing condition

(picture shows the band of heave chain only)

Fig. 5
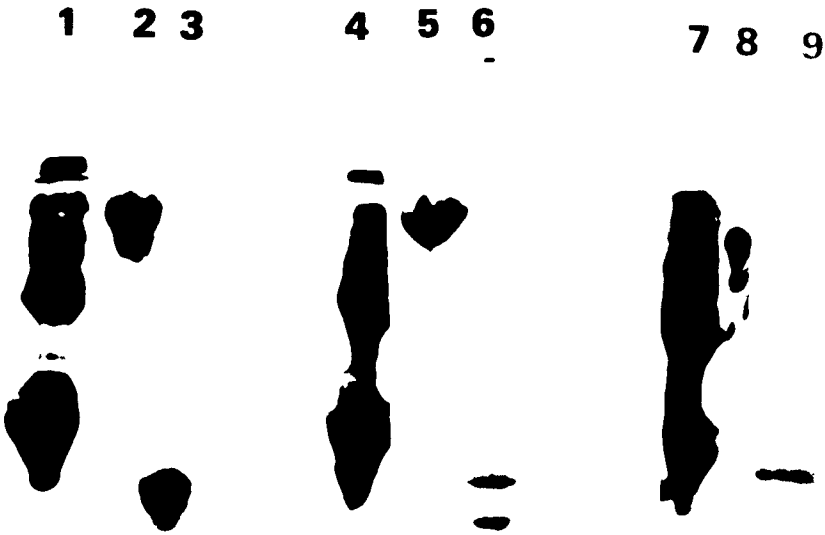
Fig. 6

Determination of the optimal conditions for the preparation of Dal B01 F(ab)'2 fragments.

Dal B01 was incubated with pepsin (1 : 40, w/w) at 37°C and under different pH conditions. Aliquots were taken out at different intervals and subjected to SDS-PAGE. Lanes 3 to 16 show the progressive digestion of Dal B01 with time at all the three different pH conditions. Note that the proportion of intact antibody decreased as the proportion of F(ab)'2 fragment increased with time. After incubation for 3 hr at pH 3.7 (Lane 6), 4 hr at pH 3.8 (Lane 11) and 6 hr at pH 4.0 (Lane 16), all the intact antibody was digested to F(ab)'2 fragment.

Lane 1	Dal B01	Lane 2	Dal B01 under reducing condition
			(picture shows the band of heave chain only)
Lanes 3 - 6	pH 3.7		
Lane 3	0.5 hr	Lane 4	1.0 hr
Lane 5	2.0 hr	Lane 6	3.0 hr
Lanes 7-11	pH 3.8		
Lane 7	0.5 hr	Lane 8	1.0 hr
Lane 9	2.0 hr	Lane 10	3.0 hr
Lane 11	4.0 hr		
Lanes 12-16	pH 4.0		
Lane 12	0.5 hr	Lane 13	1.0 hr
Lane 14	2.0 hr	Lane 15	4.0 hr
Lane 16	6.0 hr		

Fig. 6
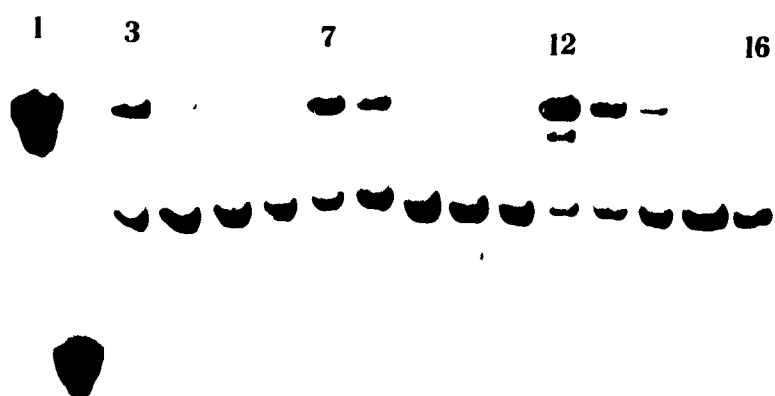
Fig. 7

Determination of the optimal conditions for the preparation of Dal B02 F(ab)'2 fragments.

Dal B02 was incubated with pepsin (1 : 40, w/w) at 37°C at pH 3.7. Aliquots were taken out at different intervals and subjected to SDS-PAGE. Lanes 2 to 8 show the progressive digestion of Dal B02 with time. Note that the proportion of intact antibody decreased as the proportion of F(ab)'2 fragment increased with time. At 6 ° (Lane 8), all the intact antibody was digested to F(ab)'2 fragment.

Lane 1	Dal B02
Lane 2	0.5 hr
Lane 3	1.0 hr
Lane 4	2.0 hr
Lane 5	3.0 hr
Lane 6	4.0 hr
Lane 7	5.0 hr
Lane 8	6.0 hr

Fig. 7
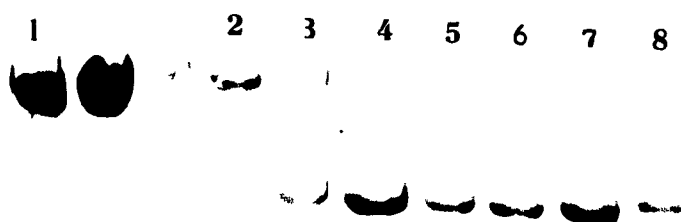
Fig. 8

Elution profiles of the products of digestion mixtures of Dal B01 or Dal B02 and pepsin after chromatography using a Sephacryl S-200 (1.6 x 90 cm) column.

Dal B01 or Dal B02 was digested with pepsin (1 : 40, w/w) at pH 3.7 for 3 or 6 hr, respectively. The digestion mixtures were then loaded on the column and eluted with 0.01 M PBS. Fractions of 3.0 ml each were collected and the O.D. of each fraction was measured at 280 nm. Two peaks were obtained after elution. Peak 1 represents the F(ab)'2 fragments while peak 2 represents the smaller fragments. Fractions in peak 1 were pooled and the protein concentration was determined by Lowry's method.

Fig. 8A   Elution profile of the products of digestion of a mixture of Dal B01 and pepsin.

Fig. 8B   Elution profile of the products of digestion of a mixture of Dal B02 and pepsin.

Fig. 8A
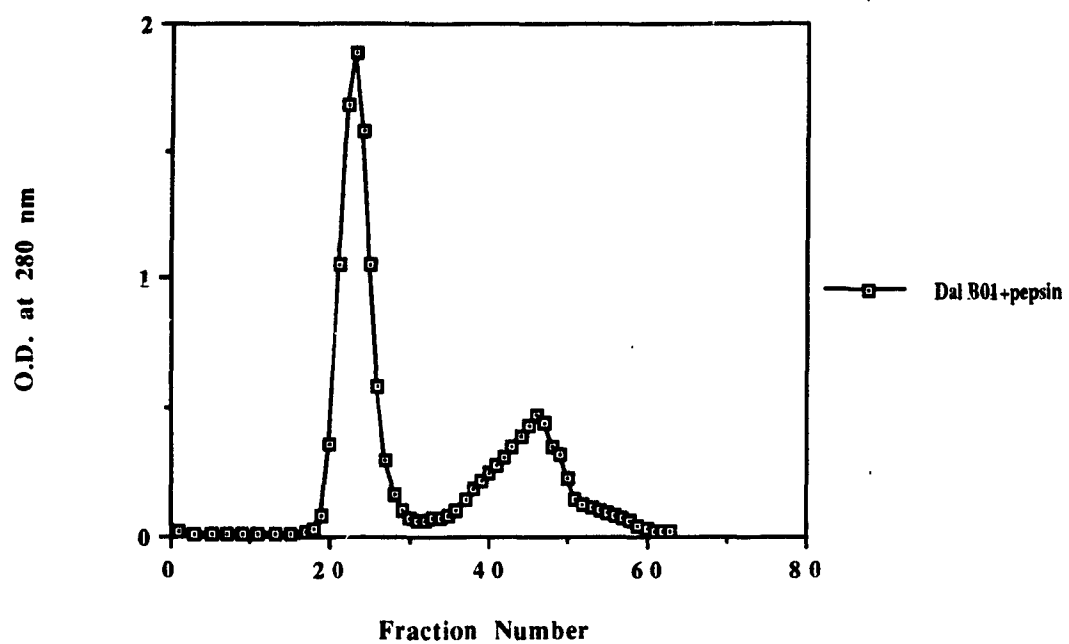
Fig. 8B
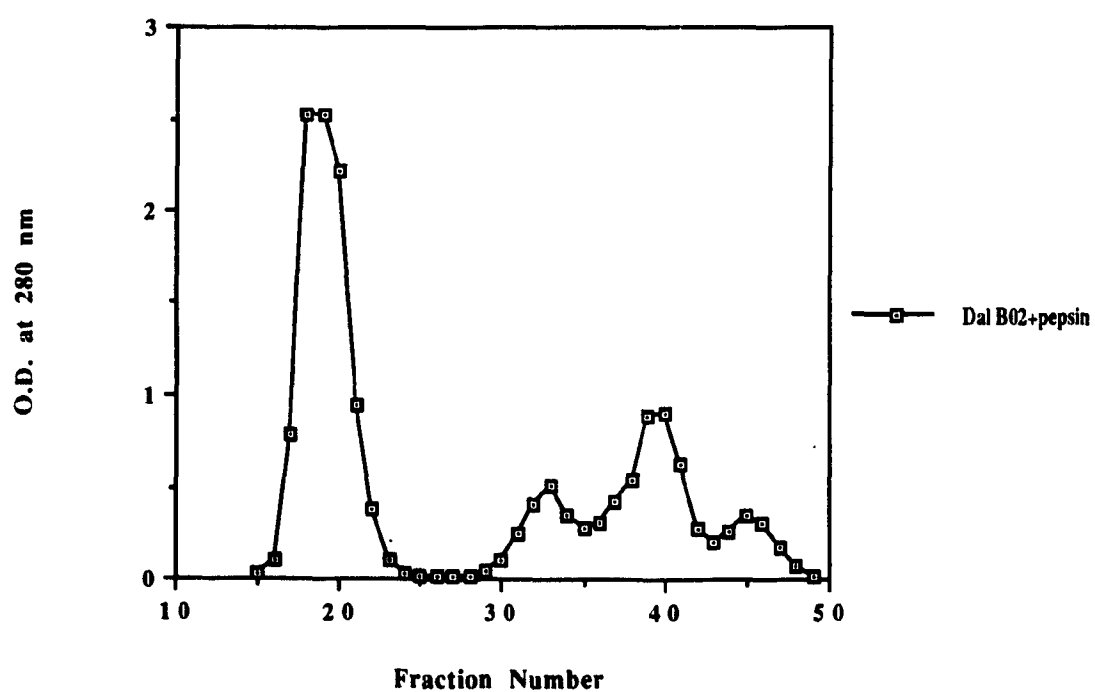
Fig. 9

SDS-PAGE analysis of pooled peak 1 fractions obtained from Dal B01 and Dal B02 preparations after the " optimal " peptic digestion.

MoAbs were digested by incubation with pepsin (40 to 1, w/w) at 37°C under optimal conditions (i.e., pH and duration) as shown in Figs. 7 and 8. The F(ab)'2 fragments were purified from digestion mixtures by gel chromatography using a Sephacryl S-200 columnm.

Lane 1	Dal B02
Lane 2	Dal B02 under reducing condition
	(picture shows the band of heave chain only)
Lane 3	Digestion mixture of Dal B02 and pepsin
Lane 4	Purified Dal B02 F(ab)'2 fragment
Lane 5	Dal B01
Lane 6	Dal B01 under reducing condition
	(picture shows the band of heave chain only)
Lane 7	Digestion mixture of Dal B01 and pepsin
Lane 8	Purified Dal B01 F(ab)'2 fragment

Fig. 9
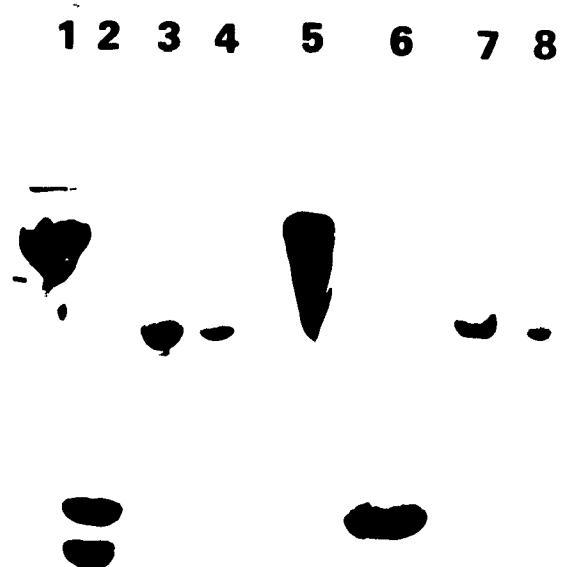
Fig. 10

Immunofluorescence photomicrographs showing membrane staining of D10-1 cells after incubation with Dal B01 or Dal B02 at 37°C for 4 hr.

D10-1 cells were incubated with either Dal B01 or Dal B02 at a concentration of 5.0 μg MoAb protein per ml medium for 30 min at 4°C. The cells were washed thrice with cold PBS and reincubated at 37°C for various periods of time. At intervals of 0, 0.5 hr, 1 hr, 2 hr and 6 hr, aliquots of cells were taken out and stained with FITC labeled GAM-IgG for 30 min. After another 3 washes with PBS, cell smears were made and examined with an immunofluorescence microscope.

(A) Immunofluorescence staining of D10-1 cells after exposure to Dal B01 for 4 hr at 37°C.

(B) and (C) Immunofluorescence staining of D10-1 cells after exposure to Dal B02 for 4 hr at 37°C.

Arrows indicate caps on D10-1 cells.

Fig. 10

a

b
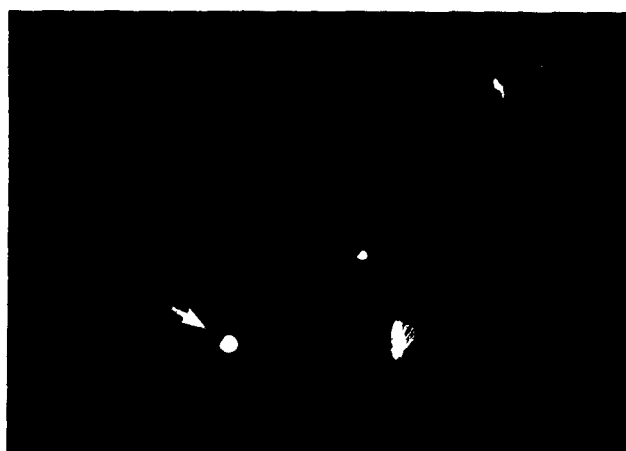
c

Table 3 **The percentages of D₁₀-₁ cells that showed caps after incubation with Dal B01 or Dal B02 at 37°C for different durations** [1]

Time (hr)	0	0.5	1.0	2.0	4.0	6.0
Dal B01 [2]	0	0	3 [3]	6	6	5
Dal B02	0	4	3	8	7	9

1. D₁₀-₁ cells were coated with Dal B01 or Dal B02 at 4°C for 30 min after which the cells were incubated at 37°C for various periods of time. At indicated intervals, aliquots of cells were taken out and stained with FITC-labeled GAM-IgG and examined with an immunofluorescence microscope.

2. Antibody concentration used was 5.0 µg/ml of either Dal B01 or Dal B02.

3. All data represent the mean of the results obtained from two separate experiments. At least 200 cells were examined in each experiment.

chloramine T increased from 2 min to 10 min. The highest iodine incorporation was achieved at 3 min after which the level of ^{125}I incorporation virtually remained unchanged when the reaction proceeded to 5 or 10 min.

1.4.2 The effect of the amount of chloramine T used in the reaction mixtures on iodine incorporation and the IRF of radioiodinated Dal B01, Dal B02 and their F(ab)'₂ fragments

Studies were carried out by the incubation of given amounts of MoAbs and radioactive ^{125}I with different amounts of chloramine T at room temperature for 2 min. As shown in Table 5, up to the concentration of 100 µg/ml of chloramine T, there was no significant decrease in the IRF of all the four MoAb preparations. Some loss of IRF was observed when the concentration of chloramine T reached 200 µg/ml (e. g., the IRF of Dal B02 decreased from 75.5% to 43% when the concentration of chloramine T increased from 50 µg/ml to 200 µg/ml). There was a direct correlation between the level of iodine incorporation and the amounts of chloramine T used in this study.

Based on these results, all the chloramine T based protein radioiodination procedures in this study were carried out by incubation of MoAbs or their F(ab)'2 fragments at a chloramine T concentration of 100 µg/ml for 2 min at room temperature.

1.4.3 The effect of different incorporation levels of radioactive iodine on the IRF of Dal B01, Dal B02 and their F(ab)'₂ fragments

Studies carried out with Dal B02 incorporating different levels of radioactive iodine (Table 6) showed that there was only a small decrease (from 83% to 75%) in the IRF of Dal B02 as the level of iodine incorporation increased from 0.25 to 4.0 µCi/µg of MoAb protein (i. e., the iodine incorporation in the antibody increased from 1 atom of ^{125}I per 54.7

molecules of IgG to 1 atom of ^{125}I per 3.4 molecules of IgG). However, there was a significant loss in IRF (from 83% to 55%) when the level of iodine incorporation increased from 0.25 µCi/µg (1 atom of ^{125}I per 54.7 molecules of IgG) to 10 µCi/µg MoAb protein (1 atom of ^{125}I per 1.4 molecules of IgG).

The F(ab)'2 fragment of Dal B02 had a lower IRF than intact Dal B02 even at an identical level of iodine incorporation, e. g., an IRF of 50% for the F(ab)'2 fragment compared to an IRF of 78% for the intact antibody at an identical level of iodine incorporation of 1 atom of ^{125}I per 8 molecules of IgG or F(ab)'2 (i. e., the specific activities were 1.73 µCi/µg protein for intact Dal B02 and 2.34 µCi/µg protein for the F(ab)'2 fragment). The IRF of the F(ab)'2 fragment preparation was also more sensitive to iodine incorporation. For example, the IRF of the F(ab)'2 fragment preparation decreased from 52.1% to 35% as the specific activity increased from 0.21 µCi/µg protein (1 atom of ^{125}I per 74.6 molecules of F(ab)'2 fragment) to 4.1 µCi/µg protein (1 atom of ^{125}I per 4.6 molecules of F(ab)'2 fragment).

Dal B01 and its F(ab)'2 fragment preparations had a lower IRF than Dal B02 and its corresponding fragment preparation. At an iodine incorporation of 0.21 to 0.23 µCi/µg protein (i.e., 1 atom of ^{125}I per 65.1 molecules of IgG or 81 molecules of F(ab)'2 fragment), the IRF of the intact Dal B01 or its F(ab)'2 fragment preparations was approximately 30% and 25%, respectively. The IRF of Dal B01 and its F(ab)'2 fragment preparations was also sensitive to the level of iodine incorporation. For example, the IRF of intact Dal B01 decreased from 30% to 11% as the specific activity of the antibody increased from 0.25 µCi/µg protein (1 atom of ^{125}I per 74.6 molecules of IgG) to 3.7 µCi/µg protein (1 atom of ^{125}I per 3.7 molecules of IgG).

Based on these studies, it could be seen that Dal B02 and its F(ab)'2 fragment had higher IRF than Dal B01 and its corresponding F(ab)'2 fragment, and intact Dal B02 had higher IRF than its F(ab)'2 fragment, at approximately the same level of iodine incorporation. An inverse correlation was observed between the loss of antibody immunoreactivity and the increase in the level of iodine incorporation.

In summary, the results obtained above indicate that important factors that determine the retention of the immunoreactivity of Dal B01, Dal B02 and their F(ab)'2 fragments during chloramine T based radioiodination procedures include (i) the reaction conditions, i. e., the amount of chloramine T used and the reaction time; (ii) the level of incorporation of radioactive iodine; and (iii) the nature of antibody preparations. i. e., variations among the two different MoAbs and their F(ab)'2 fragment preparations.

1.5 Determination of the Number of Binding Sites on D10-1 cells, the Affinity of Binding and the Immunoreactive Fraction of Radioiodinated Dal B01, Dal B02 and Their F(ab)'2 Fragments

The specific activities . 'radioiodinated Dal B01, Dal B02 and their F(ab)'2 fragments used in these studies ranged from 0.2 to 0.5 μCi/μg protein.

Figs. 11 and 12 present typical results obtained from studies carried out to determine the IRF of radiolabeled Dal B01, Dal B02 and their F(ab)'2 fragments using D10-1 cells. The IRF of antibodies was calculated from the plots of the inverse of cell concentration (in ml/millions) against the ratio of total added radioactivity over bound radioactivity. The inverse value of the Y-axis intercept gives the IRF of each MoAb or its F(ab)'2 fragment (see Materials and Methods for detailed description).

Figs. 13 and 14 present the results of typical studies on the determination of the above binding parameters of Dal B01, Dal B02 and their F(ab)'2 fragments using D10-1 cells. Scatchard analysis of data thus obtained yielded the number of binding sites per tumor cell and the affinity constant (Ka) of binding (Table 7, see Materials and Methods for the method of calculation). The number of binding sites of the two MoAbs and their F(ab)'2 fragments on tumor cells calculated from the observed data showed that Dal B02 had the largest number of binding sites, followed by Dal B02 F(ab)'2 fragment, Dal B01, and Dal B01 F(ab)'2 fragment. Since not 100% of MoAb molecules in the radioiodinated antibody preparations were immunoreactive, corrections, based on the IRF values of each antibody preparation, were made to obtain the real number of binding sites and Ka. As shown in Table 7, there was no significant difference in the number of binding sites between Dal B01 and Dal B02 on D10-1 cells. Both Dal B01 F(ab)'2 and Dal B02 F(ab)'2 fragments had approximately the same number of binding site as their corresponding intact MoAbs. Dal B01 had approximately the same Ka value compared to Dal B02, and Dal B01 F(ab)'2 fragment had approximately the same Ka value compared to Dal B02 F(ab)'2 fragment. However, the Ka values of the F(ab)'2 fragments of both Dal B01 and Dal B02 were lower than that of their corresponding intact MoAbs.

Table 4   The effect of the duration of exposure of Dal B02 to chloramine T
on   the iodine incorporation and the IRF of Dal B02 [1]

Time (min)	1.0	2.0	3.0	5.0	10.0
Specific activity [2]	0.197 [4]	0.255	0.35	0.28	0.36
IRF (%) [3]	66 [4]	65.5	51	40	33

1. Constant amounts of Dal B02, ^{125}I and chloramine T were mixed and stirred at room
temperature for different times as indicated. The radiolabeled proteins were purified by
chromatography on NAP-10 columns.

2. Specific activity is expressed as $\mu Ci / \mu g$ protein.

3. The IRF of the different radioiodinated Dal B02 preparations was determined using D10-
1 cells as described in Materials and Methods.

4. All values are the mean of 3 determinations.

Table 5 **The effect of the amount of chloramine T used in reaction mixtures on iodine incorporation and the IRF of MoAbs** [1]

Chloramine T (μg/ml)		25	50	100	200
Dal B02	Specific activity [2]	0.13 [4]	0.255	0.255	0.358
	IRF (%) [3]	75.5 [4]	72	66	43
Dal B01	Specific activity	0.205	0.213	0.294	0.455
	IRF (%)	32	30	26	30
B02 F(ab)'2	Specific activity	0.016	0.19	0.25	0.20
	IRF (%)	ND [5]	58.8	52.1	50
B01 F(ab)'2	Specific activity	0.09	0.347	0.18	0.494
	IRF (%)	ND	27	31.6	20

1. Constant amounts of Dal B01, Dal B02 or their F(ab)'2 fragments and ^{125}I were incubated with different amounts of chloramine T at room temperature for 2 min. The radiolabeled proteins were separated from free iodine using a Sephadex G-25 NAP-10 column.

2. Specific activity is expressed as μCi / μg protein.

3. The IRF of the antibodies was determined using D10-1 cells as described in Materials and Methods.

4. All values are the mean of 3 determinations.

5. Not determined.

Table 6   **The effect of different levels of iodine incorporation   on the IRF of MoAbs** [1]

	Specific activity [2]	0.25	1.23	1.90	3.90	4.02	8.0	10.0
Dal B02	(IgG/^{125}I) [3]	54.7	11.0	7.2	5.5	3.4	1.7	1.4
	IRF (%) [4]	83 [5]	80	76	71	75	60	55
	Specific activity	0.21	0.47	0.57	0.7	1.4	3.7	
Dal B01	(IgG/^{125}I)	65.1	29.1	24.0	19.5	9.8	3.7	
	IRF (%)	30	30	25	25	20	11	
	Specific activity	0.25	1.1	2.34	4.08	6.94	11.8	
B02 F(ab)'2	(IgG/^{125}I)	74.6	17.0	8.0	4.6	2.7	1.6	
	IRF (%)	52.1	50	50	35	35	25	
	Specific activity	0.13	0.23	0.57	2.0			
B01 F(ab)'2	(IgG/^{125}I)	143	81.0	32.7	9.3			
	IRF (%)	30	25	25	20			

1. Dal B01, Dal B02 or their F(ab)'2 fragments were incubated with different amounts of ^{125}I at a chloramine T concentration of 100 µg/ml for 2 min. The radiolabeled proteins were purified by chromatography using a NAP-10 column.

2. Specific activity is expressed as µCi /µg protein.

3. Iodine incorporation level expressed as numbers of IgG molecules per atom of iodine.

4. The IRF of different labeled MoAb preparations was determined using D10-1 cells as described in Materials and Methods.

5. All values are the mean of 3 determinations.

Figs. 11 and 12

Determination of immunoreactive fractions (IRF) of radiolabeled Dal B01, Dal B02 and their F(ab)'2 fragments using D10-1 cells.

These figures show typical results obtained from at least 5 studies carried out to determine the IRF of radiolabeled Dal B01, Dal B02 and their F(ab)'2 fragments using D10-1 cells. An increasing number of D10-1 cells (from 0.5 to 10 million) were incubated with a constant amount of radiolabeled Dal B01, Dal B02 or their F(ab)'2 fragments (typically 30 to 50 ng of protein) at 4°C for 90 min after which the cells were washed thrice with cold PBS and the cell associated radioactivity was determined.

The figures on the top show the binding data obtained from experiments in which the number of cells was plotted against the ratio of the amount of antibody bound to tumor cells over the total amount of antibody added. In the bottom figures, the inverse of cell concentration (ml/millions) was plotted against the ratio of the total amount of antibody added to the amount of cell-bound antibody. Linear regression of the bottom plot to determine the Y-axis intercept yielded a value equal to the inverse of the IRF in each case (see Materials and Methods for detailed description).

Fig. 11A Binding of radiolabeled Dal B01 and Dal B02 to D10-1 cells.

Fig. 11B Determination of IRF of Dal B01 and Dal B02 using D10-1 cells.

Fig. 12A Binding of radiolabeled Dal B01 F(ab)'2 and Dal B02 F(ab)'2 to D10-1 cells.

Fig. 12B Determination of IRF of Dal B01 F(ab)'2 and Dal B02 F(ab)'2 using D10-1 cells.

Fig. 11A
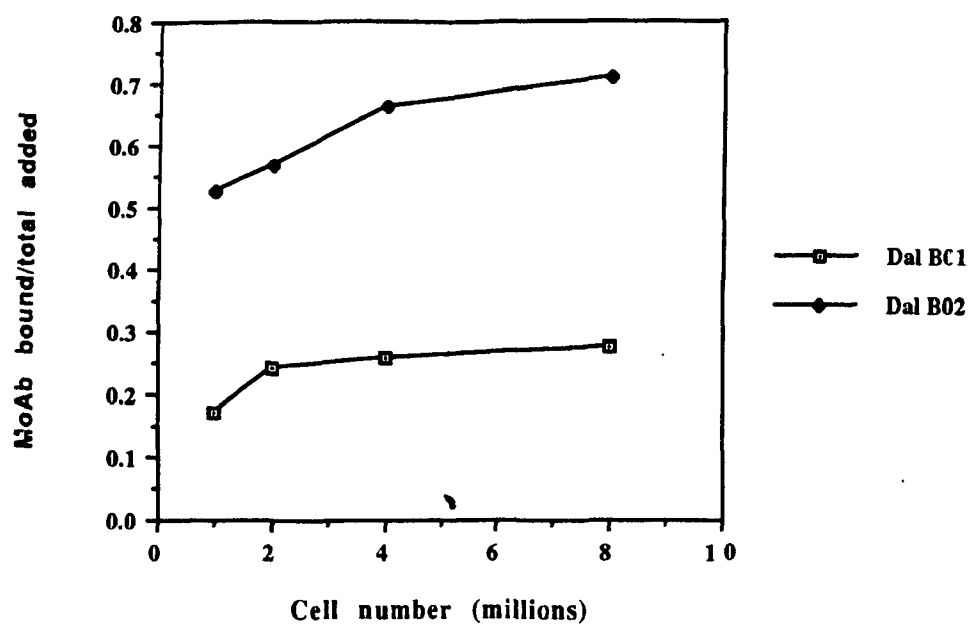
Fig. 11A

Fig. 11B

Fig. 11B
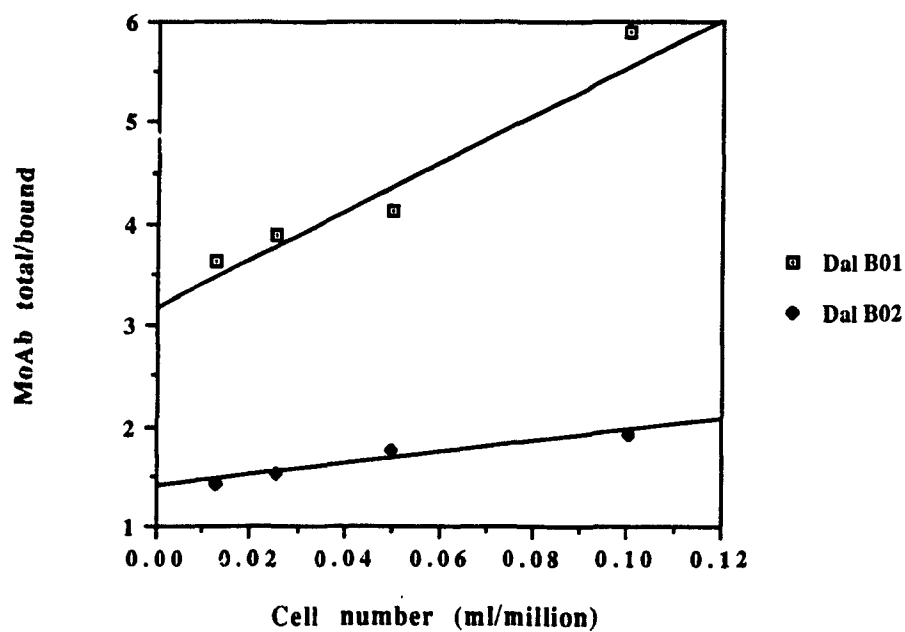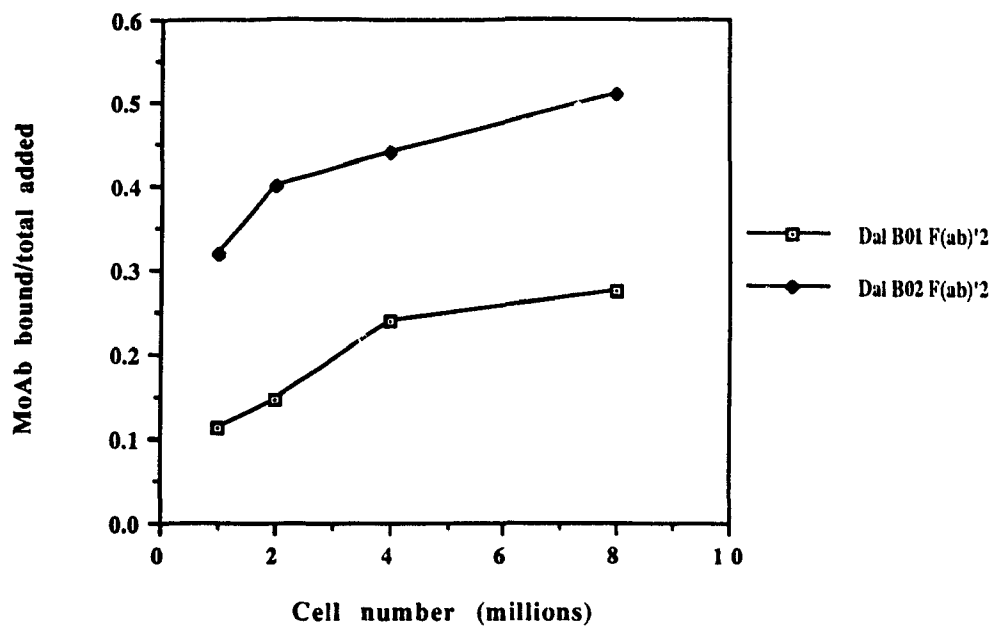
Fig. 12A

Fig. 12B
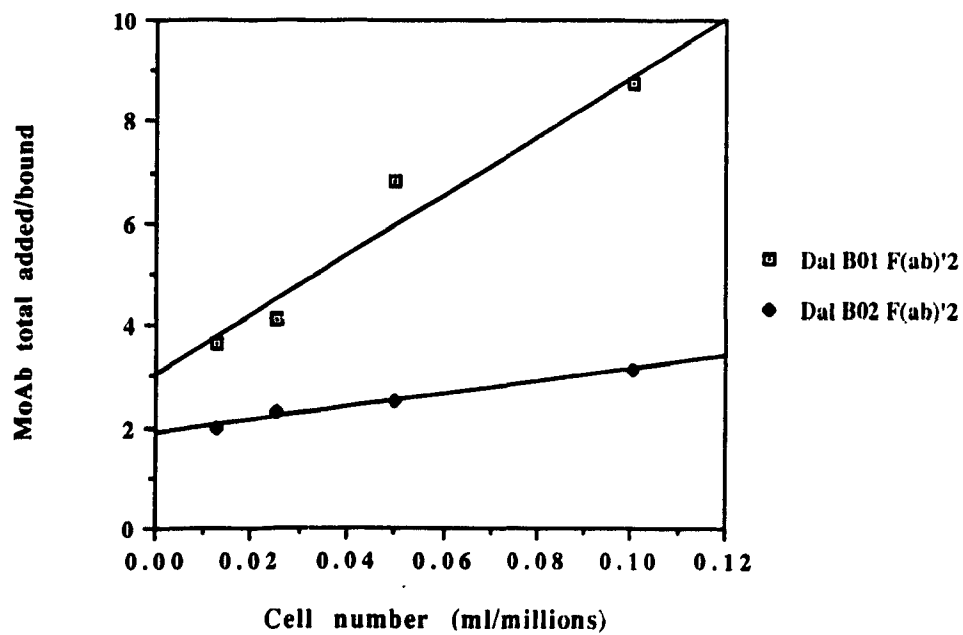
Figs. 13 and 14

Determination of the number of binding sites on D10-1 cells and Ka of binding of Dal B01, Dal B02 and their F(ab)'2 fragments.

These figures show typical results obtained from at least 5 studies carried out to determine the number of binding sites on D10-1 cells and Ka of binding of radioiodinated Dal B01, Dal B02 and their F(ab)'2 fragments. Increasing amounts of radioiodinated antibody (from 0.1 to 10 μg) were incubated with a constant number of D10-1 cells (typically 500, 000) at 4°C for 90 min after which the cells were washed thrice with cold PBS and the cell associated radioactivity was determined.

In the figures on the top, the amount of antibody added is plotted against the amount of antibody bound to D10-1 cells. In the bottom figures (Scatchard analysis), the amount of antibody bound to D10-1 cells (in pmol) is plotted against the ratio of the amount of antibody bound to tumor cells to the amount of antibody not bound to the cells (the amount of free antibody, i. e., the amount obtained by subtracting the amount of cell bound antibody from the total amount antibody added). Linear regression of the bottom plot yielded the X-axis intercept and slope from which the number of binding sites and binding affinity (Ka) were respectively calculated as described in Materials and Methods.

Fig. 13A Binding of radioiodinated Dal B01 and Dal B02 to D10-1 cells.

Fig. 13B Scatchard analysis of data from Fig. 12A to determine the number of binding sites on D10-1 cells and Ka of binding of Dal B01 and Dal B02.

Fig. 14A Binding of radioiodinated Dal B01 F(ab)'2 and Dal B02 F(ab)'2 to D10-1 cells.

Fig. 14B Scatchard analysis of data from Fig. 13A to determine the number of binding sites on D10-1 cells and Ka of binding of Dal B01 F(ab)'2 and Dal B02 F(ab)'2.

Fig. 13A
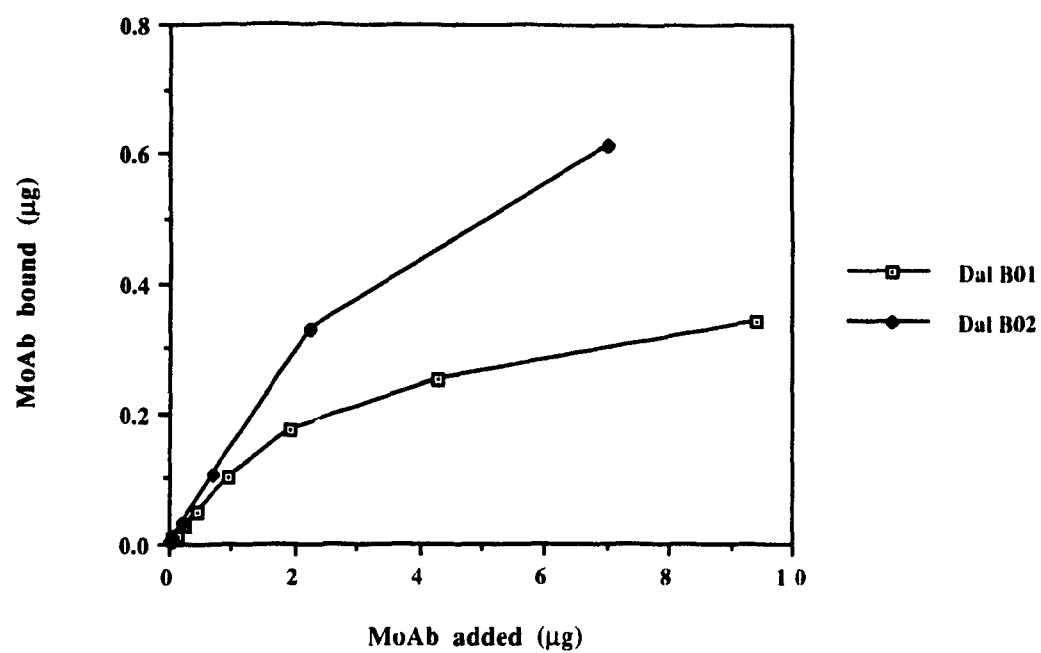
Fig. 13B
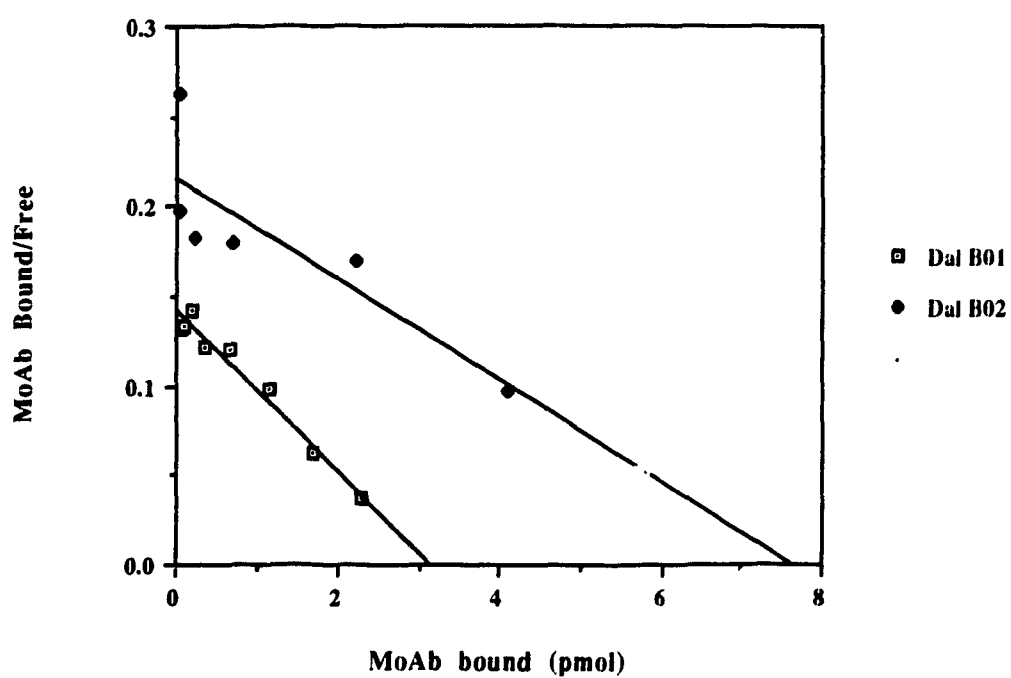
Fig. 14A
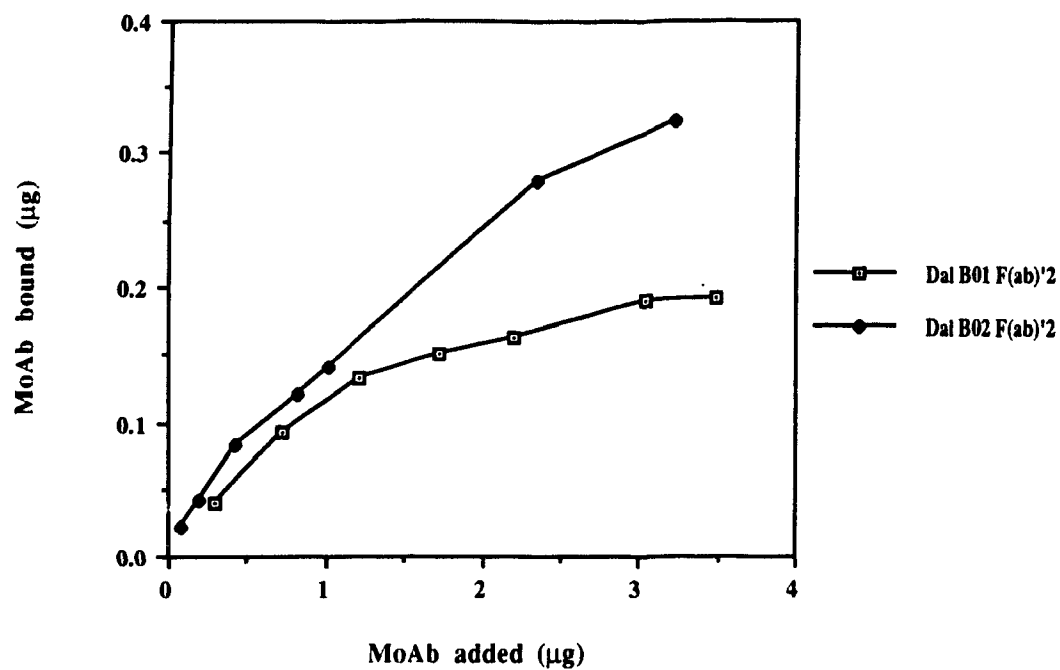
Fig. 14B
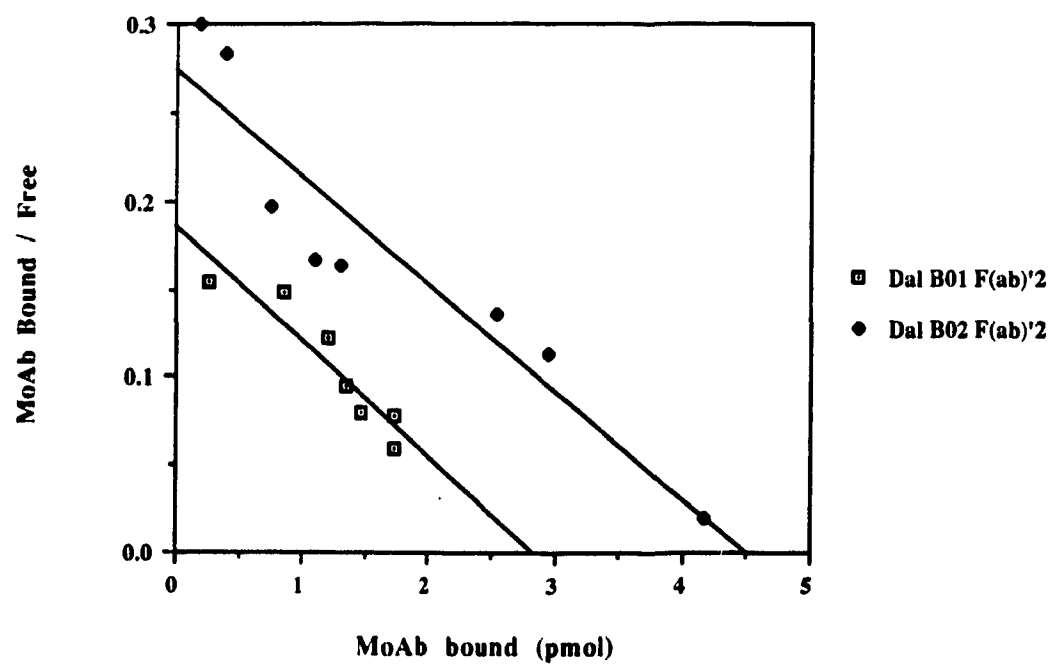
Table 7   The IRF, number of binding sites on D_{10-1} cells and Ka of

binding of Dal B01, Dal B02 and their F(ab)'2 fragments [1]

| Antibody | IRF | Number of binding sites | Binding affinity |
	(%)	(x 10^6 per cell)	(x 10^9 M $^{-1}$)
Dal B01	28.3 ± 2.6 [2]	3.5 ± 1.26 (12.4) [3]	3.6 ± 0.22 (12.7)
Dal B01 F(ab)'2	25.5 ± 4.1	3.1 ± 0.15 (12.2)	2.2 ± 0.39 (8.6)
Dal B02	73.9 ± 3.9	7.7 ± 1.1 (10.4)	7.9 ± 0.66 (10.7)
Dal B02 F(ab)'2	52.7 ± 3.6	5.8 ± 0.41 (11.0)	3.6 ± 0.33 (6.8)

1. All the parameters were determined using live D_{10-1} cells as described in Materials and Methods.

2. All values are calculated from the observed data and represent the mean ± S.D. from at least 3 determinations.

3. The figures in parenthesis represent the real values after correction for IRF of each of the MoAb preparation (see text for a detailed description).

1.6   Binding Kinetics of Dal B01, Dal B02 and Their F(ab)'₂ Fragments to D₁₀-₁ Cells

Antibody binding to cell surface associated antigen may lead to stable localization of the antibody-antigen complex on cell membrane or to modulation of the complex which may manifest itself as internalization or shedding. It is obvious that the subsequent fate of externally fixed antibody differs among different antibodies and with the target antigens expressed on cell surface. Furthermore, the metabolism of cell surface bound antibody is different compared to that of internalized antibody. In order to evaluate the potential use of MoAbs in targeted immunotherapy and radioimaging of human cancer, it is necessary to define the kinetics of interaction between MoAbs and their target tumor cells.

In this study, D₁₀-₁ cells were incubated with radioiodinated Dal B01, Dal B02 or their F(ab)'₂ fragments at 4°C or 37°C. At defined intervals, the cell bound radioactivity was determined. Figs. 15 and 16 present the binding kinetics of Dal B01, Dal B02 and their F(ab)'₂ fragments to D₁₀-₁ cells with time. At both 4°C and 37°C, the binding of either the intact Dal B01, Dal B02 or their F(ab)'₂ fragments increased rapidly during the first 10 min of incubation, and reached the plateau (maximum amount of binding) at 25 to 30 min after which the amount of antibody bound to cells remained unchanged during the period of observation of 90 to 180 min. The binding of Dal B01, Dal B02 and their corresponding F(ab)'₂ fragments to D₁₀-₁ cells was specific since no significant binding was observed when D₁₀-₁ cells were incubated with a radioiodinated non-specific IgG₁, nor when non-target K₅₆₂ cells were incubated with radioiodinated Dal B01, Dal B02 and their F(ab)'₂ fragments.

These figures also show that the amount of antibody bound to D10-1 cells was the same at either 4°C or 37°C for Dal B01, Dal B01 F(ab)'2 fragments and Dal B02. On the other hand, more Dal B02 F(ab)'2 fragment bound to D10-1 cells at 4°C than at 37°C. It is known that receptor-mediated endocytosis occurs at 37°C but not at 4°C. One of the method to calculate the amount of antibody endocytosed by target cells is to subtract the amount of cell bound antibody at 4°C from the amount of cell bound at 37°C. The data obtained here may indicate that there was no endocytosis, or internalization, of significant amount of cell surface bound Dal B01, Dal B02 or their F(ab)'2 fragments when the cells were incubated at 37°C for a period of 90 to 180 min. The significance of these binding data will be further elaborated in the Discussion section.

1.7   The Fate of Dal B02 Bound to the Surface of D10-1 Cells

As observed above, D10-1 cell bound approximately the same amount of Dal B02 at either 4°C or 37°C up to an incubation period of 180 min. This may suggest that there was no endocytosis of any significant amount of cell surface bound Dal B02 at 37°C. Two experiments were carried out to further examine the fate of D10-1 cell surface bound Dal B02 antibody.

1.7.1   Binding of Dal B02 to D10-1 cells at either 4°C or 37°C at various extracellular antibody concentrations

To determine whether the uptake of Dal B02 by target D10-1 cells may vary with different extracellular antibody concentrations, the D10-1 cells were incubated with different amounts of Dal B02 at either 4°C or 37°C for 120 min, after which the cells were washed and the cell-associated radioactivity was determined. As shown in Fig. 17, at each defined extracellular antibody concentration, there was no significant difference between the

amounts of antibody that bound to D$_{10-1}$ cells at 4°C and 37°C. This finding is consistent with the result described above.

1.7.2 Release of D$_{10-1}$ cell surface bound ^{125}I-Dal B02 in the presence of a large excess of cold Dal B02

Cell surface bound radiolabeled antibody is likely to be displaced competitively by a large excess of the cold antibody, provided that the radiolabeled antibody is not endocytosed. In this study, to examine whether the cell associated ^{125}I-Dal B02 stayed on the surface of D$_{10-1}$ cells or was endocytosed, and if so, how much was endocytosed, I used a large excess of cold Dal B02 to displace the D$_{10-1}$ cell surface bound ^{125}I-Dal B02. D$_{10-1}$ cells were first coated with ^{125}I-Dal B02 at 37°C for 120 min, after which the cells were incubated at 37°C with or without the presence of a large excess of cold Dal B02.

As a control, ^{125}I-Dal B02 coated D$_{10-1}$ cells were incubated in RPMI 1640 medium at 37°C without any cold Dal B02. At different intervals, aliquot of cells were taken out and the cell associated radioactivity and the radioactivity released in the supernatant were determined. The supernatant was treated with 10% TCA (as described in Materials and Methods) and the radioactivity in the TCA precipitated fraction and in the TCA soluble fraction was also determined. Fig. 18 shows the percentage of initially cell bound radioactivity (expressed as cpm) that remained associated with D$_{10-1}$ cells at different times after incubation at 37°C. More than 80% of the initial cell bound cpm remained associated with cells after incubation for 6 hr at 37°C. The radioactivity released in the supernatant was mostly TCA precipitable, indicating that they were associated with large protein moieties (e.g., intact antibody or its large fragments).

When the ^{125}I-Dal B02 coated D$_{10\text{-}1}$ cells were incubated in the presence of a large excess of cold Dal B02 (i. e., the concentration of cold Dal B02 was 50-fold higher than that of ^{125}I-Dal B02 used to coat D$_{10\text{-}1}$ cells), a rapid release of radioactivity into the supernatant was observed upon the addition of cold antibody (Fig. 18). At the end of the 2 hr period of incubation, greater than 80% of the initial cell bound radioactivity was found in the supernatant. Greater than 95% of this released radioactivity was TCA precipitable, indicating the radioactivity was associated with intact antibody or its large fragments.

These results suggest that (i) after binding, greater than 80% Dal B02 remained associated with D$_{10\text{-}1}$ cells after incubation at 37°C for at least 6 hr, i. e., the observation period used in this study; (ii) the majority of released radioactivity was associated with intact Dal B02 or its large catabolic fragments and could be precipitated by TCA; and (iii) the majority of cell associated Dal B02 after incubation at 37°C for 2 hr was cell surface bound and could be displaced by cold Dal B02. It is possible that the remaining Dal B02, i. e., the amount of antibody that could not be displaced by the cold antibody, was intracellullar. However, it is also possible that the remaining Dal B02 was still on the cell surface but could not be dissociated under these experimental conditions.

None of the above studies indicate internalization of significant amounts of Dal B01 or Dal B02. To further investigate the possibility of internalization of small amounts of cell surface bound Dal B01 or Dal B02, in the next study, Dal B01, Dal B02 and Dal K29 were adsorbed to colloidal gold particles, and the resulting MoAb-Au complexes were used to further elucidate the interaction between these MoAbs and their respective target cells.

Figs. 15 and 16

The time-course of binding of Dal B01, Dal B02 and their F(ab)'2 fragments to D10-1 cells at either 4°C or 37°C.

Radioiodinated Dal B01, Dal B02 or their F(ab)'2 fragments were incubated with D10-1 cells at either 4°C or 37°C. At indicated times (from 0 to 90 min), aliquots of cells were taken out and the cell bound radioactivity was determined. In these figures, the duration of incubation was plotted against the ratio of the amount of antibody bound to tumor cells to the amount of antibody not bound to tumor cells (i. e., free antibody, see legend of Figs. 13 and 14 for the method of calculation). A non-specific IgG1 and the non-target K562 cells were used in this study as negative controls.

Fig. 15A The time-course of binding of Dal B01 and a non-specific IgG1 to D10-1 cells.

Fig. 15B The time-course of binding of Dal B01 F(ab)'2 fragment to target D10-1 and non-target K562 cells.

Fig. 16A The time-course of binding of Dal B02 to target D10-1 and non-target K562 cells.

Fig. 16B The time-course of binding of Dal B02 F(ab)'2 fragment to target D10-1 and non-target K562 cells.

Fig. 15A

Legend:
- 37°C, B01
- 4°C, B01
- 37°C, IgG1
- 4°C, IgG1

Y-axis: Bound/Free (0.0 to 0.3)
X-axis: Times (min) (0 to 100)

Fig. 15B

Legend:
- 37°C, D10-1
- 4°C, D10-1
- 37°C, K562
- 4°C, K562

Y-axis: Bound/Free (0.0 to 0.2)
X-axis: Time (min) (0 to 100)
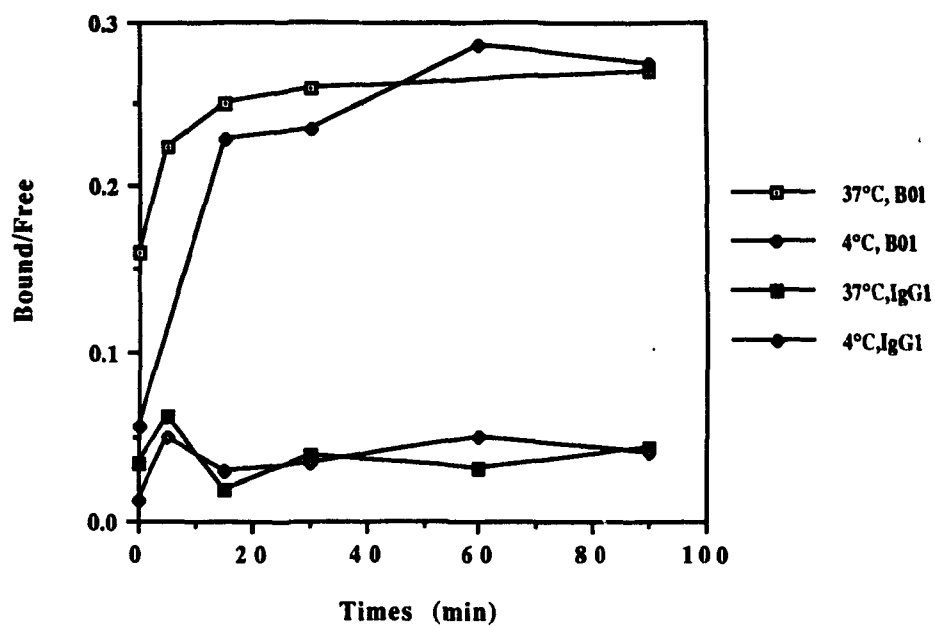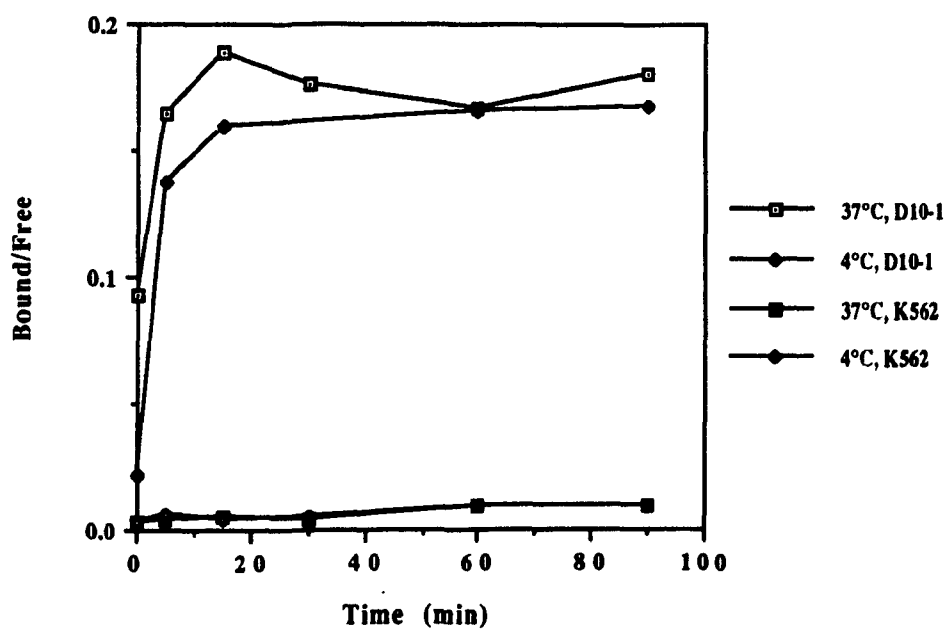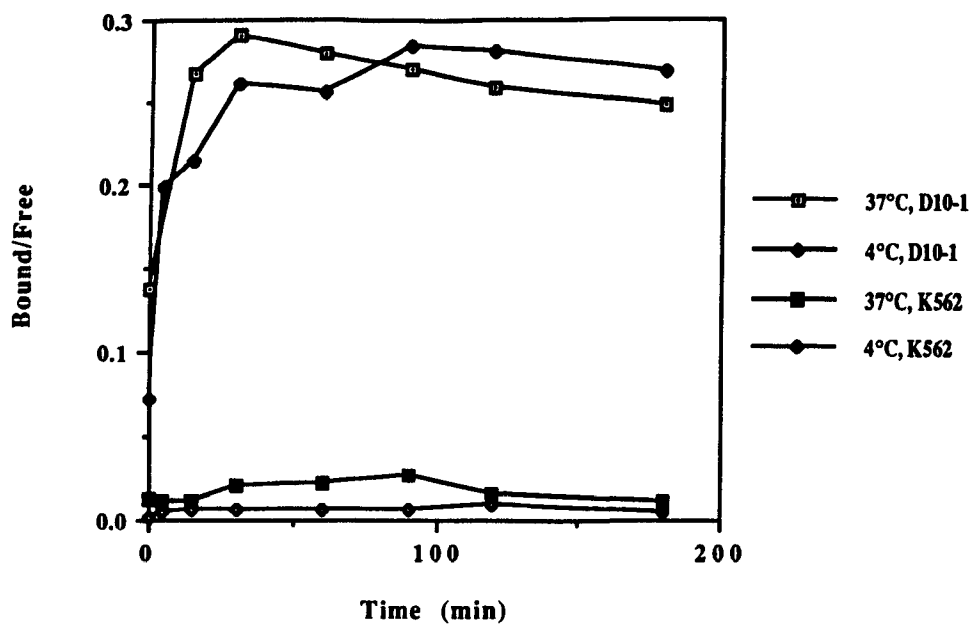
Fig. 16A

Fig. 16B
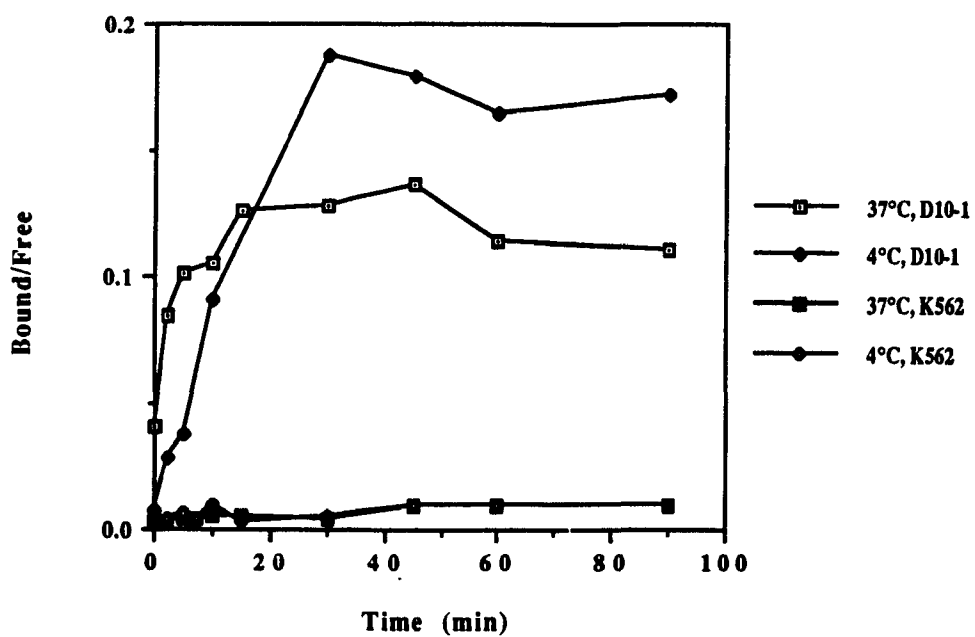
Fig. 17

The influence of temperature of incubation on the amount of Dal B02 that bound to D_{10-1} cells.

D_{10-1} cells were incubated with different amounts of radiolabeled Dal B02 at either 4°C or 37 °C for 120 min, after which the cell associated radioactivity was determined.

Fig. 17
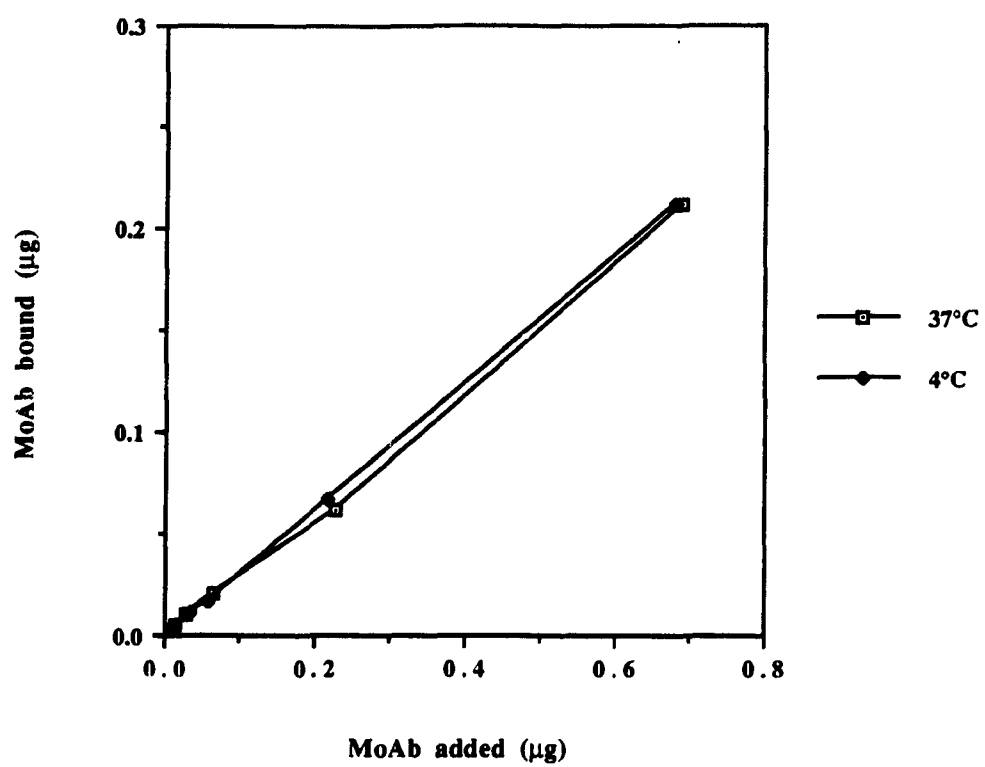
Fig. 18

The fate of D10-1 cell surface bound Dal B02.

D10-1 cells were coated with radioiodinated Dal B02 at 37°C for 120 min after which the cells were washed 3 times with PBS. The cells were then reincubated at 37°C in the presence or absence of a large excess of cold Dal B02. At indicated intervals, aliquots of cells were taken out and the radioactivity that remained associated with cells or released in the supernatant was determined. The supernatant was then treated with 10% TCA and the radioactivity in TCA precipitable fraction and in TCA soluble fraction was determined.

Note that when D10-1 cells coated with radioiodinated Dal B02 were reincubated at 37°C in the presence of a large excess of cold Dal B02, about 80% of cell associated radioactivity was released in the supernatant within 45 min.

Fig. 18

Cell-associated radioactivity (% of initial cell bound) vs Time at 37°C (min)

- cell associated
- supernatant
- TCA precipitable
- (+) cold Dal B02
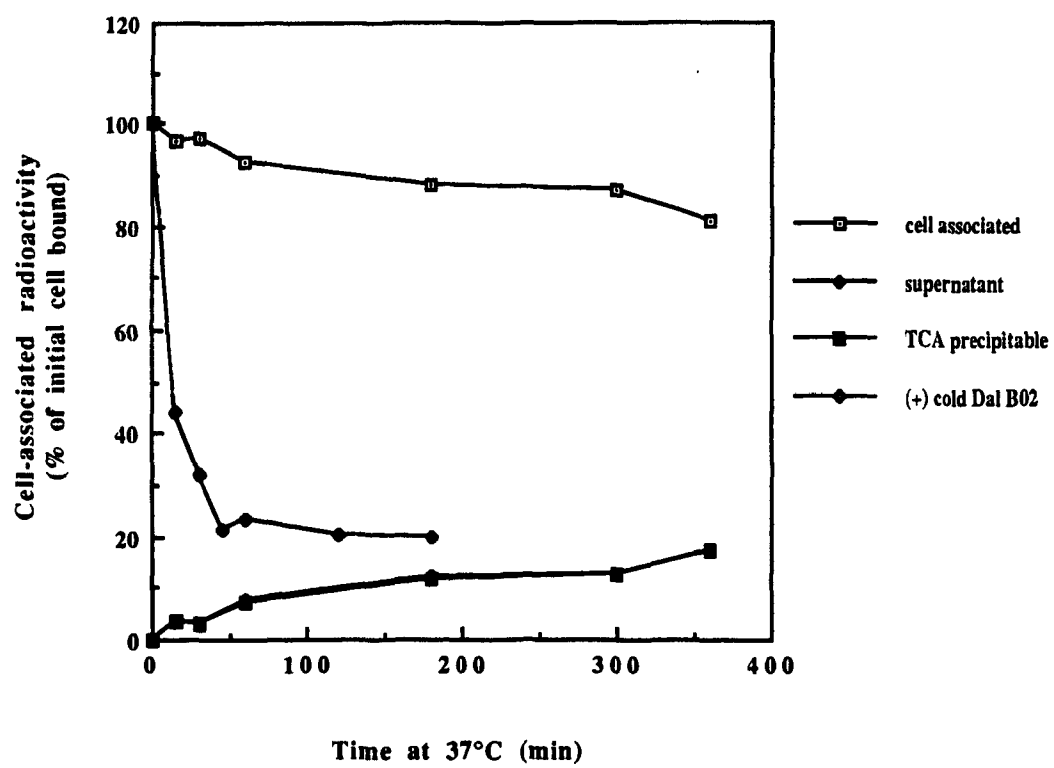
1.8   Preparation of MoAb-Au Complexes and Utilization of These Complexes to Trace the Fate of Cell Surface Bound Dal B01 and Dal B02

1.8.1   Determination of the size of gold particles and the optimal conditions for the adsorption of gold particles to MoAbs

The colloidal gold particles had a mean diameter of 15 nm as determined by electron microscopy. Preliminary studies were carried out to adsorb Dal B01, Dal B02, and Dal K29 on gold particles using two different pH conditions. It was found that the optimal pH that could stabilize MoAb-Au complexes was 7.1 for Dal B02 and Dal K29, and 9.2 for Dal B01.

The amount of antibody required to stabilize 1.0 ml of colloidal gold solution was determined as described in Materials and Methods. It was found that 50 μg of Dal ' 01 protein, 40 μg of Dal B02 protein and 60 μg of Dal K29 protein were the minimum amounts of antibody required to stabilize 1.0 ml of colloidal gold solution.

1.8.2   Preparation of Dal B01-Au, Dal B02-Au and Dal K29-Au complexes

Ten ml of colloidal gold solution were mixed with 550 μg of ^{125}I-labeled Dal B01, or 440 μg of ^{125}I-labeled Dal B02 or 660 μg of ^{125}I-labeled Dal K29 at room temperature for 3 min, after which the unbound MoAbs were washed away by ultracentrifugation (27,000 x g for 40 min). The absolute amounts of both MoAb or gold particle incorporated in final products could be determined by respectively measuring the radioactivity or optical density at 700 nm of the complexes. Table 8 presents the recovery of MoAbs and gold particles

after complex formation, as well as the number of antibody molecules adsorbed per gold particle in the complexes.

1.8.3 Immunoreactivity of Dal B01, Dal B02 and Dal K29 after adsorption to gold particles

Since the purpose was to use these MoAb-Au complexes to trace the interaction between MoAbs and their target cells, it was important to make sure that the immunoreactivity of these MoAbs was well retained after adsorption to gold particles. As shown in Table 8, the IRF of Dal B01 and Dal B02 were well retained after adsorption, whereas Dal K29 lost 50% of its original IRF after adsorption.

Two different methods were used to evaluate the immunoreactivity of gold particle-complexed Dal B01 or Dal B02. In the first method, the absolute amounts of antibody (either free or complexed to gold particles) that bound to target D10-1 cells were compared. As shown in the top figures of Figs. 19 and 20, there was no significant difference between the amounts of antibody that bound to target cells before and after the adsorption of Dal B01 or Dal B02 to gold particles.

In the second method used for the evaluation of the immunoreactivity of gold particle-complexed Dal B01 or Dal B02, ^{125}I labeled MoAbs, either free or complexed to gold particles, were evaluated for their binding to target D10-1 cells in the presence of increasing amounts of the appropriate cold parent MoAb. As shown in the bottom figures of Figs. 19 to 20, the binding of gold particle-complexed MoAbs to D10-1 cells was reduced compared to that of the respective free MoAbs. As the gold particles (with a mean diameter of 15 nm) are much larger than the free MoAbs, the reduction in the binding activity of the gold

particle complexed MoAbs may be due either to a steric hindrance and/or real loss of antibody activity after adsorption.

1.8.4   Stability of Dal BO1-Au, Dal BO2-Au and Dal 29-Au complexes

The stability of MoAb-Au complexes is an important consideration when using the gold particle as a marker to study the interaction between a MoAb and cell surface associated target antigen (s) and the subsequent fate (e. g., endocytosis or shedding) of the cell surface bound antibody. The MoAb should remain stably associated with the marker gold particles during the entire process. As shown in Table 9, all the three MoAb-Au complexes were stable when incubated at 37°C for up to 8 hr under either neutral (pH = 7.0) or an acidic (pH = 4.0) condition. These complexes were also stable during repeated freezing and thawing cycles (Table 10). However, on storage at 4°C, gradual release of antibody from gold particles was observed. After 2 weeks, only 72% of initially adsorbed Dal BO1 and 85% of initially adsorbed Dal K29 were remained associated with gold particles, and these values dropped respectively to 67% and 78% after 5 weeks (Table 11).

1.8.5   Cytotoxicity of MoAb-Au complexes

It was also very important to ascertain that MoAb-Au complexes were not cytotoxic and did not detectably damage the target cells after their incubation with these complexes. The usefulness of gold particles as marker would be greatly compromised if they induce changes in cell behavior (e.g., alterations in antigen expression, endocytosis and intracellular metabolism) because of the toxicity of the MoAb-Au complexes. Table 12 shows that all the three MoAb-Au complexes, colloidal gold solution or MoAb alone were not cytotoxic to their target cells in the concentrations used in this study.

Table 8   Percentage MoAbs and gold particles that were incorporated in the MoAb-Au complexes and the IRF of MoAbs [1]

MoAb		Dal B01	Dal B02	Dal K29
MoAb (%) [2]		6.2	11.8	12.0
Gold (%) [2]		60.6	94.1	20.0
IgG / Gold [3]		18.2	29.6	110.6
IRF (%) [4]	Free MoAb	34.0	58.0	28.0
	MoAb-Au	33.8	68.7	15.0

1. Three different MoAbs were complexed to colloidal gold particles (diameter, 15 nm) under optimal conditions defined in Result section 1.8.1.

2. The amounts of MoAbs or gold particles that were incorporated in final products (i.e., MoAb-Au complexes) expressed as the percentage of starting materials.

3. The numbers of IgG molecules complexed to one gold particle.

4. The IRF of free MoAbs or their gold complexes was determined using D_{10-1} cells for Dal B01 and Dal B02 , and Caki-1 cells for Dal K29.

Figs. 19 and 20

Determination of immunoreactivity of Dal B01 and Dal B02 after adsorption to gold particles.

Two different assays were used to evaluate the immunoreactivity of gold particle-complexed Dal B01 and Dal B02. In the first assay, the binding activity of ^{125}I-Dal B01-Au or ^{125}I-Dal B02-Au complexes to target D10-1 cells was compared directly to that of ^{125}I-Dal B01 or ^{125}I-Dal B02, respectively. In the other assay, the binding activity of ^{125}I-Dal B01-Au or ^{125}I-Dal B02-Au complexes to target D10-1 cells was compared to that of ^{125}I-Dal B01 or ^{125}I-Dal B02 in the presence of increasing amounts of appropriate cold MoAbs .

Fig.19A The binding activity to target D10-1 cells of ^{125}I-Dal B01-Au complex as compared to that of ^{125}I-Dal B01.

Fig.19B The binding activity to target D10-1 cells of ^{125}I-Dal B01-Au complex and ^{125}I-Dal B01 in the presence of increasing amounts of cold Dal B01.

Fig.20A The binding activity to target D10-1 cells of ^{125}I-Dal B02-Au complex as compared to that of ^{125}I-Dal B02.

Fig.20B The binding activity to target D10-1 cells of ^{125}I-Dal B02-Au complex and ^{125}I-Dal B02 in the presence of increasing amounts of cold Dal B02.

Inhibition (%)

Cold Dal B01 (µg)

Fig. 19B

Dal B01
Dal B01-Au

MoAb bound (µg)

MoAb added (µg)

Fig. 19A

Dal B01
Dal B01-Au

206

Fig. 20B

Inhibition (%)

Cold Dal B02 (µg)

Dal B02
Dal B02-Au

Fig. 20A

MoAb bound (µg)

MoAb added (µg)

Dal B02
Dal B02-Au

207
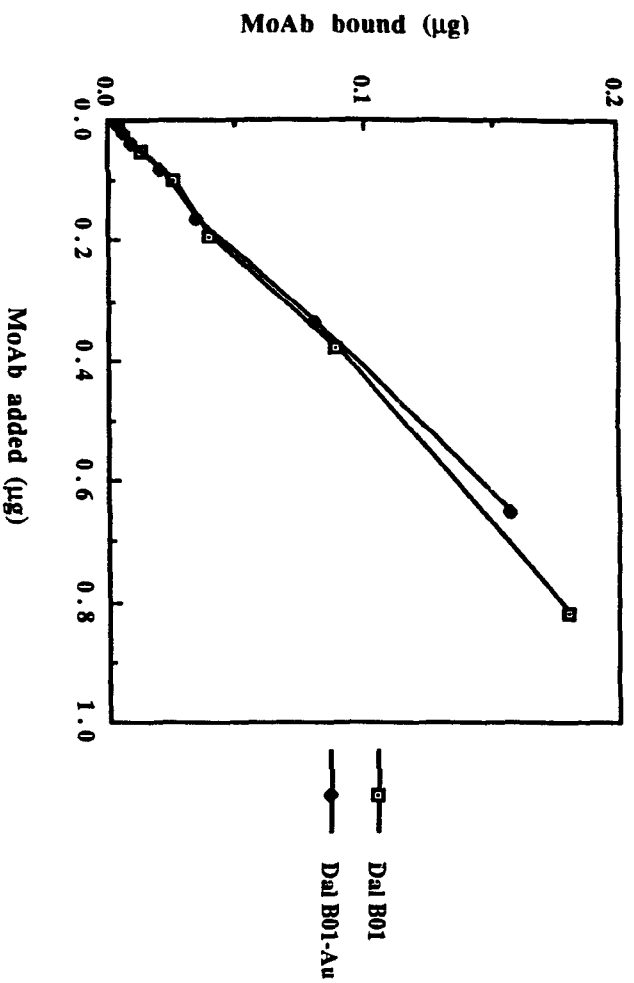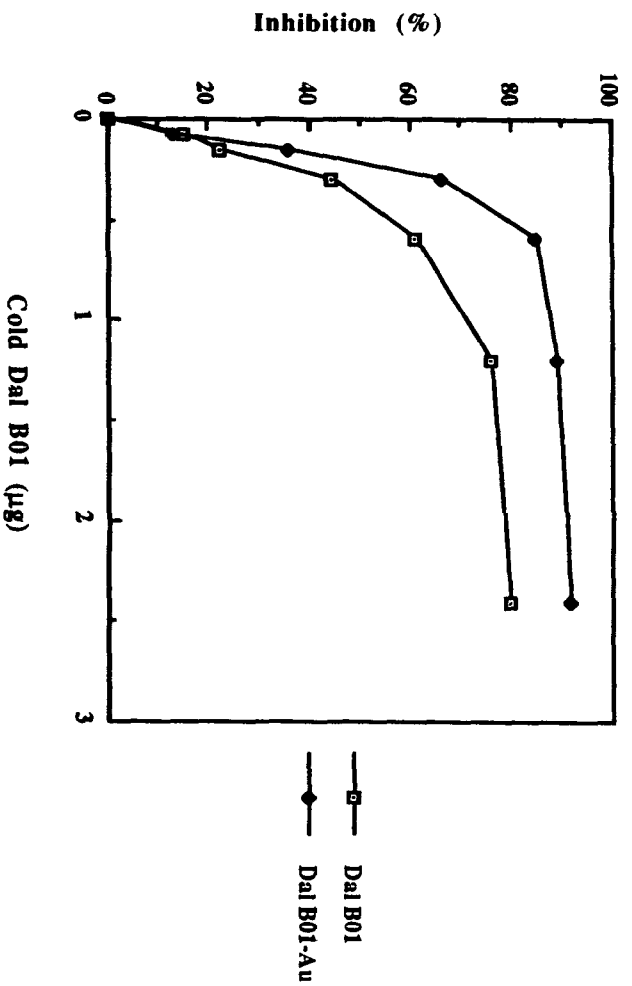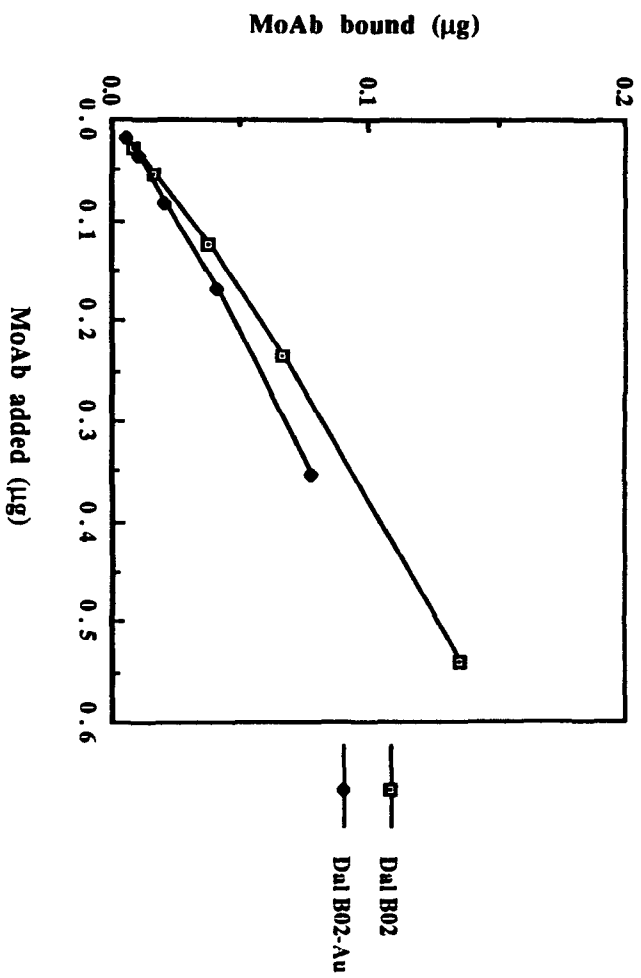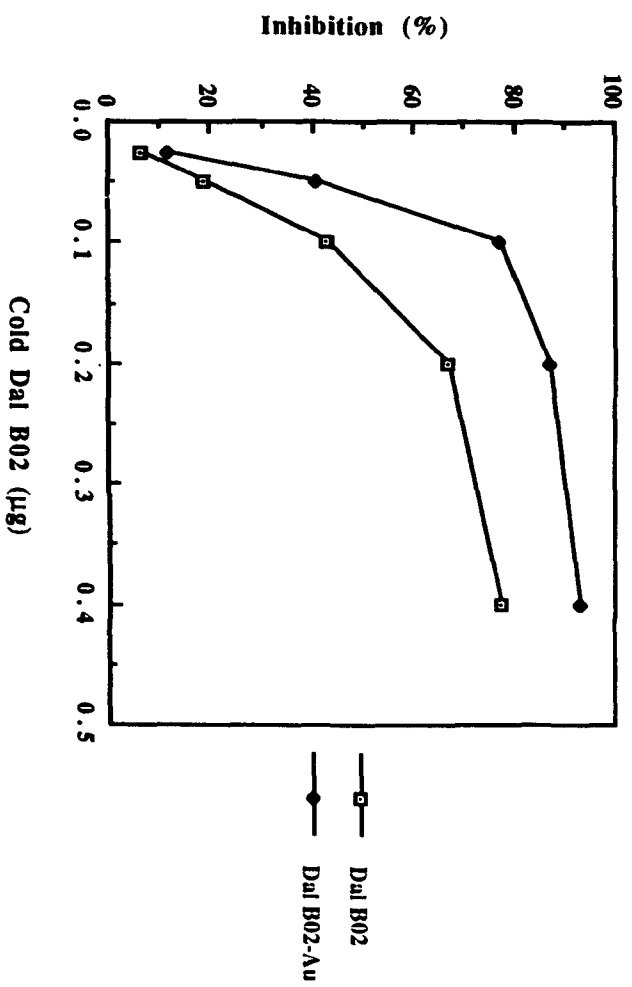
Table 9 Stability of MoAb-Au complexes in RPMI medium at 37°C [1]

(A) At pH 7.0

Time (hr)	0	0.5	1.0	2.0	4.0	6.0	8.0
Dal B01-Au	100[2]	100	94.5	95.8	95.6	97.9	95.2
Dal B02-Au	100	97.2	97.0	91.3	94.7	97.0	97.0
Dal K29-Au	100	100	100	100	100	100	100

(B) At pH 4.0

Time (hr)	0	0.5	1.0	2.0	4.0	6.0
Dal B01-Au	100	96.8	95.2	97.7	97.9	91.7
Dal B02-Au	ND[3]	ND	ND	ND	ND	ND
Dal K29-Au	100	100	100	100	100	100

1. All the three MoAb-Au complexes were incubated with RPMI medium at 37°C at defined pH conditions as stated. Aliquots were taken out at indicated intervals. The gold particles were centrifuged down at 27, 000 x g for 40 min. The radioactivity that remained associated with gold particles as well as released into the supernatant was determined using a gamma counter.

2. All values are the mean of 2 determinations and represent the percentage of radioactivity remained associated with Au particles.

3. Not determined.

Table 10 **Stability of MoAb-Au complexes during repeated freezing and thawing cycles** [1]

Cycles	0	1	2	3	4	5
Dal B01-Au	100 [2]	93.1	89.0	93.6	95.5	89.0
Dal B02-Au	100	97.2	92.3	98.1	100	98.5
Dal K29-Au	100	100	100	100	100	100

1. All the three MoAb-Au complexes were frozen at -70 °C and then thawed at 37°C rapidly. After each cycle of freezing and thawing, aliquots were taken out. The gold particles were centrifuged down at 27, 000 x g for 40 min. The radioactivity that remained associated with gold particles as well as released into the supernatant was determined using a gamma counter.

2. All values are the mean of 2 determinations and represent the percentage of radioactivity remained associated with Au particles.

Table 11 Stability of MoAb-Au complexes during storage at 4°C [1]

Time (weeks)	0	2	3	5
Dal B01-Au	100 [2]	72	72	67
Dal B02-Au	ND [3]	ND	ND	ND
Dal K29-Au	100	85	85	78

1. The MoAb-Au complexes were stored at 4°C. Aliquots were taken out at indicated intervals. The gold particles were centrifuged down at 27, 000 x g for 40 min. The radioactivity that remained associated with gold particles or released into the supernatant was determined using a gamma counter.

2. All values are the mean of 2 determinations and represent the percentage of radioactivity remained associated with Au particles.

3. Not determined.

25

Table 12   Cytotoxicity of MoAbs or MoAb-Au complexes [1]

Time (hr)	0	1.0	2.0	4.0	6.0
Dal B01 [2]	0 [4]	0	7.0	10.0	15.0
Dal B01-Au [2]	0	1.5	10.0	9.5	13.0
Dal K29 [3]	0	0	16.0	ND [5]	14.0
Dal K29-Au [3]	0	8.5	13.0	ND	20.5
Gold particles [2]	0	0	10.5	ND	9.0
PBS [2]	0	3.5	5.0	2.5	11.0

1. Appropriate tumor cells were incubated with either free MoAbs or MoAb-Au complexes under the conditions used for EM studies as described in Materials and Methods. At different intervals, aliquots of cells were taken out and the viability of cells was determined using the trypan blue exclusion assay.

2. Determined using D_{10-1} cells.

3. Determined using Caki-1 cells.

4. All values are the mean of 2 determinations and represent the percentage of dead cells at the time of assay. At least 200 cells were counted at each point.

5. Not determined.

1.8.6 The fate of Dal B01-Au and Dal B02-Au complexes bound to the surface of target D10-1 cells

The results presented above demonstrate that after adsorption to gold particles, MoAb Dal B01 and Dal B02 retained their immunoreactivity, the MoAb-Au complexes were stable and not cytotoxic to target cells during the incubation procedure. These features allowed me to use these complexes to further study the fate of cell surface bound Dal B01 and Dal B02 with the help of electron microscopy.

(A)   Binding of Dal B01-Au or Dal B02-Au complex to D10-1 cells and the release of cell surface bound complexes

The binding of ^{125}I-Dal B01-Au or ^{125}I-Dal B02-Au complex to target D10-1 cells and the release of cell surface bound complex during prolonged incubation at 37°C was investigated and compared to that of ^{125}I-Dal B01 or ^{125}I-Dal B02, respectively. D10-1 cells were first coated with ^{125}I-Dal B01-Au complex, ^{125}I-Dal B02-Au complex, or ^{125}I-Dal B02 at 4°C for 90 min after which the unbound complexes or antibody was washed away. The cells were then reincubated at 37°C in antibody free medium for up to 6 hr. At defined intervals, aliquots of cells were taken out and ^{125}I activity in the cell pellets and in the supernatants was determined. As shown in Fig. 21, a rapid release of radioactivity from target D10-1 cells was observed in the first 30 min of incubation with Dal B02-Au complex and in the first 60 min of incubation with Dal B01-Au complex, after which the cell associated radioactivity remained at stable levels. At the end of 6 hr of incubation, about 70% of the initial cell bound ^{125}I-Dal B01-Au complex and 80% of the initial cell bound ^{125}I-Dal B02-Au complex remained associated with the cells, indicating that the binding of both the Dal B01-Au and Dal B02-Au complexes to target cells was quite stable. There was no difference in the binding kinetics between free ^{125}I-Dal B02 and ^{125}I-Dal B02-Au complex.

In the case of Dal B02-Au complex, the radioactivity released into the supernatant was precipitated by 10% TCA. The majority of the radioactivity in the supernatant was TCA precipitable, indicating that the ^{125}I activity remained associated with intact antibody or their large fragments.

(B)   Binding of Dal B01-Au or Dal B02-Au complex to D10-1 cells and the fate of cell surface bound complexes as determined by electron microscopy

Preliminary immunofluorescence studies had demonstrated that the incubation of target cells with the MoAb-Au complexes produced a sequence of staining pattern (e.g., membrane staining, patching and then capping at 37°C) that was identical to the staining pattern produced by the free parent MoAbs (see Result 1.3). The aim of this study was to further examine the fate of cell surface bound Dal B01 and Dal B02 at the electron microscopic level, i. e., to study the sequence of distribution of these MoAbs on the cell surface, and then to investigate their possible internalization. A few relevant pictures are presented in Figs. 22 to 25.

After coating D10-1 cells with Dal B01-Au or Dal B02-Au complex at 4°C, the cells were incubated at 37°C. As shown in Figs. 22 to 24, at the end of incubation at 4°C, the cell bound gold particles were evenly distributed along the cell surface. The number of cell surface bound gold particles differed from MoAb to MoAb and had direct correlation with the IRF of the MoAb. The mean number of gold particles were 28.9 ± 13.2 for Dal K29-Au complex, 134 ± 57.2 for Dal B01-Au complex, and 261.7 ± 72.4 for Dal B02-Au complex per target cell. Few particles were observed inside cells. The gold particles began to from "patches" and appeared in the cell cytoplasm after incubation at 37°C for 30 min. The distribution of gold particles on cell surface became increasingly uneven, i. e., there was more "patch" formation, and the number of intracellular gold particles increased with

time of incubation at 37°C. At 4 hr after incubation at 37°C, a few "caps" were observed on cells exposed to either Dal B01-Au or Dal B02-Au complex. The maximum numbers of internalized gold particles could be seen after incubation for 2 hr with Dal B02-Au complex (63.8 ± 9.6 gold particles per cell, approximately 17.1% of total cell associated particles) and after incubation for 6 hr with Dal B01-Au complex (20.1 ± 26.8 gold particles per cell, about 14.8% of total cell associated particles) (Table 13).

Compared to Dal B01 and Dal B02, much smaller number of Dal K29-Au particles were observed associated with target Caki-1 cells (Fig. 24). However, the Dal K29-Au complex showed the internalization of a higher proportion of gold particles by Caki-1 cells. For example, 17.2% and 24.1% of cell associated gold particles were internalized into Caki-1 cells upon incubation at 37°C for 1 hr and 6 hr, respectively.

No cell surface associated or internalized gold particles could be detected in any of the control preparations incubated at either 4°C or 37°C incubation (Fig. 25), indicating that the binding of the MoAb-Au complexes to their respective target cells and their subsequent internalization are antibody-dependent .

In conclusion, Dal B01 and Dal B02 retained their immunoreactivity after adsorption to gold particles. Both the MoAb-Au complex preparations bound specifically to target D10-1 cells, but not to non-target MOLT-3 or M21 cells. After incubation with D10-1 cells at 37°C for 6 hr, about 14 - 15% of initial cell bound Dal B01-Au or Dal B02-Au complex were endocytosed. A larger number of Dal B02 complexed gold particles bound to and were endocytosed by D10-1 cells compared to the number of Dal B01 complexed gold particles that bound to and were endocytosed by D10-1 cells.

Fig. 21

Release of cell surface bound Dal B01-Au or Dal B02-Au complexes from D10-1 cells.

D10-1 cells were coated with ^{125}I-Dal B01-Au complex, or ^{125}I-Dal B02-Au complex, or ^{125}I-Dal B02 at 4°C for 90 min, after which the cells were washed 3 times and incubated at 37°C. At indicated intervals, aliquots of cells were taken out and the ^{125}I radioactivity that remained associated with cells and released into the supernatant was determined. In the case of Dal B02-Au complex, the supernatant was treated with 10% TCA and the ^{125}I activity in the TCA precipitable and soluble fractions was determined (Fig. 21B).

Radioactivity
(% of initial cell bound)

Fig. 21B

Time (min)

- ■ TCA-precipitable
- ◆ Supernatant
- ☐ Cell-associated

Cell-associated radioactivity
(% of initial cell bound)

Fig. 21A

Time (min)

- │ Dal B01-Au
- ■ Dal B02-Au
- ◆ Dal B02-Au
- ☐ Dal B02

216
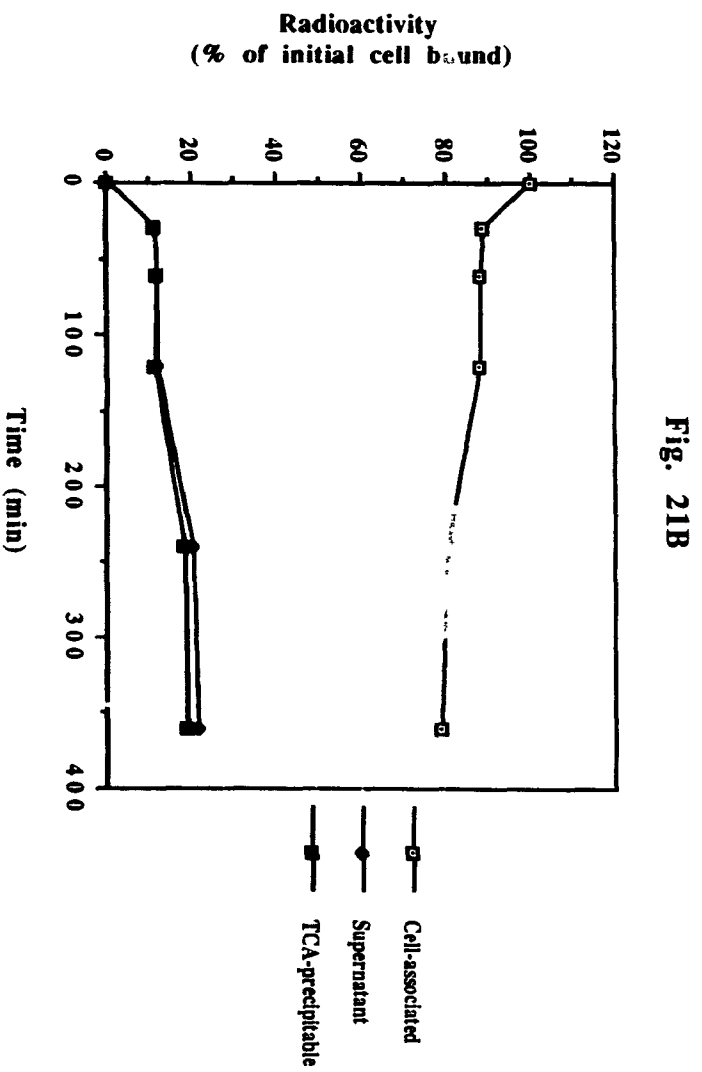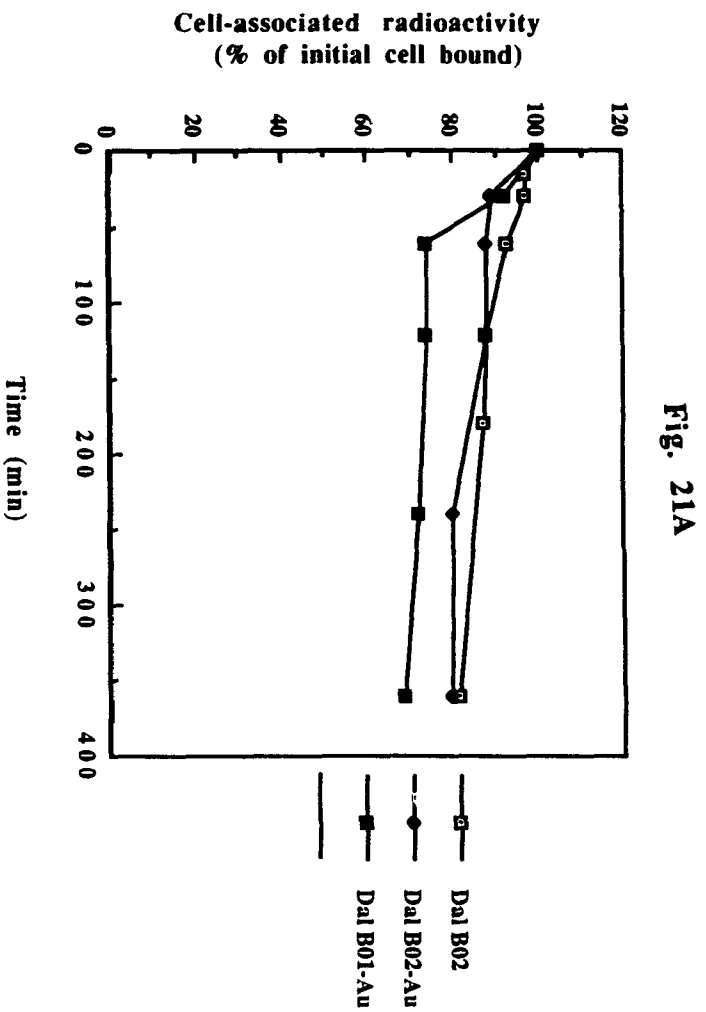
Figs. 22 to 25

The fate of cell surface bound Dal B01-Au, Dal B02-Au or Dal K29-Au complexes.

D10-1 or Caki-1 cells were coated with the appropriate MoAb-Au complex at 4°C for 60 min after which the cells were washed 3 times and incubated at 37°C. At intervals of 0, 0.5, 1, 2, 4 and 6 hr, aliquots of cells were taken out and processed for TEM examination (see Materials and Methods for detailed description).

Fig. 22 The fate of D10-1 cell surface bound Dal B01-Au complex. (A) 0 time at 37°C (i. e., at the end of incubation at 4°C); (B) 1.0 hr; (C) 4.0 hr; and (D) 6.0 hr at 37°C.

Fig. 23 The fate of D10-1 cell surface bound Dal B02-Au complex. (A) 0 time at 37°C (i. e., at the end of incubation at 4°C); (B) 0.5 hr ; (C) 1.0 hr; (D) 2.0 hr; (E) and (F) 4.0 hr (Fig. F shows a cap formed on D10-1 cell surface); (G) and (H) 6.0 hr at 37°C.

Fig. 24 The fate of Caki-1 cell surface bound Dal K29-Au complex. (A) 0 time at 37°C (i. e., at the end of incubation at 4°C); (B) 1.0 hr; (C) 4.0 hr; and (D) 6.0 hr at 37°C.

Fig. 25 Control preparations for this study included the following:

(A) D10-1 cells incubated with gold particles;

(B) D10-1 cells incubated with Anti-BSA IgG-Au complex;

(C) MOLT-3 cells incubated with gold particles;

(D) MOLT-3 cells incubated with Dal B02-Au complex;

(E) M21 cells incubated with Dal B01-Au complex;

(F) M21 cells incubated with Dal K29-Au complex.

Fig. 22

Fig. 23

A   B

C   D
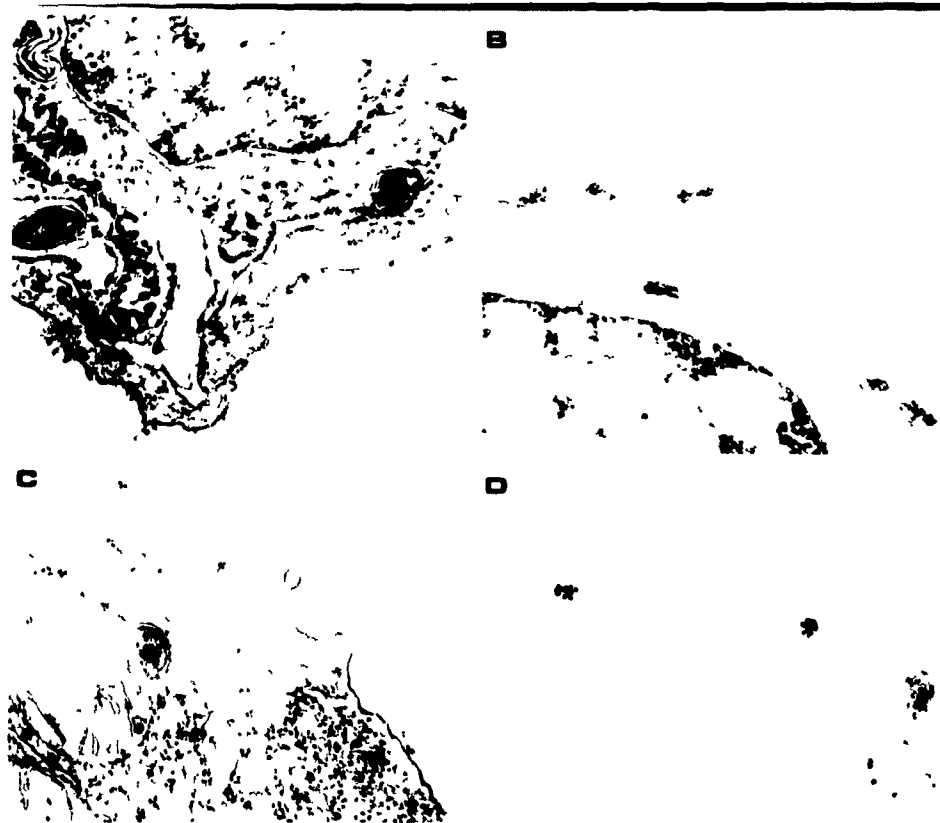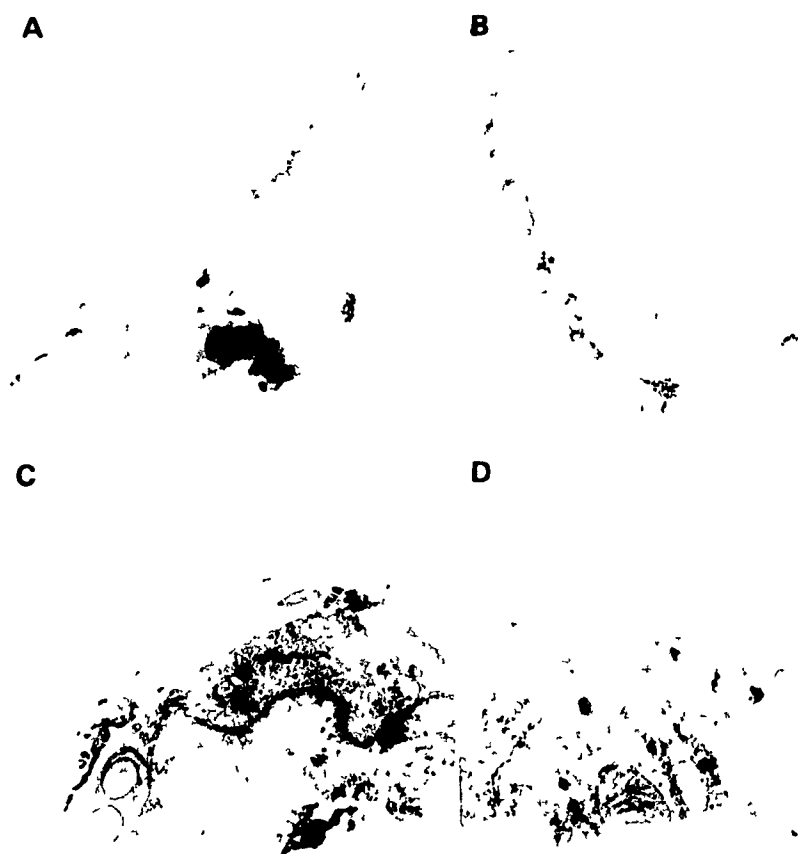
Fig. 23
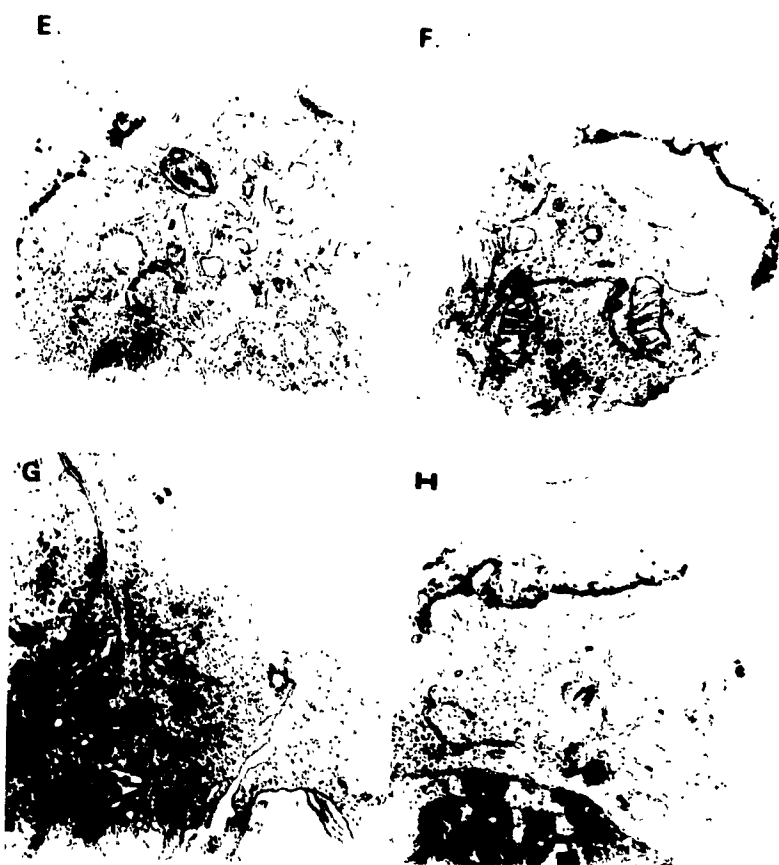
Fig. 24

Fig. 25
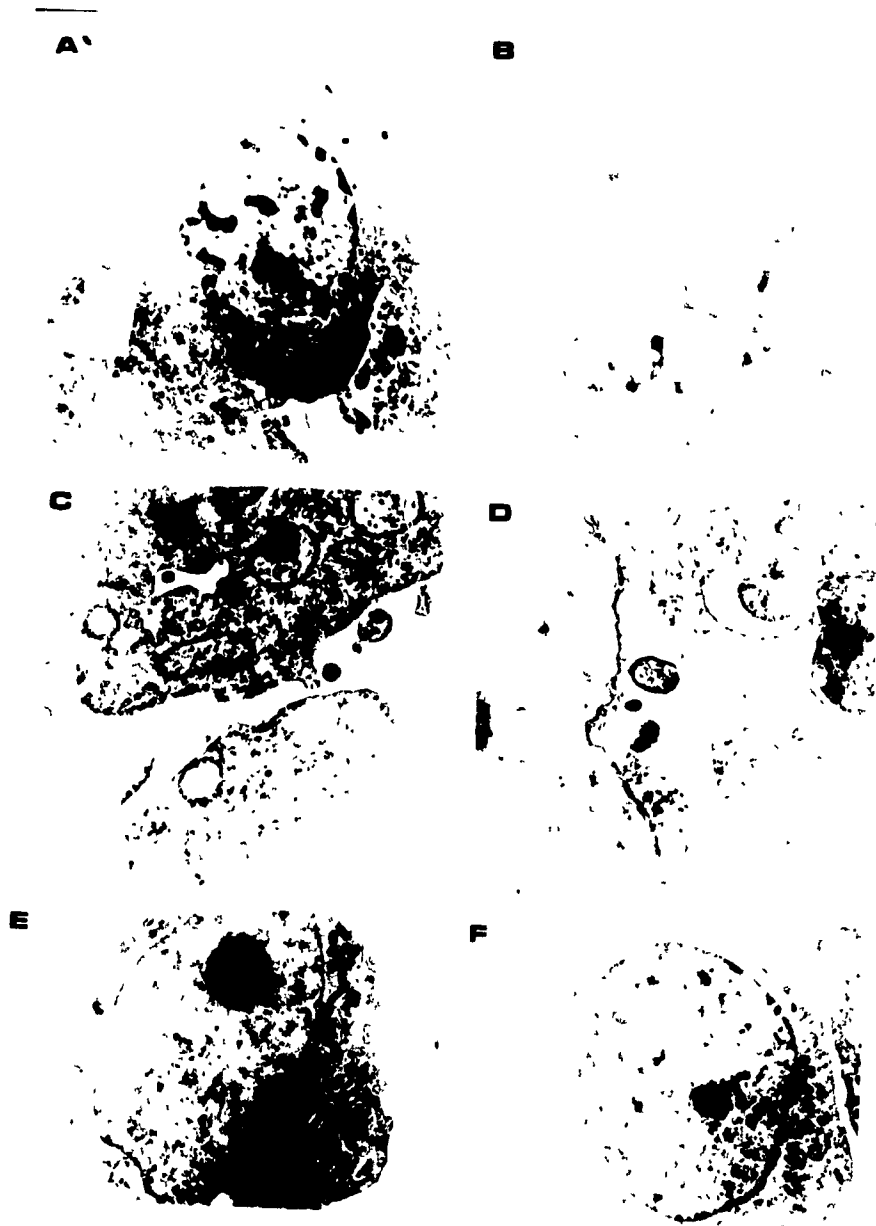
Table 13 **The number of MoAb-Au particles internalized by target cells after incubation at 37°C for various times** [1]

(A) The number of gold particles bound to cell surface or internalized [2]

Time (hr)		0 [3]	0.5	1.0	2.0	4.0	6.0
Dal B01-Au	Out	134±57.2	122±45.1	115.5±37.8	125.4±45.2	134.6±38	113.2±36.8
	In [4]	0.4±0.4	0.6±1.2	2.1±3.0	12.5±10.2	6.5±7.7	20.1±26.8
Dal B02-Au	Out	261.7±72.4	250.1±103	183.3±44.2	144.3±38.6	144.5±38.6	158.4±27.2
	In	39.2±19.8	44±24.1	63.8±9.6	62.1±18.7	53.8±13.5	57.3±16.6
Dal K29-Au	Out	28.9±13.2	20.3±7.9	19.7±8.7	23.5±10.5	22.1±6.4	17.6±7.7
	In	4.1±2.8	3.8±3.5	8.3±5.3	7.9±3.0	6.1±3.1	10.1±9.0

1. Dal B01-Au, Dal B02-Au and Dal K29-Au complexes were allowed to bind to their respective target D_{10-1} or Caki-1 cells at 4°C for 60 min. After 3 washes with cold PBS, the cells were reincubated at 37°C for up to 6 hr. At indicated intervals, aliquots of cells were taken out and processed for TEM examination (see Materials and Methods for detailed description).

2. All data represent the number of gold particles found associated with one cell and are the mean ± S.D. of the numbers counted from 15 randomly selected cells.

3. Time 0 at 37°C, i. e., at the end of incubation at 4°C.

(Continued)

(B) The percentage of cell associated gold particles that were found in the cytoplasm of the target cells [5]

Time (hr)	0	0.5	1.0	2.0	4.0	6.0
Dal B01-Au	0	0.2	1.5	8.8	6.2	14.8
Dal B02-Au	0	2.0	12.3	17.1	14.1	13.6
Dal K29-Au	0	3.3	17.2	12.8	9.2	24.1

4. "Out " represent the number of gold particles bound on cell surface, while " In" represent the number of gold particles found inside the cell.

5. The percentage of intracytoplasmic gold particles at any defined time (T) was calculated as following:

$$\frac{\text{Number of intracytoplasmic gold particles at time T - Number of intracytoplasmic gold particles at time 0}}{\text{Number of cell surface bound gold particles at time T+Number of intracytoplasmic gold particles at time T}} \times 100$$

Section 2 **Pharmacokinetics, Biodistribution and Tumor Localization of Radioiodinated Dal B01, Dal B02 and Their F(ab)'2 Fragments after Injection into Human B-cell Chronic Lymphocytic Leukemia Xenograft Bearing Nude Mice**

2.1 Immunoreactivity of Dal B01, Dal B02 and Their F(ab)'2 Fragments after Radioiodination

After radioiodination using chloramine T and purification using a NAP-10 column, the specific activity of all the antibody preparations was approximately of 0.5 to 1.0 µCi / µg protein. TCA precipitation demonstrated that more than 97% of radioactivity in antibody preparations was protein bound. The IRF and specificity of target cell binding of radioiodinated Dal B01, Dal B02 and their F(ab)'2 fragment preparations were examined in vitro using D10-1 cells. The highest IRF was obtained with Dal B02 (73.9%), followed by Dal B02 F(ab)'2 (52.7%), Dal B01 (28.3%) and Dal B01 F(ab)'2 fragment (25.5%). Iodine-125 labeled non-specific IgG2a, IgG1 and their F(ab)'2 fragments preparations were used in this study as controls respectively for Dal B01, Dal B02 and their F(ab)'2 fragments. In vitro studies showed that the binding of these non-specific Ig preparations to D10-1 cells was always less than 1% of the total radioactivity added.

2.2 Pharmacokinetics of Radiolabeled Dal B01, Dal B02 and Their F(ab)'2 Fragments in D10-1 Xenograft Bearing Nude Mice

Nude mice were inoculated s.c. with 5 to 10 x 10^6 D10-1 cells into the right flank 48 - 72 hr after receiving 400 rad TBI (see Materials and Methods for detailed description). The biodistribution studies were carried out at approximately 10 days post tumor cell inoculation, i. e., when the size of the s.c. tumors ranged from 0.5 to 0.8 g (Fig. 26). The

xenograft bearing nude mice were given i.v. via the tail vein ^{131}I labeled Dal B01, Dal B02 or their F(ab)'2 fragments mixed with ^{125}I labeled isotype-matched non-specific IgGs or their F(ab)'2 fragment preparations. Samples of blood were obtained from these mice at indicated times after the administration of radioiodinated protein preparations. The clearance of radioactivity from blood with time as the percentage of initial radioactivity is presented in Figs. 27 to 30. The kinetics of clearance from the blood of either intact antibodies or their F(ab)'2 fragments were found to follow a biphasic curve: first there was a rapid exponential decrease, and this was followed by a less steep exponential decrease. The intact MoAbs were cleared from blood much slower than their F(ab)'2 fragments. For example, at 24 hr post i.v. injection, about 22 to 30% of initial radioactivity in blood remained in the circulation after i.v. administration of radiolabeled intact Dal B01 or Dal B02, while only 2.8 to 6.0% of the initial radioactivity in blood remained in the circulation after the i.v. administration of their F(ab)'2 fragments. Calculations of pharmacokinetic parameters based on the mathematical model described in Materials and Methods confirmed that intact Dal B01 and Dal B02 had 3 to 5-fold longer half-lives (both t $1/2\alpha$ and t $1/2\beta$) than their respective F(ab)'2 fragments. These two intact MoAbs were cleared from the circulation of the nude mice 4 to 6 times slower than their F(ab)'2 fragments. Since the total dose of antibody protein given to the mice was different for each antibody preparation, no direct comparison of the AUC can be made among these antibody preparations. However, from the available AUC data (Table 14), it can be estimated that intact Dal B01 and Dal B02 had approximately 5 to 6-fold larger AUC than their respective F(ab)'2 fragments at equivalent doses of administered proteins. There was no significant difference between specific and non-specific IgG preparations, as well as between specific and non-specific F(ab)'2 fragment preparations, as regards the above pharmacokinetic parameters. Among all the four F(ab)'2 fragment preparations, non-specific Dal Br 7 F(ab)'2 fragment preparation showed the longest half-life (both t $1/2\alpha$ and t $1/2\beta$) and the lowest clearance rate (CL).

Figs. 27 to 30 also present the total body ^{131}I activity of the mice given radiolabeled antibody preparations over time as the percentage of the total ^{131}I activity administered. These results demonstrate that intact Dal B01 and Dal B02 were cleared from mouse body at a much slower rate than their respective F(ab)'2 fragments. For example, at 24 hr post i.v. injection, about 45 to 50% of the administered radioactivity was retained in the mice given ^{131}I labeled intact MoAb, but only 10 to 13% of the administered radioactivity was retained in the mice given F(ab)'2 fragments.

2.3 Biodistribution of Radiolabeled Dal B01, Dal B02 and Their F(ab)'2 Fragments after Intravenous Administration into D10-1 Xenograft Bearing Nude Mice

The biodistribution of radioiodinated Dal B01, Dal B02 and their F(ab)'2 fragments in D10-1 xenograft bearing mice is shown in Figs. 31 to 47. All the four antibody preparations, i.e., intact Dal B01, Dal B02 and their F(ab)'2 fragments showed a markedly higher percentage of the injected dose per gram tissue (% ID / g tissue) in tumors than in all other organs (except blood) at all times examined. The highest tumor localization was observed at 48 hr for intact Dal B01 and Dal B02 MoAbs (7.85 and 13.7 % ID / g tissue, for Dal B01 and Dal B02, respectively) and at 24 hr for their F(ab)'2 fragments (2.06 and 2.33 % ID / g tissue, for Dal B01 F(ab)'2 and Dal B02 F(ab)'2 fragments, respectively). The clearance of Dal B01 and Dal B02 from xenografted tumors followed the same kinetic order. At 96 and 168 hr after administration of radiolabeled antibody preparations, there were 7.3% and 2.9 % ID / g tumors in mice given ^{131}I-Dal B02, while only 4.8% and 2.1% ID / g tumors in mice given ^{131}I-Dal B01, respectively. The clearance of Dal B02 F(ab)'2 fragment from xenografted tumors was slower compared to that of Dal B01 F(ab)'2 fragment. At 72 and 120 hr after administration, there were 0.83% and 0.2% ID / g tumors in mice given Dal B02 F(ab)'2 fragment, while only 0.34% and 0.11% ID / g tumors in

mice given Dal B01 F(ab)'2 fragment, respectively. On comparing the rate of clearance of tumor-localized antibody, it was found that the F(ab)'2 fragments were cleared from the xenografted tumor at a faster rate than their respective parent intact antibody.

Compared to their respective isotype-matched non-specific IgGs, both Dal B01 and Dal B02 showed a significantly higher % ID / g in D10-1 xenografts, although the distribution in normal organs of these preparations (i. e., either specific MoAbs or non-specific IgGs), was quite similar. Furthermore, the tumor localization of both Dal B01 F(ab)'2 fragment and Dal B02 F(ab)'2 fragments was also significantly higher than their respective isotype-matched IgG F(ab)'2 fragments. When the tumor to normal tissue ratios (T / NT ratios) were calculated (Figs. 31 to 47), the specific Dal B01, Dal B02 and their F(ab)'2 fragments showed much higher T / NT ratios than their non-specific counterparts. For intact Dal B01 and Dal B02, the T / NT ratios usually increased over time, indicating that the clearance of these two specific MoAbs from xenografts was relatively slower than their clearance from normal mouse tissues. The highest T / NT ratios were obtained at 168 hr (i. e., the period of observation in the study) after the i.v. administration of these two intact MoAbs. For both Dal B01 F(ab)'2 and Dal B02 F(ab)'2 fragments, the highest T / NT ratios were obtained between 48 to 72 hr after antibody administration. These T / NT ratios decreased with time till the end of the observation period of 120 hr.

All the above data suggest that the tumor localization of Dal B01, Dal B02 and their F(ab)'2 fragments is tumor specific. This was further confirmed by the calculation of localization indices (LI). As shown in Figs. 34, 38, 42 and 47, the LI of these specific antibody preparations in tumor is always greater than 3.0 (except Dal B01 F(ab)'2 at 120 hr), indicating a high specificity of tumor localization of Dal B01, Dal B02 and their F(ab)'2 fragments. Among the four specific antibody preparations, the LI of Dal B02 and its

corresponding F(ab)'2 fragment were higher than that of Dal B01 and its corresponding F(ab)'2 fragment, respectively.

2.4 Gamma-Camera Imaging of Xenografted D10-1 Tumors

Gamma camera images of D10-1 xenografts were obtained at 24, 48 and 72 hr after i.v. administration of ^{131}I-labeled F(ab)'2 fragments, and at 24, 48, 72, 96 and 192 hr after i.v. administration of ^{131}I labeled intact antibodies. A clear tumor image with moderate background activity was obtained at 24 hr after injection of ^{131}I-Dal B02 F(ab)'2 fragment (Fig. 48A). The image of the tumor became more clear at 48 hr as the radioactivity in blood and other normal organs decreased further (Fig. 48B). However, at 72 hr, the total amount of radioactivity in the tumor was too low to produce a defined tumor image (Fig. 48C). After the administration of ^{131}I-Dal B02, a poorly defined image of the tumor with high background activity could be obtained at 24 hr (Fig. 49A). From day 2 to day 8, the tumor images became increasingly clear as the radioactivity in blood and other normal organs decreased (Figs. 49B, 49C and 49D). At Day 8, excellent, sharply defined tumor images were obtained (Fig. 49D).

The quality of tumor images obtained with ^{131}I-Dal B01 was not as good as that obtained with Dal B02. As shown in Figs. 50A to D, tumors could be seen at 48 hr after antibody administration and the images became increasingly clear with time. However, even at Day 8, the background radioactivity was still quite high compared to that in mice given ^{131}I-Dal B02 (Fig. 50D). Dal B01 F(ab)'2 failed to yield clear tumor images at all time points (i.e., 24, 48 and 72 hr post i.v. administration of ^{131}I labeled fragment) examined (Fig. 51A to C)

2.5 Reactivity of MoAbs Recovered from the Serum of D10-1 Xenograft Bearing Nude Mice

After elution from a NAP-10 column, all samples of serum obtained form D10-1 xenograft bearing nude mice injected i.v. with radioiodinated MoAb preparations yielded a single radioactive fraction. The elution profile of above samples of serum was identical with that of the parent MoAb preparations, indicating that there was no detectable free radioactive iodine or radioiodine-containing small fragments in the circulation at the time of obtaining the samples of serum. There was about a 30 to 50% decrease in the IRF of the serum-derived MoAb fractions compared to that of the parent MoAb preparations.

2.6 Autoradiography of Xenografted D10-1 Tumors after the Administration of ^{131}I Labeled Dal B01, Dal B02 or Their F(ab)'2 Fragments

At 96 hr after i.v.administration of ^{131}I labeled intact Dal B01 or Dal B02, or 48 hr after the administration of ^{131}I labeled Dal B01 F(ab)'2 fragment or Dal B02 F(ab)'2 fragment, two mice in each group were sacrificed. The xenografted tumors were taken out and cryostat sections (5 μm thick) were cut. After fixation in formaldehyde vapor overnight, the sections were subjected to autoradiography. Figs. 52 and 53 show the microautoradiographs of cryostat sections of these tumor tissues. Clusters of high grain density were observed on tumor cell surface as well as in the intercellular matrix. These results indicate the accessibility of tumor cells in the s. c. D10-1 xenografts to i.v. administered radiolabeled Dal B01, Dal B02 and their F(ab)'2 fragments.

In conclusion, both Dal B01, Dal B02 and their F(ab)'2 fragments have been shown to have a large number of binding sites on D10-1 cells (i.e., 10 to 12 million binding sites per

cell) with high Ka of binding (i.e., 6.8 to 12.7 x 10^9 M^{-1}). Upon injection into D$_{10-1}$ xenograft bearing nude mice, these antibodies showed selective localization in tumor xenografts. The F(ab)'2 fragments were cleared from the xenograft bearing nude mice at a much faster rate than their parent MoAbs. The absolute amounts of antibody that localized in tumors were higher for the two intact MoAbs than their respective F(ab)'2 fragments. Excellent tumor images were obtained in D$_{10-1}$ xenograft bearing nude mice using ^{131}I-labeled intact Dal B02 or its F(ab)'2 fragment. Based on these results, Dal B02 may be potentially useful for the radioimmunodetection and radioimmunotherapy of human B-cell CLL.

Fig. 26

Photograph of a nude mouse bearing a s.c. D10-1 tumor in its right flank.

Nude mice were inoculated s.c. with 5×10^6 D10-1 cells 48 to 72 hr after 400 rad TBI. Hundred percent of nude mice developed a s.c. solid tumor at the site of inoculation within 7 to 10 days. Biodistribution studies of radiolabeled Dal B01, Dal B02 and their F(ab)'2 fragments were carried out at about 10 days after tumor inoculation, when the size of the tumors ranged from 0.5 to 0.8 g.

Fig. 26

Figs. 27 to 30

Clearance of radioiodinated Dal B01, Dal B02 and their F(ab)'2 fragments in D10-1 xenograft bearing nude mice.

D10-1 xenograft bearing nude mice were given i.v. ^{131}I labeled specific Dal B01, Dal B02 or their F(ab)'2 fragments mixed as appropriate with ^{125}I labeled isotype-matched non-specific IgGs or their F(ab)'2 fragments. At indicated intervals, samples of blood were obtained from the mice and ^{131}I and ^{125}I activities in the blood were determined using a dual-window gamma counter. The total body ^{131}I activity of the mice was also monitored using a whole body gamma counter.

Fig. 27 The clearance of radioiodinated Dal B01 in D10-1 xenograft bearing nude mice.

(A) Clearance of ^{131}I and ^{125}I activities from blood;

(B) Clearance of total body ^{131}I activity.

Fig. 28 The clearance of radiolabeled Dal B01 F(ab)'2 fragment in D10-1 xenograft bearing nude mice. --- Clearance of ^{131}I and ^{125}I activities from blood;

Fig. 29 The clearance of radiolabeled Dal B02 in D10-1 xenograft bearing nude mice.

(A) Clearance of ^{131}I and ^{125}I activities from blood;

(B) Clearance of total body ^{131}I activity.

Fig. 30 The clearance of radiolabeled Dal B02 F(ab)'2 fragment in D10-1 xenograft bearing nude mice.

(A) Clearance of ^{131}I and ^{125}I activities from blood;

(B) Clearance of total body ^{131}I activity.

Fig. 27A

Fig. 27B

Radioactivity in blood
(% of initial activity)

Time (hr)

Fig. 28

Br-7 F(ab)'2

B01 F(ab)'2

Total body radioactivity
(% of initial activity)

Radioactivty in blood
(% of initial acuvity)

Fig. 29B

Fig. 29A

Time (hr)

Time (hr)

Dal B02

Dal B02

IgG1

**Total body radioactivity
(% of initial activity)**

Fig. 30B

Time (hr)

□ B02 F(ab)'2

**Radioactivity in blood
(% of initial activity)**

Fig. 30A

Time (hr)

□ B02 F(ab)'2

♦ IgG1 F(ab)'2
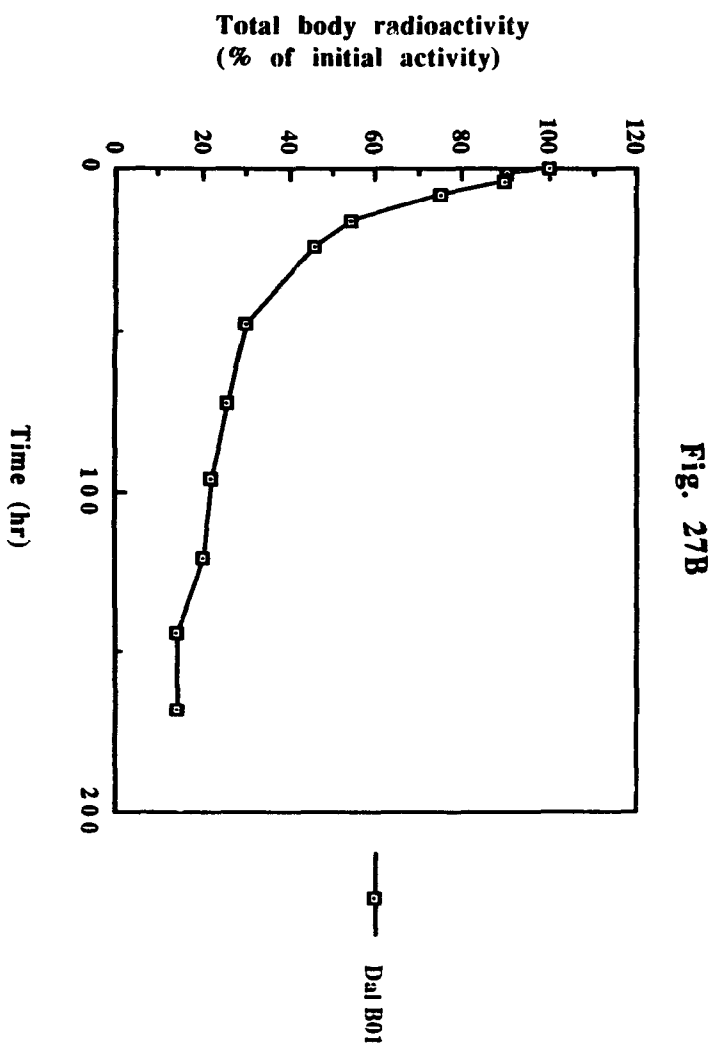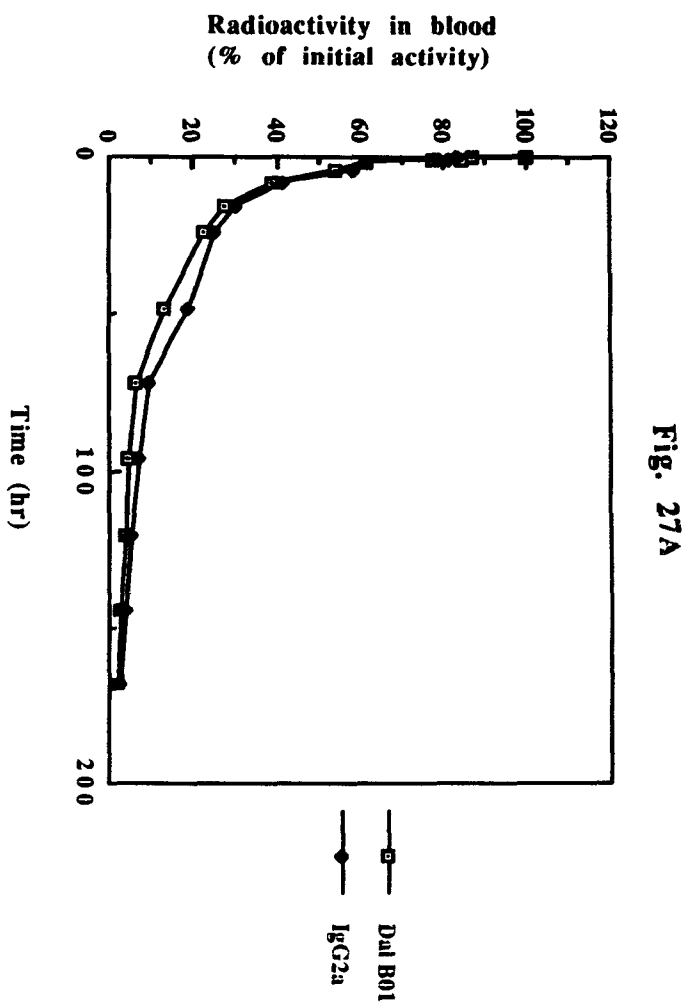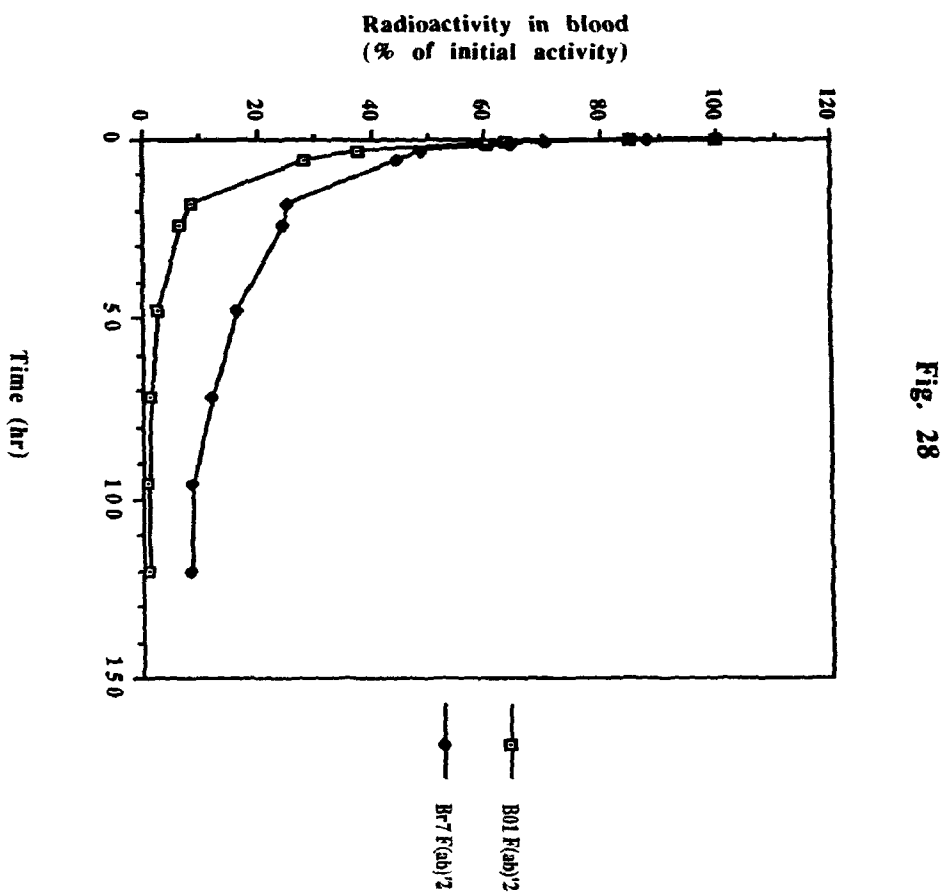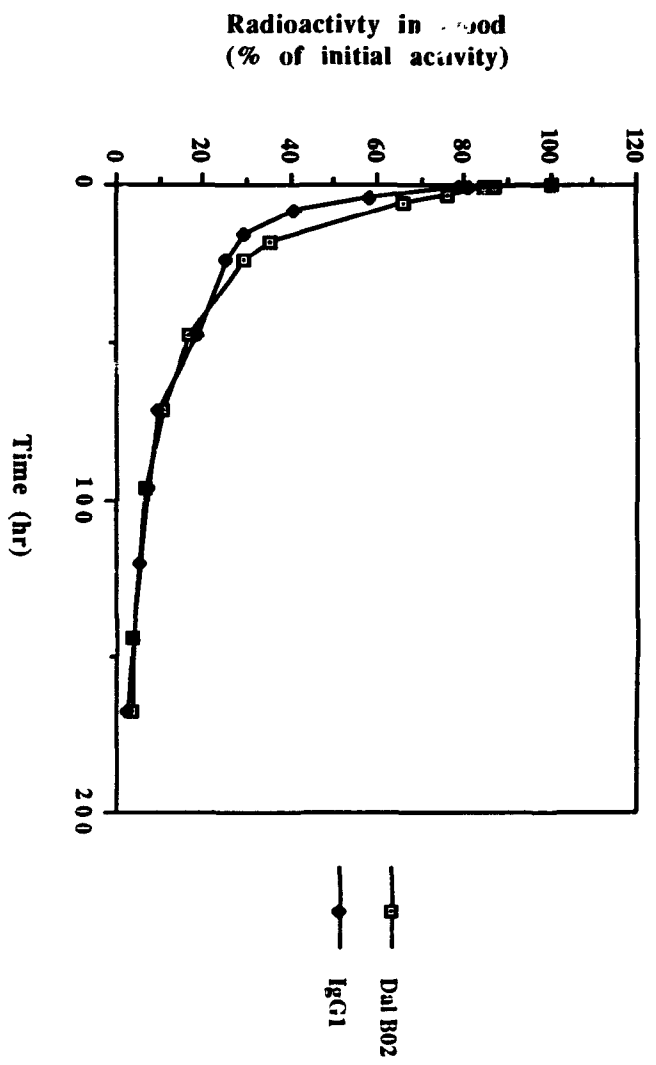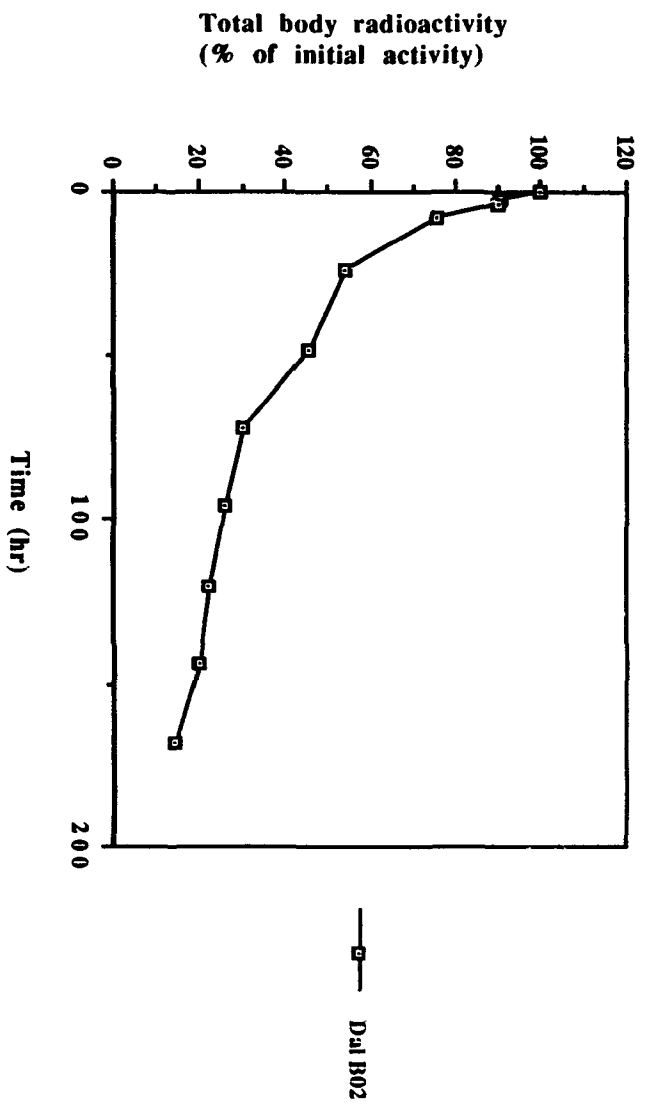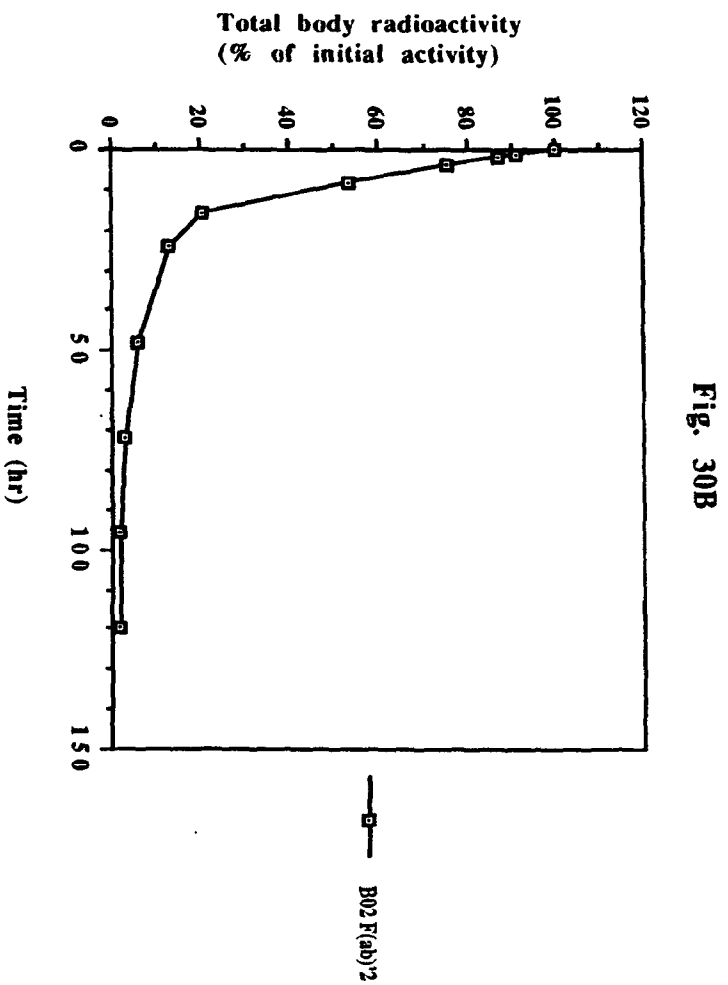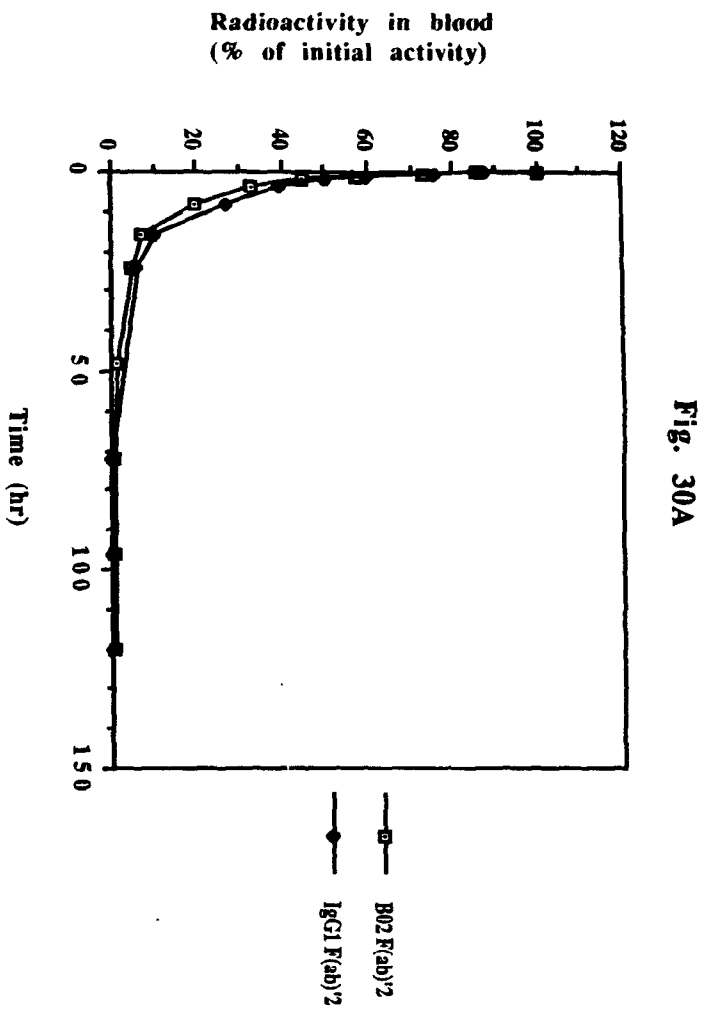
Table 14 Pharmacokinetic parameters of intravenously (i.v.) injected radioiodinated antibodies and their F(ab)'2 fragments in D10-1 xenograft bearing nude mice [1]

Antibody	Vd (ml)	T1/2α (hr)	T1/2β (hr)	AUC (μCi·h/ml)	CL (μl/h)
Dal B01 [2]	3.80 [3]	1.53	25.1	343.7	105
IgG2a	4.15	2.01	36.4	50.6	80
Dal B02	4.38	2.60	39.1	656	61.2
Dal B01 F(ab)'2	4.39	0.42	7.28	37.9	417
Dal Br 7 F(ab)'2	6.42	0.53	30.8	34.5	145
Dal B02 F(ab)'2	3.53	0.50	5.83	121.5	420
IgG1 F(ab)'2	3.09	0.44	6.82	74.7	315

1. D10-1 xenograft bearing mice were given ^{131}I labeled specific MoAbs or their F(ab)'2 fragments mixed with ^{125}I labeled isotype-matched non-specific IgGs or their F(ab)'2 fragments. Samples of blood were obtained at defined intervals and ^{131}I and ^{125}I activities in the blood were determined using a dual-window gamma counter.

2. Radioactivity given to mice were: (i) Dal B01 (30 μCi) plus non-specific IgG2a (5 μCi); (ii) Dal B02 (50 μCi) plus non-specific IgG1 (10 μCi); (iii) Dal B01 F(ab)'2 (15 μCi) plus Dal Br 7 F(ab)'2 (5 μCi); (iv) Dal B02 F(ab)'2 (50 μCi) plus non-specific IgG1 F(ab)'2 (25 μCi). Dal Br 7 is an anti-human breast carcinoma MoAb of the IgG2b subclass that does not bind to D10-1 cells.

3. All parameters were calculated from the mean values of antibody concentrations in the blood of 3 mice obtained at defined intervals (see Methods section 7.3 for a detailed description).

Figs. 31 to 34

Biodistribution of radioiodinated Dal B01 after i.v. injection into D10-1 xenograft bearing nude mice.

D10-1 xenograft bearing nude mice were given ^{131}I labeled Dal B01 (IRF 28.3%) mixed with an ^{125}I labeled isotype-matched non-specific IgG1 i.v. . Groups of 3 mice were sacrificed at 48, 96 and 168 hr post antibody administration. The xenografted tumor and normal mouse tissues were taken out, weighed and tissue associated ^{131}I and ^{125}I activities were determined using a dual-window gamma counter. The % ID / g tissue and the T / NT ratios were then calculated as described in Methods section 7.4.

Fig. 31 Biodistribution of radioiodinated Dal B01 in D10-1 xenograft bearing mice at 48 hr after antibody administration.   (A) % ID / g tissue;   (B) T / NT ratios.

Fig. 32 Biodistribution of radioiodinated Dal B01 in D10-1 xenograft bearing mice at 96 hr after antibody administration.   (A) % ID / g tissue;   (B) T / NT ratios.

Fig. 33 Biodistribution of radioiodinated Dal B01 in D10-1 xenograft bearing mice at 168 hr after antibody administration.   (A) % ID / g tissue;   (B) T / NT ratios.

Fig. 34 The localization index (LI) of radioiodinated Dal B01 in D10-1 tumor-bearing nude mice at 48, 96 and 168 hr after antibody administration.

Fig. 31A

Fig. 31B

Fig. 32A

Fig. 32A

Fig. 32B

Fig. 32B

Fig. 33A

% ID / g tissue

Fig. 33B

T / NT Ratio

Fig. 34

Localization Index (LI)
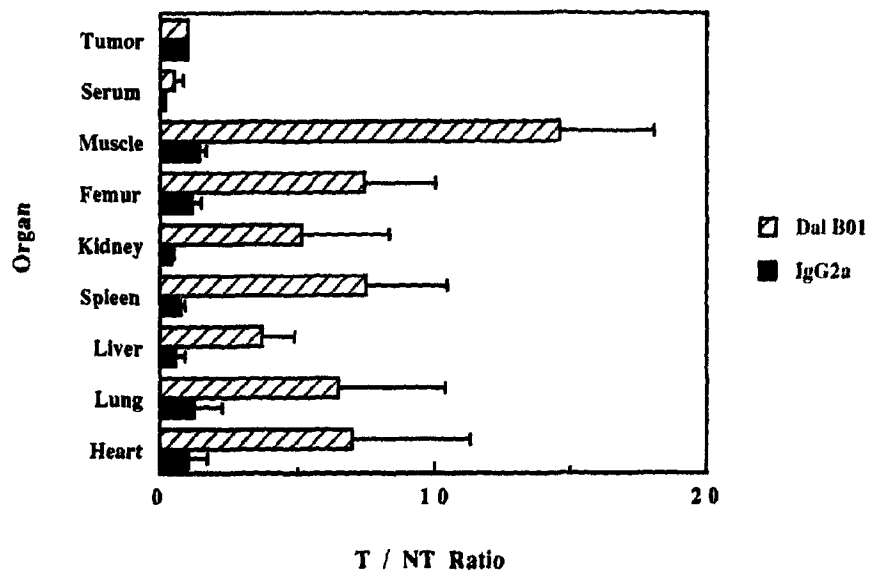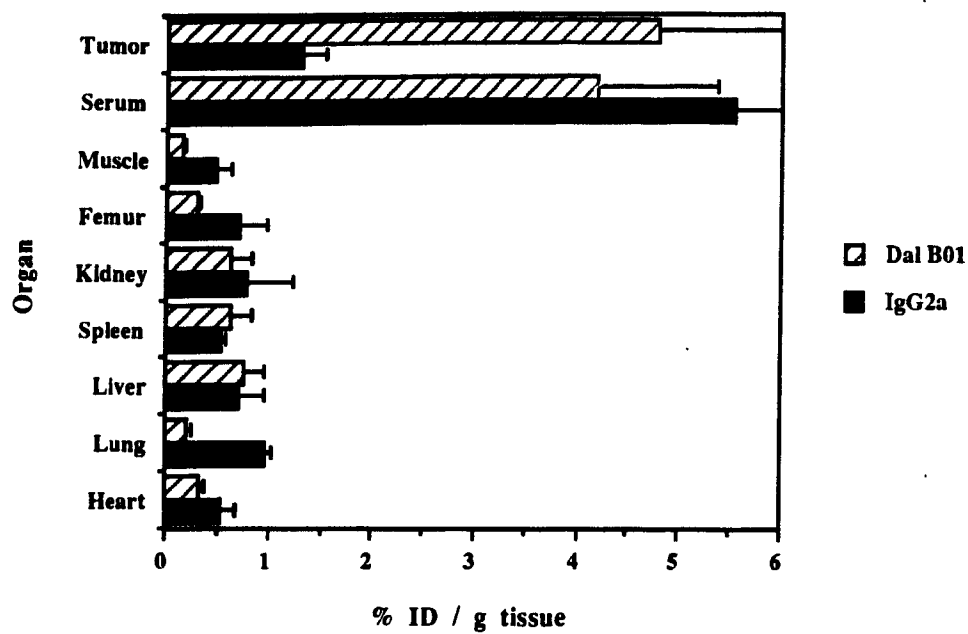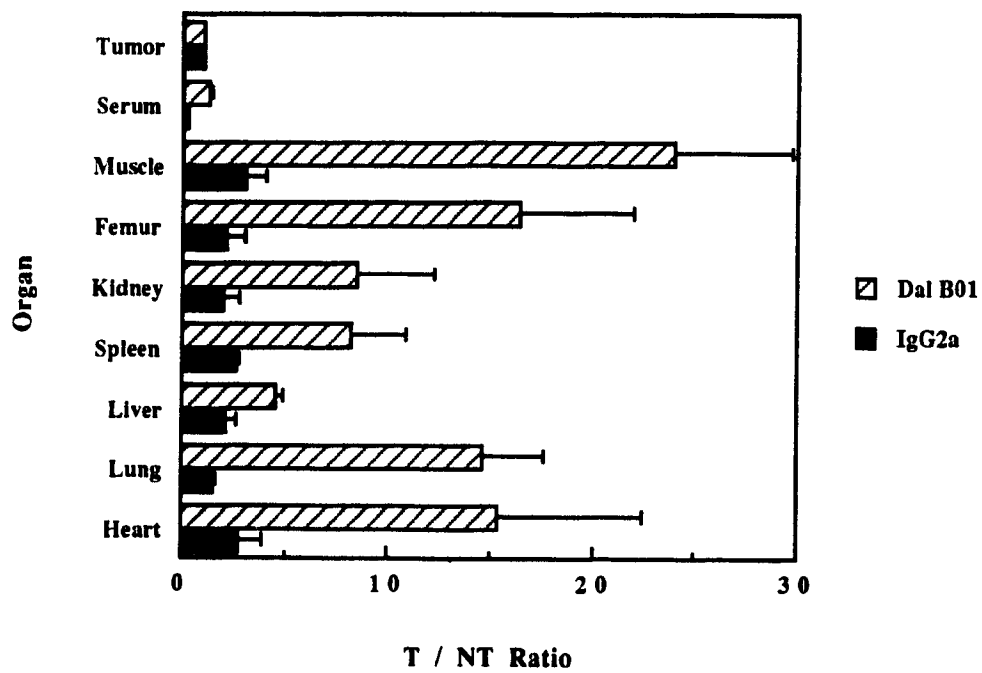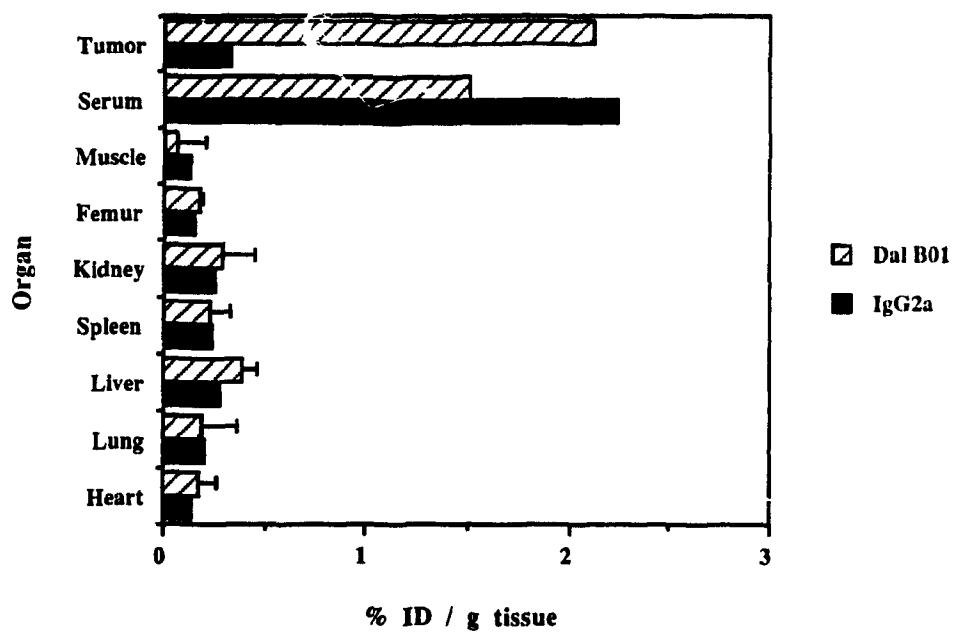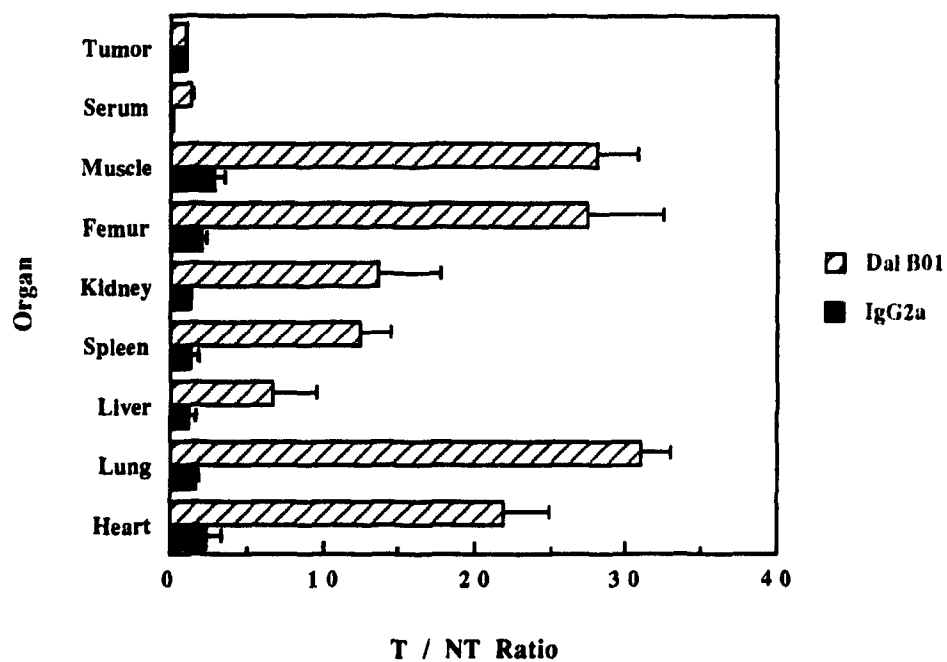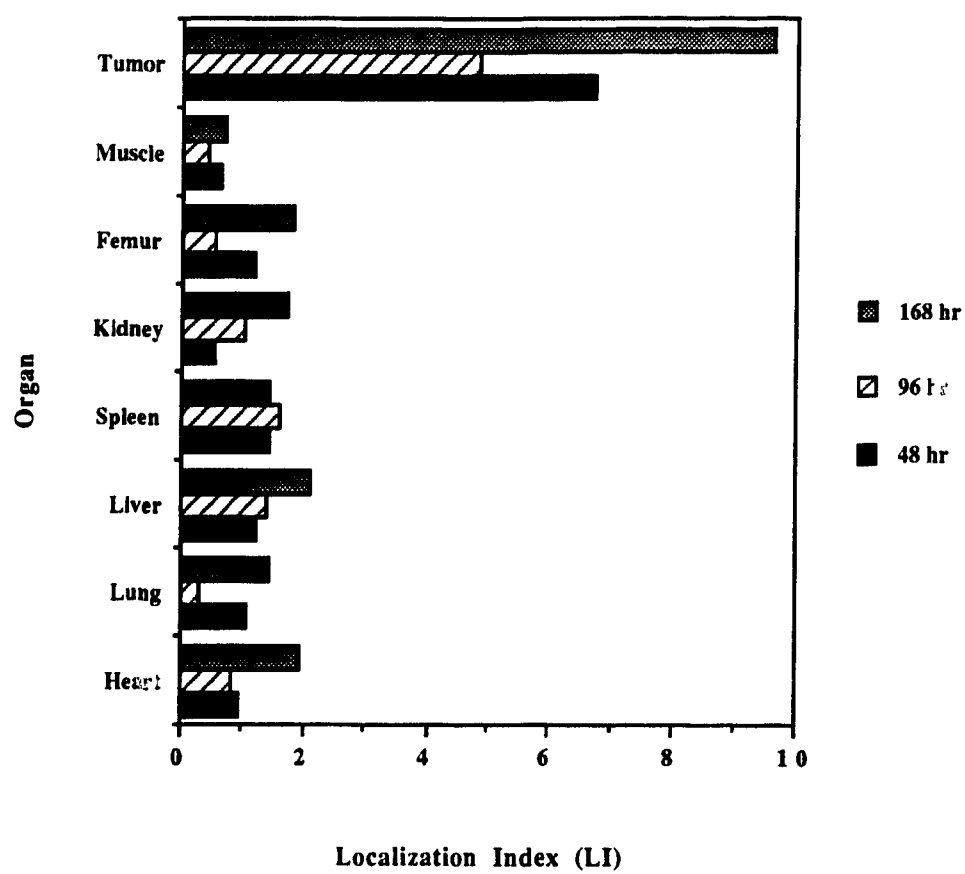
Figs. 35 to 38

Biodistribution of radioiodinated Dal B01 F(ab)'2 fragment after i.v. injection into D10-1 xenograft bearing nude mice.

D10-1 xenograft bearing nude mice were given ^{131}I labeled Dal B01 F(ab)'2 fragment (IRF 25.5%) mixed with an ^{125}I labeled IgG2b F(ab)'2 fragment (i. e., Br 7 F(ab)'2 fragment) i.v.. Groups of 3 mice were sacrificed at 24, 72 and 120 hr post antibody administration. The xenografted tumor and normal mouse tissues were taken out, weighed and tissue associated ^{131}I and ^{125}I activities were determined using a dual-window gamma counter. The % ID / g tissue and the T / NT ratios were then calculated as described in Methods section 7.4.

Fig. 35 Biodistribution of radioiodinated Dal B01 F(ab)'2 fragment in D10-1 xenograft bearing mice at 24 hr after antibody administration. (A) % ID / g tissue; (B) T / NT ratios.

Fig. 36 Biodistribution of radioiodinated Dal B01 F(ab)'2 fragment in D10-1 xenograft bearing mice at 72 hr after antibody administration. (A) % ID / g tissue; (B) T / NT ratios.

Fig. 37 Biodistribution of radioiodinated Dal B01 F(ab)'2 fragment in D10-1 xenograft bearing mice at 120 hr after antibody administration. (A) % ID / g tissue; (B) T / NT ratios.

Fig. 38 The localization index (LI) of radioiodinated Dal B01 F(ab)'2 fragment in D10-1 xenograft bearing nude mice at 24, 72 and 120 hr after antibody administration.

Fig. 35A

% ID / g tissue

Legend:
- B01 F(ab)'2
- Br7 F(ab)'2

Fig. 35B

T / NT Ratio

Legend:
- B01 F(ab)'2
- Br7 F(ab)'2

Fig. 36A

Fig. 36B

Fig. 37A

% ID / g tissue

Legend:
- B01 F(ab)'2 (hatched)
- Br7 F(ab)'2 (black)

Fig. 37B

T / NT Ratio

Legend:
- B01 F(ab)'2 (hatched)
- Br7 F(ab)'2 (black)

Fig. 38

Localization Index (LI)
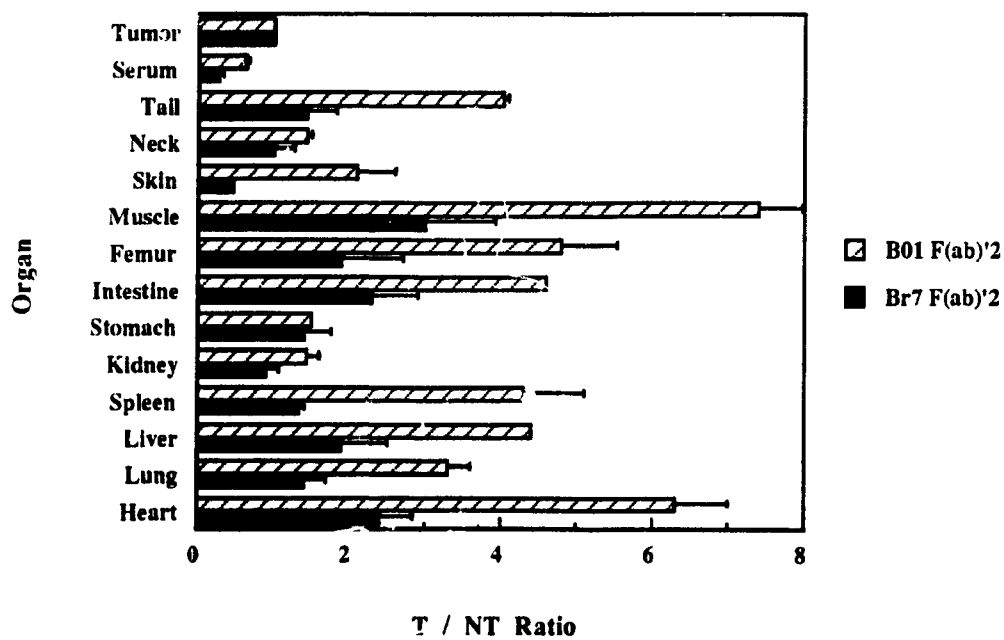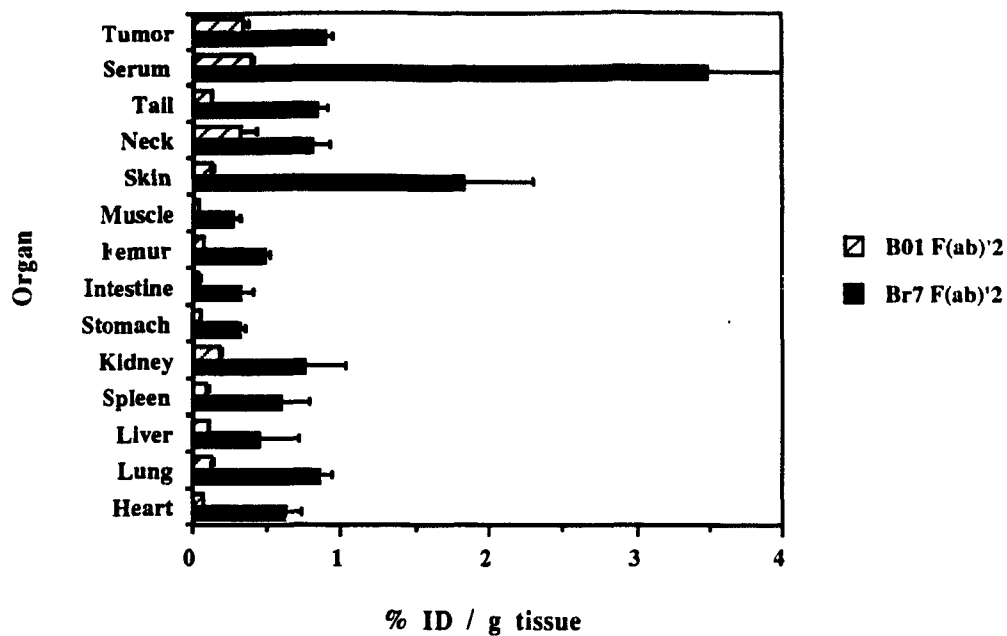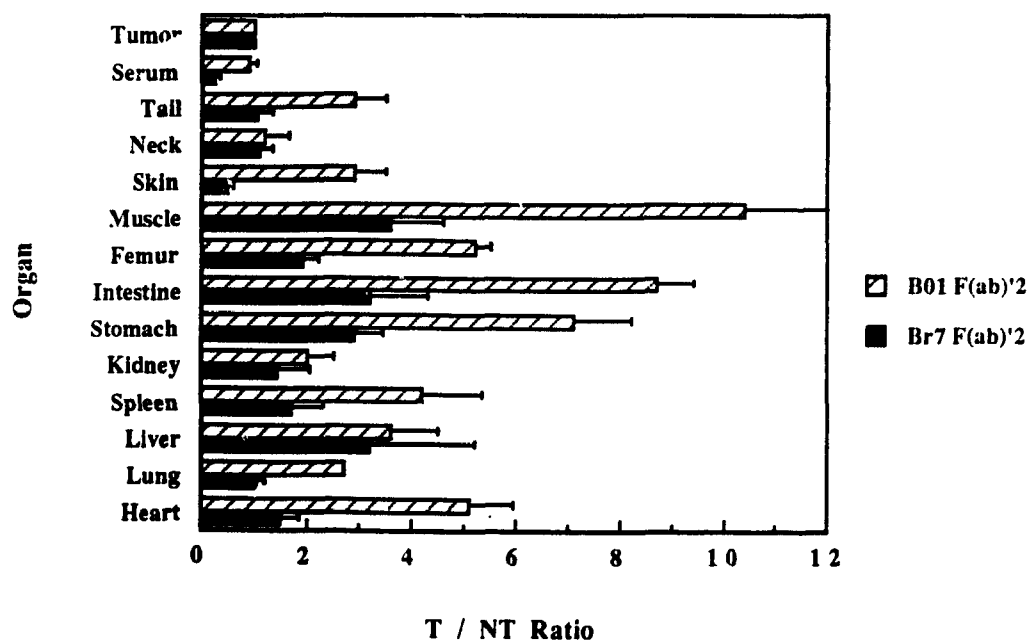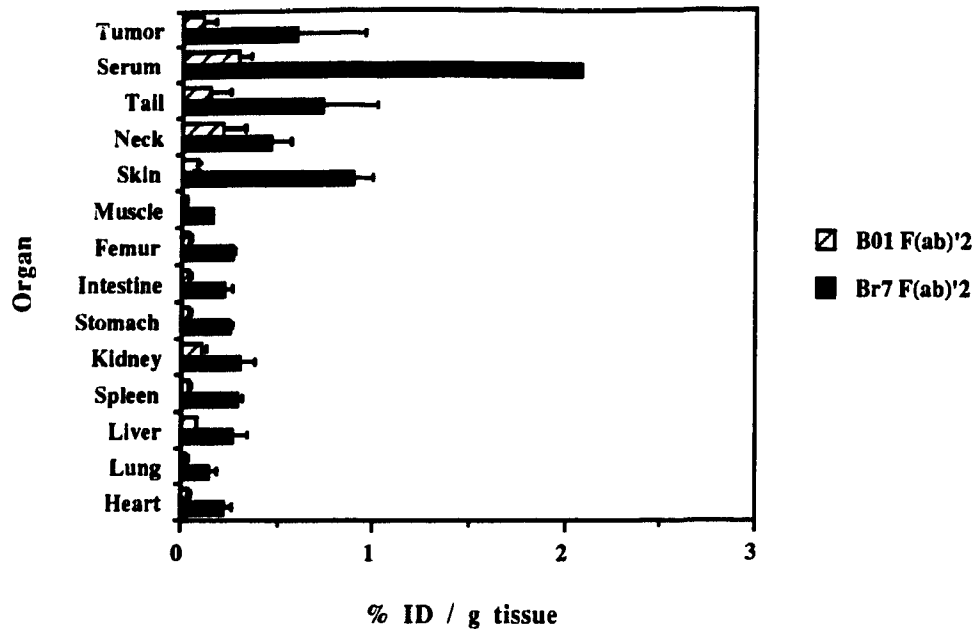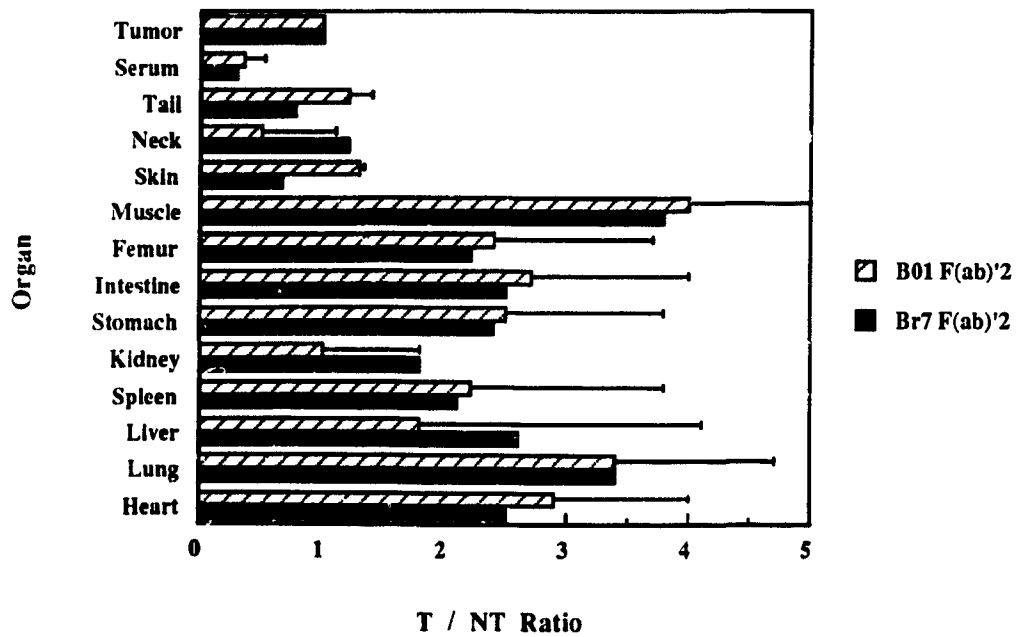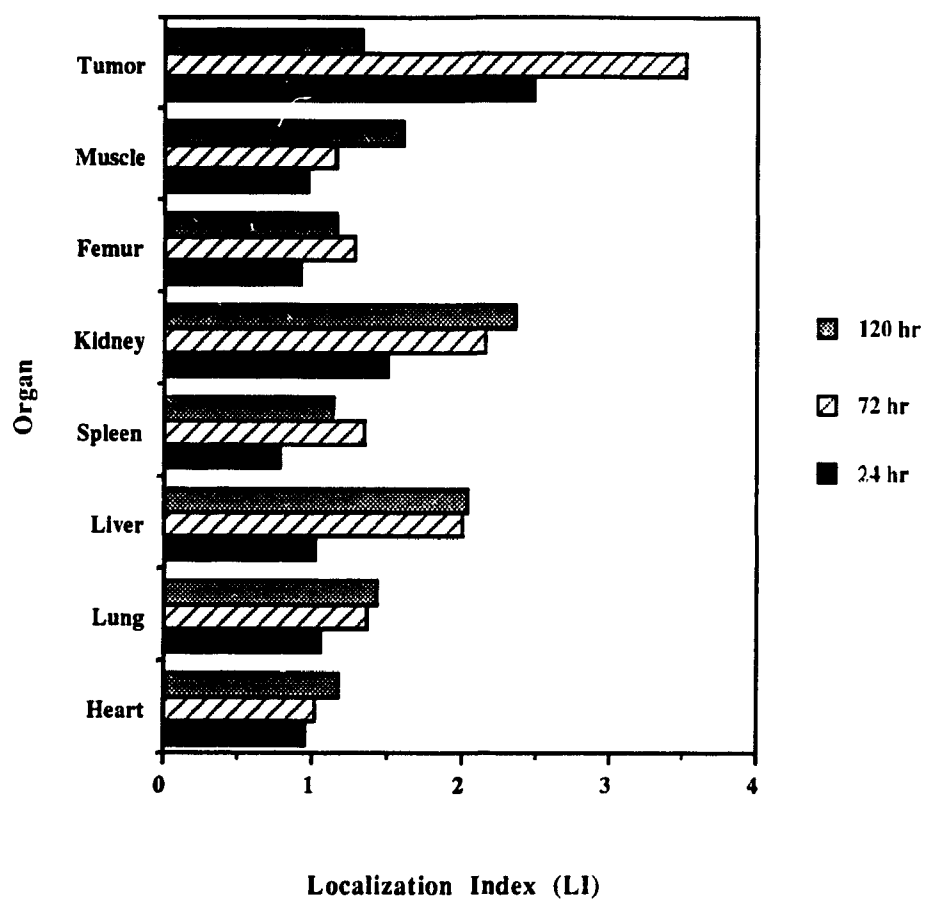
Figs. 39 to 42

Biodistribution of radioiodinated Dal B02 after i.v. injection into $D_{10\text{-}1}$ xenograft bearing nude mice.

$D_{10\text{-}1}$ xenograft bearing nude mice were given ^{131}I labeled Dal B02 (IRF 73.9%) mixed with an ^{125}I labeled isotype-matched non-specific IgGi i.v. . Groups of 3 mice were sacrificed at 48, 96 and 168 hr post antibody administration. The xenografted tumor and normal mouse tissues were taken out, weighed and tissue associated ^{131}I and ^{125}I activities were determined using a dual-window gamma counter. The % ID / g tissue and the T / NT ratios were then calculated as described in Methods section 7.4.

Fig. 39 Biodistribution of radioiodinated Dal B02 in $D_{10\text{-}1}$ xenograft bearing mice at 48 hr after antibody administration.   (A) % ID / g tissue;   (B) T / NT ratios.

Fig. 40 Biodistribution of radioiodinated Dal B02 in $D_{10\text{-}1}$ xenograft bearing mice at 96 hr after antibody administration.   (A) % ID / g tissue;   (B) T / NT ratios.

Fig. 41 Biodistribution of radioiodinated Dal B02 in $D_{10\text{-}1}$ xenograft bearing mice at 168 hr after antibody administration.   (A) % ID / g tissue;   (B) T / NT ratios.

Fig. 42 The localization index (LI) of radioiodinated Dal B02 in $D_{10\text{-}1}$ xenograft bearing nude mice at 48, 96 and 168 hr after antibody administration.
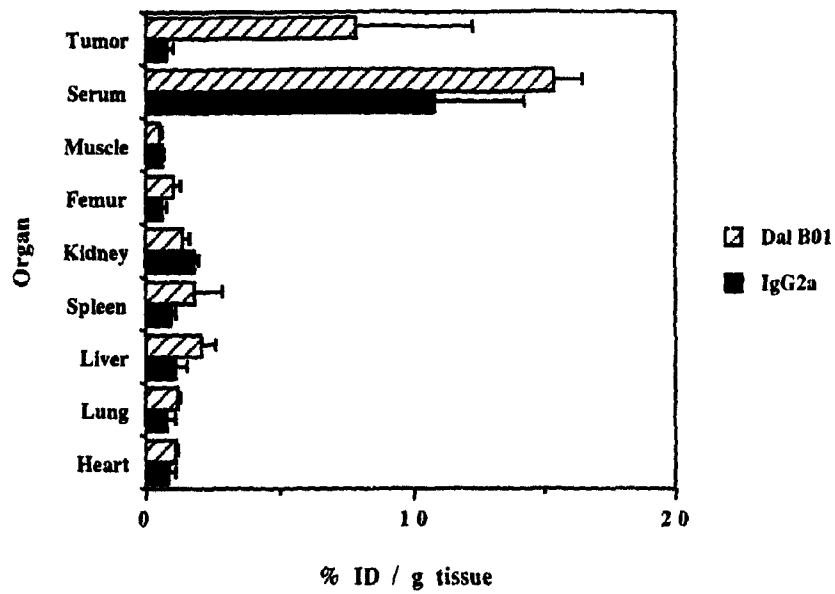
Fig. 39A

% ID / g tissue

☑ Dal B02
■ IgG1

Fig. 39B

T / NT Ratio

☑ Dal B02
■ IgG1

Fig. 40A

% ID / g tissue

Fig. 40B

T / NT Ratio

Fig. 41A

Dal B02
IgG1

% ID / g tissue

Organ

Tumor
Serum
Muscle
Femur
Kidney
Spleen
Liver
Lung
Heart

0   1   2   3

Fig. 41B

Dal B02
IgG1

T / NT Ratio

Organ

Tumor
Serum
Muscle
Femur
Kidney
Spleen
Liver
Lung
Heart

0   1 0   2 0

Fig. 42

Localization Index (LI)
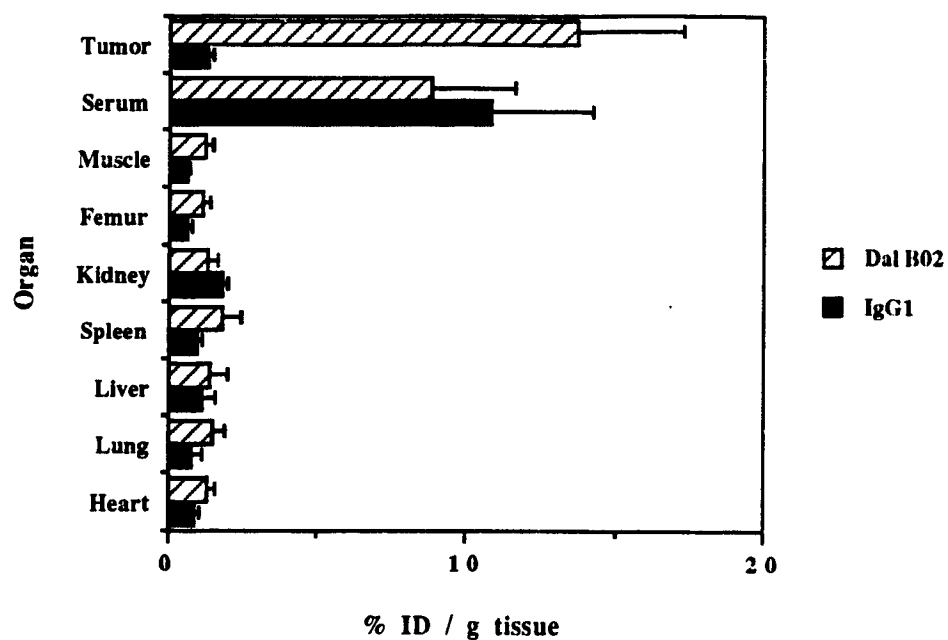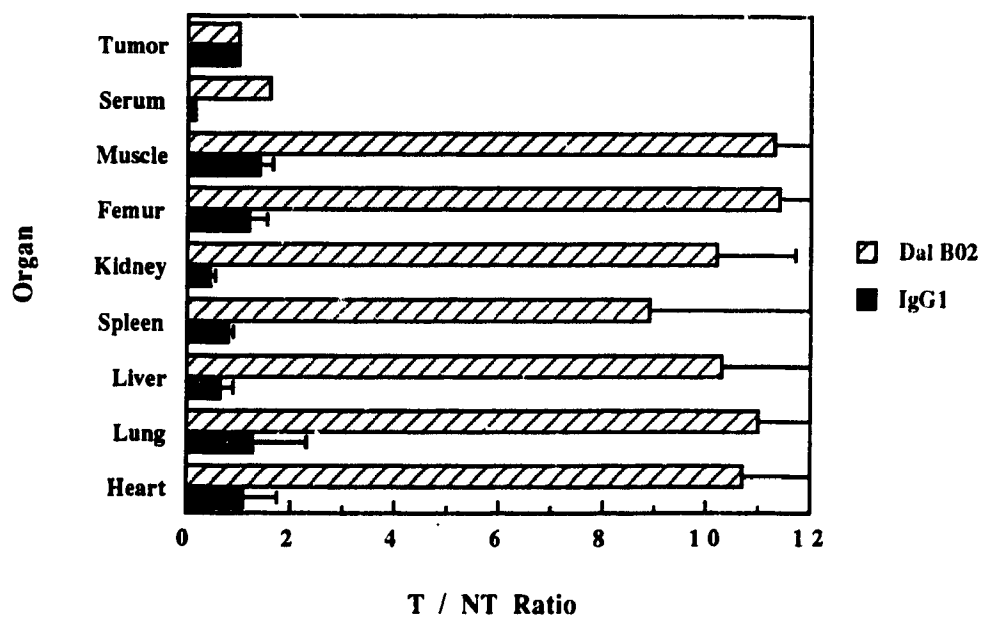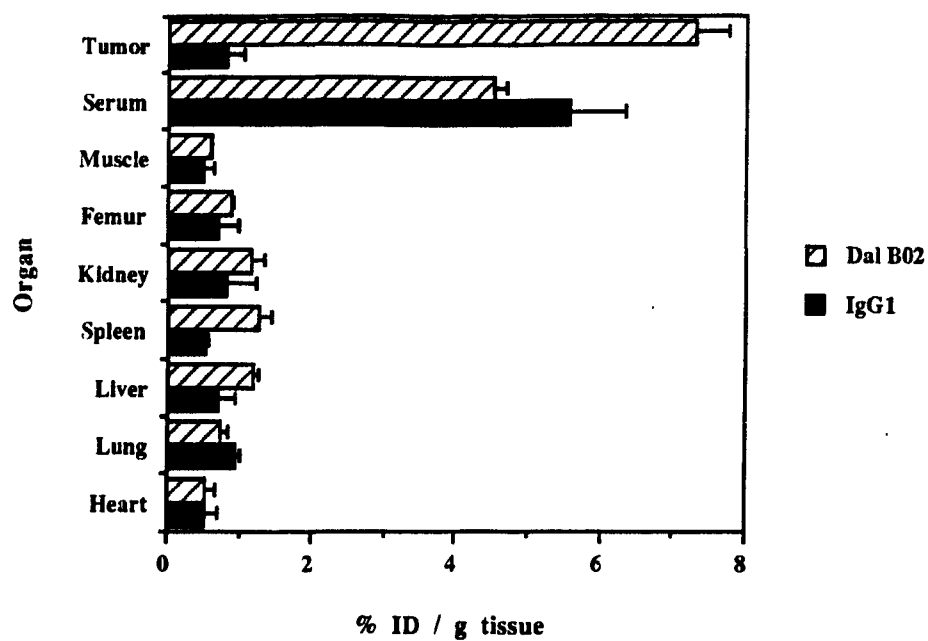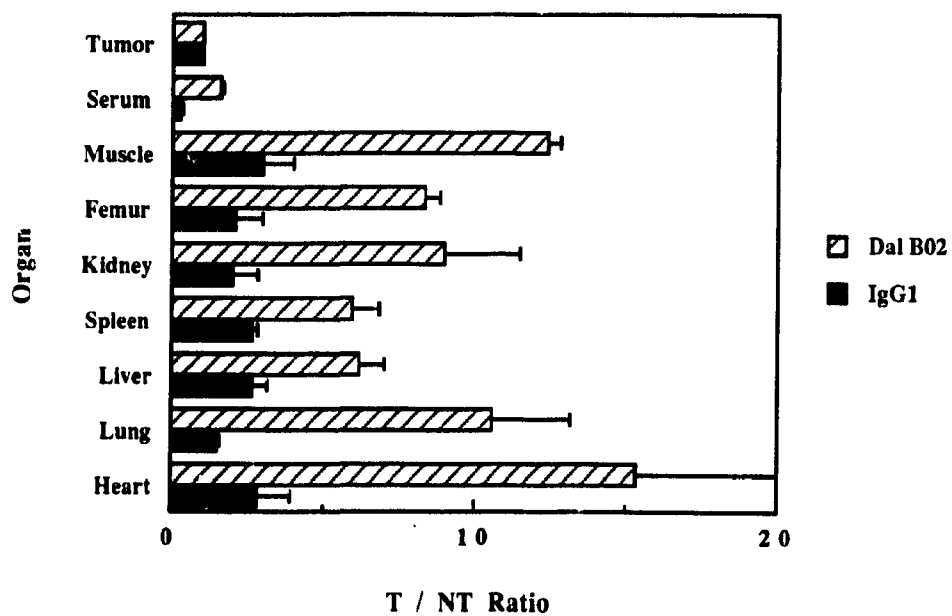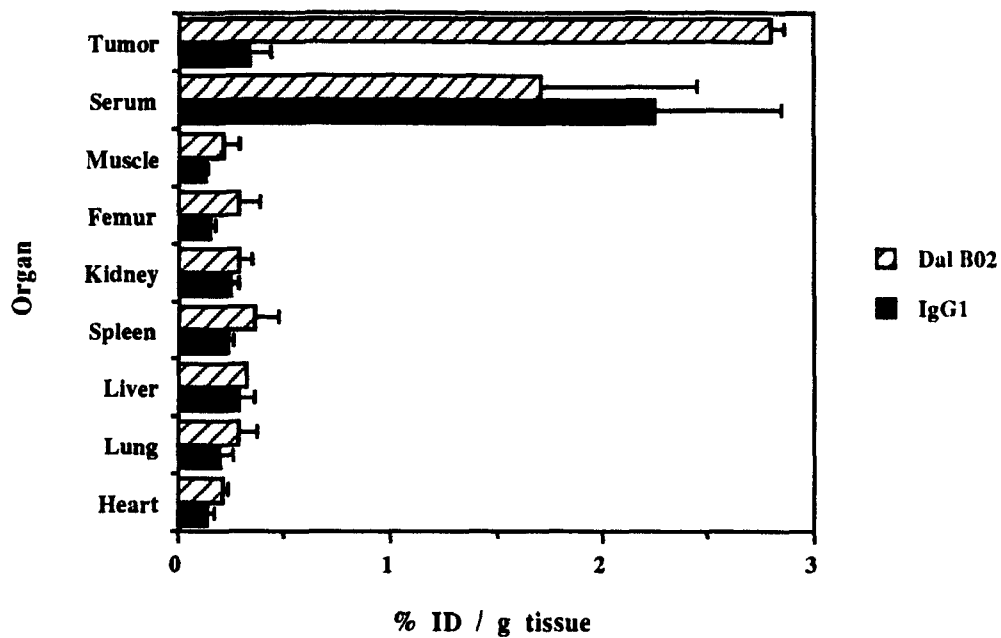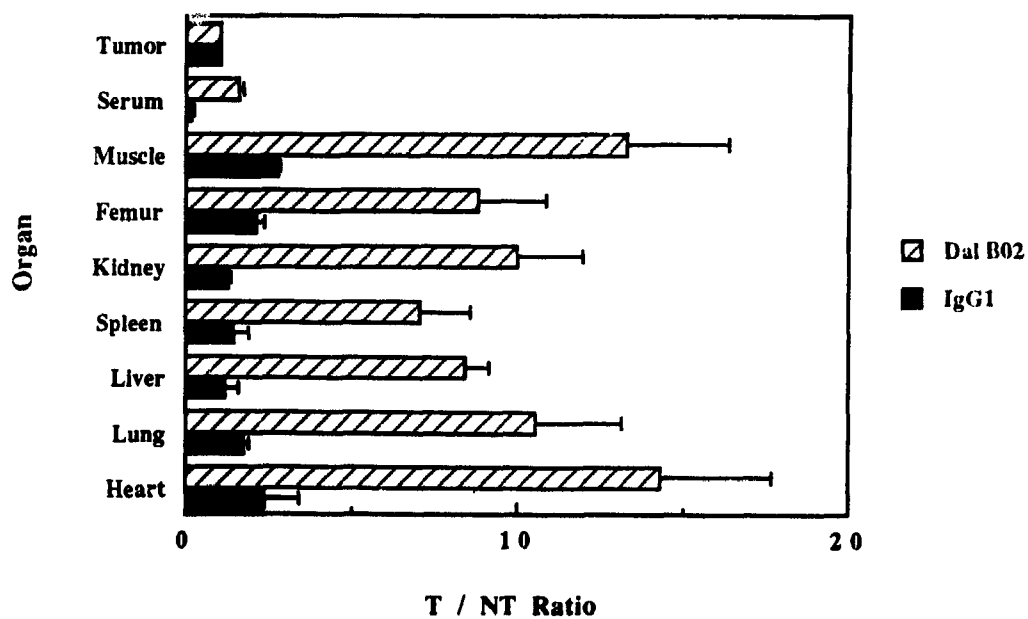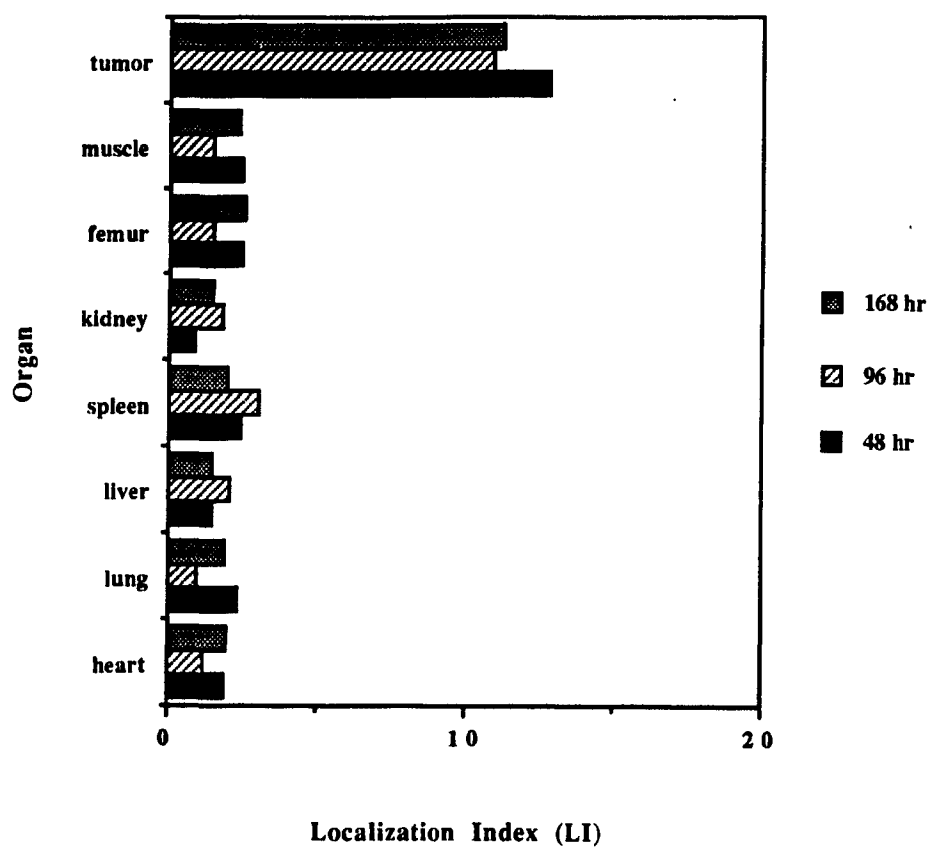
Figs. 43 to 47

Biodistribution of radioiodinated Dal B02 F(ab)'2 fragment after i.v. injection into D10-1 xenograft bearing nude mice.

D10-1 xenograft bearing nude mice were given ^{131}I labeled Dal B01 F(ab)'2 fragment (IRF 52.7%) mixed with an ^{125}I labeled isotype-matched non-specific IgG1 F(ab)'2 fragment i.v.. Groups of 3 mice were sacrificed at 24, 48, 72 and 120 hr post antibody administration. The xenografted tumor and normal mouse tissues were taken out, weighed and tissue associated ^{131}I and ^{125}I activities were determined using a dual-window gamma counter. The % ID / g tissue and the T / NT ratios were then calculated as described in Methods section 7.4.

Fig. 43   Biodistribution of radioiodinated Dal B02 F(ab)'2 fragment in D10-1 xenograft bearing mice at 24 hr after antibody administration. (A) % ID / g tissue; (B) T / NT ratios.

Fig. 44   Biodistribution of radioiodinated Dal B02 F(ab)'2 fragment in D10-1 xenograft bearing mice at 48 hr after antibody administration. (A) % ID / g tissue; (B) T / NT ratios.

Fig. 45   Biodistribution of radioiodinated Dal B02 F(ab)'2 fragment in D10-1 xenograft bearing mice at 72 hr after antibody administration. (A) % ID / g tissue; (B) T / NT ratios.

Fig. 46   Biodistribution of radioiodinated Dal B02 F(ab)'2 fragment in D10-1 xenograft bearing mice at 120 hr after antibody administration. (A) % ID / g tissue; (B) T / NT ratios.

Fig. 47   The localization index (LI) of radioiodinated Dal B02 F(ab)'2 fragment in D10-1 tumor-bearing nude mice at 24, 48, 72 and 120 hr after antibody administration.
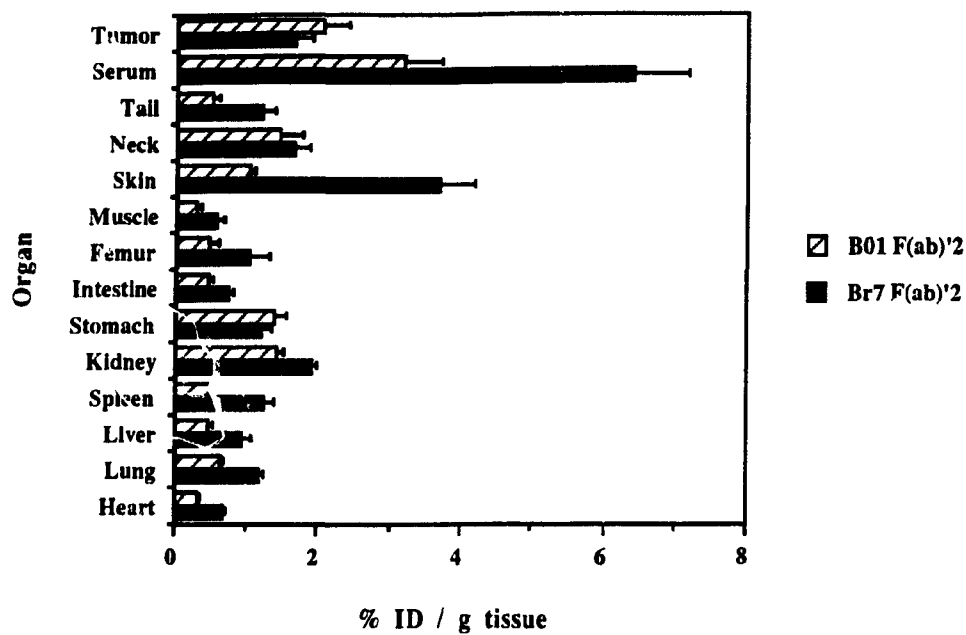
Fig. 43A

% ID / g tissue

Fig. 43B

T / NT Ratio

Fig. 44A

Fig. 44B

Fig. 45A

% ID /g tissue

Organ axis labels (top to bottom): Tumor, Serun, Tail, Neck, Skin, Muscle, Femur, Intestine, Stomach, Kidney, Spleen, Liver, Lung, Heart

☑ B02 F(ab)'2
■ IgG1 F(ab)'2

Fig. 45B

T / NT Ratio

Organ axis labels (top to bottom): Tumor, Serun, Tail, Neck, Skin, Muscle, Femur, Intestine, Stomach, Kidney, Spleen, Liver, Lung, Heart

☑ B02 F(ab)'2
■ IgG1 F(ab)'2

Fig. 46A

% ID / g tissue

Legend:
- B02 F(ab)'2
- IgG1 F(ab)'2

Organ axis (top to bottom): Tumor, Serun, Tail, Neck, Skin, Muscle, Femur, Intestine, Stomach, Kidney, Spleen, Liver, Lung, Heart

X-axis: 0.0, 0.1, 0.2, 0.3

Fig. 46B

T / NT Ratio

Legend:
- B02 F(ab)'2
- IgG1 F(ab)'2

Organ axis (top to bottom): Tumor, Serun, Tail, Neck, Skin, Muscle, Femur, Intestine, Stomach, Kidney, Spleen, Liver, Lung, Heart

X-axis: 0, 2, 4, 6, 8, 10

Fig. 47

Localization Index (LI)

Figs. 48 to 51

Radioimmunoimaging of D10-1 xenografts in nude mice using ^{131}I labeled Dal B01, Dal B02 or their F(ab)'2 fragments.

D10-1 xenograft bearing nude mice were given ^{131}I-Dal B01, ^{131}I-Dal B02, ^{131}I-Dal B01 F(ab)'2 fragment, or ^{131}I-Dal B02 F(ab)'2 fragment i.v.. At 24, 48, 72, 98 and 192 hr post antibody administration, the mice were subjected to gamma camera imaging using a computerized gamma scanner (see Methods section 7.5 for a detailed description).

Fig. 48   Images of a D10-1 xenograft in a nude mouse at (A) 24 hr; (B) 48 hr; and (C) 72 hr after the administration of ^{131}I-Dal B02 F(ab)'2 fragment.

Fig. 49   Images of a D10-1 xenograft in a nude mouse at (A) 24 hr; (B) 48 hr; (C) 96 hr; and (D) 192 hr after the administration of ^{131}I-Dal B02.

Fig. 50   Images of a D10-1 xenograft in a nude mouse at (A) 24 hr; (B) 48 hr; (C) 96 hr; and (D) 192 hr after the administration of ^{131}I-Dal B01.

Fig. 51   Images of a D10-1 xenograft in a nude mouse at (A) 24 hr; (B) 48 hr; and (C) 72 hr after the administration of ^{131}I-Dal B01 F(ab)'2 fragment.

Fig. 48

a.

b

c

Fig. 49

a

b

c

d

264
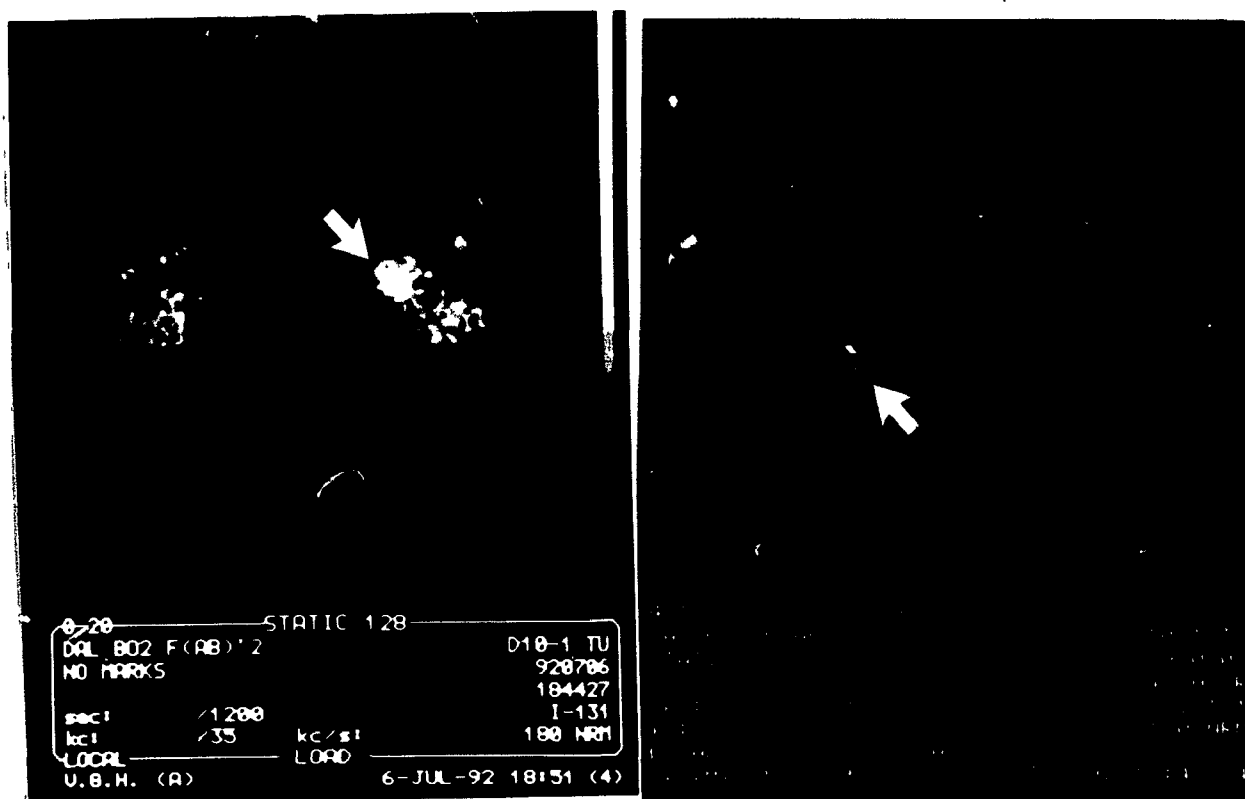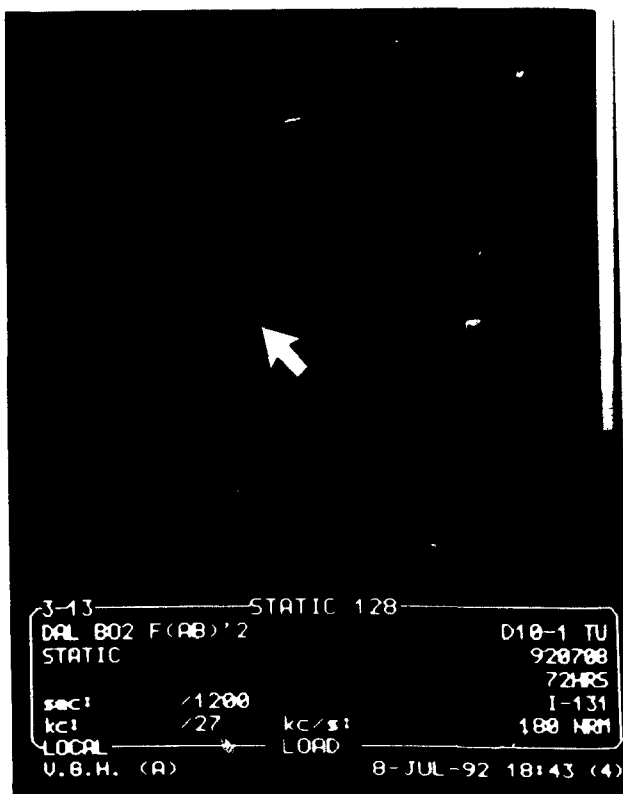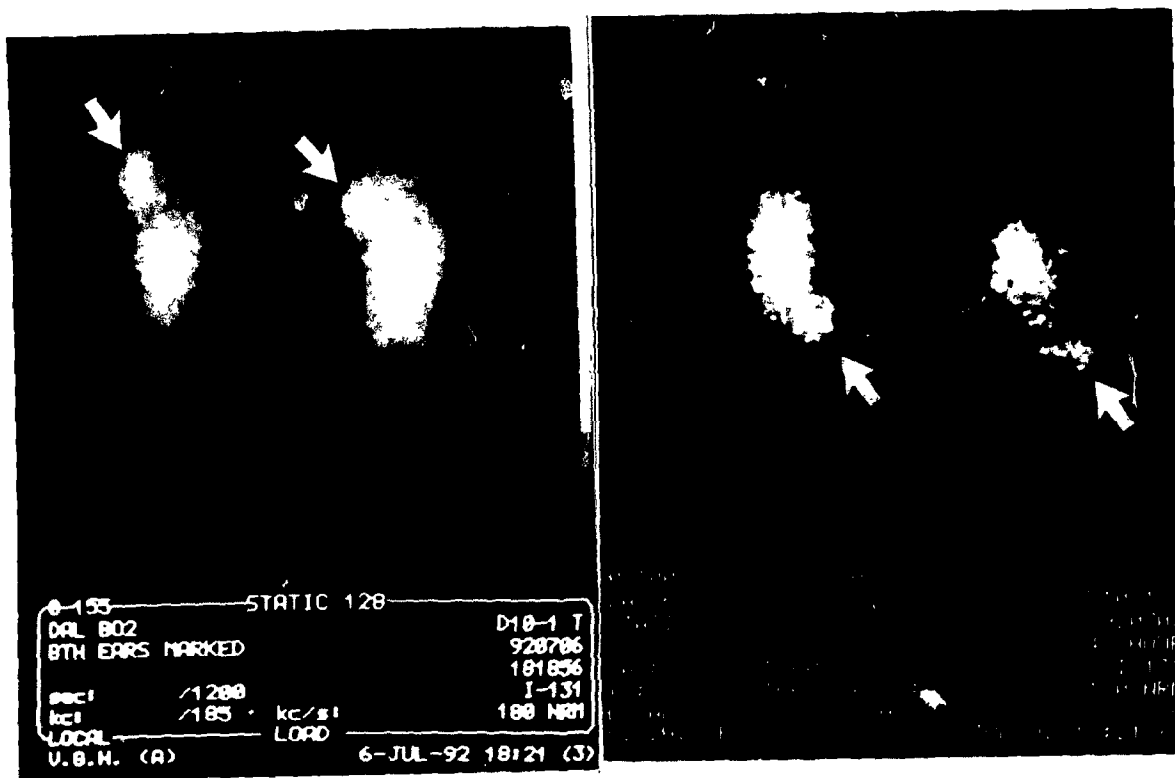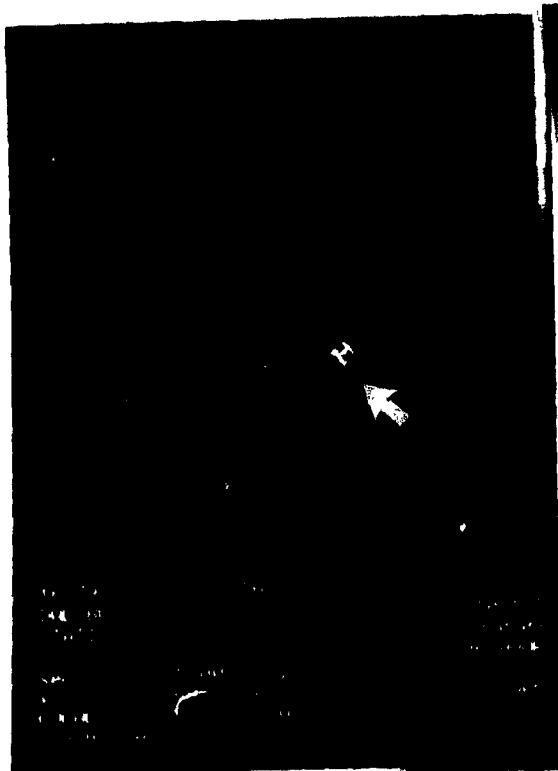
Fig. 50
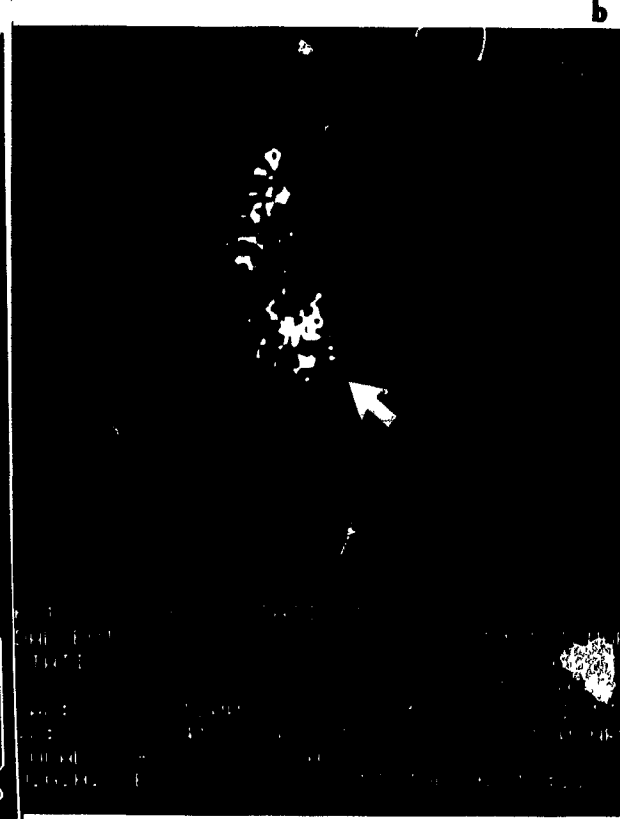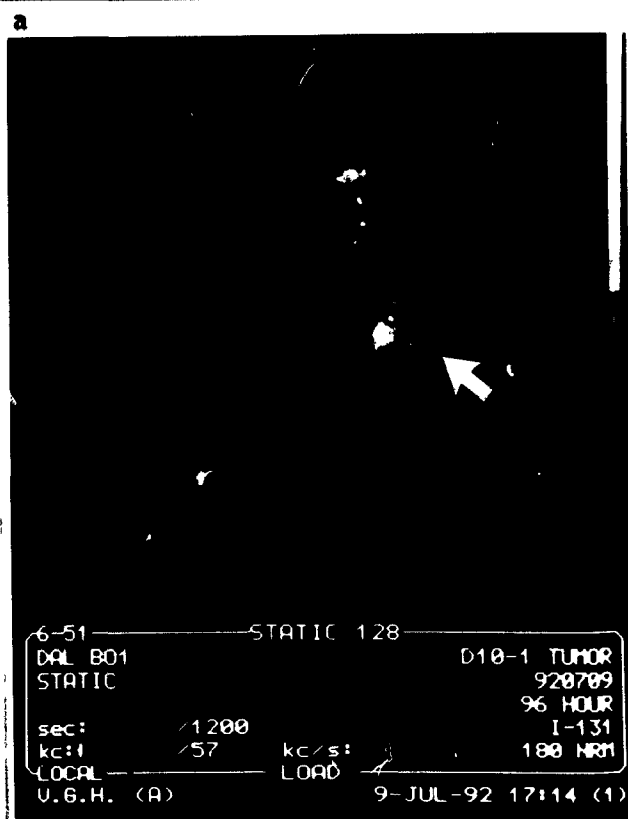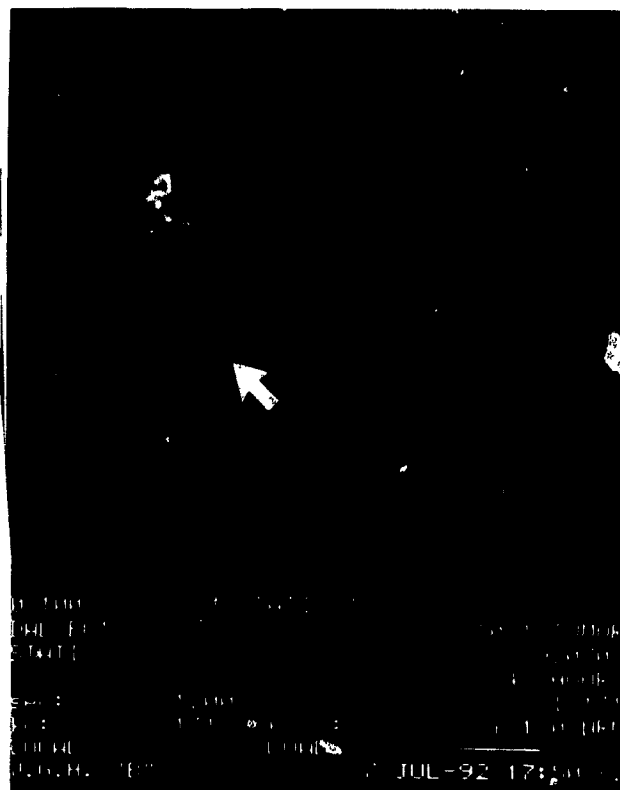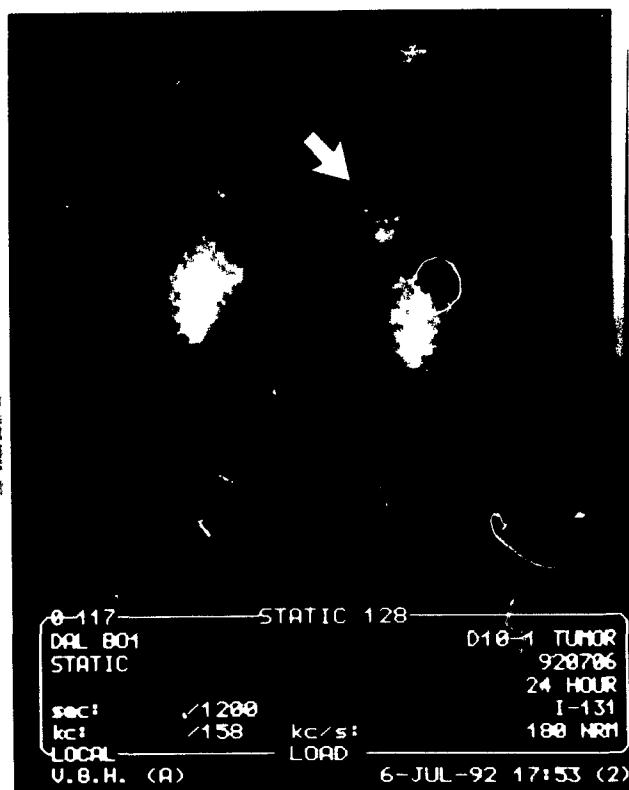
Fig. 51
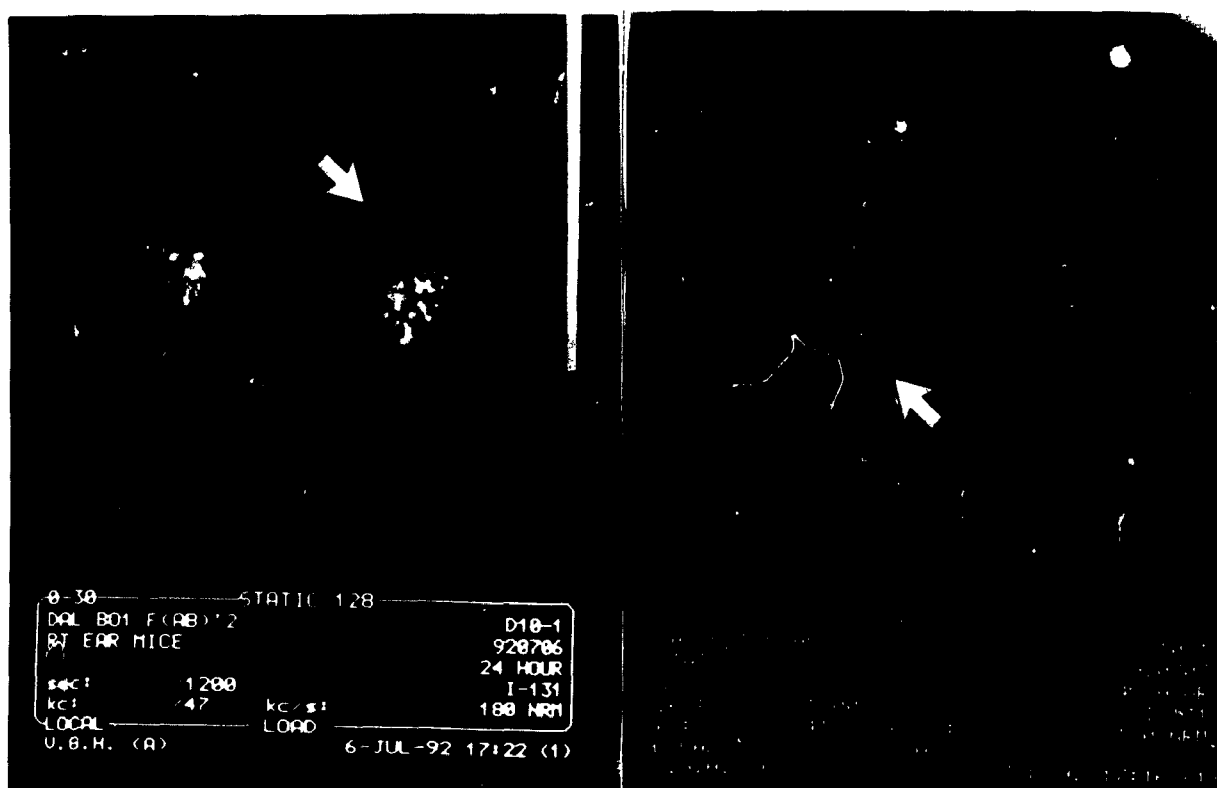
a

b
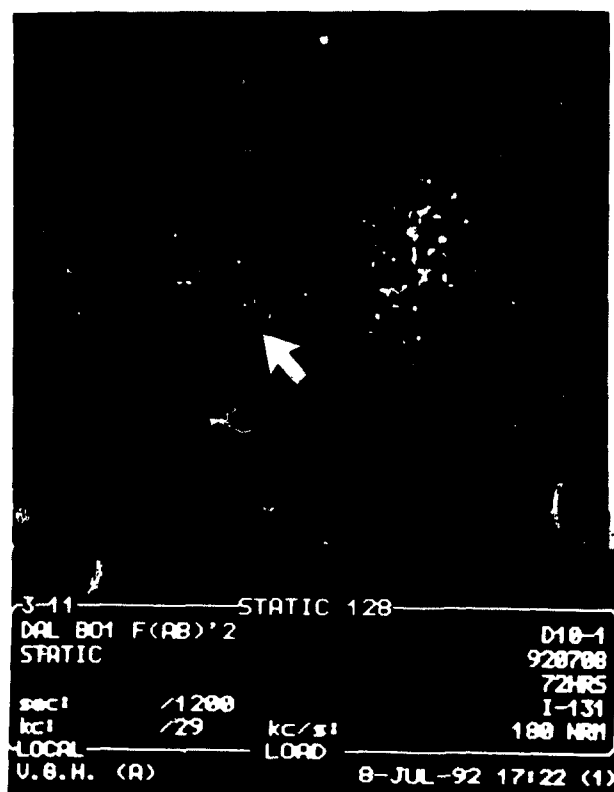
c

Figs. 52 and 53

Autoradiographs of D10-1 xenografts after i.v. injection of ^{131}I labeled Dal B01, Dal B02, or their F(ab)'2 fragments.

D10-1 xenograft bearing mice were sacrificed 48 hr post i.v. administration of ^{131}I-Dal B01 F(ab)'2 fragment or ^{131}I-Dal B02 F(ab)'2 fragment, or 96 hr post i.v. administration of ^{131}I-Dal B01 or ^{131}I-Dal B02. The tumor xenografts were taken out, and cryostat sections (5 μm thick) were cut and fixed in formaldehyde vapor overnight. The sections were then subject to autoradiography as described in Methods section 7.7.

Fig. 52A   Autoradiograph of 5 μm cryostat sections of a D10-1 xenograft at 96 hr after i.v. injection of ^{131}I-Dal B01.

Fig. 52B   Autoradiograph of 5 μm cryostat sections of a D10-1 xenograft at 48 hr after i.v. injection of ^{131}I-Dal B01 F(ab)'2 fragment.

Fig. 53A   Autoradiograph of 5 μm cryostat sections of a D10-1 xenograft at 96 hr after i.v. injection of ^{131}I-Dal B02.

Fig. 53B   Autoradiographs of 5 μm cryostat sections of a D10-1 xenograft at 48 hr after i.v. injection of ^{131}I-Dal B02 F(ab)'2 fragment.

Fig. 52

a
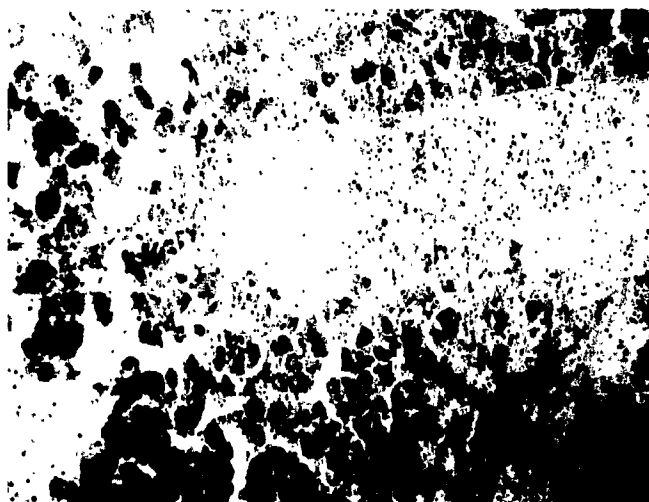
b

Fig. 53

a
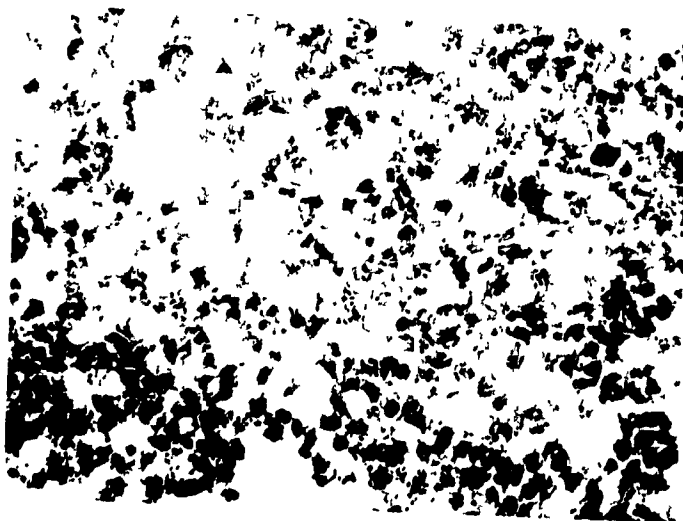
b

Section 3   Comparison of the Reactivity, Stability, Pharmacokinetics and Biodistribution of Dal B02 after Radioiodination by Three Different Iodination Methods

The purpose of this study was to evaluate the effects of three different protein radioiodination procedures, i.e., N-succinimidyl-para-iodobenzoate (PIB), Bolton-Hunter (B-H) and Chloramine-T (Chl. T), as regards to the stability of incorporated radioiodine, retention of antibody activity, as well as their pharmacokinetics and biodistribution in D_{10-1} xenograft bearing nude mice after i.v. administration of radioiodinated Dal B02 preparations.

3.1. Efficiency   of   Radioiodination   and   Immunoreactivity   of Radioiodinated Dal B02

As shown in Table 15, the Chloramine T method yielded the highest iodine incorporation, which is about two-folds higher than in the products of the PIB and Bolton-Hunter methods. However, the use of PIB and Bolton-Hunter methods resulted in products with higher antibody IRF. When comparing their immunoreactivity, i.e., the ability of different iodinated Dal B02 preparations to bind to target D_{10-1} cells, using either a direct binding assay or a competition assay, it was observed that ^{125}I-Dal B02 (PIB) retained the highest immunoreactivity (Fig. 54). All the three antibody preparations had a radiochemical purity > 97% , as determined by TLC or TCA precipitation. The specific activities of the three differently labeled antibody preparations varied from 0.24 - 0.36 $\mu Ci/\mu g$ protein.

3.2. Stability of the Radioiodinated Dal B02 Preparations in vitro

The in vitro stability of the incorporated radioiodine in the three ^{125}I-Dal B02 preparations was determined by incubation at 37°C with (i) freshly isolated human serum; (ii) mouse liver homogenate; and (iii) human thyroid homogenate. At defined intervals, aliquots were taken out from the incubation mixtures and the radioactivity that remained associated with Dal B02 protein and released into the supernatant was determined using TCA precipitation or ITLC.

3.2.1   Stability of radioiodinated Dal B02 preparations after incubation with human serum

^{125}I-Dal B02 (PIB) and ^{125}I-Dal B02 (B-H) preparations were quite stable in human serum. More than 99% of radioactivity remained associated with Dal B02 protein up to 168 hr of incubation. There was also no significant decrease in the IRF of these two ^{125}I-Dal B02 preparations. Approximately 7% radioactivity was released into the supernatant after 168 hr incubation of ^{125}I-Dal B02 (Chl.T). The IRF of this Dal B02 preparation was markedly reduced, i. e., from 52% to 36%   (Fig. 55).

3.2.2   Stability of radioiodinated Dal B02 preparations after incubation with mouse liver homogenate

There was a gradual release of radioactivity from all the three types of ^{125}I-Dal B02 preparations after incubation with mouse liver homogenate. The major proportion of the released radioactivity came off the protein during the first 72 hr of incubation, after which the deiodination process became much slower (Fig. 56A). At 168 hr, about 83.4%, 71% and 60.8% of radioactivity remained associated with ^{125}I-Dal B02 (PIB), ^{125}I-Dal B02 (B-H) and ^{125}I-Dal B02 (Chl. T), respectively. Reduction of IRF was also observed in all the

three types of preparations (Fig. 56B). The ^{125}I-Dal B02 (PIB) showed a better retention of IRF than ^{125}I-Dal B02 (B-H) and ^{125}I-Dal B02 (Chl. T). While the ^{125}I-Dal B02 (PIB) still had an IRF of 52.7% (an 18% decrease compared to the IRF of the preparation before incubation), the ^{125}I-Dal B02 (B-H) and ^{125}I-Dal B02 (Chl. T) only had IRF of 41.5% and 34.2%, respectively (a 34% decrease compared to the IRF of the respective preparation before incubation).

3.2.3 Stability of radioiodinated Dal B02 preparations after incubation with human thyroid homogenate

About 92-95% of radioactivity was found still assoiated with Dal B02 in all the three types of ^{125}I-Dal B02 preparations after incubation with thyroid homogenate at 37°C for up to 72 hr. However, there were 18%, 28% and 38% of decrease in antibody IRF in ^{125}I-Dal B02 (PIB), ^{125}I-Dal B02 (B-H) and ^{125}I-Dal B02 (Chl. T) preparations, respectively (Fig. 57).

3.3   In vivo Pharmacokinetics and Biodistribution

The biodistribution studies were carried out in s.c. D10-1 xenograft bearing nude mice. The biodistribition of the three types of radioiodinated Dal B02 preparations were determined separately in two experimental groups. In one group, ^{131}I-Dal B02 (PIB) was paired with an equal amount of ^{125}I-Dal B02 (Chl. T), while in the other group, ^{131}I-Dal B02 (PIB) was paired with an equal amount of ^{125}I-Dal B02 (B-H). Each mouse received a total of 80 µg of protein. At indicated intervals, samples of blood were obtained from 3 mice in each group and ^{131}I and ^{125}I activities were determined. Fig. 58 shows Dal B02 concentrations in blood of nude mice at different times after i.v. administration of the three different types of radioiodinated Dal B02 preparations. Table 16 shows various pharmacokinetic parameters after i.v. injection of the three types of radioiodinated Dal B02 preparations. No

significant difference was found among these three types of preparations as regards their

pharmacokinetic parameters, e.g, volume of apparent distribution (Vd), area under curve

(AUC), serum half life (t 1/2 α and t 1/2β) and clearance from circulation (CL).

At 48, 96 and 168 hr post administration of radioiodinated Dal B02 preparations, three

mice from each group were sacrificed. Figs. 59 to 64 show the organ distribution (% ID / g

tissue) of the three different types of radioiodinated Dal B02 preparations. A similar

distribution of radioactivity was observed in most organs among the three types of

radioiodinated Dal B02 preparations in D10-1 xenograft bearing mice with the following

exceptions: (i) there was a higher % ID / g tissue in liver and spleen in mice given ^{131}I-Dal

B02 (PIB); (ii) there was a higher % ID / g tissue in the thyroid in mice given ^{125}I-Dal B02

(B-H) and ^{125}I-Dal B02 (Chl. T); and (iii) there was no difference in the uptake of

radioactivity by tumor tissue at 48 and 96 hr after injection of the three types of Dal B02

preparations. However, at 168 hr, the mice given ^{125}I-Dal B02 (Chl. T) showed a lower %

ID / g tissue in tumor than the mice given the ^{131}I-Dal B02 (PIB) did. On comparing the T /

NT ratios among the mice given the three types of Dal B02 preparations, the mice given

[131]I-Dal B02 (PIB) showed a higher tumor / thyroid tissue ratio, but the mice given [125]I-

Dal B02 (B-H) and ^{125}I-Dal B02 (Chl. T) had higher tumor / liver and tumor/spleen ratios.

3.4 Stability, IRF and Immunoreactivity of Dal B02 Recovered from the Serum of D10-1 Xenograft Bearing Nude Mice Injected with Radioiodinated Dal B02 Preparations

Samples of serum from D10-1 xenograft bearing nude mice injected with different types of

radioiodinated Dal B02 preparations were collected at 48 and 96 hr post i.v.antibody

administration. After elution from a NAP-10 column, all samples of serum yielded a single

radioactive fraction. This elution profile was identical with that of the parent Dal B02

preparations, indicating that there was no detectable free radioactive iodine (^{131}I or ^{125}I) or radioiodine-containing small fragments in the circulation at the time of obtaining these samples of serum.

When the IRF and immunoreactivity were examined, it was found that there was no decrease in antibody IRF in ^{131}I-Dal B02 (PIB) and ^{125}I-Dal-B02 (B-H) preparations even up to 168 hr after i.v. injection, but there was a 26 % decrease in IRF (from 51 % to 37.9 %) in ^{125}I-Dal B02 (Chl. T) preparation (Table 17). The immunoreactivity of Dal B02 was also well retained in ^{131}I-Dal B02 (PIB) and ^{125}I-Dal B02 (B-H) preparations. However, there was a significant decrease in immunoreactivity in ^{125}I-Dal B02 (Chl. T) preparation at 96 hr after i.v. administration (Fig. 65).

3.5 The Influence of Tumor Weight on the Amount of Intratumoral Dal B02 Localization

In this study, a total of 27 D10-1 xenograft bearing nude mice were injected i.v. with radioiodinated Dal B02 preparations. The tumor weight in these mice varied from 0.1 to 0.5 g at the beginning of the study. All D10-1 xenograft bearing nude mice were given radioiodinated Dal B02 at day 0. The % ID / g tumor tissue of Dal B02 were obtained from 9 mice at each time point examined (i. e., 48, 96 and 168 hr post antibody administration). As shown in Fig. 66, there was an inverse correlation between the tumor weight and the % ID / g tissue of Dal B02 that localized in the tumor, i.e., the smaller the tumor mass, the higher % ID /g tumor tissue. This correlation could be seen at all the three time points examined, i.e., 48 hr, 96 hr and 168 hr after i.v. injection of radioiodinated Dal B02. However, the absolute amounts of Dal B02 that localized in the smaller tumors was not always greater than that localized in the larger tumors. The absolute amount of Dal B02 that

localized in a specific tumor was dependent on both the tumor weight and the % ID / g
tumor tissue, i.e., it equals the product of tumor weight (g) and the % ID / g tumor tissue.

3.6   Comparison of i.v. and i.p. Routes of Dal B02 Administration as Regards to Tumor Localization and Concentration in Blood of Dal B02

In this study, three D10-1 xenograft bearing nude mice were given a mixture of 40 μg of
^{131}I-Dal B02 (PIB) and 40 μg of ^{125}I-Dal B02 (Chl. T) i.p., while the other three mice
were given the same mixture i.v.. Samples of blood were obtained at indicated intervals
and ^{131}I and ^{125}I activities in the blood were determined with a dual-window gamma
counter. At 168 hr post antibody administration, all mice were sacrificed and the
distribution of ^{131}I and ^{125}I activities in the tumors as well as in different normal mouse
tissues were determined.

Fig. 67A shows the concentrations of Dal B02 in blood as % ID / ml blood. After i.v.
injection, the highest antibody concentration was achieved immediately after antibody
administration. This concentration of Dal B02 then declined rapidly. Less than 30% of
initial radioactivity remained in the blood of nude mice given Dal B02 i.v. at 24 hr post
antibody administration. In contrast to i.v. injection, the blood concentration of the
radioactivity increased gradually after i.p. antibody administration, and the peak level was
achieved at 24 hr. At about 16 hr post antibody administration, the Dal B02 concentration
in the blood of nude mice given antibody i.p. exceeded the Dal B02 concentration in the
blood of nude mice given antibody i.v.. The Dal B02 concentration in the blood of mice
given antibody preparation i.p. was consistently higher than that in the blood of mice given
antibody preparation i.v. afterward.

Fig. 67B shows that the total body radioactivity of mice given radioiodinated Dal B02 by the i.v. route declined slightly faster than that of the mice given the antibody i.p., indicating that Dal B02 given via the i.v. route was cleared faster than Dal B02 given via the i.p. route.

When the % ID / g tissue and the T / NT ratios were compared, it was found that the mice injected by the i.p. route had higher amount of radioactivity in tumors, serum, as well as in most other organs except in liver and spleen, compared to the mice given the Dal B02 by the i.v. route (Figs. 68 and 69). When both ^{131}I-Dal B02 (PIB) and ^{125}I-Dal B02 (Chl. T) were given i.p., the former had higher radioactivity in the tumor xenograft, serum, liver and spleen, while the latter had higher radioactivity in thyroid. This is consistent with the results obtained in the mice given the same mixture by the i.v. route as described in the Results section 3.3.

In conclusion, radioiodination of Dal B02 using the PIB method yielded a preparation that retained higher antibody immunoreactivity, was more stable, and which after i.v. administration showed higher tumor localization and less nonspecific uptake of radioiodine by the thyroid, as compared to the radiolabeled products obt.. ed using Bolton-Hunter and Chloramine-T methods. There was an inverse correlation between the tumor weight and the % ID / g tumor of radioiodinated Dal B02 preparation.

Table 15 Efficiency of radioiodination and IRF of Dal B02 preparations after radioiodination using the three different methods [1]

Method	Radioiodine Incorporation (%)	Specific Activity ($\mu Ci/\mu g$)	IRF of Dal B02 (%)
PIB method	15.3 ± 3.0 [2]	0.29 ± 0.03	64.1 ± 3.4
B-H method	11.8 ± 1.6	0.27 ± 0.05	63.0 ± 0.4
Chl.T method	34.3 ± 6.1	0.36 ± 0.02	53.7 ± 3.1

1. Dal B02 was labeled with ^{125}I using PIB, Bolton-Hunter reagent or Chloramine T as described in Materials and Methods. Radiolabeled Dal B02 was purified from the reaction mixture using a NAP-10 column. IRF of Dal B02 was determined using D_{10-1} cells.

2. Data are the percentage of total added radioiodine that was incorporated into Dal B02 protein after radioiodination and represent the mean ± S. D. of 3 determinations.

Fig. 54

The immunoreactivity of Dal B02 after radioiodination by three different iodination methods.

Dal B02 was radiolabeled by one of the three protein iodination methods, i. e., PIB, Bolton-Hunter and Chloramine T. Two types of assays were used to determine the retention of antibody activity after radioiodination. In the first assay, the ability of the different radioiodinated Dal B02 preparations to bind to target D_{10-1} cells was compared. In the other assay, the ability of different radioiodinated Dal B02 preparations to compete with cold Dal B02 for binding to target D_{10-1} cells was compared.

Fig. 54A   Ability to bind to target D_{10-1} cells of ^{125}I-Dal B02 (PIB), ^{125}I-Dal B02 (B-H) and ^{125}I-Dal B02 (Chl. T) preparations.

Fig. 54B   Competition of different radioiodinated Dal B02 preparations with cold Dal B02 for binding to D_{10-1} cells.

Fig. 54A
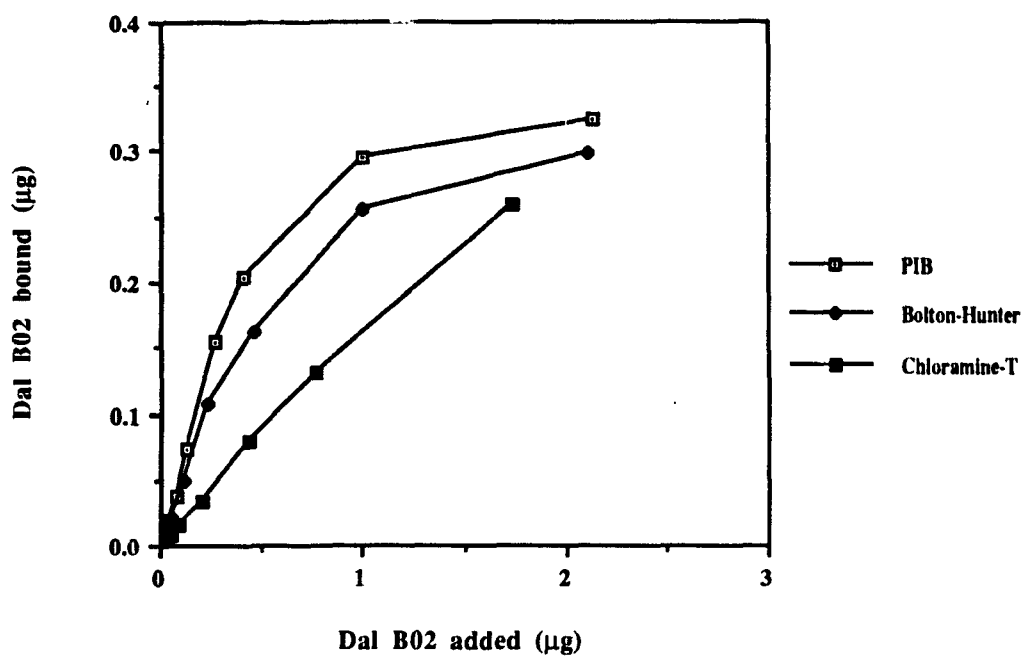
Fig. 54B
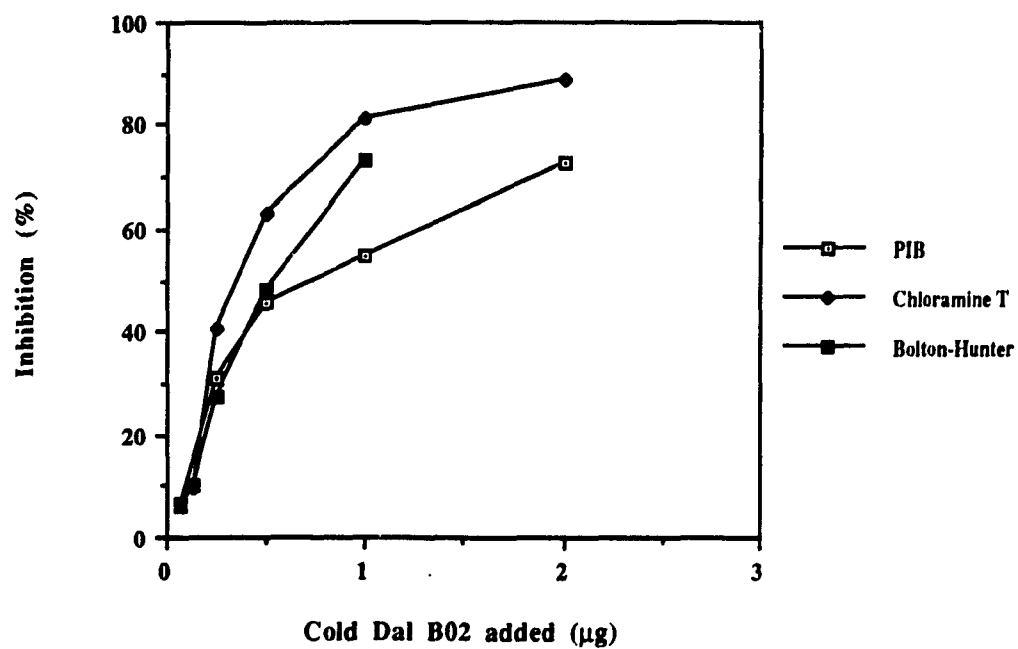
Fig. 55

Stability of ^{125}I-Dal B02 (PIB), ^{125}I-Dal B02 (B-H) and ^{125}I-Dal B02 (Chl. T)
preparations after incubation in human serum.

Aliquots of Dal B02, radioiodinated by the three different methods, were incubated with
freshly isolated human serum at 37°C. Aliquots were taken out at indicated intervals.
Protein-bound and free ^{125}I activity released into the supernatant was determined by 10%
TCA precipitation or ITLC assay. The IRF of Dal B02 after different periods of incubation
was also determined using D10-1 cells.

Fig. 55A
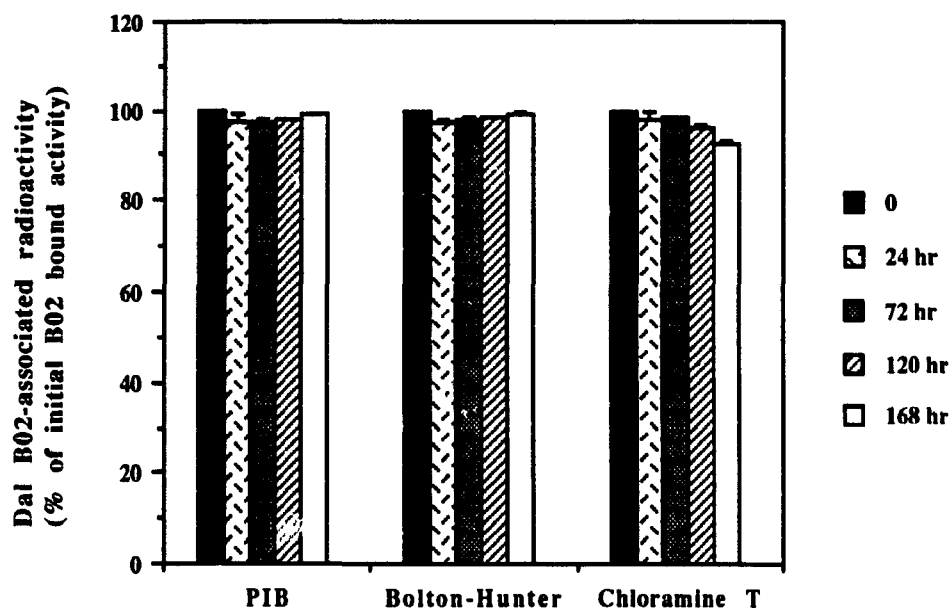
Fig. 55B
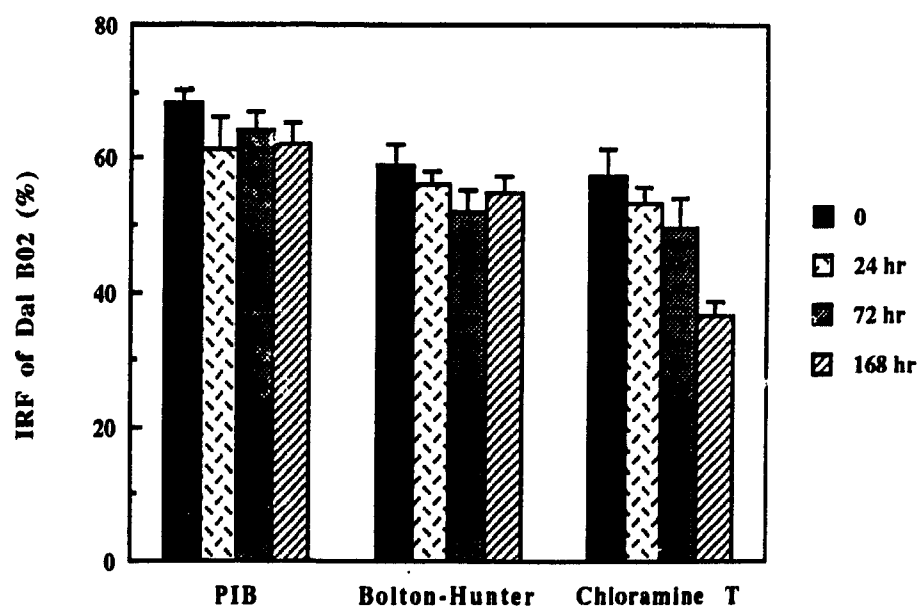
Fig. 56

Stability of ^{125}I-Dal B02 (PIB), ^{125}I-Dal B02 (B-H) and ^{125}I-Dal B02 (Chl. T) preparations after incubation in mouse liver homogenate.

Aliquots of Dal B02, radioiodinated by the three different methods, were incubated with mouse liver homogenate at 37°C. Aliquots were taken out at indicated intervals. Protein-bound and free ^{125}I activity released into the supernatant was determined by 10% TCA precipitation or ITLC assay. The IRF of Dal B02 after different periods of incubation was also determined using D$_{10-1}$ cells.

Fig. 56A
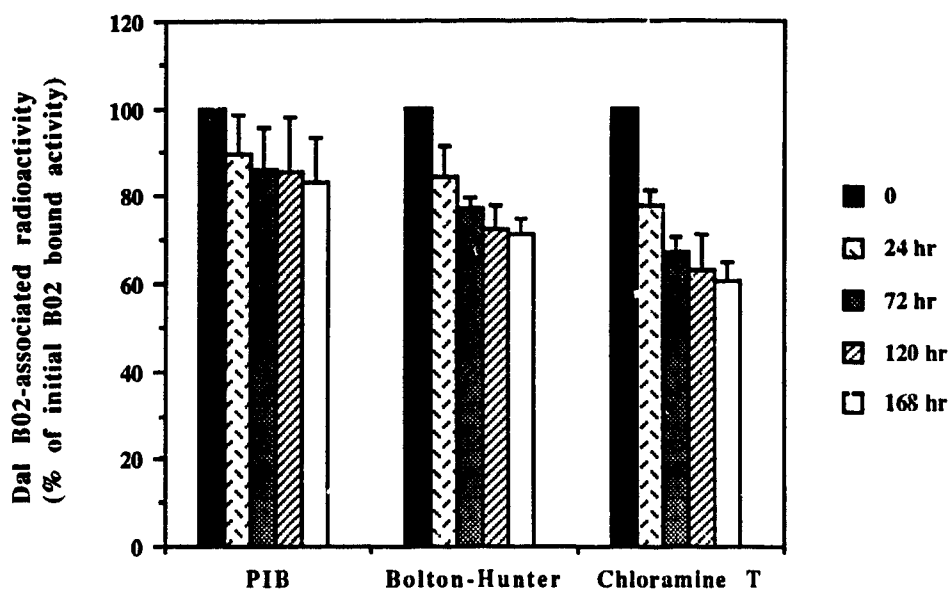
Fig. 56B
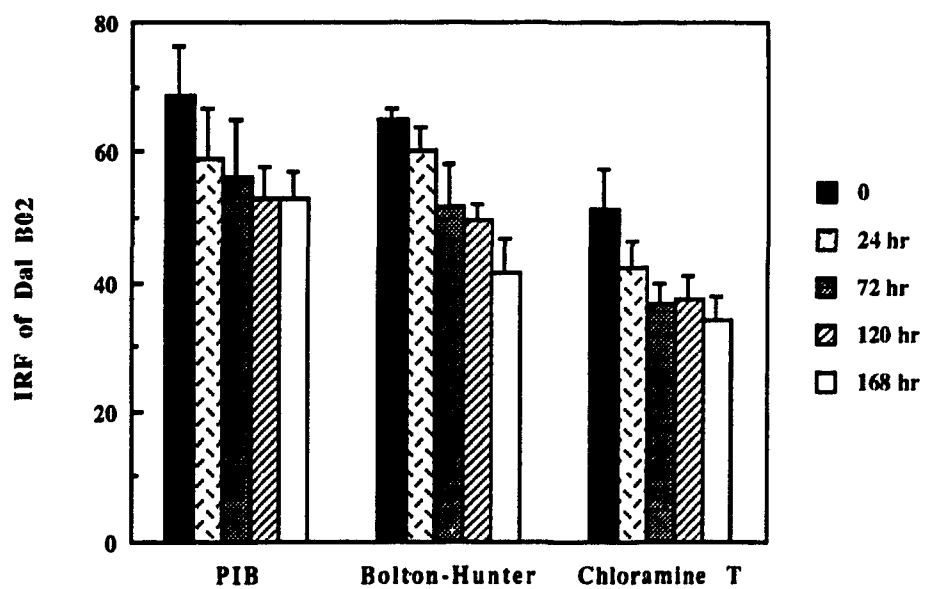
Fig. 57

Stability of ^{125}I-Dal B02 (PIB), ^{125}I-Dal B02 (B-H) and ^{125}I-Dal B02 (Chl. T) preparations after incubation in human thyroid homogenate.

Aliquots of Dal B02, radioiodinated by the three different methods, were incubated with human thyroid homogenate at 37°C. Aliquots were taken out at indicated intervals. Protein-bound and free ^{125}I activity released into the supernatant was determined by 10% TCA precipitation or ITLC assay. The IRF of Dal B02 after different periods of incubation was also determined using D10-1 cells.

Fig. 57A
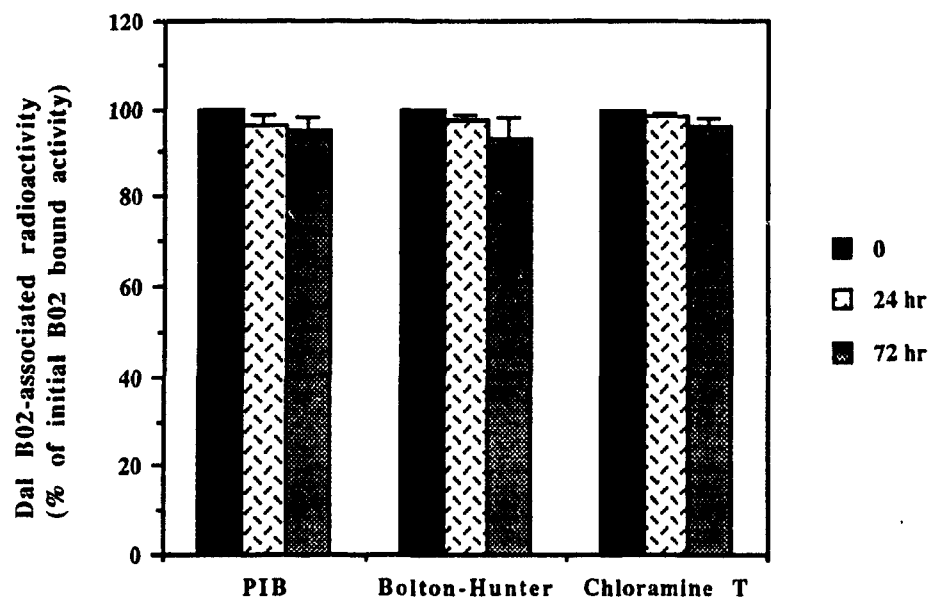
Fig. 57B
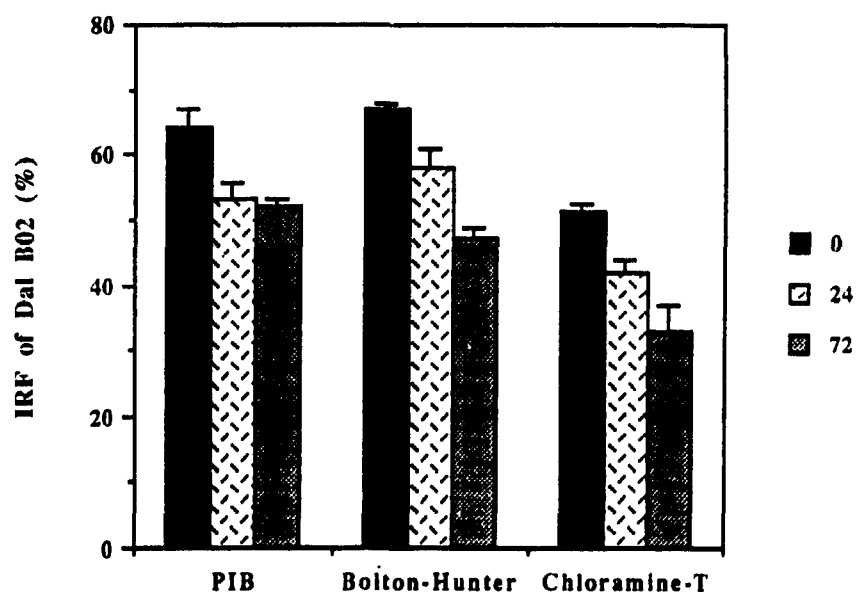
Fig. 58

Clearance of i.v. injected ^{131}I-Dal B02 (PIB), ^{125}I-Dal B02 (B-H) and ^{125}I-Dal B02 (Chl. T) preparations from the blood of D10-1 xenograft bearing mice.

Each D10-1 xenograft bearing nude mouse was given i.v. 40 μg ^{131}I-Dal B02 (PIB) mixed with 40 μg of ^{125}I-Dal B02 (B-H) or 40 μg of ^{125}I-Dal B02 (Chl. T). At indicated intervals, samples of blood were obtained from the mice and ^{131}I and ^{125}I activities in the blood were determined with a dual-window gamma counter. All points represent the mean obtained from three to six mice.

Dal B02 concentration in blood (μg/ml)

Fig. 58

Time (hr)

Chloramine-T

Bolton-Hunter

PIB
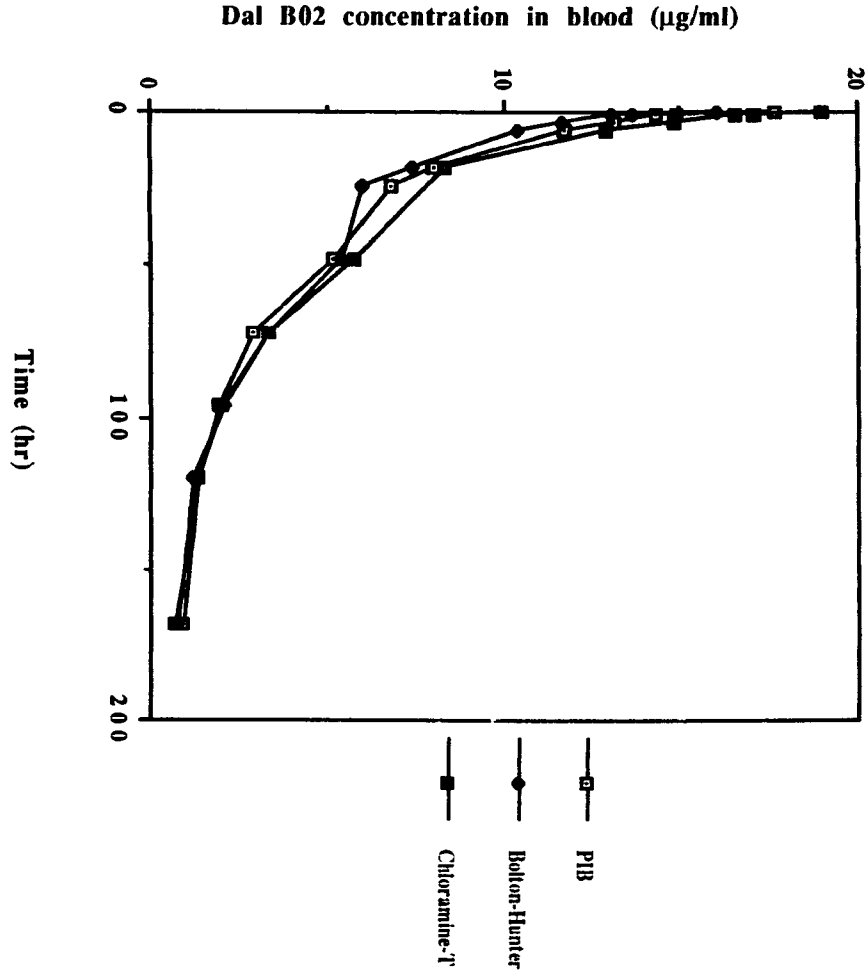
Table 16　Pharmacokinetic parameters of ^{131}I-Dal B02 (PIB), ^{125}I-Dal B02 (B-H) and ^{125}I-Dal B02 (Chl. T) after i.v. injection into D10-1 xenograft bearing nude mice [1]

Methods	Vd (ml)	T1/2α (hr)	T1/2β (hr)	AUC (μCi·hr/ml)	CL (μl/h)
PIB	3.47 [2]	2.52	38.7	644	620
B-H	3.92	2.10	43.9	647	618
Chl.T	4.38	2.60	39.1	656	612

1. Each nude mouse was given a mixture of 40 μg of ^{131}I-Dal B02 (PIB) and 40 μg of ^{125}I-Dal B02 (B-H) or 40 μg of ^{125}I-Dal B02 (Chl. T). Samples of blood were obtained at indicated intervals and ^{131}I and ^{125}I activities in the blood were determined.

2. All parameters were calculated from the mean values of antibody concentration in the blood obtained from 3 to 6 mice. See detailed description in Materials and Methods.

Figs. 59 to 61

Biodistribution of i.v. injected ^{131}I-Dal B02 (PIB) and ^{125}I-Dal B02 (Chl. T) in D10-1 xenograft bearing nude mice.

Each D10-1 xenograft bearing nude mouse was given i.v. 40 μg ^{131}I-Dal B02 (PIB) mixed with 40 μg of ^{125}I-Dal B02 (Chl. T). Groups of 3 mice were sacrificed at 48, 96 and 168 hr post antibody administration. The xenografted tumor and normal mouse tissues were taken out, weighed and the tissue associated ^{131}I and ^{125}I activities were determined using a dual-window gamma counter. The % ID / g tissue and the T / NT ratios were then calculated as described in Materials and Methods.

Fig. 59   Biodistribution of ^{131}I-Dal B02 (PIB) and ^{125}I-Dal B02 (Chl. T) in D10-1 xenograft bearing nude mice at 48 hr post i.v. antibody administration.

Fig. 60   Biodistribution of ^{131}I-Dal B02 (PIB) and ^{125}I-Dal B02 (Chl. T) in D10-1 xenograft bearing nude mice at 96 hr post i.v. antibody administration.

Fig. 61   Biodistribution of ^{131}I-Dal B02 (PIB) and ^{125}I-Dal B02 (Chl. T) in D10-1 xenograft bearing nude mice at 168 hr post i.v. antibody administration.

Fig. 59A

% ID / g tissue

Fig. 59B

T / NT Ratio

Fig. 60A

% ID / g tissue

Fig. 60B

T / NT Ratio

Fig. 61A

% ID / g tissue

Fig. 61B

T / NT Ratio
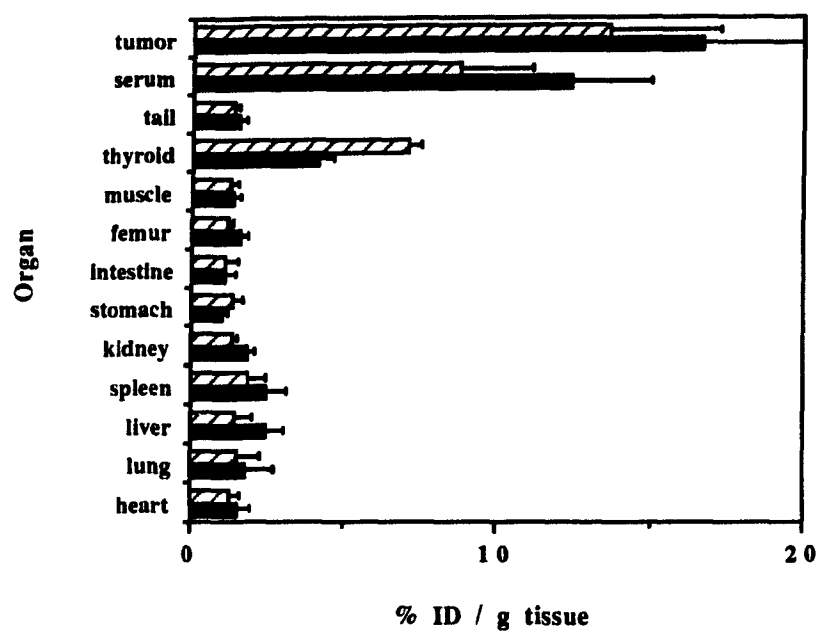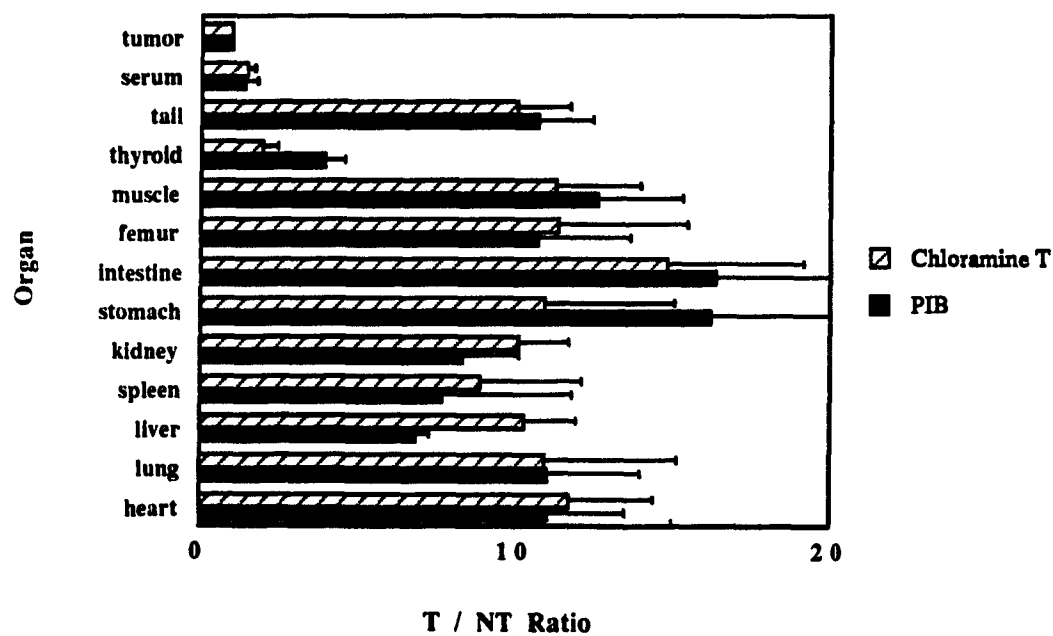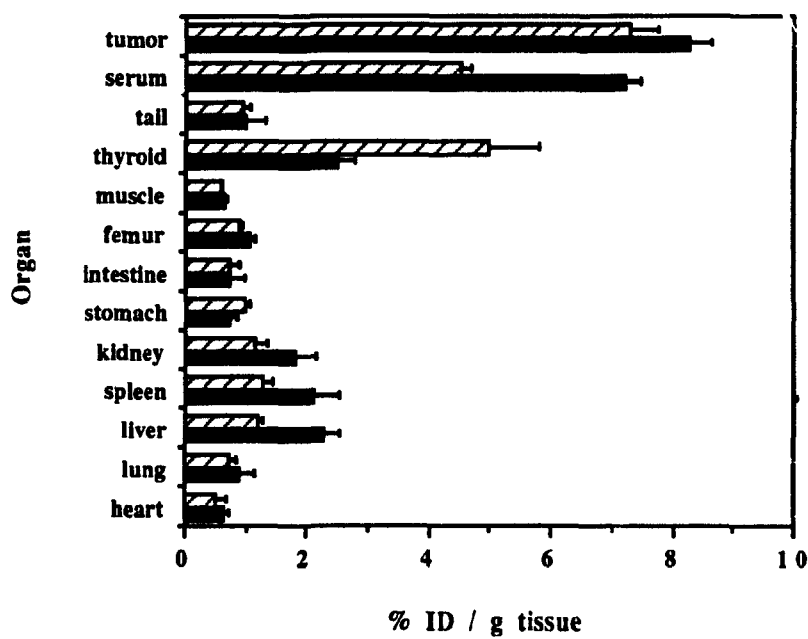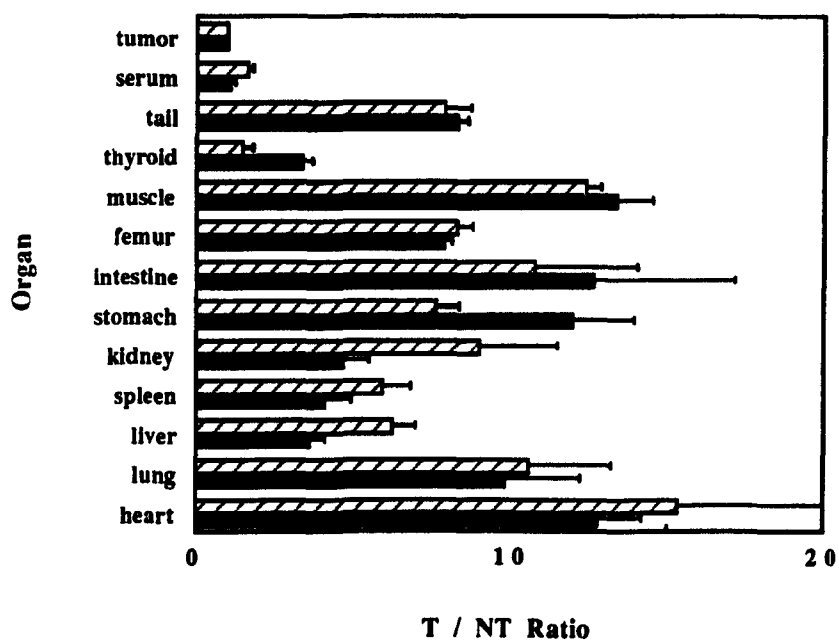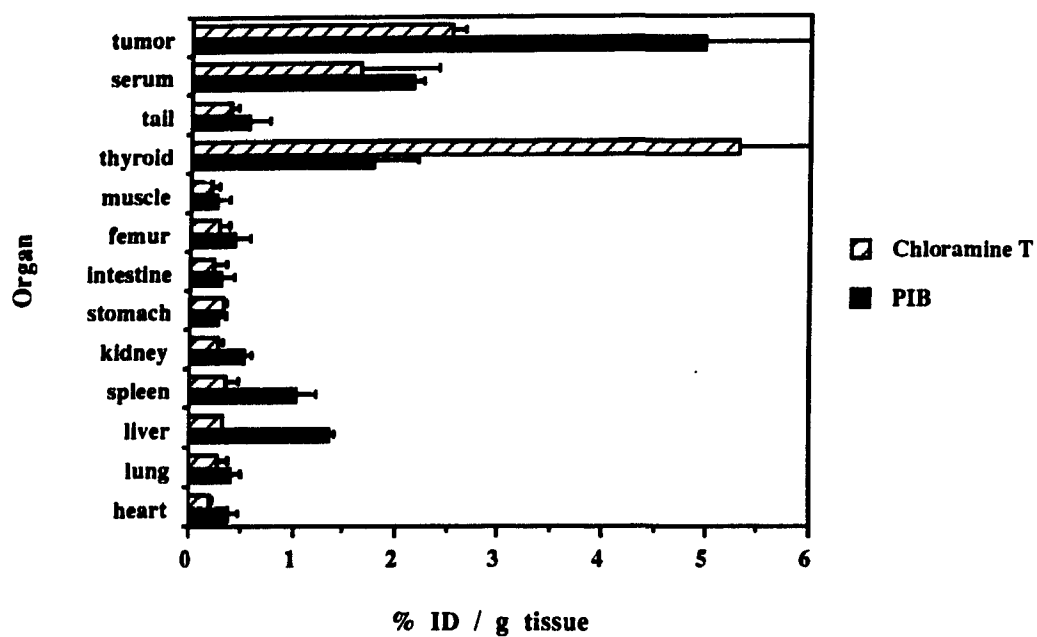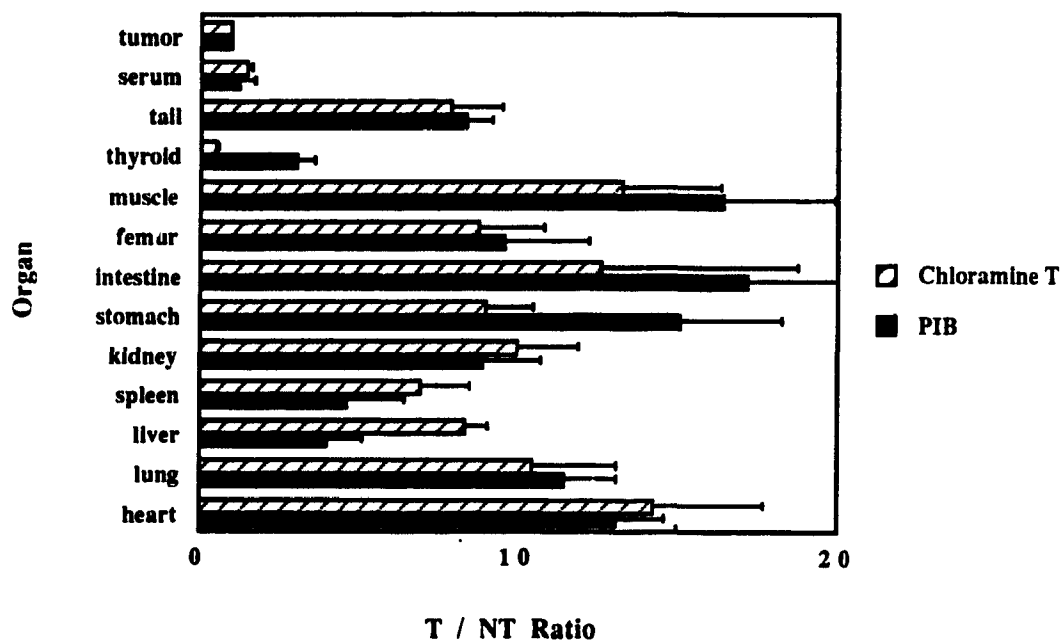
Figs. 62 to 64

Biodistribution of i.v. injected ^{131}I-Dal B02 (PIB) and ^{125}I-Dal B02 (B-H) in D$_{10-1}$ xenograft bearing nude mice.

Each D$_{10-1}$ xenograft bearing nude mouse was given i.v. 40 μg ^{131}I-Dal B02 (PIB) mixed with 40 μg of ^{125}I-Dal B02 (B-H). Groups of 3 mice were sacrificed at 48, 96 and 168 hr post antibody administration. The xenografted tumor and normal mouse tissues were taken out, weighed and the tissue associated ^{131}I and ^{125}I activities were determined using a dual-window gamma counter. The % ID / g tissue and the T / NT ratios were then calculated as described in Materials and Methods.

Fig. 62 Biodistribution of ^{131}I-Dal B02 (PIB) and ^{125}I-Dal B02 (B-H) in D$_{10-1}$ xenograft bearing nude mice at 48 hr post i.v. antibody administration.

Fig. 63 Biodistribution of ^{131}I-Dal B02 (PIB) and ^{125}I-Dal B02 (B-H) in D$_{10-1}$ xenograft bearing nude mice at 96 hr post i.v. antibody administration.

Fig. 64 Biodistribution of ^{131}I-Dal B02 (PIB) and ^{125}I-Dal B02 (B-H) in D$_{10-1}$ xenograft bearing nude mice at 168 hr post i.v. antibody administration.

Fig. 62A

Organ (y-axis)

tumor, serum, tail, thyroid, muscle, femur, intestine, stomach, kidney, spleen, liver, lung, heart

% ID / g tissue (x-axis): 0, 10, 20

Legend: ▨ Bolton-Hunter ■ PIB

Fig. 62B

Organ (y-axis)

tumor, serum, thyroid, muscle, femur, intestine, stomach, kidney, spleen, liver, lung, heart

T / NT Ratio (x-axis): 0, 2, 4, 6, 8, 10, 12
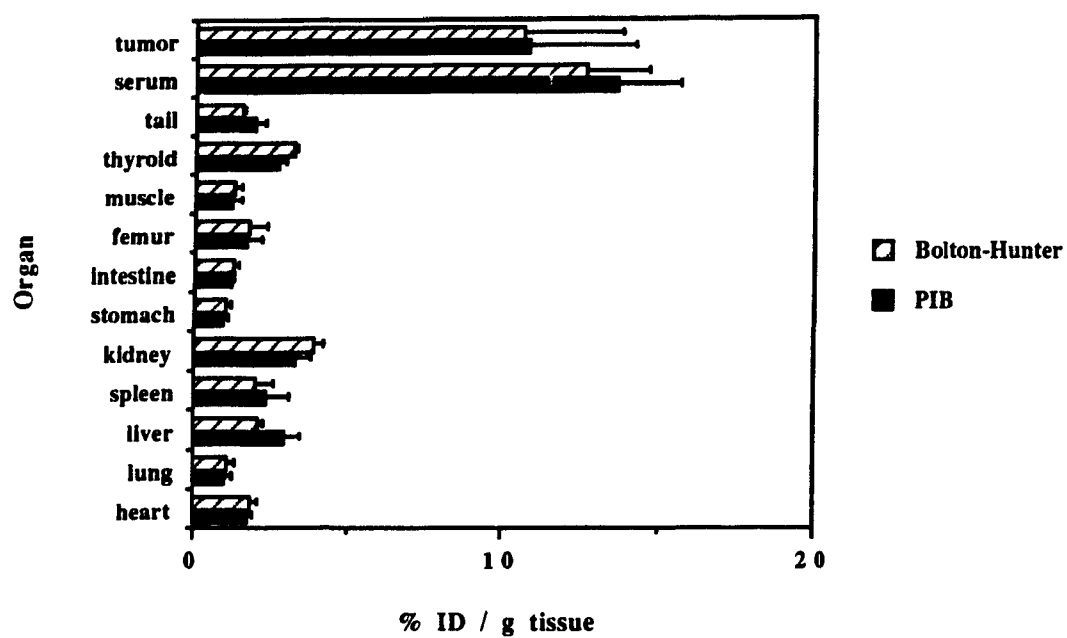
Legend: ▨ Bolton-Hunter ■ PIB
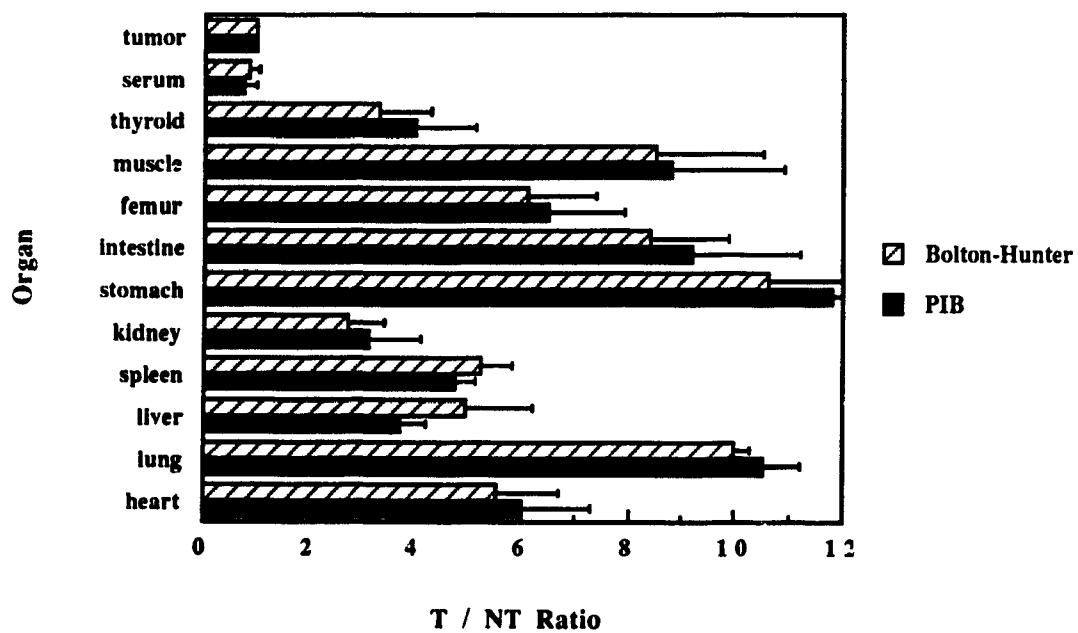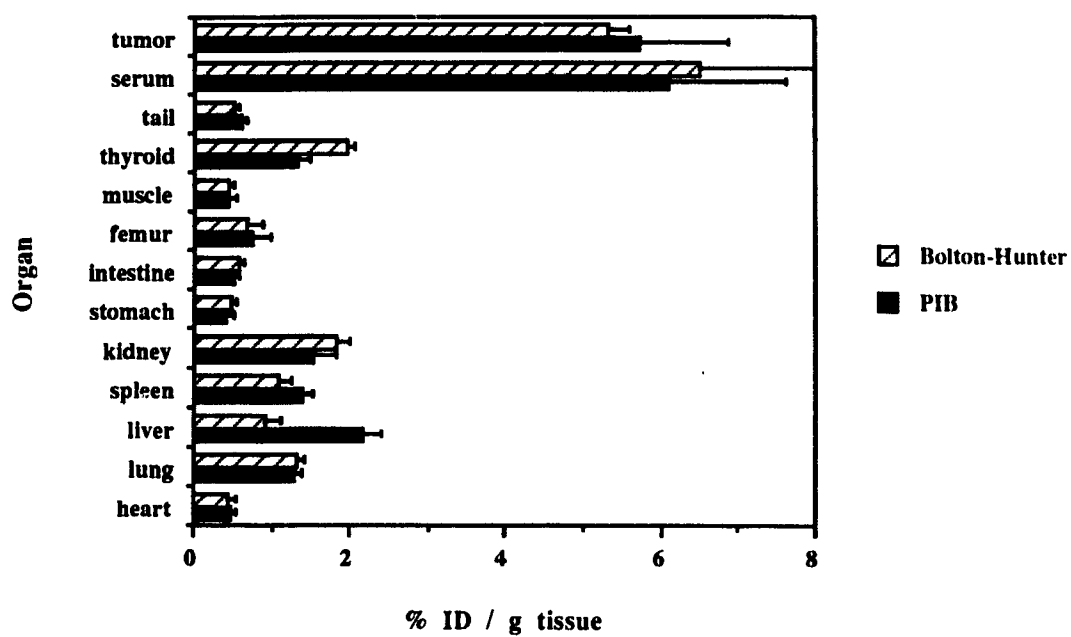
Fig. 63A

Fig. 63B
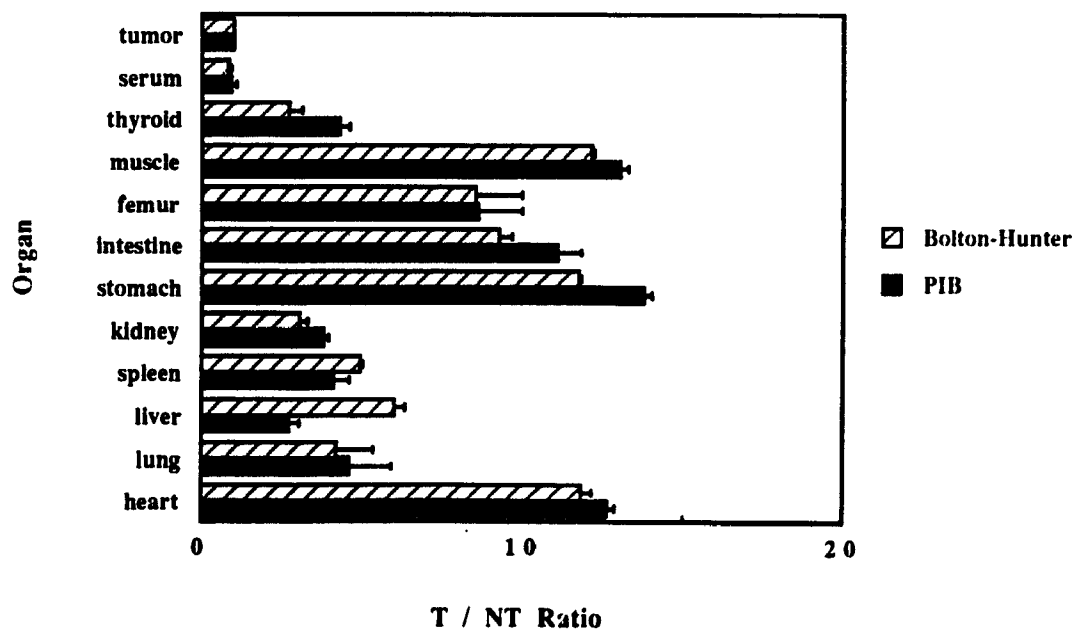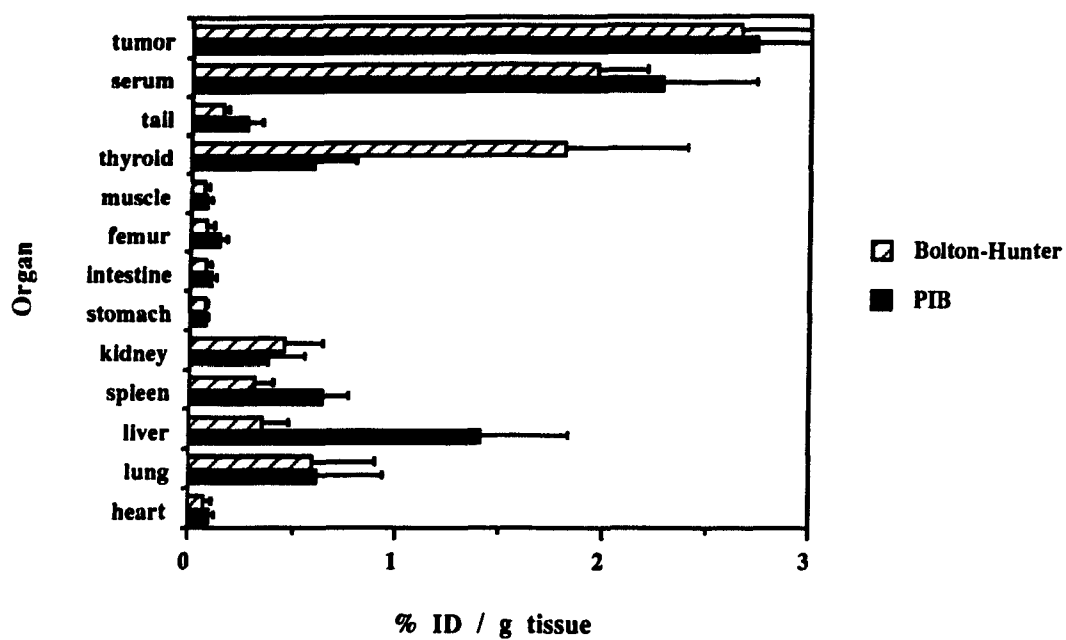
Fig. 64A

Fig. 64B
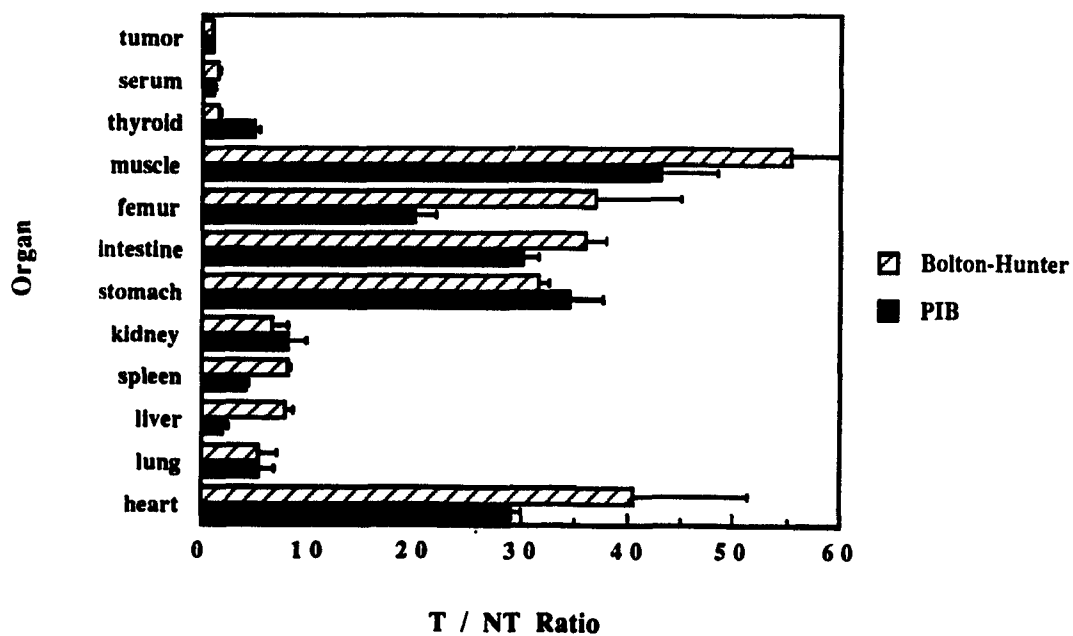
Fig. 65

Retention of immunoreactivity of ^{131}I-Dal B02 (PIB), ^{125}I-Dal B02 (B-H) and ^{125}I-Dal B02 (Chl. T) recovered from the serum of D10-1 xenograft bearing nude mice.

Each D10-1 xenograft bearing nude mouse was given 40 μg ^{131}I-Dal B02 (PIB) mixed with 40 μg of ^{125}I-Dal B02 (B-H) or 40 μg of ^{125}I-Dal B02 (Chl. T). Samples of serum were collected from the nude mice at 48 and 96 hr post antibody administration. The ability to bind to target cells of ^{131}I-Dal B02 (PIB), ^{125}I-Dal B02 (B-H) and ^{125}I-Dal B02 (Chl. T) in the serum was determined using D10-1 cells as described in Materials and Methods.

Top figure: Dal B02 (PIB).

Middle figure: Dal B02 (B-H).

Bottom figure: Dal B02 (Chl. T).

Fig. 65A
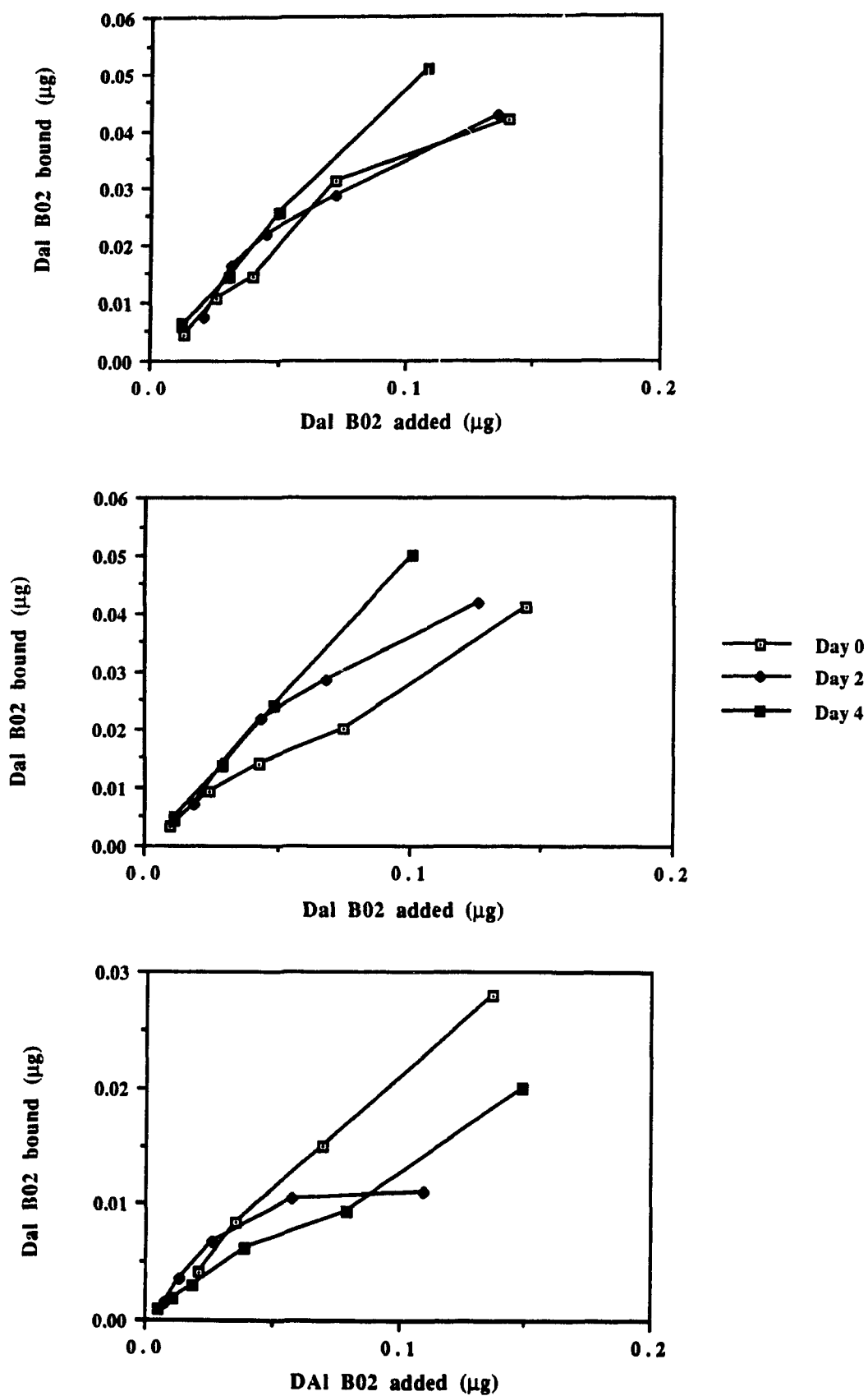
Table 17   IRF of ^{131}I-Dal B02 (PIB), ^{125}I-Dal B02 (B-H) and ^{125}I-Dal B02 (Chl. T) recovered from the serum of D10-1 xenograft bearing mice [1]

Time (hr)	0	48	96	168
PIB	76.5	86.8	81.8	77.0
B-H	63.2	83.8	81.9	67.6
Chl.T	51.0	48.8	47.0	37.9

1. Samples of serum were obtained f·. m D10-1 xenograft bearing nude mice given ^{131}I-Dal B02 (PIB) mixed with ^{125}I-Dal B02 (B-H) or ^{125}I-Dal B02 (Chl. T) at indicated intervals. The IRF of Dal B02 in the serum was determined using D10-1 cells as described in Materials and Methods.

Fig. 66

The influence of tumor weight on the percentage of the injected dose of radioiodinated Dal B02 that localized in the tumor.

Nude mice bearing D10-1 xenografts of different weight were given radioiodinated Dal B02 i.v.. At 48, 96 and 168 hr post antibody administration, 9 mice were sacrificed and the % ID / g tumor of Dal B02 was determined.

In these figures, the tumor weight in gram was plotted against the percentage of the injected dose of radioiodinated Dal B02 that localized in the tumor (% ID / g tumor). An inverse correlation between the tumor weight and the % ID / g tumor tissue was observed, i.e., the smaller the tumor, the higher the % ID / g tumor. This correlation was observed at all the three time points examined, i.e., at 48 hr (A), 96 hr (B), and 168 hr (C) after i.v. administration of radioiodinated Dal B02.

Fig. 66A
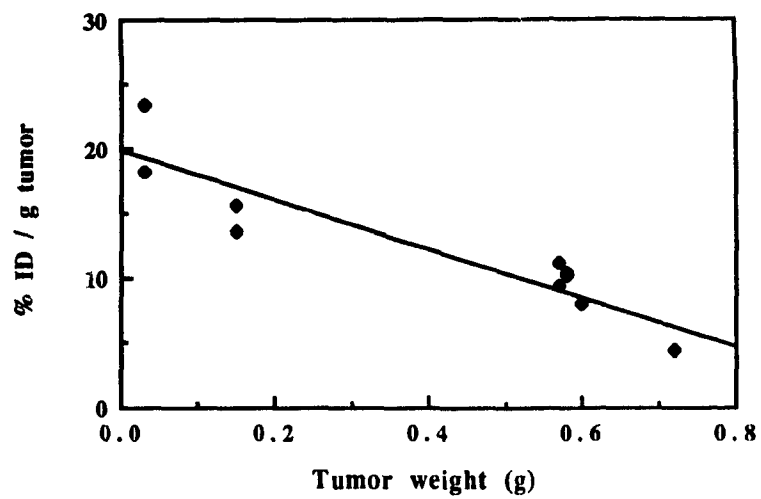
Fig. 66B
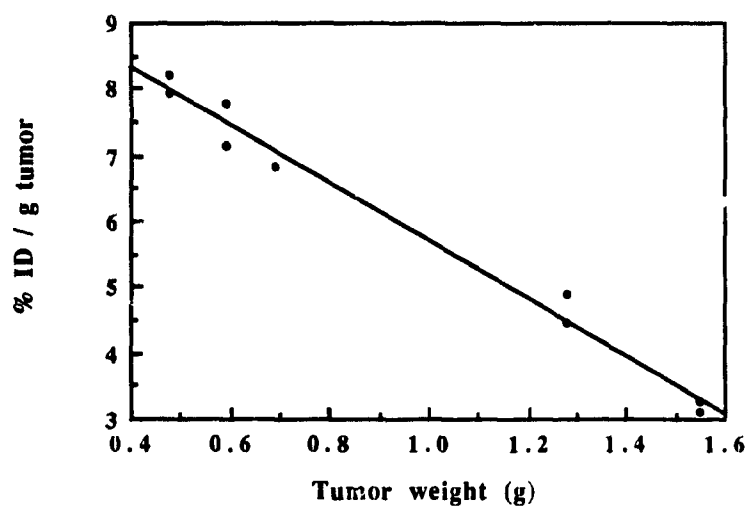
Fig. 66C
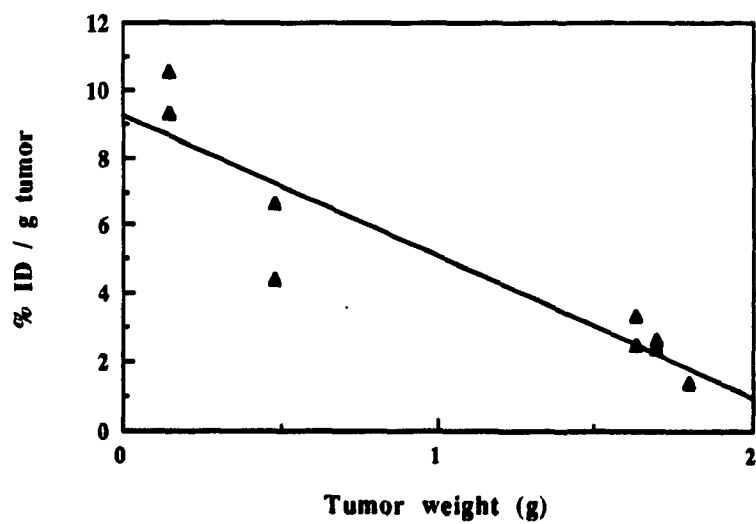
Fig. 67

Comparison of the effects of i.p. and i.v. routes of administration of radioiodinated Dal B02 on the blood concentration of Dal B02 and total body radioactivity.

D10-1 xenograft bearing nude mice were given radioiodinated Dal B02 via either the i.v. or i.p. route. At indicated intervals, samples of blood were obtained and the % ID / ml blood determined. The total body radioactivity of the mice was also monitored with a calibrator. Each point represents the mean of data obtained from 3 mice.

Fig. 67A The concentration of Dal B02 in the blood of D10-1 xenograft bearing nude mice after injection of radioiodinated Dal B02 via either the i.v. or the i.p. route.

Fig. 67B Total body radioactivity of D10-1 xenograft bearing nude mice after injection of radioiodinated Dal B02 via either the i.v. or the i.p. route.

Total body radioactivity
(% of initial activity)

Time (hr)

Fig. 67B

i.v. Injection
i.p Injection

Dal B02 in blood
(% ID / ml blood)

Time (hr)

Fig. 67A

i.v. Injection
i.p. Injection
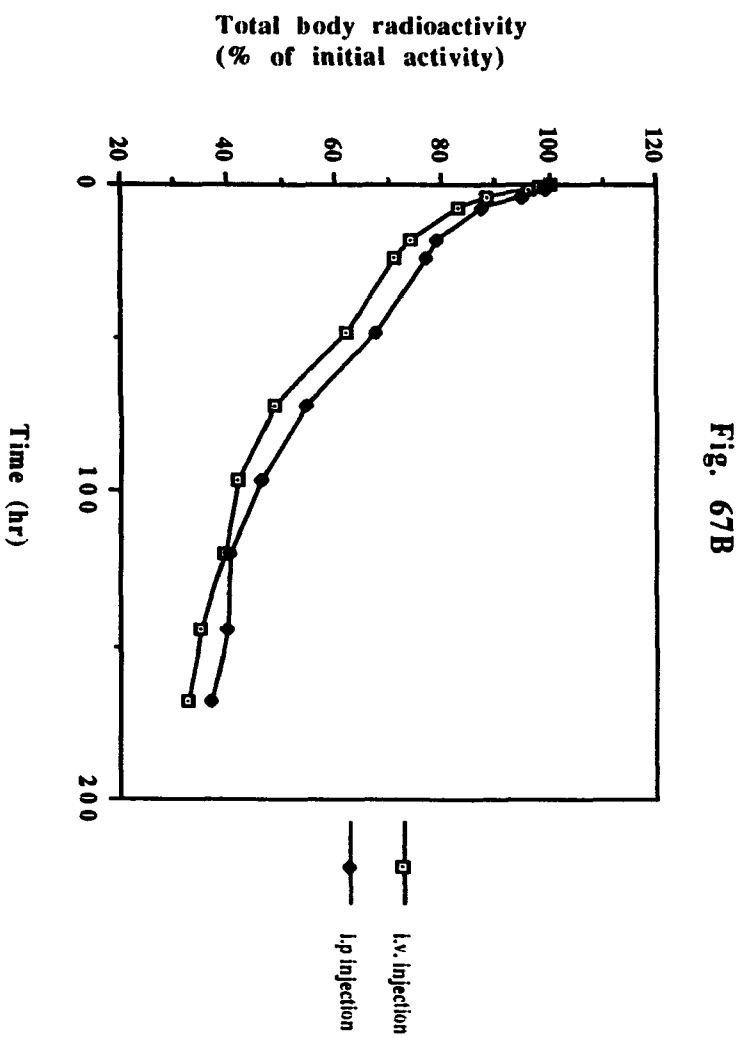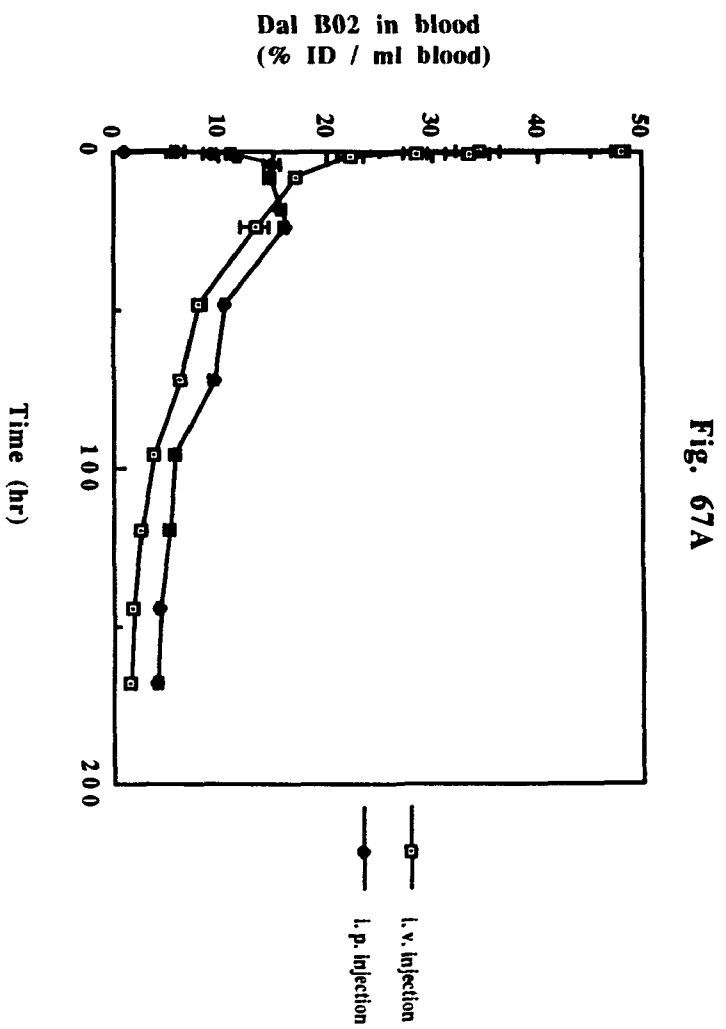
Figs. 68 and 69

Comparison of biodistribution and tumor localization of radioiodinated Dal B02 after administration into D10-1 xenograft bearing nude mice via either the i.v. or the i.p. route.

D10-1 xenograft bearing nude mice were given radioiodinated Dal B02 via either the i.v. or the i.p. route. The mice were sacrificed at 168 hr post antibody administration and the biodistribution of radioiodinated Dal B02 was determined.

Fig. 68   Biodistribution of ^{131}I-Dal B02 (PIB) after injection into D10-1 xenograft bearing nude mice via either the i.v. or i.p. route.

Fig. 69   Biodistribution of ^{125}I-Dal B02 (Chl. T) after injection into D10-1 xenograft bearing nude mice via either the i.v. or i.p. route.

Fig. 68A

% ID / g tissue

Fig. 68B

T / NT Ratio

Fig. 69A

% ID / g tissue
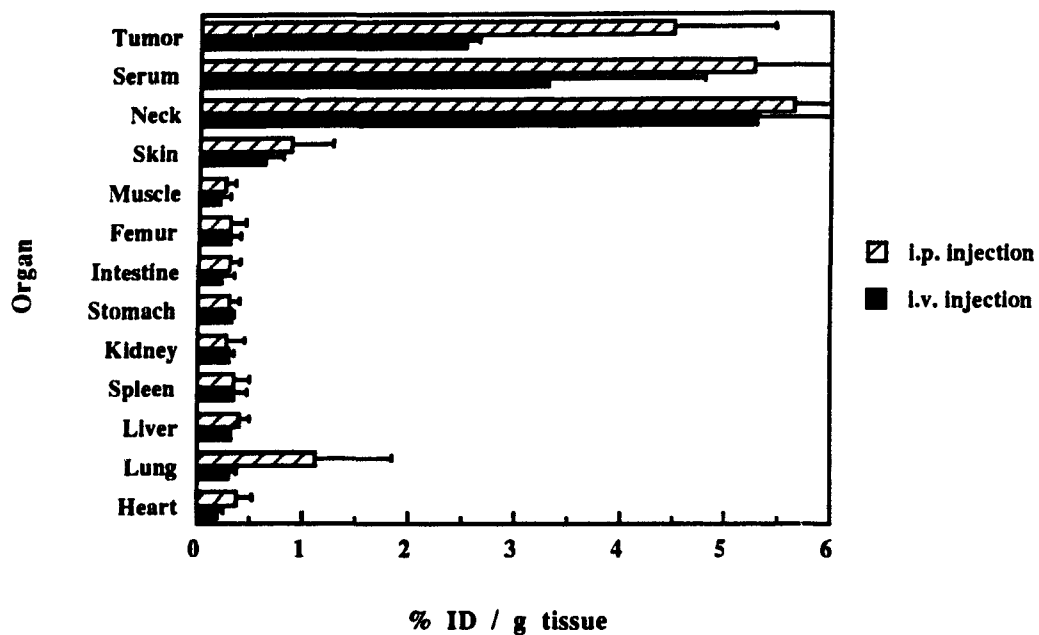
Fig. 69B
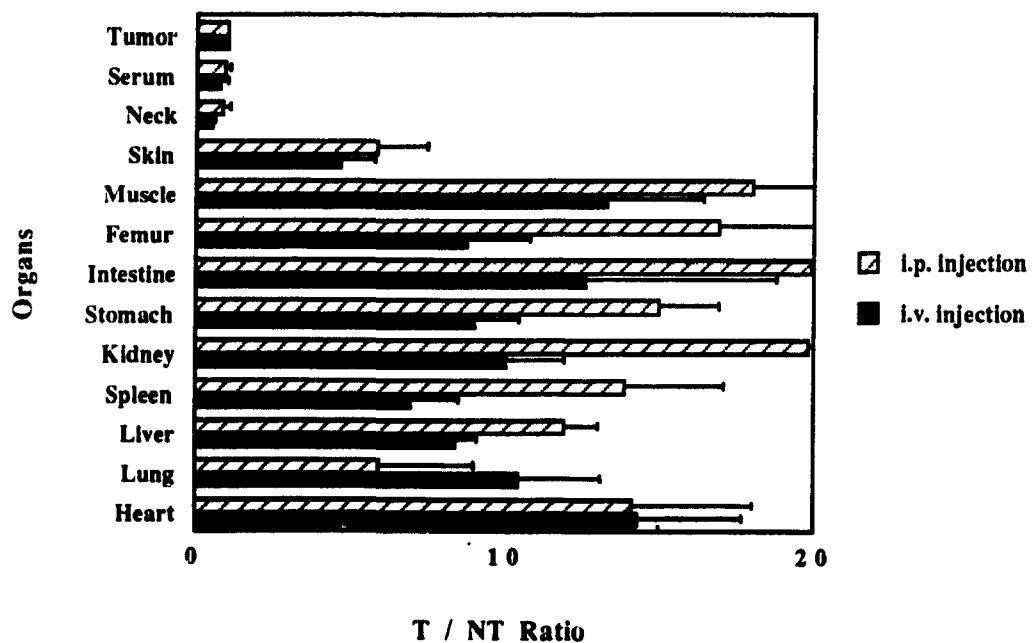
T / NT Ratio

Section 4 Preparation of Dal B01-MTX and Dal B02-MTX Immunoconjugates, Their Cytotoxicity in vitro and the Uptake of Dal B01 or Dal B02 Conjugated MTX by Tumor Cells

Previous investigations from this laboratory have demonstrated that when linked to an MoAb against tumor associated cell surface antigen (e.g., anti-renal cell carcinoma MoAbs and anti-melanoma MoAbs), the cytotoxicity of conjugated MTX towards target tumor cells was much greater compared to their cytotoxicity towards non-target cells (Ghose et al., 1988). The aim of this study was to prepare Dal B01-MTX conjugates and Dal B02-MTX conjugates via different linkages and to evaluate these conjugates as regards (i) retention of antibody and drug activities; (ii) anti-tumor potency in vitro; and (iii) their uptake by target D10-1 cells and non-target MOLT-3 cells.

4.1 Preparation of Dal B01-MTX and Dal B02-MTX Conjugates

In this study, MTX was linked to Dal B01 and Dal B02 via either active ester or hydrazone linkage. The resulting conjugates are respectively referred as MoAb-MTXAE conjugate and MoAb-MTXH conjugate.

4.1.1 Preparation of active ester based MoAb-MTX conjugates (MoAb-MTXAE)

The NHS active ester based method entails activation of the carboxyl group of MTX by means of NHS and DCC in DMF and then reaction of the active ester (MTX-AE) with nucleophilic groups in the MoAb protein in an aqueous medium at neutral pH. Conjugation of MTX to Dal B02 did not result in significant precipitation of the protein. However, considerable amounts of precipitates were observed with Dal B01. This resulted in the low recovery of Dal B01 protein (less than 30% of the amount of protein added) after

conjugation. The IgG/MTX molar ratio in both Dal B01-MTXAE and Dal B02-MTXAE conjugates was approximately 1 to 4 or 1 to 5 (i.e., one IgG molecule was loaded with 4 to 5 molecules of MTX).

4.1.2 Preparation of MoAb-MTX conjugates by site-specific hydrazone linkage (MoAb-MTXH)

As discussed in Introduction, this method of coupling is likely to avoid MTX incorporation in the antigen binding site of antibodies since carbohydrate moieties are mostly located in the Fc portion of the IgG molecule. Conjugation of MTX to the oligosaccharide moieties of antibody involves two steps: (i) generation of reactive aldehyde groups in oligosaccharides, and (ii) subsequent reaction of the polyaldehyde antibody with MTX hydrazide (MTXH) to form a hydrazone linkage. Compared to the active ester method, this method did not result in significant precipitation of Dal B01 during conjugation. The IgG/MTX molar ratio in both Dal B01-MTXH and Dal B02-MTXH conjugates was approximately 1 to 5 or 1 to 6 (i.e.,one IgG molecule was loaded with 5 to 6 molecules of MTX).

4.2 Retention of Antibody Activity

Retention of antibody activity in MoAb-MTX conjugates depends on avoiding the incorporation of drug molecules in the antigen binding sites of MoAbs and/or avoiding any conformational change as a result of drug loading that might interfere with antigen binding. Membrane immunofluorescence was used routinely in this study to determine the titers of MoAbs before and after conjugation with MTX. No significant difference in the titers (minimal antibody concentration that stains 50% of target D10-1 cells) was observed between Dal B02-MTXAE and Dal B02-MTXH conjugates, or between the parent Dal B02 and its conjugates (the parent Dal B02 and its conjugates had a titer of approximately 0.1

μg/ml). The titer of Dal B01-MTXAE conjugate (0.6 μg/ml) was somewhat higher than that of free Dal B01 and Dal B01-MTXH conjugate (0.3 μg/ml).

4.3 Retention of Drug Activity

Retention of drug activity in conjugates was assayed by inhibition of DHFR in a cell free system following the method described in Materials and Methods. Comparison of the DHFR inhibitory activity of free MTX with that of MoAb conjugated MTX showed that the IC_{50} values (MTX concentration required to inhibit 50% activity of DHFR) for all conjugates, irrespective of the MoAb used and the method of linkage, were 5 to 6-fold higher than that of free MTX. These observations can be attributed to steric factors since the molecular size of MoAb-MTX conjugate is much larger than that of free MTX.

4.4 In vitro Cytotoxicity of Dal B01-MTX and Dal B02-MTX Conjugates

A preliminary investigation had demonstrated that both Dal B01 and Dal B02 were not toxic to target D_{10-1} cells, or to the non-target MOLT-3 cells up to a concentration of 500 μg/ml. The maximum amount of conjugated MoAbs used in this study was below 250 μg per ml of cell culture medium.

When cells were exposed continuously for 72 hr to test agents in vitro (Figs. 70 and 72), free MTX was the most effective inhibitor of proliferation for both D_{10-1} and MOLT-3 cells. Exposure to a mixture of MTX plus Dal B01 or Dal B02 did not alter the cytotoxicity of MTX in the mixtures. Compared to free MTX, all MoAb conjugated MTX preparations were less inhibitory towards both target and non-target cells in this continuous exposure assay.

Considering the target D10-1 cells, both types of Dal B02-MTX conjugates, i.e., Dal B02-MTXAE and Dal B02-MTXH, were almost equally inhibitory (the IC_{50} values of the conjugates were 0.0387 µg/ml and 0.0359 µg/ml, respectively). However, these two conjugates were about 5-fold less inhibitory than free MTX. The Dal B01-MTXH conjugate (IC_{50}, 0.198 µg/ml) was about 30 times less inhibitory than free MTX. The least potent conjugate was Dal B01-MTXAE (IC_{50}, 0.328 µg/ml) which was about 50 times less inhibitory than free MTX.

MOLT-3 cells were more sensitive to free MTX than D10-1 cells. The IC_{50} of free MTX for MOLT-3 cells (0.00285 µg/ml) is 2.5-fold lower than that for D10-1 cells. In contrast to free MTX, Dal B01 or Dal B02-linked MTX was much less toxic towards the non-target MOLT-3 cells. The IC_{50} values of Dal B02-MTXAE and Dal B02-MTXH were 0.0296 µg/ml and 0.0875 µg/ml, which were about 10 and 30 times higher than that of free MTX, respectively. The IC_{50} values of Dal B01-MTXH and Dal B01-MTXAE conjugates was about 70 and 120 times higher than that of free MTX, respectively.

As shown in Table 18, the selectivity ratios of MoAb-MTX conjugates to target D10-1 cells over non-target MOLT-3 cells ranged from 1.8 to 5.7. When free MTX was simply mixed with (i.e., not covalently linked with) Dal B01, the selectivity ratio was below 1.0. These results indicate a selective cytotoxicity of MoAb-MTX conjugates towards antibody reactive target cells. The order of inhibitory potency of these agents towards target D10-1 cells was: MTX (free or plus MoAb) > Dal B02-MTXH > Dal B02-MTXAE > Dal B01-MTXH > Dal B01-MTXAE (Table 18).

In another study, the cells were exposed to test agents for only 6 hr after which the cells were washed thrice and then incubated in drug free medium for an additional period of 72 hr. This pulse exposure assay only measures the inhibitory effect of those amounts of drug

(either free or conjugated to MoAbs) that have entered the cells or that are bound to the cell

surface (due to the binding of the MoAb to tumor cell surface antigen) after the exposure. It

is believed that this is much closer to the clinical situation when the free drug or its

conjugate is given to patients by a bolus injection or a single infusion, after which the

concentration of the drug (either in free form or conjugated to MoAbs) in blood and/or

tumors decline rapidly because of drug metabolism and/or clearance. The results of this

pulse exposure assay are somewhat different from those obtained in continuous exposure

assay. Considering the target D10-1 cells, the Dal B02-MTXAE conjugate (IC50, 0.445

µg/ml) was somewhat more potent than free MTX (IC50, 0.775 µg/ml), and the Dal B01-

MTXAE conjugate (IC50, 2.15 µg/ml) is only about 3-fold less potent (instead of 50 times

less potent in the continuous exposure assay) than the free drug (Figs. 71 and 73). The

cytotoxicity of these two MoAb-MTX conjugates to non-target MOLT-3 cells was

significantly less in this pulse exposure assay. The IC50 of Dal B02-MTXAE conjugate to

MOLT-3 cells was 2.09 µg/ml, which was 22-fold higher than that of free MTX. For Dal

B01-MTXAE conjugate, a MTX concentration of 4.5 µg/ml (which is about 50 times

higher than the IC50 of free MTX to MOLT-3 cells) only yielded a 21% inhibition of cell

growth compared to the proliferation of untreated control cells (Table 18). The selectivity

ratios of both the MoAb-MTX conjugates to target D10-1 cells over non-target MOLT-3

cells were significantly increased (up to 43.5) in this pulse exposure assay compared to the

selectivity ratio obtained in continuous exposure assay. This result further confirms the

selective cytotoxicity of Dal B01-MTX and Dal B02-MTX conjugates towards target D10-1

cells.

In conclusion, after conjugation to Dal B01 or Dal B02, MTX was more cytotoxic to D10-1

cells than to MOLT-3 cells, although MOLT-3 cells were more sensitive to free MTX than

D10-1 cells. These results indicate that a selective cytotoxicity of MTX against target D10-1

cells was achieved after the conjugation of MTX to Dal B01 or Dal B02. The selectivity in

Figs. 70 and 71

Cytotoxicity of MTX, Dal B01-MTXAE and Dal B01-MTXH conjugates towards target D10-1 and non-target MOLT-3 cells.

Aliquots of D10-1 or MOLT-3 cells (5×10^5 cells in 100 μl of medium) were grown in a 96 well plate overnight, after which the stated amounts of free MTX or Dal B01-MTX conjugates (in 100 μl of PBS) were added to each well. In the continuous exposure assay, cells were incubated with the test agents for 72 hr. In the pulse exposure assay, cells were incubated with the test agents for 6 hr, then washed thrice and reincubated in fresh medium for an additional 72 hr. The total number of cells in each well were counted and inhibition of cell growth was determined as described in Methods section 9.4.

Fig. 70   Inhibition of cell proliferation after continuous exposure for 72 hr to test agents.

(A) D10-1 cells;   (B) MOLT-3 cells.

Fig. 71   Inhibition of cell proliferation after pulse exposure for 6 hr to test agents.

(A) D10-1 cells;   (B) MOLT-3 cells.

Fig. 70A
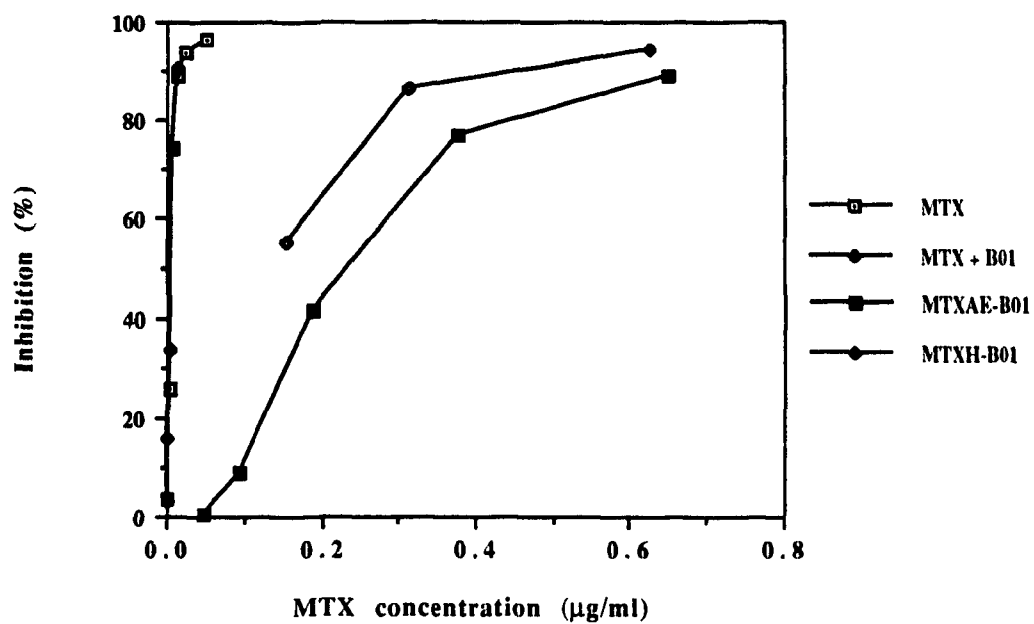
Fig. 70B
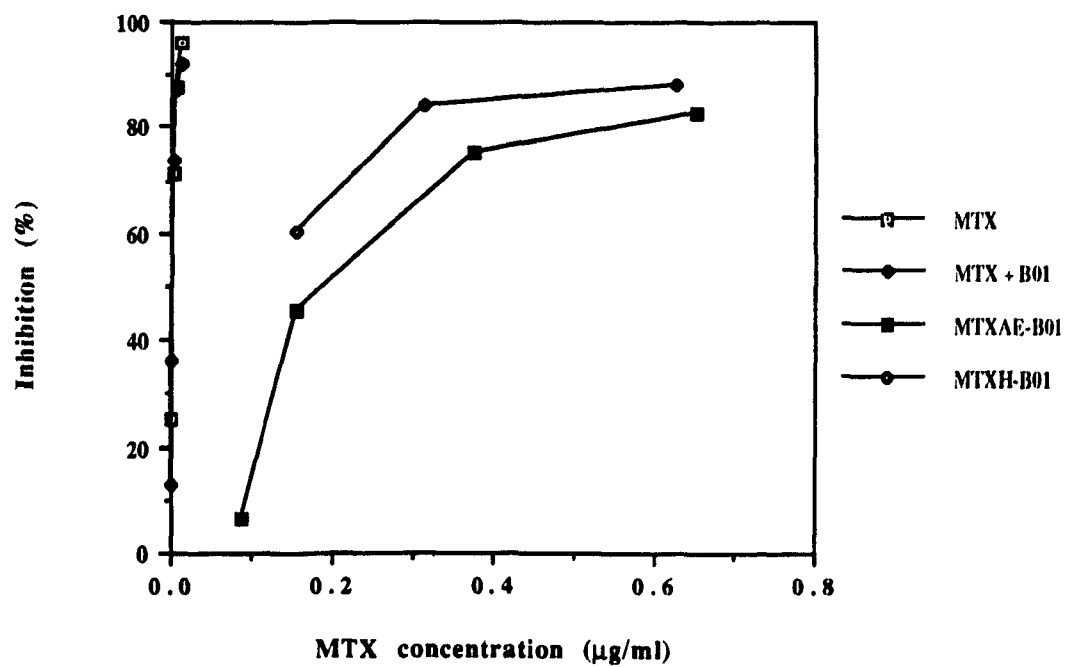
Fig. 71A
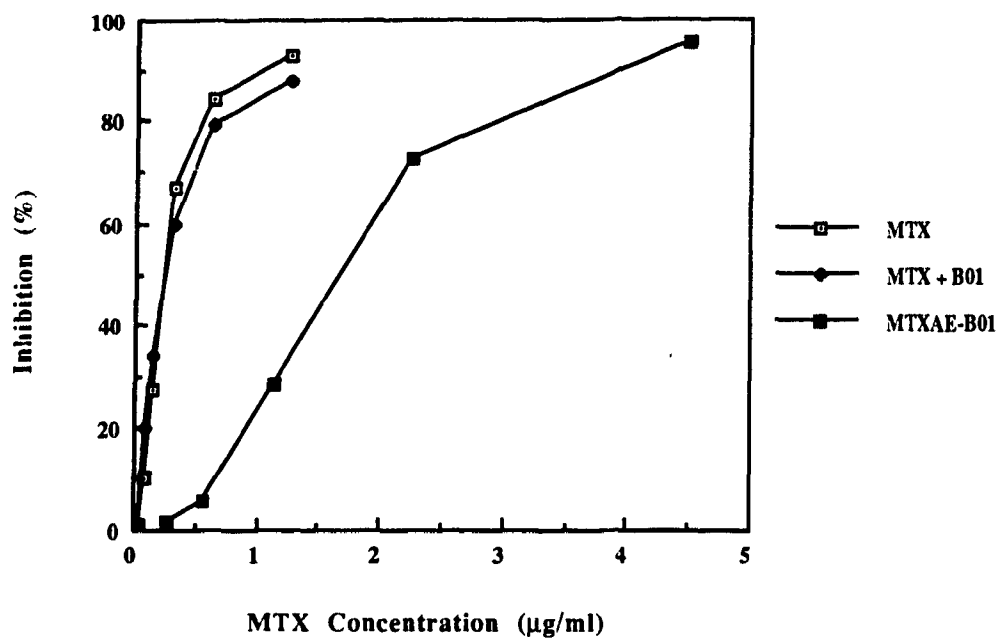
Fig. 71B
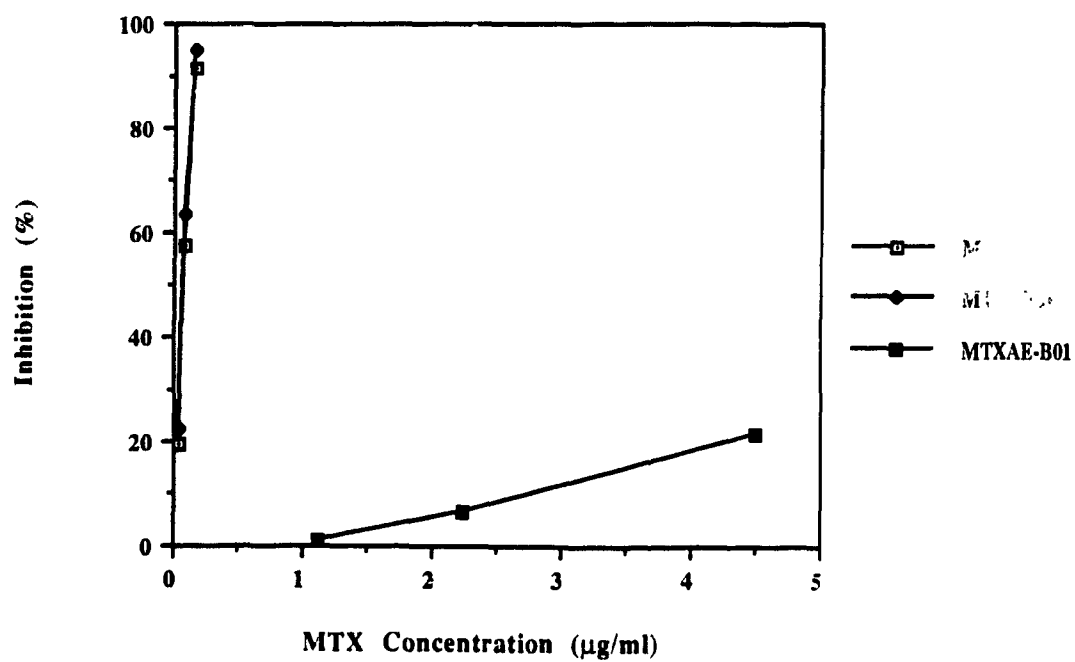
Figs. 72 and 73

Cytotoxicity of MTX, Dal B02-MTXAE and Dal B02-MTXH conjugates towards target D10-1 and non-target MOLT-3 cells.

Aliquots of D10-1 or MOLT-3 cells (5×10^5 cells in 100 µl of medium) were grown in a 96 well plate overnight, after which the stated amounts of free MTX or Dal B02-MTX conjugates (in 100 µl PBS) were added to each well. In the continuous exposure assay, cells were incubated with the test agents for 72 hr. In the pulse exposure assay, cells were incubated with the test agents for 6 hr, then washed thrice and reincubated in fresh medium for an additional 72 hr. The total number of cells in each well were counted and inhibition of cell growth was determined as described in Methods section 9.4.

Fig. 72   Inhibition of cell proliferation after continuous exposure for 72 hr to test agents.

(A) D10-1 cells;   (B) MOLT-3 cells.

Fig. 73   Inhibition of cell proliferation after pulse exposure for 6 hr to test agents.

(A) D10-1 cells;   (B) MOLT-3 cells.

Fig. 72A
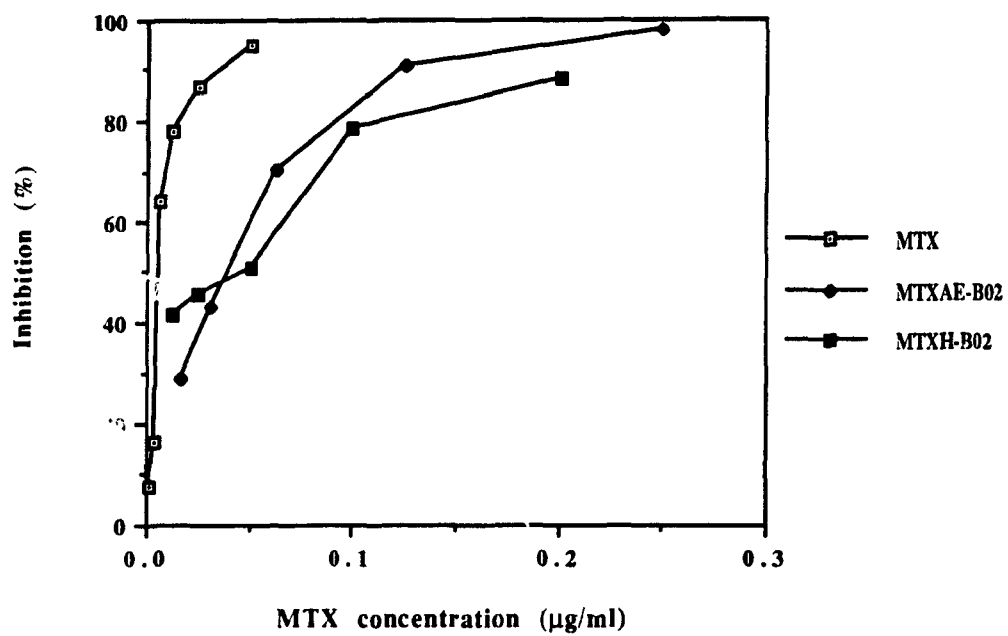
Fig. 72B
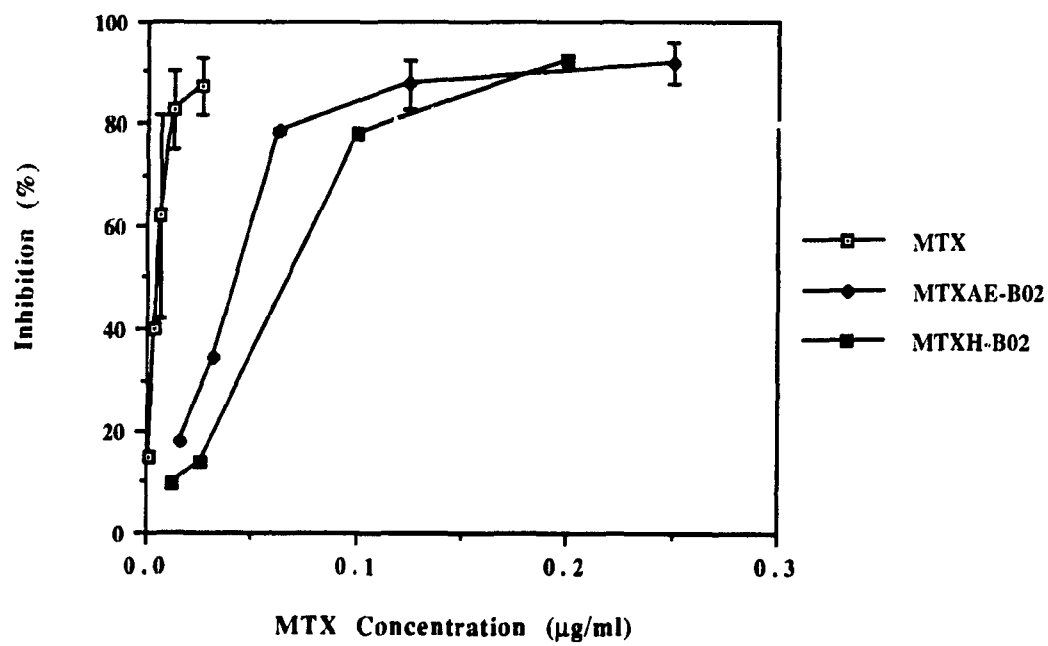
Fig. 73A
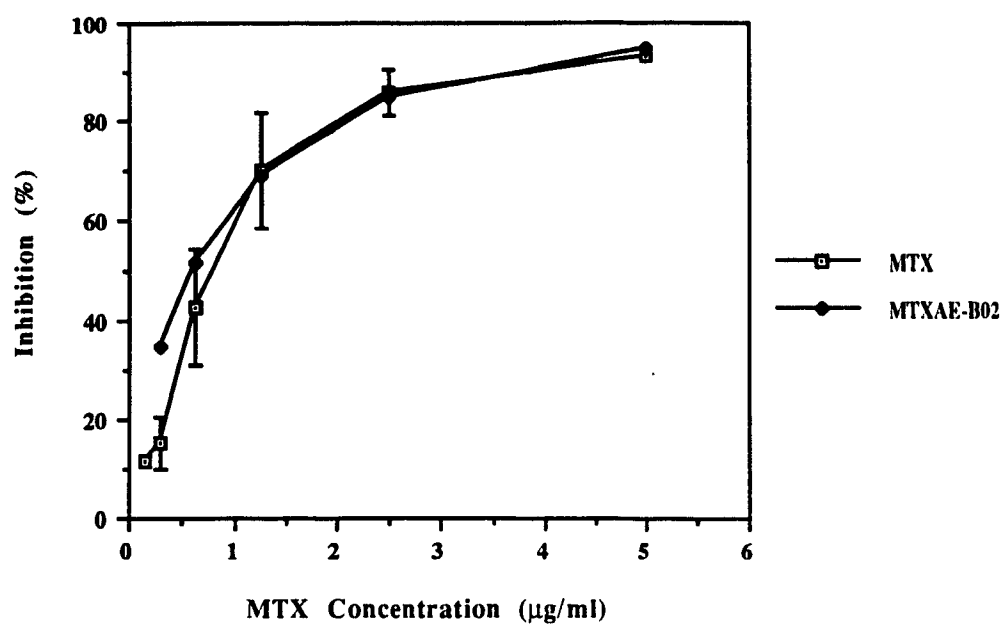
Fig. 73B
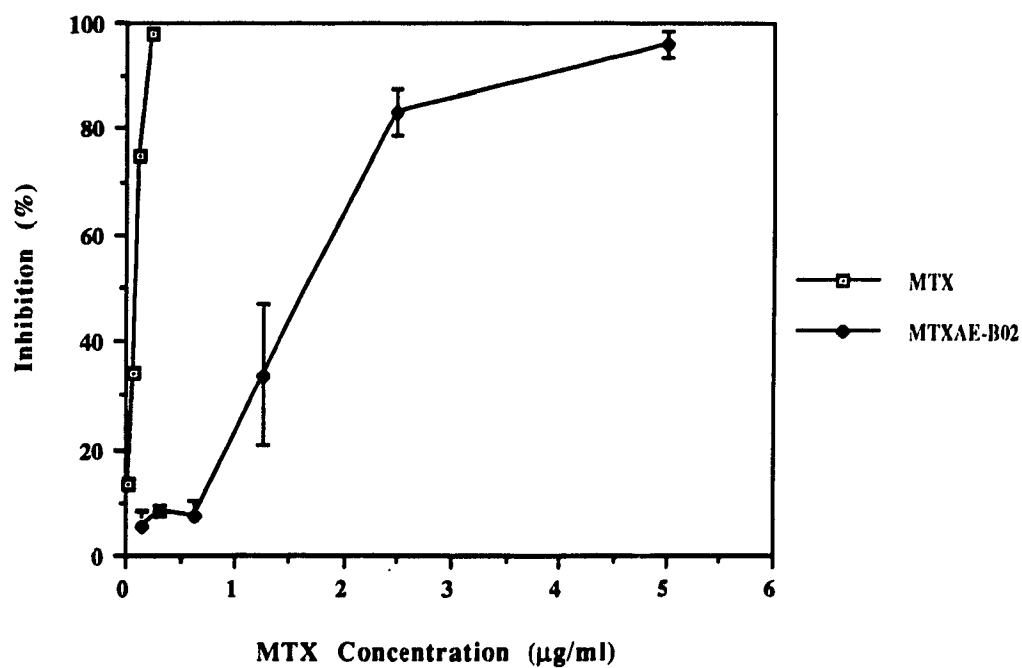
Table 18   IC$_{50}$ values of MTX, Dal B01-MTX and Dal B02-MTX conjugates for D$_{10-1}$ and MOLT-3 cells [1]

(A) 72 hr continuous exposure

	D$_{10-1}$ cells	MOLT-3 cells	Selectivity Ratio [4]
MTX	0.0068 ± 0.0014 [2] (1.0) [3]	0.00285 ± 0.0002 (1.0)	1.0
MTX + Dal B01 [5]	0.0071 ± 0.0008 (0.96)	0.0027 ± 0.0003 (1.0)	0.91
Dal B01-MTXAE [6]	0.328 ± 0.061 (0.021)	0.361 ± 0.008 (0.008)	2.7
Dal B01-MTXH [7]	0.198 ± 0.031 (0.034)	0.21 ± 0.06 (0.014)	2.5
Dal B02-MTXAE [6]	0.0387 ± 0.006 (0.176)	0.0296 ± 0.008 (0.096)	1.8
Dal B02-MTXH [7]	0.0359 ± 0.003 (0.189)	0.0875 ± 0.009 (0.033)	5.7

1. The cytotoxicity of free MTX and its conjugates was assayed using target D$_{10-1}$ cells and non-target MOLT-3 cells as described in Materials and Methods.

2. The values represent μg of MTX (in free or conjugated form) per ml medium and are the mean ± S.D. of at least 3 determinations.

3. The figures inside parenthesis represent the sensitivity ratio which can be calculated as follow :

$$\text{Sensitivity ratio} = \frac{\text{The IC}_{50}\text{ value of test agent to the cells}}{\text{The IC}_{50}\text{ value of free MTX to the cells}}$$

(Continued)

(B) 6 hr pulse exposure

	D10-1 cells	MOLT-3 cells	Selectivity Ratio
MTX	0.775 ± 0.276 (1.0)	0.093 ± 0.016 (1.0)	1.0
MTX + Dal B01	0.585 (1.32)	0.073 (1.27)	1.04
Dal B01-MTXAE	2.15 (0.36)	> 4.5 [8] (< 0.02)	> 18
Dal B02-MTXAE	0.445 (1.74)	2.09 (0.04)	43.5

4. The selectivity ratio was calculated by

$$\text{Selectivity ratio} = \frac{\text{The sensitivity ratio of the test agent to target cells}}{\text{The sensitivity ratio of the test agent to non-target cells}}$$

5. The mixture of free MTX and free MoAb contained the same IgG/MTX molar ratio as in the MoAb-MTX conjugate.

6. MTX was linked to MoAb via active ester linkage (non-site specific linkage).

7. MTX was linked to MoAb via hydrazone linkage (site-specific linkage).

8. A concentration of 4.5 µg/ml yielded an inhibition of 21% only.

cytotoxicity of both Dal B01-MTX and Dal B02-MTX conjugates was higher in pulse exposure assay compared to that in continuous exposure assay. The IC_{50} values of DHFR inhibition were 5 to 6 times higher for all the four MoAb-MTX conjugates compared to that of free MTX. Except for the Dal B02-MTX conjugate in 6 hr pulse exposure assay, all other 3 three MoAb-MTX conjugates used in this study were less inhibitory to cell proliferation compared to free MTX. No significant difference was observed between MoAb-MTXAE conjugates and MoAb-MTXH conjugates regarding the retention of antibody and drug activities.

4.5 Uptake of Free MTX, Dal B01 or Dal B02 Conjugated MTX by D10-1 and MOLT-3 Cells

As discussed in the Introduction section, MTX binds to its target enzyme DHFR and inhibits the conversion of dihydrofolic acid to tetrahydrofolic acid. For inhibition of cell proliferation, the intracellular concentration of MTX has to exceed the intracellular level of DHFR. To determine whether the conjugation of MTX to anti-tumor MoAbs will lead to the uptake of higher amount of MTX by target cells, it is necessary to compare the kinetics of uptake and efflux of MoAb conjugated MTX with that of free MTX. In this study, experiments were carried out to determine the (i) uptake of free [^{3}H]-MTX by D10-1 and MOLT-3 cells; (ii) uptake of Dal B01 and Dal B02 conjugated [^{3}H]-MTX by D10-1 and MOLT-3 cells; (iii) efflux of free [^{3}H]-MTX from D10-1 and MOLT-3 cells; and (iv) the release of free [^{3}H]-MTX or [^{3}H]-MTX containing MoAbs (or their fragments) from target D10-1 cells after the cells were incubated with either Dal B01-MTX conjugate or Dal B02-MTX conjugate.

4.5.1 Uptake of free [^{3}H]-MTX by D10-1 and MOLT-3 cells

In this in vitro study, cell surface associated [^{3}H]-MTX, either free or conjugated to MoAbs, were distinguished from the internalized [^{3}H]-MTX by deducting cell associated [^{3}H] radioactivity after incubation at 4°C (a temperature at which endocytosis does not take place) from cell associated [^{3}H] radioactivity after incubation at 37°C. The amounts of cell associated [^{3}H] radioactivity at 37°C will include both surface associated and endocytosed [^{3}H]-MTX but the cell associated radioactivity at 4°C will measure only the cell surface associated drug.

The time-course of uptake of free [^{3}H]-MTX by D10-1 and MOLT-3 cells incubated at either 4°C or 37°C was determined using an extracellular concentration of 10 μM of [^{3}H]-MTX. As shown in Fig. 74, both cells took up much more free drug at 37°C than at 4°C. The net uptake of free [^{3}H]-MTX by D10-1 cells was rapid and leveled off at about 15 min, which was earlier than the time needed for reaching the plateau of uptake of free [^{3}H]-MTX by MOLT-3 cells which was about 45 to 60 min. However, the maximum uptake of free [^{3}H]-MTX by MOLT-3 cells at the end of incubation (15 pmol MTX/mg protein) was higher than the amount of MTX taken up by D10-1 cells (10 pmol MTX/mg protein).

In another experiment to obtain Eadie-Hoftsee plots, D10-1 and MOLT-3 cells were incubated for 3 min either at 37°C or 4°C with various concentrations of [^{3}H]-MTX, i.e., ranging from 0.156 to 80 μM. As shown in Figs. 75 and 76 , D10-1 cells took up slightly more [^{3}H]-MTX than MOLT-3 cells under these conditions. This is well in agreement with the fact that D10-1 cells took up free [^{3}H]-MTX more rapidly than MOLT-3 cells at the first 10 min of incubation (as described above). From the Y-axis intercepts of the Eadie-Hoftsee plots, the Vmax (i.e., rate of maximum uptake) for D10-1 cells was determined to be 9.76 pmol MTX/mg protein/min, and for MOLT-3 cells the Vmax was 7.42 pmol MTX/mg protein/min. From the slope of the plots, the Km values (i.e., [^{3}H]-MTX concentration

giving half maximum uptake) for D10-1 cells was calculated to be 8.37 μM, and for MOLT-3 cells was calculated to be 8.52 μM.

4.5.2 Efflux of free [³H]-MTX from D10-1 and MOLT-3 cells

For inhibition of cell proliferation, the intracellular concentration of MTX has to exceed the level of intracellular DHFR. Hence it is important to know how much MTX remains inside the exposed cells (bound to DHFR) after incubation with a defined extracellular concentration of MTX. In this study, efflux of [³H]-MTX from D10-1 and MOLT-3 cells was determined after loading the cells with free [³H]-MTX at an extracellular concentration of 10 μM. The amounts of [³H]-MTX that remained associated with D10-1 or MOLT-3 cells at various times after incubation in MTX free efflux medium were determined. Since MTX binds stoichiometrically to intracellular DHFR, the molar amount of MTX that remains inside cells after the completion of efflux equals to that of intracellular DHFR.

D10-1 and MOLT-3 cells were first loaded with [³H]-MTX by incubation with 10 μM of free [³H]-MTX at 37°C for 2 hr. The cells were then washed and reincubated for another 2 hr in fresh, MTX free efflux medium. Aliquots of cells were collected at defined intervals, washed and cell associated radioactivity was determined. As shown in Fig. 77, MOLT-3 cells initially took up more free [³H]-MTX than D10-1 cells did (i.e., 23 pmol MTX/mg protein in MOLT-3 cells versus 18 pmol MTX/mg protein in D10-1 cells). The efflux of free MTX from D10-1 cells stopped at about 10 to 15 min after incubation in the efflux medium (which is earlier than the time needed by MOLT-3 cells which stopped at about 45 to 60 min), after which the cell associated [³H]-MTX remained at a constant level. At the end of efflux, the levels of intracellular [³H]-MTX was about 11 pmol MTX/mg protein for D10-1 cells, and was about 8 pmol MTX/mg protein for MOLT-3 cells. These results show that the level of intracellular DHFR in D10-1 cells is higher than that in MOLT-3 cells.

Fig. 74

The time-course of uptake of free [^{3}H]-MTX by D10-1 and MOLT-3 cells.

Ten million cells were incubated with [^{3}H]-MTX at an extracellular concentration of 10 µM either at 4°C or 37°C for up to 120 min. At indicated intervals, aliquots of cells were taken out, washed 6 times with cold PBS and cell associated [^{3}H] activity was determined. The protein content of the cell pellet was determined by Lowry's method.

Fig. 74A The time-course of uptake of [^{3}H]-MTX by D10-1 cells.

Fig. 74B The time-course of uptake of [^{3}H]-MTX by MOLT-3 cells.

Fig. 74A
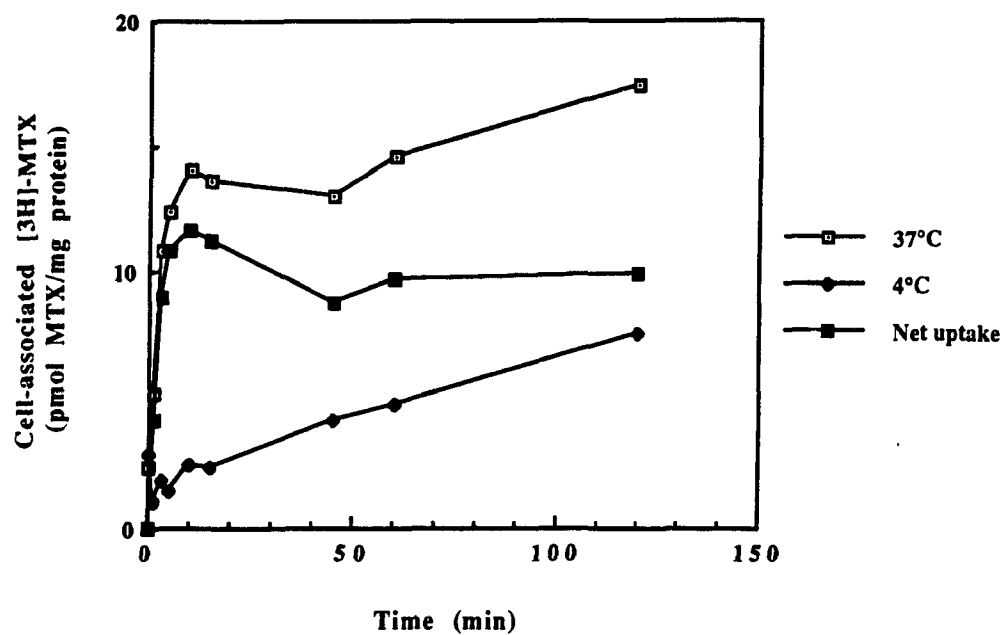
Fig. 74B
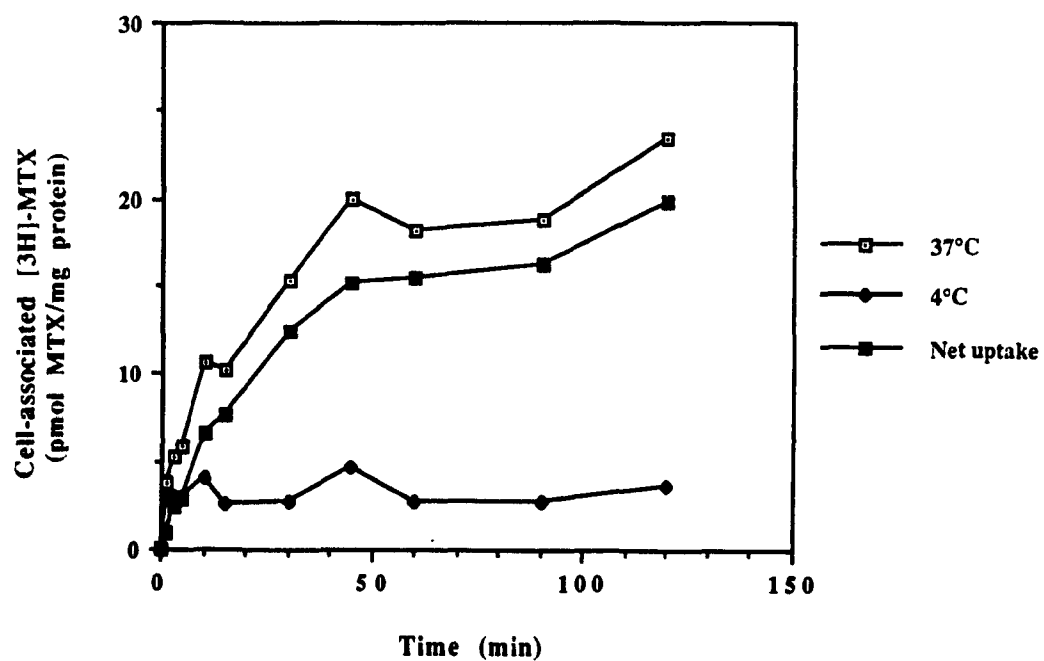
Figs.75 and 76

Rate of uptake of [^{3}H]-MTX by D10-1 and MOLT-3 cells.

One million D10-1 or MOLT-3 cells were incubated with various extracellular concentrations of [^{3}H]-MTX at either 4°C or 37°C for 3 min. At the end of incubation, the cells were washed 6 times with cold PBS and cell associated [^{3}H] activity was determined.

Fig. 75A Uptake of [^{3}H]-MTX by D10-1 cells.

Fig. 75B Eadie-Hoftsee ; ; t of data from Fig. 75A, from which the Vmax (the Y-axis intercept) and Km (the slope) values were determined.

Fig. 76A Uptake of [^{3}H]-MTX by MOLT-3 cells.

Fig. 76B Eadie-Hoftsee plot of data from Fig.76A, from which the Vmax (the Y-axis intercept) and Km (the slope) values were determined.

Fig. 75A
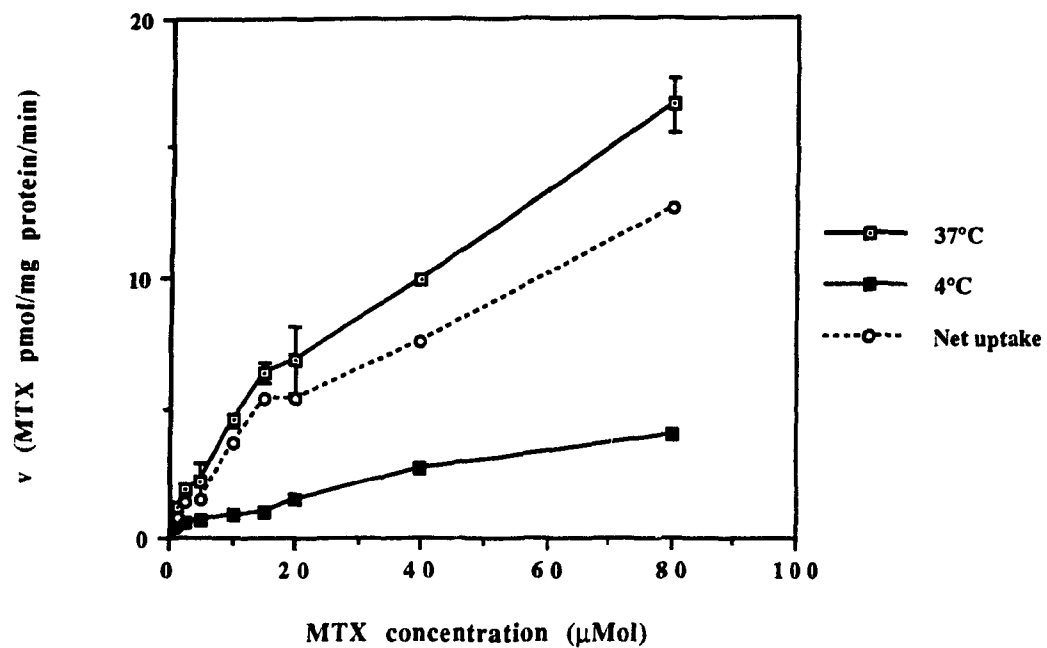
Fig. 75B
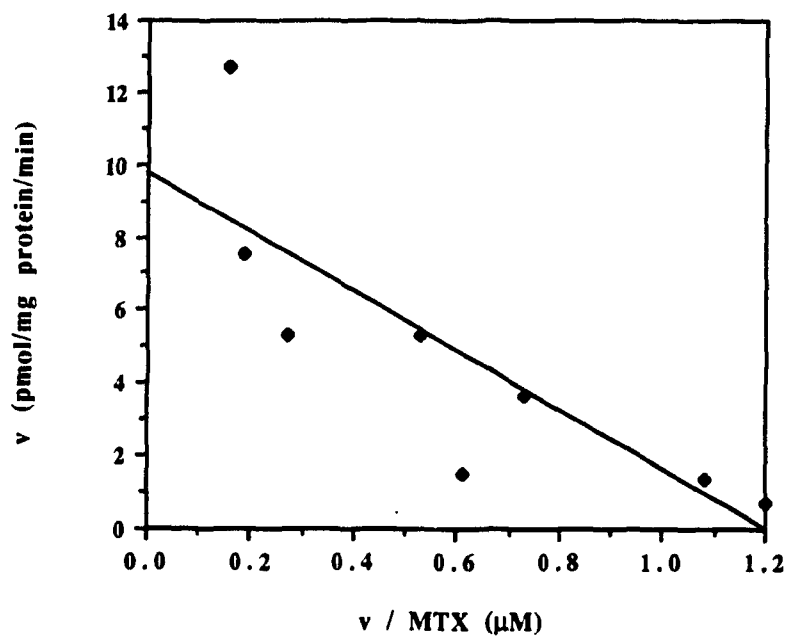
Fig. 76A
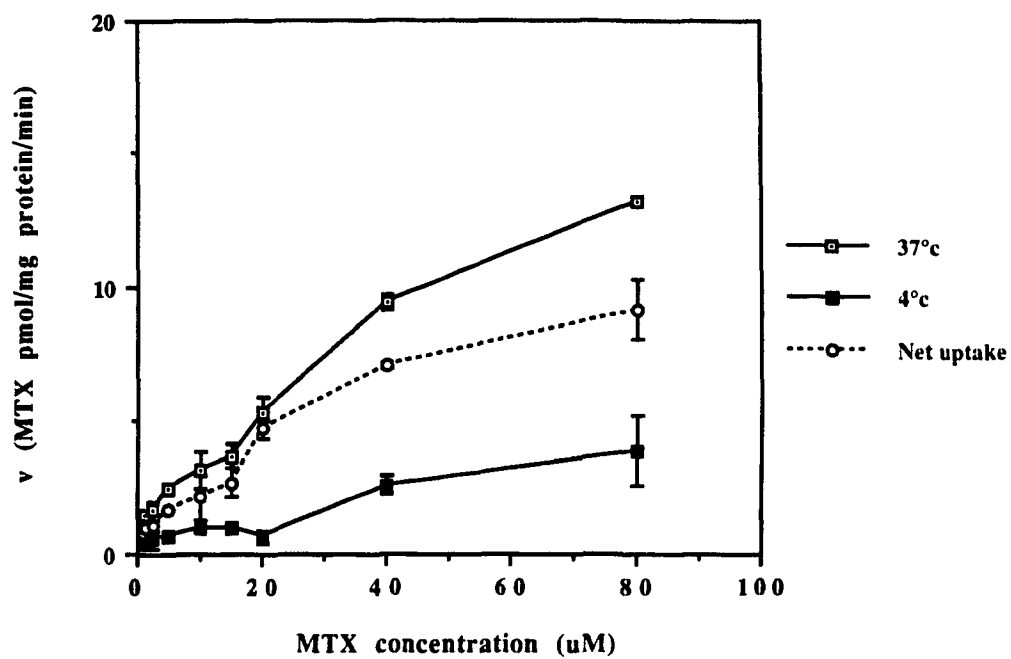
Fig. 76A

Fig. 76B

Fig. 76B
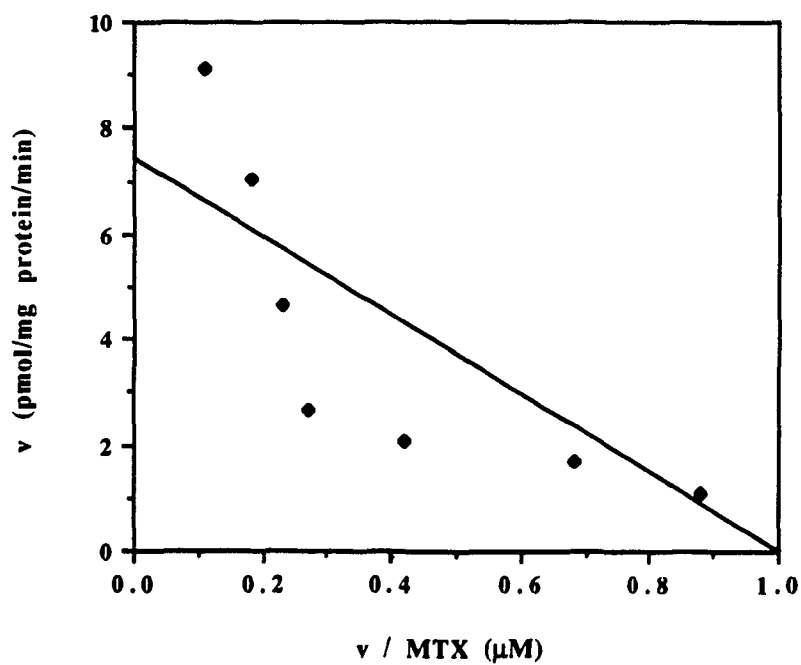
Fig.77

Efflux of [^{3}H]-MTX from D$_{10\text{-}1}$ and MOLT-3 cells.

Ten million D$_{10\text{-}1}$ or MOLT-3 cells were incubated with [^{3}H]-MTX at an extracellular concentration of 10 µM for 120 min at 37°C. At the end of incubation, the cells were washed 6 times with cold PBS and reincubated in drug free medium at 37°C for a period of 120 min. At indicated intervals, aliquots of cells were taken out and the cell associated [^{3}H] activity was determined.

**Cell-associated [3H]-MTX
(pmol MTX/ mg protein)**

Time (min)

Fig. 77

D10-1

MOLT-3

328
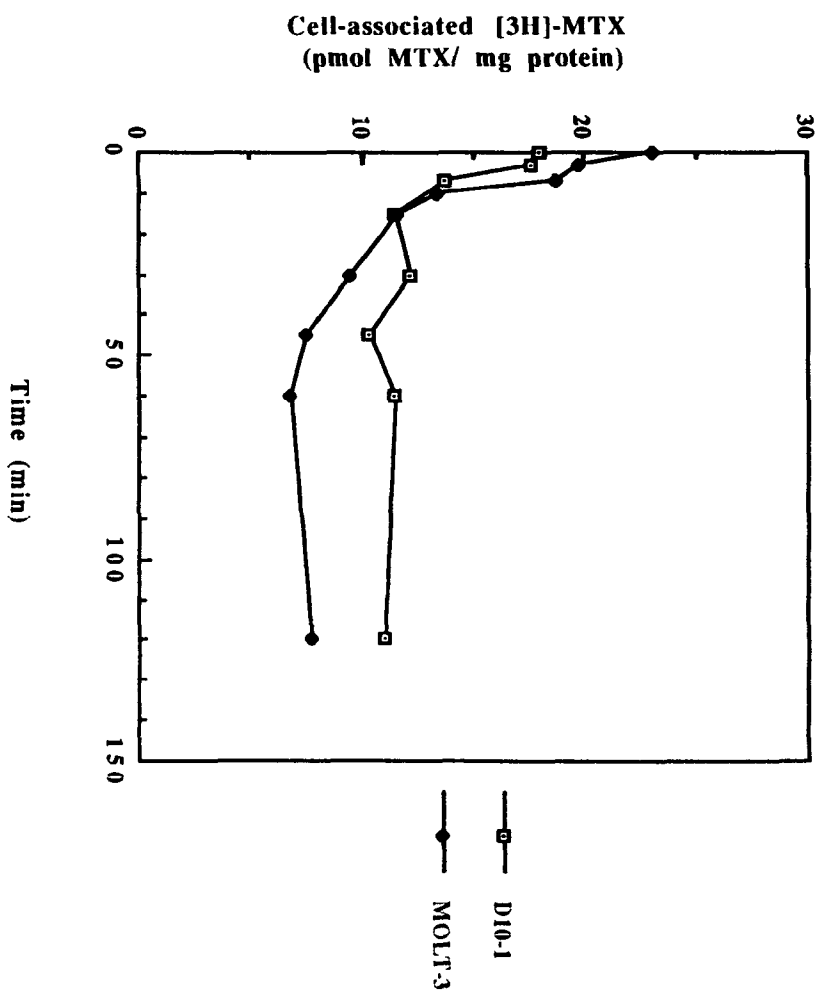
4.5.3 Uptake of Dal B01 or Dal B02 conjugated [³H]-MTX by D10-1 and MOLT-3 cells

The time-course of uptake of Dal B01 and Dal B02 conjugated [³H]-MTX by D10-1 cells was determined at an extracellular [³H]-MTX concentration of 10 μM. As shown in Fig. 78, the binding of either Dal B01-MTX or Dal B02-MTX conjugate to D10-1 cells was rapid. The maximum binding (i.e., plateau) was reached within the first 5 min of incubation either at 4°C or 37°C, and then remained unchanged during the incubation period of 3 hr. Approximately 3 to 4-fold more [³H]-MTX conjugated to Dal B02 bound to D10-1 cells compared to [³H]-MTX conjugated to Dal B01 at all extracellular concentrations of the conjugates investigated. When the net amounts of uptake were calculated, it was found that the maximum amount of uptake was 78 pmol MTX/mg protein for [³H]-MTX conjugated to Dal B01 and 125 pmol MTX/mg protein for [³H]-MTX conjugated to Dal B02. This is about 8-fold higher for Dal B01-MTX conjugate, and 12-fold higher for Dal B02-MTX conjugate than the uptake of free [³H]-MTX by D10-1 cells.

Fig. 79 shows the uptake of [³H]-MTX, either free or conjugated to Dal B01 or Dal B02, by D10-1 and MOLT-3 cells at different extracellular [³H]-MTX concentrations at either 4°C or ³7°C for 90 min. The net uptake of MoAb conjugated [³H]-MTX at 37°C was calculated by subtracting the amount of MTX bound at 4°C from the total amount of MTX bound at 37°C. Comparison of the net uptake of MoAb conjugated [³H]-MTX (Figs. 79 A and B) with the net uptake of free [³H]-MTX (Fig. 79 C) by D10-1 cells revealed that the uptake of the conjugated drug exceeded that of free drug at equivalent extracellular drug concentrations by approximately 10 to 20 times (for Dal B01-MTX conjugate) and 30 to 40 times (for Dal B02-MTX conjugate). Even though MOLT-3 cells took up slightly more free [³H]-MTX than D10-1 cells (Fig. 79C and D), target D10-1 cells took up much more MoAb conjugated MTX than non-target MOLT-3 cells (Fig. 79B).

The results show that D10-1 cell took up more [^{3}H]-MTX when conjugated to Dal BO2 than to Dal BO1. This is consistence with the observation that 4 to 6 times more of Dal BO2-MTX conjugate bound to D10-1 cells than Dal BO1-MTX conjugate did. This result is well in agreement with our earlier observation that Dal BO2 preparation had a higher IRF and ^{125}I labeled Dal BO2 bound more to D10-1 cells than ^{125}I labeled Dal BO1 did. From Fig. 79 B, it can be seen that the non-target MOLT-3 cells also took up a substantial amount of Dal BO2-MTX conjugate. This suggests that, in addition to specific binding and uptake of MoAb conjugated MTX, there may also be non-specific binding and uptake of MoAb-MTX conjugates by tumor cells.

As shown in Figs. 79A and B, the amounts of [^{3}H]-MTX conjugated to either Dal BO1 or Dal BO2 that remained associated with D10-1 cells leveled off (i.e., reached a plateau) at an extracellular concentration of 20 μM of [^{3}H]-MTX for both Dal BO1-MTX and Dal BO2-MTX conjugates. The maximum amount of [^{3}H]-MTX that bound to D10-1 cells after incubation for 90 min at 37°C was approximately 1000 pmol MTX/mg protein for Dal BO1-MTX conjugate, and 4000 pmol MTX/mg protein for Dal BO2-MTX conjugate. The maximum net uptake was approximately 250 pmol MTX/mg protein for Dal BO1 conjugated [^{3}H]-MTX and 862 pmol/mg protein for Dal BO2 conjugated [^{3}H]-MTX. Again, it can be seen that the amount of uptake of Dal BO2 conjugated [^{3}H]-MTX by D10-1 cells was about 3 to 4-fold higher than the uptake of Dal BO1 conjugated [^{3}H]-MTX.

4.5.4 Uptake of free or MoAb conjugated [^{3}H]-MTX by D10-1 and MOLT-3 cells after pulse exposure for 6 hr

The purpose of this study was to determine the absolute amounts of [^{3}H]-MTX, either free or conjugated with MoAbs, that remained associated with target D10-1 or non-target MOLT-

3 cells (either intracellularly or bound to cell surface) after pulse exposure for 6 hr to various extracellular concentrations of free or MoAb conjugated [^{3}H]-MTX. The [^{3}H]-MTX concentrations (either free or conjugated to MoAb) used in this study were the same as those used to determine the IC$_{50}$ values in the proliferation assay described above. From Table 18, it can be seen that the IC$_{50}$ values for D$_{10-1}$ cells in the 6 hr pulse exposure assay were approximately 1.4 µM for free MTX, 3.9 µM for Dal B01-MTX conjugate and 0.8 µM for Dal B02-MTX conjugate. In this study, the MTX concentrations (either free or conjugated to MoAb) used ranged from 1.25 µM to 10.0 µM.

As shown in Fig. 80, after pulse exposure for 6 hr to various extracellular concentrations of free or MoAb conjugated [^{3}H]-MTX, approximately 50 to 150 times more [^{3}H]-MTX linked to Dal B01, and 150 to 300 times more [^{3}H]-MTX linked to Dal B02, remained associated with D$_{10-1}$ cells than free [^{3}H]-MTX did. Since no parallel study was carried out at 4°C to determine the amount of cell surface bound MoAb-MTX conjugate, we could not determine the absolute amount of MoAb-MTX conjugate that were endocytosed by the cells. However, these results indicate that much more MTX remained associated with target D$_{10-1}$ cells after pulse exposure of the cells to MoAb conjugated MTX compared to the amount of cell associated MTX after pulse exposure of the cells to free MTX. The uptake of free [^{3}H]-MTX by MOLT-3 cells was approximately 2-fold higher than the uptake by D$_{10-1}$ cells. However, the amount of MoAb conjugated [^{3}H]-MTX that bound to MOLT-3 cells was always 2 to 5 times lower than that bound to D$_{10-1}$ cells. These results again suggest that the binding of MoAb conjugated [^{3}H]-MTX to D$_{10-1}$ cells is a MoAb-based specific event. The non-specific uptake of substantial amounts of MoAb-MTX conjugates by non-target MOLT-3 cells is likely to be responsible for the inhibition effect of the conjugates to these cells observed in the proliferation inhibition assay.

4.5.5. The fate of Dal B01-MTX and Dal B02-MTX conjugates bound to D10-1 cell surface

To further examine the fate of cell surface bound MoAb-MTX conjugates, D10-1 cells were incubated with either Dal B01-[³H]-MTX or Dal B02-[³H]-MTX conjugate at an extracellular concentration of 5 μM for 2 hr either at 4°C or 37°C. The cells were then washed thrice with cold PBS and reincubated at 37°C in conjugate free efflux medium with or without the presence of a large excess of unconjugated cold appropriate MoAb for 60 min. The concentration of unconjugated cold MoAbs was 50-fold higher than that of MoAbs in the conjugates. At intervals of 0, 5, 10, 15, 30 and 60 min, aliquots of cells were taken out and the cell associated [³H]-MTX activity was determined.

When MoAb-[³H]-MTX conjugate incubated D10-1 cells were reincubated in conjugate free efflux medium at 37°C without any unlabeled free MoAb, there was a rapid release of [³H] radioactivity from the cells during the first 10 to 15 min of incubation, following which a relatively constant level of cell associated [³H] radioactivity was established (Fig. 81). The rates of release of [³H]-MTX activity from D10-1 cells were different depending upon the temperature at which the cells were initially incubated with the conjugates. The release of [³H]-MTX activity from D10-1 cells that were initially incubated with the conjugates at 37°C was faster than that from D10-1 cells that were initially incubated with the conjugates at 4°C. At the end of the 60 min period of incubation, about 87.3% of [³H]-MTX activity of Dal B01-MTX conjugate and 74.3% of [³H]-MTX activity of Dal B02-MTX conjugate remained associated with the cells that were initially incubated with the conjugates at 4°C. The amount of cell associated MTX at the end of efflux were 317 pmol MTX/mg protein for Dal B01-MTX conjugate and 1080 pmol MTX/mg protein for Dal B02-MTX conjugate. When the cells were initially incubated with the conjugates at 37°C, only 77.1% of [³H]-MTX activity of Dal B01-MTX conjugate and 63.6% of [³H]-MTX activity of Dal B02-MTX conjugate remained associated with the cells. The amount of cell associated MTX at

the end of efflux were 289 pmol MTX/mg protein for Dal B01-MTX conjugate and 939 pmol MTX/mg protein for Dal B02-MTX conjugate.

To determine whether these cell associated, MoAb conjugated MTX remained on the cell surface or were internalized, in another experiment, the conjugate-loaded D_{10-1} cells were reincubated at 37°C in the presence of a large excess of the unconjugated cold parent MoAb. Our previous experiment (see Fig. 18) had shown that the incubation of D_{10-1} cells with a large excess of appropriate cold free MoAb replaced approximately 80% of the cell surface bound radiolabeled MoAb. As shown in Fig. 81, large amounts of cell associated [^{3}H] radioactivity were displaced from the cell surface by the unconjugated cold parent MoAb. This process proceeded rapidly and was completed within 30 min, after which the cell associated [^{3}H] radioactivity remained at constant levels. At the end of incubation, approximately 12% of [^{3}H]-MTX activity of Dal B01-[^{3}H]-MTX conjugate and 15% of [^{3}H]-MTX activity of Dal B02-[^{3}H]-MTX conjugate remained associated with the cells that were initially incubated with the conjugates at 4°C for 2 hr. Although the amounts of [^{3}H] radioactivity that remained associated with D_{10-1} cells were slightly higher (approximately 5% higher) in cells that were initially incubated with MoAb-MTX conjugates at 37°C than that in cells that were initially incubated with MoAb-MTX conjugates at 4°C, the difference was not significant.

The fate of cell bound Dal B02-[^{3}H]-MTX conjugate was compared with that of ^{125}I-labeled Dal B02. In this study, D_{10-1} cells were initially incubated with either Dal B02-[^{3}H]-MTX conjugate or ^{125}I-Dal B02 at 37°C for 2 hr, after which the cells were washed three times and reincubated at 37°C with or without the presence of a large excess of unlabeled free Dal B02. At intervals of 0, 5, 15, 30, 45, 60 and 120 min, cell associated radioactivity ([^{3}H] or ^{125}I) was determined. As shown in Fig. 82, in the absence of any cold free antibody, the release of [^{3}H]-MTX activity from D_{10-1} cells was much faster tha

the release of ^{125}I-Dal B02 activity. Approximately 88% of the initial cell bound ^{125}I-Dal B02 radioactivity remained associated with the cells at the end of 120 min of incubation, while approximately 64% of the initial cell bound $[^3H]$-MTX activity remained associated with the cells at the end of 120 min of incubation. The possible explanations for this observation may include (i) a decrease in the binding avidity of Dal B02 MoAb after conjugation to MTX leading to the release of intact Dal B02-MTX conjugate from cell surface; (ii) the catabolism of Dal B02-$[^3H]$-MTX conjugate either on the cell surface or after internalization and subsequent efflux of free $[^3H]$-MTX or $[^3H]$-MTX-containing small fragments of the carrier MoAb. In the presence of unconjugated cold Dal B02, about 80% of both the initial cell bound Dal B02-$[^3H]$-MTX and ^{125}I-Dal B02 radioactivities were displaced from the surface of D10-1 cells within 45 to 60 min.

In conclusion, these results show that when the target D10-1 cells were incubated at 37°C with Dal B01 or Dal B02 linked MTX, more of the drug was taken up by the cells than they were incubated with free MTX. The uptake of Dal B01 or Dal B02 conjugated MTX by target D10-1 cells was much higher than the uptake of the conjugates by the non-target MOLT-3 cells, although MOLT-3 cells took up more free MTX than D10-1 cells. These results indicate that the uptake of MoAb conjugated MTX was a MoAb-based specific event. Furthermore, the higher IRF of Dal B02 preparation led to more binding of conjugated MTX to target cells followed by higher uptake of conjugated MTX compared to the binding and uptake of MTX linked to Dal B01 preparation that had a lower IRF. Efflux studies showed that MTX when linked to Dal B01 or Dal B02 stayed long r with the target cells in larger amounts compared to equivalent amounts of free MTX.

Fig. 78

The time-course of uptake of Dal B01 or Dal B02 conjugated [^{3}H]-MTX by D10-1 cells.

Ten million D10-1 cells were incubated with either Dal B01-MTX or Dal B02-MTX conjugate at an extracellular concentration of 10 μM (of MTX) at either 4°C or 37°C for a period of up to 180 min. At indicated intervals, aliquots of cells were taken out, washed 4 times with cold PBS and cell associated [^{3}H] activity was determined.

Fig. 78A The time-course of uptake of Dal B01 conjugated [^{3}H]-MTX by D10-1 cells.

Fig. 78B The time-course of uptake of Dal B02 conjugated [^{3}H]-MTX by D10-1 cells.

Fig. 78A
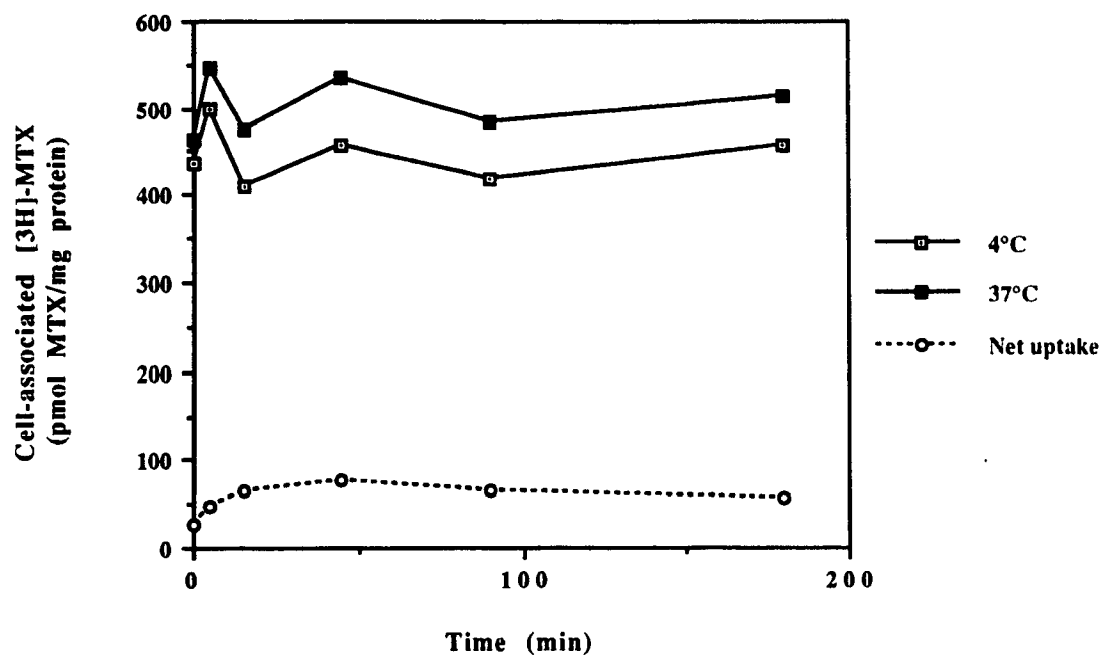
Fig. 78B
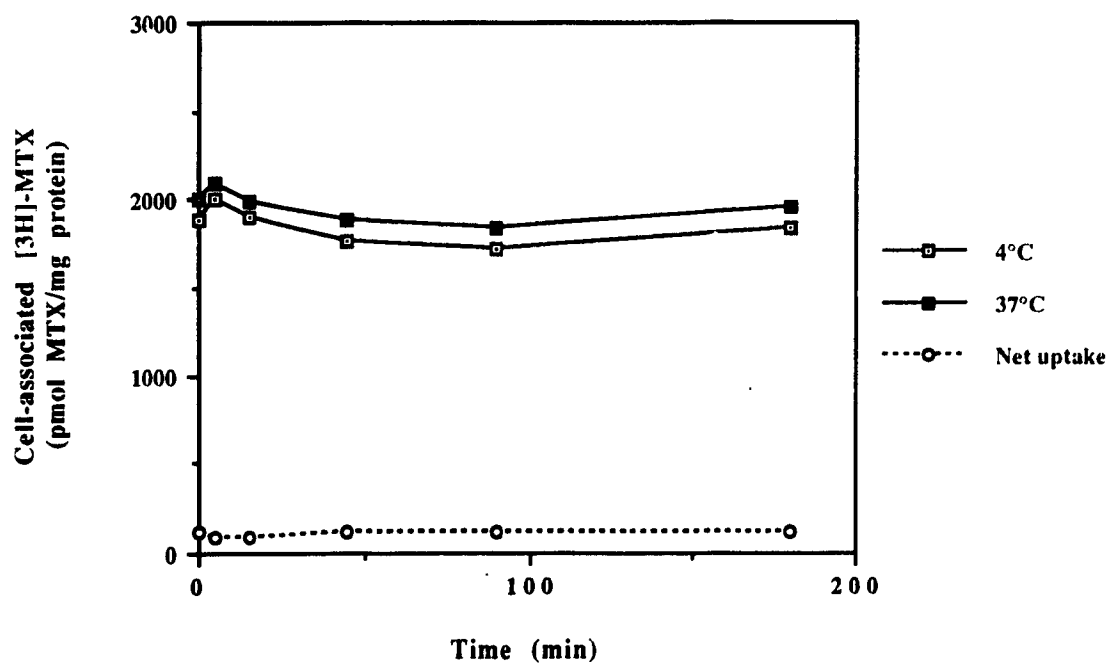
Fig. 79

Uptake of free [^{3}H]-MTX, Dal B01 or Dal B02 conjugated [^{3}H]-MTX by D10-1 and MOLT-3 cells.

One million cells were incubated with various extracellular concentrations of [^{3}H]-MTX, Dal B01-[^{3}H]-MTX, or Dal B02-[^{3}H]-MTX conjugates at either 4°C or 37°C for 90 min. At the end of incubation, the cells were washed 6 times with cold PBS and cell associated [^{3}H] activity was determined.

Fig. 79A Uptake of Dal B01 conjugated [^{3}H]-MTX by D10-1 cells at either 4°C or 37°C.

Fig. 79B Uptake of Dal B02 conjugated [^{3}H]-MTX by D10-1 and MOLT-3 cells at either 4°C or 37°C.

Fig. 79C Uptake of free [^{3}H]-MTX by D10-1 cells at either 4°C or 37°C.

Fig. 79D Uptake of free [^{3}H]-MTX by MOLT-3 cells at either 4°C or 37°C.

Fig. 79A
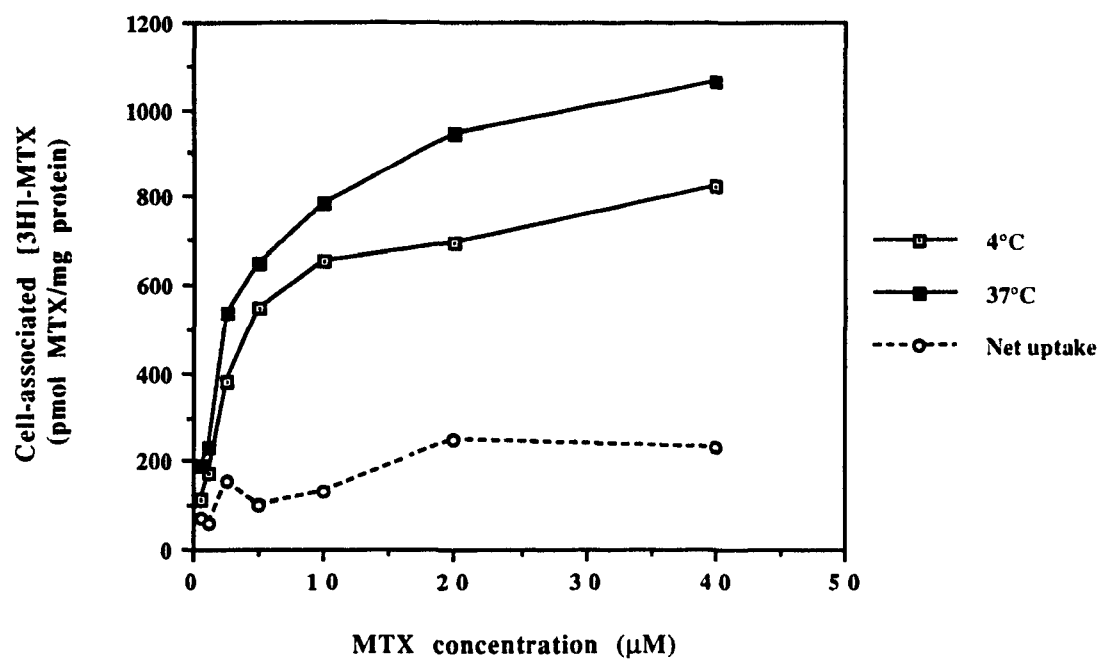
Fig. 79B
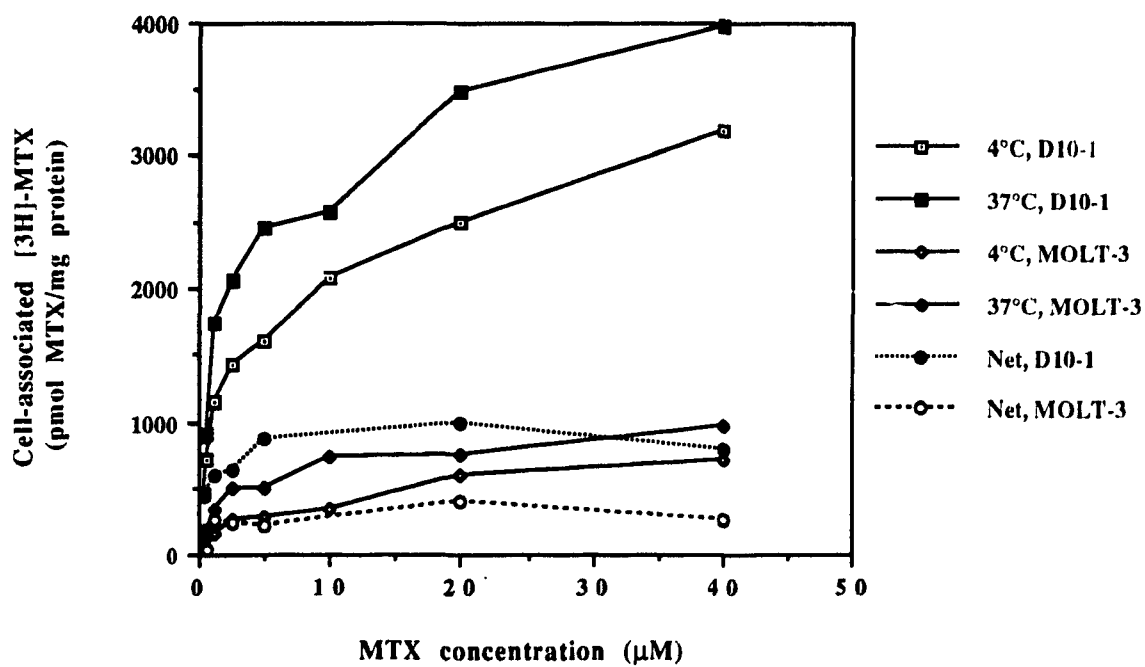
Fig. 79D
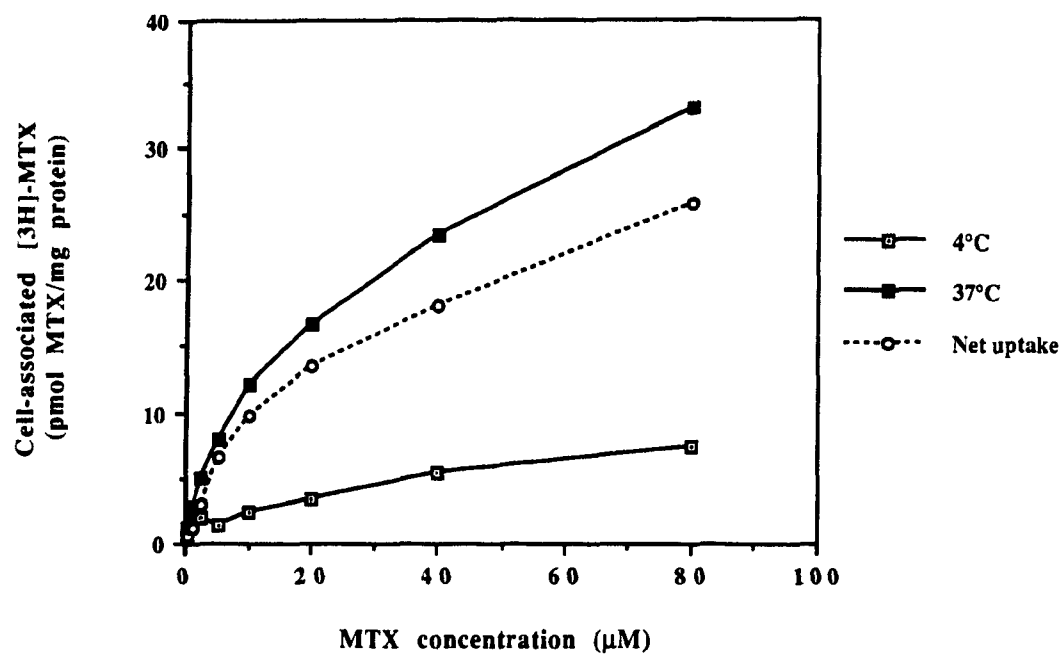
Fig. 79C
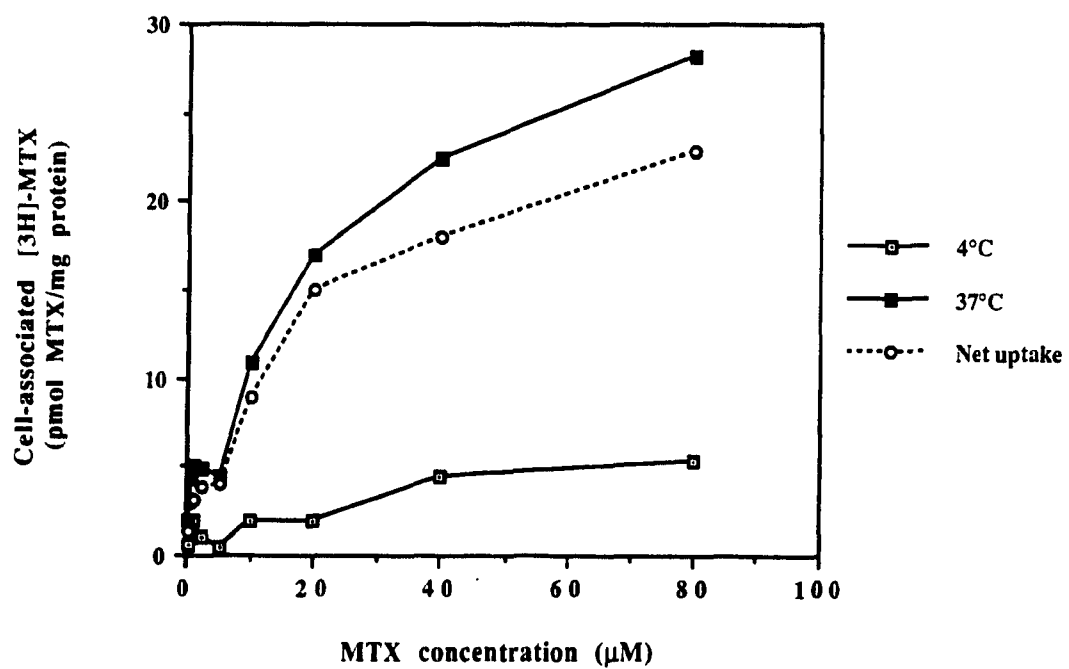
Fig. 80

Uptake of free [³H]-MTX, Dal B01 or Dal B02 conjugated [³H]-MTX by D10-1 and MOLT-3 cells after pulse exposure for 6 hr at 37°C.

One million cells were incubated with various extracellular concentrations of [³H]-MTX, Dal B01-[³H]-MTX, or Dal B02-[³H]-MTX conjugates at 37°C for 6 hr. At the end of incubation, the cells were washed 6 times with cold PBS and cell associated [³H] activity was determined.

Fig. 80A Uptake of Dal B01 or Dal B02 conjugated [³H]-MTX by D10-1 and MOLT-3 cells after pulse exposure for 6 hr at 37°C.

Fig. 80B Uptake of free [³H]-MTX by D10-1 and MOLT-3 cells after pulse exposure for 6 hr at 37°C.

Fig. 80A
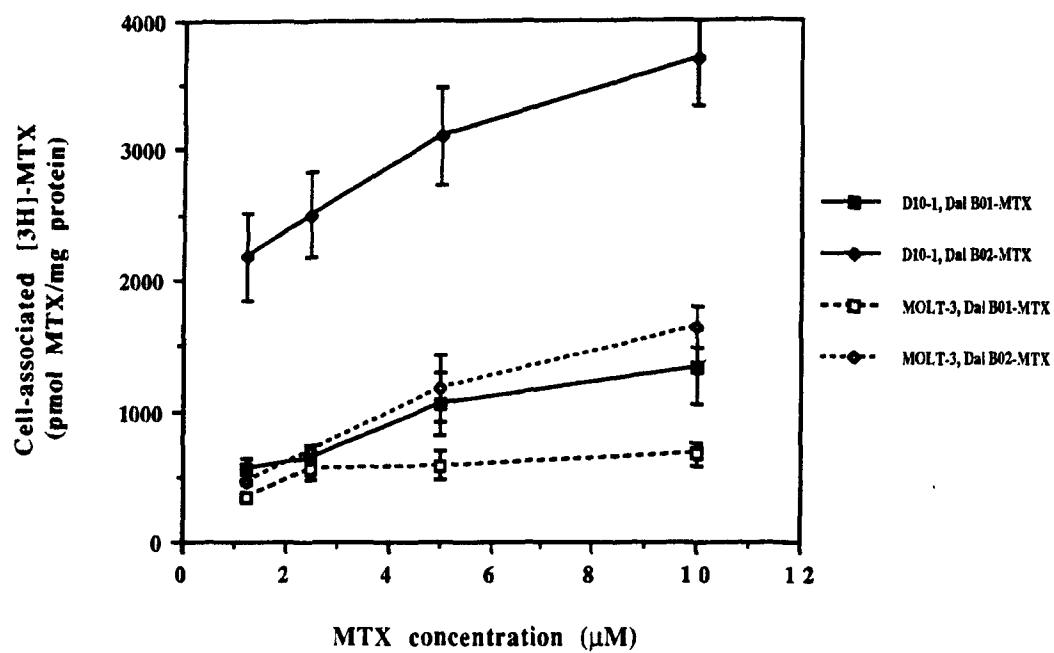
Fig. 80B
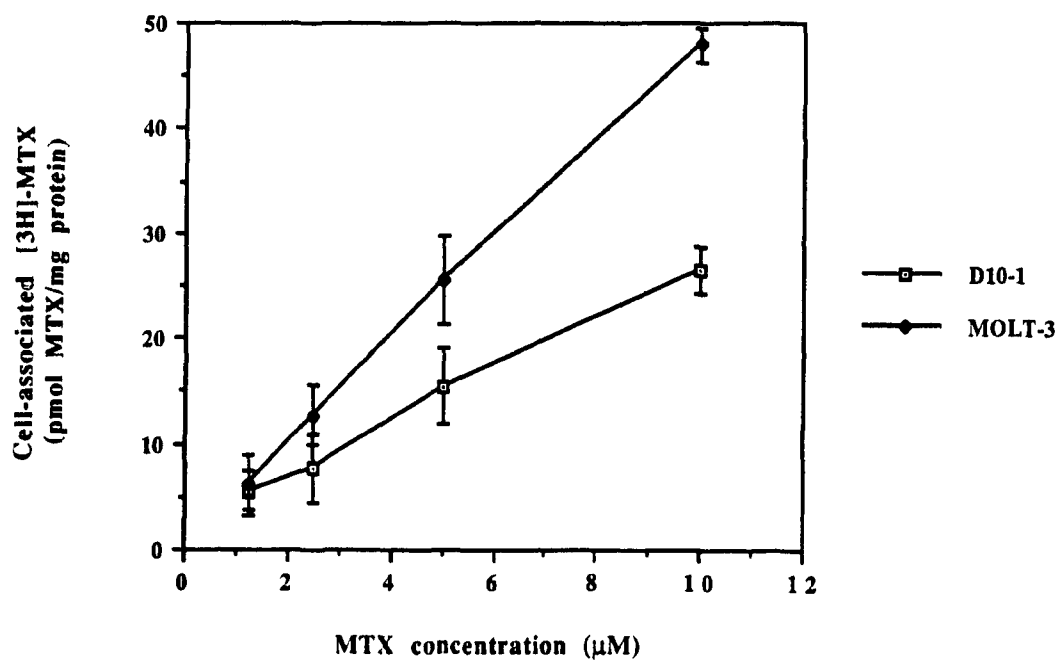
Fig. 81

The fate of D10-1 cell surface bound Dal B01-[^{3}H]-MTX or Dal B02-[^{3}H]-MTX conjugates.

D10-1 cells were preloaded with Dal B01-[^{3}H]-MTX or Dal B02-[3H]-MTX conjugates (MTX concentration, 5.0 µM) for 2 hr a either 4°C or 37°C. The conjugate coated cells were then reincubated in conjugate free medium at 37°C for up to 60 min with or without the presence of a large excess of appropriate unconjugated cold MoAb (the concentration of unconjugated cold MoAb was 50 times higher than that in MoAb-[^{3}H]-MTX conjugate) . At indicated intervals, aliquots of cells were taken out, washed 4 times with cold PBS and cell associated [^{3}H] activity was determined.

Fig. 81A Release of Dal B01 conjugated [^{3}H]-MTX from D10-1 cells in the presence or absence of a large excess of unlabeled free Dal B01.

Fig. 81B Release of Dal B02 conjugated [^{3}H]-MTX from D10-1 cells in the presence or absence of a large excess of unlabeled free Dal B02.

Cell-associated [3H]-MTX
(% of initial bound activity)

Cell-associated [3H]-MTX
(% of initial bound activity)

Fig. 81B

Fig. 81A

Time (min)

Time (min)

4°C x 2 hr

37°C x 2 hr

4°C x 2 hr + B02

37°C x 2 hr + B02

4°C x 2 hr

37°C x 2 hr

4°C x 2 hr + B01

37°C x 2 hr + B01

343
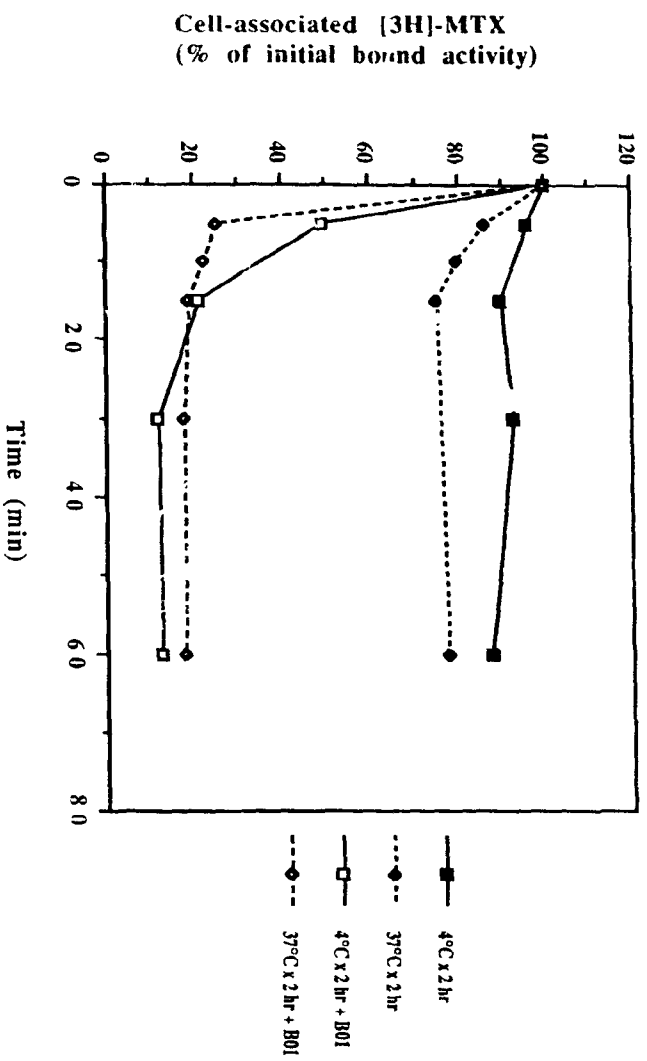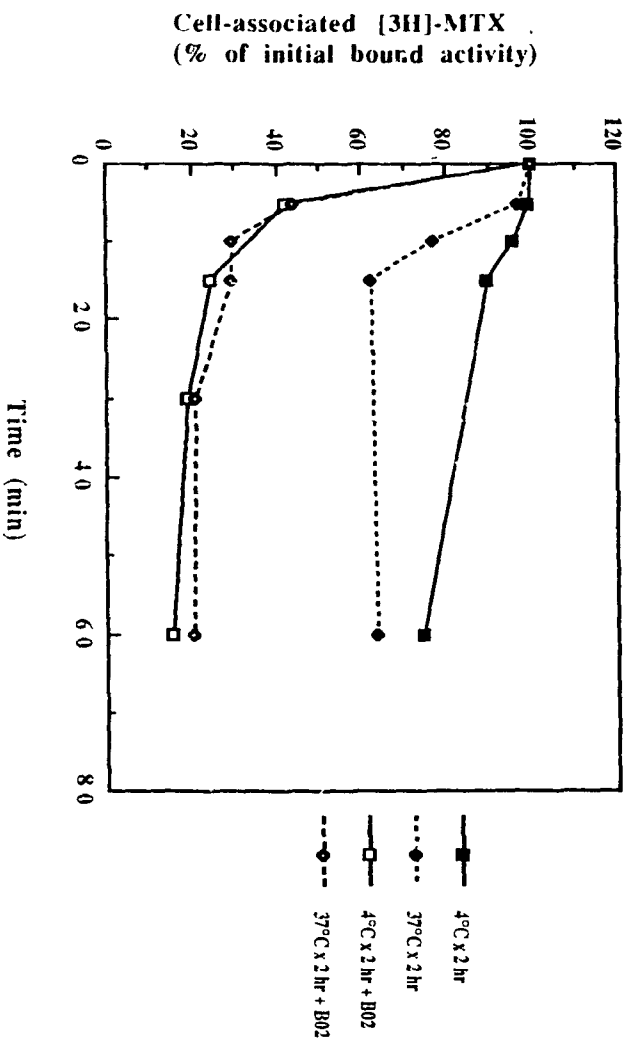
Fig. 82

The fate of D10-1 cell surface bound Dal B02-[^{3}H]-MTX conjugate and ^{125}I-Dal B02.

D10-1 cells were preloaded with ^{125}I-Dal B02 or Dal B02-[^{3}H]-MTX conjugates at 37°C for 2 hr. The antibody coated cells were then reincubated in fresh medium at 37°C for up to 120 min with or without the presence of a large excess of unlabeled free Dal B02 (the antibody concentration of unconjugated cold Dal B02 was 50 times higher than that of radiolabeled Dal B02 or its conjugate). At indicated intervals, aliquots of cells were taken out, washed 4 times with cold PBS and cell associated ^{125}I or [^{3}H] activity was determined.

Cell-associated radioactivity
(% of initial bound activity)

Fig. 82

Time (min)

[3H]-MTX-B02 + B02

[3H]-MTX-B02

125I-Dal B02 + B02

125I-Dal B02

345
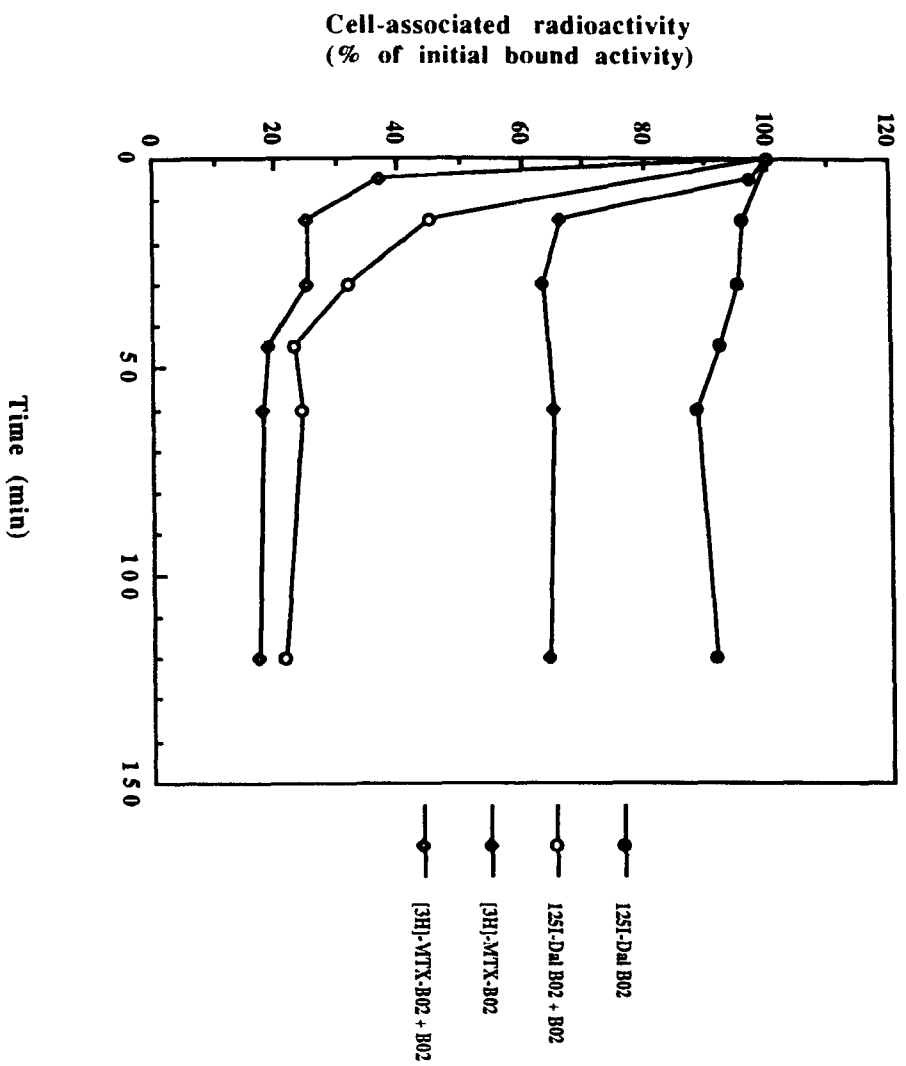
Section 5 Preparation, Cytotoxicity, In Vivo Tumor Localization and Anti-Tumor Activity of Dal B01-ADR and Dal B02-ADR Immunoconjugates

Results presented in Results section 1 have shown that both Dal B01 and Dal B02 MoAbs were poorly internalized after their binding to the surface of target D10-1 cells. It is therefore likely that both Dal B01 and Dal B02 are not suitable as tumor-specific carriers for those drugs that need internalization to exert their cytotoxic effect. In this part of my study, I therefore used ADR as the test chemotherapeutic agent to prepare Dal B01-ADR and Dal B02-ADR conjugates, because it is known that one of the mechanism of cytotoxic action of ADR is its deleterious effects on the plasma membrane (Triton and Yee, 1982). Four different types of Dal B01-ADR and Dal B02-ADR conjugates were prepared using several different linkages. These conjugates were evaluated as regards to their retention of antibody activity and cytotoxicity in vitro. The anti-tumor activity of the most potent conjugate was further evaluated in vivo in D10-1 xenograft bearing nude mice.

5.1 Preparation of Dal B01-ADR and Dal B02-ADR Conjugates

Four types of antibody-ADR conjugates were prepared with MoAb Dal B01, Dal B02 and a non-specific myeloma IgG1 using different conjugation methods. These conjugates were: (i) ADR linked to MoAbs via a CAA spacer using an amide bond (Dal B01-CAA-ADR and Dal B02-CAA-ADR conjugates); (ii) ADR linked to MoAbs via its C13 moi· ·y using a hydrazone bond (Dal B01-C13-ADR and Dal B02-C13-ADR conjugates); (iii) ADR linked to Dal B02 or non-specific IgG1 with the use of an intermediate carrier, i.e.,dextran T-40. In these conjugates, oxidised dextran T-40 was first linked to IgG site-specifically (i.e., via the carbohydrate residues of the IgG molecule), and then loaded with ADR via the C13 moiety of the drug molecule using a hydrazone bond (Dal B02-Dex-ADR (ss) or IgG1-

Dex-ADR (ss) conjugates); and (iv) ADR linked to Dal B02 using dextran T-40 as intermediate carrier (Dal B02-Dex-ADR (nss) conjugate). In this conjugate, ADR was first linked to oxidised dextran T-40 via its amino sugar group, the Dex-ADR was then liked to Dal B02 randomly using a Schiff's base bond. (see Fig. 4 for the schemes for the preparation of different antibody-ADR conjugates). The ADR to IgG molar ratio in these conjugates, ranged from 4 to 6 (ADR) to 1 (IgG) in conjugates prepared with direct linkages (i.e., CAA and C13 conjugates), and were approximately 1/1.2/25 (IgG/Dex/ADR) in Dal B02-Dex-ADR (ss) conjugate, 1/1.4/30 (IgG/Dex/ADR) in IgG₁-Dex-ADR (ss) conjugate, and 1/1.8/41 (IgG/Dex/ADR) in Dal B02-Dex-ADR (nss) conjugate.

5.2 The Retention of Antibody Activity in the Conjugates

The antibody activity of MoAbs (i.e., Dal B01 and Dal B02) in the conjugates prepared by direct linkages (i.e., CAA and C13) was determined by indirect membrane immunofluorescence using D10-1 cells as described for MoAb-MTX conjugates. There were no significant difference in titers of all these MoAb-ADR conjugates and their respective parent MoAbs.

The antibody activity of Dal B02 in Dal B02-Dex-ADR conjugates was determined by a competition assay. The conjugates were used to compete with ^{125}I labeled unconjugated Dal B02 for binding to target D10-1 cells. As shown in Fig. 83, there was no significant difference in the binding of ^{125}I labeled unconjugated Dal B02 to target D10-1 cells, in the presence of either unconjugated cold Dal B02 or Dal B02 conjugated to ADR, indicating that Dal B02 retained its full antigen binding activity even after loading with large numbers of drug molecules (25 to 41 ADR molecules per IgG molecule).

5.3 Inhibition of D10-1 Cell Proliferation in vitro by Dal B01-ADR and Dal B02-ADR Conjugates

Figs. 84 to 89 show the in vitro anti-tumor activity of different MoAb-ADR conjugates against both target D10-1 and non-target MOLT-3 cells. The IC50 values of these conjugates for both the cell lines are presented in Table 19 .

In the 48 hr continuous exposure assay, the IC50 values of free ADR was 0.012 μg/ml for D10-1 cells and 0.081 μg/ml for MOLT-3 cells. The addition of free Dal B01 or Dal B02 to free ADR did not significantly affect the cytotoxicity of the free drug. The cytotoxicity of MoAb-CAA-ADR conjugates towards both target D10-1 and non-target MOLT-3 cells was about 10 times less than that of free ADR. The cytotoxicity of conjugates prepared by the C13 linkage was comparable to that of free ADR towards target D10-1 cells and was about 5 times less than that of the free drug towards non-target MOLT-3 cells. The selectivity ratio was 2.1 for Dal B01-C13-ADR conjugate and 5.1 for Dal B02-C13-ADR conjugate, indicating a selective cytotoxicity of these conjugates towards target D10-1 cells.

The most potent conjugate was Dal B02-Dex-ADR (ss) conjugate. In this conjugate, the oxidised dextran T-40 was first conjugated to Dal B02 via site-specific linkage to carbohydrate residues and then loaded with ADR via the C13 moiety of the ADR molecule using a hydrazone bond. The IC50 value of this conjugate to target D10-1 cells (0.0035 μg/ml) was 5 times lower than that of free drug (IC50, 0.012 μg/ml), whereas the IC50 value of this conjugate to non-target MOLT-3 cells (0.456 μg/ml) was 6 times higher than that of free drug (IC50, 0.081 μg/ml). The selectivity ratio achieved was as high as 19.1, indicating a highly specific cytotoxicity towards target tumor cells. When ADR was linked to dextran T-40 via its amino sugar group instead of its C13 moiety, and the ADR loaded dextran T-40 was conjugated to Dal B02 via non-site specific linkage using an amide bond,

the resulting conjugate (Dal B02-Dex-ADR (nss)) was about 20 times less potent towards target D10-1 cells than Dal B02-Dex-ADR (ss) conjugate. The IC50 value of Dal B02-Dex-ADR (nss) conjugate to target D10-1 cells was 0.069 μg/ml. This was 5 times higher than that of free ADR.

The non-specific IgG1-Dex-ADR (ss) conjugate was found to be as cytotoxic as the free drug to D10-1 cells, but less cytotoxic than specific Dal B02-Dex-ADR (ss) conjugate to D10-1 cells. The cytotoxicity of both Dal B02-Dex-ADR (ss) conjugate and IgG1-Dex-ADR (ss) conjugate was almost equal towards the non-target MOLT-3 cells. The IC50 values of both the conjugates were about 5 times higher than that of the free drug, indicating a loss of ADR activity after conjugation to non-specific protein carriers. The Dex-ADR binary conjugate with higher ADR incorporation (i.e., Dex/ADR ratio, 1/30) was more cytotoxic than the binary conjugate with lower ADR incorporation (i.e., Dex/ADR ratio, 1/15). Both binary conjugates were much less cytotoxic towards D10-1 cells than free ADR and Dal B02-Dex-ADR (ss) conjugate. However, These two binary conjugates were almost equal cytotoxic towards MOLT-3 cells compared to Dal B02-Dex-ADR (ss) conjugate. The IC50 values of Dex-ADR (Dex/ADR molar ratio, 1/30) and of Dal B02-Dex-ADR (ss) (IgG/Dex/ADR molar ratio, 1/1.2/25) for MOLT-3 cells were 0.54 μg/ml and 0.456 μg/ml, respectively. Thus, the order of potency of these test agents to D10-1 cells is: Dal B02-Dex-ADR (ss) > ADR (alone or mixed with MoAb) > Dal B02-C13-ADR > IgG1-Dex-ADR (ss) > Dal B01-C13-ADR > Dal B02-Dex-ADR (nss) > Dal B02-CAA-ADR > Dal B01-CAA-ADR > Dex-ADR (higher ADR incorporation) > Dex-ADR (lower ADR incorporation).

In 6 hr or 3 hr pulse exposure assays, the IC50 values of free ADR for both D10-1 and MOLT-3 cell lines were 2 to 5 times higher than that obtained in the 48 hr continuous

exposure assay. Again, the addition of free Dal B01 or Dal B02 to free ADR did not significantly affect the cytotoxicity of the free drug.

Considering target D_{10-1} cells, both Dal B01-CAA-ADR and Dal B02-CAA-ADR conjugates were approximately 35 to 40 times less potent than free ADR. The IC50 values for D_{10-1} cells were about 10 times higher with Dal B01-C13-ADR conjugate and 2 times higher with Dal B02-C13-ADR conjugate than that with free ADR. Again, the Dal B02-Dex-ADR (ss) conjugate was found to be the most potent preparation in these pulse exposure assays. The IC50 value of this conjugate was approximately 1.3 to 2.7-fold lower than that of free ADR. Consistent with the results of the continuous exposure assay, Dal B02-Dex-ADR (nss) conjugate was about 20 to 30 times less potent than Dal B02-Dex-ADR (ss) conjugate, and was 11 to 16 times less potent than free ADR. Again, the non-specific IgG1-Dex-ADR (ss) conjugate was found to be as potent as free ADR. The order of potency of these test agents to D_{10-1} cells in this pulse exposure assay is the same as that listed above in the continuous exposure assay.

Considering the non-target MOLT-3 cells, all types of Dal B01-ADR and Dal B02-ADR conjugates prepared via direct linkages (i.e., CAA and C13) were about 30 to 50 times less potent than free ADR. The IC50 value of Dal B02-Dex-ADR (ss) conjugate was 7 to 10 times higher than that of free ADR. The Dal B02-Dex-ADR (nss) conjugate was found to be 25 to 40 times less potent than free ADR, and 2 to 5 times less potent than Dal B02-Dex-ADR (ss) conjugate. The cytotoxicity of non-specific IgG1-Dex-ADR (ss) conjugate was almost equal to that of Dal B02-Dex-ADR (ss) conjugate, which was about 10 times less potent than free ADR. The selectivity ratios of Dal B02-Dex-ADR (ss) conjugate were 29.7 (in the 6 hr pulse exposure assay) and 9.4 (in the 3 hr pulse exposure assay), indicating a highly selective cytotoxicity towards target D_{10-1} cells.

Two observations need special mention: (i) unlike the results obtained with of MoAb-MTX conjugates, the pulse exposure of D10-1 cells to MoAb-ADR conjugates resulted in a decrease in the selectivity ratio of most of the conjugates. The selectivity ratio of MoAb-CAA-ADR conjugates was less than 1.0 in most of cases (except for Dal B02-CAA-ADR conjugate in the 3 hr pulse exposure assay), indicating lack of selectivity in their cytotoxicity towards target cells; and (ii) free ADR was 5-fold more cytotoxic to D10-1 cells than to MOLT-3 cells, however, the non-specific IgG1-Dex-ADR (ss) conjugate was found to be 25 to 50-fold more toxic to D10-1 cells than to MOLT-3 cells.

In conclusion, four types of MoAb-ADR conjugates were prepared using different linkages. Both Dal B01 and Dal B02 MoAbs retained their immunoreactivity after conjugation to ADR using these different linkage methods. The conjugates based on linkage via the C13 moiety of ADR molecule were more potent than conjugates prepared using the CAA spacer. The Dal B02-Dex-ADR (ss) conjugate linked via the the C13 moiety of ADR molecule using a hydrazone bond was much more potent than Dal B02-Dex-ADR (nss) conjugate linked via the amino sugar moiety of ADR molecule using a Schiff's base bond. All MoAb-ADR conjugates were more potent inhibitors of D10-1 cells than the Dex-ADR binary conjugate. Of the six Dal B01-ADR and Dal B02-ADR conjugates studied, Dal B02-Dex-ADR (ss) conjugate was the most potent tumor inhibitor. This conjugate also demonstrated a highly selective cytotoxicity to target D10-1 cells. Therefore, the Dal B02-Dex-ADR (ss) conjugate was chosen for further in vivo evaluation in D10-1 xenograft bearing nude mice.

Fig. 83

Competition between Dal B02-Dex-ADR conjugates and ^{125}I-Dal B02 in their binding to target D10-1 cells.

D10-1 cells were incubated with given amounts of ^{125}I-Dal B02 in the presence of increasing amounts of cold free Dal B02, cold Dal B02-Dex-ADR (ss) conjugate, or cold Dal B02-Dex-ADR (nss) conjugate at 4°C for 90 min. The cell associated radioactivity was determined after 4 washes with cold PBS. The inhibition of target cell binding of ^{125}I-Dal B02 by cold Dal B02 or Dal B02-Dex-ADR conjugates was determined and compared to the binding of control preparation.

353

Fig. 83

Cold Dal B02 added (µg)
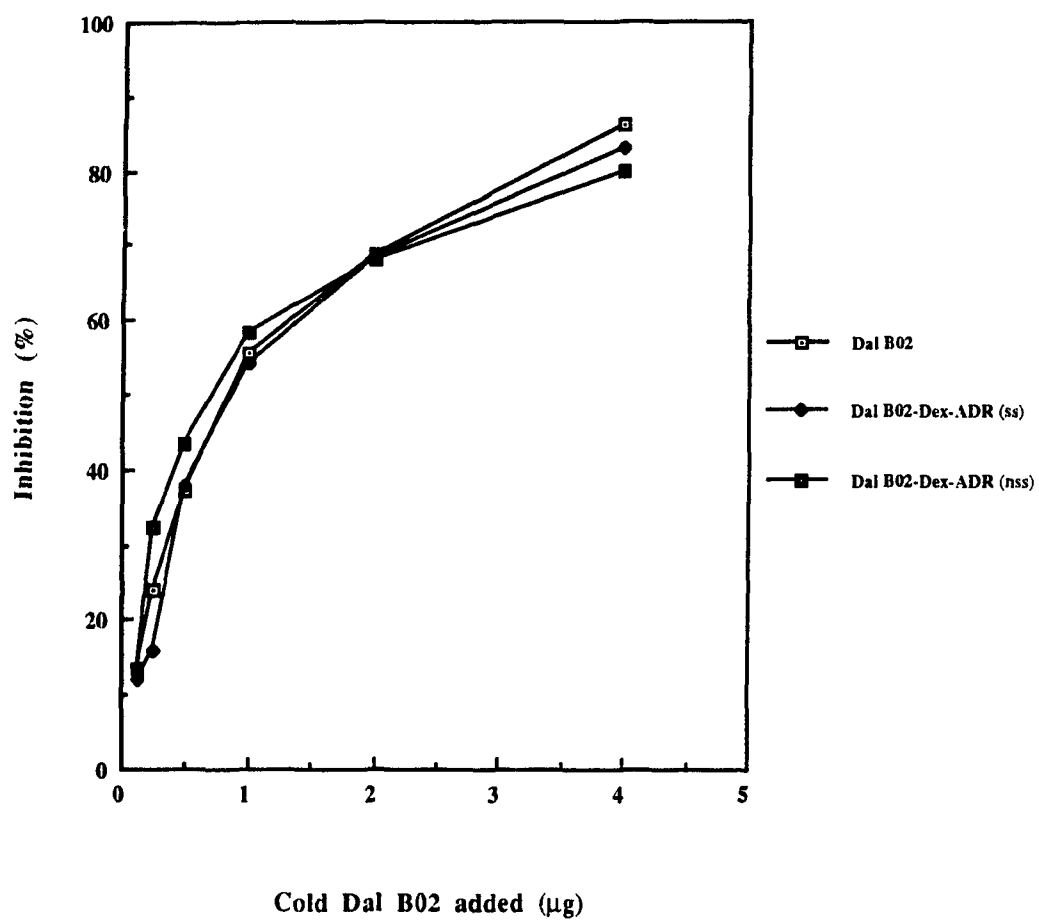
Figs. 84 to 86

Cytotoxicity of free ADR and different Dal B01-ADR conjugates towards target D10-1 and non-target MOLT-3 cells.

Five x 10^5 D10-1 or MOLT-3 cells (in 100 μl of medium) were cultured in a 96 well plate overnight, after which stated amounts of free ADR or Dal B01-ADR conjugates were added (in 100 μl PBS). The cells were incubated with the test agents for 48 hr in the continuous exposure assay. For pulse exposure, the cells were incubated with test agents for 6 hr or 3 hr after which the cells were washed thrice and reincubated in fresh medium for an additional 48 hr. The total number of cells in each well was counted and the inhibition of cell proliferation was calculated and compared to the control preparations that were not exposed to any test agents.

Fig. 84   Inhibition of cell proliferation after continuous exposure for 48 hr.

(A) D10-1 cells;   (B) MOLT-3 cells.

Fig. 85   Inhibition of cell proliferation after pulse exposure for 6 hr.

(A) D10-1 cells;   (B) MOLT-3 cells.

Fig. 86   Inhibition of cell proliferation after pulse exposure for 3 hr.

(A) D10-1 cells;   (B) MOLT-3 cells.

Fig. 84A

Fig. 84B

Fig. 85A

ADR concentration (µg/ml)

- □ ADR
- ◆ ADR + B01
- ■ ADR-B01(CAA)
- ◇ ADR-B01(C13)

Fig. 85B

ADR concentration (µg/ml)

- □ ADR
- ◆ ADR + B01
- ■ ADR-B01(CAA)
- ◇ ADR-B01(C13)
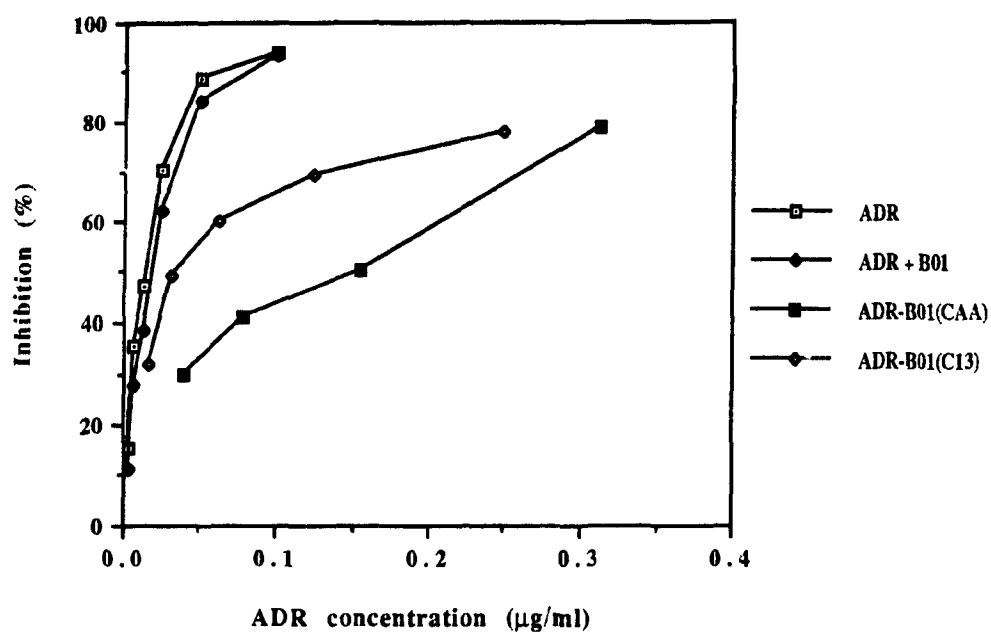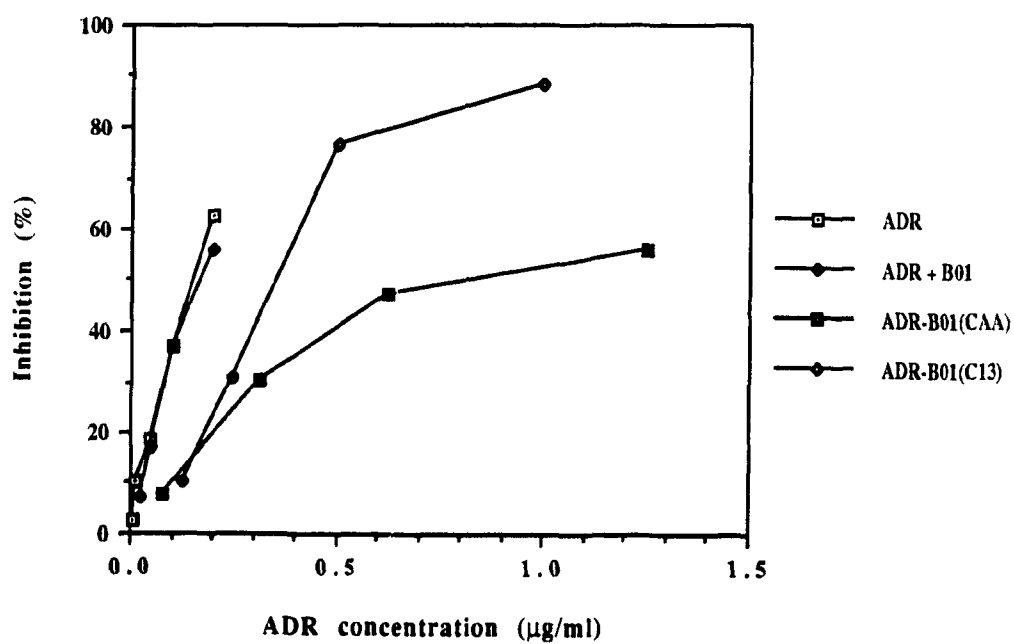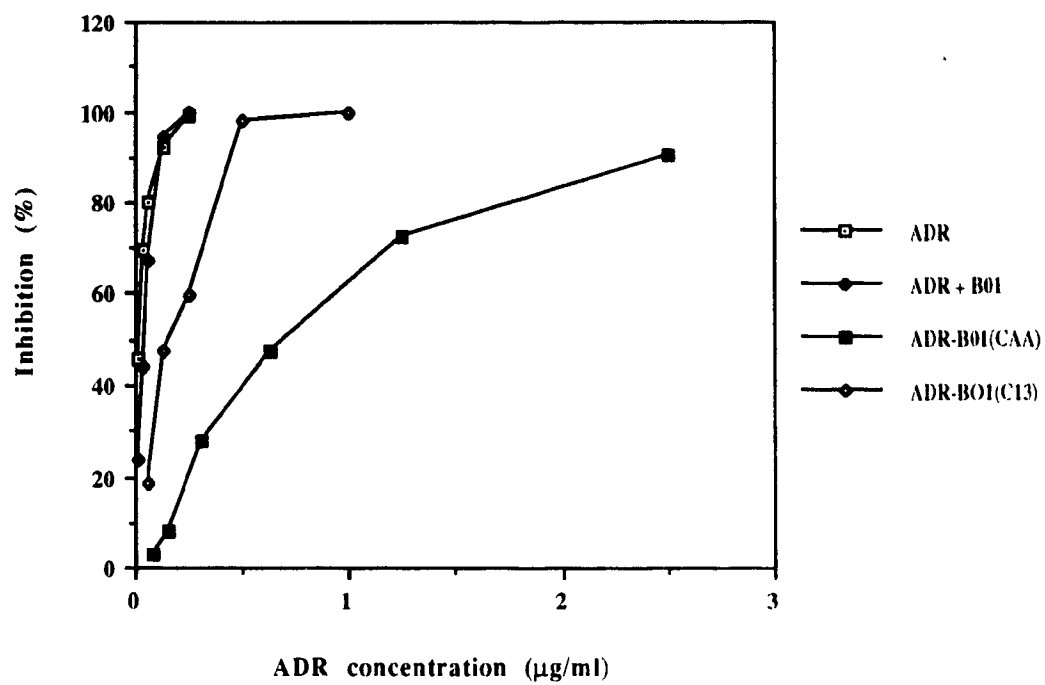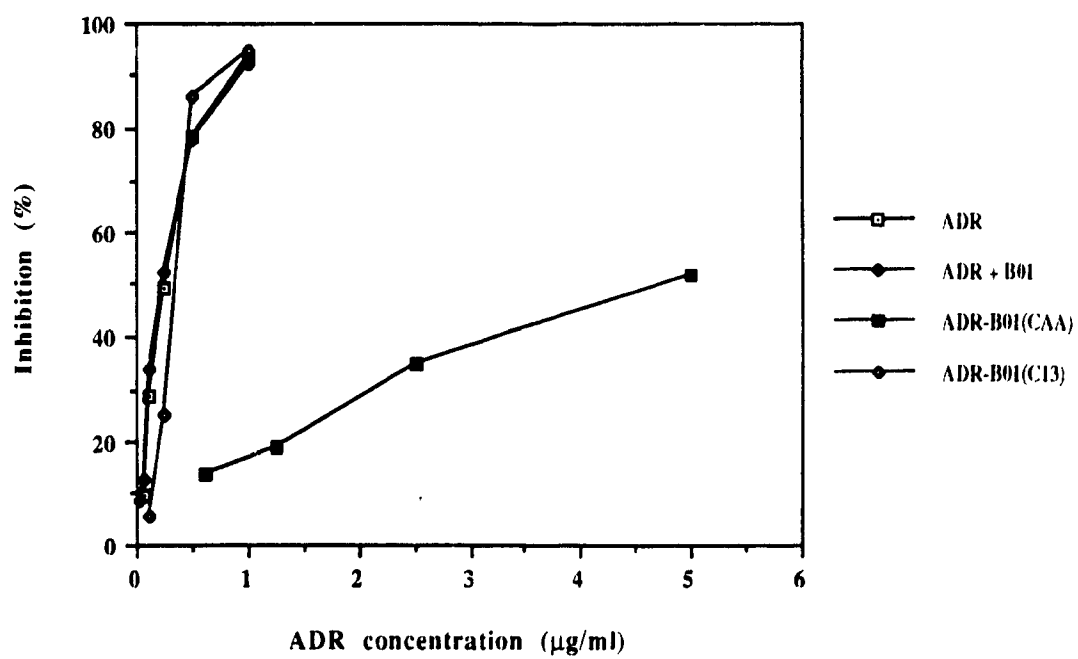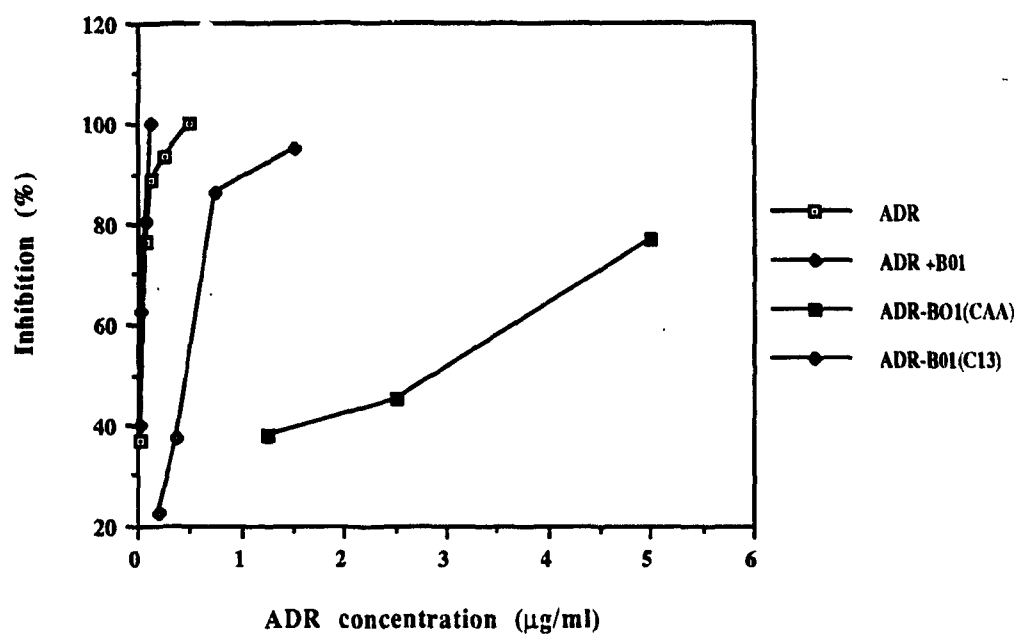
Fig. 86A

Fig. 86B
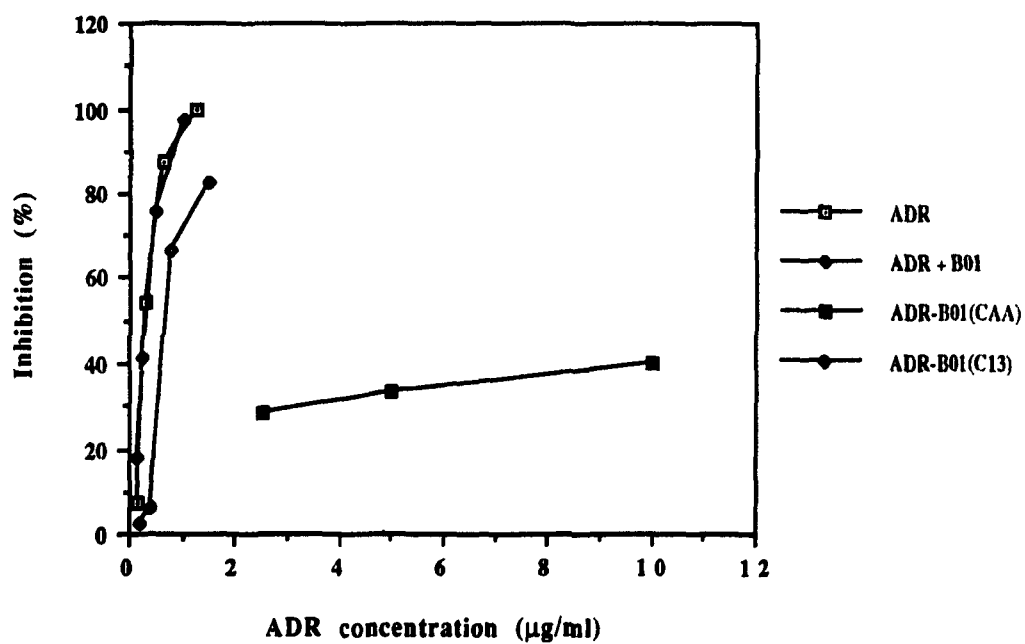
Figs. 87 to 89

Cytotoxicity of free ADR and different Dal B02-ADR conjugates towards target D10-1 and non-target MOLT-3 cells.

Five x 10^5 D10-1 or MOLT-3 cells (in 100 µl of medium) were cultured in a 96 well plate overnight, after which stated amounts of free ADR or Dal B02-ADR conjugates were added (in 100 µl PBS). The cells were incubated with the test agents for 48 hr in the continuous exposure assay. For pulse exposure, the cells were incubated with test agents for 6 hr or 3 hr after which the cells were washed thrice and reincubated in fresh medium for an additional 48 hr. The total number of cells in each well was counted and the inhibition of cell proliferation was calculated and compared to the control preparations that were not exposed to any test agents.

Fig. 87　Inhibition of cell proliferation after continuous exposure for 48 hr.

(A) D10-1 cells;　(B) MOLT-3 cells.

Fig. 88　Inhibition of cell proliferation after pulse exposure for 6 hr.

(A) D10-1 cells;　(B) MOLT-3 cells.

Fig. 89　Inhibition of cell proliferation after pulse exposure for 3 hr.

(A) D10-1 cells;　(B) MOLT-3 cells.

Fig. 87A

ADR
ADR + B02
ADR-B02(CAA)
ADR-B02(C13)
ADR-Dex-B02 (ss)
ADR-Dex-B02 (nss)
ADR-Dex-IgG1 (ss)
ADR-Dex

Fig. 87B

ADR
ADR-B02(CAA)
ADR-B02(C13)
ADR-Dex-B02 (ss)
ADR-Dex-B02 (nss)
ADR-Dex-IgG1 (ss)
ADR-Dex
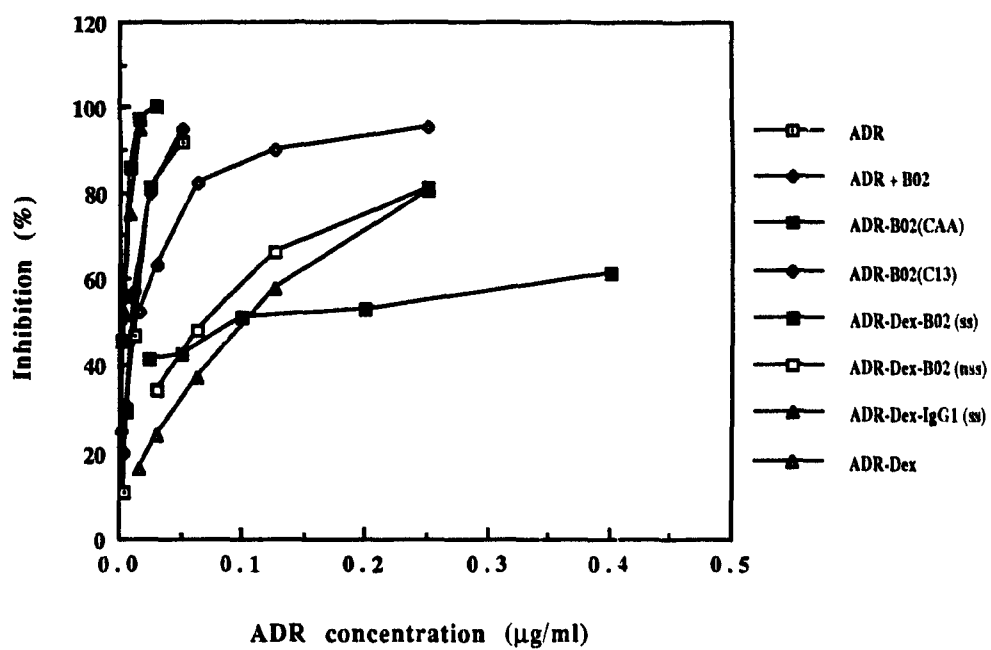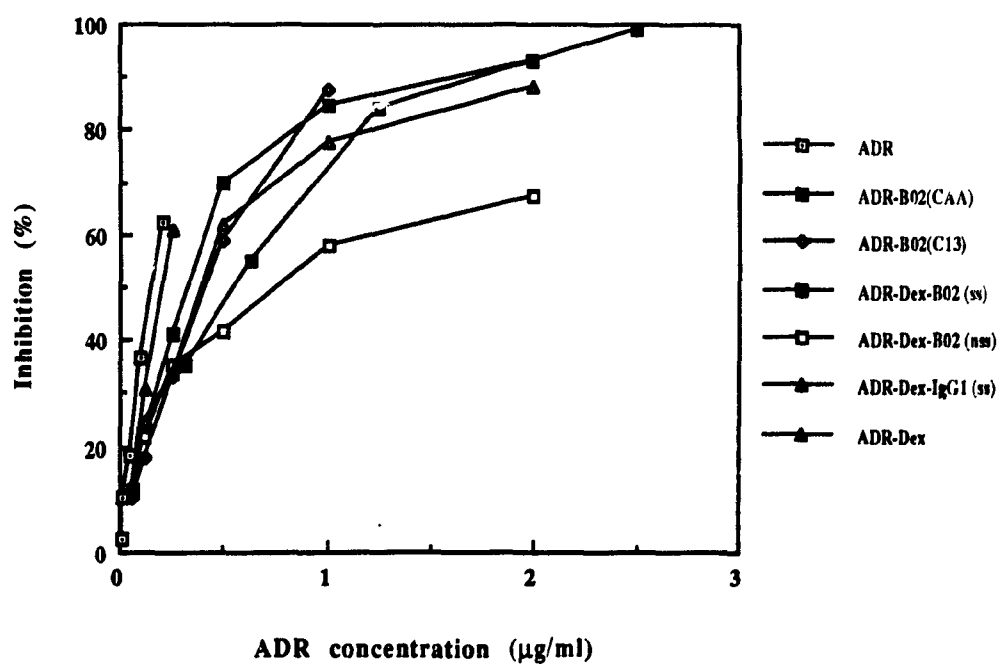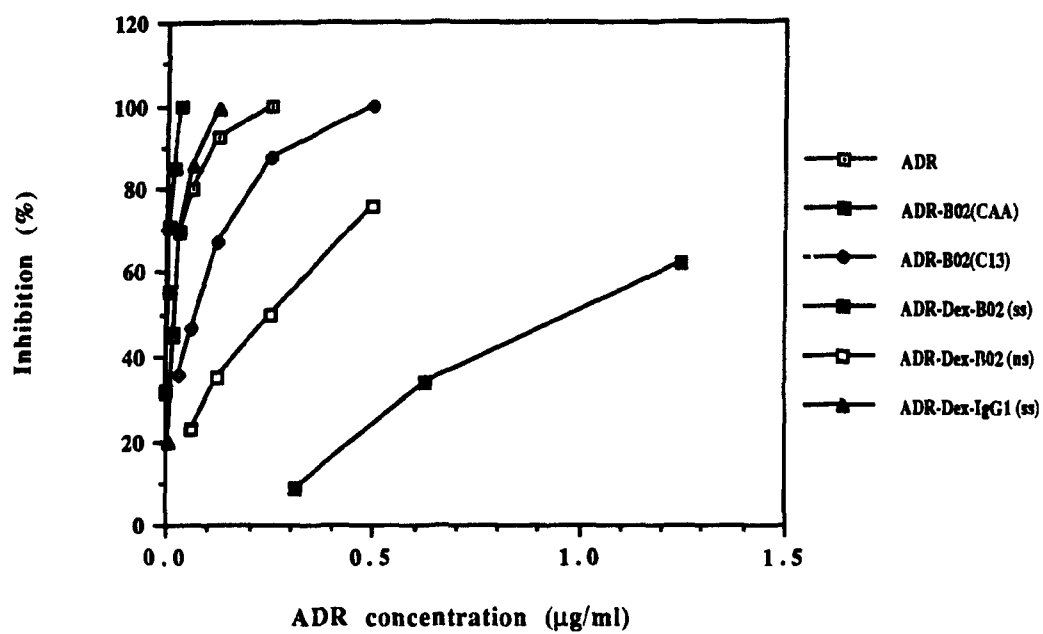
Fig. 88A

Fig. 88B
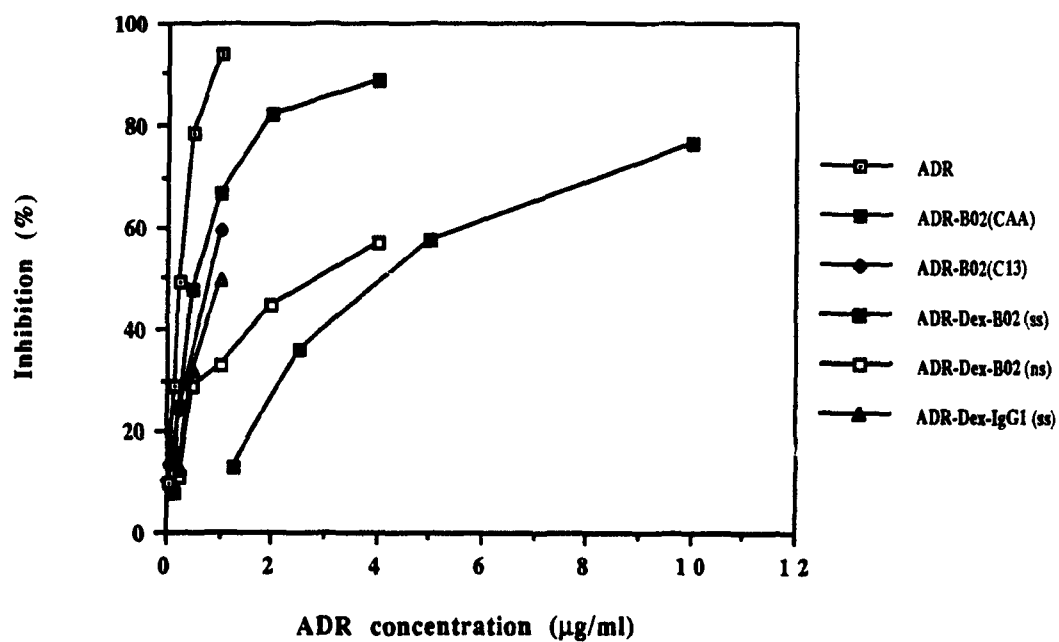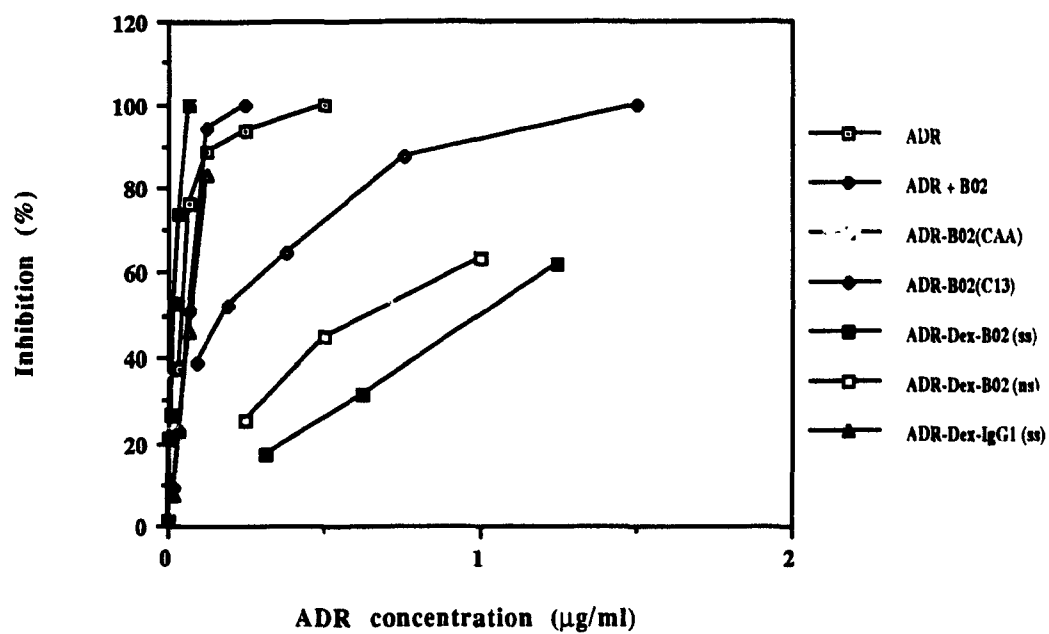
Fig. 89A

Fig. 89B
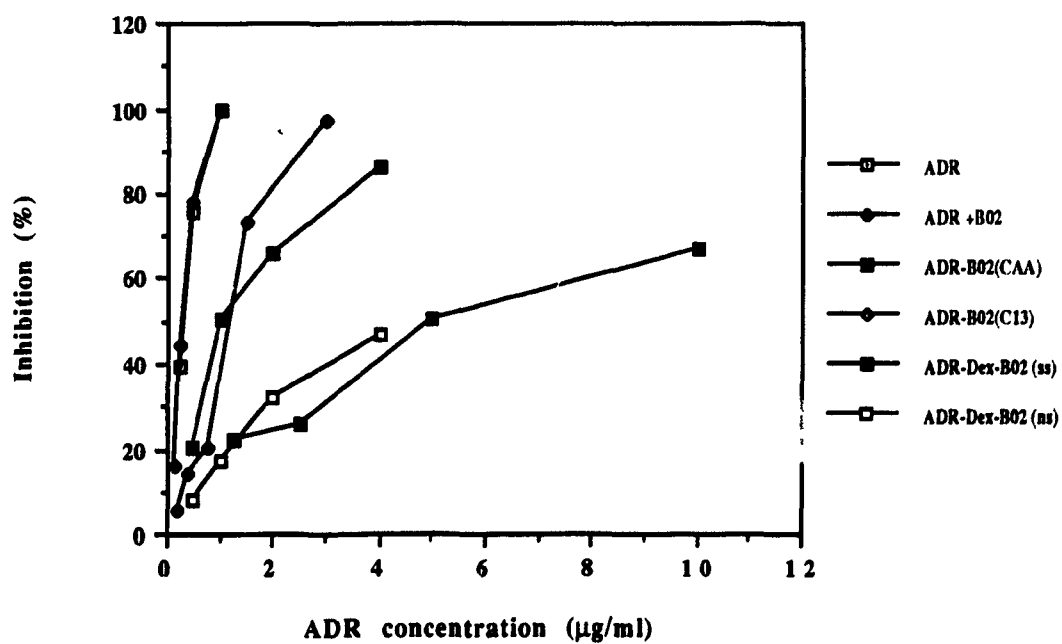
Table 19   The IC50 values of ADR, Dal B01-ADR and Dal B02-ADR

conjugates

(A) 48 hr continuous exposure

	D10-1 cells	MOLT-3 cells	Selectivity Ratio [4]
ADR	0.012 [2] (1.0) [3]	0.081 (1.0)	1.0
ADR + Dal B01 [5]	0.029 (0.41)	0.17 (0.48)	0.85
ADR + Dal B02 [5]	0.013 (0.92)	0.15 (0.54)	1.7
Dal B01-CAA-ADR [6]	0.15 (0.08)	0.95 (0.85)	0.94
Dal B01-C13-ADR [7]	0.032 (0.38)	0.44 (0.18)	2.1
Dal B02-CAA-ADR [6]	0.10 (0.12)	0.45 (0.18)	0.67
Dal B02-C13-ADR [7]	0.014 (0.86)	0.49 (0.17)	5.1
Dal B02-Dex-ADR (ss) [8]	0.0035 (3.43)	0.456 (0.18)	19.1
Dal B02-Dex-ADR (nss) [9]	0.069 (0.17)	1.25 (0.065)	2.6
IgG1-Dex-ADR (ss) [10]	0.018 (0.67)	0.41 (0.20)	3.4
Dex-ADR (1/30) [11]	0.11 (0.11)	0.54 (0.15)	0.73
Dex-ADR (1/15) [12]	0.18 (0.067)	0.75 (0.11)	0.61

1. The cytotoxicity of free ADR or its conjugates was determined using target D10-1 cells and non-target MOLT-3 cells as described in Materials and Methods.

(Continued)

(B) 6 hr pulse exposure

	D_{10-1} cells	MOLT-3 cells	Selectivity Ratio
ADR	0.029 (1.0)	0.14 (1.0)	1.0
ADR + Dal B01	0.043 (0.68)	0.37 (0.38)	1.8
Dal B01-CAA-ADR	1.13 (0.026)	4.64 (0.03)	0.87
Dal B01-C13-ADR	0.20 (0.147)	0.44 (0.32)	0.46
Dal B02-CAA-ADR	0.97 (0.03)	5.33 (0.03)	1.0
Dal B02-C13-ADR	0.06 (0.49)	0.81 (0.18)	2.8
Dal B02-Dex-ADR (ss)	0.011 (2.67)	1.50 (0.09)	29.7
Dal B02-Dex-ADR (nss)	0.32 (0.09)	3.46 (0.04)	2.5
IgG1-Dex-ADR (ss)	0.033 (0.89)	1.94 (0.07)	12.7

2. All values are μg/ml and represent the mean of at least 3 determinations.

3. The values inside the parenthesis represent the sensitivity ratio which was calculated as follows:

$$\text{Sensitivity ratio} = \frac{\text{The IC50 value of the test agent}}{\text{The IC50 value of free ADR}}$$

4. The value represents the selectivity ratio which was calculated by

$$\text{Selectivity ratio} = \frac{\text{The sensitivity ratio of the test agent to target cells}}{\text{The sensitivity ratio of the test agent to non-target cells}}$$

(Continued)

(C) 3 hr pulse exposure

	D$_{10-1}$ cells		MOLT-3 cells		Selectivity Ratio
ADR	0.058	(1.0)	0.26	(1.0)	1.0
ADR + Dal B01	0.046	(1.26)	0.43	(0.61)	2.1
ADR + Dal B02	0.032	(1.81)	0.36	(0.72)	2.5
Dal B01-CAA-ADR	4.93	(0.012)	16.4	(0.016)	0.75
Dal B01-C13-ADR	0.52	(0.11)	0.87	(0.3)	0.37
Dal B02-CAA-ADR	1.00	(0.06)	6.35	(0.04)	1.5
Dal B02-C13-ADR	0.13	(0.45)	1.39	(0.19)	2.4
Dal B02-Dex-ADR (ss)	0.044	(1.32)	1.82	(0.14)	9.4
Dal B02-Dex-ADR (nss)	0.824	(0.07)	9.83	(0.026)	2.7
IgG$_1$-Dex-ADR (ss)	0.074	(0.78)	2.50	(0.1)	7.8

5. The mixture of free ADR and free MoAb at the same molar ratio as in MoAb-ADR conjugates.

6. ADR was linked to MoAbs via a CAA spacer using an amide bond.

7. ADR was linked to MoAbs via C13 moiety of ADR molecule using a hydrazone bond.

8. Oxidised dextran was first linked to MoAb site-specifically and then loaded with ADR via the C13 moiety of ADR molecule using a hydrazone bond.

9. ADR was first linked to oxidised dextran via its amino group. The ADR loaded dextran was then linked to Dal B02 randomly using a Schiff's base bond.

10. A non-specific IgG$_1$-Dex-ADR conjugate prepared by the method described in (8).

11. Dex-ADR binary conjugate using C13 linkage at a Dex/ADR molar ratio of 1 to 30.

12. Dex-ADR binary conjugate using C13 linkage at a Dex/ADR molar ratio of 1 to 15.

5.4 The Pharmacokinetics and Biodistribution of Dal B02-Dex-ADR (ss) Conjugate after Intravenous Administration into D10-1 Xenograft Bearing Mice

Results presented above have shown that the Dal B02-Dex-ADR (ss) conjugate is the most potent inhibitor of D10-1 cell proliferation in vitro. This conjugate also demonstrated a good retention of antibody activity and an excellent selective cytotoxicity towards the target D10-1 cells. We therefore selected this conjugate for further evaluation of its anti-tumor activity in vivo in D10-1 xenograft bearing nude mice. Before evaluating the anti-tumor activity of this conjugate in vivo, I first studied the pharmacokinetics and biodistribution of this conjugate and unconjugated parent Dal B02 in D10-1 xenograft bearing nude mice.

Both the parent Dal B02 and Dal B02-Dex-ADR (ss) conjugate were labeled with ^{131}I using chloramine T following the method described in Materials and Methods. No free ADR was released from the conjugate during radioiodination as monitored by TLC assay. The IRF and immunoreactivity of radiolabeled Dal B02-Dex-ADR (ss) conjugate were examined using D10-1 cells. The IRF was 63.8% for ^{131}I labeled unconjugated Dal B02, and 56.9% for ^{131}I labeled Dal B02-Dex-ADR (ss) conjugate. As shown in Fig. 90, there was no difference between ^{131}I-Dal B02-Dex-ADR (ss) conjugate and ^{131}I-Dal B02 as regards the amounts of antibody that bound to target D10-1 cells when both the ^{131}I labeled preparations were incubated with D10-1 cells at 4°C for 2 hr. Results of these in vitro studies indicate that Dal B02 retained its full immunoreactivity after conjugation to ADR.

The pharmacokinetics and biodistribution of the ^{131}I-Dal B02-Dex-ADR (ss) conjugate was examined in D10-1 s.c. xenograft bearing nude mice and compared to that of unconjugated ^{131}I-Dal B02. A non-specific IgG1 antibody was labeled with ^{125}I and was used as a control preparation. The study was carried out as described in Methods section 7.

Both Dal B02 and Dal B02-Dex-ADR (ss) conjugate had the same pharmacokinetic pattern. As shown in Fig. 91 A, the kinetics of clearance of ^{131}I-Dal B02 and ^{131}I-Dal B02-Dex-ADR (ss) conjugate from blood followed a biphasic pattern: there was a rapid exponential decrease in the first few hours, and this was followed by a less steep exponential decrease. No significant difference was found between ^{131}I-Dal B02 and ^{131}I-Dal B02-Dex-ADR (ss) conjugate as regards to their half-lives (t $1/2\alpha$ and t $1/2\beta$), distribution volume (Vd) and area under curve (AUC). The ^{131}I activity associated with both the preparations were cleared from the body of xenograft bearing mice almost at the same rate (half-lives of total body activity for both free Dal B02 and Dal B02-Dex-ADR (ss) were approximately 24 hr), as shown in Fig.91 B.

Figs. 92 and 93 show the tissue distribution of ^{131}I-Dal B02 and ^{131}I-Dal B02-Dex-ADR (ss) conjugate 96 hr after administration of the radiolabeled preparations. Both preparations demonstrated much higher localization in D10-1 tumors compared to the localization of the non-specific control IgG1 preparation. The percentage of the injected dose (% ID) of both the ^{131}I-Dal B02 and ^{131}I-Dal B02-Dex-ADR (ss) conjugate that localized in xenografted tumor was also much higher than the percentage of the injected dose of both the preparations that localized in any normal mouse tissues. The T / NT ratios obtained with both the preparations ranged from 5.0 to 63 in most organs (with the exception of blood) of the tumor bearing mice given either the ^{131}I labeled preparation. No significant difference was observed between ^{131}I-Dal B02 and ^{131}I-Dal B02-Dex-ADR (ss) conjugate as regards the % ID of antibody that localized in tumors. The % ID / g tumor tissue was 2.96 ± 0.99 % for ^{131}I-Dal B02 and 2.81 ± 0.26 % for ^{131}I-Dal B02-Dex-ADR (ss) conjugate.

5.5 Inhibition of Tumor Growth in vivo by Dal B02-Dex-ADR (ss) Conjugate in D10-1 Xenograft Bearing Nude Mice

5.5.1 Determination of the maximum tolerated dose (MTD), optimal schedule and optimal route of administration of ADR and its conjugates for the treatment of D10-1 tumor-bearing nude mice

The toxicity of the free drug or its conjugates to mice was determined on the basis of loss of body weight of the treated mice: minor toxicity was defined as a loss of 5 to 10% of the initial body weight; moderate toxicity was defined as a loss of body weight that ranged between 11 to 15% of the initial body weight; severe toxicity was considered when the loss exceeded 15% of the initial body weight necessitating withdrawal of treatment. Preliminary studies to determine the MTD of free ADR, Dex-ADR binary conjugate and NMG-Dex-ADR (ss) conjugate were carried out in normal CD1 mice.

As shown in Table 20, no significant toxicity was observed at the maximum dose of free ADR used (5.0 mg/kg x q2d x 5, i.v., total dose: 25 mg ADR/kg) in these CD1 mice. This observation differed from the results of our previous studies on the toxicity of ADR in nude mice. Considering that there may be a difference in drug sensitivity among different strains of mice, we repeated this study in nude mice. In nude mice, the MTD of free ADR was dependent on the route and schedule of administration. Furthermore, the sensitivity to free ADR was different between normal nude mice and D10-1 xenograft bearing nude mice. The MTD was significantly higher when ADR was given by the i.v. route than when given by the i.p. route. In normal nude mice, at total dose of 25 mg ADR/kg, given 5.0 mg/kg x q2d x 5 i.v. did not cause any significant toxicity. The same total dose following the identical schedule but given i.p. killed all mice. Furthermore, the same total dose of ADR given i.v. following a different schedule, i.e., 8.5 mg/kg x q2d x 3, killed all mice. At a total dose of

22.5 mg ADR/kg, given 7.5 mg/kg x q2d x 3 i.p. caused significant toxicity and killed all mice, but the same total dose following the same schedule but given i.v. did not cause any death. A total dose of 17.5 mg ADR/kg was not lethal irrespective of whether the drug was given i.v. following schedules of 3.5 mg/kg x q2d x 5 or 8.5 mg/kg x q2d x 2, however, moderate toxicity was observed with the latter schedule. Tumor-bearing nude mice were more sensitive to ADR than their normal counterparts. A total dose of 25 mg ADR/kg when given 5.0 mg/kg x q2d x 5 by the i.v. route, did not show any toxicity in normal nude mice, but caused severe toxicity in tumor-bearing nude mice. All mice lost 10 to 15% of their body weight and barely survived the treatment. A total dose of 17.5 mg ADR/kg, when given 3.5 mg/kg x q2d x 5 by the i.v. route, did not cause any toxicity in tumor bearing nude mice.

For NMG-Dex-ADR (ss) conjugate and the Dex-ADR binary conjugate (Table 21), a total dose of 50 mg ADR/kg when given 10 mg/kg x q2d x 5 by the i.v. route did not cause any toxicity in normal CD1 mice. Because of the limited availability of Dal B02-Dex-ADR (ss) conjugate, we evaluated the toxicity of two different total doses of this conjugate and administered the conjugates i.v. into D10-1 xenograft bearing nude mice following two different schedules. The use of these two different total doses and schedules of administration of the conjugate was based on the results of previous studies carried out in this laboratory. It was found that xenograft bearing nude mice were more sensitive to these conjugates than normal CD1 mice. The schedule of administration of these conjugates had a significant effect on their systemic toxicity. For example, at total dose of 25 mg ADR/kg, given i.v. as Dal B02-Dex-ADR (ss) conjugate, or as IgG1-Dex-ADR (ss) conjugate, or as Dex-ADR binary conjugate, following the schedule of 5.0 mg/kg x q2d x 5, did not cause any significant toxicity in tumor-bearing mice. However, wl :n the same conjugates were given following the schedule of 8.5 mg/kg x q2d i.v., only 2 injections (i.e., a total dose of 17.0 mg ADR/kg) caused severe toxicity in xenograft bearing nude mice (loss of body

weight 10 to 15%), and death of 1 of 5 mice given the IgG1-Dex-ADR (ss) conjugate and 2 of 4 mice given the Dex-ADR binary conjugate. No death was observed in the mice given the Dal B02-Dex-ADR (ss) conjugate.

Thus, the MTD of free ADR and its conjugates was dependent on the total dose of ADR (free or conjugated), as well as the route and schedule of administration. The MTD also varied among different strains of mice, and was different in normal or xenograft bearing nude mice. The nude mice were more sensitive to ADR and its conjugates than CD1 mice, and xenograft bearing nude mice were more sensitive to free ADR and its conjugates than normal nude mice.

5.5.2 Treatment of D10-1 xenograft bearing nude mice with ADR and Dal B02-Dex-ADR (ss) conjugate

As discussed above, the MTD of either free ADR or its conjugates was significantly higher when administered by the i.v. route than by the i.p. route. All preparations were therefore given to tumor-bearing nude mice by the i.v. route.

When D10-1 xenograft bearing nude mice were treated with free ADR following the schedule of 5.0 mg ADR/kg x q2d, severe toxicity was observed and the treatment had to be terminated after 5 injections to prevent the death of these mice. In this study, we therefore used this MTD and another non-lethal total dose dose, i.e.,17.5 mg ADR/kg following the schedule of 3.5 mg/kg x q2d x 5, to treat tumor-bearing nude mice.

For Dal B02-Dex-ADR (ss) conjugates, it was known that a protocol of 8.5 mg ADR/kg x q2d caused severe toxicity after 2 injections (total dose, 17.0 mg ADR/kg) necessitating the termination of the treatment. However, another protocol, i.e., 5.0 mg ADR/kg x q2d, 5

injections (total dose 25.0 mg ADR/kg) did not cause mortality or severe toxicity in the treated mice. Both these protocols were used in this study. Several other appropriate control preparations were also given to groups of D10-1 xenograft bearing nude mice. These control preparations include: (i) non-specific IgG1-Dex-ADR (ss) conjugate; (ii) Dex-ADR binary conjugate; (iii) free Dal B02 at a dose of 100 mg/kg; (iv) free Dal B02 plus Dex-ADR binary conjugate (i.e., a mixture of Dal B02 and Dex-ADR binary conjugate).

The anti-tumor activity of free ADR and its conjugates in D10-1 xenograft bearing nude mice is presented in Figs. 94 to 100.

When equal amounts of ADR, either free or as conjugates, were given to tumor-bearing nude mice following a schedule of 5.0 mg ADR/kg x q2d x 5 (total dose, 25.0 mg ADR/kg), the highest anti-tumor activity was achieved with free ADR. In this group, there was one complete cure and one partial tumor regression out of a total of four mice. Severe toxicity was observed in this group requiring termination of the treatment after the fifth injection. Treatment with conjugates at this dose level did not cause any toxicity. All conjugates, as well as free Dal B02, caused various degrees of delays in the progressive growth of the tumors in a proportion of treated mice. However, no cure was achieved. The administration of free Dal B02, Dex-ADR binary conjugate or IgG1-Dex-ADR (ss) conjugates, prevented progressive tumor growth at an early stage, i.e.,during the period of treatment that lasted from day 10 (the start of treatment) to day 20 (the termination of treatment). The tumor in all these groups of mice started to grow rapidly as soon as treatment stopped. Compared to the mice given these control preparations, the mice given specific Dal B02-Dex-ADR (ss) conjugate had a much longer duration of tumor growth inhibition, i.e., up to 30 days in three out of four mice.

When the conjugates were given to D$_{10-1}$ xenograft bearing nude mice following the schedule of 8.5 mg ADR/kg x q2d x 2, a significant increase in the anti-tumor effect of the conjugates was observed, even though the total dose used here (17.0 mg ADR/kg) was less than the total dose of drug (i.e., 25.0 mg ADR/kg) used in the previous protocol. Treatment with Dal B02-Dex-ADR (ss) conjugate following this protocol resulted in complete cure in three out of five mice, and long delays (up to 40 days) in the resumption of progressive tumor growth in the other two mice. Non-specific IgG$_1$-Dex-ADR (ss) conjugate also showed some anti-tumor activity leading to one complete cure and significant delays (up to 30 days) in in the resumption of progressive tumor growth in three of five mice. One mouse died of toxicity in this group. Treatment with Dex-ADR binary conjugate killed two of four mice as a result of toxicity. The two surviving mice showed significant delays (one mouse up to 30 days and the other up to 50 days) in the resumption of tumor growth. To avoid severe toxicity and mortality, the total dose of free ADR (17.0 mg ADR/kg) was given following a schedule of 3.5 mg/kg x q2d x 5 in this study. This schedule did not cause any significant toxicity. The treatment resulted in one complete cure and one partial tumor regression out of four mice and delays in progressive tumor growth in other two mice. However, the therapeutic efficacy of this dose of ADR (i.e., a total dose of 17.0 mg ADR/kg) was less potent than that of a total dose of 25.0 mg ADR/kg, indicating that both toxicity and anti-tumor activity of free ADR are dose-dependent.

Fig. 90

Reactivity of ^{131}I-Dal B02-Dex-ADR (ss) conjugate with D10-1 cells compared to that of ^{131}I-Dal B02.

Five x 10^5 D10-1 cells were incubated with different amounts of ^{131}I-Dal B02 or ^{131}I-Dal B02-Dex-ADR (ss) conjugate at 4°C for 90 min. The cell associated radioactivity was determined after 4 washes with cold PBS.

Fig. 90

Dal B02 added (μg)
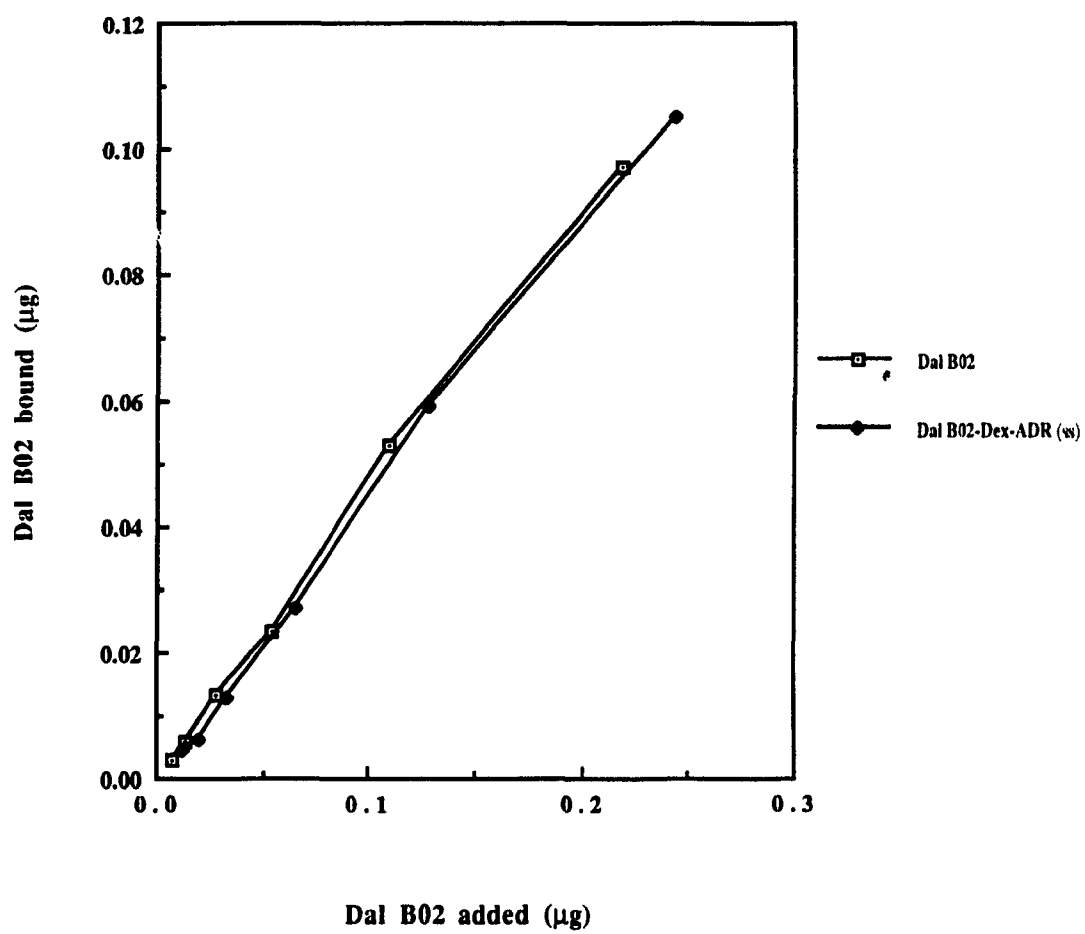
Fig. 91

Clearance of ^{131}I-Dal B02 or ^{131}I-Dal B02-Dex-ADR (ss) conjugate in D10-1 xenograft bearing nude mice.

D10-1 xenograft bearing nude mice were given either ^{131}I-Dal B02 or ^{131}I-Dal B02-Dex-ADR (ss) conjugate mixed with ^{125}I labeled non-specific IgG1 by the i.v. route. Blood samples were obtained at given intervals and the ^{131}I and ^{125}I activities in the blood were determined using a dual-window gamma counter. The total body ^{131}I activity of the mice was monitored using a calibrator.

Fig. 92A Clearance of ^{131}I-Dal B02 or ^{131}I-Dal B02-Dex-ADR (ss) conjugate from blood.

Fig. 92B Total body ^{131}I activity of D10-1 xenograft bearing mice given ^{131}I-Dal B02 or ^{131}I-Dal B02-Dex-ADR (ss) conjugate.

Total body radioactivity
(% of initial activity)

Radioactivity in blood
(% of initial activity)

Fig. 91B

Fig. 91A

Time (hr)

Time (hr)

Dal B02

Dal B02-Dex-ADR (ss)

Dal B02

Dal B02-Dex-ADR (ss)

375
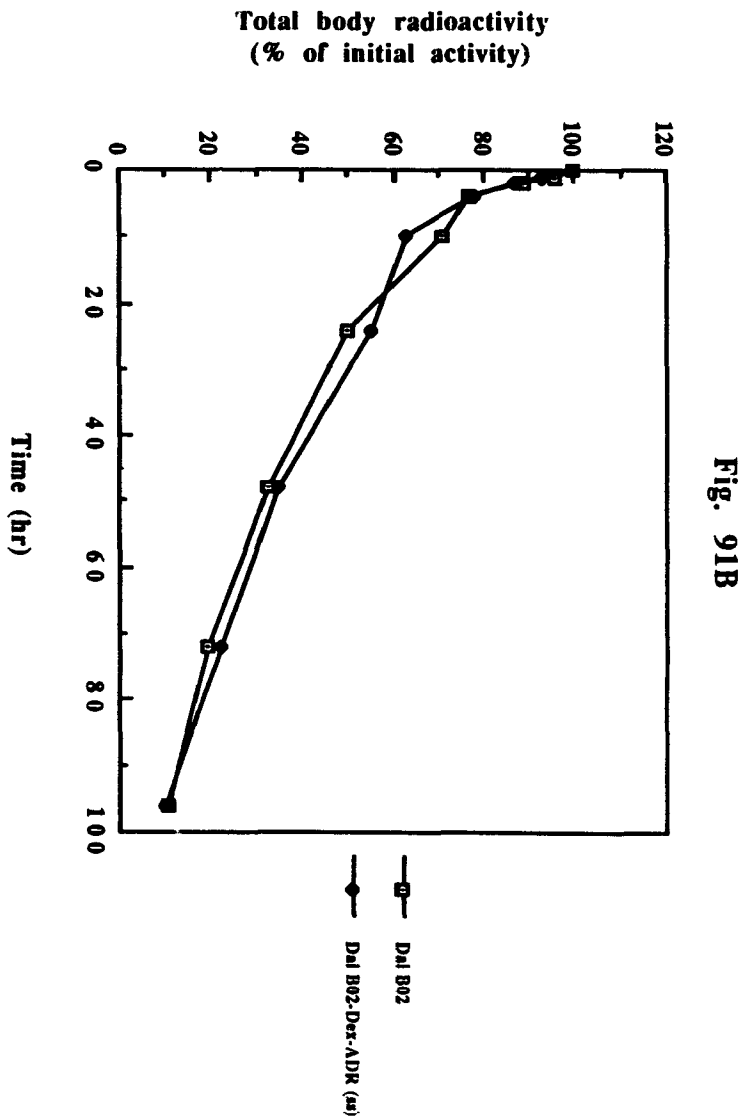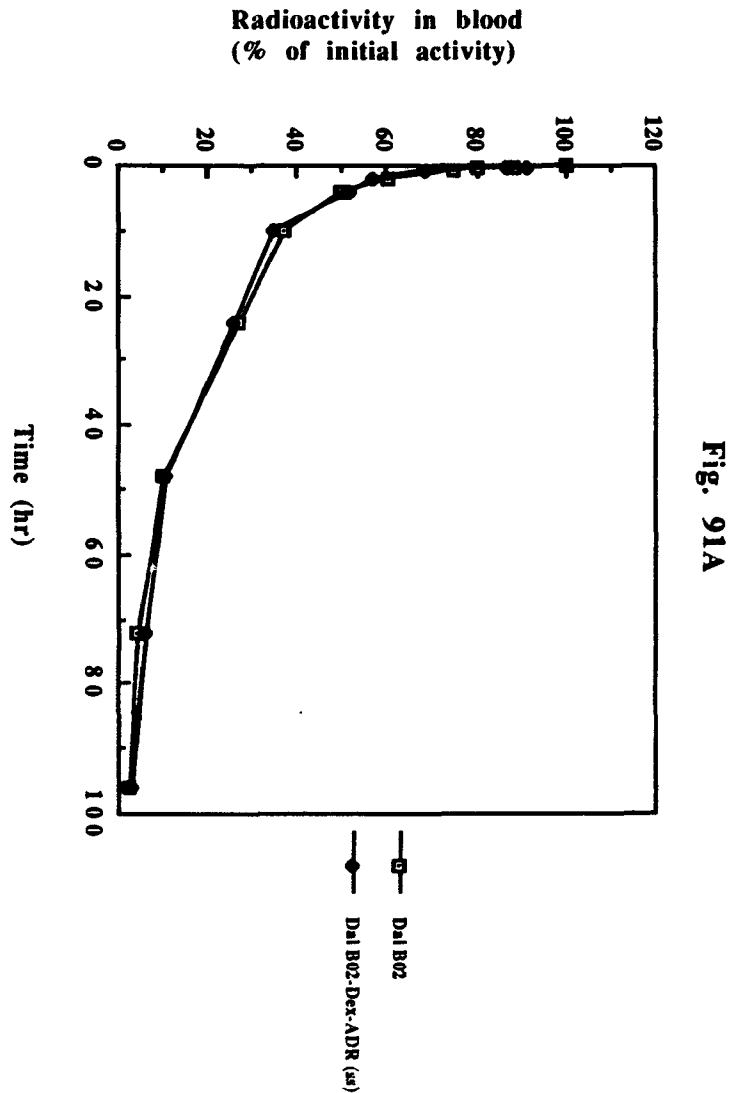
Figs. 92 and 93

Biodistribution of ^{131}I-Dal B02 and ^{131}I-Dal B02-Dex-ADR (ss) conjugate in D10-1 xenograft bearing nude mice.

D10-1 xenograft bearing nude mice were given either ^{131}I-Dal B02 or ^{131}I-Dal B02-Dex-ADR (ss) conjugate mixed with ^{125}I labeled non-specific IgG1 by the i.v. route. The mice were sacrificed at 96 hr post antibody administration. The xenografted tumor and normal mouse tissues were taken out, weighed, and the tissue associated ^{131}I and ^{125}I activities were determined using a dual-window gamma counter. The % ID / g tissue and T / NT ratio were then calculated.

Fig. 92 Biodistribution of ^{131}I-Dal B02 in D10-1 xenograft bearing nude mice at 96 hr post administration of the antibody.

Fig. 93 Biodistribution of ^{131}I-Dal B02-Dex-ADR (ss) conjugate in D10-1 xenograft bearing nude mice at 96 hr post administration of the conjugate.

Fig. 92A

% ID / g tissue

Legend:
- IgG1
- Dal B02

Fig. 92B

T / NT Ratio

Legend:
- IgG1
- Dal B02

Fig. 93A

Organ (y-axis, top to bottom): tumor, serum, tail, neck, skin, muscle, femur, intestine, stomach, kidney, spleen, liver, lung, heart

% ID / g tissue

- ▨ IgG1
- ■ Dal B02-Dex-ADR (ss)

Fig. 93B

Organ (y-axis, top to bottom): tumor, serum, tail, neck, skin, muscle, femur, intestine, stomach, kidney, spleen, liver, lung, heart

T / NT Ratio

- ▨ IgG1
- ■ Dal B02-Dex-ADR (ss)
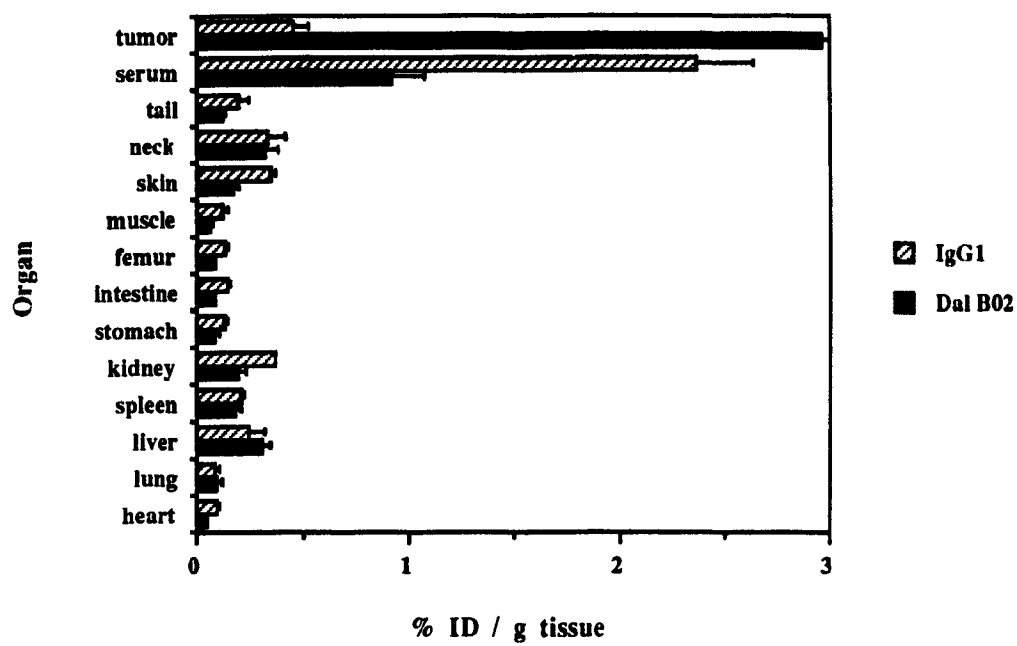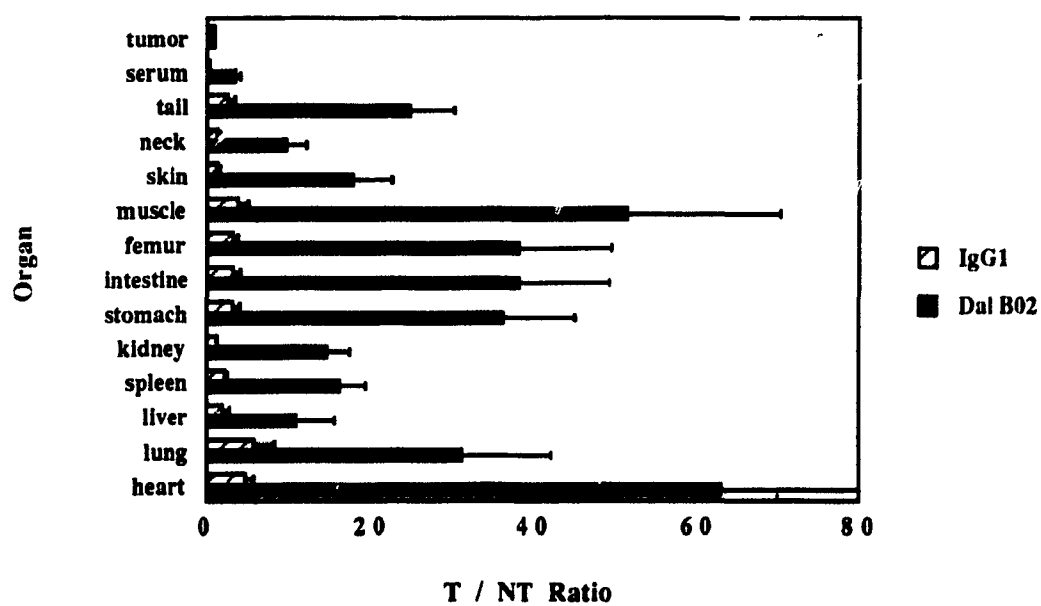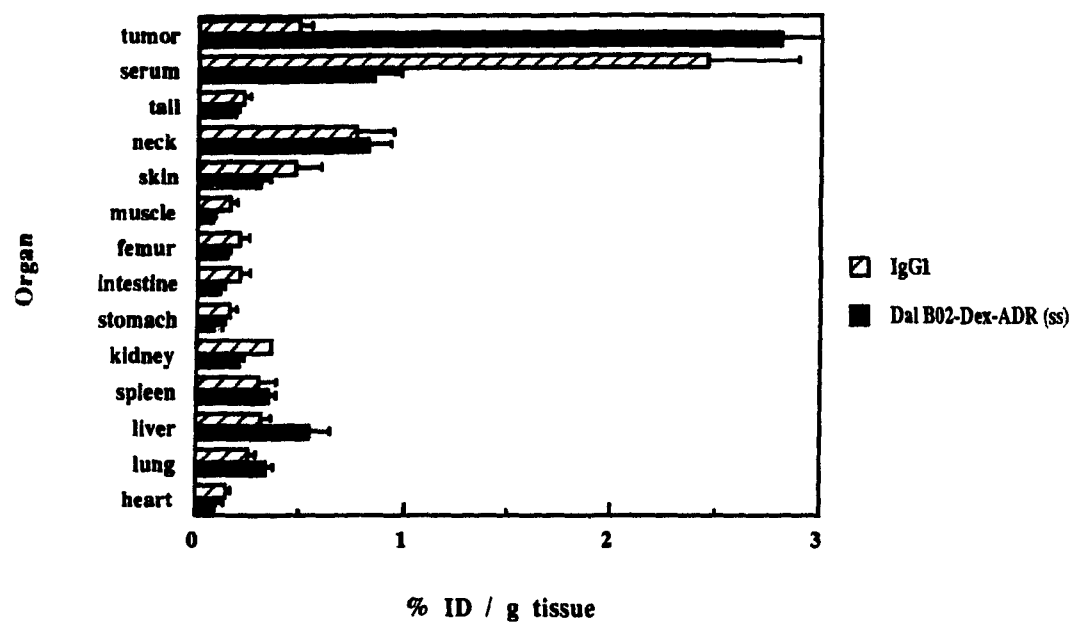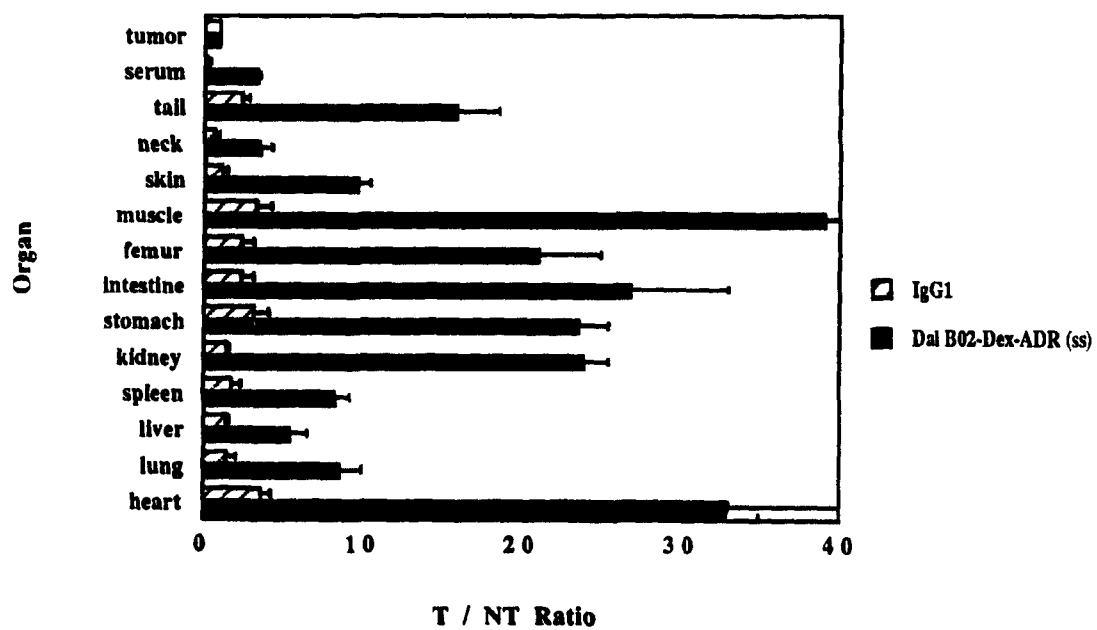
Table 20   Toxicity of free ADR to normal CD1 mice, nude mice and

D10-1 xenograft bearing nude mice

Total dose (mg/kg)	Schedule (mg/kg)	Route [1]	Toxicity Loss of weight [2]	Death [3]
(A) normal CD1 mice				
25.0	5.0 x 5, q2d	i.v.	-	0 / 5
17.5	3.5 x 5, q2d	i.v.	-	0 / 5
(B) normal nude mice				
25.0	5.0 x 5, q2d	i.v.	-	0 / 4
	8.5 x 3, q2d	i.v.	+++	3 / 3
	5.0 x 5, q2d	i.p.	+++	4 / 4
22.5	7.5 x 3, q2d	i.v.	++	0 / 3
	7.5 x 3, q2d	i. p.	+++	4 / 4
17.5	8.5 x 2, q2d	i.v.	+	0 / 3
	3.5 x 5, q2d	i.v.	-	0 / 3
(C) D10-1 xenograft bearing nude mice				
25.0	5.0 x 5, q2d	i.v.	++	0 / 4
17.5	3.5 x 5, q2d	i.v.	-	0 / 4

1. ADR was dissolved in 0.01 M sterile PBS and given to mice via either the i.p. or the i.v. route.

2. Loss of body weight at the end of treatment: (+) between 5-10%; (++) 11 to 15%; and (+++) more than 15% loss of initial body weight.

3. Number of mice dead out of total mice in the group.

Table 21   Toxicity of Dex-ADR, NMG-Dex-ADR (ss), IgG1-Dex-ADR (ss), or Dal B02-Dex-ADR (ss) conjugates to normal CD1 mice and D10-1 xenograft bearing nude mice

Total dose (mg/kg)	Schedule (mg/kg)	Conjugate [1]	Toxicity Loss of weight [2]	Death [3]
(A) normal CD1 mice				
50.0	10.0 x 5, q2d	NMG-Dex-ADR	-	0 / 5
25.0	5.0 x 5, q2d	NMG-Dex-ADR	-	0 / 5
50.0	10.0 x 5, q2d	Dex-ADR	-	0 / 5
25.0	5.0 x 5, q2d	Dex-ADR	-	0 / 5
(B) D10-1 xenograft bearing nude mice				
25.0	5.0 x 5, q2d	Dal B02-Dex-ADR (ss)	-	0 / 4
		IgG1-Dex-ADR (ss)	-	0 / 4
		Dex-ADR	-	0 / 4
17.0	8.5 x 2, q2d	Dal B02-Dex-ADR (ss)	++	0 / 5
		IgG1-Dex-ADR (ss)	+++	1 / 5
		Dex-ADR	+++	2 / 4

1. All conjugates were dialysed against 0.01 M PBS, sterilized by filtration through a 0.22 μm filter and given to mice via the i. v. route.

2. Loss of body weight at the end of treatment: (+) between 5-10%; (++) 11 to 15%; and (+++) more than 15% of loss of initial body weight.

3. Number of mice dead out of total mice in the group.

Figs. 94 to 100

In vivo anti-tumor activity of free ADR, free Dal B02, Dex-ADR, mixture of Dal B02 and Dex-ADR, Dal B02-Dex-ADR (ss) and IgG1-Dex-ADR (ss) conjugates in D10-1 xenograft bearing nude mice.

The nude mice were given 400 rad TBI 48 hr prior to tumor inoculation. Each mouse received 5 x 10⁶ D10-1 cells s.c.. The treatment started at about 10 days after tumor inoculation when the tumor volume reached 60 to 200 mm³. All the injections were given i.v. in a volume of 0.2 to 0.4 ml. The tumors were measured twice a week and the tumor volume was calculated as described in Materials and Methods.

Fig. 94   Control group (no treatment).

Fig. 95A   Free ADR, 3.5 mg/kg x q2d x 5

Fig. 95B   Free ADR, 5.0 mg/kg x q2d x 5

Fig. 96A   Dex-ADR conjugate, 8.5 mg/ kg x q2d x 2

               (arrows indicate the death of 2 mice)

Fig. 96B   Dex-ADR conjugate, 5.0 mg/kg x q2d x 5

Fig. 97A   Dal B02-Dex-ADR (ss) conjugate, 8.5 mg/kg x q2d x 2

Fig. 97B   Dal B02-Dex-ADR (ss) conjugate, 5.0 mg/kg x q2d x 5

Fig. 98A   IgG1-Dex-ADR (ss) conjugate, 8.5 mg/kg x q2d x 2

               (arrow indicates the death of one mouse)

Fig. 98B   IgG1-Dex-ADR (ss) conjugate, 5.0 mg/kg x q2d x 5

Fig. 99   Dex-ADR conjugate plus Dal B02 (mixture),

               5.0 mg/kg of ADR and 100 mg/kg of Dal B02 x q2d x 5

Fig. 100   Dal B02, 100 mg/kg x q2d x 5

Fig. 94

Time (days)
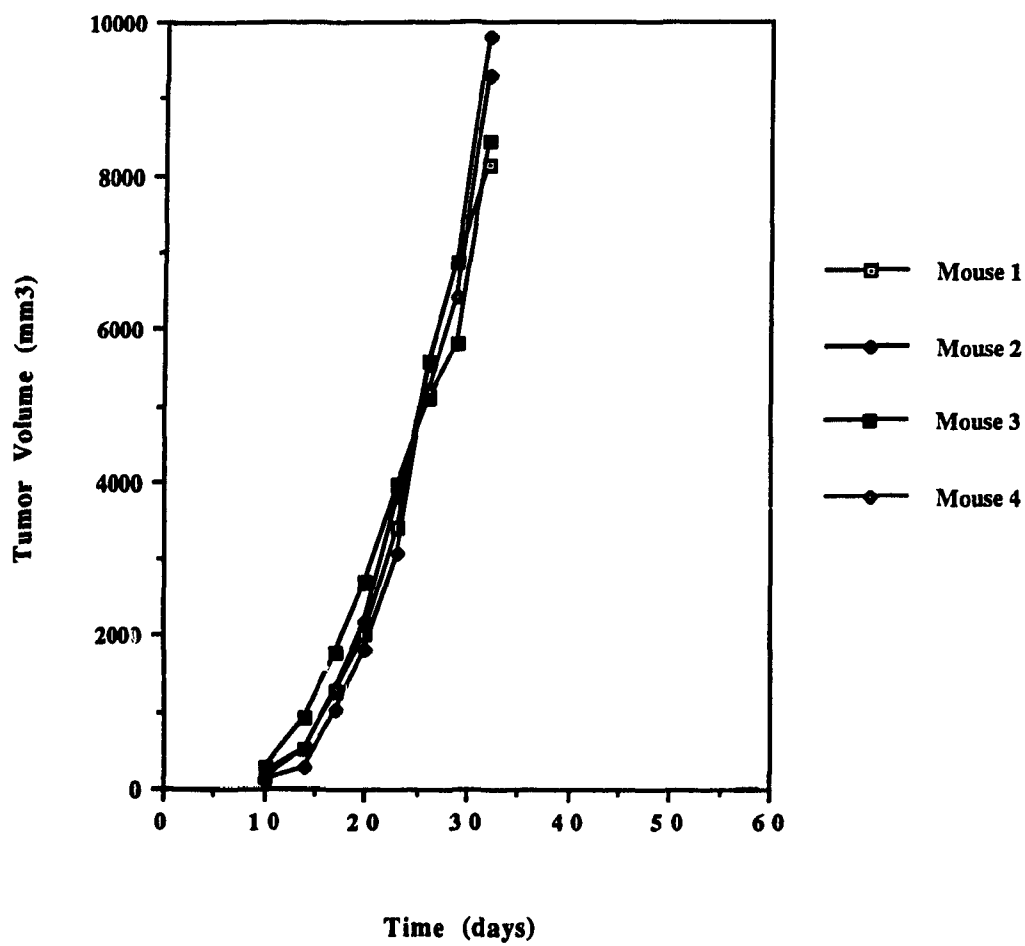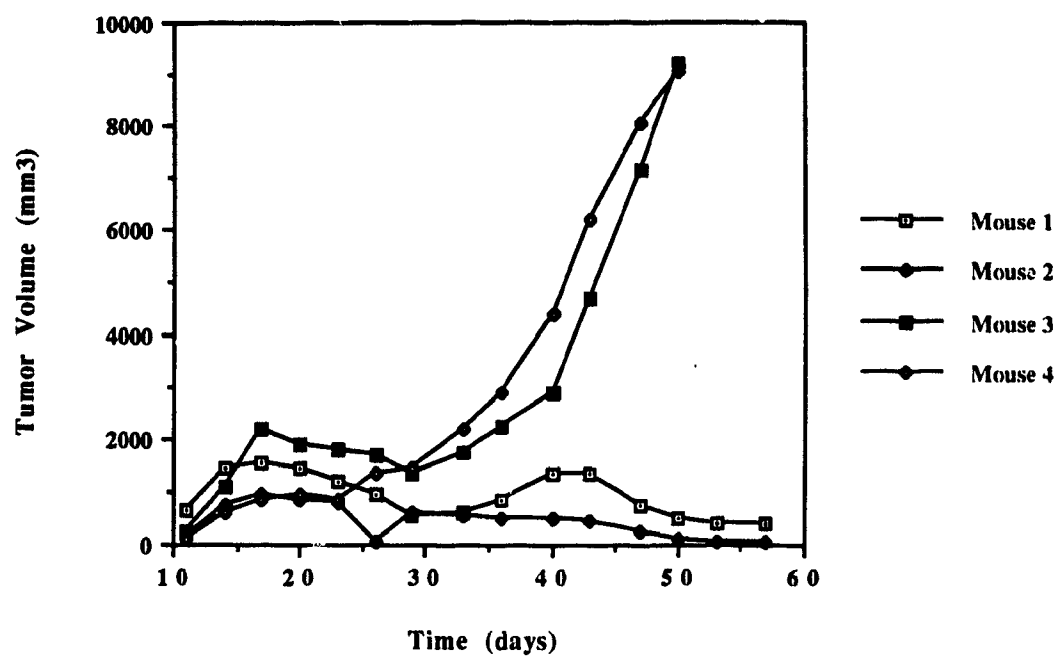
Fig. 95A

Fig. 95B
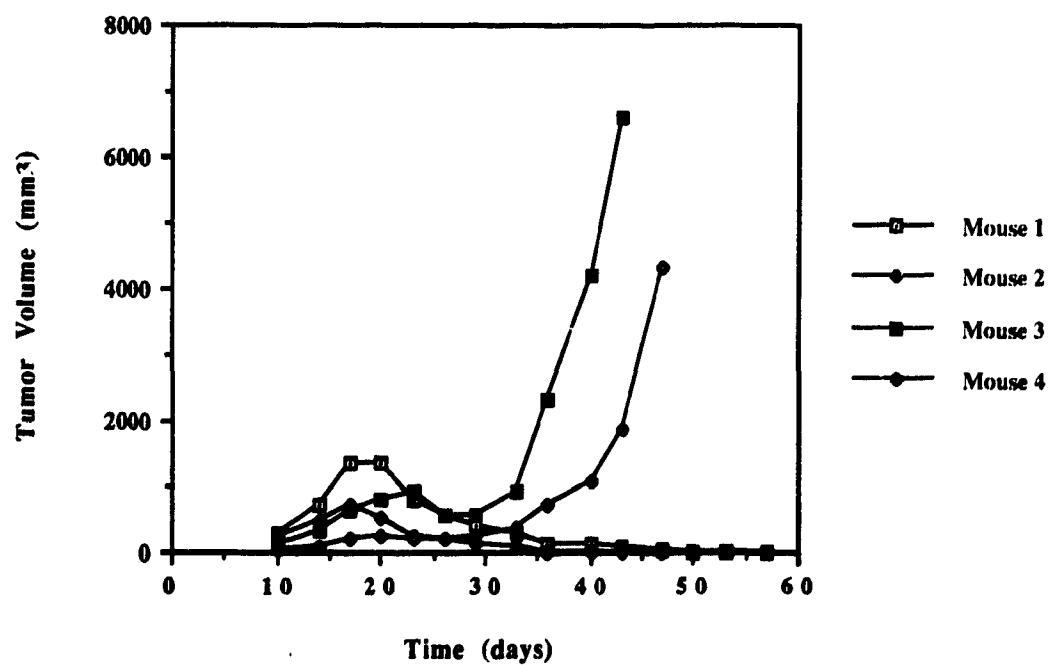
Fig. 96A
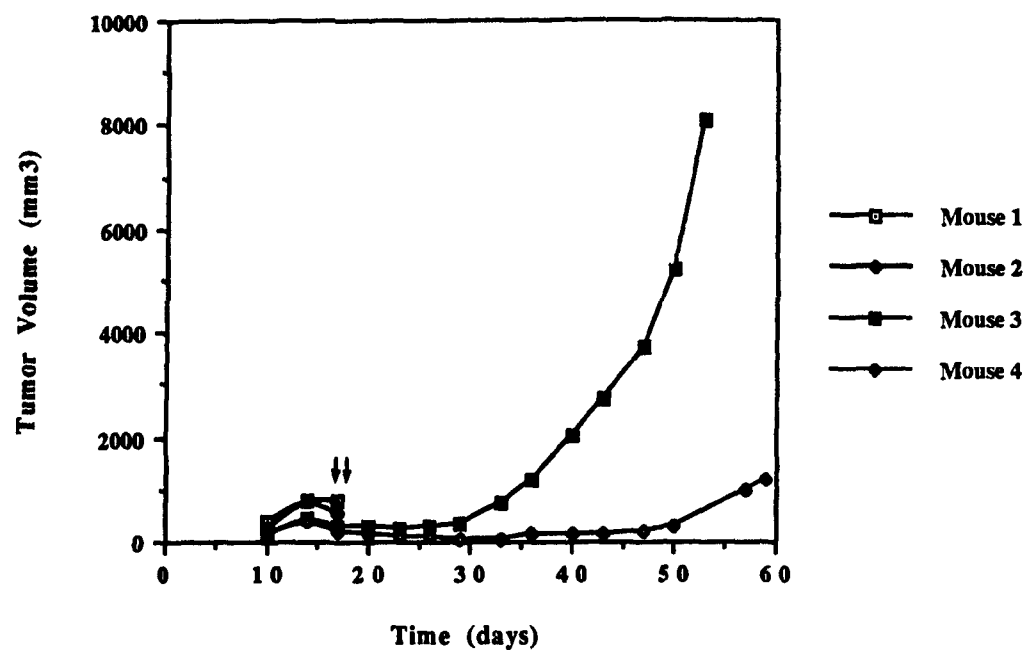
Fig. 96B
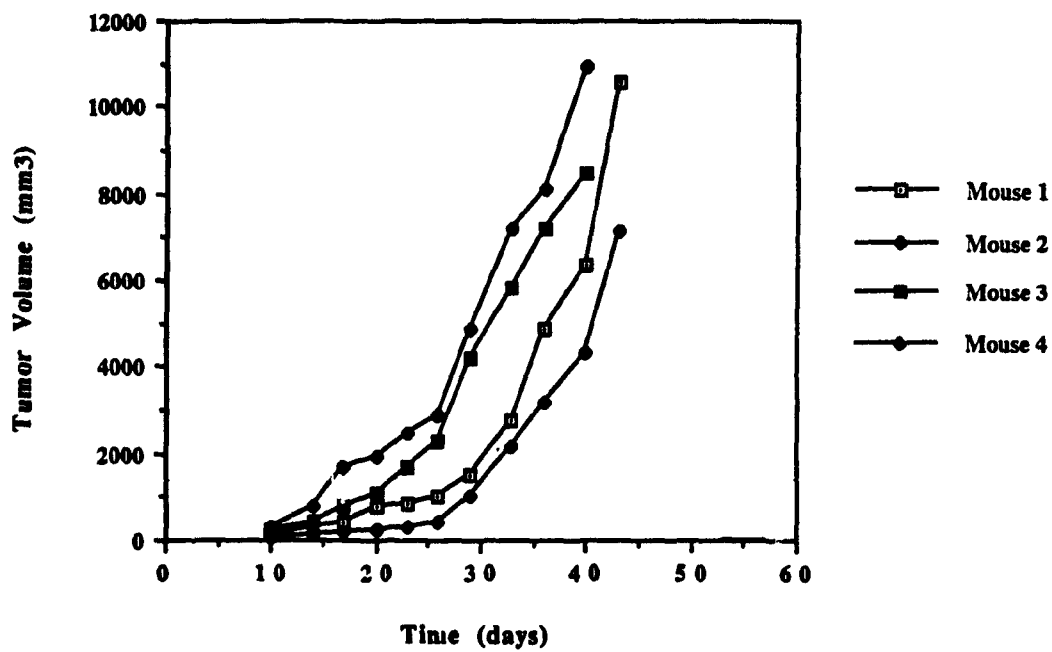
Fig. 97A
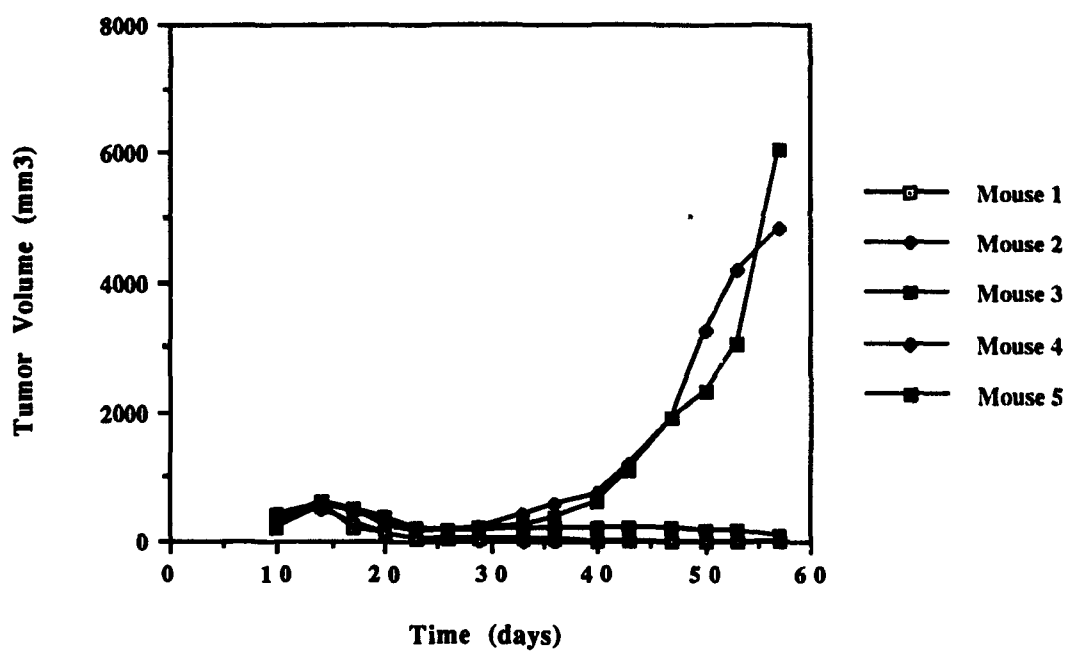
Fig. 97B
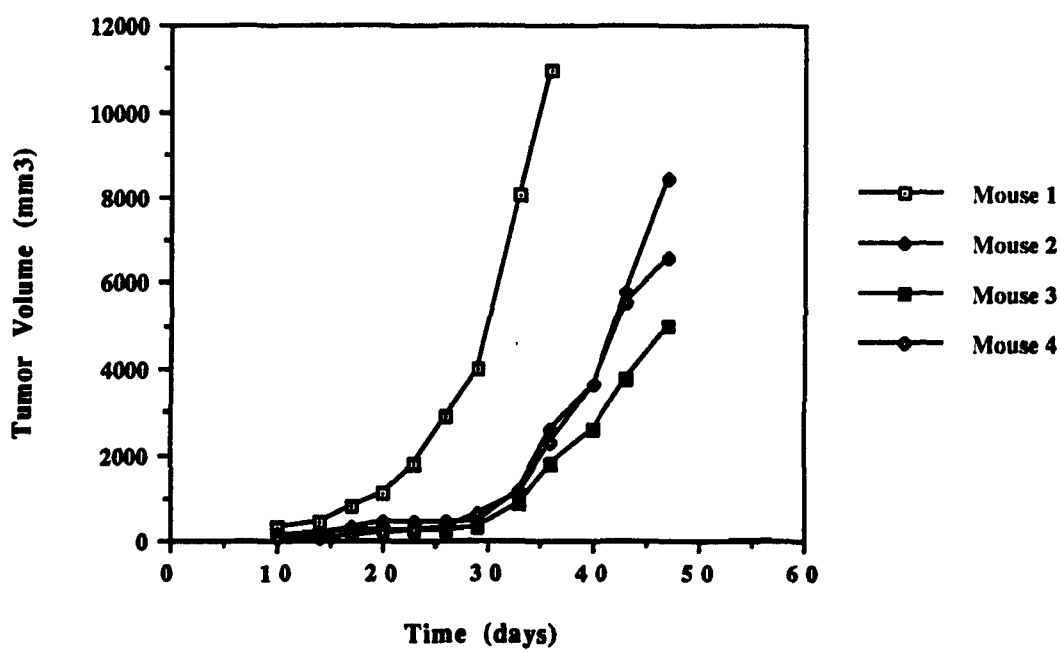
Fig. 98A
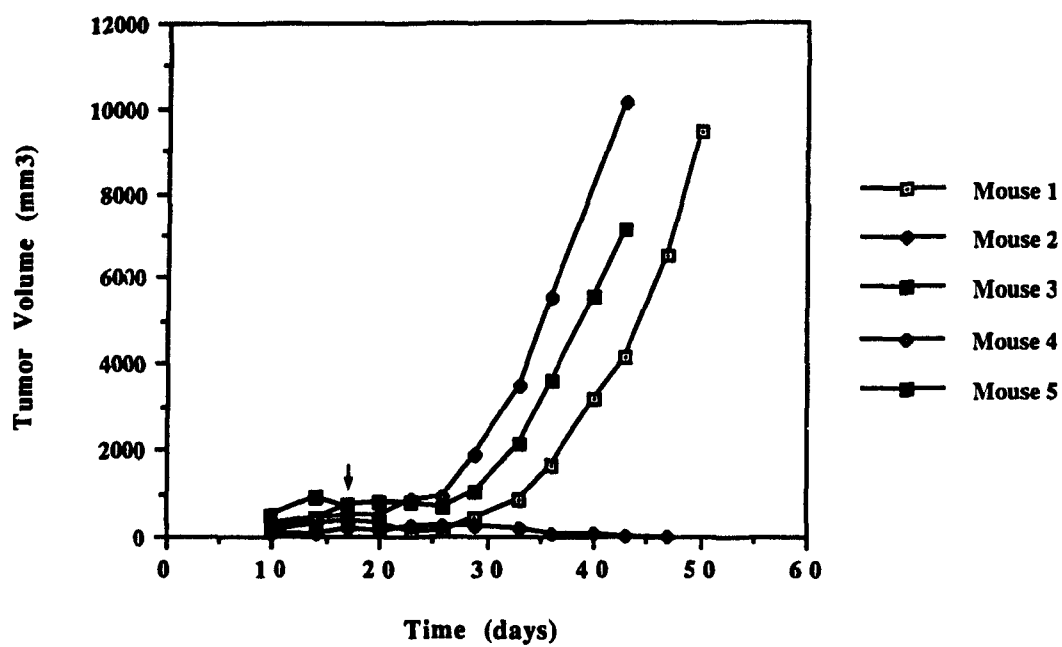
Fig. 98A

Fig. 98B

Fig. 98B
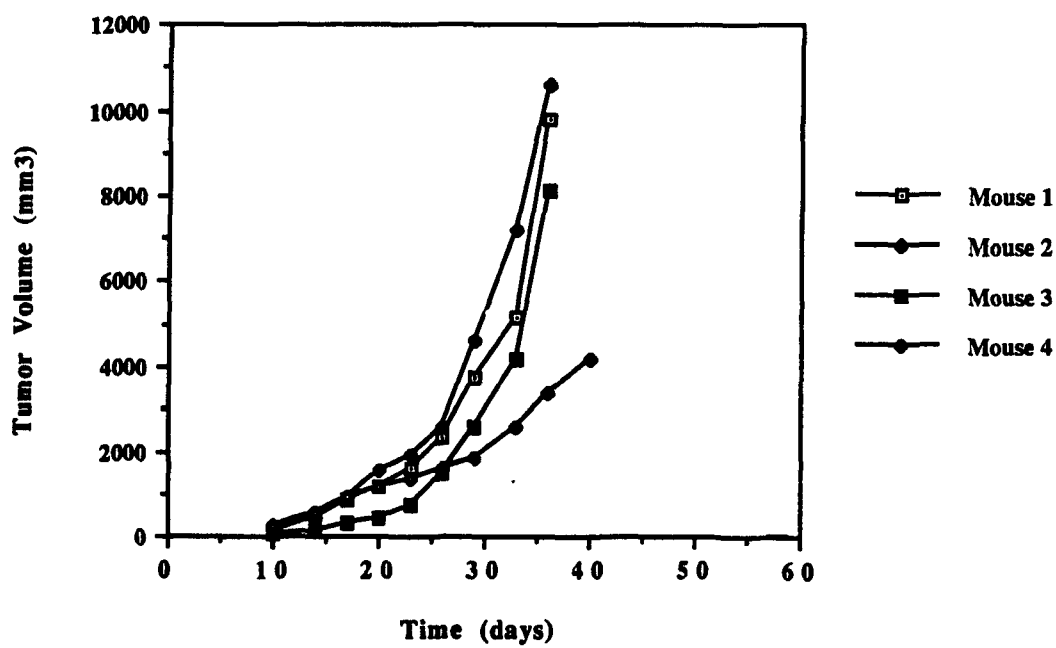
Fig. 99
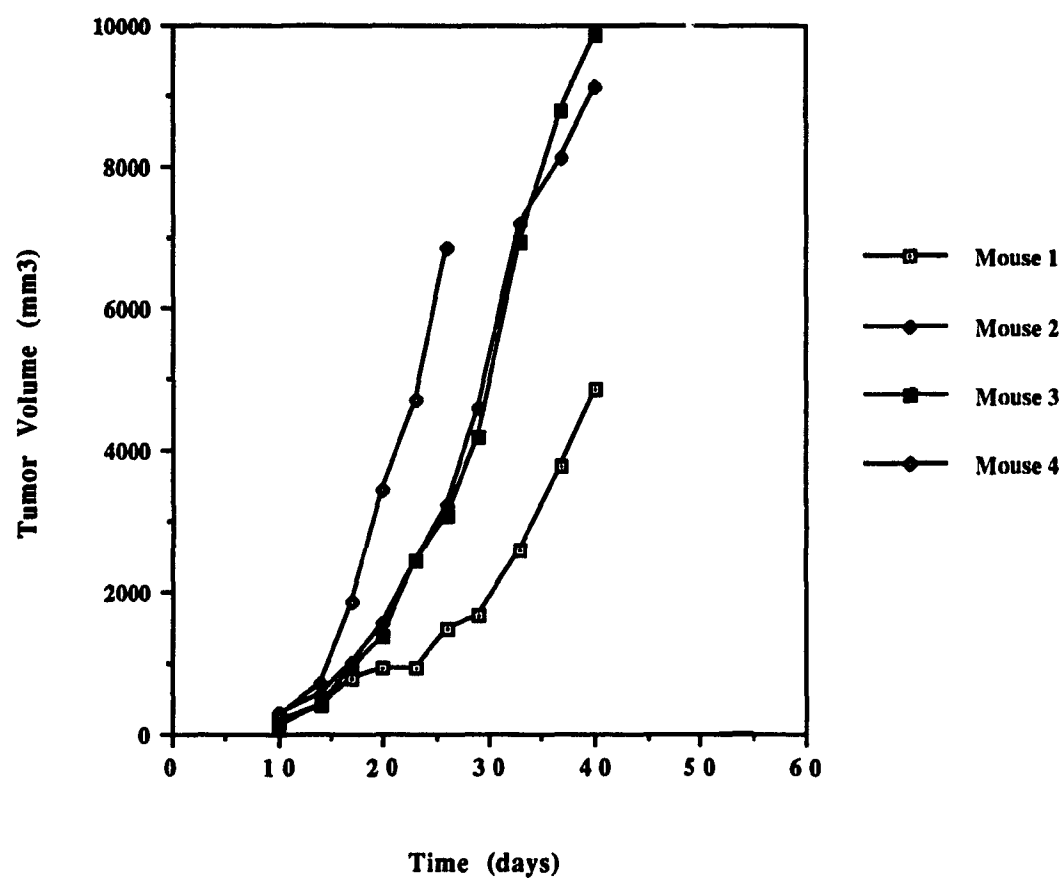
Fig. 100
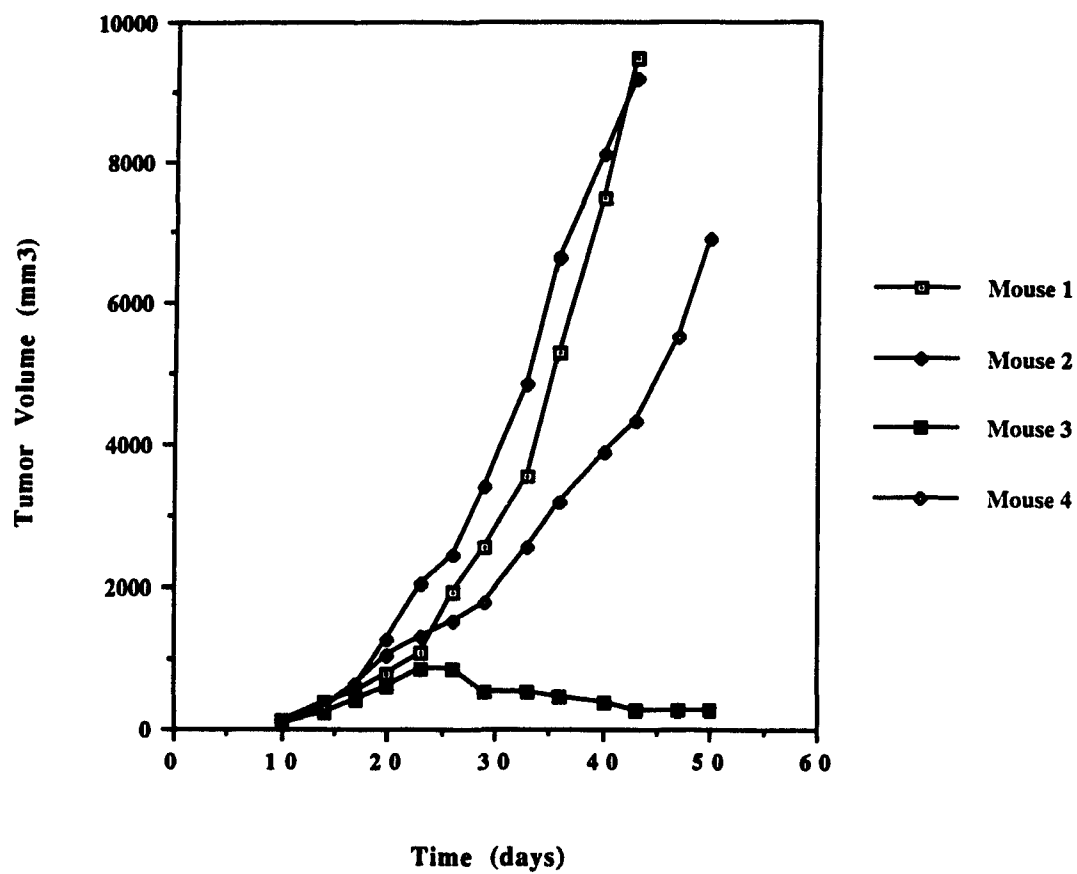
Section 6   Establishment of Human B-cell Chronic Lymphocytic Leukemia in Immunodeficient Nude and SCID Mice

Previous studies in Dr. Ghose's laboratory had established an EBV-transformed human B-cell chronic lymphocytic leukemia cell line (Lee et al., 1986). On s.c. inoculation in nude mice, this cell line produced progressively growing s.c.xenografts (Ghose et al., 1988b). In other studies, it was found that a clonal subline with partial duplication of chromosome 1q, i.e., 46, XY, dup (1) (q11--q32), which was designated as D_{10-1} (Lee et al., 1988), was more tumorigenic, grew faster and produced more metastases compared to the parent clones when inoculated s.c.in nude mice (Ghose et al., 1990). These results encouraged us to develop new B-cell CLL models to appropriately evaluate the efficacy of MoAb-based immunotherapy of this disease. To mimic the different clinical manifestations of human B-cell CLL, i.e., proliferation of tumor cells subcutaneously as solid tumors, intraperitoneally as ascites tumor, or as intravascular and/or systemically disseminated leukemia, we injected D_{10-1} cells s.c., i. v., or i.p. into SCID and irradiated nude mice and produced several different types of B-cell CLL models with progressively growing lethal tumors often accompanied with widespread metastases of leukemic cells.

In a preliminary study, we gave 5×10^6 to 10×10^6 D_{10-1} cells either via the i.v. route to non-irradiated nude mice, or via the i.p. route to non-irradiated nude mice either primed or not with one or two i.p. injections of pristane. None of these mice developed solid tumors or ascites during an observation period of 12 months. As TBI had facilitated the engraftment of the parent EBV-CLL-1 cells in nude mice in the early studies carried out in this laboratory (Ghose et al., 1990), we subjected the nude mice to TBI 48 to 72 hr prior to tumor cell inoculation. We found that TBI led to the successful engraftment of D_{10-1} cells in 100% of nude mice.

6.1 Growth of D10-1 after i.p. or i.v. Inoculation in Irradiated Nude Mice

After i.p. inoculation of 5 x 10^6 D10-1 cells/mouse, 10/10 (100%) of irradiated nude mice developed large amounts of ascites (Fig. 101) and died at 35.3 ± 11.9 days (range from 17 to 56 days). The mean volume of ascites at the time of sacrifice was 4.3 ± 1.9 ml (range from 2.0 to 8.0 ml per mouse). The ascites fluid was viscous, grayish or bloody in appearance, clotted easily and contained large numbers of tumor cells (1.0 ± 0.39 x 10^8 per ml ascites, range from 0.6 to 1.4 x 10^8 cells per ml). Large solid tumors were also found inside the peritoneal cavity of these mice, usually involving the entire mesentery. Both kidneys were embedded in solid tumor tissue. Most peritoneal and mediastinal lymph nodes were enlarged. On histological examination, normal lymph node structure was completely replaced with large, deeply stained monomorphic lymphocytes. Necrotic areas were seen in the center of large tumor masses. Lymphocytic infiltration could be seen along the edge of solid tumors. Solid sheets of tumor cells could be seen wrapping the spleen and both the kidneys but there was no parenchymal invasion. Metastatic foci of tumor cells were observed in the pancreas (Fig. 102). Total peripheral white blood cell (WBC) counts were increased to 94.0 ± 32.6 x 10^3 per ml at the terminal stage. The majority of these cells were neutrophils (94.9 ± 2.9%).

All the eight mice (100%) given 5 x 10^6 D10-1 cells/mouse via the i.v. route developed solid s.c. tumors on the back, mostly as a single tumor mass around the neck or in the shoulder area (Fig. 103). A few mice also developed tumors in the axillae. The mean survival of these mice was 45.1 ± 12.0 days (range from 30 to 60 days). Autopsy revealed enlarged mediastinal and peritoneal lymph nodes. On gross examination, there was no evidence of other visceral organ involvement but in two mice, tumor deposits were seen

around the renal capsule. Histological examination of enlarged lymph nodes revealed the replacement of normal lymph node architecture by tumor tissue as described above. Tumor invasion along the bronchi was also observed in the lungs of all mice (Fig. 104). Total WBC count was slightly elevated ($18.3 \pm 6.7 \times 10^3$ per ml). The differential count was within the normal range ($62.1 \pm 8.7\%$ cells in the peripheral blood were lymphocytes).

In both the models, the spleen appeared to be small and atrophic. There was no staining of cells when the cells from the bone marrow and spleen of tumor-bearing nude mice were stained with FITC-labeled goat anti-human Ig λ light chain antibodies. No cells with the morphology of D10-1 cells could be detected in the peripheral blood smears from these tumor-bearing nude mice.

6.2 Growth of D10-1 Cells after i.p. or i.v. Inoculation into SCID Mice

All the six SCID mice given i.p. inoculation of 5×10^6 D10-1 cells/mouse developed large amounts of ascites (1.8 to 4.8 ml per mouse, mean volume 3.0 ml/mouse) and were sacrificed between 21 to 26 days after tumor cell inoculation. The ascites had the same appearance as described above and contained large numbers of tumor cells (2.1 to 2.6 x 10^8 cells per ml). Large tumor masses were found inside the peritoneal cavity. All abdominal viscera were surrounded by solid tumor tissue. Mediastinal and intra-abdominal lymph nodes were enlarged. In contrast to our observation in nude mice, the spleen was somewhat enlarged in all the SCID mice inoculated with D10-1 cells i. p.. Histological examination revealed large tumor deposits in all the enlarged lymph nodes, disseminated tumor cells throughout the mesentery, and tumor deposits in the pancreas, in the renal parenchyma, and around small blood vessels in the liver (Fig. 105)

In the SCID mice inoculated with 5 x 10^6 D10-1 cells/mouse i. v., 5/5 mice developed paralysis of both the hind legs from 27 to 40 days after tumor inoculation. In contrast to the tumors observed in the nude mice, no solid tumor was found in the back of these SCID mice. Both peritoneal and mediastinal lymph nodes were enlarged in all these mice. Only in one mouse, a tumor was found involving the stomach and the mesentery along with the production of ascites. However, on histological examination of these mice, a number of internal organs showed parenchymal tumor invasion: lungs (around bronchi), liver (perivascular), kidneys, spleen, and in one mouse, the stomach. All enlarged mediastinal and peritoneal lymph nodes were completely replaced by tumor cells (Fig . 106)

Immunofluorescence examination using FITC-labeled goat anti-human Ig λ chain antibody revealed λ chain positive cells in the bone marrow and spleen of these SCID mice. Consistent with the observation in nude mice, D10-1 cell inoculated SCID mice also showed an increase in the number of neutrophils in the peripheral blood. No cells with the morphology of D10-1 cells could be detected in the peripheral blood smears from these tumor-bearing nude mice.

6.3   Growth of D10-1 Cells after s.c. Inoculation into SCID Mice

Five SCID mice were inoculated s.c. with 5 x 10^6 D10-1 cells. All mice developed a s.c. solid tumor at the site of inoculation within 10 days. The tumors grew rapidly and the mice were sacrificed within 3 weeks. Autopsy showed enlarged mediastinal lymph nodes, but no evidence of tumor invasion could be seen in any internal organ. Histological examination revealed large collection of monomorphic tumor cells in the lymph node. Small metastatic tumor foci were also seen in the liver along small vessels. No tumor was detected in other organs.

6.3   In vitro Characterization of the Tumors Cells Obtained from the Ascites or Solid Tumors in Nude and SCID Mice Inoculated with D10-1 Cells

Cytogenetic analysis carried out by Dr. C. Lee showed that tumor cells obtained from the ascites fluid or solid tumors in D10-1 cell inoculated nude or SCID mice had human chromosomes and possessed the same karyotype as D10-1 cells, i.e., 46, XY, dup (1) (q11-- q32). On immunofluorescence assay, all these cells, i.e., parent D10-1 cells and tumor cells obtained from the ascites fluid or solid tumors in D10-1 inoculated nude mice, reacted with Dal B01 and Dal B02 antibodies.

The doubling times of growth in vitro of parent D10-1 cells, tumor cells obtained from the ascites fluid or solid tumors in D10-1 cell inoculated nude mice were 29.4, 31.5 and 31.4 hr, respectively. The IC50 values in a continuous exposure assay (72 hr for MTX and 48 hr for ADR) for D10-1 cells, tumor cells obtained from ascites fluid or solid tumors for MTX were 0.008, 0.01, 0.011µg/ml, and for ADR were 0.05, 0.06, 0.07µg/ml, respectively.

Fig. 101

Photograph of a nude mouse bearing D10-1 ascites tumor after i.p. inoculation of D10-1 cells.

Nude mice were primed with pristane i.p. twice (14 days apart) and given 400 rad TBI one week after the second pristane injection. The mice were then inoculated i.p. with 5×10^6 D10-1 cells 48 to 72 hr after TBI. Hundred percent of the mice developed ascites within 4 weeks and died within 35.3 ± 11.9 days after tumor inoculation.

The picture shows a nude mouse with a large amount of ascites 30 days after inoculation with D10-1 cells via the i.p. route.

Fig. 101

Fig. 102

Microphotographs of sections of tissues from nude mice bearing D10-1 ascites tumor after i.p. inoculation of D10-1 tumor cells.

Ascites bearing nude mice were sacrificed at a terminal stage. Tissues were fixed in 10% formaldehyde. Five µm thick sections were cut from paraffin blocks and stained with H & E.

(A) An enlarged mediastinal lymph node: Normal structure of the lymph node is replaced by large, monomorphic, deeply stained tumor cells.

(B) Mesentery and pancreas: Disseminated tumor cells can be seen in the mesentery and the pancreas.

(C) Kidney: Arrows indicate the tumor cells around renal capsule.

(D) Peripheral blood smear of the ascites-bearing nude mice (Top) and normal nude mice (Bottom) after Wright's staining. The number of neutrophils in the peripheral blood of tumor-bearing mice was markedly increased compared to that in the peripheral blood of normal mice.

Fig. 102
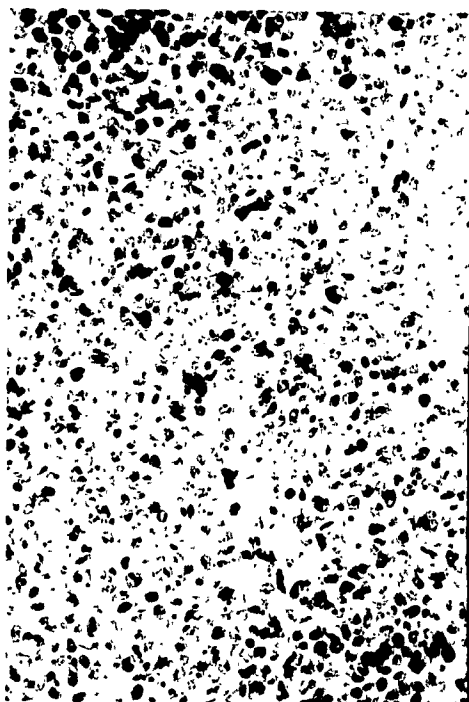
a
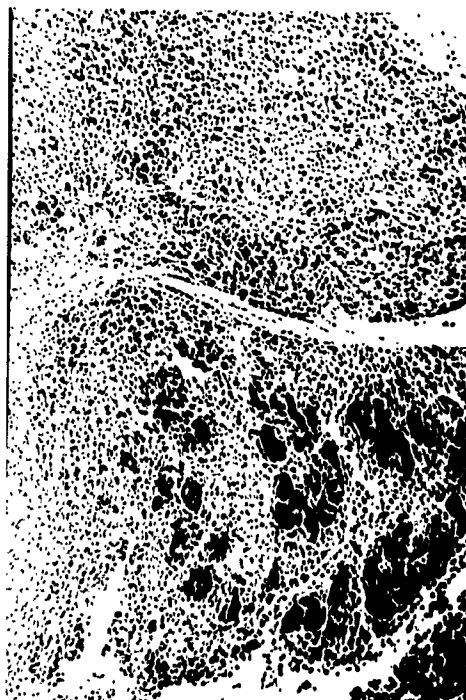
b
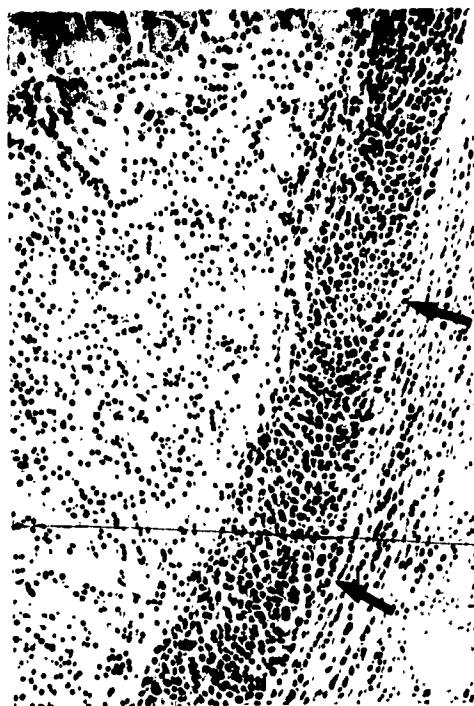
c
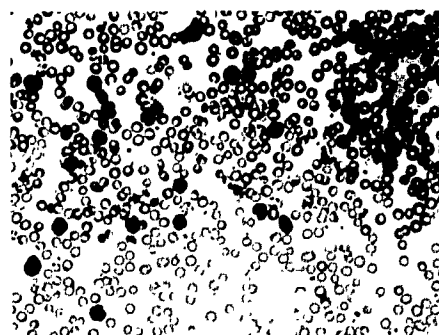
d

Fig. 103

Photograph of a nude mouse that developed a solid tumor on the back after i.v. inoculation of D10-1 tumor cells.

Nude mice were given 400 rad TBI 48 to 72 hr prior to the inoculation of 5×10^6 D10-1 cells i.v.. Hundred percent of the mice developed a solid tumor on the back within 4 to 5 weeks and died at 45.1 ± 12.0 days after tumor inoculation.

The picture shows a solid tumor on the back of the nude mouse 35 days after inoculation of D10-1 tumor cells via the i.v. route.

Fig. 103

Fig. 104

Microphotographs of sections of tissues from nude mice bearing s.c. solid tumor after i.v. inoculation of D10-1 tumor cells.

D10-1 tumor-bearing nude mice were sacrificed at a terminal stage. Tissues were fixed in 10% formaldehyde. Five μm thick sections were cut from paraffin blocks and stained with H & E.

(A) A solid s.c.tumor: The tumor consists of large, monomorphic, deeply stained tumor cells.

(B) An enlarged mediastinal lymph node: Normal structure of the lymph node is replaced by large, monomorphic, deeply stained tumor cells.

(C) Lung: Picture shows infiltrating tumor cells along the bronchi.

(D) Kidney: Arrows indicate tumor cells around renal capsule.

Fig. 104

a
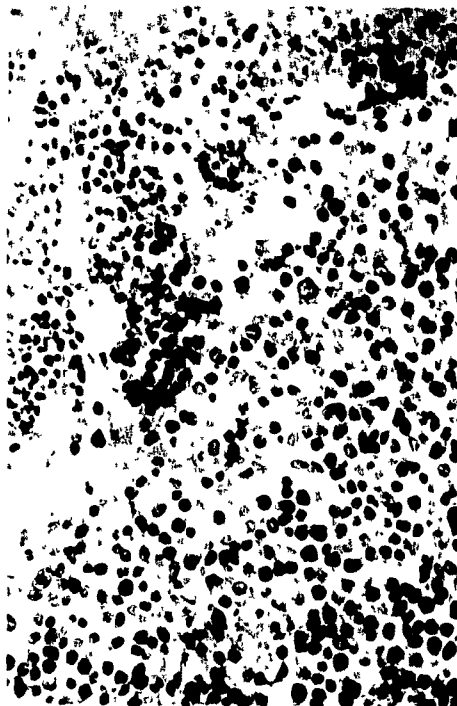
b

c
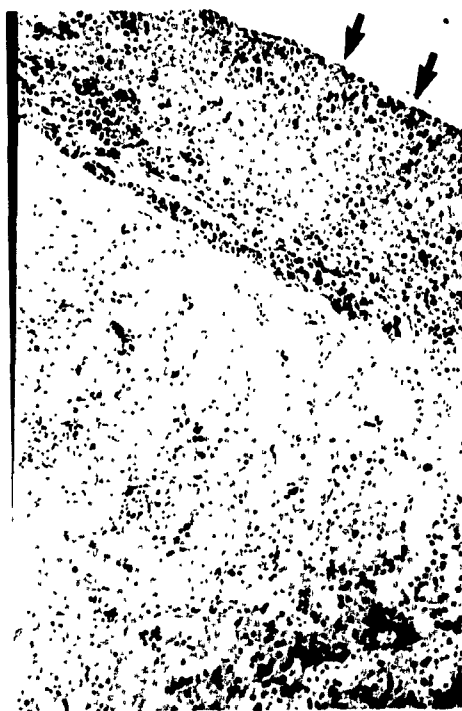
d

Fig. 105

Microphotographs of sections of tissues from SCID mice bearing D$_{10-1}$ ascites tumor after i.p. inoculation of D$_{10-1}$ tumor cells.

Ascites bearing SCID mice were sacrificed at a terminal stage. Tissues were fixed in 10% formaldehyde. Five µm thick sections were cut from paraffin blocks and stained with H & E.

(A) An enlarged mediastinal lymph node around the trachea: Normal structure of the lymph node is replaced by large, monomorphic, deeply stained tumor cells.

(B) Mesentery and pancreas: Disseminated tumor cells can be seen in the mesentery and the pancreas.

(C) Kidney: Arrows indicate infiltrating tumor cells in the renal parenchyma.

(D) Liver: Arrows indicate infiltrating tumor cells in the liver parenchyma.

Fig. 105

a

b

c

d

Fig. 106

Microphotographs of sections of tissues from SCID mice inoculated i.v. with D10-1 tumor cells.

D10-1 tumor bearing SCID mice were sacrificed once the mice developed paralysis of hind legs (28 to 40 days after tumor cell inoculation). Tissues were fixed in 10% formaldehyde. Five μm thick sections were cut from paraffin blocks and stained with H & E.

(A) Enlarged mediastinal lymph node: Normal structure of the lymph node is replaced by large, monomorphic, deeply stained tumor cells.

(B) Lung: Arrows indicate foci of tumor cells along the bronchi.

(C) A mesenteric lymph node: Normal structure of the lymph node and replaced by large, monomorphic, deeply stained tumor cells.

(D) Kidney: Arrows indicate infiltrating tumor cells in the renal parenchyma.

(E) Liver: Arrows indicate infiltrating tumor cells in the liver parenchyma.

(F) Stomach: Arrows indicate foci of tumor cells in the stomach.

Fig. 106
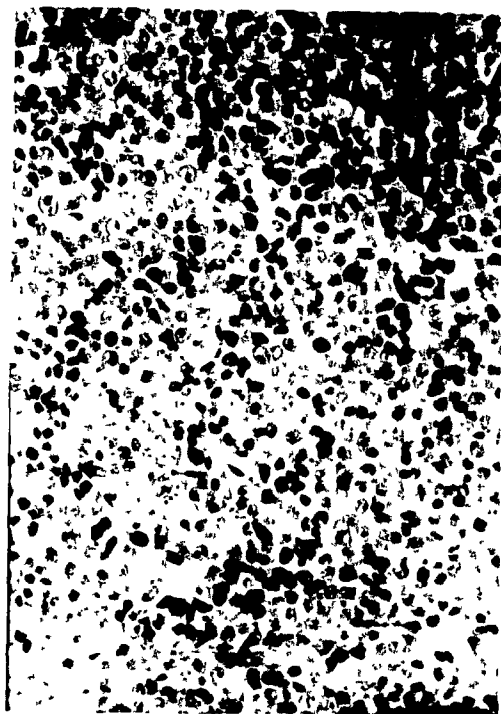
a
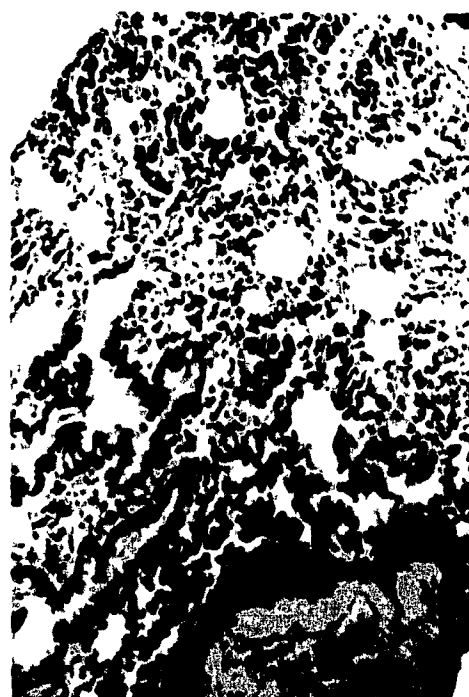
b
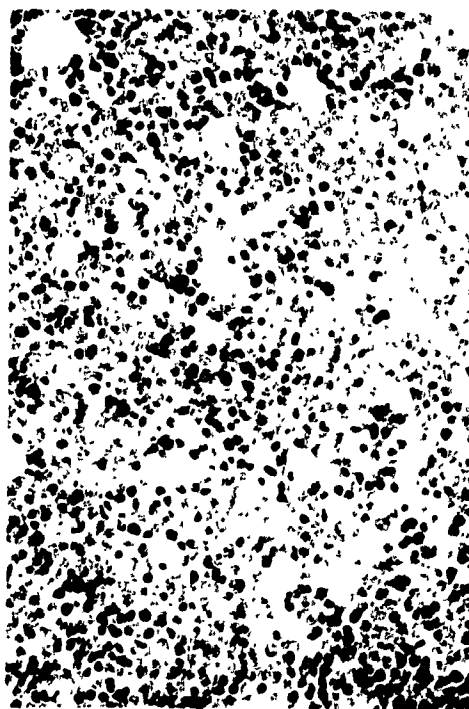
c

d

f
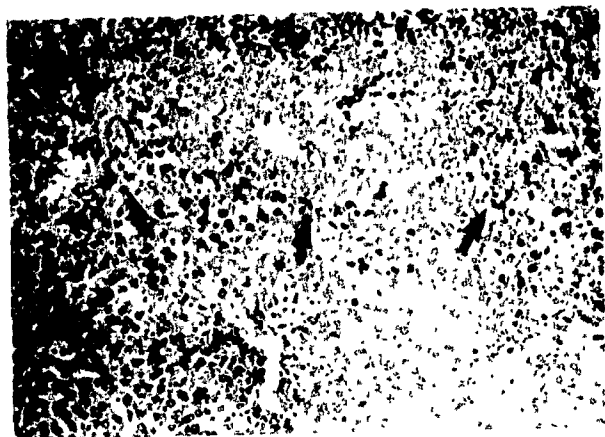
e

Section 7   Monoclonal Antibody-Based Targeted Radiotherapy of Human B-cell Chronic Lymphocytic Leukemia in Immunodeficient Nude and SCID Mice

Radiolabeled MoAbs have been extensively used in recent years for tumor radioimmunoimaging and radioimmunotherapy in animal models and in patients. Since tumors differ in their radiosensitivity, and leukemias and lymphomas are relatively radiosensitive (Badger and Berstein, 1986; Houghton and Scheinberg, 1988), they may be more susceptible to radioimmunotherapy. I have already shown that, Dal B02, a MoAb directed against human B-cell CLL, binds specifically to D_{10-1} cells in vitro with a relatively high Ka of binding and a large number of binding sites, and selectively localizes in the xenografts of D_{10-1} cells in nude mice. Furthermore, the binding of Dal B02 to D_{10-1} cell surface is quite stable and dose not induce internalization of significant amount of cell surface bound MoAb, i.e., the cell surface bound Dal B02 is cleared slowly from the surface of D_{10-1} cells. These features made Dal B02 an ideal candidate for using as a carrier to specifically deliver radionuclides (e.g., ^{131}I) for the treatment of human B-cell CLL.

After the establishment of human B-cell CLL models in nude and SCID mice (see Results section 6), in this study, I evaluated the anti-tumor activity of Dal B02, either used alone or labeled with ^{131}I, in vivo in these xenograft models.

7.1 In vitro Cytotoxic Effect of Unmodified Dal B02 on D_{10-1} Cells

As described in the Results section 4, no significant cytotoxicity was observed when Dal B02 was incubated with D_{10-1} cells in vitro for 72 hr up to an antibody concentration of 500 µg/ml. I, then, investigated whether Dal B02 was cytotoxic to D_{10-1} cells in the

presence of splenic cells or peritoneal macrophages obtained from either nude or SCID mice.

ADCC assay revealed that effector cells (i.e., splenic cells and macrophages) obtained from SCID mice were more potent in mediating ADCC in the presence of Dal B02, compared to the effector cells obtained from nude mice. Only 12.9% of D10-1 cells were lysed when splenic cells of nude mice were used as effector cells, even at a very high E/T ratio (200 to 1). Using splenic cells of SCID mice, 20.6% of D10-1 cells were lysed at an E/T ratio of 100 to 1 (Table 22). When peritoneal macrophages of nude mice were used as effector cells at an E/T ratio of 100 to 1, 14.7% of D10-1 cells were lysed. At the same E/T ratio (i.e., 100 to 1), macrophages of SCID mice lysed 55.8% of D10-1 cells (Table 23). These ADCC-mediated cytolysis were MoAb-based specific processes since neither a non-specific IgG1 along with the above effector cells caused any lysis of D10-1 cells, nor did the splenic cells and macrophages lyse D10-1 cells in the absence of Dal B02.

The CDC effect of Dal B02 was also studied. When rabbit complement was used, about 15.2% of D10-1 cells were lysed at a Dal B02 concentration of 5.0 µg/ml (Table 24). Again, this CDC on D10-1 cells was Dal B02 mediated. No cell lysis was observed when Dal B02 was replaced by a non-specific IgG1, nor when Dal B02 coated D10-1 cells were incubated with inactivated complement.

7.2   Sensitivity of D10-1 Cells to External Gamma Radiation

D10-1 cells in culture (i.e., in 1.0 ml medium containing 1.0×10^5 cells/well in 24 well cell culture plates) were exposed to different doses of gamma radiation from a ^{60}Co source after which the cells were grown in vitro for an additional 5 days. Cells were counted in triplicate every day. As shown in Fig. 107, 200 rad of gamma radiation significantly

inhibited the growth of D10-1 cells, and cell proliferation was completely inhibited when the radiation dose went up to 600 rad.

7.3 Radioiodination of Dal B02 and Its F(ab)'2 Fragments

In all experiments, the specific activity of radioiodinated Dal B02 or its F(ab)'2 fragments ranged from 5 to 8 μCi/μg protein. Greater than 97% of radioactivity was found associated with the protein moiety as determined by 10% TCA precipitation. The IRF of radioiodinated Dal B02 was approximately 70%, whereas the IRF of Dal B02 F(ab)'2 fragments was approximately 50%.

7.4 Targeted Radiotherapy of Human B-cell CLL in D10-1 Xenograft Models

Nude or SCID mice that had received D10-1 cells i.p. were treated using the i.p. route, and mice that had received tumor cells i.v. were treated via the i.v. route. Nude mice with s.c. xenografts were treated via the i.v. route.

7.4.1 Targeted radiotherapy of s.c. D10-1 xenograft in nude mice with Dal B02 or its F(ab)'2 fragment

Groups of four mice bearing a s.c. D10-1 xenograft (tumor volumes ranged from 60 to 200 mm^3) were given i.v. (i) PBS; (ii) 50 μg of unlabeled Dal B02; (iii) 50 μg of Dal B02 labeled with 300 μCi of ^{131}I; (iv) 100 μg of Dal B02 F(ab)'2 fragment labeled with 500 μCi of ^{131}I; (v) 50 μg of non-specific IgG1 labeled with 300 μCi of ^{131}I; or (vi) 50 μg of unlabeled Dal B02 mixed with 50 μg of non-specific IgG1 labeled with 300 μCi of ^{131}I. Two injections were given to tumor-bearing mice. For F(ab)'2 fragment, the second

injection was given 4 days after the first injection, i.e., when the total body radioactivity of the mice was lower than 10 μCi per mouse. For intact Dal B02, it took 15 days for the total body radioactivity to be reduced to about 10 to 15 μCi per mouse. Therefore, the second injection was given 16 days after the first injection.

Figs. 108 to 113 show the results of these treatments of individual mouse. Without any treatment, the tumor grew very rapidly and reached the average volume of 8000 mm^3 within 32 days. Mice treated with ^{131}I labeled Dal B02 produced complete cure in three out of four mice, and a significant delay in progressive tumor growth in the other mouse. This mouse was found to clear total body radioactivity at a much faster rate than the other three mice in the group (Fig. 114). Treatment with unlabeled Dal B02 only resulted in moderate delay in progressive tumor growth in one of three mice. Mice treated with ^{131}I labeled Dal B02 F(ab)'2 fragment resulted in tumor regression as well as significant inhibition of progressive tumor growth in all the four mice in the early stage (up to 26 days), after which the tumors regained their rapid growth. Radiolabeled non-specific IgG1 also showed some inhibition of tumor growth in the early stage. However, no tumor regression was observed. The mixture of radiolabeled non-specific IgG1 and Dal B02 was not a more effective inhibitor of tumor growth compared to radiolabeled non-specific IgG1 alone. These results indicate that the increased anti-tumor efficacy of radiolabeled Dal B02 was a MoAb dependent specific effect, and due neither to the carrier effect of IgG molecule (i.e., the increased biological half-life of ^{131}I activity after linkage to IgG), nor the radiosensitization of tumor cells by Dal B02.

7.4.2   Targeted radiotherapy of D10-1 ascites tumors with ^{131}I labeled Dal B02 or its F(ab)'2 fragment in nude and SCID mice

As shown in Fig. 115, 10/10 (100%) of untreated nude mice given 5 x 10^6 D10-1 cells i.p. developed ascites tumor and died within 35.3 ± 11.9 days after tumor inoculation. The radiolabeled non-specific IgG1 preparation did not show any therapeutic effect. Unmodified Dal B02 demonstrated a significant anti-tumor effect. Three of six mice in this group survived tumor-free for longer than 150 days, while the other three mice died of tumor with a longer duration of survival (mean survival, 88.3 ± 31.2 days). The best therapeutic effect was achieved with ^{131}I labeled Dal B02, a single i.p. injection of 50 µg of Dal B02 labeled with 300 µCi of ^{131}I resulted in long-term tumor-free survival of five of six mice (Table 25).

When nude mice were inoculated i.p. with 15 x 10^6 D10-1 cells per mouse (instead of 5 x 10^6 cell per mouse as was in the studies described above), all untreated mice developed ascites and died within 23.3 ± 2.4 days. As described above, a single injection of 50 µg of unmodified Dal B02 significantly inhibited tumor growth in nude mice inoculated i.p. with 5 x 10^6 D10-1 cells. However, the same amount of Dal B02 could not inhibit the formation of visible ascites or prolong the survival of the mice inoculated with 15 x 10^6 tumor cells per mouse. Treatment with 150 µg of unmodified Dal B02 or Dal B01 resulted in prolonged survival of the mice but no cure was achieved. When 500 µg of unmodified Dal B02 was used, two out of three mice survived tumor-free over 150 days, while the other died of tumor at 90 days after tumor inoculation. Compared to unmodified antibody, a single injection of 50 µg Dal B02 labeled with 300 µCi of ^{131}I resulted in a long term tumor free survive of three out of five mice. The other two mice died with tumor 47 and 50 days after tumor inoculation, i.e., there was a 2-fold increase in the duration of survival compared to untreated control tumor-bearing mice (Fig.116 and Table 26).

Administration of a single dose of Dal BO2 F(ab)'2 fragment (100 μg/mouse), either unmodified or labeled with 500 μCi of ^{131}I, to nude mice inoculated i.p. with 5 x 10^6 D10-1 cells did not show any anti-tumor effect. As shown in Figs. 117 and 118, the durations of survival were comparable irrespective of whether the mice were given one or two injections of unmodified Dal BO2 F(ab)'2 fragment, or one injection of ^{131}I labeled Dal BO2 F(ab)'2 fragment preparation, or two injections of ^{131}I labeled Dal BO2 F(ab)'2 fragment preparation administered 7 days apart (Table 27). Although there was one mouse survived tumor free in each of the group treated with Dal BO2 F(ab)'2 (two injections), ^{131}I-Dal BO2 F(ab)'2 (one injection), or ^{131}I-Dal BO2 F(ab)'2 (two injections given 7 days apart), the difference among these groups and control group in total survival rate (including the duration of survival) is not significant. However, in the group given two injections of ^{131}I labeled Dal BO2 F(ab)'2 fragment preparation administered 4 days apart, the duration of survival of treated mice was significantly prolonged compared to control group and group treated with one injection of unmodified Dal BO2 F(ab)'2 fragment preparation (Table 27).

Fig. 119 shows the results from D10-1 cell i.p. inoculated SCID mice (5 x 10^6 cells/mouse) treated with unmodified Dal BO2, ^{131}I labeled Dal BO2, or ^{131}I labeled non-specific IgG1. All control mice died of tumor within 24.2 ± 1.8 days. Treatment with unmodified Dal BO2 significantly prolonged the survival of these mice (mean survival, 52.4 ± 5.3 days). However, in contrast to the results obtained in nude mice, all the SCID mice eventually died of tumor. Treatment with 300 μCi of ^{131}I conjugated either to Dal BO2 or a non-specific IgG1 resulted in the early death of 100% of the mice (mean survival, 10 to 15 days), before the development of detectable ascites tumor (Table 28). Autopsy and histological examination showed advanced atrophic changes in the bone marrow and spleen of these mice, indicating that they died of radiation toxicity.

7.4.3   Targeted radiotherapy of i.v. inoculated D10-1 cells with Dal B02 or its F(ab)'2 fragment in nude and SCID mice

All untreated nude mice given 5 x 10⁶ D10-1 cells i.v. developed solid tumors in the back and died within 45.1 ± 12.0 days after tumor inoculation. Consistent with our observation in the i.p. model, the radiolabeled non-specific IgG1 preparation did not show any therapeutic effect. When treatment was given 3 days after tumor inoculation, unmodified intact Dal B02 and its ^{131}I labeled counterpart demonstrated an equal anti-tumor effect. Administration of either type of preparation resulted in the long term tumor-free survival of four out of five mice in both the groups (Fig. 120 and Table 29). However, when the treatment was given 7 days, instead of 3 days after tumor inoculation, ^{131}I labeled Dal B02 demonstrated a much better anti-tumor effect than the parent unmodified Dal B02 (Fig. 121). Three out of five mice treated with ^{131}I labeled Dal B02 had a long term tumor-free survival, the other two mice developed a solid tumor in the back at about 45 days after tumor inoculation. The tumors in these two mice had a very slu rate of growth and regressed spontaneously 90 to 120 days after tumor inoculation. All the 5 mice in this group survived over 150 days. Only one of five mice treated with unmodified Dal B02 survived tumor free longer than 150 days, the other four mice developed tumor and died within 57.5 ± 8.8 days (Table 29).

Consistent with the results obtained in the i.p. model, administration of a single dose of Dal B02 F(ab)'2 fragment (100 µg/mouse), either unmodified or labeled with 500 µCi of ^{131}I, or two injections of unmodified Dal B02 F(ab)'2 fragment did not show any anti-tumor activity when the mice were inoculated i.v. with 5 x 10⁶ D10-1 cells (Fig. 122). There was no difference in the durations of survival of tumor inoculated nude mice irrespective of whether the mice were given one single injection, or two injections of unmodified Dal B02

F(ab)'2 fragment, or one injection of ^{131}I labeled Dal B02 F(ab)'2 fragment preparations. However, two injections of ^{131}I labeled Dal B02 F(ab)'2 fragment significantly prolonged the survival of the treated mice (Table 30).

Fig. 123 shows the results obtained from SCID mice inoculated with D10-1 cells i.v. . Consistent with the results obtained in nude mice, all untreated mice died with tumors within 34 ± 4.1 days. In the group of mice given unmodified Dal B02, survival was prolonged (mean survival, 53 ± 6.0 days) but there was no cure. Interestingly, all the five untreated SCID mice developed paralysis of hind legs without palpable solid tumors in the back at the terminal stage (as was described in Results section 6.2), whereas all the 5 mice treated with unmodified Dal B02 developed a solid tumor in the back (as those seen in untreated, i.v. D10-1 cell inoculated nude mice) but had no paralysis. All the SCID mice given unmodified Dal B02 finally died of large solid tumors in their back. Consistent with the observations with SCID mice inoculated with D10-1 cells i.p., administration of 300 µCi of ^{131}I (conjugated to either specific Dal B02 or non-specific IgG1) to SCID mice inoculated with D10-1 cells i.v. resulted in the early death of all the mice (range of survival, 10 to 15 days), before the development of paralyses or palpable solid tumors (Table 31). Autopsy and histological examination revealed advanced atrophic changes in the spleen and bone marrow of these mice, suggesting that they also died of radiation toxicity.

Table 22   ADCC of Dal B02 on D10-1 cells in the presence of splenic cells of nude or SCID mice determined using a ^{51}Cr release assay [1]

Target cells	Antibody [2]	E / T ratio			
		200:1	100:1	50:1	25:1

(A) Effector cells: splenic cells of nude mice

Target cells	Antibody	200:1	100:1	50:1	25:1
D10-1	Dal B02	12.9 ± 2.4 [3]	6.3 ± 2.2	4.9 ± 2.6	2.2 ± 1.5
D10-1	IgG1 [4]	0	0	0	0
D10-1	Nil	1.1	0.4	0.3	0.1
Yac	Nil	34.5 ± 3.9	21.0 ± 0.9	10.2 ± 0.8	1.8 ± 1.0

(B) Effector cells: splenic cells of SCID mice

Target cells	Antibody	200:1	100:1	50:1	25:1
D10-1	Dal B02	ND [5]	20.6 ± 6.2	9.8 ± 4.4	5.4 ± 1.4
D10-1	IgG1	ND	4.8 ± 2.0	1.5 ± 1.5	1.5 ± 1.5
Yac	Nil	ND	50.8 ± 3.3	ND	ND

1. Nude or SCID mice were primed i.p. with 100 units of poly IC 24 hr before harvesting the effector cells (see Methods section 4 for a detailed description).

2. Antibody concentration used: 5.0 µg/ml.

3. Data represent the percentage of ^{51}Cr released from D10-1 cells and are the mean ± S.D. of at least 3 determinations.

4. Non-specific IgG1.

5. ND: not determined.

Table 23   ADCC of Dal B02 on D_{10-1} cells in the presence of peritoneal macrophages of nude or SCID mice determined using a ^{51}Cr release assay [1]

Target cells	Antibody [2]	E / T ratio			
		200:1	100:1	50:1	25:1

(A) Effector cells: macrophages of nude mice

Target cells	Antibody	200:1	100:1	50:1	25:1
D_{10-1}	Dal B02	ND [3]	14.7 ± 2.1 [4]	6.9 ± 1.2	3.0 ± 0.9
D_{10-1}	IgG$_1$ [5]	ND	0	0	0
D_{10-1}	Nil	ND	2.4	1.5	0.6
Yac	Nil	ND	13.6 ± 1.8	7.8 ± 1.2	4.7 ± 0.9

(B) Effector cells: macrophages of SCID mice

Target cells	Antibody	200:1	100:1	50:1	25:1
D_{10-1}	Dal B02	61.8 ± 4.6	55.8 ± 6.8	25.4 ± 2.3	10.6 ± 3.9
D_{10-1}	IgG$_1$	6.7 ± 2.5	4.3 ± 0.5	2.5 ± 1.5	0.4 ± 0.1
D_{10-1}	Nil	0	0	0	0

1. Nude and SCID mice were primed i.p. with 0.1 ml incomplete Frenud's adjuvant 24 hr before harvesting the effector cells (see Methods section 4 for a detailed description).

2. Antibody concentration used: 5.0 μg/ml.

3. ND: not determined.

4. Data represent the percentage of ^{51}Cr released from target cells and are the mean ± S.D. of 3 determinations.

5. Non-specific IgG$_1$.

Table 24 Complement-dependent cytotoxicity (CDC) of Dal B02 on D_{10-1} cells determined using a ^{51}Cr release assay [1]

Target cells	Antibody [2]	Complement [3]	^{51}Cr release (%)
D_{10-1}	Dal B02	C [4]	15.8 ± 2.3 [6]
D_{10-1}	Dal B02	IC [5]	0
D_{10-1}	Dal B02	Nil	0
D_{10-1}	Nil	C	0
D_{10-1}	IgG$_1$ [7]	C	0
D_{10-1}	IgG$_1$	IC	0
HL$_{60}$	HI98 [8]	C	30.7 ± 6.8
HL$_{60}$	HI98	IC	0
HL$_{60}$	HI98	Nil	0
HL$_{60}$	Dal B02	C	0

1. The CDC effect of MoAbs was determined using appropriate ^{51}Cr labeled target cells.

2. Antibody concentration used: 5.0 μg/ml.

3. Complement dilution: 1 to 10.

4. Fresh complement.

5. Inactivated complement (inactivated by incubation at 56°C for 30 min).

6. Data represent the percentage of ^{51}Cr released from target cells and are the mean ± S.D. of at least 3 determinations.

7. Non-specific IgG$_1$.

8. An IgM class MoAb that is known to be cytotoxic to HL$_{60}$ cells.

Fig. 107

In vitro sensitivity of D10-1 cells to external gamma radiation.

D10-1 cells were exposed to different doses of gamma radiation from a ^{60}Co source after which the cells were incubated in growth medium for 5 days. Cells were counted in triplicate every 24 hr.

Note that the inhibition of cell growth by gamma radiation was dose-dependent. Two hundred rad of gamma radiation significantly inhibited the proliferation of D10-1 cells. Proliferation of D10-1 cells stopped after exposure to 600 rad of radiation.

Fig. 107

Cell numbers (x 100,000/ml)

Time (days)

control
200 Rad
400 Rad
600 Rad
800 Rad
1200 Rad
1600 Rad
2000 Rad
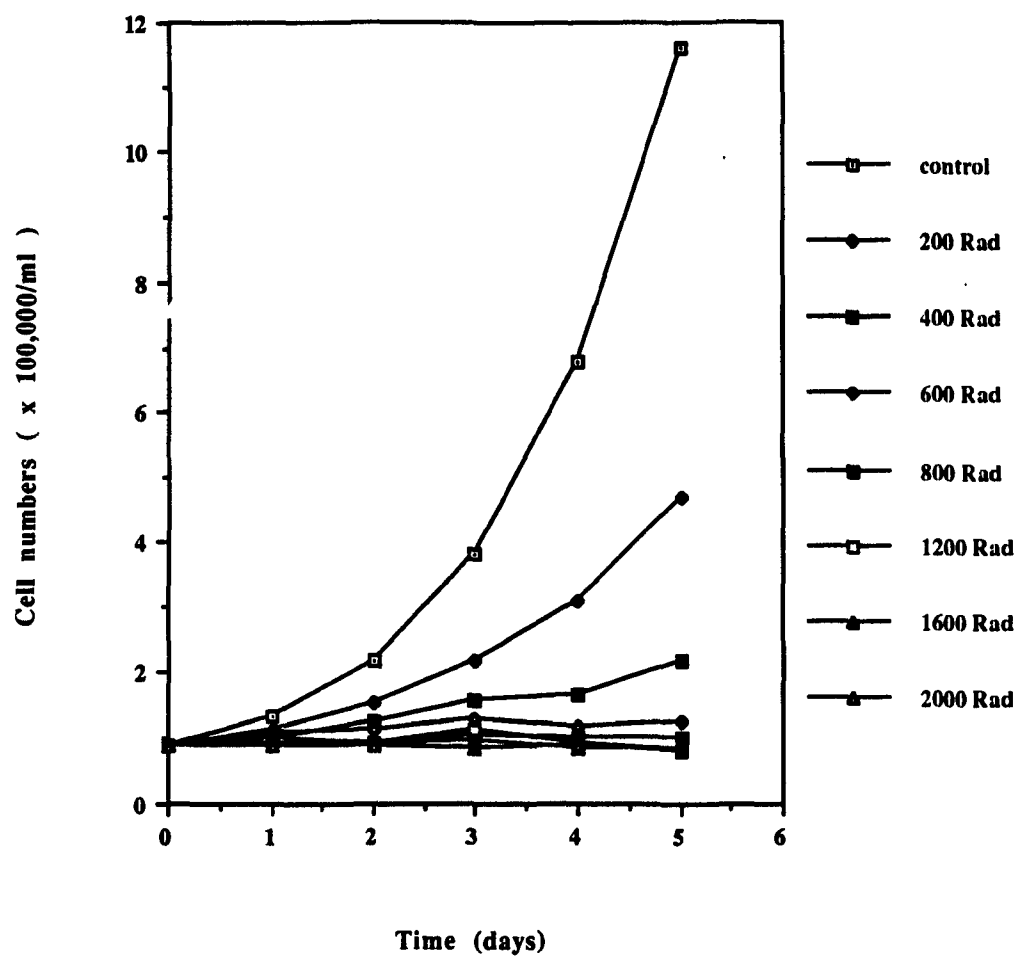
Figs. 108 to 113

Results of administration of ^{131}I labeled Dal B02 and its F(ab)'2 fragment in s.c. D10-1 xenograft bearing nude mice.

Nude mice were inoculated with 5×10^6 D10-1 cells via the s.c. route (into the right flank) 48 to 72 hr after 400 rad TBI. Treatment was started at about 10 days after tumor cell inoculation when the tumor volume was between 60 to 200 mm^3. All mice received two injections i.v.. Tumors were measured twice a week and the tumor volume was calculated as described in Materials and Methods. See text for detailed description of the results depicted in these figures.

Fig. 108	Control group (no treatment);
Fig. 109	Mice given unlabeled Dal B02 (50 μg x 2);
Fig. 110	Mice given ^{131}I labeled Dal B02 (300 μCi / 50 μg protein x 2);
Fig. 111	Mice given ^{131}I labeled Dal B02 F(ab)'2 fragment (500 μCi / 100 μg protein x 2). Arrow indicates the death of one mouse;
Fig. 112	Mice given ^{131}I-nonspecific IgG1 (300 μCi / 50 μg protein x 2);
Fig. 113	Mice given ^{131}I -nonspecific IgG1 (300 μCi / 50 μg protein) plus 50 μg unlabeled Dal B02 x 2.

Fig. 108

Fig. 109

Fig. 110

Tumor Volume (mm3) vs Time (days)

Mouse 1
Mouse 2
Mouse 3
Mouse 4

Fig. 111

Tumor Volume (mm3) vs Time (days) graph with legend: Mouse 1, Mouse 2, Mouse 3, Mouse 4
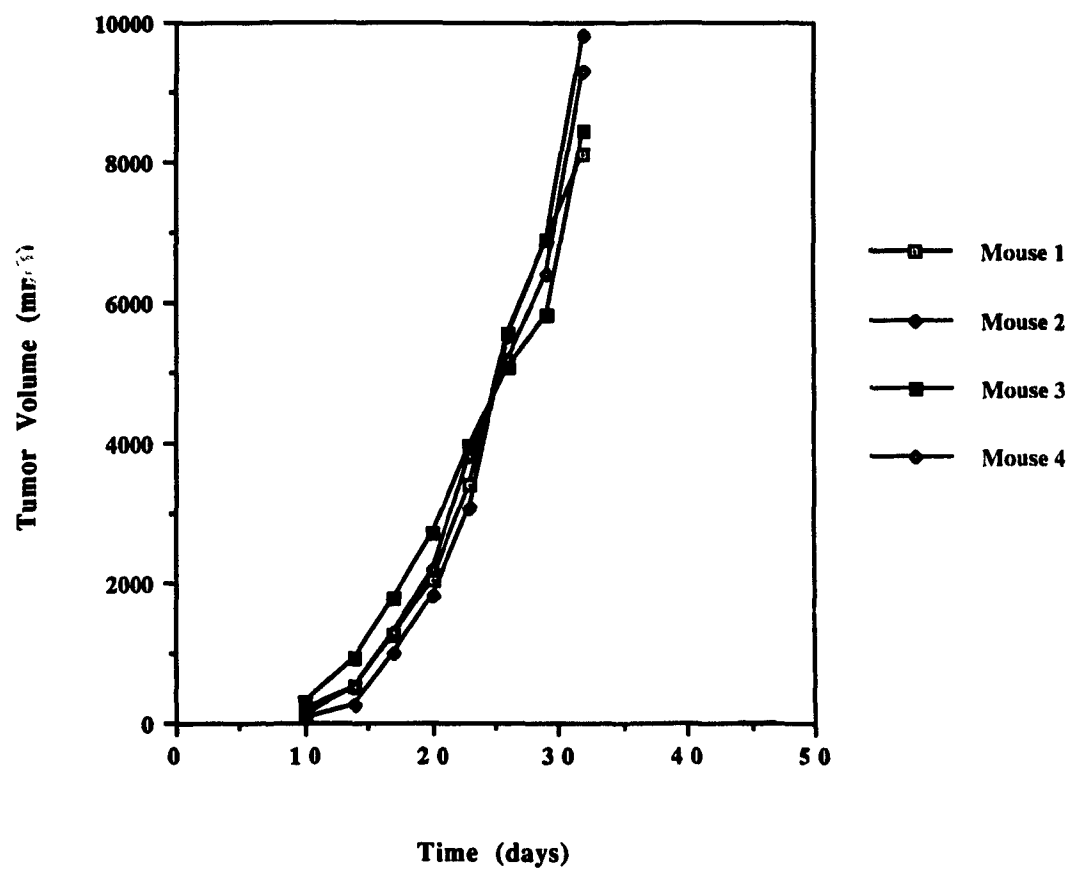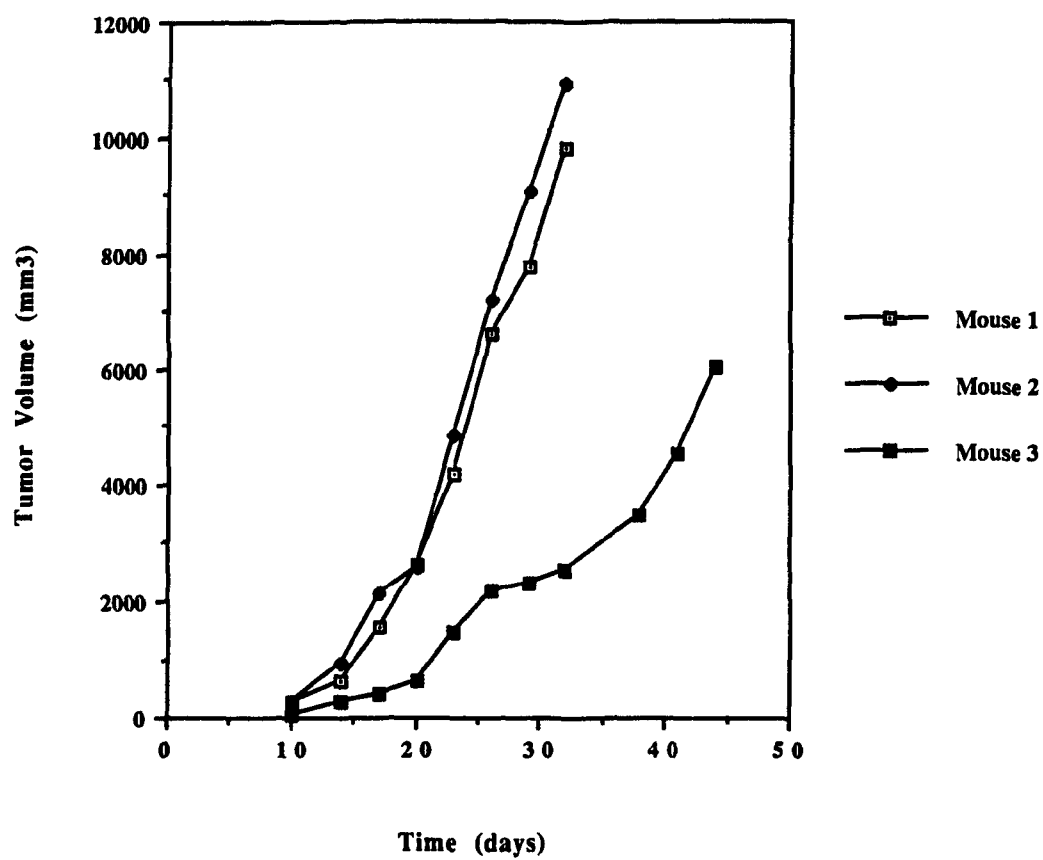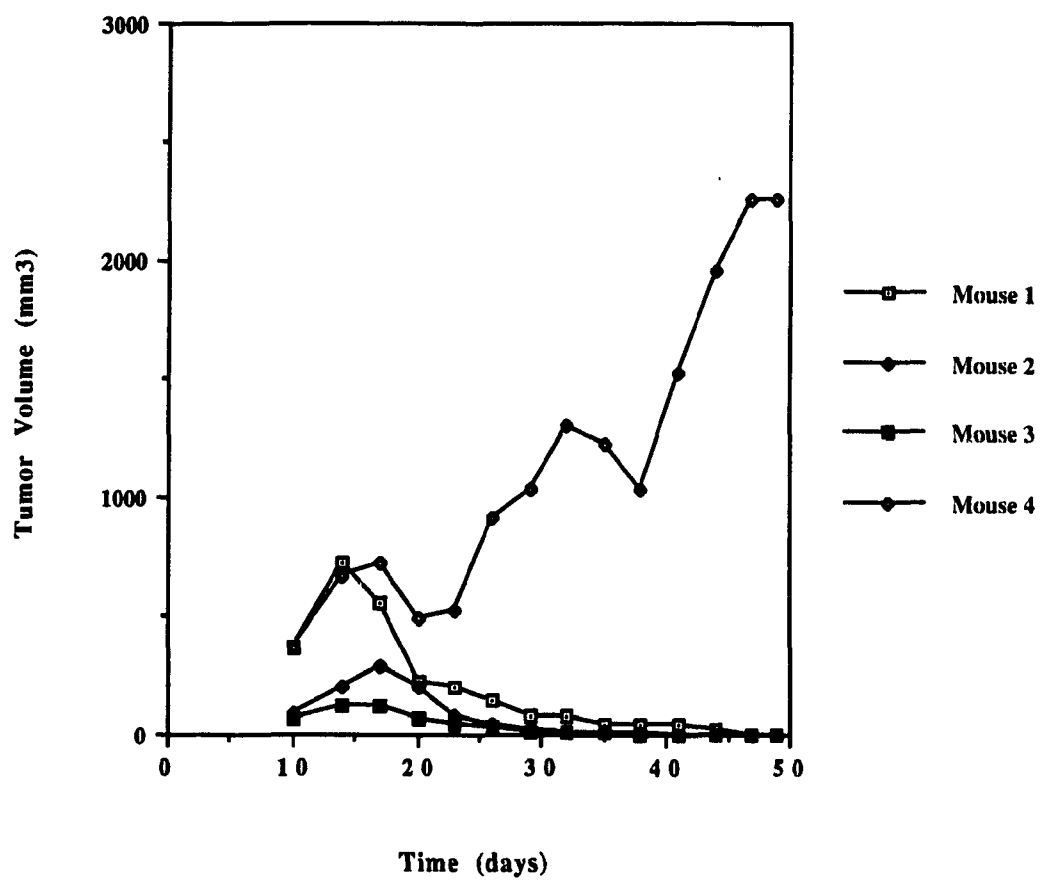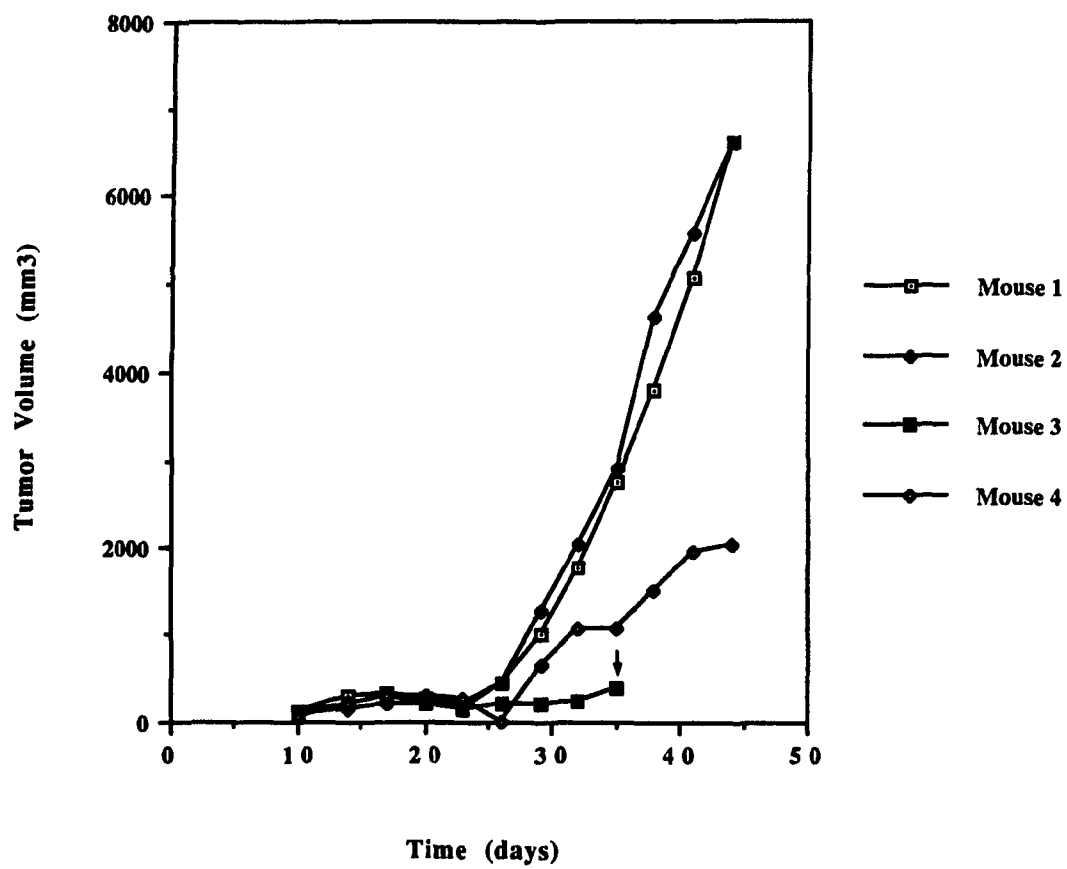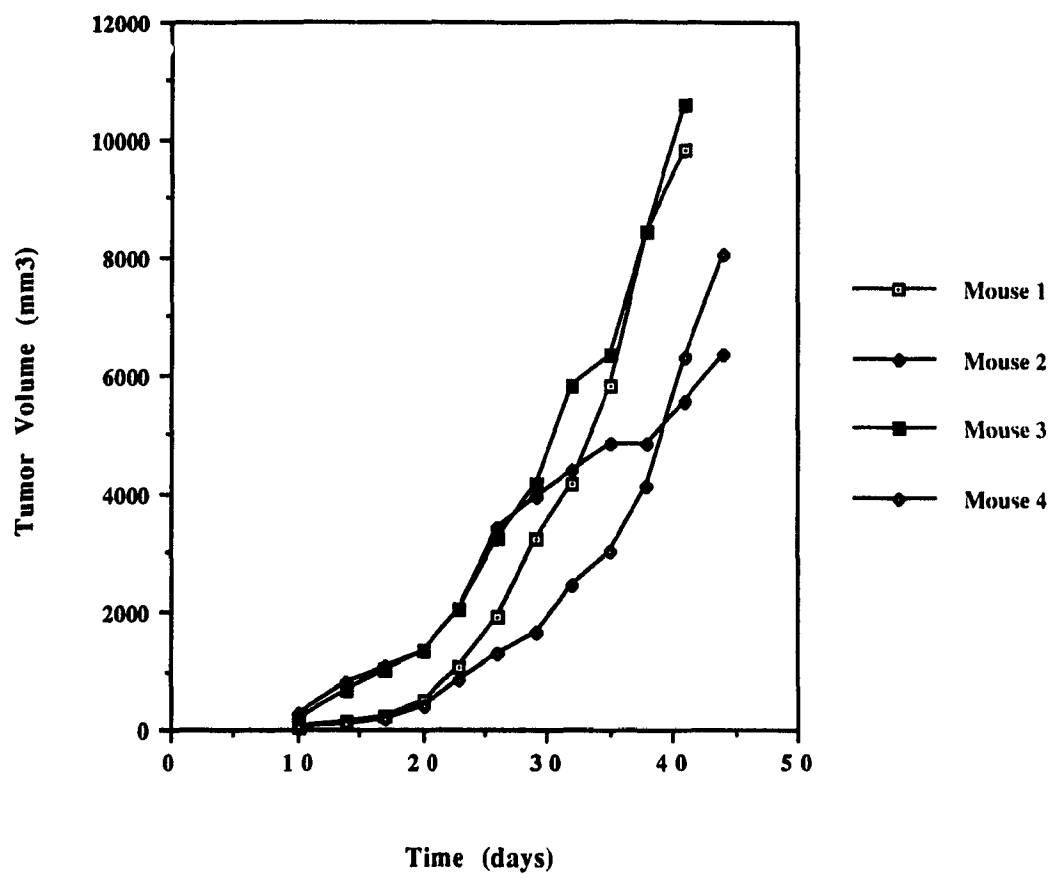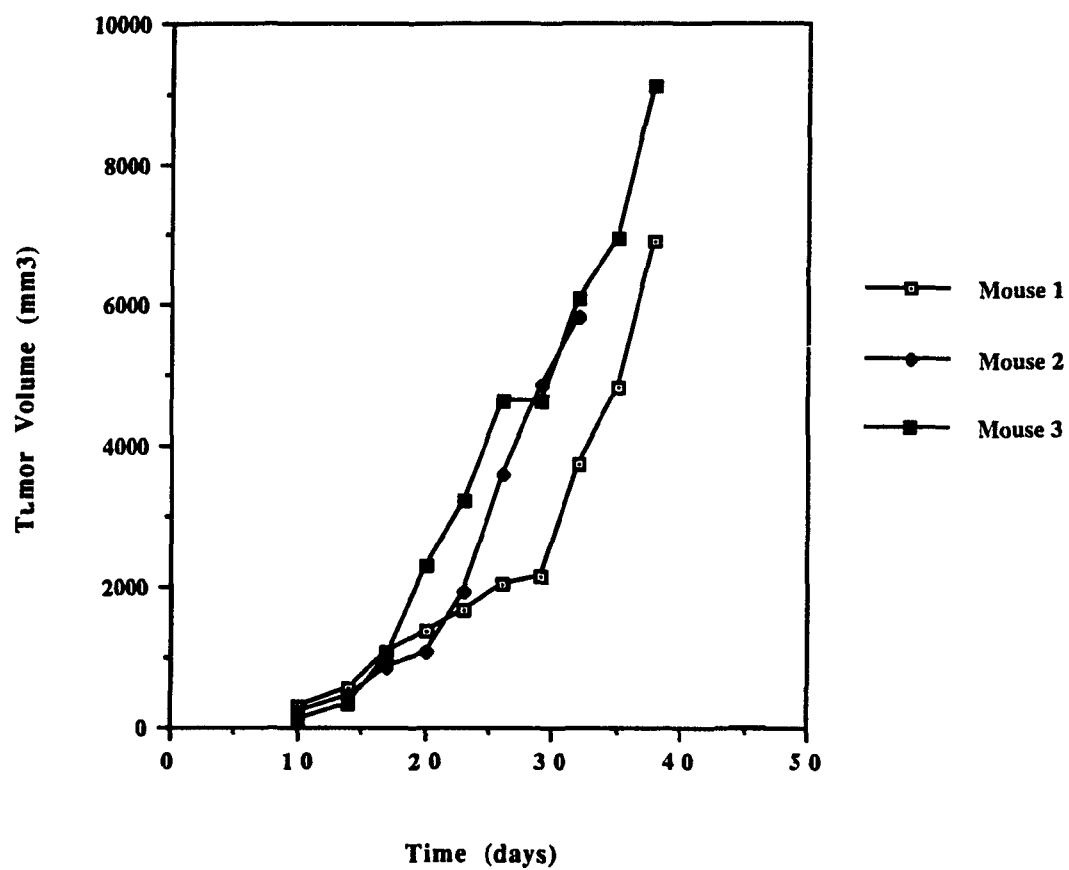
Fig. 112

Fig. 113

Fig. 114

Total body radioactivity of D10-1 xenograft bearing nude mice treated with ^{131}I labeled antibodies.

D10-1 s.c.tumor bearing nude mice were treated with ^{131}I labeled antibodies as described in the legend of Fig. 110 to 115. The total body radioactivity of these mice was monitored with a calibrator at indicated intervals.

(A) Total body radioactivity of D10-1 xenograft bearing nude mice treated with two injections of ^{131}I labeled Dal B02, ^{131}I labeled Dal B02 F(ab)'2 fragment, or ^{131}I labeled non-specific IgG1 (alone or mixed with unlabeled Dal B02). Arrows indicate the time when the radiolabeled antibody preparations were given to the nude mice (thin arrow: ^{131}I-Dal B02 F(ab)'2 fragment; thick arrow: ^{131}I-Dal B02 or ^{131}I-IgG1).

(B) Total body radioactivity of D10-1 xenograft bearing nude mice treated with two injections of ^{131}I labeled Dal B02. Note the clearance of radioactivity in mouse No. 4 was much faster than the clearance of radioactivity in the other three mice of the same group.

Fig. 114A
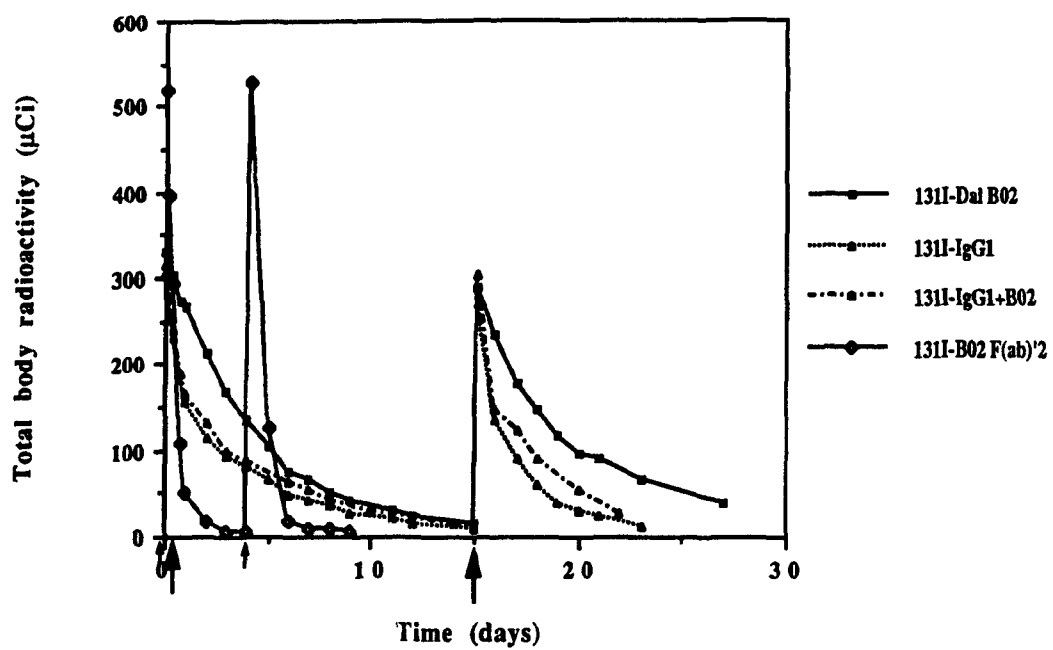
Fig. 114B
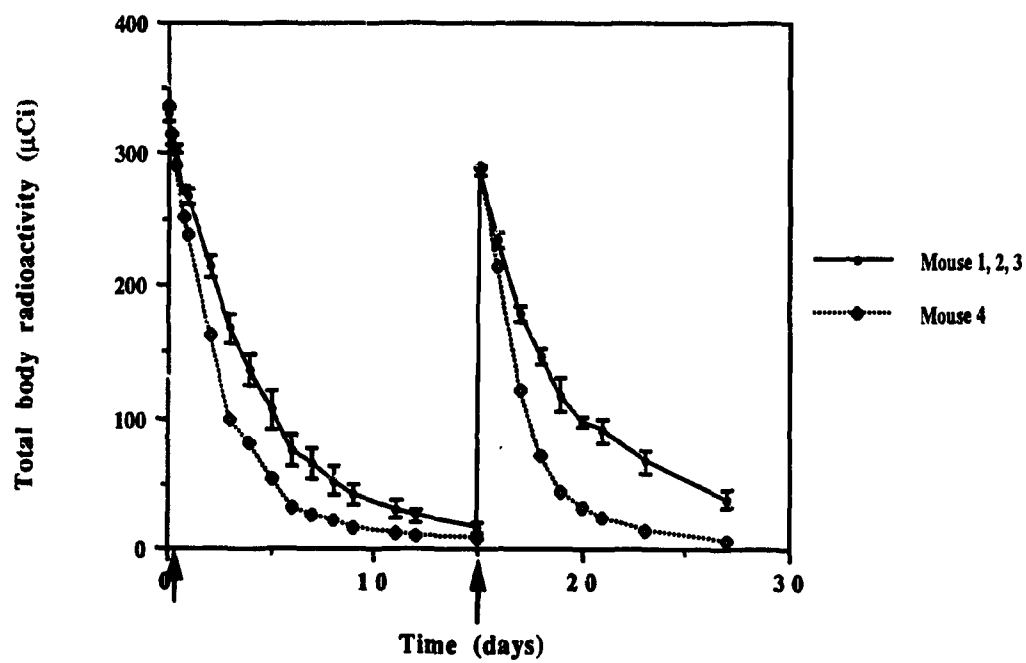
Figs. 115 to 119

Results of administration of ^{131}I labeled Dal B02 and its F(ab)'2 fragment in nude or SCID mice inoculated **i.p.** with D10-1 tumor cells.

D10-1 cell inoculated nude or SCID mice were treated i.p. with unmodified Dal B02, ^{131}I-Dal B02, ^{131}I-Dal B02 F(ab)'2 fragment, or ^{131}I-non-specific IgG1 3 days after tumor inoculation. The mice were observed for the appearance of ascites tumor and survival.

Fig. 115 Survival of nude mice inoculated i.p. with **5 x 10⁶** D10-1 cells and treated with unmodified 50 μg of Dal B02, 300 μCi of ^{131}I linked to 50 μg of Dal B02, or 300 μCi of ^{131}I labeled 50 μg of non specific IgG1.

Fig. 116 Survival of nude mice inoculated i.p. with **15 x 10⁶** D10-1 cells and treated with unlabeled Dal B02 (50 μg, 150 μg, or 500 μg), or 300 μCi of ^{131}I linked to 50 μg of Dal B02.

Fig. 117 Survival of nude mice inoculated i.p. with **5 x 10⁶** D10-1 cells and treated with either labeled or unlabeled Dal B02 F(ab)'2 fragment.

PBS:	Control group;
F(ab)'2 (1):	One injection of 100 μg of unlabeled Dal B02 F(ab)'2 fragment;
F(ab)'2 (2):	Two injections of 100 μg of unlabeled Dal B02 F(ab)'2 fragment given 4 days apart;
^{131}I-F(ab)'2 (1):	One injection of 500 μCi of ^{131}I linked to 100 μg of Dal B02 F(ab)'2 fragment;
^{131}I-F(ab)'2 (2):	Two injections of 500 μCi of ^{131}I linked to 100 μg of Dal B02 F(ab)'2 fragment given 4 days apart;

Fig. 118 Survival of nude mice inoculated i.p. with 5×10^6 D10-1 cells and treated with radiolabeled Dal B02 F(ab)'2 fragment.

PBS:	Control group;
^{131}I-F(ab)'2 (5):	Two injections of 500 μCi of ^{131}I linked 100 μg of Dal B02 F(ab)'2 fragment given 4 days apart (i.e., on day 5 after the first injection) ;
^{131}I-F(ab)'2 (8):	Two injections of 500 μCi of ^{131}I linked 100 μg of Dal B02 F(ab)'2 fragment given 7 days apart (i.e., on day 8 after the first injection).

Fig. 119 Survival of SCID mice inoculated i.p. with 5×10^6 D10-1 cells and treated with unlabeled Dal B02, 300 μCi of ^{131}I linked 50 μg of Dal B02, or 300 μCi of ^{131}I linked 5 μg of non-specific IgG1.

Fig. 115
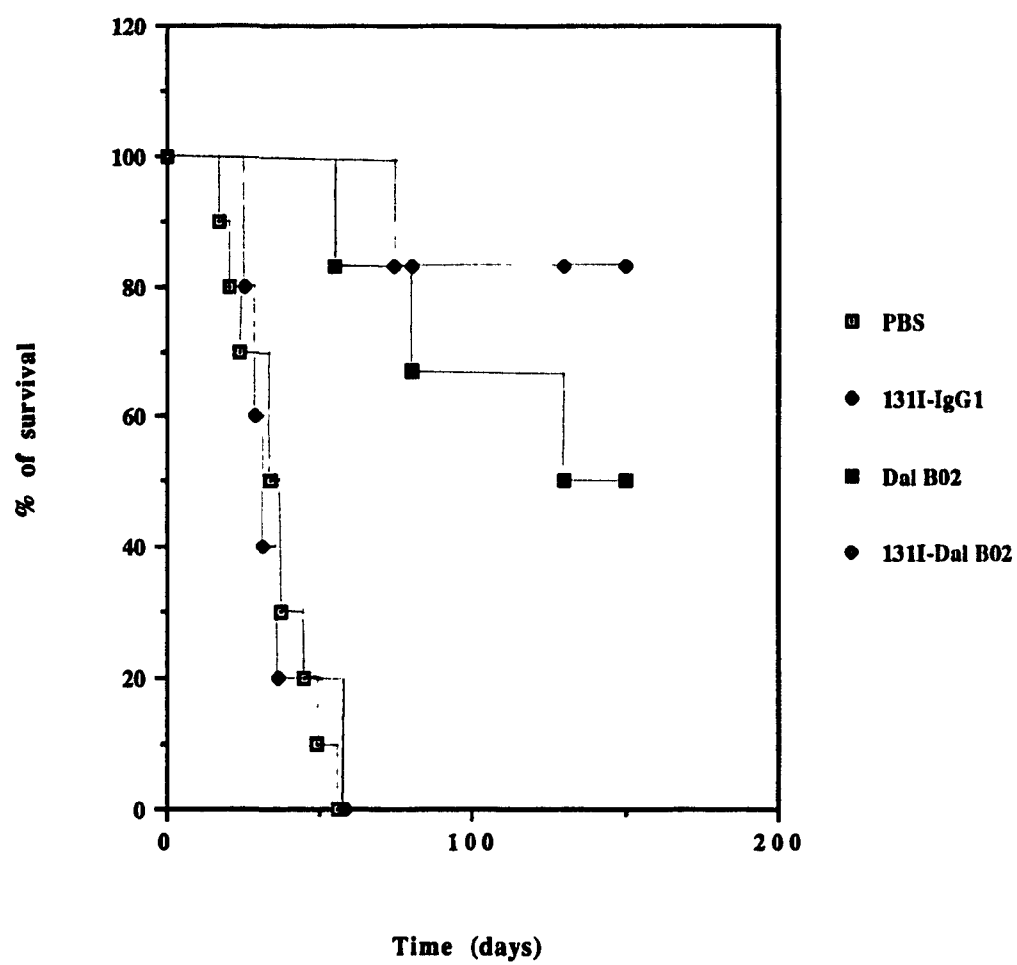
Fig. 116
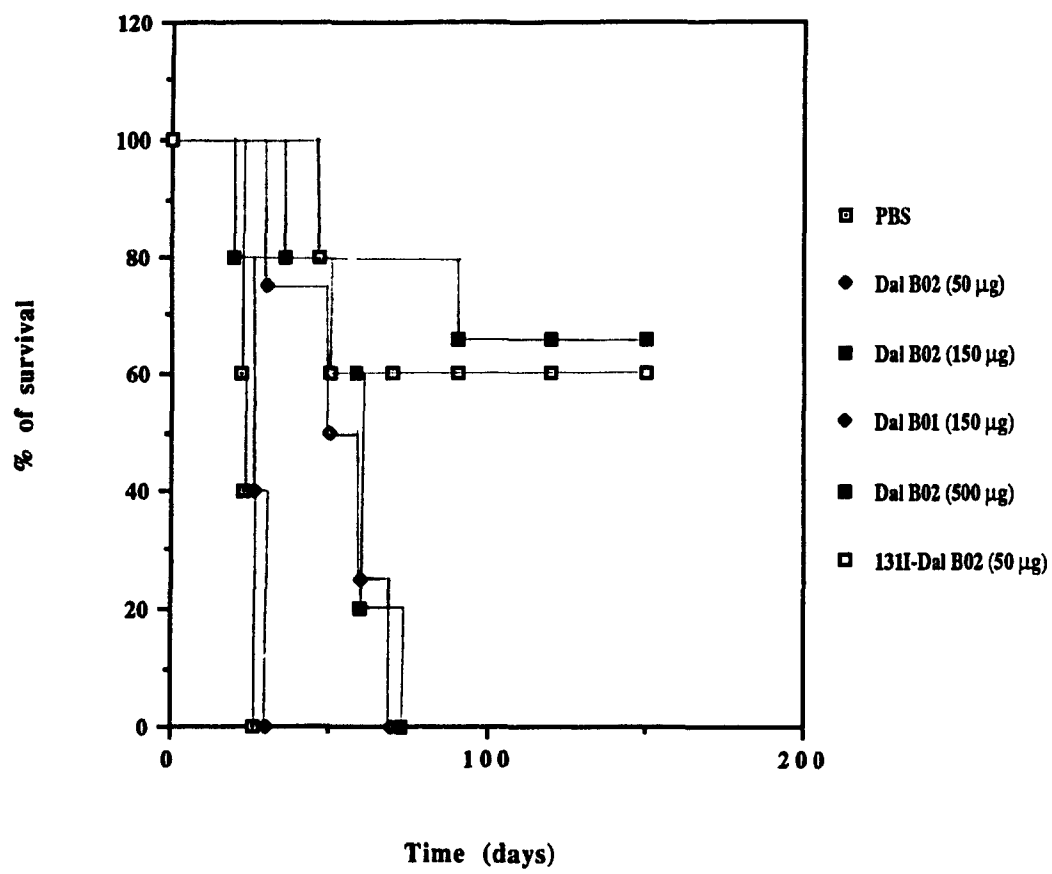
Fig. 117
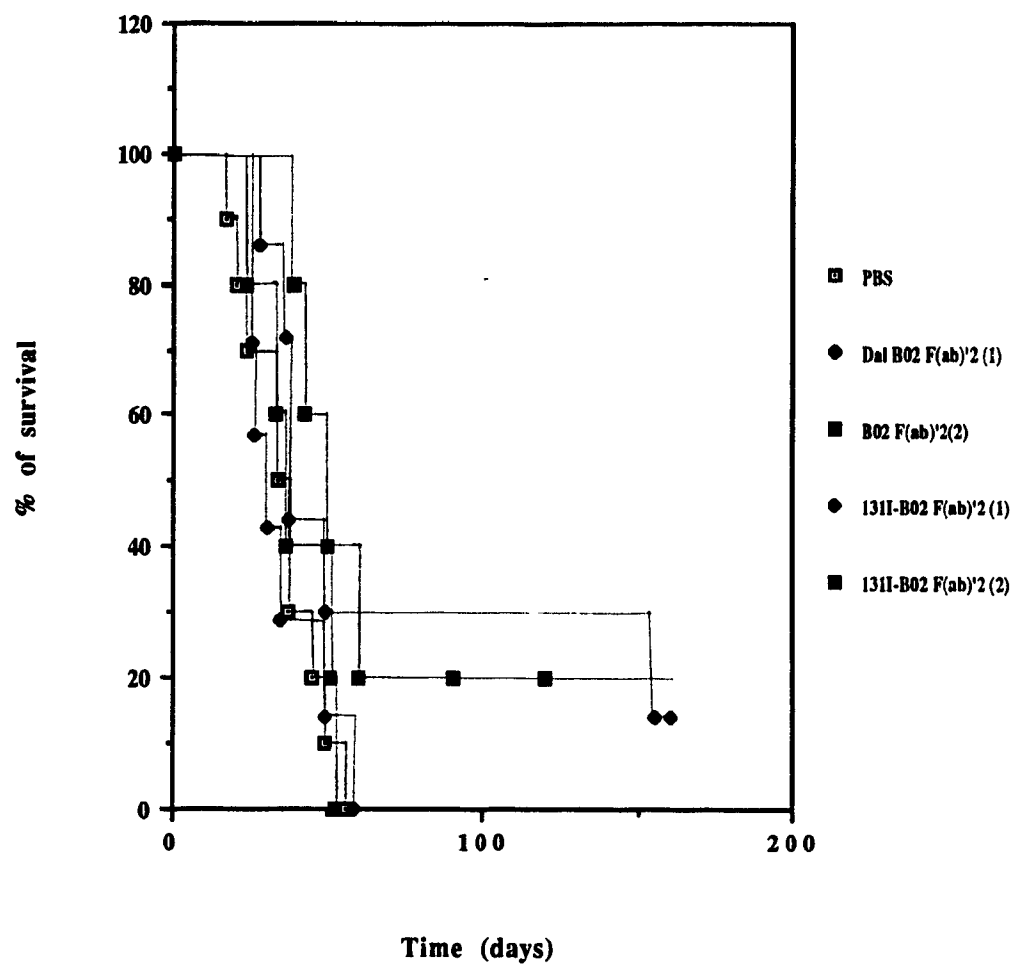
Fig. 118
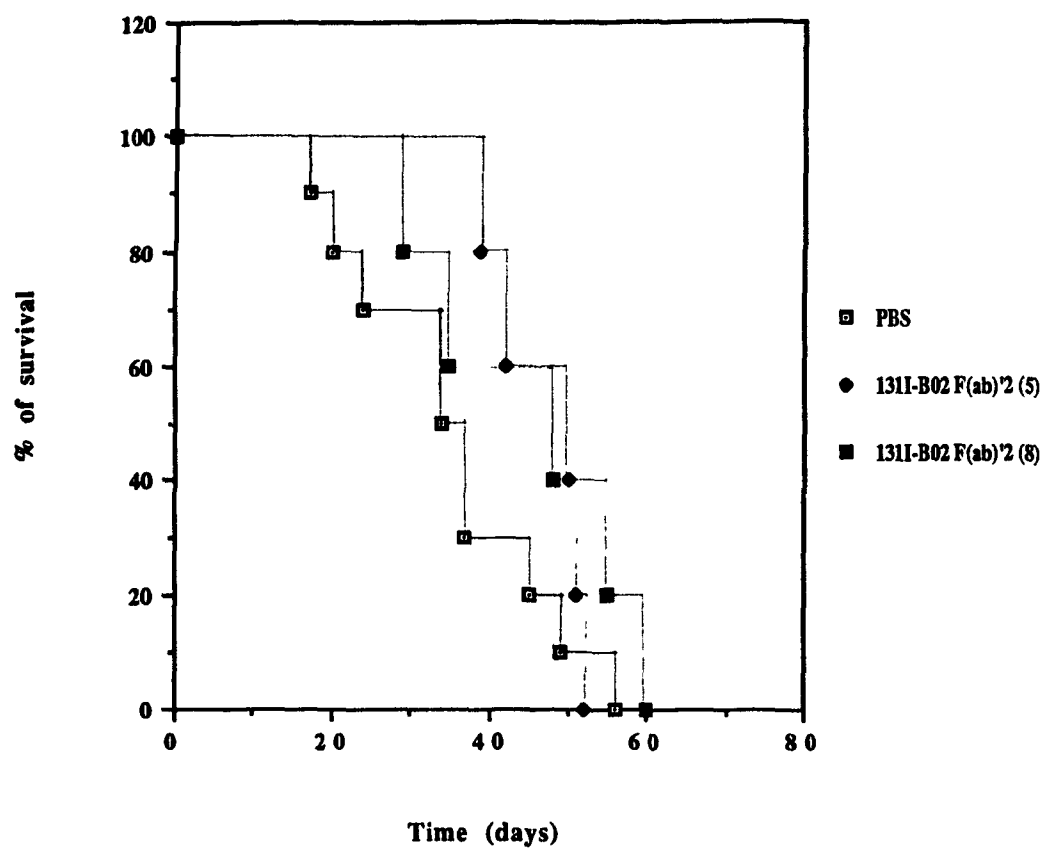
Fig. 119
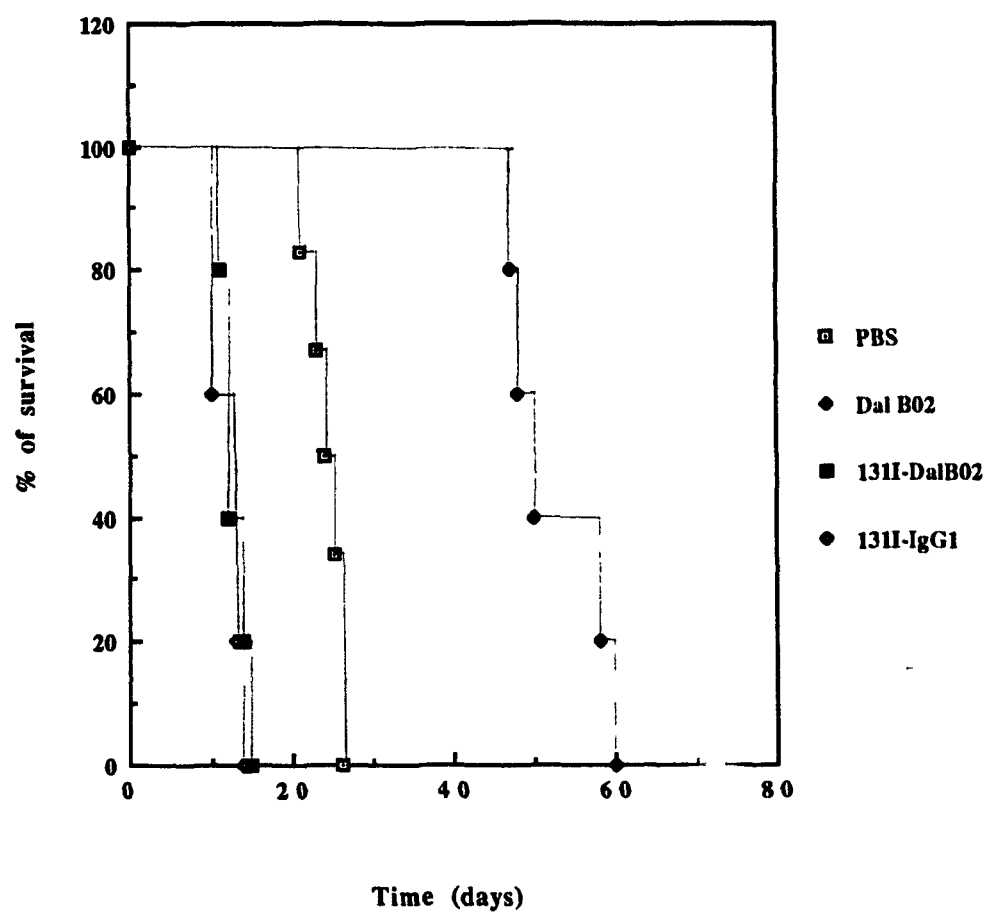
Table 25 Inhibition of D10-1 tumor growth by ^{131}I labeled Dal B02 (I)

--- Nude mice i.p. model [1]

Treatment	Tumor / Total mice	Survival (days) [2]	P values [3]
(1) PBS	10 / 10	35.3 ± 11.9 (17 - 56)	
(2) Dal B02	3 / 6	88.3 ± 31.2 (55 - 130)	P < 0.01
(3) ^{131}I-IgG1	5 / 5	35.4 ± 11.9 (25 - 58)	P > 0.05
(4) ^{131}I-Dal B02	1 / 6	74, others > 150	P < 0.01

1. Treatment started 3 days after the nude mice were inoculated with 5×10^6 D10-1 cells via the i.p. route. Each mouse was given one injection of PBS; 50 μg of unlabeled Dal B02; 50 μg of Dal B02 labeled with 300 μCi of ^{131}I; or 50 μg of non-specific IgG1 labeled with 300 μCi of [131]I.

2. Data represent the mean ± S.D. and the range of survival.

3. The significance of the difference in the survival of mice between different groups was tested by the logrank test. P values shown are calculated between the indicated experimental group and the control group.

Additional P values:

P < 0.01 between group 4 and group 1 , group 2 and group 1; group 4 and group 3, group 2 and group 3; P > 0.05 between group 1 and group 3, group 4 and group 2.

Table 26   Inhibition of D10-1 tumor growth by ^{131}I labeled Dal B02 (II)

--- Nude mice i.p. model [1]

Treatment	Tumor / Total mice	Survival (days) [2]	P value [3]
(1) PBS	5 / 5	23.4 ± 2.3 (20 - 26)	
(2) Dal B02 (50 μg)	5 / 5	26.8 ± 3.0 (22 - 30)	P > 0.05
(3) Dal B02 (150 μg)	5 / 5	57.4 ± 12.0 (36 - 73)	P < 0.01
(4) Dal B01 (150 μg)	4 / 4	50.0 ± 16.3 (30 - 70)	P < 0.01
(5) Dal B02 (500 μg)	1 / 3	90, others > 150	P < 0.01
(6) ^{131}I-Dal B02	2 / 5	47, 50, others > 150	P < 0.01

1. Treatment started 3 days after the nude mice were inoculated with 15 x 10^6 D10-1 cells via the i.p. route. Each mouse was given one injection of PBS; 50 μg, 150 μg, or 500 μg of unlabeled Dal B02; 150 μg unlabeled Dal B01; or 50 μg of Dal B02 labeled with 300 μCi of ^{131}I.

2. Data represent the mean ± S.D. and the range of survival.

3. The significance of the difference in the survival of mice between different groups was tested by the logrank test. P values shown are calculated between the indicated experimental group and the control group.

Additional P values: P > 0.05 between group 3 and group 4, group 5 and group 6; P = 0.05 between group 3 and 5, group 4 and group 5; P < 0.05 between group 3 and group 6, group 4 and group 6; P < 0.01 between group 2 and group 3, group2 and group 4, group 2 and group 5, group 2 and group 6.

Table 27 Inhibition of D10-1 tumor growth by ^{131}I labeled Dal B02 F(ab)'2 fragment   --- Nude mice i.p. model [1]

Treatment	Schedule [2]	Tumor / Total mice	Survival (days) [3]	P value [4]
(1) PBS	Day 3	10 / 10	35.3 ± 11.9 (17 - 56)	
(2) Dal B02 F(ab)'2	Day 3	7 / 7	35.4 ± 12.1 (25 - 58)	P > 0.05
(3) Dal B02 F(ab)'2	Day 3, Day 7	4 / 5	38.3 ± 13.3 (24 - 60)	P > 0.05
(4) ^{131}I-B02 F(ab)'2	Day 3	6 / 7	37.0 ± 6.8 (28 - 49)	P > 0.05
(5) ^{131}I-B02 F(ab)'2	Day 3, Day 7	5 / 5	46.2 ± 4.7 (39 - 50)	P < 0.05
(6) ^{131}I-B02 F(ab)'2	Day 3, Day 10	4 / 5	41.8 ± 10.3 (29 - 55)	P > 0.0⁵

1. Treatment started 3 days after the nude mice were inoculated with 5×10^6 D10-1 cells via the i.p. route. Each mouse was given one or two injections (4 days or 7 days apart) of PBS; 100 μg of unlabeled Dal B02 F(ab)'2 fragment; or 100 μg of Dal B02 F(ab)'2 labeled with 500 μCi of [131]I.

2. The first injection was given to mice on day 3, and the second was given on either day 7 (i.e., 4 days apart from the first injection), or day 10 (i.e., 7 days apart from the first injection) post D10-1 cell inoculation as indicated.

2. Data represent the mean ± S.D. and the range of survival.

3. The significance of the difference in the survival of mice between different groups was tested by the logrank test. P values shown are calculated between the indicated experimental group and the control group.

Additional P values: P = 0.05 between group 2 and group 5;

P > 0.05 among all other groups.

Table 28   Inhibition of D10-1 tumor growth by ^{131}I labeled Dal B02
--- SCID mice i.p. model [1]

Treatment	Tumor / Total mice	Survival (days) [2]	P value [3]
(1) PBS	5 / 5	24.2 ± 1.8 (21 - 26)	
(2) Dal B02	5 / 5	52.4 ± 5.3 (47 - 60)	P < 0.01
(3) ^{131}I-IgG1	5 / 5	12.0 ± 1.8 (10 - 15) [4]	ND [5]
(3) ^{131}I-Dal B02	5 / 5	11.8 ± 1.7 (10 - 15) [4]	ND

1. Treatment started 3 days after the SCID mice were inoculated with 5 x 10^6 D10-1 cells via the i.p. route. Each mouse was given one injection of PBS; 50 µg of unlabeled Dal B02; 50 µg of Dal B02 labeled with 300 µCi of ^{131}I; or 50 µg of non-specific IgG1 labeled with 300 µCi of ^{131}I.

2. Data represent the mean ± S.D. and the range of survival.

3. The significance of the difference in the survival of mice between different groups was tested by the logrank test. P values shown are calculated between the indicated experimental group and the control group.

4. All mice died before the development of ascites tumor.

5. ND: not determined.

Figs. 120 to 123

Results of administration of ^{131}I labeled Dal B02 and its F(ab)'2 fragment in nude or SCID mice inoculated i.v. with D10-1 cells.

D10-1 cell inoculated nude or SCID mice were treated i.v. with Dal B02, ^{131}I-Dal B02, ^{131}I-Dal B02 F(ab)'2 fragment, or ^{131}I-non-specific JσG1 3 days (or 7 days in Fig. 121) after D10-1 cell inoculation. The mice were observed for the appearance of solid tumor and survival.

Fig. 120 Survival of nude mice inoculated i.v. with 5 x 10^6 D10-1 cells and treated with 50 g of unmodified Dal B02, 300 μCi of ^{131}I linked to 50 μg of Dal B02, or 300 μCi of ^{131}I linked to 50 μg of non-specific IgG1 **three days** after tumor cell inoculation.

Fig. 121 Survival of nude mice inoculated i.v. with 5 x 10^6 D10-1 cells and treated with 50 μg of unmodified Dal B02, 300 μCi of ^{131}I linked to 50 μg of Dal B02, or 300 μCi of ^{131}I linked to 50 μg of non-specific IgG1 **seven days** after tumor inoculation.

Fig. 122 Survival of nude mice inoculated i.v. with 5 x 10^6 D10-1 cells and treated 3 days after tumor inoculation with PBS; one injection of 100 μg of unlabeled F(ab)'2 fragment (1); two injections of 100 μg of unlabeled F(ab)'2 fragment given 4 days apart (2); one injection of 500 μCi of ^{131}I linked to 100 μg of F(ab)'2 fragment (1); or two injections of 500 μCi of ^{131}I linked to 100 μg of F(ab)'2 fragment given 4 day apart (2).

Fig. 123 Survival of SCID mice inoculated i.v. with 5 x 10^6 D10-1 cells and treated 3 days after tumor inoculation with unlabeled Dal B02; 300 ''Ci of ^{131}I linked to 50 μg of Dal B02; or 300 μCi of ^{131}I linked to 50 μg of non-specific IgG1.

Fig. 120

Fig. 121

Fig. 121

Fig. 122

Graph with y-axis "% of survival" (0 to 120) and x-axis "Time (days)" (0 to 200).
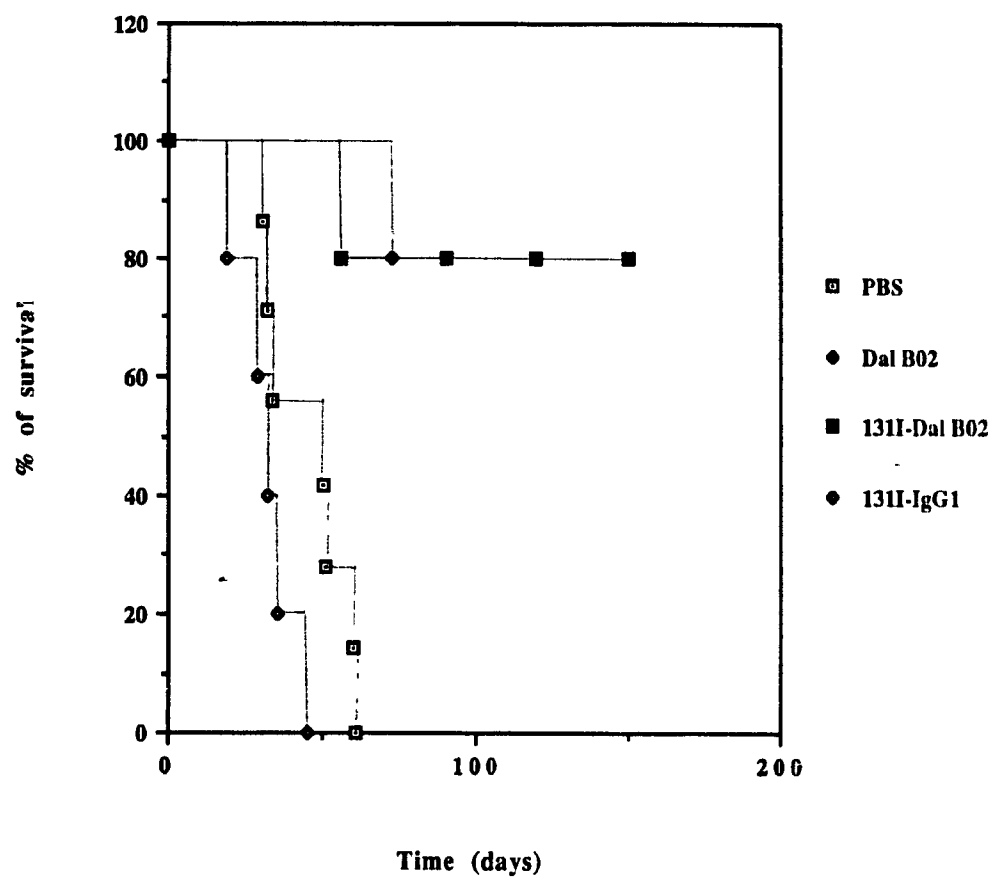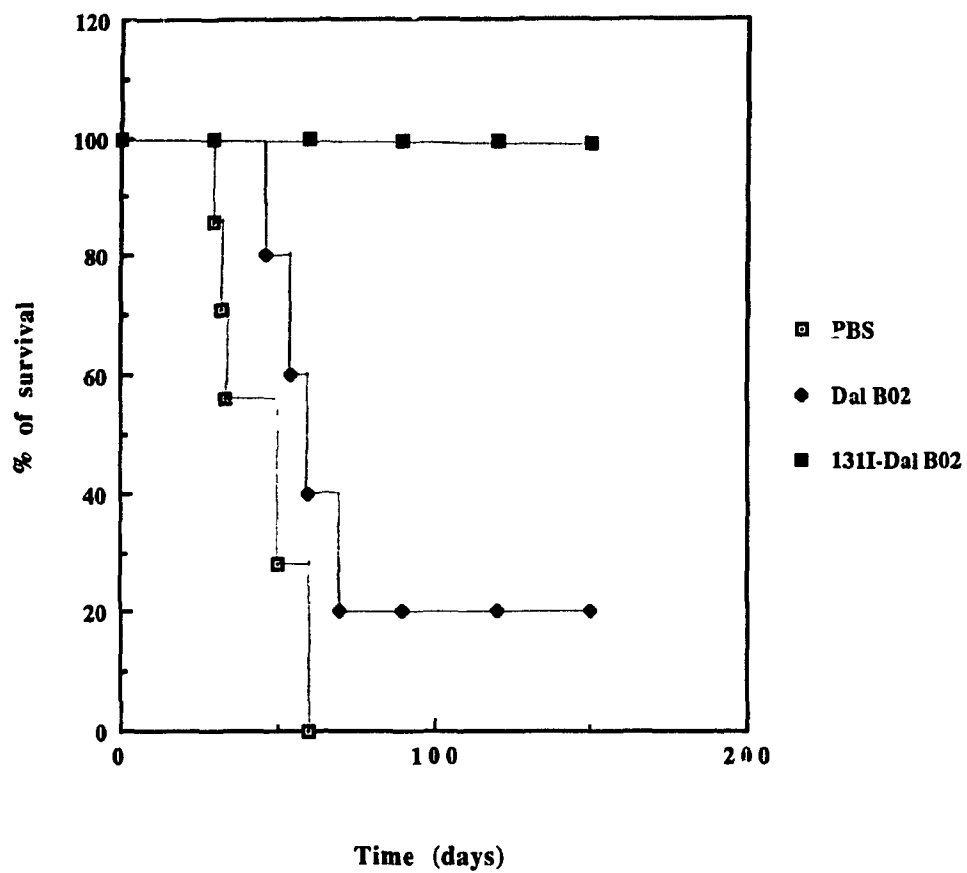
Legend:
- □ PBS
- ◆ B02 F(ab)'2 (1)
- ■ B02 F(ab)'2 (2)
- ◆ 131I-B02 F(ab)'2 (1)
- ■ 131I-B02 F(ab)'2 (2)
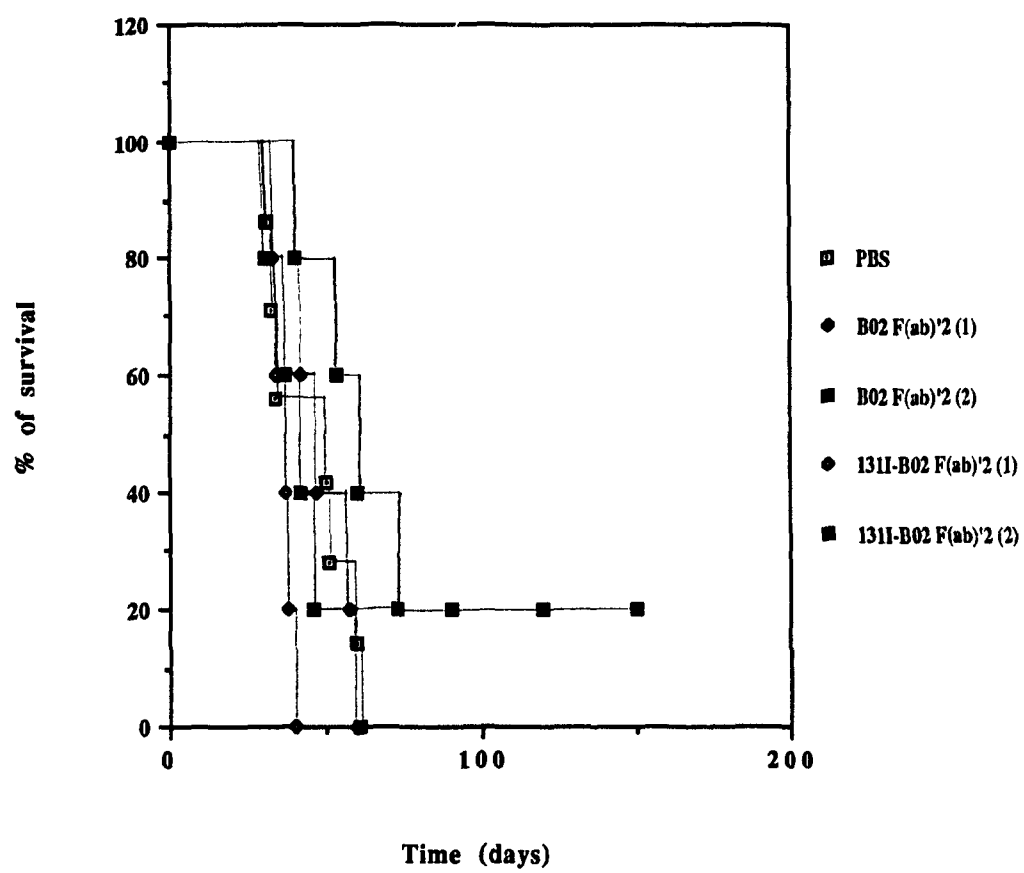
Fig. 123
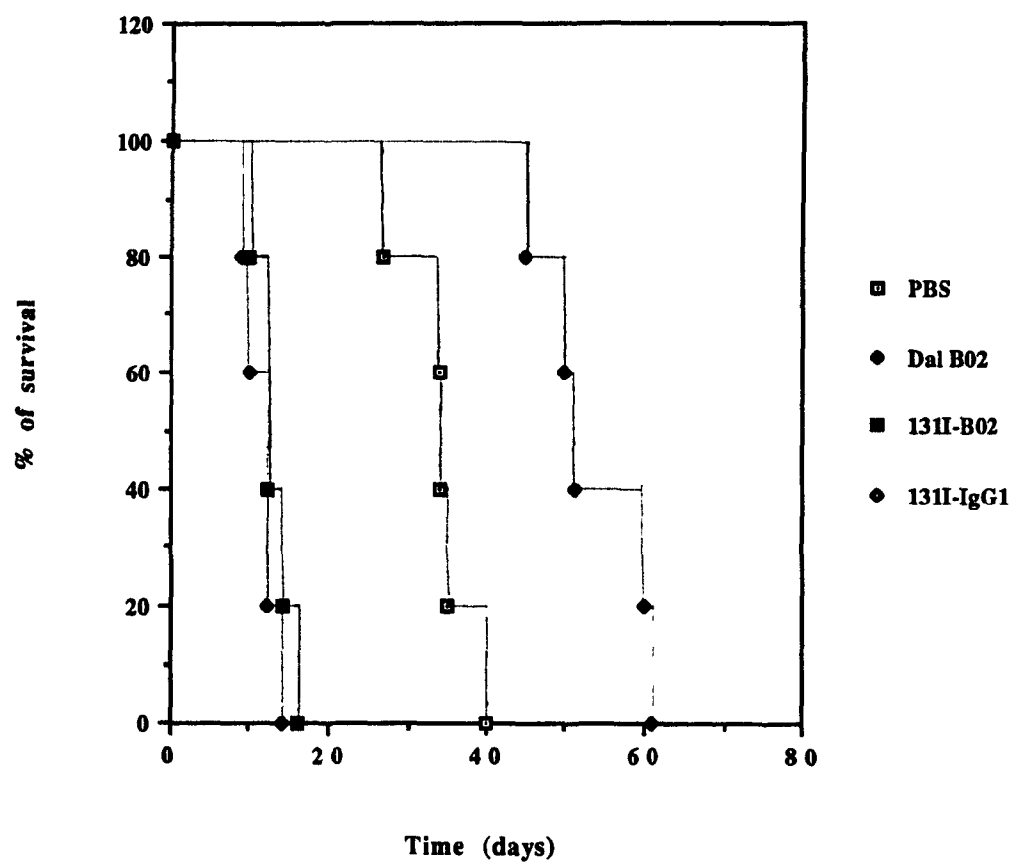
Table 29   Inhibition of D10-1 tumor growth by ^{131}I labeled Dal B02

--- Nude mice i.v. model [1]

Treatment	Schedule	Tumor / Total mice	Survival (days)[2]	P value [4]
(1) PBS	Day 3	8 / 8	45.1 ± 12.0 (30 - 60)	
(2) ^{131}I-IgG1	Day 3	5 / 5	32.0 ± 8.4 (19 - 45)	P > 0.05
(3) Dal B02	Day 3	1 / 5	72, others > 150	P < 0.01
(4)^{131}I-Dal B02	Day 3	1 / 5	56, others > 150	P < 0.01
(5) Dal B02	Day 7	4 / 5	57.5 ± 8.8 (46 - 70)	P = 0.05
(6)^{131}I-Dal B02	Day 7	2 / 5 [3]	All > 150	P < 0.01

1.Treatment started 3 or 7 days after the nude mice were inoculated with 5 x 10^6 D10-1 cells

via the i.v. route. Each mouse was given one injection of PBS; 50 μg of unlabeled Dal

B02; 50 μg of Dal B02 labeled with 300 μCi of ^{131}I; or 50 μg of non-specific IgG1 labeled

with 300 μCi of ^{131}I at time indicated.

2. Data represent the mean ± S.D. and the range of survival.

3. The tumors in these two nude mice regressed spontaneously 90 to 120 days after tumor

inoculation.

4. The significance of the difference in the survival of mice between different groups was

tested by the logrank test. P values shown are calculated between the indicated experimental

group and the control group. Additional P values: P > 0.05 among groups 3, 4, 6; P <

0.01 between group 2 and all other groups (except group 1), P < 0.01 between group 5

and group 6;   P < 0.05 between group 5 and group 3, group 5 and group 4;

Table 30 Inhibition of D10-1 tumor growth by ^{131}I labeled Dal B02 F(ab)'2 fragment --- Nude mice i.v. model [1]

Treatment	Schedule [2]	Tumor / Total mice	Survival (days) [3]	P value [4]
(1) PBS	Day 3	8 / 8	45.1 ± 12.0 (30 - 60)	
(2) Dal B02 F(ab)'2	Day 3	5 / 5	47.6 ± 10.2 (32 - 60)	P > 0.05
(3) Dal B02 F(ab)'2	Day 3, Day 7	4 / 5	38.8 ± 6.0 (30 - 46)	P > 0.05
(4) ^{131}I-B02 F(ab)'2	Day 3	5 / 5	36.2 ± 2.5 (33 - 40)	P > 0.05
(5) ^{131}I-B02 F(ab)'2	Day 3, Day 7	4 / 5	56.5 ± 11.9 (40 - 73)	P = 0.05

1. Treatment started 3 days after the nude mice were inoculated with 5 x 10^6 D10-1 cells via the i.v. route. Each mouse was given one or two injections (4 days apart) of PBS; 100 µg of unlabeled Dal B02 F(ab)'2 fragment; or 100 µg of Dal B02 F(ab)'2 labeled with 500 µCi of ^{131}I.

2. The first injection was given to mice on day 3, and the second was given on day 7 post D10-1 cell inoculation as indicated.

3. Data represent the mean ± S.D. and the range of survival.

3. The significance of the difference in the survival of mice between different groups was tested by the logrank test. P values shown are calculated between the indicated experimental group and the control group.

Additional P values: P < 0.05 between group 4 and group 5;

P > 0.05 among all other groups;

Table 31   Inhibition of D10-1 tumor growth by ^{131}I labeled Dal B02

--- SCID mice i.v. model [1]

Treatment	Tumor / Total mice	Survival (days) [2]	P value [4]
(1) PBS	5 / 5	34.0 ± 4.1 (27 - 40)	
(2) Dal B02	5 / 5	53.0 ± 6.0 (45 - 60)	P < 0.01
(3) ^{131}I-IgG1	5 / 5	12.5 ± 1.6 (10 - 15) [3]	ND [5]
(3) ^{131}I-Dal B02	5 / 5	11.6 ± 2.5 (10 - 15) [3]	ND

1. Treatment started 3 days after the SCID mice were inoculated with 5×10^6 D10-1 cells via the i.v. route. Each mouse was given one injection of PBS; 50 µg of unlabeled Dal B02; 50 µg of Dal B02 labeled with 300 µCi of ^{131}I; or 50 µg of non-specific IgG1 labeled with 300 µCi of ^{131}I.

2. Data represent the mean ± S.D. and the range of survival.

3. All mice died before the development of tumor.

4. The significance of the difference in the survival of mice between different groups was tested by the logrank test. P values shown are calculated between the indicated experimental group and the control group.

5. ND: not determined.

Section 8   Inhibition of Intraperitoneal Human Renal Cell Carcinoma Xenografts in Nude Mice with A Heteroconjugate (K29 - OKT3) Reacting with Human Renal Cell Carcinoma and T-Cell Receptor Complex CD3

8.1   Preparation of K29-OKT3 Heteroconjugate

The heteroconjugate was prepared by Dr. Kerr et al. as described in Methods section 13.1. The purity and molecular weight of the heteroconjugate were analyzed by SDS-PAGE. Antibody dimers (m.w. 300, 000) and larger heteroconjugates (m.w. varying from 600, 000 to 1000, 000) were used in this study. In vitro studies had demonstrated that this heteroconjugate was tumor inhibitory in the presence of PBL or tumor infiltrating lymphocytes (TIL) from patients with renal cell carcinoma (Kerr et al., 1991).

8.2   Assay for the Dual Specificity of K29-OKT3 Heteroconjugate

Membrane immunofluorescence showed that the K29-OKT3 heteroconjugate reacted with both Nu-caki-1 line of human renal cell carcinoma cells and human T lymphocytes, including freshly isolated human peripheral blood T lymphocytes and the human T-cell leukemia line MOLT-3 (Fig. 124). Table 32 compares the reactivity of Dal K29, K29-OKT3 heteroconjugate and Dal B02 with human peripheral blood T lymphocytes and several human tumor cell lines.

FACS analysis further confirmed that the K29-OKT3 heteroconjugate reacted with both Nu-caki-1 cells and human T lymphocytes. Table 33 shows that both Dal K29 and K29-

OKT3 heteroconjugate reacted with Nu-caki-1 cells and T lymphocytes in a concentration-dependent manner. However, only about 80% of either Nu-caki-1 cells or human T lymphocytes could be stained by the K29-OKT3 heteroconjugate, even when a high concentration of the heteroconjugate (up to 40 μg/ml) was used.

When K29-OKT3 heteroconjugate coated Nu-caki-1 cells were incubated with freshly isolated human T lymphocytes, rosette formation, in which T cells adhered around the surface of Nu-caki-1 cells, was observed. There was no rosette formation when the heteroconjugate coated Nu-caki-1 cells were incubated with D10-1 cells. These results indicate that the K29-OKT3 heteroconjugate could specifically cross-link the target cells (i.e., Nu-caki-1 cells) to T lymphocytes.

In an assay to demonstrate that the heteroconjugate indeed contained both Dal K29 (an IgG1) and OKT3 (an IgG2a), Nu-caki-1 cells were first coated with the heteroconjugate and then stained with GAM subclass antibodies conjugated to HRP. It was found that K29-OKT3 heteroconjugate coated Nu-caki-1 cells reacted with both GAM IgG1 and IgG2a subclass antibodies. This result confirmed that Dal K29 and OKT3 antibodies were firmly linked together in the heteroconjugate.

8.3 Determination of Antibody Activity of Dal K29 and the K29-OKT3 Heteroconjugate

Using immunofluorescence, the titers of reactivity of Dal K29 and the K29-OKT3 heteroconjugate with Nu-caki-1 cells were determined. The titers were observed to be 0.625 μg/ml for Dal K29 and 1.25 μg/ml for the K29-OKT3 heteroconjugate.

Table 32 Immunofluorescence assay of the binding of MoAb Dal K29, OKT3 or K29-OKT3 heteroconjugate to various human tumor cell lines and peripheral blood T lymphocytes [1]

	Nu-caki-1	MOLT-3	T lymphocytes	D10-1
Dal K29 [2]	+	-	-	-
OKT3	-	+	+	-
K29-OKT3	+	+	+	-
Dal B02	-	-	-	+

1. Indirect membrane immunofluorescence assay was performed on viable tumor cells or freshly isolated human peripheral blood T lymphocytes as described in Methods section 1.6.

2. The concentration of various MoAbs and the heteroconjugate was 5.0 µg/ml.

■

Table 33   FACS assay of the binding of MoAb Dal K29 or K29-OKT3 heteroconjugate to Nu-caki-1 cells and peripheral blood T lymphocytes [1]

Antibody Concentration (µg/ml)	Dal K29		K29-OKT3	
	Nu-caki-1	T cells	Nu-caki-1	T cells
40.0	ND [2]	ND	79.6 [3]	76.6
20.0	76.9	2.7	79.1	78.0
10.0	77.9	3.9	74.2	76.0
5.0	77.6	5.1	70.0	72.6
2.5	72.3	4.8	58	55.4
1.25	62.0	4.9	51.1	32.8
0.625	55.4	6.4	ND	ND

1. Immunofluorescence staining was carried out using viable Nu-caki-1 and T lymphocytes. The fluorescence stained cells were analyzed using a FACS as described in Methods section 13.2. Human B-cell CLL line D10-1 cells were used as negative control cells.

2. Not determined.

3. Percentage of immunofluorescence positive cells.

Fig. 124

Immunofluorescence staining of Nu-caki-1 cells, MOLT-3 cells and human T lymphocytes by the K29-OKT3 heteroconjugate.

Note that this K29-OKT3 heteroconjugate reacted with the human renal cell carcinoma cell line Nu-caki-1 cells (A), human T-cell leukemia line MOLT-3 cells (B) and human peripheral blood T lymphocytes (C). Dal K29 only reacted to Nu-caki-1 cells.

Antibody concentration used: 5.0 μg/ml.

Fig. 124
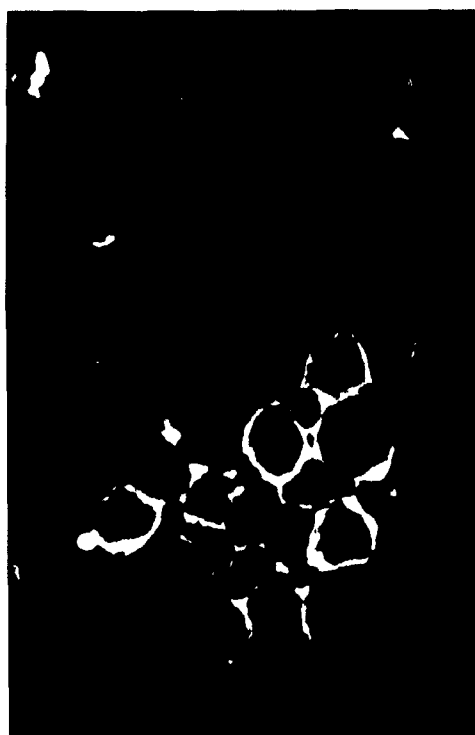
a

b

c

ELISA was also carried out using Nu-caki-1 cells to confirm the retention of reactivity of MoAb Dal K29 in K29-OKT3 heteroconjugate. As shown in Fig. 125, the IC50 values (i.e., the antibody concentration that yielded 50% of the maximum absorbance) were approximately 0.5 µg/ml ʼ · K̄ 9-OKT3 heteroconjugate, and 0.3 µg/ml for Dal K29. This result is in consistent with the observation obtained in immunofluorescence assay, and indicates that the Dal K29 antibody in K29-OKT3 heteroconjugate retains its immunoreactivity.

8.4 Biodistribution of Dal K29 and the K29-OKT3 Heteroconjugate after Intravenous Injection into Nu-caki-1 Xenograft Bearing Nude Mice

Both Dal K29 and K29-OKT3 heteroconjugate were labeled with ^{131}I using the chloramine T method. The specific activity of ^{131}I-Dal K29 and ^{131}I-K29-OKT3 heteroconjugate was 2.0 µCi/µg and 1.7 µCi/µg protein, respectively. The IRF of the antibodies, using Nu-caki-1 cells as target cells, was 38.5% for Dal K29, and 36.8% for the K29-OKT3 heteroconjugate. The Nucaki-1 xenograft bearing nude mice were given i.v. 15 µg of either ^{131}I-Dal K29 (30 µCi) or ^{131}I-K29-OKT3 heteroconjugate (25 µCi), mixed with 5 µg of ^{125}I-Dal B02, an isotype-matched non-specific antibody. Samples of blood were obtained at indicated intervals and the ^{131}I and ^{125}I activities in blood were determined. Groups of three mice were sacrificed at 24, 48, 96 and 168 hr post antibody administration. The distribution of Dal K29 or K29-OKT3 heteroconjugate in xenografted tumor as well as in normal mouse tissues was determined as described in Methods section 7.

8.4.1   Pharmacokinetics of Dal K29 and K29-OKT3 heteroconjugate

The pharmacokinetics of radiolabeled antibodies were determined by measuring the ^{131}I and ^{125}I activities in samples of blood at indicated intervals. Fig. 126A shows the ^{131}I and

[125]I activities (expressed as a percentage of the initial activity) in blood over time after i.v. administration of ^{131}I-Dal K29 or ^{131}I-K29-OKT3 heteroconjugate. The heteroconjugate was cleared much faster from the circulation than Dal K29 and the control MoAb Dal B02. Approximately 21.4% of the initial blood radioactivity remained in circulation 60 min after i.v. injection of ^{131}I-K29-OKT3 heteroconjugate, while 52.9% of the initial blood radioactivity still remained in the circulation of mice given ^{131}I-Dal K29. At 24 hr, only 4.2% of the initial blood radioactivity remained in the circulation of mice given ^{131}I-K29-OKT3 heteroconjugate, while 25% of the initial blood radioactivity remained in the circulation of mice given ^{131}I-Dal K29. As shown in Fig. 126B, the total body radioactivity of mice injected with the K29-OKT3 heteroconjugate also decreased much faster than that of mice injected with Dal K29, indicating that the heteroconjugate was cleared at a faster rate than Dal K29.

8.4.2   Biodistribution of Dal K29 and K29-OKT3 heteroconjugate

Biodistribution studies (Figs. 127 to 130) showed that the amount of K29-OKT3 heteroconjugate that localized in Nu-caki-1 xenografts was lower than the amount of tumor-localized Dal K29. Maximum tumor localization of the heteroconjugate was seen at 48 hr after i.v. injection. The % ID / g tumor tissue of the heteroconjugate was 0.93, 1.91, 1.04 and 0.47, at 24, 48, 96 and 168 hr after antibody administration, respectively. Maximum tumor localization of Dal K29 was seen at 24 hr after i.v. injection. The % ID / g tumor tissue of Dal K29 was 3.33, 2.48, 2.11, and 1.14, at 24, 48, 96 and 168 hr after antibody administration, respectively. Compared to Dal K29, the heteroconjugate showed the localization of a higher percentage of injected dose in liver and spleen. For example, at 24 hr after i.v. injection, the % ID of the heteroconjugate in the liver and spleen were 2.6% / g and 4.03% / g, and the % ID of Dal K29 in the liver and spleen were 1.06% / g and 1.3% / g, respectively. Dal K29 showed a higher T / NT ratios for most organs at 24 and 48 hr

after i.v. injection compared to the T / NT ratios of the K29-OKT3 heteroconjugate. However, the difference became less significant with time, i.e., at 96 and 168 hr after i.v. injection.

8.4.3   Stability of ^{131}I Dal K29 and ^{131}I-K29-OKT3 heteroconjugate in xenografted Nu-caki-1 tumors and normal mouse tissues

The xenografted tumors as well as internal organs (i.e., liver, spleen, kidney and thyroid) of xenograft bearing nude mice given ^{131}I-Dal K29 or ^{131}I-K29-OKT3 heteroconjugate were taken out and homogenized. The tissue homogenates were then precipitated with 10% TCA and the radioactivity in the precipitates and in the supernatant was determined (Table 34). It was found that in the normal mouse organs obtained from the mice given Dal K29 or the non-specific MoAb Dal B02, most of the tissue-radioactivity (i.e., 95 to 99%) was TCA precipitable. However, in the xenografted tumors of these mice, only 84 to 89 % of the tumor-localized Dal K29 radioactivity (compared to 93 to 98% of tumor-localized non-specific ^{131}I-Dal B02 radioactivity) could be precipitated. In the mice given the K29-OKT3 heteroconjugate, the percentages of precipitable radioactivity were lower in all organs (including the tumors), compared to the percentage of precipitable radioactivity in the organs of mice given Dal K29 or the non-specific ^{131}I-Dal B02. For example, at 48 hr after antibody administration, 72 to 87% of mouse tissue-associated radioactivity could be precipitated in the organs (except of blood) of mice given ^{131}I-K29-OKT3 heteroconjugate, compared to 93 to 96% of TCA precipitable radioactivity in the organs of mice given ^{131}I-Dal K29 or the non-specific ^{131}I-Dal B02. In the xenografted tumor, about 77% of tumor-localized radioactivity in mice given ^{131}I-K29-OKT3 heteroconjugate could be precipitated, compared to 89% of tumor-localized radioactivity in mice given ^{131}I-Dal K29 and 93% of tumor-localized radioactivity in mice given non-specific ^{131}I-Dal B02. These results indicate that (i) Nu-caki-1 xenograft tumors catabolize tumor-localized specific Dal

K29 and K29-OKT3 heteroconjugate; and (ii) Dal K29-OKT3 heteroconjugate is more susceptible to be catabolized by Nu-caki-1 tumors, as well as organs rich in reticulo-endothelial cells (e.g., liver and spleen), compared to the parent MoAb Dal K29.

The IRF of Dal K29 and K29-OKT3 heteroconjugate recovered from the serum of xenograft bearing nude mice was also determined. As shown in Table 35, both Dal K29 and the K29-OKT3 heteroconjugate retained their original IRF even after staying in the circulation of these mice for up to 168 hr.

8.4.4 Autoradiography of xenografted Nu-caki-1 tumor tissues after i.v. injection of ^{131}I-Dal K29 or ^{131}I-K29-OKT3 heteroconjugate

Groups of Nu-caki-1 xenograft bearing nude mice were sacrificed at 48 hr and 96 hr after i.v. injection of ^{131}I-Dal K29 or ^{131}I-K29-OK1 5 heteroconjugate. Cryostat sections of the xenografts were obtained and subject to autoradiography (see Methods section 7.7). As shown in Figs. 131 to 132, high density clusters of silver grain were observed on tumor cell surface, as well as in the intercellular matrix in tumors obtained from nude mice given either ^{131}I-Dal K29 or ^{131}I-K29-OKT3 heteroconjugate. This result indicates that both Dal K29 and K29-OKT3 heteroconjugate had good access to Nu-caki-1 cells in the s.c tumor xenografts in nude mice.

8.5 Treatment of Intraperitoneal Xenografts of Nu-caki-1 Cells with K29-OKT3 Heteroconjugate and Human PBL

Nude mice inoculated with 5 x 10^6 Nu-caki-1 cells i.p. were treated 24 hr later with PBS; the K29-OKT3 heteroconjugate alone; K29-OKT3 heteroconjugate plus human PBL (at two different E/T ratios, i.e. , 3 to 1 and 10 to 1); or a mixture of Dal K29 and OKT3

antibodies plus human PBL (E/T ratio, 10 to 1). As shown in Fig. 133, all mice treated with PBS developed ascites as well as solid tumors in the peritoneal cavity and died within 18 to 31 days (mean survival, 27.6 ± 4.9 days). Heteroconjugate alone slightly prolonged the survival of tumor bearing mice (mean survival, 40.8 ± 9.0 days. P = 0.05). No animal in this group surviving beyond 51 days. In the group treated with the mixture of Dal K29 and OKT3 plus PBL, three of four mice died within 38 days (30.3 ± 5.6 days), the other mouse survived for 110 days (P > 0.05). The survival of mice treated with the K29-OKT3 heteroconjugate plus PBL varied with the different E/T ratios used. When a E/T ratio of 3 to 1 was used, four out of five mice died of tumor within 34 days after tumor inoculation (mean survival, 30.5 ± 2.2 days, P > 0.05). The fifth mouse died of tumor 110 days after tumor cell inoculation. When the E/T ratio was increased to 10 to 1, there was a significant prolongation of survival, i.e., two of four mice survived tumor free over 150 days, while the other two mice died at 53 and 70 days after tumor inoculation, respectively (Table 36, P < 0.05).

Fig. 125

Comparison of the binding of Dal K29 and the K29-OKT3 heteroconjugate to Nu-caki-1 cells by ELISA.

Fig. 125

O. D. at 493nm

Antibody added (µg)
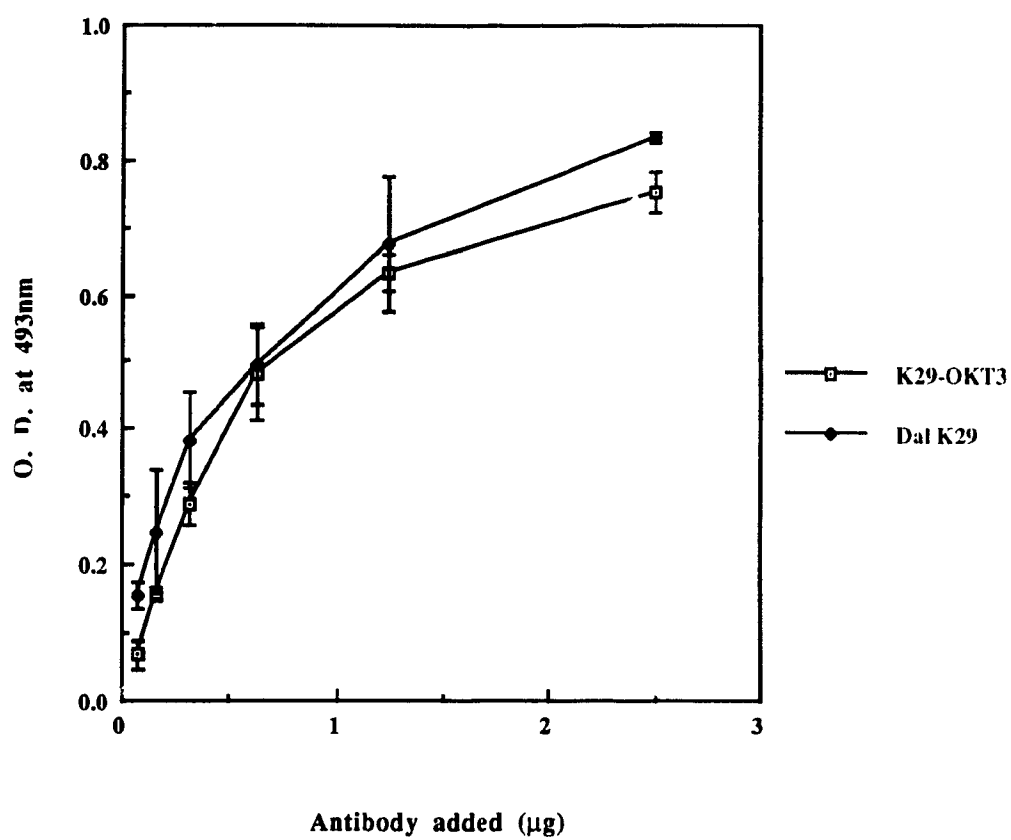
□ K29-OKT3

◆ Dal K29

Fig. 126

Clearance of ^{131}I-Dal K29 and ^{131}I-K29-OKT3 heteroconjugate in s.c. Nu-caki-1 xenograft bearing nude mice.

Nu-caki-1 s.c.xenograft bearing nude mice were given ^{131}I-Dal K29 or ^{131}I-K29-OKT3 heteroconjugate mixed with ^{125}I-Dal B02 via the i.v. route. At indicated intervals, samples of blood were obtained and ^{131}I and ^{125}I activities in the blood were determined. The total body radioactivity of the xenograft bearing mice was also monitored.

Fig. 126A Clearance of ^{131}I-Dal K29, ^{131}I-K29-OKT3 heteroconjugate and ^{125}I-Dal B02 from the blood.

Fig. 126B Clearance of total body ^{131}I activity.

Total body radioactivity
(% of initial activity)

Fig. 126B

Time (hr)

Dal K29

K29-OKT3

Radioactivity in blood
(% of initial activity)

Fig. 126A

Time (hr)

Dal B02

Dal K29

K29-OKT3

462
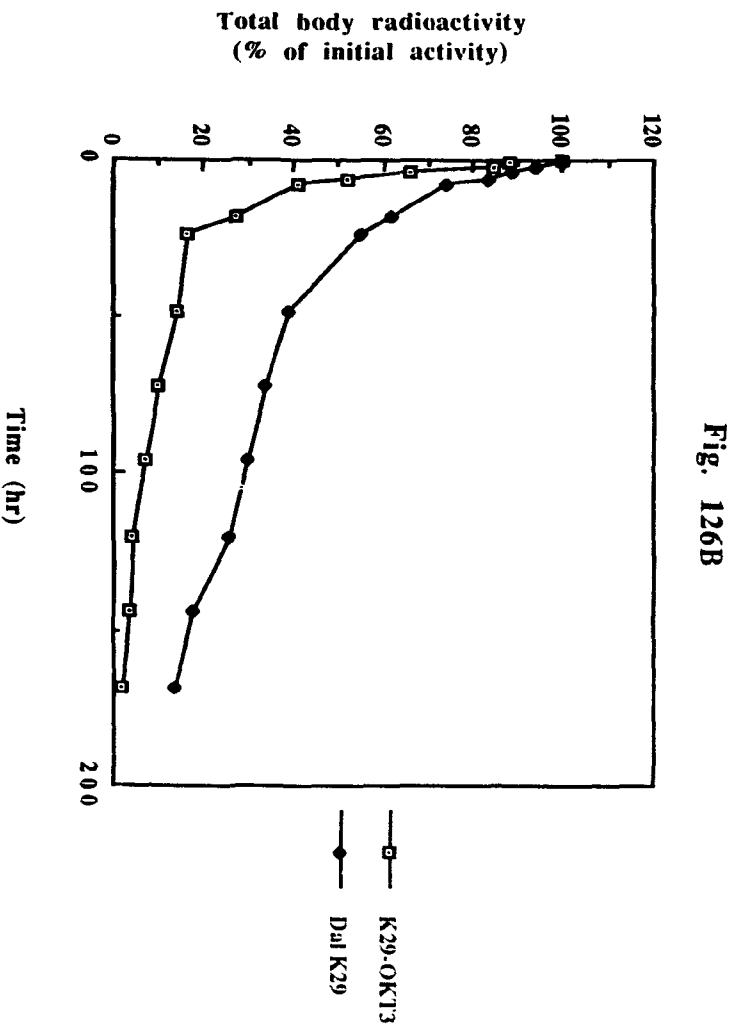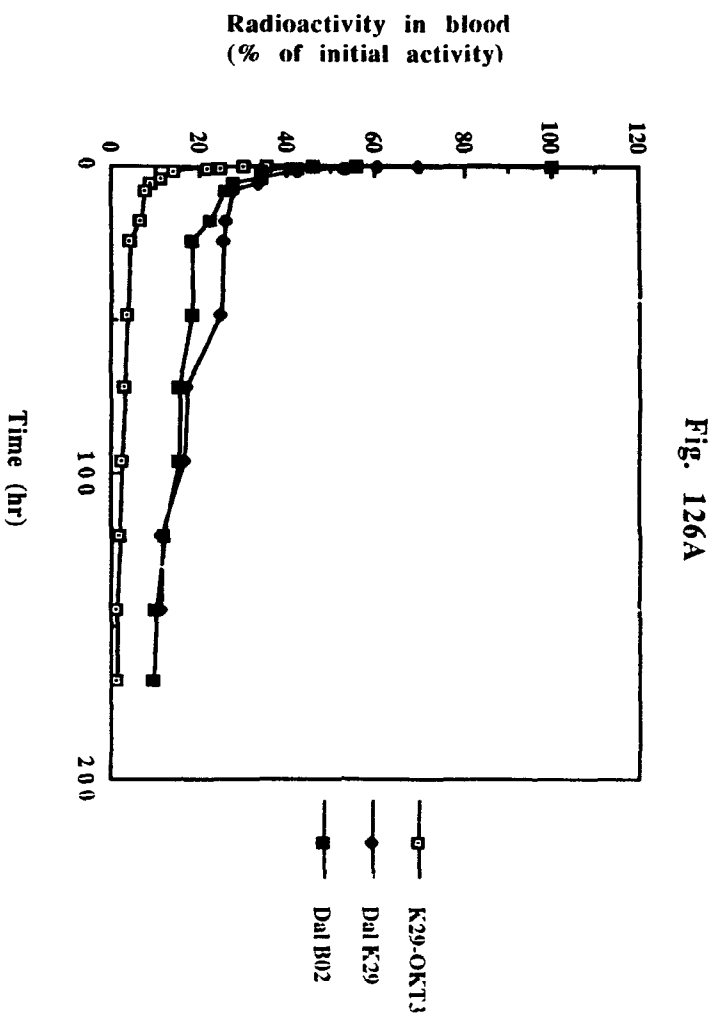
Figs. 127 to 130

Biodistribution of ^{131}I-Dal K29 and ^{131}I-K29-OKT3 heteroconjugate in s.c. Nu-caki-1 xenograft bearing mice.

S.c. Nu-caki-1 xenograft bearing nude mice were given ^{131}I-Dal K29 or ^{131}I-K29-OKT3 heteroconjugate via the i.v. route. Groups of three mice were sacrificed at 24, 48, 96 and 168 hr after antibody administration. The xenografted tumor and normal mouse tissues were taken out and weighed. Tissue associate radioactivity was determined with a gamma counter. The % ID / g tissue and the T / NT ratios were then calculated.

Fig. 127   Biodistribution of Dal K29 and K29-OKT3 heteroconjugate in s.c. Nu-caki-1 xenograft bearing nude mice at 24 hr after antibody administration.

(A) % ID / g tissue;   (B) T / NT ratio.

Fig. 128   Biodistribution of Dal K29 and K29-OKT3 heteroconjugate in s.c. Nu-caki-1 xenograft bearing nude mice at 48 hr after antibody administration.

(A) % ID / g tissue;   (B) T / NT ratio.

Fig. 129   Biodistribution of Dal K29 and K29-OKT3 heteroconjugate in s.c. Nu-caki-1 xenograft bearing nude mice at 96 hr after antibody administration.

(A) % ID / g tissue;   (B) T / NT ratio.

Fig. 130   Biodistribution of Dal K29 and K29-OKT3 heteroconjugate in s.c. Nu-caki-1 xenograft bearing nude mice at 168 hr after antibody administration.

(A) % ID / g tissue;   (B) T / NT ratio.

Fig. 127A

% ID / g tissue

Dal K29
K29-OKT3

Fig. 127B

T / NT Ratio

Dal K29
K29-OKT3

Fig. 128A

% ID / g tissue

Fig. 128B

T / NT Ratio
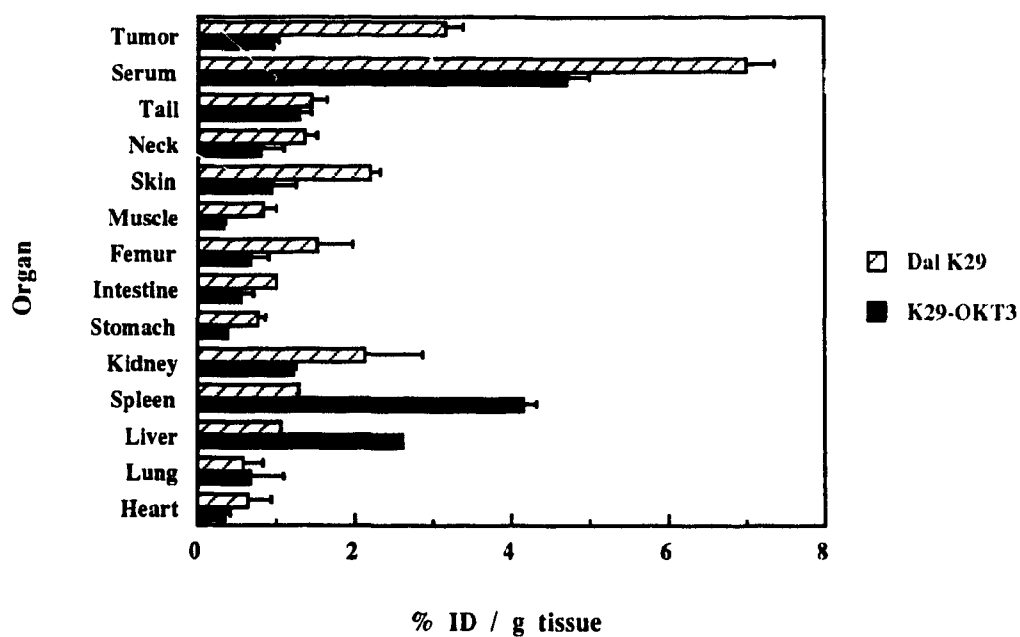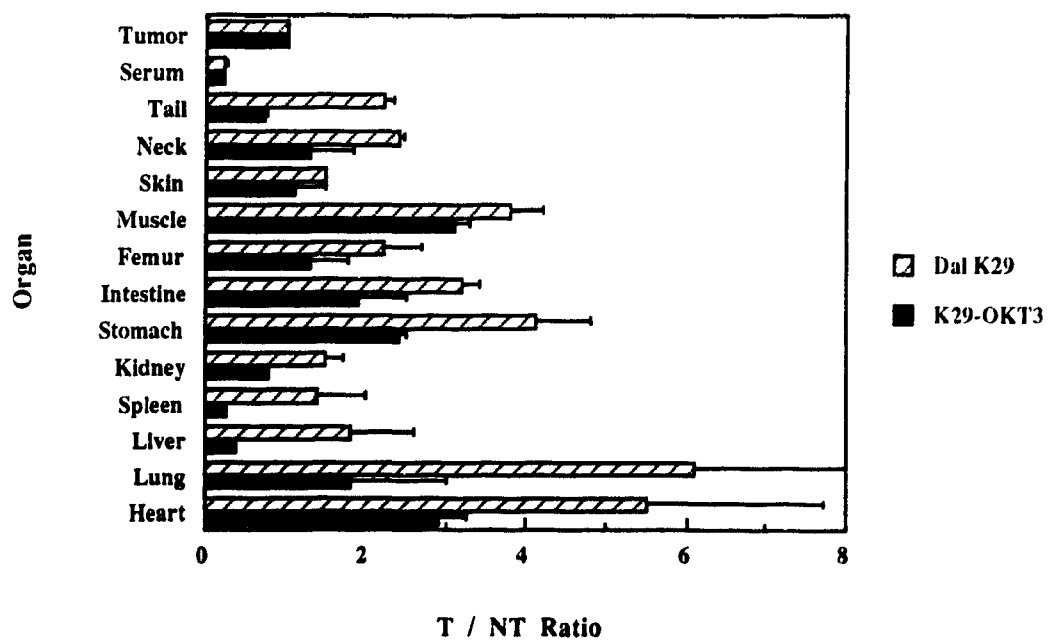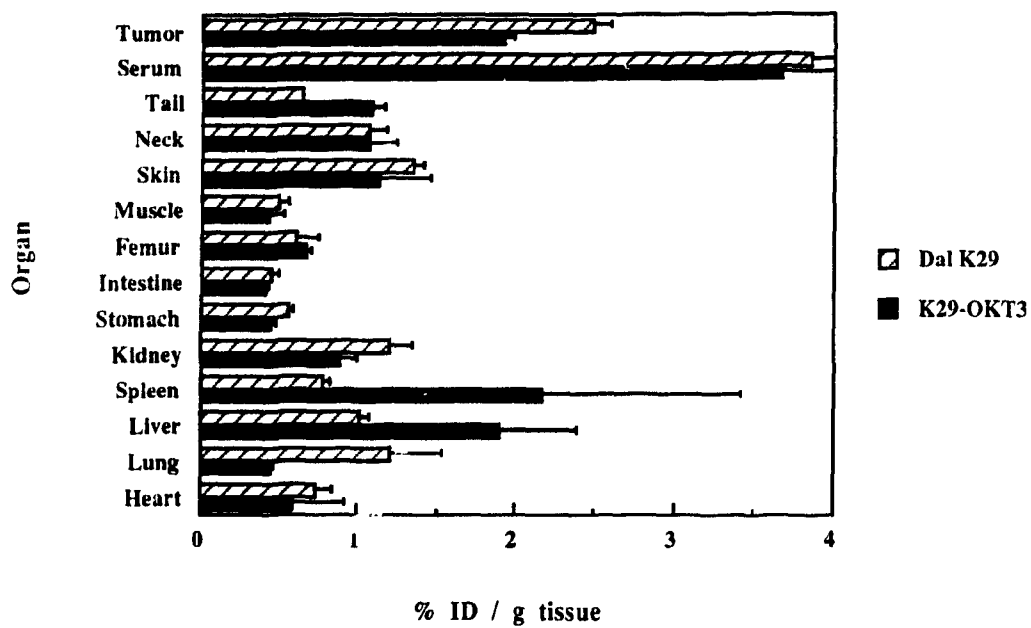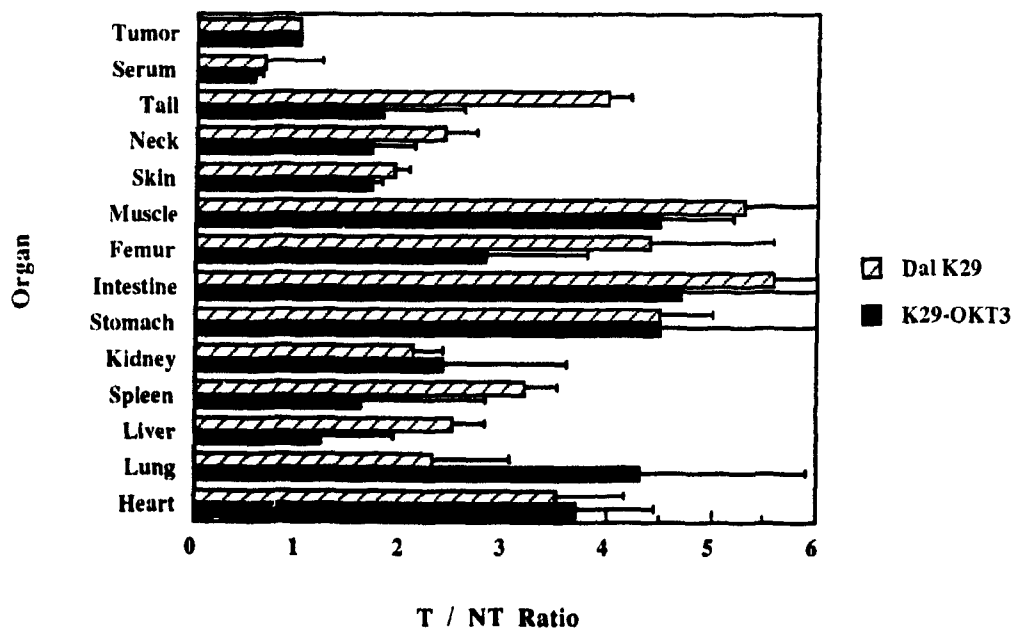
Fig. 129A

Fig. 129B

Fig. 130A

% ID / g tissue
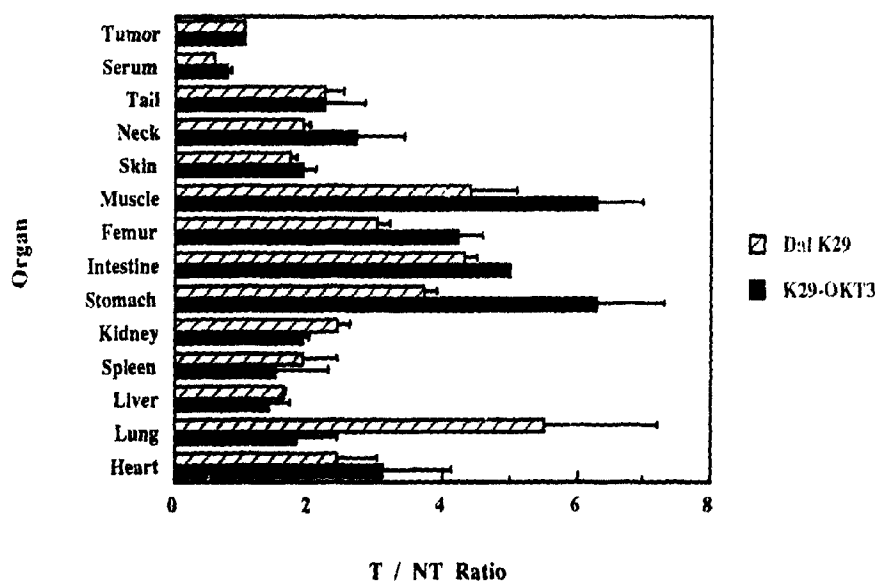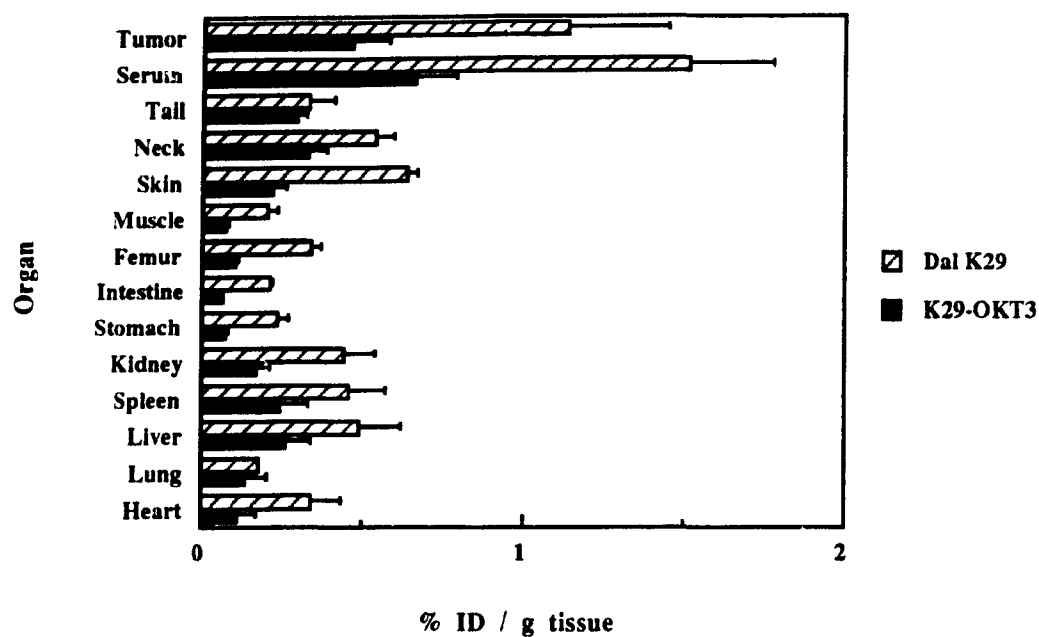
Fig. 130B
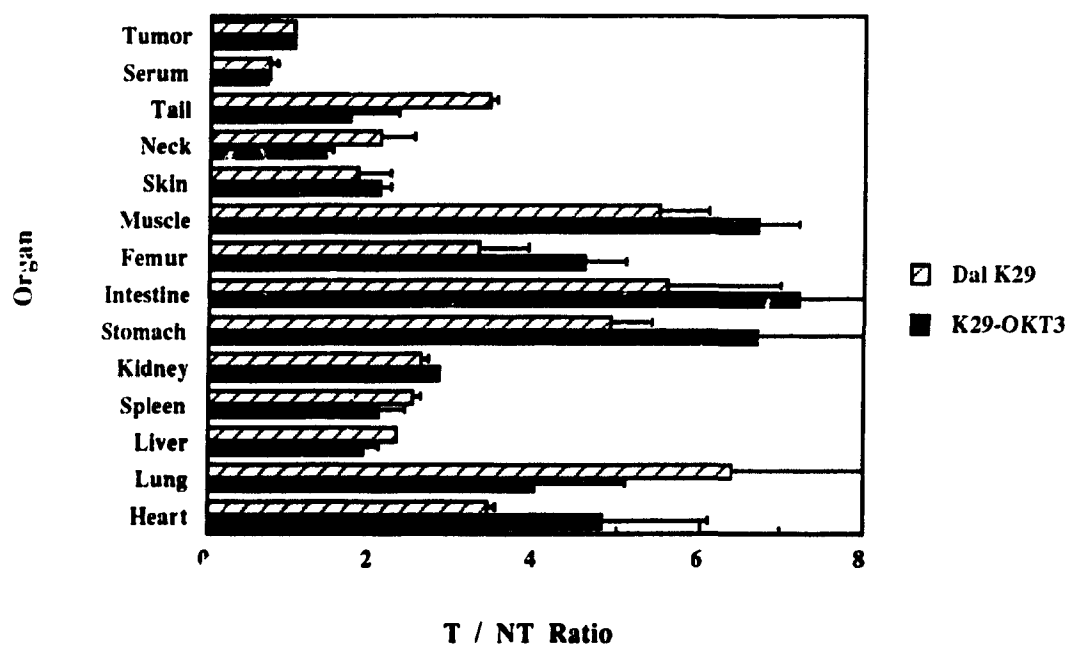
T / NT Ratio

Table 34   TCA   precipitable ^{131}I   radioactivity   in   the   supernatant   of homogenized   organs   and   xenografted   Nu-caki-1   tumors   from   nude   mice given ^{131}I-Dal   K29   or ^{131}I-K29-OKT3   heteroconjugate [1]

(A)   48   hr   after   i.v.   administration   of ^{131}I-Dal   K29   or ^{131}I-K29-OKT3 heteroconjugate

Organ	Dal K29	K29-OKT3	Dal B02
Liver	94.4 ± 0.84 [2]	78.2 ± 3.6	94.1 ± 1.7
Spleen	93.4 ± 2.5	72.4 ± 5.2	91.3 ± 2.2
Kidney	95.0 ± 0.5	74.0 ± 0.9	94.5 ± 2.4
Neck	96.1 ± 0.4	87.7 ± 1.3	97.3 ± 1.6
Serum	99.0 ± 0.1	94.0 ± 0.6	98.3 ± 0.1
Tumor	88.8 ± 0.3	77.1 ± 8.3	92.8 ± 2.6

(Continued)

(B) 96 hr after i.v. administration of ^{131}I-Dal K29 or ^{131}I-K29-OKT3 heteroconjugate

Organ	Dal K29	K29-OKT3	Dal BO2
Liver	96.5 ± 0.3	81 ± 2.3	97.2 ± 1.3
Spleen	96.5 ± 1.3	78.8 ± 2.0	96.8 ± 1.5
Kidney	95.8 ± 1.8	84.1 ± 2.3	96.8 ± 1.7
Neck	95.0 ± 2.5	89.1 ± 1.1	97.4 ± 2.3
Serum	99.0 ± 0.7	93.1 ± 1.4	98.7 ± 0.1
Tumor	84.0 ± 1.9	77.1 ± 4.7	96.6 ± 2.8

(Continued)

(C)   168 hr after i.v. administration of ^{131}I-Dal K29 or ^{131}I-K29-OKT3 heteroconjugate

Organ	Dal K29	K29-OKT3	Dal B02
Liver	97.2 ± 2.5	81.6 ± 3.4	98.7 ± 1.4
Spleen	95.6 ± 5.6	69.7 ± 7.5	99.0 ± 1.2
Kidney	97.3 ± 0.9	86.0 ± 0.5	97.9 ± 1.3
Neck	97.4 ± 0.8	84.2 ± 5.4	98.8 ± 1.5
Serum	99.3 ± 0.4	94.8 ± 0.5	99.5 ± 0.3
Tumor	84.0 ± 1.9	81.7 ± 4.3	97.8 ± 1.3

1. Organs and xenografted tumors from Nu-caki-1 xenograft bearing nude mice given ^{131}I-Dal K29 or ^{131}I-K29-OKT3 heteroconjugate preparation were taken out and homogenized. The supernatant of tissue homogenates was precipitated by 10% TCA as described in Methods section.

2. All values are the percentage of radioactivity in the tissue homogenate that could be precipitated by 10% TCA and represent the mean ± S.D. of 3 determinations performed using tissues from at least 2 mice.

Table 35   IRF of Dal K29 and K29-OKT3 heteroconjugate recovered from the serum of Nu-caki-1 xenograft bearing nude mice [1]

Time (hr) [2]	0	48	96	168
Dal K29	38.5 [3]	33.6	48.9	40.4
K29-OKT3	36.8	39	38.9	32.9

1. Sera were obtained from Nu-caki-1 xenograft bearing nude mice given ^{131}I-Dal K29 or ^{131}I-K29-OKT3 heteroconjugate at indicated intervals.

2. Hours after the administration of ^{131}I-Dal K29 or ^{131}I-K29-OKT3 heteroconjugate preparation at which the samples of serum were obtained.

3. The IRF of Dal K29 or K29-OKT3 heteroconjugate in the serum was determined using Nu-caki-1 cells as described in Methods section 5.3.

Figs. 131 and 132

Autoradiographs of Nu-caki-1 xenografts after i.v. injection of ^{131}I-Dal K29 or ^{131}I-K29-OKT3 heteroconjugate.

S.c Nu-caki-1 xenograft bearing nude mice were sacrificed at 48 and 96 hr after the administration of ^{131}I-Dal K29 or ^{131}I-K29-OKT3 heteroconjugate. The xenografts were taken out, and 5 μm thick cryostat sections were cut and fixed in formaldehyde vapor overnight. The sections were then subject to autoradiography as described in Methods section 7.7.

Fig. 131   Autoradiographs of 5 μm thick cryostat section of a Nu-caki-1 xenograft at (A) 48 hr; and (B) 96 hr after i.v. injection of ^{131}I-Dal K29.

Fig. 132   Autoradiographs of 5 μm thick cryostat section of a Nu-caki-1 xenograft at (A) 48 hr; and (B) 96 hr after i.v. injection of ^{131}I-K29-OKT3 heteroconjugate.

Fig. 131
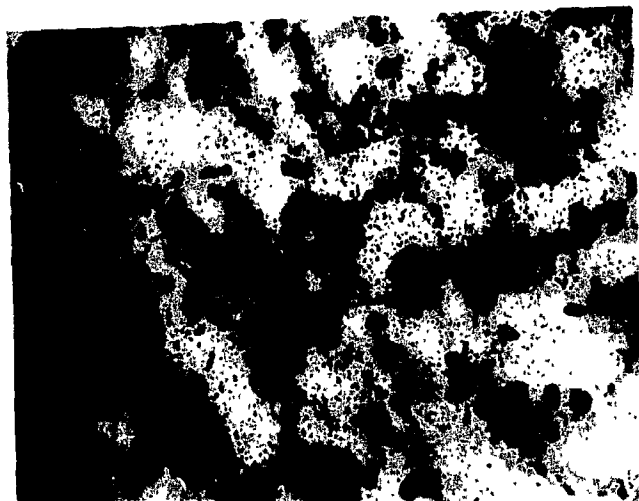
a
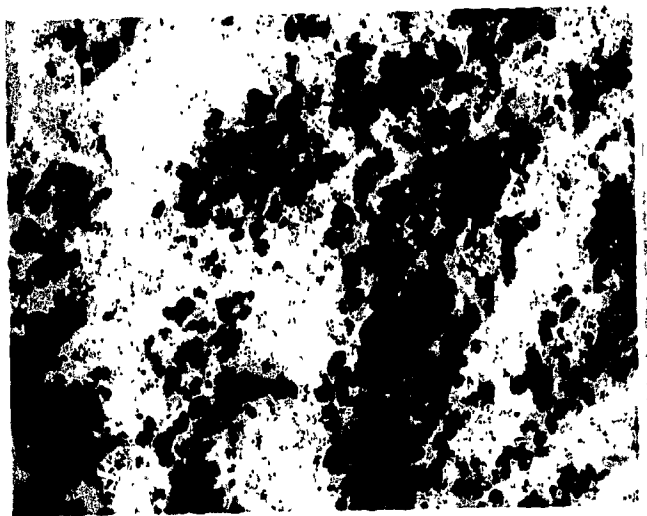
b

Fig. 132
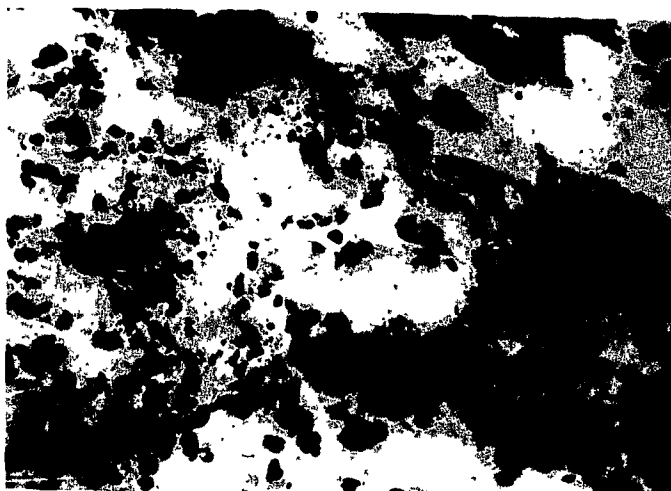
a
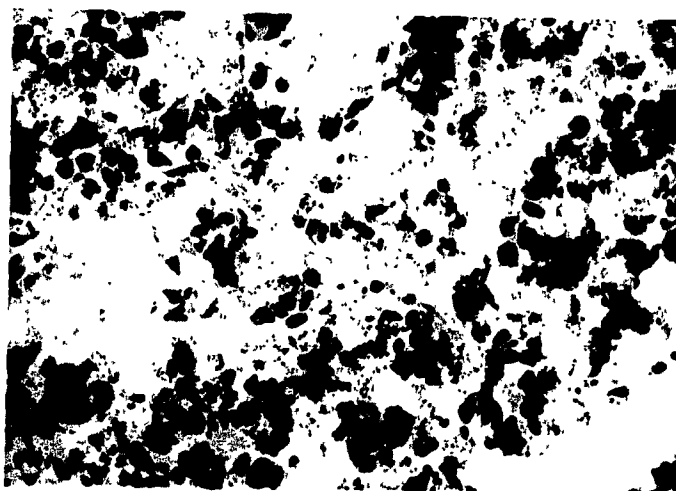
b

Fig. 133

Inhibition of intraperitoneal Nu-caki-1 ascites tumor in nude mice after treatment with K29-OKT3 heteroconjugate and human PBL.

Nude mice inoculated with 5×10^6 Nu-caki-1 cells i.p. were treated 24 hr after tumor inoculation with (i) K29-OKT3 heteroconjugate alone; (ii) K29-OKT3 heteroconjugate plus human PBL (E / T ratio 3 to 1, or 10 to 1); and (iii) a mixture of Dal K29 and OKT3 (i.e., unlinked) plus human PBL at an E / T ratio of 10 to 1. The mice were observed for the appearance of ascites tumor and survival.

Fig. 133
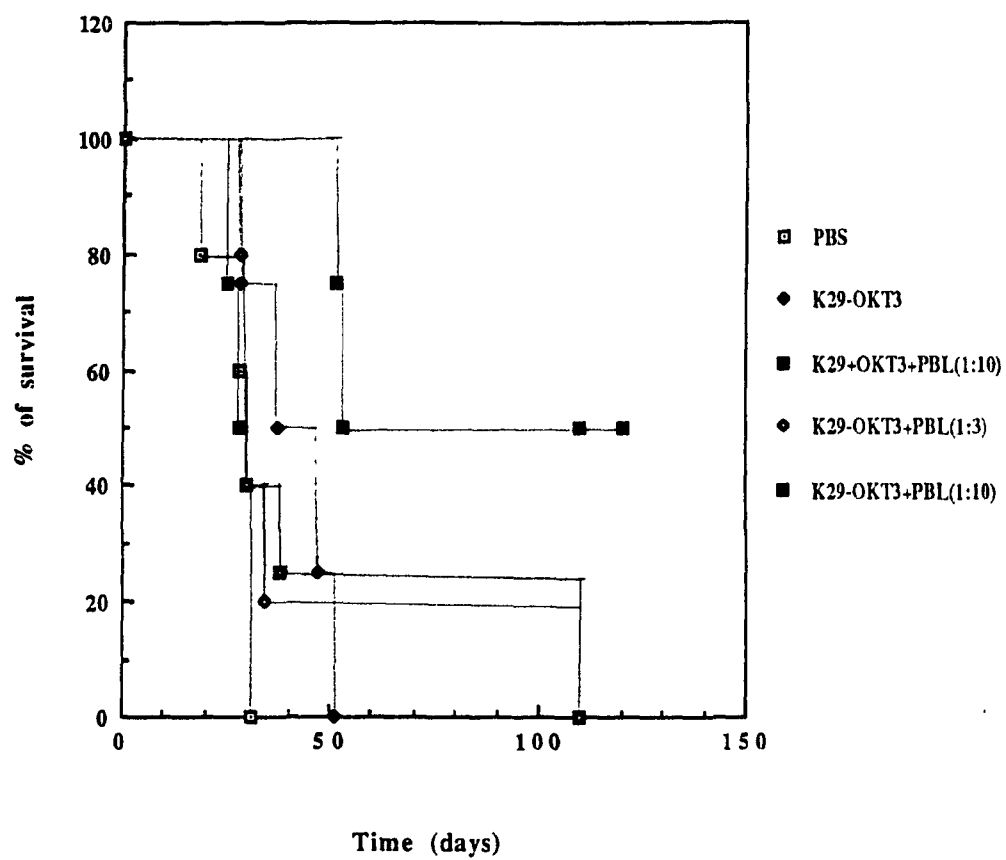
Table 36   Inhibition of intraperitoneal Nu-caki-1 ascites tumor after treatment with K29-OKT3 heteroconjugate and human PBL [1]

Treatment	Ascites / total mice	Survival (days)
(1) PBS	5 / 5 [2]	18, 28, 30, 31, 31 [5]
(2) K29-OKT3 [3]	4 / 4	28, 37, 47, 51
(3) Dal K29+OKT3+PBL (E/T, 10/1) [4]	4 / 4	25, 28, 38, 110
(4) K29-OKT3 + PBL (E/T, 3/1)	5 / 5	28, 30, 30, 34, 110
(5) K29-OKT3 + PBL (E/T, 10/1)	2 / 4	53, 70, other two > 150

1. Nude mice were given the preparations i.p. 24 hr after inoculation with Nu-caki-1 cells $(5 \times 10^6$ cells/mouse i. p.).

2. The number of nude mice that developed ascites tumor out of the total number of nude mice in the group.

3. The amount of K29-OKT3 heteroconjugate used in all groups was 30 μg.

4. A mixture of Dal K29 (15 μg), OKT3 (15 μg) and PBL.

5. The difference in the survival of mice between different groups was tested by the logrank test. P values are calculated between experimental groups and the control group. $P < 0.05$ between group 5 and all other groups except group 3; $P > 0.05$ group 4 and 1, group 4 and 2, group 3 and 1, group 3 and 2; $P = 0.05$ between group 3 and group 5, group 2 and group 1;

DISCUSSION

1. MoAb-Based Targeted Radioimmunotherapy of Human B-Cell Chronic Lymphocytic Leukemia in Experimental Models

Since the discovery of Kohler and Milstein in 1975, the hybridoma technique has been widely used to produce numerous MoAbs against various human cancers. Once constructed, hybridomas can be grown either in vitro in cell culture or in vivo in the peritoneal cavity of appropriate animals (e.g., syngeneic BALB/c mice). The secreted MoAb is then purified from the supernatant of cell culture or from mouse ascites fluid. In vitro culture methods have several advantages over growing the hybridomas in the peritoneal cavity of appropriate animals. The supernatant of the cell culture contains only defined MoAb and no mouse antibody or other mouse proteins. The problem associated with the large amounts of FCS used in the culture medium now can be avoided by the use of serum free medium (e.g., ITES). Furthermore, the hybridomas can be easily grown in a pyrogen-free system, which may reduce the chance of pyrogen contamination during antibody production. There are several disadvantages of in vitro culture method: (i) large amounts of medium are needed and the MoAb concentration in the supernatant is usually low (10 to 50 μg range per ml medium); and (ii) it may also require special equipment (e.g., perfusion bioreactor or hollow-fiber system) for the production of adequate amounts of MoAb needed for clinical application. Such equipment is usually expensive and may not be available in every laboratory. On the other hand, growth of hybridoma cells in the peritoneal cavity of appropriate animals is relatively a much simpler procedure. No special instruments are required and the MoAb can be readily purified from mouse ascites fluid. Also, the yield of MoAb from the mouse ascites fluid (from 1 to 10 mg/ml of ascites) is usually much higher than that from the supernatant obtained from cell cultures.

Several methods are being employed to purify MoAb from mouse ascites fluid or from cell culture supernatant, including ammonium sulfate precipitation, caprylic acid precipitation,

and chromatography (e.g., affinity, ion-exchange or size exclusion chromatography). Among them, the caprylic acid method is simple and inexpensive for purifying IgG (Mckinney and Parkinson, 1987). Caprylic acid forms insoluble complexes with plasma proteins (particularly α and β globulins), leaving a major portion of IgG in a soluble form, which can be further isolated by subsequent precipitation with 40% of ammonium sulfate. Most investigators, as well as ourselves, have found that the caprylic acid method is suitable for the purification of murine IgG1 and IgG2b, but not IgG3, while the Protein A affinity chromatography method is more suitable for the purification of murine IgG2a. HPLC and FPLC provide quick methods for obtaining highly purified MoAbs. Both methods are mostly used for analytic or preparatory purpose. It also requires more expensive equipments that are not likely to be available in every laboratory. In this study, Protein A chromatography was used to purify Dal B01, an IgG2a MoAb, and caprylic acid precipitation followed by 40% ammonium sulfate precipitation was used to purify Dal B02, an IgG1 MoAb harvested from mouse ascites fluid. SDS-PAGE analysis showed that both methods yielded highly purified MoAbs.

For the preparation of F(ab)'2 fragments from intact murine MoAb, it was found that the optimal conditions (e.g., pH conditions and the time required for complete digestion at a defined pH condition) for complete digestion of IgG molecules by pepsin varied with different MoAbs (Lamoyi and Nisonoff, 1983). The overall susceptibility to degradation is IgG2b > IgG3 > IgG 2a > IgG1 (Parham, 1983). In this study, with a defined pepsin/IgG ratio of 1/40 (w/w) and at pH 3.7, it took 3 hr for the complete digestion of Dal B01, an IgG2a subclass MoAb, and 6 hr for Dal B02, an IgG1 subclass MoAb. This result is well in agreement with those reported in the literature (Kurkela et al., 1988; Parham, 1983).

Radiolabeled MoAbs are being increasingly used in the diagnosis and treatment of tumors in animal models and patients (Buchsbaum and Lawrence, 1990; Sfakianakis, 1990; Larson, 1991). Because of commercial availability and the ease of chemical manipulation of proteins for radiolabeling by standard procedures (Regoeczi, 1984), radioisotopes of iodine, i.e., ^{123}I, ^{125}I and ^{131}I are the radionuclides of choice of most investigators for MoAb-based tumor radioimmunoimaging and radioimmunotherapy (Langmuir, 1992). A variety of methods for radioiodination of proteins are available (Wilbur, 1992) and the ideal one may differ with different antibodies and their intended application, and to some extent, the preference of each investigator. However, the iodination procedure should not damage antibody activity and the bond between the carrier antibody and radionuclide should be stable.

Chloramine T method was initially chosen in this study to iodinate Dal B01, Dal B02 and their F(ab)'2 fragments because of the simplicity of the iodination procedure and the reliable iodination efficiency obtained from past studies (Osterman, 1984). Chloramine T method is known to iodinate protein by directly iodinating the tyrosine residues in the protein (Wilbur, 1992). It may damage antibody activity by involving the tyrosine residues in the complementarity determining regions (CDRs) that are required for antigen binding (Osterman, 1984). Since different antibodies or F(ab)'2 fragments may have different susceptibility to protein iodination by chloramine T, the extent of loss of immunoreactivity after iodination varies from MoAb to MoAb, and from a given intact MoAb to its F(ab)'2 fragment. Some antibodies may tolerate chloramine T well while others may lose their activity completely after this radioiodination procedure (Eary et al., 1989). Based on this consideration, preliminary studies were carried out to determine the optimal conditions for iodination of MoAb Dal B01 and Dal B02 using chloramine T.

When Dal B02 was radioiodinated with ^{125}I using chloramine T, it was found that the IRF of Dal B02 decreased significantly when the MoAb was exposed to chloramine T for longer than 3 min (Table 4), or when the MoAb was exposed to high concentrations of chloramine T (e.g., 200 µg/ml) (Table 5). The increase in the level of ^{125}I incorporation in Dal B02 is unlikely to be the major cause of the decrease of IRF in both cases. Firstly, as shown Table 4, the specific activity (i.e., the level of iodine incorporation) of Dal B02 preparation in this experiment was almost the same irrespective of whether the MoAb was exposed to chloramine T for 3 min or 10 min (i.e., 0.35 versus 0.36 µCi/µg, approximately 1 atom of ^{125}I per 40 molecules of IgG). However, the IRF of the antibody was markedly decreased (i.e., 66% versus 33%) after an exposure period of 10 min. Secondly, as shown in Table 5, when a high concentration of chloramine T (200 µg/ml) was used, the IRF of Dal B02 decreased to 43% when the specific activity of the antibody was only 0.36 µCi/µg (1 atom of ^{125}I per 40 molecules of IgG). In fact, as shown in Table 6, Dal B02 had an IRF of 75% at a specific activity as high as 4.0 µCi/µg (1 atom of ^{125}I per 3.4 molecules of IgG) when the MoAb was radioiodinated at a lower concentration of chloramine T (i.e., 100 µg/ml) for 2 min in the presence of a larger amount of ^{125}I. It seems that in studies described above, the amount of chloramine T used and the duration of exposure of the MoAb to chloramine T played a critical role in the retention of antibody IRF, at least at these low levels of iodine incorporation (i.e., specific activities ranged from 0.1 to 0.5 µCi/µg as in Tables 4 and 5).

Although the results described above showed that at these low specific activities, the levels of iodine incorporation was not a major factor in the decrease of IRF of Dal B02, studies with radioiodinated Dal B01, Dal B02 and their F(ab)'2 fragments with increased levels of radioiodine incorporation did demonstrate the decrease of IRF of these MoAbs and their F(ab)'2 fragments at higher levels of ^{125}I incorporation (Table 6). Since all radioiodinations in this study were carried out following the same procedure (i.e., at a chloramine T

concentration of 100 μg/ml for 2 min), it was possible to investigate the sole effect of levels

of radioiodine incorporation on the retention of IRF of Dal B01, Dal B02 and their F(ab)'2

fragments. The extent of decrease of antibody IRF with increasing levels of iodine

incorporation varied from MoAb to MoAb, and from a given intact MoAb to its F(ab)'2

fragment. In this study, Dal B02 and its F(ab)'2 fragment seem to be more sensitive to the

increase in the level of iodine incorporation than Dal B01 and its F(ab)'2 fragment.

To obtain radioiodinated MoAbs with high specific activity using the chloramine T method,

at least three approaches are possible: (i) to increase the duration of iodination reaction; (ii)

to increase the amount of chloramine T in the reaction mixture; and (iii) to increase the

amount of radioactive iodine in the reaction mixture. In this study, all these three

approaches were attempted using Dal B02 and ^{125}I. The first approach not only failed to

increase the level of iodine incorporation in the MoAb, but also resulted in the loss of

MoAb IRF as the reaction proceeded beyond 3 min (Table 4). In the second approach, a

direct correlation was observed between the increase in the amount of chloramine T used

and the increase in the level of iodine incorporation. However, high concentrations of

chloramine T caused significant decrease of MoAb IRF (Table 5). The third approach, i.e.,

using a moderate concentration of chloramine T (100 μg/ml) and a period of 2 min and

increase the amount of ^{125}I in the reaction mixture, yielded radioiodinated Dal B02

preparation with high levels of iodine incorporation and high IRF (Table 6). Therefore, for

in vivo radioimmunotherapy with ^{131}I-Dal B02, Dal B02 was iodinated using 100 μg/ml of

chloramine T for 2 min with the desired amount of ^{131}I.

Results showed that both Dal B01 and Dal B02 MoAbs have almost the same number of

binding sites on D10-1 cells. There was no significant difference in the number of binding

sites on D10-1 cells for both Dal B01 F(ab)'2 and Dal B02 F(ab)'2 fragments compared to

their parent intact MoAbs. However, both F(ab)'2 fragments had lower affinity of binding

compared to their parent intact MoAbs. The loss of antibody affinity with F(ab)'2 fragments is likely to be due to their higher susceptibility to this iodination procedure. As observed by Singh (1989), SDS-PAGE of radiolabeled F(ab)'2 fragment showed some breakdown of the molecule to lower molecular weight fragments after radioiodination. Other possibilities include steric changes in the antigen binding site of the antibody after fragmentation and/or damage to this site by the peptic digestion.

When the same amounts of intact MoAbs or their F(ab)'2 fragments (of approximately the same level of iodine incorporation) were incubated with target D10-1 cells, higher proportions of Dal B02 or its F(ab)'2 fragment bound to D10-1 cells compared to the proportions of Dal B01 or its respective F(ab)'2 fragment that bound to D10-1 cells. As stated, there was no difference in the number of binding sites between all these four antibody preparations. Furthermore, Dal B01 has approximately the same Ka of binding as Dal B02, and Dal B01 F(ab)'2 fragment has approximately the same Ka of binding as Dal B02 F(ab)'2 fragment. Therefore, the difference in the proportions of antibodies bound to target cells is due to the difference in the IRF of these antibody preparations.

Once anti-tumor MoAb binds to cell surface antigen(s) of tumor cells, the fate of the resulting antibody-antigen complex might be (i) retention on cell surface as a stable complex; (ii) endocytosis; (iii) shedding; or (iv) catabolism on cell surface. Internalization of individual antibody may follow different pathways (Pastan and Willingham, 1983). The major mode of antibody internalization is receptor-mediated endocytosis (Garnett and Baldwin, 1986; Shawler et al., 1988). Other mechanisms by which cells uptake surface-bound antibodies include fluid phase uptake (e.g., pinocytosis) (Frankel, 1988) and via membrane utilization or membrane biosynthesis (Steinman et al., 1983). Receptor-mediated endocytosis permits cells to internalize macromolecules needed for cellular functions or provides a route by which potential injurious molecules can be removed and/or detoxified

from biological fluids (Pastan and Willingham, 1983). The steps in this multiphase process involve (i) binding of the ligand (e.g., antibody) to its receptor (e.g., antigen) expressed on cell surface; (ii) clustering (patching) of the ligand-receptor complexes; (iii) capping, which involves the translocation of the complexes to one or two polar regions of the cell (this step requires energy and can be inhibited by metabolic inhibitor such as potassium cyanide, sodium azide and low temperature); (iv) endocytosis of the capped complexes and/or shedding of the complexes; and finally (v) recycling of the receptor. Most ligand-receptor complexes are internalized via clathrin-coated pits (Goldstein et al., 1988). Once internalized, ligand-receptor complexes are localized in a structure defined as endosome. The endosome is an acidic non-lysosomal compartment where uncoupling or dissociation of ligand-receptor complexes occurs. The ligand may be further routed to other intracellular organelles (such as lysosomes and the Golgi apparatus) or released into cytosol. The ligand can then either be degraded (e.g., in the lysosome) and/or exert its effect on intracellular target molecules (e.g., toxin in cytosol) (Pastan and Willingham, 1983). Since antibodies that do not undergo "capping" are usually not endocytosed in significant amount, the "capping" phenomenon may serve as a useful guide in predicting which antibody will be endocytosed and when this event is likely to occur (Guclu, et al., 1975). This is very important in selecting an antibody as a carrier to specifically deliver those therapeutic drugs or toxins whose targets are intracellularly distributed (see Introduction sections 4.2.2 and 4.3.1 for a detailed discussion).

Three major types of binding kinetics of antibodies to cell surface antigens were described by Matzku et al. (1986) using anti-melanoma MoAbs: (i) the amount of antibody bound to target cells was approximately the same at either 4°C or 37°C; (ii) the amount of binding at 37°C was higher than that at 4°C; and (iii) the amount of binding at 37°C was lower than that at 4°C. As already stated, receptor-mediated endocytosis does not occur at 4°C. One of the most common way to calculate the amount of antibody endocytosed by target cells is to

subtract the amount of cell bound antibody at 4°C from the total amount of cell bound antib~dy at 37°C. However, due to the complexity of the interaction between MoAbs and their target antigens (and this may also vary with different MoAbs and target antigens), in some situations, the difference in the amount of antibody bound to target cells at 37°C and at 4°C, may not always correlate with the rate of internalization (Tilgen and Matzku, 1990). This may be due to the following facts: (i) some types of cells do not internalize a particular cell surface bound MoAb even at 37°C, although there might be a marked increase in the amount of antibody binding at 37°C compared to the amount of bound at 4°C (Matzku et al., 1988); (ii) the increase in the dissociation constant with temperature may exceed the increase in the association constant leading to the dissociation of larger amounts of the antibody from target cells (Johnstone et al., 1990); and (iii) the metabolism of the internalized antibody and subsequent efflux of the breakdown small catabolic fragments resulting in the loss of radioactivity from the target cells (Geissler et al., 1991). In both (ii) and (iii), the loss of radioactivity from cells may mask the possible enhanced binding and internalization of the radiolabeled antibody by the cells at 37°C. Finally, shedding of antibody-antigen complex from tumor cell surface at increased temperature may also cause the loss of cell-surface bound antibody (Tilgen and Matzku, 1990);

My results (Figs. 15 and 16) show that the kinetics of binding of Dal B01, its F(ab)'2 fragment, as well as that of Dal B02 to D10-1 cells followed the first mode, i.e., the amounts of antibody that bound to target cells were basically the same at either 4°C or 37°C. The binding kinetics of Dal B02 F(ab)'2 followed the third mode, i.e., the amount of antibody bound to target cells was greater at 4°C than that at 37°C. As discussed above, the difference in the amounts of antibodies bound to D10-1 cells at 37°C and 4°C does not provide conclusive evidence as to whether cell associated antibody were surface bound or internalized.

Several methods are available to either qualitatively or quantitatively identify cell surface bound MoAbs and those that are endocytosed. For qualitative determination, immunocytological staining methods are used most often (Singh, 1989). Cells are first incubated with the antibody (Ab1) against cell surface associated antigen(s) at either 37°C or 4°C. At different intervals, the cells are fixed and sections are cut. The enzyme or gold-linked anti-Ab1 antibody (Ab2) is then used to locate the distribution of Ab1. For quantitative determination, two methods are commonly used. In the first method, MoAb-coated cells are treated with a iso-osmolar low pH buffer (e. g., pH 2.8) (Matzku et al., 1986). In other method, MoAb-coated cells are treated with enzymes such as trypsin (Kyriakos et al, 1992). Both treatments are known to dissociate cell surface bound MoAb, and thus allow for the discrimination between surface bound and internalized antibody. However, these methods do not provide definite evidence of internalization of MoAb. In some situations, the cell surface bound antibodies may not be completely removed by these treatments. Furthermore, the damage and/or increase in the permeability of cells brought about by these treatments may dislocate cell surface bound antibodies into the cytoplasm.

Press et al. (1989b) have studied the in vitro binding parameters of a panel MoAbs directed against different B-cell differentiation antigens on Daudi cells. These antibodies differed substantially in their behavior after binding to target cells. Basically, two modes of binding and internalization of antibody to target cells were observed. In the first mode, the cell bound MoAbs, such as anti-IgM (μ chain), anti-CD22 and anti-CD19 MoAbs, were rapidly internalized resulting in the disappearance of radioactivity from the cell surface and appearance of the label in the intracellular compartment. TCA soluble radioactivity (in free form or associated with small catabolic fragments) in supernatant appeared rapidly after incubation of antibody coated cells at 37°C and accounted for 70 to 80% of initial total cell associated cpm at 24 hr. In the other mode, cell bound MoAbs, such as anti-CD37, anti-class II and anti-CD20 MoAbs, were retained longer on the cell surface with a slower

intracellular accumulation of the label. Less than 10% of radioactivity in supernatant was TCA soluble after 24 hr incubation with these MoAbs, suggesting that the disappearance of these MoAb from cell surface was primarily due to dissociation rather than catabolism. Similar results have also been reported by Kyriakos et al. (1992), who used a number of MoAbs directed against several tumor cell lines, including melanoma and carcinomas of ovarian, lung and kidney.

The interaction of Dal B02 with D10-1 cells is consistent with the second mode described by Press (1989). When D10-1 cells coated with radiolabeled Dal B02 were incubated at 37°C for 6 hr, over 80% of cell bound radioactivity remained associated with the cells. Greater than 95% of the radioactivity released into the supernatant was TCA precipitable, indicating that this radioactivity was associated with intact Dal B02 or its large fragments (Fig. 18). This result suggests that the binding of Dal B02 to its target antigen was quite stable and the major mode of release of cell surface bound Dal B02 is dissociation rather then intracellular catabolism.

In another experiment in which D10-1 cells were first coated with radiolabeled Dal B02 at 37°C for 2 hr and then exposed to a large excess of cold Dal B02. About 80% of initial cell associated radiolabeled Dal B02 was displaced by cold Dal B02, indicating the majority of D10-1 cell-associated Dal B02 remained on cell surface after incubation at 37°C for 2 hr. It is possible that the amount of radiolabeled Dal B02 that could not be displaced by the cold antibody was intracellular. However, it is also possible that this proportion of radiolabeled Dal B02 still remained on the cell surface but could not be dissociated under these experimental conditions.

Thus, none of the above studies firmly established internalization of any significant amount of Dal B01 or Dal B02. Therefore, MoAbs Dal B01 and Dal B02 were adsorbed to

colloidal gold particles, and the MoAb-labeled gold particles were used as a marker to trace the interaction between Dal B01, Dal B02 and their target cells and to ascertain the existence of antibody internalization (if any, the proportion of internalization).

The stability of the MoAb-Au complexes is an important consideration for their effective use in this study. The adsorption of MoAb to colloidal gold particles is a complex phenomenon. The formation of stable MoAb-Au complexes is dependent on the stability of the colloidal gold itself, the concentration, conformation and isoelectric point of the antibody and the ionic strength, pH and temperature of the suspending medium (De Meij, 1983). Thus, the optimal conditions for the preparation of stable MoAb-Au complexes varies from MoAb to MoAb. It is necessary that the coupling procedure be carried out in a pH environment that is at, or near to the isoelectric point of the antibody. The amount of antibody that is required to stabilize a given amount of colloidal gold solution also varies from MoAb to MoAb. For example, Martin et al. (1990) reported that 6 μg of GAM IgG was adequate to stabilize 1 ml colloidal gold solution (diameter of the gold particle, 40 nm). In my study, 40 to 60 μg of the three different MoAbs were the minimum amounts needed to stabilize 1 ml colloidal gold solution.

Before the use of these gold particle complexed MoAbs, it was important to examine the IRF of the MoAbs, the stability of the adsorption between MoAbs and gold particles and the cytotoxicity of the MoAb-Au complexes.

Three methods were used to determine the immunoreactivity of the gold particle-adsorbed MoAbs. Dal B01 and Dal B02 retained their original IRF after adsorption to gold particles, whereas about a 50% decrease of original IRF was observed after adsorption of Dal K29 to gold particles. There was no significant difference in the absolute amount of ^{125}I labeled MoAbs that bound to target cells between unadsorbed parent ^{125}I-MoAb and gold particle-

adsorbed ^{125}I-MoAbs when both the preparations were incubated with appropriate target cells at 4°C for 2 hr. However, in a competition assay, it was found that the ability of gold particle-adsorbed ^{125}I-MoAbs to bind to target cells was decreased in the presence of respective cold free MoAbs, compared to respective unadsorbed ^{125}I-MoAbs (Figs. 19 and 20).

The stability and cytotoxicity of MoAb-Au complexes are two other important factors for the effective use of these complexes. The MoAb should remain stably associated with the marker gold particles during the entire procedure (i.e., incubation, cell fixation and section cutting). Furthermore, the MoAb-Au complexes should not be cytotoxic and damage the target cells during incubation. The usefulness of MoAb-Au complexes would be severely compromised if the MoAb dissociates from the gold particles and/or if the MoAb-Au complexes damage the cells. The results obtained in this study demonstrate that all the three MoAb-Au complexes were stable and not cytotoxic to target cells during the period of incubation. All these features, i.e., good stability of the complexes, retention of immunoreactivity, and lack of cytotoxicity, allowed me to use these MoAb-Au complexes to study the fate of cell surface bound Dal B01 and Dal B02 using electron microscopy.

After incubation of cells with appropriate MoAb-Au complex at 4°C, the gold particles were found to be evenly distributed on the cell surface. The mean numbers of cell surface bound particles differed with different MoAb-Au complexes, i.e., ranging from 29 for Dal K29-Au complex, 134 for Dal B01-Au complex to 262 for Dal B02-Au complex per cell (Table 13). As endocytosis is not likely to take place at 4°C, the small numbers of gold particles that appeared " inside " cells before incubation at 37°C could have been due to the plane of cell section, e.g., a transverse section of membrane invagination might be viewed as an intracellular organelle in 2-dimensional sections and the gold particles inside the invaginations are likely to be counted as " intracellular". As stated, the amount of

internalization of gold particles at 37°C at any defined time point was calculated by subtracting the number of goid particles found to be " intracellular " at 4°C incubation from the total number of intracellular gold particles at 37°C.

When MoAb-Au complex coated cells were incubated at 37°C, the distribution of cell surface-bound gold particles became increasingly uneven. A few caps were observed after incubation at 37°C for 4 hr on D10-1 cells exposed to either Dal B01-Au or Dal B02-Au complex. The total number of cell surface bound gold particles decreased with time while the number of intracellular gold particles increased. The loss in the number of surface bound gold particles exceeded the increase in the number of intracellular gold particles, indicating both internalization and shedding could have taken place. This was observed with all the three MoAb-Au complexes and their respective target cells. When the rate of shedding between ^{125}I-Dal B02 and ^{125}I-Dal B02-Au complex was compared, it was found that the shedding was faster for the complex (Fig. 20), suggesting the binding avidity of the complex was reduced compared to that of the free antibody.

After incubation for 6 hr at 37°C, about 14 to 15% of total cell-associated Dal B01-Au or Dal B02-Au particles were observed in the cytoplasm of the target D10-1 cells. A higher percentage (i.e., 24.1%) of cell-associated Dal K29-Au particles was internalized by target Caki-1 cells after an incubation period of 6 hr. Immunofluorescence staining revealed that a larger proportion of Caki-1 cells formed caps when the cells were incubated with Dal K29 at 37°C. The higher rate of internalization of the Dal K29-Au particles by Caki-1 cells may be associated with this higher rate of " capping ", since the " capping " phenomenon is likely to be one of the important steps in inducing receptor-mediated endocytosis (Guclu et al., 1975).

The corelation between the parameters of binding of anti-tumor MoAbs to target tumor cells in vitro and their accumulation in the tumor in vivo remains to be established. However, it is undoubted that these binding parameters are important when selecting a MoAb either use alone or as a carrier to specifically deliver therapeutic agents for the treatment of cancer (see Introduction section 4.2 for detailed discussion). It is possible that, on the basis of parameter analysis, Dal B01 and Dal B02 may be well suited for in vivo application as a carrier for radionuclides (such as ^{131}I and ^{90}Y) for tumor imaging and radioimmunotherapy, and for those chemotherapeutic agents (e.g., ADR) which exert their cytotoxic effect via membrane mechanism for chemoimmunotherapy, because these two MoAbs (i) are highly specific for B-CLL cells; (ii) have large number of binding sites on target cells; and (iii) are cleared slowly from the surface of target tumor cells (i.e., both Dal B01 and Dal B02 had a low rate of endocytosis and degradation). However, the low IRF of Dal B01 preparation (i.e., less than 30%) constitutes a major disadvantage of the therapeutic use of this antibody.

A number of MoAbs directed against human tumor antigens are being investigated for their potential as carriers in tumor immunoimaging and immunotherapy (Grossbard, 1992). To determine whether an antibody is suitable for tumor detection and targeted therapy in vivo, it is essential to study the biodistribution of these carrier antibodies, especially their pharmacokinetics, their tumor localization, as well as normal tissue distribution in xenograft bearing animal models.

In this study, I have examined the in vivo distribution and tumor localization of these two MoAbs, i.e., Dal B01 and Dal B02, and their F(ab)'2 fragments in D10-1 xenograft bearing nude mice. After i.v. administration, a much higher percentage of the Dal B01, Dal B02 and their F(ab)'2 fragments localized in the tumor than in normal organs (with the exception of blood). On comparing the localization of co-injected isotype-matched, non-specific

control IgGs or their F(ab)'2 fragments, it was clear that the tumor uptake of Dal B01, Dal B02 or their fragments was specific, since the localization indices in the tumor xenografts were greater than 3 in all cases (with the exception of the localization of Dal B01 F(ab)'2 fragment at 24 and 120 hr post antibody administration).

Consistent with the results of other studies (Ghose et al., 1982a; Guha et al., 1991), this study shows that F(ab)'2 fragments were cleared from circulation more rapidly than the intact parent antibody. This is likely due to the smaller size of the fragment and hence ease of transcapillary passage and renal clearance. F(ab)'2 fragment is believed to have some advantages in tumor imaging, because their rapid clearance from blood and other normal organs reduces the background activity and yields higher T / NT ratios than the intact parent antibody. This allows early tumor imaging and yields clear tumor images (Goldenberg, 1988). However, in this study, we did not observe any improved T / NT ratios with F(ab)'2 fragments compared to their intact parent counterpart. This is likely due to the lower IRF and Ka of the fragments compared to the intact MoAbs. As stated,the loss of antibody activity of Dal B01 F(ab)'2 and Dal B02 F(ab)'2 fragments may be due to antibody damage during peptic digestion and / or increased susceptibility of these fragments to partial denaturation during radiolabeling (Singh, 1989).

Several factors influence the quality of antibody-based tumor imaging (Ghose, et al., 1982b). T / NT ratios are regarded as one of the important determinants (Bradwell et al., 1985). The absolute amount of tumor localized radioactivity, as well as the localization index (LI) are two other important factors that affect the quality of images (Ghose, et al., 1982a and 1982b). In my imaging study, although the intact Dal B02 showed a much higher percentage (% ID / g tissue) of tumor localization than its F(ab)'2 fragments at 24 and 48 hr after administration of radioiodinated antibody preparations, the latter produced better images because of the lower background activity. However, the rapid decrease in the

amount of tumor-associated ^{131}I radioactivity of Dal B02 F(ab)'2 fragment adversely affected the quality of images obtained later. At 72 hr after antibody administration, the absolute amount of radioactivity that localized in the tumor in mice given F(ab)'2 fragment was too low (less than 1.0 % ID / g) to yield tumor images, even though the T / NT ratios were maintained at almost the same level as at 24 and 48 hr. With intact Dal B02, the tumor images were obtained starting at 24 hr and became increasingly clear as the background activity gradually declined. In contrast to its F(ab)'2 fragment, there was still approximately 2.8 % ID of Dal B02 / g tumor at day 8, whereas only 0.2 to 0.4 % ID / g remained in normal tissues (except the blood). This yielded an excellent tumor image. The lower quality of images obtained after administration of ^{131}I-Dal B01 intact antibody is likely to be due to the lower T / NT ratios and LI in tumors, as well as the lower % ID / g tumor obtained with Dal B01, compared to those obtained after administration of ^{131}I-Dal B02. These facts may also explain the failure of Dal B01 F(ab)'2 fragment to yield good images. These results show that the high T / NT ratios, as well as high % ID / g tissue and LI value in tumor improve the sensitivity of tumor images.

Consistent with the observations made during a previous study with an anti-human renal cell carcinoma (RCC) MoAbs in human RCC xenografts (Guha et al., 1991), assay of the serum of mice given radioiodinated Dal B02 or its F(ab)'2 fragment showed that, after i.v. administration of antibody, there was no detectable free radioiodine or iodine-containing small molecules in the circulation up to 120 or 168 hr period of observation. However, the ^{131}I-Dal B02 or ^{131}I-Dal B02 F(ab)'2 fragment in the circulation had lower immunoreactivity compared to the parent preparations used for injection. It is pertinent to state that the use of chloramine T for radiolabeling of Dal B02 and its F(ab)'2 fragment had yielded radioimmunoconjugates that lost their immunoreactivity in the circulation of the tumor bearing nude mice.

The ideal radioiodination method may differ with different antibodies and their intended application (i.e., diagnostic versus therapeutic). However, the labeling procedure should not interfere with antibody activity and the bond between the carrier antibody and the radionuclide should be stable. A variety of methods for radioiodination of proteins are available but none is fully satisfactory (Powe, 1986; Wilbur, 1992). The major problems associated with the currently used procedures for antibody iodination are: (i) the loss of antibody activity during radiolabeling; (ii) the denaturation of antibody which results in altered biodistribution and catabolism; and (iii) in vivo deiodination of antibody. All of these may lead to a decrease in the tumor localization of radioiodine. The Chloramine-T method of radioiodination employs a single-step reaction by directly iodinating the tyrosine residues in the antibody (Fig. 2C). This method is relatively easy and can yield a high iodine incorporation (Osterman, 1984). However, it may also damage antibody activity by iodinating the tyrosine residues in the complementarity determining regions (CDRs) that are required for antigen binding. Furthermore, the iodinated tyrosine is a substrate for multiple dehalogenase enzymes in vivo (Eary et al., 1989; Zalutsky et al., 1985). The Bolton-Hunter method of radioiodination of protein uses N-succinimidyl-para-hydroxyphenylpropionate under mild conditions (Bolton and Hunter, 1973). Instead of tyrosine, radioiodine is incorporated in the lysine residues. However, in this method, the radioiodine is attached to a phenyl group which is structurally similar to iodinated tyrosine residues (Fig. 2B). Thus Bolton-Hunter method based radioiodine labeled antibodies are also subject to deiodination in vivo. There is an ongoing search for methods for radioiodination of antibodies that are not susceptible to dehalogenation (Ali et al., 1988; Zalutsky and Narula, 1988; Wilbur et al., 1991; Wilbur, 1992). A new approach employs a radioiodinated small molecule intermediate that does not have the ortho-iodophenol moiety (e.g., tyrosine). It is expected that an antibody labeled with radioiodine attached to a nonphenolic aromatic ring might not be susceptible to dehalogenase activity. Several such approaches have been developed in recent years (see Introduction section 4.4.3 for a

detailed discussion). A typical example of these approaches is the use of N-succinimidyl para-iodobenzoate (PIB), a product of iodination of N-succinimidyl 4-tri-n-butylstannylbenzoate, as an intermediate to iodinate proteins (Wilbur et al., 1989) (Fig. 2A).

In this study, I have shown that antibody activity was best preserved with Dal B02 (PIB) preparation, whereas the Dal B02 (Chl. T) preparation had the lowest IRF. This finding is contrary to other reports (Wilbur et al., 1989) in which the antibodies radioiodinated using the Chloramine-T method had the same IRF as the antibodies radioiodinated using the PIB method. This is likely to be due to the differences in the antibodies studied.

My results on the stability of radioiodinated Dal B02 after incubation of labeled antibodies in human serum, mouse liver and human thyroid homogenates show that Dal B02 (PIB) preparation was more stable in vitro than Dal B02 (B-H) and Dal B02 (Chl. T) preparations. Dal B02 (PIB) also retained the highest IRF among all the three preparations. Interestingly, no significant deiodination was observed when all the three types of radioiodine labeled antibody preparations were incubated with thyroid homogenate in the presence of DTT and NADPH. This is not consistent with the finding of Wroblewski et al. (1991), who observed a significant deiodination after incubation of ^{131}I-labeled hCG with thyroid homogenate in vitro. Again, this is likely to be due to the differences in the nature of proteins studied.

Biodistribution studies demonstrated that there was no difference in the rate of serum clearance and other pharmacokinetic parameters, among the three types of radioiodinated antibody preparations (Table 16). Since free radioiodine is known to accumulate in the thyroid, preferential uptake of iodine by the thyroid would be indicative of greater antibody deiodination in vivo, provided that the uptake of free radioiodine by thyroid is not blocked

prior to the administration of radioiodinated antibody preparations. As illustrated in Figs. 59 to 64, the paired label experiments showed that the PIB method based linkage reduced thyroid uptake of radioiodine by 3-fold compared to Bolton-Hunter and Chloramine-T method based preparations. Wilbur et al.(1989) reported a 7.5-fold reduction in the uptake of radioiodine by the thyroid 192 hr after injection of PIB based antibody preparations compared to that of Chloramine-T based antibody preparations (1.12% vs 8.38%). By using N-(m-[^{125}I/^{131}I] iodophenyl) bromoacetamide (IPB) as an intermediate, Khawli et al. (1991) reduced the thyroid uptake of radioiodine by about 2-fold compared to the uptake of radioiodine by the thyroid after the administration of Chloramine-T method based preparations (9.3% vs 17.3%). These results and those presented here have shown that the use of an intermediate with radioactive iodine attached to a nonphenolic aromatic ring, markedly reduces dehalogenation of radioiodinated antibodies in vivo.

There was no significant difference in the tumor uptake of radioiodinated Dal B02 at 48 hr and 96 hr after administration of the three different types of preparations. However, a⁺ 168 hr, Dal B02 (PIB) preparation demonstrated a much higher tumor localization than the Dal B02 (Chl. T) preparation. This is consistent with the observation of Zalutsky et al. (1987b) but not with that of Wilbur et al. (1989). These conflicting results may be due to differences in the antibody preparations and tumor models studied. In fact, on comparing the IRF and immunoreactivity of Dal B02 recovered from the serum of xenograft bearing mice, it was found that Dal B02 (PIB) had a higher IRF and immunoreactivity than Dal B02 (Chl. T). It is interesting to note that retention of radioiodine in liver and spleen is higher in mice given Dal B02 (PIB). The nonspecific uptake of Dal B02 (PIB) preparation by organs rich in reticulo-endothelial cells (RES) is a likely explanation (Zalutsky et al., 1987b).

Thus, radioiodination of Dal B02 using the PIB method yielded a protein that retained higher antibody activity, was more stable, and which after i.v. administration showed higher tumo: localization and less nonspecific uptake of radioiodine by the thyroid, as compared to radiolabeled products obtained using the Bolton-Hunter reagent or Chloramine-T. One major disadvantage associated with the PIB method is the low efficiency of radioiodine incorporation, i.e., only about 10 to 15% of the ^{131}I used in the labeling reaction was incorporated into the final product. When therapeutic amounts of MoAb linked ^{131}I activity (e. g, several mCi) are necessary, a large amount of ^{131}I will be needed to radioiodinate carrier MoAbs with the PIB method. This will not only result in considerable waste of the radioisotope, but also cause problems such as radiation hazardous to investigators. Based on these considerations, we chose the chloramine T method for the radioiodination of Dal B02 for radioimmunotherapy. Preliminary study had shown that radiolabeling efficiencies of 65 to 85% could be achieved when chloramine T was used to iodinate Dal B02 with ^{131}I. The problem associated with the accumulation of large amounts of ^{131}I activity in the thyroid of xenograft bearing nude mice could be overcome by giving the mice Lugol's iodine 72 hr prior to the administration of radioiodinated MoAb.

One of the major obstacles in the study of B-cell CLL has been the difficulty in developing a suitable animal model of this disease. This is important for the elucidation of the biology of this leukemia and the evaluation of new therapeutic strategies. In recent years, a number of MoAbs directed against human B-cell malignancies have been produced (Epstein et al., 1987; Pawlak-Byczkowska et al., 1989; Guha et al., 1990). Some of these MoAbs have been evaluated for their tumor localization in vivo in experimental models (Epstein et al., 1985; Buchsbaum et al., 1988; Faguet et al., 1990). A s.c. D10-1 xenograft model has been produced in this laboratory by injecting D10-1 cells subcutaneously in both irradiated and non-irradiated nude mice, and this model has been used to evaluate the therapeutic

efficacy of MTX and chlorambucil (CBL) (Ghose et al., 1988b). In this study, tw ɔ additional reproducible human B-cell CLL models that are very similar to the clinical conditions of the disease were established by inoculating tumor cells i.p. or i.v. into immunodeficient nude or SCID mice.

No ascites or solid tumors developed after i.p. or i.v. injection of D_{10-1} cells in nude mice that were not exposed to TBI. However, TBI was not necessary for the SCID mice, since all SCID mice that received the same number of tumor cells (i.e. $5 \times 10^6 D_{10-1}$ cells per mouse) developed progressive tumors. Also, i.v. injection of D_{10-1} cells in SCID mice led to the development of disseminated tumors in a number of visceral organs and multiple lymph nodes. The tumors in this model was more widely disseminated compared to the distribution of tumors in nude mice. Because TBI brings about a wide range of structural and functional change in the host, such as atrophic changes in the spleen and other lymphoid organs, and may affect tumor growth and spread (Olch et al., 1957; Fidler et al., 1978), xenografts of D_{10-1} cells in SCID mice provides a better model for studying the progression of human B-cell CLL and for evaluating various therapeutic agents for this disease.

It is important to distinguish xenografted tumor cells from tumor cells of host origin. Karyological studies of all tumor cells, irrespective of whether they were recovered from ascites or solid tumors of D_{10-1} cell inoculated mice, revealed that these tumor cells originated from the parent human B-cell CLL cell line D_{10-1}, i.e., they had human chromosomes and possessed the same karyotype as D_{10-1} cells (46, XY, dup (1) (q11 - q32). Membrane immunofluorescence staining with anti-human B-cell CLL MoAbs and anti-human Ig λ chain antibodies further confirmed their D_{10-1} cell origin. These cells also retained their pattern of growth in vitro (i.e., they had same doubling time as the parent D_{10-1} cells) and sensitivity to therapeutic agents like MTX and ADR. These data indicate

that these experimental models are suitable to be used to evaluate different anti-human B-cell CLL therapeutic agents.

After i.v. inoculation of D10-1 cells, all SCID mice but not nude mice developed paralysis of the hind legs at the terminal stage. At present, we have not been able to elucidate the pathogenesis of this condition in this model. Small metastatic lesions in the central nervous system (i.e., brain or spinal cord) may be one explanation.

Several authors have recently reported the establishment of acute human B-cell leukemia (B-ALL) in SCID mice (Kamel-Raid et al., 1989; Ghetie et al., 1990). In one recent study, Jansen et al.(1992) produced a disseminated and fatal leukemia in SCID mice by i.v. injection of the pre-B ALL cell line MALM-6-UM1, and Uckun et al. used this model to successfully evaluate the therapeutic efficiency of an immunotoxin (1992). Several studies have shown that SCID mice injected with lymphoid cells from donors who are EBV positive usually develop fatal B-cell lymphomas of human lymphoid origin (Okana et al., 1990; Cannon et al., 1990). However, to our knowledge, no reproducible experimental models of human B-cell CLL have been reported to date. In one recent report, Kobayashi et al. (1992) transferred B-CLL cells from patients into SCID mice that had received 300 rad TBI. Greater than 97% of these B-CLL cells express CD5 and CD19. No tumor cells survived longer than 5 weeks after i.v. inoculation, whereas tumor cells inoculated i.p. survived at least 10 weeks in these SCID mice. Furthermore, these i.p. tumor inoculated SCID mice developed human B-cell tumors at about 78 ± 19 days after tumor injection. However, these tumors were CD5 negative and were not clonally related to the original CLL cells, indicating that they differ biologically from the original population of injected CLL cells. The authors therefore suggest that these tumors are derived from spontaneous transformation of B cells latently-infected with EBV and are similar to EBV-associated lymphoproliferative syndrome observed after organ transplantation (Zutter et al., 1988),

rather than the engraftment of the inoculated B-CLL cells. As stated, we believe that the establishment of B-cell CLL nude and SCID mice models will provide a good opportunity to study the progress of and to evaluate various new therapeutic agents for human B-cell CLL.

In spite of advances in the field of chemo- or radiotherapy of cancer, most currently used anticancer agents have a low therapeutic index (Holland, 1983), i.e., they damage neoplastic as well as normal proliferating cells at therapeutic dose levels. Because of their specificity, MoAbs directed against tumor-specific or associated antigens are likely to be of help in overcoming this obstacle. Some MoAbs have demonstrated tumoricidal effects themselves. Specific passive immunotherapy of human cancer by injecting MoAbs into cancer patients has been attempted for more than a decade. The majority of such studies have been focused on the treatment of hematological neoplasms. Unfortunately, in most of these studies, the anti-tumor efficacy of MoAbs were observed sporadically and the effect (if any) were brief. However, there are two exceptions, i.e., the use of anti-idiotype MoAbs in nodular B-cell lymphoma and in few cases, with T-cell lymphoma, where a higher rate of response (including CR) have been achieved. To date, the overall rate of response after the administration of MoAbs alone in cancer patients is 5%, 16% and 17%, for CR, PR and minor responses, respectively (Jansen et al., 1989) (see Introduction section 4.1 for a detailed discussion).

MoAbs have several other potential applications in cancer therapy, e.g., they can be used as carriers to specifically deliver radioisotopes (Goldenberg, 1988), chemotherapeutic drugs (Ghose et al., 1987) or toxins (Ramakrishnan, 1992), or to focus tumoricidal effector cells to the tumors (Songsivilai and Lachmann, 1990) (see Introduction section 4). Leukemias and lymphomas are believed the preferred diseases for MoAb-based immunotherapy because of their radiosensitivity and chemosensitivity, the well developed vascularization of

lymphomas and the patient been immunosuppressed, thus having infrequent HAMA responses (Badger and Bernstein, 1986). Different types of cytotoxic agents, such as chemotherapeutic drugs (e.g., MTX and ADR), radioisotopes (e.g., ^{131}I and ^{90}Y) and toxins (e. g., ricin and PE), have been covalently linked to different anti-tumor MoAbs and evaluated for the treatment of these malignant diseases. To date, promising results have been obtained in the therapy of human xenografts in animal models (Wessels, 1990). However, the results obtained from the limited number of clinical trials are less impressive (Britton, 1991; Grossbard, 1992).

The use of MoAbs as carriers of radioisotopes to deliver radiation selectively to tumor cells has been attempted for several decades. In an early study, Ghose et al. (1967) showed that an antibody against the mouse Ehrlich ascites carcinomas (EAC) could be conjugated with enough ^{131}I to prevent the in vivo growth of EAC cells exposed in vitro to the radioiodinated antibody. In another study, the same group demonstrated that the exposure of EAC cells to anti-EAC antibody renders them more sensitive to external X-irradiation (Ghose and Cerini, 1969). All these studies in Dr. Ghose's laboratory led to the first report of targeted radiotherapy in vivo in an animal model (Ghose and Guclu, 1974), in which they demonstrated that the injection of ^{131}I-labeled polyclonal anti-EL4 lymphoma antibodies could prolong the survival and produce cure in a proportion of tumor-bearing mice. In 1980, Order et al. reported some success in treating human hepatoma with ^{131}I-labeled antiferritin antibodies. In recent years, radiolabeled MoAbs have been extensively used to treat various human tumors in animal models as well as in patients. A number of studies have been carried out in several medical centers to treat patients with B-cell malignancies using radiolabeled anti-pan B-cell MoAbs. The response rates in these studies has varied and shown various degree of tumor regression, including CR, PR and minor responses (see Introduction section 4.4.4 for a review).

There is disagreement about the ideal radioisotopes suitable for coupling to anti-tumor MoAb to be used for therapeutic purpose. As stated, because of its commercial availability, ease of protein labeling and its successful use in the treatment of carcinoma of thyroid, ^{131}I is still the choice of most investigators. The doses of ^{131}I used for radioimmunotherapy in nude mouse xenograft models have varied from a total of 230 μCi (administered in two separated doses) (Chiou et al., 1988) to 840 μCi (as single dose) (Gerresten et al., 1992) when linked to intact IgG antibodies, and from 400 μCi (Buchegger et al., 1989) to 3000 μCi (Colapinto et al., 1990) when linked to F(ab)'2 fragments derived from IgG antibodies. In contrast to the finding of Gerresten et al. (1992), who showed that the injection of 840 μCi of ^{131}I linked to intact IgG antibody into a nude mouse caused no other adverse reaction except a 10% loss in body weight , in my preliminary study, the injection of 500 μCi ^{131}I linked to Dal B02 resulted in the death of 100% of D10-1 xenograft bearing nude mice. This was comparable to the finding of Schlom et al. (1990b), in their case, a single dose of 600 μCi of ^{131}I linked to intact IgG killed 60% of the injected nude mice. The high mortality in our study could be due to the fact that the nude mice had received 400 rad of TBI (in order to facilitate the engraftment of human leukemia cells) 5 days before the administration of ^{131}I-labeled Dal B02. The histological findings indicate that these mice died of supervening radiation toxicity, as evidenced by the markedly atrophic changes in spleen and bone marrow.

In this study, experiments were carried out to determine the anti-tumor effect of ^{131}I labeled Dal B02 or its F(ab)'2 fragment in three different types of human B-cell CLL xenograft models in nude or SCID mice. Based on the observation described above, in both the i.p. and i.v. models, all xenograft bearing mice were treated with a single injection of reduced does of 300 μCi (but not 500 μCi) of ^{131}I when linked to intact IgG antibody. When F(ab)'2 fragment was used as carrier, the ^{131}I dose remained at 500 μCi. In the s.c. tumor model, all mice were given a total dose of 600 μCi of ^{131}I linked to intact IgG antibody or

1000 µCi of ^{131}I linked to F(ab)'2 fragment, but these total dose was administered in two dose fractions.

In the s.c. model, 600 µCi of ^{131}I linked to Dal B02 was given to each xenograft bearing nude mice. To avoid lethality, this total dose was divided into two fractions. Most investigators usually give the second injection of radioiodinated antibody between 7 to 10 days after the first injection (Schlom et al., 1990b), i.e., when the total body activity decreased to a level below 15 µCi/mouse. In this study, it took 15 days after the administration of 300 µCi of ^{131}I linked to Dal B02 for the total body radioactivity to be reduced to a level below 15 µCi/ mouse, and therefore, the second injection was given to these mice 16 days after the first injection. This treatment resulted in complete cure of the s.c. xenografts of D10-1 cells in 3 of 4 mice. There was a significant delay in progressive tumor growth in the other mouse. This latter mouse (mouse No.4) showed a much faster rate of clearance in total body radioactivity after i.v. administration of radiolabeled Dal B02. This rapid clearance of radioactivity might have contributed to the reduced anti-tumor activity of the radioiodinated Dal B02 in this mouse.

Treatment with ^{131}I labeled Dal B02 F(ab)'2 fragment caused reduction in tumor size and significant delays in the resumption of progressive tumor growth in all the 4 treated mice. However, no complete cure was achieved. All the tumors resumed their fast rate of growth once the treatment stopped. Measurement of total body radioactivity in these mice showed that the clearance of radioactivity from the mice given radiolabeled F(ab)'2 fragment was much faster compared to mice given radiolabeled intact Dal B02. As discussed in the Introduction section 4.2.2, although the use of F(ab)'2 fragments may have some advantages in tumor imaging, the intact MoAb may be better carrier in radioimmunotherapy. As already stated, the absolute amount of radioactivity that localizes in tumors is much higher for intact antibody than its F(ab)'2 fragment. Also, the increased

exposure of tumors to antibody-linked radioisotopes, due to the longer half-life of tumor localization of intact antibody, may provide an enhanced therapeutic effect. As shown in Table 14, the intact Dal B02 indeed had a 5 to 6-fold longer serum half-life, as well as 5 to 6-fold larger AUC compared to its F(ab)'2 fragment. Furthermore, the percentages of the injected dose of radioactivity that localized in per g of tumors were respectively 13.5%, 7.3% and 2.8% at 48, 96 and 168 hr after i.v. administration of radiolabeled intact Dal B02. On the o..ier hand, the percentages of the injected dose that localized in per g of tumors were respectively 2.33%, 1.33%, 0.825% and 0.2% at 24, 48, 96 and 120 hr after i.v. administration of radiolabeled Dal B02 F(ab)'2 fragment. These localization data suggest that when labeled with ^{131}I, intact Dal B02 MoAb is able to deliver a much higher dose of radiation to targeted D10-1 xenografts compared to its F(ab)'2 fragment.

Iodine-131 labeled non-specific IgG1 also demonstrated a substantial anti-tumor activity. This is likely to be due to radiation delivered to the tumor by the radiolabeled IgG1 that localized in the tumor and surrounding tissues. Our localization studies revealed that 1.31%, 0.82% and 0.33% of the injected dose of radioactivity linked to non-specific IgG1 localized in per g of D10-1 xenografts respectively at 48, 96 and 168 hr after i.v. antibody administration. These % ID / g tumor were approximately 10-fold lower than the percentage of specific Dal B02 localized in the tumors. My results of exposure of D10-1 cells to external gamma radiation had shown that D10-1 cells are very sensitive to gamma radiation. A radiation dose of as low as 200 rad was able to significantly inhibit the growth of D10-1 cells, and a radiation dose of 600 rad completely stopped the proliferation of the cells (Fig. 107). This high radiosensitivity of D10-1 cells might account for the tumor inhibition caused by ^{131}I labeled non-specific IgG1.

Unlabeled Dal B02 did not show any anti-tumor effect at this low dose level (50 µg/mouse). Furthermore, a mixture of unlabeled Dal B02 and ^{131}I labeled non-specific

IgG₁ did not add to the tumor inhibitory effect of ^{131}I labeled non-specific IgG₁. All these

results indicate that the superior therapeutic efficacy of ^{131}I labeled Dal B02 is due to the

targeted delivery of radioactivity to tumors by the specific binding of Dal B02 to tumor

associated antigen, and the change in pharmacokinetics of the radioisotope (e.g. increased

half-life) because of the linkage of ^{131}I to a macromolecular carrier like IgG, but not to the

radiosensitization of the tumor cells by Dal B02. Although the radiation dose delivered to

tumors by different types of radiolabeled antibody preparations was not determined in this

study, our results suggest a direct correlation between the dose of radiation delivered to

tumors (i.e., % ID of radioactivity that localized in the tumors) and the effectiveness of the

radiolabeled antibody preparations.

Unlike the observation in the s.c. model, i.e., 50 μg of unlabeled Dal B02 had no tumor

inhibitory effect, administration of 50 μg of unlabeled Dal B02 in the i.p. and the i.v.

models showed a significant anti-tumor effects. An equal anti-tumor effect (i.e., long-term

tumor free survival of 4 out of 5 mice) was obtained with 50 μg of Dal B02, either alone or

labeled with 300 μCi of ^{131}I, in the i.v. model. In the i.p. model, treatment with

unlabeled Dal B02 resulted in long-term tumor free survival of 3 of 6 mice, compared to

long-term tumor free survival of 5 of 6 mice treated with Dal B02 labeled with 300 μCi

^{131}I. It is possible that the difference in the therapeutic effectiveness of unlabeled Dal B02

in these three models is due to the differences in the tumor burden. Although in all of these

three models, each nude mouse was initially given 5 x 10⁶ D₁₀-₁ cells s.c., i.p., or i.v.,

the treatment in the i.p. and the i.v. models started at 48 to 72 hr after tumor inoculation,

while in the s.c. model, the treatment was not given to the mice until a period of 10 days

after tumor inoculation, i.e., when a palpable solid tumor was seen. It is clearly that the

tumor burden in the s.c. model is much heavier than that in the i.p. and the i.v. models.

Two other observations in this study further confirm the influence of tumor burden on the

therapeutic effectiveness of unlabeled Dal B02. First, a single dose of 50 μg of unlabeled

Dal B02 could not stop or even delay the development of ascites tumors in nude mice if the mice were inoculated i.p. with 15×10^6 D10-1 cells (instead of 5×10^6 D10-1 cells). Second, a single dose of 50 μg of unlabeled Dal B02 could not stop the development of solid tumors (in the back of nude mice) if the treatment was given to the mice 7 days (instead of 3 days) after i.v. inoculation with 5×10^6 D10-1 cells. Another possibility that may account for the difference in the therapeutic efficacy of unlabeled Dal B02 in these three models is the difference in the accessibility of the inoculated tumor cells to the subsequent administered Dal B02. The accessibility is clearly not a problem in both the i.p. and the i.v. models since both the tumor cells and the MoAb were given to the mice followed the same route (i.e., intraperitoneally or intravenously). In the s.c. model, (with a solid tumor of size of 60 mm^3 to 200 mm^3) additional factors such as extravasation and penetration of MoAb in the tumor tissue may significantly reduce the accessibility of the xenografted tumor cells to i.v. administered Dal B02 (see Introduction section 4.2.3 for a detailed discussion).

As discussed in the Introduction section 4.1.3, unmodified anti-tumor MoAbs can inhibit the growth of appropriate tumors via several different mechanisms, e.g., ADCC, CDC, anti-growth factor receptor and anti-idiotype effects. We had demonstrated that Dal B02, an IgG1, did not induce a strong ADCC or CDC in the presence of effector cells (i.e., splenic cells or peritoneal macrophages) from nude mice or rabbit complement (Tables 22 to 24). Therefore, it is likely that effector mechanism (s) oth : ., ... ADCC and CDC have also contributed to the anti-tumor effect of unmodified Dal B02.

Several observations revealed that the tumor inhibitory effect of ^{131}I labeled Dal B02 was not solely due to the effector mechanism (s) of unlabeled MoAb: (i) as stated, when nude mice were inoculated i.p. with 15×10^6 D10-1 cells, a single injection of 50 μg of unlabeled Dal B02 could not stop or even delay the development of ascites tumors in these mice. On

the contrary, 50 µg of Dal B02 when labeled with 300 µCi ^{131}I produced 3 long-term tumor free survival out of 5 mice; (ii) when the treatment was given 7 day after i.v inoculation of 5 x 10⁶ D10-1 cells, 4 of 5 mice treated with unlabeled Dal B02 (50 µg per mouse) developed tumor and died within 8 weeks (the other one died of tumor at 150 days) after tumor inoculation, whereas in the group treated with the same dose of Dal B02 linked to 300 µCi ^{131}I, all the 5 mice survived longer than 150 days. Although 2 of these mice developed tumor within 8 weeks of tumor inoculation in this group, both tumors regressed spontaneously within 120 days after tumor inoculation.

In contrast to the intact Dal B02, Dal B02 F(ab)'2 fragments, either used alone or radiolabeled with ^{131}I, did not demonstrate any significant anti-tumor effect in both the i p and the i.v. models. There may be several explanations for the ineffectiveness of the F(ab)'2 fragment in this study. Firstly, as stated, Dal B02 F(ab)'2 fragment was cleared much faster from tumor bearing nude mice than intact Dal B02. This resulted in much less of accumulation of radioactivity in the tumors, as well as shorter period of retention of tumor-localized radioactivity, compared to those obtained with intact antibody. Therefore, with the doses of radioactivity and the schedules used in this study, the F(ab)'2 fragment was not able to deliver tumoricidal dose of radiation to tumor cells. Secondly, my results show that unmodified intact Dal B02 itself has a considerable anti-tumor effect. Therefore, the depletion of Fc portion of the IgG molecule might have contributed to the decreased effectiveness of Dal B02 F(ab)'2 fragment. It is known that the Fc portion of antibody molecules usually plays an important role in the anti-tumor effect of unmodified intact MoAbs. The importance of the Fc portion is two-fold: it recruits the effector mechanisms of tumor host (e. g., ADCC and CDC) and prolongs the half-life of the antibody preparation. The depletion of Fc portion renders F(ab)'2 fragment unable to induce ADCC and CDC. The short half-life of F(ab)'2 fragment not only decreases the radiation dose delivered to

tumors (provided that the fragment was radiolabeled), but also reduces the chance by which the fragment recruits host's effector mechanisms to eradicate the tumors.

In SCID mice, 300 μCi of ^{131}I linked to either Dal B02 or the non-specific IgGi killed all treated mice within 2 weeks. It has been shown that SCID mice are approximately 2 to 3-fold more sensitive to radiation than normal mice (Fulop and Phillip, 1986). In our study, advanced atrophic changes were observed in bone marrow and spleen of these mice, indicating that they died of radiotoxicity.

A prolonged survival of D10-1 cell inoculated SCID mice was obtained in the groups treated with unlabeled Dal B02, in both the i.p. and the i.v. models. However, no cure was achieved. The mechanisms of tumor inhibition caused by Dal B02, as discussed above, is not clear. Assay of ADCC in vitro using Dal B02 and splenic cell or peritoneal macrophages from SCID mouse showed that SCID mice had higher splenic NK cell activity as well as higher peritoneal macrophage activity compared to nude mice (Tables 22 and 23). However, the anti-tumor activity of Dal B02 demonstrated in SCID mouse models was much lower than that in nude mouse models. It is known that SCID mice have normal NK cell activity (Dorshkind et al., 1985) and normal number of macrophages. The phenotype of these macrophages are the same as in the immunocompetent parent mice, and these macrophages response appropriately to exogenous T cell-derived stimuli in vitro (Bancroft et al., 1991). However, in contrast to macrophages in immunocompetent mice, the macrophages in SCID mice are only responsive to bacterial antigens, but not to immunogenic proteins (Bancroft et al., 1991). Thus, the strong ADCC effect induced by SCID macrophages and Dal B02 is likely to be the reflection of activation of the peritoneal macrophages of SCID mice by Frenud's adjuvant, the agent used to prime the SCID mice at 24 hr prior to collection of peritoneal macrophages. Therefore, the strong ADCC effect induced by adjuvant-stimulated SCID macrophages in vitro may not reflect the anti-tumor

potency of these cells in vivo. It is possible that in D10-1 cell inoculated SCID mice, the macrophages were not appropriately activated by the administration of Dal B02. Furthermore, due to the lack of both T and B lymphocytes, the immunoregulatory network in SCID mice may be too weak to mount an efficient immune response to destroy the inoculated tumor cells.

2. MoAb-Based Targeted Chemoimmunotherapy of Human B-Cell Chronic Lymphocytic Leukemia in Experimental Models

MoAbs may also be used as carriers to specifically deliver chemotherapeutic agents to tumors. A number of chemotherapeutic agents have been conjugated to MoAbs. These agents include alkylating drugs such as chlorambucil (Ghose et al., 1977; Smyth et al., 1988) and mitomycin (Noguchi et al., 1991), anthracyclines such as daunomycin (Arnon et al., 1982; Dillman et al., 1988) and adriamycin (Braslawsky et al., 1990; Shih et al., 1991), anti-metabolites such as methotrexate (Kulkarni et al., 1981; Kanellos et al., 1985; Pimm et al., 1988a) and 5-fluorouracil (Hurwitz et al., 1985), vinca alkaloids such as vindesine and vinblastine (Rowland et al., 1985; Starling et al., 1991), and cis-platium (Schechter et al., 1987).

MTX was the first drug to be used for conjugation to anti-tumor antibodies (Mathe et al, 1958). Because of its wide clinical use and well elucidated mode of action, structure-action relationship, and mechanisms of toxicity and drug resistance (Johns and Bertino, 1982), MTX has been used widely for the preparation of antibody-drug immunoconjugates (Ghose et al., 1983a; Ghose et al., 1988a). Antibody-MTX conjugates have been produced using several different covalent linkages. Ghose, et. al. (1988a) have evaluated several methods of linkage of MTX to anti-tumor antibodies. These methods include coupling

using either amide linkages via water-soluble carbodiimides (EDCI), reactive intermediate derivatives of MTX (e.g., the active ester intermediary formed by reaction with N-hydroxysuccinimide), or a mixed anhydride reaction, or via hydrazide linkages. Conjugates retaining drug and antibody activity were produced using EDCI, active esters, and hydrazides. However, the hydrazide method was more effective as regard to retention of antibody activity and yield of conjugated protein. In my study, both the active ester and hydrazide methods were used to conjugate MTX to Dal B01 or Dal BG2 MoAb. The retention of drug and antibody activities and the cytotoxicity of all the four conjugates were compared.

Several factors may contribute to the reduction of drug activity after coupling to MoAb. These factors include: (i) steric hindrance caused by the linkage of the drug to a relatively large IgG molecule; (ii) the use of functional group(s), which are required for the activity of the drug, for conjugation of the drug to antibody; and (iii) damage of drug molecule during the coupling procedure. Retention of MTX activity in conjugates can be determined by a method of assay based on the inhibition of its target enzyme DHFR. In this study, the DHFR inhibitory capacity of all four conjugates were 15 - 20% of that of free MTX. This loss of ability to inhibit DHFR in an in vitro assay system may not necessarily indicate loss of anti-tumor activity in vivo, since catabolism in vivo may give products that regain drug activity. If catabolism occurs in the milieu of the target tumor, the conjugate may display full cytotoxic potential of MTX towards tumor cells in culture or in tumor-bearing animals. Kralovec et al. (1989b) have demonstrated that incubation of a MoAb-MTX (produced via a hydrazone linkage) with cell homogenate led to the release of free MTX with full DHFR inhibitory capacity of the parent drug. Complementary to this report, Ghose et al. (1988a) showed a fraction of catabolic fragments of antibody-MTX conjugate resulting from the action of cell homogenate gave DHFR inhibition approximately equal to the conjugate from which the fraction was derived, i.e., the DHFR inhibitory capacity of the catabolic

fragments was 5 to 6 times weaker than that of free MTX. Thus, the restoration of DHFR inhibitory capacity of MTX when the drug is delivered to tumor cells as antibody-MTX conjugate depends on whether the catabolism of antibody-MTX conjugates by the tumor cells will release free MTX or MTX-containing small fragments.

The causes of the loss of antibody activity in conjugates include (i) interference with the antigen binding site by the incorporated drug; (ii) induction of conformational changes in antibody molecule as a result of drug loading leading to interference with antigen binding; and (iii) denaturation of the antibody during the conjugation procedure. In this study, MoAb-MTX conjugates have been produced by linking MTX molecules either randomly to IgG molecule or site-specifically to the carbohydrate residues of the IgG molecules. Earlier studies had shown that when MTX was linked to antibodies randomly via direct linkage, there was a rapid decline in antibody activity when the molar incorporation of MTX exceeded 10 (Kulkarni et al., 1985). It was expected that better retention of antibody activity would probably be achieved by linkage of MTX to antibody via carbohydrate residues because the carbohydrate residues are infrequent in the antigen binding sites of antibody (Beale and Feinstein, 1976). However, in this study, the use of carbohydrate residues for conjugating MTX to Dal B01 or Dal B02 did not yield conjugates with incorporation of more than 7 molecules of MTX per molecule of IgG. This was not greater than those achieved with the active ester method. For this level of MTX incorporation, both the active ester and the carbohydrate residue based methods of linkages yielded conjugates that retained good antibody activity compared to their parent unconjugated MoAbs.

Conjugation of cytotoxic drugs to MoAbs can often result in a substantial reduction of drug activity. Quantitative cytotoxicity study carried out by Endo et al. (1987) with MTX conjugated to MoAbs showed 5 to 10-fold reduction in the cytotoxicity of conjugates compared to that of free drug. However, some exceptions were also observed. For

example, Garnett et al. (1983) and Embleton (1986) reported that MoAb-HSA-MTX conjugates were more toxic to target osteosarcoma cells than free MTX. In my study, Dal B01-MTX and Dal B02-MTX conjugates showed respectively 30-fold and 5-fold reduction in their cytotoxicity to D10-1 cells compared to free MTX in a 72 hr continuous exposure assay. However, in a 6 hr pulse exposure assay, the Dal B02-MTX conjugate was found to be slightly more potent than free MTX, whereas Dal B01-MTX conjugate was 3-fold less potent than the free drug. The conjugates were much less toxic to MOLT-3 cells than to D10-1 cells, despite the fact that MOLT-3 cells are more sensitive to free MTX. Furthermore, the cytotoxicity of both the conjugates to non-target MOLT-3 cells was much lower than that of free MTX. For example, in the 6 hr pulse exposure assay, Dal B01-MTX conjugate was 100-fold less potent and Dal B02-MTX conjugate was 20-fold less potent than the free drug to non-target MOLT-3 cells. The selectivity ratios of cytotoxicity of the conjugates to D10-1 cells over MOLT-3 cells were as high as 40 to 50, indicating a very specific cytotoxicity of the conjugates to antibody reactive cells. Since in this pulse exposure assay, cells were washed thrice after exposure to test agents for 6 hr, only cell surface bound and endocytosed drug (free or conjugated to MoAbs) was retained during the subsequent period of incubation. These results suggest that the cytotoxicity of Dal B01-MTX and Dal B02-MTX conjugates to D10-1 cells was a MoAb-based specific event. This specific cytotoxicity of conjugates to target cells is likely due to (i) delivery of larger amounts of MTX to target cells when MTX is conjugated to MoAbs; (ii) longer retention of MoAb-linked MTX by target cells (either on the cell surface or inside cells); and (iii) slow, prolonged release of MTX from the surface bound or endocytosed conjugates, rendering it into a sustained release dosage form.

The change in the cytotoxicity of MTX after conjugation to MoAbs is probably due to altered mechanisms of uptake of the MoAb coupled drug. Free MTX enters cells mainly by a single high-affinity influx mechanism that probably depends on the function of specific

intramembrane protein(s) (see Introduction section 4.3.3). Several studies have shown that MoAb-MTX conjugates are endocytosed by target cells via receptor-mediated endocytosis and transported to the lysosomal compartment where digestion of the conjugates releases free drug. The free drug then diffuses to its site (i. e., cytosol) of action, i.e., bind to its target enzyme DHFR (Garnett and Baldwin, 1986). Treatment of tumor cells with ammonium chloride and thiol proteinase inhibitors (e. g., leupeptin and LRE 64) reduces the cytotoxicity of MoAb-MTX conjugates, while the same treatment had no effect on the cytotoxicity of free MTX (Garnett and Baldwin, 1986; Endo et al., 1987). These results indicate the involvement of lysosomal degradation of the MoAb-MTX conjugates for their cytotoxic action.

My study shows that the uptake of free MTX by D10-1 cells was more rapid than its uptake by MOLT-3 cells. The uptake of MTX by D10-1 cells reached the plateau (i.e., maximum uptake) at 10 min of incubation, while the uptake of MTX by MOLT-3 cells reached plateau at 45 min. However, the maximum amount of cell associated MTX at the end of incubation was higher in MOLT-3 cells than in D10-1 cells. The Km values of uptake of free MTX normally vary with the cell lines investigated. For exan. ple, Goldman et al. (1968) observed the Km value of uptake of MTX to be 15 μM for L1210 cells, while Uadia et al. (1985) reported the Km value of uptake of MTX to be 5 μM for M21 cells. In this study, it was found that the Km values of uptake of MTX were 8.37 μM for D10-1 cells and 8.52 μM for MOLT-3 cells. In the efflux study, it was found that D10-1 cells retained more MTX than MOLT-3 cells did after efflux in drug free medium, indicating that D10-1 cells have a higher level of intracellular DHFR than MOLT-3 cells. These features of D10-1 cells, i.e., lower uptake of MTX and higher level of intracellular DHFR (compared to that of MOLT-3 cells), suggest that D10-1 cells would be less sensitive to free MTX than MOLT-3 cells. This was confirmed in cytotoxicity assay. As shown in Table 18 , the IC50 value of MTX for D10-1 cells was about 3-fold higher than the value for MOLT-3 cells.

The amount of uptake of MoAb linked MTX by tumor cells after incubation with MoAb-MTX conjugates depends upon: (i) specific binding of the conjugates to tumor antigen(s) on cell surface and subsequent endocytosis; (ii) non-specific binding to cell surface and endocytosis by mechanisms independent of specific transport carriers, e.g., pinocytosis; (iii) efflux of free MTX or MTX containing small fragments produced by intracellular catabolism, and (iv) catabolic release of free MTX or MTX containing fragments mediated by proteolytic enzymes on the surface of tumor cells. From the uptake studies with Dal B01-MTX conjugate and Dal B02-MTX conjugates, it can be seen that the uptake of MoAb linked MTX by target D_{10-1} cells was much higher than the uptake of free MTX. The uptake of Dal B01 or Dal B02 linked MTX was a MoAb-based specific process, since the uptake of the MoAb linked MTX by target D_{10-1} cells was much higher than the uptake by non-target MOLT-3 cells, although MOLT-3 cells took up more MTX than D_{10-1} cells when incubated with free MTX. Also, the difference between the amount of Dal B01 or Dal B02 linked MTX taken up by D_{10-1} cells at 4°C and 37°C was not as significant as the difference between the amount of free MTX taken up by D_{10-1} cells at 4°C and 37°C, indicating the mechanism of uptake of MoAb linked MTX is different from that of free MTX. The higher uptake of MTX when linked to anti-tumor MoAbs has also been reported by several investigators with the use of different MoAbs and other tumor cell lines (Uadia et al., 1983; Garnett and Baldwin, 1986; Endo et al., 1987). It is worth noting that non-target MOLT-3 cells also took up a substantial amount of Dal B02 linked MTX. This is likely to be responsible for the toxicity of the conjugates towards MOLT-3 cells observed in proliferation inhibition assays.

In my study, the IRF of the MoAbs can be correlated with the uptake of MoAb linked MTX. The uptake of Dal B02 linked MTX by D_{10-1} cells was approximately 3 to 4 times higher than the uptake of Dal B01 linked MTX. As stated, Dal B02 and Dal B01 have

approximately the same number of binding sites on D10-1 cells with approximately the same Ka of binding, but the IRF of the Dal B02 preparation was about 2.5-fold higher than that of Dal B01 preparation. These results indicate that MoAb preparations with higher IRF are likely to lead to the binding of a larger proportion of MoAb-MTX conjugates and hence higher uptake of MoAb linked MTX by target cells.

Release of Dal B01 or Dal B02 linked MTX from D10-1 cells differed from that of free MTX. There was a rapid efflux of MTX from D10-1 cells that were loaded with free MTX. The efflux stopped at about 10 min after incubation at 37°C in efflux medium with a steady state of intracellular MTX, i.e., approximately 9 pmol MTX/mg protein. To investigate the release of [^{3}H]-MTX from D10-1 cells that were loaded with Dal B01-[^{3}H]-MTX or Dal B02-[^{3}H] MTX conjugate, the cells were first incubated with either of the conjugate for 2 hr at either 4°C or 37°C. The conjugate-loaded cells were then reincubated at 37°C in the efflux medium with or without the presence of a large excess free MoAb. The efflux of [^{3}H]-MTX activity from D10-1 cells that were loaded with Dal B01-[^{3}H]-MTX or Dal B02-[^{3}H]-MTX conjugate depended on the temperature at which the cells were initially incubated with the conjugates. Like the efflux of free MTX, the release of [^{3}H]-MTX activity from conjugate-loaded D10-1 cells in the absence of any cold free MoAb stopped at about 10 to 15 min. The release of [^{3}H]-MTX activity form the cells that were initially incubated with the conjugates at 37°C was faster than the release of [^{3}H]-MTX activity from cells that were initially incubated with the conjugates at 4°C. This may indicate that a small proportion of cell surface bound Dal B01-[^{3}H]-MTX or Dal B02-[^{3}H]-MTX conjugate was internalized into the cells after incubation at 37°C for 2 hr. The increased rate of release of [^{3}H]-MTX activity from these cells is likely to be the reflection of efflux of free [^{3}H]-MTX or [^{3}H]-MTX-containing small fragments resulting from the intracellular catabolism of the conjugates. The steady state levels of cell-associated [^{3}H]-MTX activity at the end of efflux was much higher in cells incubated with MoAb-MTX conjugates (i.e., 30

times higher for Dal B01-MTX conjugate and 100 times higher for Dal B02-MTX conjugate) than that in cells incubated with free MTX.

To ascertain whether cell associated MoAb-MTX conjugates were cell surface bound or were endocytosed, Endo, et. al. (1987) treated the conjugate-loaded cells with a low pH buffer to remove cell surface bound conjugate. However, this method may introduce an error in the determination of the endocytosed drug because the low pH buffer might damage the cells and make the cells more permeable to cell surface bound conjugate. In my study, a large amount of cold free MoAb was used to displace cell surface bound MoAb-MTX conjugates. When the cells were initially incubated with Dal B01-MTX or Dal B02-MTX conjugates at 4°C for 2 hr, over 85 - 87% of the initial cell bound [^{3}H]-MTX activity could be displaced by appropriate cold free MoAbs. The uneluted [^{3}H]-MTX activity (i.e., about 13 to 15% of initial cell associated activity) after this treatment could have been the result of resistance of cell surface bound conjugates to this treatment for elution rather than the internalization of the conjugates. When the cells were initially incubated with the conjugates at 37°C for 2 hr, the percentage of [^{3}H]-MTX activity that remained associated with cells after displacement was about 5% higher for both the conjugates than the percentage of cell associated [^{3}H]-MTX activity in cells that were initially incubated with the conjugates at 4°C. My immunogold studies have shown that about 8.8% of Dal B01-Au and 17.1% of Dal B02-Au complexes were internalized by D10-1 cells after incubation at 37°C for 2 hr (Table 13). Therefore, the results obtained here suggest: (i) internalization of a small proportion of cell surface bound Dal B01-MTX or Dal B02-MTX conjugates after incubation at 37°C for 2 hr; and (ii) intracellular catabolism of internalized Dal B01-MTX or Dal B02-MTX conjugates and subsequent efflux of free [^{3}H]-MTX and/or [^{3}H]-MTX-containing small fragments.

In this study, we did not determine the absolute amount of intracellular MTX after the D10-1 cells were exposed to various extracellular concentrations of Dal B01-MTX or Dal B02-MTX conjugates at 37°C for 6 hr. Studies with immunogold complexes have revealed that about 15% of cell surface bound Dal B01 or Dal B02 was internalized after incubation at 37°C for 6 hr (Table 13). This allowed us to estimate the amount of intracellular MTX after the D10-1 cells were exposed to Dal B01-MTX or Dal B02-MTX conjugates at 37°C for 6 hr. For example, after incubation with an extracellular concentration of conjugates containing 5 μM of MTX at 37°C for 6 hr, the D10-1 cell associated [^{3}H]-MTX activity was 1047 pmol MTX/mg cell protein for Dal B01-MTX conjugate and 3110 pmol MTX/mg protein for Dal B02-MTX conjugate (Fig. 80). Assuming that 15% of these conjugates were endocytosed (as observed in Results section 1.8.6 with gold particle-complexed Dal .J1 or Dal B02), it can be calculated that the amounts of endocytosed conjugates are 157 pmol MTX/ mg protein for Dal B01-MTX conjugate and 467 pmol MTX/mg protein for Dal B02-MTX conjugate. From the study on the uptake of free MTX under the same conditions, it was found that uptake of free MTX by D10-1 cells was approximately 26.5 pmol MTX/mg protein. It could be seen that the uptake of MoAb linked MTX by D10-1 cells was 6-fold higher for Dal B01-MTX conjugate and 18-fold higher for Dal B02-MTX conjugate than the uptake of free MTX. However, in the cytotoxicity study using the 6 hr pulse exposure assay, it was observed that the IC50 value of Dal B01-MTX conjugate (2.15 μg/ml, i.e., 3.9 μM) was approximately 3-fold higher than that of free MTX (0.775 μg/ml, i.e., 1.4 μM), whereas the IC50 value of Dal B02-MTX conjugate (0.445 μg/ml, i.e., 0.81 μM) was about 1.7-fold lower than that of free MTX. It was thus clear that the cytotoxicity of Dal B01 or Dal B02 linked MTX was lower than that of free MTX. As stated, for its cytostatic effect, MTX has to bind to its target enzyme DHFR and inhibit the conversion of dihydrofolic acid to tetrahydrofolic acid. For inhibition of cell proliferation, the intracellular concentration of MTX has to exceed the level of DHFR. The binding ability of MoAb-MTX conjugate to DHFR might be much lower than that of free MTX due to the

steric hindrance caused by the carrier IgG molecule (Ghose et al., 1988). In this study, this was confirmed by DHFR inhibition assay in vitro in a cell free system. The IC$_{50}$ values for inhibition of DHFR of both the MoAb-MTX conjugates were about 5 to 6 times higher than that of free MTX. Early studies have also shown that, to restore the full inhibitory activity of MTX, endocytosed MoAb-MTX conjugates have to be cleaved in the lysosomal compartment to release free MTX or MTX-containing small fragments (Garnett and Baldwin, 1986; Endo et al., 1987; Ghose et al., 1988). Therefore, the lower potency of the Dal B01-MTX and Dal B02-MTX conjugates compared to the potency of free MTX might be due to both the inefficiency of the binding of the conjugates to DHFR and the inefficiency of the cleavage process. One fact that should be considered is that the above calculations on the amount of intracellular MoAb-MTX conjugates did not consider the efflux of intracellularly released free MTX or MTX-containing small fragments that could result from the catabolism of the internalized conjugate. Thus, the absolute amounts of intracellular MTX might be lower than those estimated based on the above calculation. Therefore, the above postulations are tentative and should be considered with cautions.

As stated, both Dal B01 and Dal B02 MoAbs are poorly internalized after their binding to the surface of target D$_{10-1}$ cells. It was thought that these two MoAbs were not likely to yield effective immunoconjugates with those drugs that need internalization to exert their cytotoxic effect. Results regarding the uptake and cytotoxicity of Dal B01-MTX and Dal B02-MTX conjugates discussed above support this hypothesis. I therefore used the chemotherapeutic agent ADR (a drug that is known to exert its cytocidal effect at least partly via its actions on the plasma membrane) to prepare Dal B01 and Dal B02 immunoconjugates (see Introduction section 4.3.4 for the detailed description of the mechanisms of action of ADR).

Several linkage methods have been used to couple ADR to antibodies. Most of these methods utilize the amino sugar moiety of ADR for coupling (Hurwitz et al. 1975). ADR has been linked to antibodies directly using either carbodiimide mediated linkage of the amino sugar to a carboxyl group on antibodies (Hurwitz et al. 1975; Arnon et al, 1982), or by cross-linking amino groups of the drug and antibody using glutaraldehyde (Hurwitz et al. 1975; Levy et al., 1975), or indirectly with the use of polyaldehyde dextrans as an intermediate carrier (Tsukada et al., 1981; Pimm et al., 1982). Unfortunately, most of these methods yielded MoAb-ADR conjugates with significant loss of drug activity. It is known that the amino sugar of adriamycin was involved in its binding to DNA (Neidle, 1979). Modification of the amino sugar of adriamycin has been shown to decrease the cytotoxicity of the drug (Yamamoto et al., 1972; DiMarco, 1975). Therefore, to prepare an active MoAb-ADR conjugate, the amino sugar of the drug should preferably, not be disturbed by the coupling procedure, or alternatively, the conjugate should be able to release free ADR from the carrier MoAb after endocytosis. The low retention of drug activity of MoAb-ADR conjugates prepared using the amino sugar moiety of the drug might result from the difficulty in the release of free ADR from the carrier MoAb due to steric hindrance preventing access of intralysosomal peptidases to the linkage between the drug and the carrier MoAb (Trouet et al., 1982). As discussed in the Introduction section 4.3.2, the introduction of a cis-aconityl group as an acid-sensitive spacer (Yang and Reisfeld, 1988) or the use of hydrazone bond (Greenfield et al., 1990) between ADR and the MoAb alleviates this problem by providing a reversible linkage, i.e., the drug is released from the spacer group unaltered and, hence without loss of its cytotoxic potency, when in the acidic environment of the lysosome (Shen and Ryser, 1981). Once released inside the target cells, the ADR molecule is small enough to exit the lysosomal compartment into the cytosol and thus exert its cytotoxic effects. An alternative approach to couple ADR to MoAbs without disturbing the amino group of the drug is to use other functional group(s) of the drug molecule, e.g., C13 or C14 moiety, as sites of attachment to MoAbs. Using this approach,

a number of investigators have reported the production of several different MoAb-ADR conjugates with high in vitro and in vivo activity (Gallego et al., 1984; Pietersz et al., 1988; Greenfield et al., 1990; Braslawsky et al., 1990).

In this study, four different types of MoAb-ADR conjugates were produced. Both antibody and drug activities of these various conjugates were compared in vitro before their evaluation in vivo. ADR was coupled to Dal B01 or Dal B02 by the following different methods: (i) via its amino sugar group with the use of a CAA spacer (MoAb-CAA-ADR); (ii) via its C13 moiety using a hydrazone bond (MoAb-C13-ADR); (iii) site-specifically to carbohydrate residuals in the carrier MoAb with the use of dextran T-40 as an intermediate carrier via the C13 moiety of ADR (MoAb-Dex-ADR (ss)); and (iv) non-site specifically with the use of dextran as an intermediate carrier via the amino sugar group of ADR (MoAb-Dex-ADR (nss)). In the last case, cyanoborohydride was used to stabilize the Schiff's bases formed between ADR and dextran and between dextran and MoAb (see Fig. 4 for the schemes of the synthetic pathways for the production of these conjugates).

Dal B01-CAA-ADR and Dal B02-CAA-ADR conjugates were much less potent to both target D10-1 and non-target MOLT-3 cells than free ADR. Furthermore, no selective cytotoxicity was observed with these two conjugates. Our results are not in agreement with those reported by Dillman et al. (1988) and Yang and Reisfeld (1988). Dillman et al observed that an anti-CD5 MoAb T101-CAA-ADR conjugate (IgG/ADR molar ratio, 1/25) was equally cytotoxic to target cells compared to free ADR, while in Yang and Reisfeld's study, a MoAb-CAA-ADR conjugate (IgG/ADR molar ratio, 1/10) directed against human melanoma was found to be 100-fold more cytotoxic to target cells than the free drug. As discussed in Introduction section 4.3.4, one of the mechanism of cytotoxicity of ADR is via its intercalation to DNA (in which the hydrogen of the amino group of ADR weakly binds to the negatively charged oxygen on the DNA backbone). Modification of the basic

amino group of ADR to a neutral amide by the linkage reactions used here could conceivably decrease the binding of ADR to DNA and therefore result in low drug activity. The restoration of the cytotoxicity of ADR in target cells requires its release by hydrolysis in the lysosomal compartment. Therefore, the low potency of our conjugates compared to those reported by Dillman and Yang may be due to (i) the difference in the nature of MoAbs and target cell line used; (ii) the lower drug substitution (i. e., IgG/ADR molar ratio) in the conjugates; (iii) insufficient internalization of the conjugates; and (iv) inefficient hydrolysis of the internalized conjugates to generate active forms of the drug, even though the acid-sensitive CAA spacer was used.

The potency of Dal B01-C13-ADR and Dal B02-C13-ADR conjugates was comparable to that of free ADR, and was higher than that of respective Dal B01-CAA-ADR and Dal B02-CAA-ADR conjugates. This is in consistent with the observation of Greenfield et al (1990). The higher potency of the MoAb-C13-ADR conjugates may be due to (i) the preservation of the free amino sugar of the drug in these conjugates; (ii) in addition to the acid-sensitive hydrazone bond which is attached to the C13 moiety of the ADR molecule, the linkage of ADR-hydrazide to MoAb also leads to the formation of a disulfide bond in the middle of the linker arm connecting ADR to MoAb (Fig. 4B). Both the acid-labile hydrazone bond and the reducible disulfide bond between the drug and IgG molecule may provide sites of cleavage for the release of free ADR. It has been shown that MoAb-hydrazide-MTX conjugate was not as stable as MoAb-ester-MTX conjugate, and the former released more free drug when incubated with target cells in vitro (Singh, 1989). As stated, Dal B01 and Dal B02 were poorly internalized after binding to target cells. The high potency of the Dal B01-C13-ADR and Dal B02-C13-ADR conjugates suggests that the low rate of internalization of the conjugate did not constitute a major problem in inducing target cell killing by these conjugates. It is thus possible that the Dal B01 or Dal B02-linked ADR is likely to exert its cytotoxicity via mechanisms acting on plasma membrane. Braslawsky et

al. (1991) reported that ADR linked via its C13 moiety to an internalizing MoAb was more potent than a conjugate prepared with a non-internalizing MoAb. They concluded that the internalization of MoAb-C13-ADR conjugates and release of free ADR from the MoAb in acidic intracellular compartments was an important step in the mechanism of action of the conjugates. However, in their study, no comparison was made between the cytotoxicity of free ADR and the conjugates. Also, further analysis of the data given in the paper revealed that the difference between IC_{50} values of the internalizing MoAb-ADR conjugate and non-internalizing MoAb-ADR conjugate was not as significant as that proposed by the authors (IC_{50} values were 4.4 μg/ml and 5.2 μg/m, respectively). Therefore, the conclusion made by the authors remains controversial. Furthermore, in the study of Yang and Reisfeld (1988), it has been demonstrated that a conjugate of ADR linked to an anti-melanoma MoAb 9.2.27 (a MoAb directed against a slow internalizing target antigen) was much more cytotoxic than free ADR and a mixture of ADR and the MoAb.

As discussed in Introduction section 4.3.2, in order to deliver adequate amounts of a drug to target cells by MoAbs, it is desirable to attach a maximum number of drug molecules to an antibody molecule while preserving antibody activity. Most studies have shown that the substitution of more than 10 drug residues per antibody molecule usually cause unacceptable loss of antibody activity and / or loss of solubility of the conjugate (Ghose and Blair, 1987). The use of dextran as an intermediate carrier circumvents these problems. Dextran T-40 has been previously used to prepare antibody-ADR conjugates (Hurwitz et al., 1978). However, in most of the previous studies, the conjugates prepared by this method were usually less potent than the free drug. Two factors are likely to contribute to the loss of drug activity after conjugation to antibody in these studies: (i) the use of the amino sugar of the drug as the functional group for conjugation; and (ii) the use of borohydride or cyanoborohydride to reduce the Schiff's bases formed between ADR and dextran carrier or between dextran and the carrier antibody. The reduction procedure may

significantly damage the activity of ADR (Ghose et a., 1981). However, in some cases, very potent conjugates (i.e., as potent as, or even more potent than the free drug) has been obtained even after borohydride reduction (Hurwitz et al., 1975). These conflicting results are likely to be due to (i) differences in the nature of the antibody and the target cells used; and (ii) differences in the type and the concentration of reducing agents used, and the duration of the reduction reaction.

In this study, a Dal B02-Dex-ADR (ss) conjugate was prepared, in which the dextran was first site-specifically linked to Dal B02 and then loaded with ADR via the C13 moiety of the drug molecule. This conjugate has several novel characteristics compared to other MoAb-ADR or MoAb-Dex-ADR conjugates previously reported: (i) an oxidised dextran was used as an intermediate carrier, which greatly increased the number of drug molecules that could be coupled to one IgG molecule without significant damage of antibody activity; (ii) the dextran carrier was linked to IgG site-specifically via the carbohydrate residues of the antibody, i.e., leaving the antigen-binding Fab portion free; (iii) the C13 moiety of ADR was used as the site of attachment, i.e., leaving the amino sugar of the drug free; (iv) ADR was coupled to dextran via an acid-labile hydrazone bond instead of an amide bond or a Schiff's base. For comparison, another conjugate, i.e., Dal B02-Dex-ADR (nss) was prepared following the method described by Hurwitz et al. (1978), in which ADR was first coupled to dextran via its amino sugar group, and the formed dextran-ADR binary conjugate was then linked to Dal B02 randomly (i. e., non-site specifically) via the amino groups in the protein. Finally, cyanoborohydride was used to reduce the formed Schiff's bases.

Both Dal B02-Dex-ADR (ss) conjugate and Dal B02-Dex-ADR (nss) conjugate retained full antibody activity compared to the unconjugated parent antibody, indicating that both the conjugation procedures favor the retention of antibody activity. In fact, with the use of

dextran as an intermediate carrier, only 1.2 to 1.8 molecules of ADR loaded dextran were coupled to one IgG molecule in both types of conjugates, although approximately 25 to 41 molecules of ADR were loaded on one IgG molecule. At these low substitution ratios, the possible advantages of site-specific linkage over non-site specific linkage regarding the retention of antibody activity could not be determined.

When the cytotoxicity of the two conjugates were compared, Dal B02-Dex-ADR (ss) conjugate was found to be 20-fold more potent than Dal B02-Dex-ADR (nss) conjugate. The former was 3.5-fold more potent than free ADR, whereas the latter was 6-fold less potent than free drug. As stated, no difference in the antibody activity was observed between these two types of conjugates. We suggest that the difference in the conjugation chemistry in the latter conjugate, i.e., the use of amino sugar group of the drug for coupling and the use of cyanoborohydride for the reduction of Schiff's bases, is mainly responsible for the loss of drug activity in the Dal B02-Dex-ADR (nss) conjugate.

Several evidences indicate that the increased cytotoxicity of Dal B02-Dex-ADR (ss) conjugate to target D_{10-1} cells was a MoAb-based specific event. These include: (i) the Dal B02-Dex-ADR (ss) conjugate was 5-fold more toxic to target D_{10-1} cells than the non-specific IgG_1-Dex-ADR (ss) conjugate, while both Dal B02--Dex-ADR (ss) and non-specific IgG_1-Dex-ADR (ss) were equally toxic to the non-target MOLT-3 cells. The selectivity ratio of cytotoxicity of Dal B02-Dex-ADR (ss) conjugate towards D_{10-1} cells over MOLT-3 cells was 19.1, indicating a highly selective cytotoxicity to antibody-reactive target cells; and (ii) the Dex-ADR binary conjugate used to construct the Dal B02-Dex-ADR (ss) conjugate had significantly lower cytotoxicity towards D_{10-1} cells than free ADR and the Dal B02-Dex-ADR (ss) conjugate. However, both the Dal B02-Dex-ADR (ss) conjugate and the Dex-ADR binary conjugate were approximately equally toxic to non-target MOLT-3 cells. The increased cytotoxicity against D_{10-1} cells of Dex-ADR binary

conjugate after conjugation to Dal B02 is likely to be due to a more effective delivery of Dex-ADR to the target tumor cells.

In this study, a non-specific IgG1-Dex-ADR (ss) conjugate was found to be as toxic as free ADR to D10-1 cells. This is in contrast to the results of several other studies (Greenfield et al., 1990; Trail et al., 1992), but in agreement with studies reported by Dillman et al. (1986d) and Braslawsky et al. (1991). Surprisingly, in my study, the non-specific IgG1-Dex-ADR (ss) conjugate also demonstrated a selective cytotoxicity towards D10-1 cells, i.e., it is more cytotoxic to D10-1 cells than to MOLT-3 cells. The strong cytotoxicity of this IgG1-Dex-ADR (ss) conjugate towards D10-1 cells is likely to be due to the high non-specific cytotoxicity caused by the conjugate. This may be result from the difference in sensitivity of different tumor cell lines to ADR or its conjugates (e.g., as we have seen in this study that D10-1 cells were more sensitive to ADR than MOLT-3 cells). Several other factors might have also contributed to this non-specific cytotoxicity. These include: (i) binding and/or uptake of free ADR via ADR receptors. Free drug can be either a contaminant in the conjugate preparation or released from the conjugate during the exposure; (ii) the high level of ADR incorporation in IgG1-Dex-ADR (ss) conjugate. Because of the high level of ADR incorporation in this conjugate, the binding of the IgG1-Dex-ADR (ss) conjugate to cell surface via ADR receptors may result in the binding of much larger amounts of ADR on the surface of D10-1 cells compared to the amount of ADR bound to the cell surface when the cells were incubated with free ADR. As stated, one of the mechanisms of cytotoxicity of ADR is mediated by its interaction with the plasma membrane of exposed cells (Tritton et al., 1982). Therefore, the binding of much larger amounts of IgG1 conjugated ADR to cell surface via ADR receptors after incubation of cells with the IgG1-Dex-ADR (ss) conjugate may induce a significant cytotoxicity. The effect of the level of ADR incorporation in the conjugates on the potency of the conjugates has been confirmed by the cytotoxicity study using Dex-ADR binary conjugates with different levels

of ADR incorporation. As shown in Table 19, Dex-ADR binary conjugate with a Dex/ADR molar ratio of 1 to 30 is more potent than Dex-ADR binary conjugate with a Dex/ADR molar ratio of 1 to 15; (iii) uptake of the conjugate by mechanisms other than antibody-mediated specific uptake, such as via Fc receptor on tumor cell surface that bind to the Fc region of the IgG (Witz et al., 1973; Braslawsky et al., 1976; Nio et al., 1989), pinocytosis and membrane utilization (Steinman et al., 1983); and (iv) depot effect of the macromolecular carrier, i.e., slow release of free drug from the conjugate (Ghose and Blair, 1978).

It has been difficult in some cases to demonstrate MoAb directed specific cytotoxicity of MoAb-ADR conjugates in vitro (for reasons discussed above). The accessibility of the target tumor cells, the volume of distribution and the metabolism of free ADR and MoAb-ADR conjugate in tissue culture are different form those in vivo. Also, there are no carrier proteins to take the dissociated drug away and no organs of RES to remove the conjugates in cell culture. Therefore, therapy-induced tumor regressions in animal models are crucial for establishing a rationale for clinical application of immunoconjugates. In recent years, human tumor xenografts in nude mice provided suitable experimental models for evaluating the anti-tumor activity as well as toxicity of immunoconjugates.

In sever; ' earlier studies, a number of MoAb-ADR conjugates have been evaluated for their anti-tumor efficacy in xenografted human tumors in nude mice. In general, these conjugates have been shown to be active in vivo. Two major limitations associated with most of these studies are: (i) many investigators have treated the tumor inoculated mice with conjugate at the time (or within 24 hr) of tumor inoculation (Levy et al., 1975; Tsukada et al., 1982). Others have treated the tumor cells with MoAb-ADR conjugates in vitro followed by their transplantation into mice (Aboud-Pirak et al., 1989). Such treatment are not comparable to therapy in mice with established tumors and the therapeutic efficacy of conjugates in above

models are in fact, evaluation of inhibition of tumor engraftment rather than of inhibition of tumor growth; and/or (ii) in most studies, tumor-bearing mice were treated with conjugates following an arbitrary dose and schedule and the anti-tumor activity of conjugates was compared with those obtained with equivalent amount of free drug, rather than the optimal dose and schedule of administration of free drug (Dillman et al., 1986d; 1988, Yang and Re ·ñ   i988). It has been demonstrated that MoAb-ADR conjugates are usually less toxic than the parent drug in animal models. For example, Trail et al (1992) reported that a dose of 10 mg of free ADR/kg (q4d x 3) was the LD50 dose for L2987 human lung carcinoma xenograft bearing nude mice, while a dose of 35 mg ADR/kg when given as a MoAb-ADR conjugate following the same schedule as free drug did not kill any mouse. Furthermore, it is known that both the dose and the schedule of administration are important factors in determining the anti-tumor activity as well as the toxicity of free ADR and its conjugates, and that the optimal dose and schedule of administration for conjugates may well be different from those of the free drug. Therefore, it is important to compare the efficacy of the free drug and its conjugate on the basis of their therapeutic indices, i.e., the maximum anti-tumor effect that could be achieved by either agent in relation to their toxicity, provided both agents are given in their optimal dose following optimal schedules.

In this study, the anti-tumor activity of Dal B02-Dex-ADR (ss) conjugate was compared to (i) the maximum anti-tumor activity that could be achieved with free ADR, given in its optimal dose and schedule; and (ii) the anti-tumor activity that could be achieved by an equivalent dose of free ADR. For free ADR, a dose-dependent anti-tumor activity as well as toxicity was observed. A protocol of 5 mg ADR/kg x q2d x 5 (total dose, 25 mg ADR/kg) yielded a more pronounced anti-tumor effect accompanied by a more severe toxicity compared to a protocol of 3.5 mg ADR/kg x q2d x 5 (total dose, 17 mg ADR/kg). When an equivalent dose of ADR (either free or conjugated) was given to tumor-bearing mice following a schedule of 5.0 mg/kg x q2d x 5 (total dose 25 mg ADR/kg), free ADR

showed a higher anti-tumor activity than Dal B02-Dex-ADR (ss) conjugate did. However, at this dose level and schedule, the anti-tumor activity of specific Dal B02-Dex-ADR (ss) conjugate was much higher than that of (i) non-specific IgG1-Dex-ADR (ss) conjugate; (ii) Dex-ADR binary conjugate; (iii) Dal B02 alone; and (iv) a mixture of Dex-ADR binary conjugate and Dal B02. As stated, toxicity studies have shown that this dose is the MTD for free ADR (but not for the conjugate) (Tables 20 and 21). Thus, the anti-tumor activity of free ADR obtained at this dose level constituted the maximum anti-tumor activity that could be achieved by the maximum permissible dose of the free drug. To determine whether the anti-tumor activity could be further improved with Dal B02-Dex-ADR (ss) conjugate, the conjugate was given to tumor-bearing mice following another protocol, i.e., 8.5 mg ADR/kg x q2d. The treatment in this group had to be stopped after two injections because of the severe toxicity. We did not carry out further experiments in this study to determine the optimal dose and the schedule of administration of the conjugates. However, it was clear that when this protocol was used, the therapeutic efficacy of the conjugate was superior to (i) the therapeutic efficacy achieved with an equivalent dose of free ADR (total dose, 17 mg ADR/kg); (ii) the maximum anti-tumor activity achieved with the optimal dose and schedule of administration of free drug (i.e., 5 mg ADR/kg x q2d x 5, total dose, 25 mg ADR/kg); and (iii) the therapeutic efficacy achieved with an equivalent dose of non-specific IgG1-Dex-ADR (ss) ternary conjugate or Dex-ADR binary conjugate. The superior anti-tumor efficacy of the Dal B02-Dex-ADR (ss) conjugate was demonstrated in terms of both delayed tumor growth and an increase in proportion of mice with tumor regression and complete cure. It is possible that a more pronounced anti-tumor activity can be obtained with Dal B02-Dex-ADR (ss) conjugate when the optimal dose and schedule of administration of the conjugate are defined.

ADR conjugated to high-molecular-weight non-tumor specific carriers has been shown to be more active than the free drug in vivo in animal models (Winer et al ., 1971). In my

study, experiments were carried out to determine whether the superior anti-tumor activity of the Dal B02-Dex-ADR (ss) conjugate was due to a carrier effect in which the IgG or dextran served as depots for the slow sustained release of free ADR in xenograft bearing mice. A non-specific IgG1-Dex-ADR (ss) conjugate and a Dex-ADR binary conjugate were prepared and administered to D10-1 xenograft bearing mice using the same dose and schedule of administration as those for specific conjugate. Consistent with results obtained form the previous study on radioimmunotherapy (see Results section 7.4.1), a moderate anti-tumor effect was obtained with both the non-specific IgG1-Dex-ADR (ss) ternary conjugate and the Dex-ADR binary conjugate. However, both the non-specific conjugates were much less potent than the specific Dal B02-Dex-ADR (ss) conjugate. This is consistent with the results of Greenfield et al. (1990) and Braslawsky et al. (1990). The difference in the anti-tumor activity of these specific and non-specific conjugates is likely to be due to the difference in the uptake mechanisms of these conjugates by target tumor. As shown in Figs. 92 and 93, the study on the biodistribution of radiolabeled Dal B02, Dal B02-Dex-ADR (ss) conjugate and non-specific IgG1 demonstrated that the percentage of the injected dose of Dal B02 or its conjugate that localized in D10-1 xenografts was approximately 5 to 6-fold higher than the percentage of tumor-localized non-specific IgG1. Therefore, the improved anti-tumor activity of the Dal B02-Dex-ADR (ss) conjugate appears to be associated with a more effective delivery of MoAb linked ADR to target tumors.

Because unmodified MoAbs have been shown to be active against tumor xenografts (Dillman et al., 1986d; Herlyn and Koproski, 1982), it is also possible that the anti-tumor activity of the Dal B02-Dex-ADR (ss) conjugate could have been mediated by effector mechanisms of the MoAbs (rather than the targeted delivery of cytotoxic drugs). Also, a mixture of an anti-tumor MoAb and free ADR has also been shown to have greater anti-tumor activity than an equivalent amount of free drug (Dillman et al., 1986d), indicating

that the anti-tumor activity of the conjugate might be due to the synergism between the MoAb and the free drug, i.e., the sensitization of the target tumor cells to free drugs by the binding of anti-tumor MoAbs, and/or vice versa. To address above questions, in this study, Dal B02 alone as well as a mixture of Dal B02 and Dex-ADR binary conjugate were used to treat D10-1 xenograft bearing mice following the same dose and schedule of administration as those used for the specific conjugate. Results showed that Dal B02 alone in a high dose (100 mg/kg) indeed had some anti-tumor activity. The mixture of Dal B02 and Dex-ADR binary conjugate, however, did not yield an anti-tumor activity that was greater than anti-tumor activity obtained with Dex-ADR alone, indicating that the superior anti-tumor activity of Dal B02-Dex-ADR (ss) conjugate was not due to the synergism between the MoAb and the free drug. Several other studies have also demonstrated the ineffectiveness of mixtures of anti-tumor MoAb and free ADR in animal models (Yang and Reisfeld, 1888; Trail et al., 1992).

Thus, several mechanisms could have contributed to the increased anti-tumor efficacy of Dal B02-Dex-ADR (ss) conjugate. The possible mechanisms, which are not mutually exclusive, include: (i) the role of Dal B02 as a tumor-specific carrier leading to delivery of ADR to tumor cells specifically by binding to tumor-associated antigen(s) on the surface of target tumor cells, i.e., intratumoral localization of a higher percentage of the injected dose of ADR when linked to Dal B02 than when linked to non-specific carrier such as dextran and non-specific IgG1, or than when free ADR was administered alone; (ii) changes in the pharmacokinetics of ADR after conjugation to Dal B02, i.e., prolonged half-life in circulation and depot effect (i.e., slow release of free ADR from carrier Dal B02 in target tumors); and (iii) the effector mechanisms of Dal B02, this was also observed during my study on radioimmunotherapy (see Results section 7.4.1).

The anti-tumor activity obtained with Dal B02-Dex-ADR (ss) conjugate compares favorably with other reports using MoAb-ADR conjugate prepared via a CAA spacer (Yang and Reisfeld, 1988; Dillman et al., 1988). Both Yang (1988) and Dillman (1988) used small tumors (tumor volume < 10 mm^3) and compared the anti-tumor activity of MoAb-CAA-ADR conjugates with that of free drug at equimolar doses rather than at the maximum permissible doses. In our study, tumors were much larger (tumor volume ranged from 60 to 200 mm^3) before the initiation of treatment. Even at this high tumor burden, Dal B02-Dex-ADR (ss) conjugate showed superior anti-tumor activity compared to the free ADR, non-specific IgG$_1$-Dex-ADR (ss) conjugate, Dex-ADR binary conjugate, and a mixture of Dal B02 and Dex-ADR binary conjugate. Our specific ternary conjugate is also superior to those conjugates prepared via direct C13 linkage (Braslawsky et al., 1990; Trail et al., 1992). Both Braslawsky (1990) and Trail (1992) treated breast carcinoma xenograft bearing nude mice with MoAb-C13-ADR conjugates and compared the anti-tumor activity of the conjugates with the maximum tumor inhibition that could be achieved by the free drug. Both studies showed that the specific conjugates were superior to free ADR in inhibiting the growth of the xenografted tumors. One major limitation of their conjugates was the low level of ADR incorporation. For clinical application, large amounts of MoAb will be required for the preparation of an adequate amount of immunoconjugate. For example, in Trail's study, the molar ratio of IgG/ADR in the MoAb BR64-ADR conjugate was 1/4 to 1/8. For administrating the highest dose of MoAb linked ADR (35 mg ADR/kg) in their study, 46 mg of MoAb was needed per injection for a mouse of 25 g. In my study, at the therapeutically effective dose level, the actual amount of Dal B02 given to each mouse was less than 2.5 mg per injection per mouse, i.e., an amount that is 20-fold less than the amount used by Trail.

3. Targeting Human Peripheral Blood Lymphocytes with A Heteroconjugate to Intraperitoneal Human Renal Cell Carcinoma Xenografts in Nude Mice

New strategies are being developed to target effector cells like NK cells, LAK cells and CTLs with bispecific antibodies to tumor cells. As stated, for targeting cytolytic effector cells to tumor cells, bispecific antibodies (irrespective of whether they are produced by chemical cross-linking of two antibody molecules or by fusion of two different hybridomas), should have two different antigen-specific binding sites, one for the tumor-associated antigen (target binding arm) and the other for the effector cell. Bispecific antibodies bridge effector cells to the target cell and may also simultaneously activate the effector cell's lytic machinery. This occurs with antibodies that recognize sites on effector cells involved in their activation, such as CD3 (Garrido et al., 1990), CD2 (Scott et al., 1988) and CD16 (de Palazzo et al., 1992). Of these molecules, CD3 is the most commonly used one for a number of reasons. Firstly, CD3, which is in close physical association with the T cell antigen receptor (TCR), is present on all T cells. Secondly, the binding of anti-CD3 antibody to T cells has been shown to augment IL-2 induced T cell proliferation, lymphokine production and the cytotoxicity of the T cells (Bolhuis et al., 1986). The anti-CD3 antibody component of such bispecific antibodies binds to any TCR bearing lymphocytes regardless of the specificity of the TCR and initiates the activation of the cell's lytic mechanism. The anti-tumor antigen component binds to tumor cells, thereby joining the activated T lymphocytes with tumor cells. The antibody-mediated association of the T cell with tumor cell results in the lysis of the tumor cell. The cytolysis of tumor cells is independent of the original specificity of the TCR of the CTL and is not MHC-restricted. Thus T lymphocytes of varying specificities can be directed with the bispecific antibody to kill tumor cells in a highly specific and effective manner. Bispecific antibodies have been found to be potent augmentor of in vitro tumor lysis by relevant effector cells. For

example, encouraging results have been obtained with bispecific antibodies in syngeneic murine models (Brissinck et al., 1991; Demaner et al., 1991; Weiner et al., 1991). Several reports have also demonstrated that, when administered with human effector cells, bispecific antibodies can significantly inhibit the growth of human tumor xenografts grown in nude mice (Garrido et al., 1990; de Palazzo et al., 1992; Weiner et al.,1993).

In this study, a MoAb directed against human renal cell carcinoma (RCC), Dal K29, was chemically cross-linked to a monoclonal antibody directed against CD3 molecule on T cells to form a K29-OKT3 heteroconjugate. Previous in vitro studies had demonstrated that this heteroconjugate was capable of mediating a high level of killing of RCC cells in the presence of PBL or TIL from RCC patients (Kerr et al., 1990). The objectives of my study were: (i) to investigate the pharmacokinetics and biodistribution of K29-OKT3 heteroconjugate in s.c. Nu-caki-1 xenograft bearing nude mice; and (ii) to investigate the anti-tumor activity of K29-OKT3 heteroconjugate in the presence of human PBL in Nu-caki-1 cell inoculated nude mice.

Studies on the localization of these antibody preparations after i.v. administration demonstrated that the parent Dal K29 antibody as well as the K29-OKT3 heteroconjugate specifically localized in xenografted Nu-caki-1 tumors. However, less of the heteroconjugate (i.e., % ID / g tissue) localized in the xenografted tumor than parent Dal K29. This is in agreement with the results reported by Nelson et al. (1990) who studied in vivo tumor localization of several different anti-tumor MoAb-anti-CD3 heteroconjugates. Compared to parent Dal K29 MoAb, the heteroconjugate was more rapidly cleared from the circulation as well as from the whole body of tumor host. Mice given the heteroconjugate also showed the accumulation of a higher percentage of the administered radioactivity in the liver and the spleen at the first 48 hr after antibody administration compared to the accumulation of administered parent Dal K29 MoAb. Similar results were also observed by

Winkler et al. (1990) who studied the biodistribution in mice of anti-melanoma MoAb-OKT3 heteroconjugate. The differences between K29-OKT3 heteroconjugate and parent Dal K29 MoAb as regards to the pattern of biodistribution and the rate of clearance are likely to be due to the higher molecular weight of the heteroconjugate (i.e., 300, 000 to 1000,000 dalton) compared to the parent MoAb Dal K29. It may be more difficult for the relative large heteroconjugate molecule to pass through the capillary wall and to penetrate tumor tissue. Furthermore, the large molecular size of the heteroconjugate renders them more susceptible to phagocytosis by reticulo-endothelia cells. Finally, because of the considerable heterogeneity in the size of the heteroconjugate, heteroconjugate prepared by chemically cross-linking contains a significant proportion of molecules that can present two Fc domains for binding to Fc receptors. This may increase the rate of elimination of the heteroconjugate by reticulo-endothelia cells.

Several approaches have been made to optimize the tumor localization of heteroconju·ites. In one approach, heteroconjugates have been constructed using the F(ab)'2 fragments. These heteroconjugates have yielded better tumor localization, i.e., higher T / NT ratios, as compared to intact IgG heteroconjugates because they were cleared from the blood and normal tissues more rapidly (van Dijk et al., 1991). One of the disadvantage of the F(ab)'2 heteroconjugates is the lower percentage of the injected dose of F(ab)'2 heteroconjugates localize in the tumor compared to the tumor localization of intact IgG heteroconjugates (van Dijk et al., 1991). However, in one report, there was no difference between F(ab)'2 heteroconjugate and intact IgG heteroconjugate as regards to their tumor localization (Nelson et al., 1990). Another approach to increase the tumor localization of heteroconjugate is the use of regional administration. Regional administration of heteroconjugates usually lead to higher and prolonged localization of the antibody in tumors. For example, in an intraperitoneal ovarian cancer xenograft model, the i.p. injection of heteroconjugate produced higher antibody localization in the tumors than after

i.v. injection (Moseley et al., 1988). In another i.p. xenograft model, no such difference was observed between i.p. and i.v. injections when intact anti-human colon carcinoma antibody-anti-CD3 heteroconjugates were used. However, with the F(ab)'2 heteroconjugates, i.p. administration resulted in superior T / NT ratios than i.v. administration (Nelson, et al., 1990).

Lymphocyte trafficking (including distribution and extravasation into tissues) is regulated by the presence of homing receptors on lymphocytes and corresponding ligands in the post capillary venules (Duijvestijn and Hamann, 1989). Lymphocyte homing varies with lymphocyte subsets and the target organs. As regards the localization of lymphocytes in targeted tumor tissues, the problem appears to be the accessibility of the tumor cells to the lymphocytes (Nelson et al, 1990). Systemic injection of cultured ^{111}In-labeled PBL in mice produced sequential peaks of radioactivity in the lung, liver and spleen, but the level of radioactivity in the tumor was low (Weiner et al., 1993). According to Weiner et al. (1993), in SCID mice, only 3.5% of transfused lymphocytes were present in blood 18 hr after administration. The localization of substantial proportions of i.v. injected lymphocytes (cultured in vitro with IL-2) in the lung, liver and spleen of the host have also been reported by Takai et a[1] (1988). Repetitive i.v. injections of effector cells may be necessary to maintain an effective level of effector cells in the circulation of mice. To circumvent this problem, some investigators prefer the regional administration of effector cells. Nelson et al. (1990) observed that after i.p. injection of ^{111}In-labeled PBL, there was a very high localization of the injected PBL in the intraperitoneal xenograft of human colon carcinoma, along with low localization of these PBL in normal organs. A number of investigators have successfully treated nude mice bearing intraperitoneal xenografts with i.p. administration of T lymphocytes and bispecific antibodies reacting with tumor cells and CD3 (Titus et al., 1987; Mezzanzanica et al., 1991). Other investigators have also observed tumor inhibition

after i.v. administration of bispecific antibodies and effector cells in s.c. xenograft models (de Palazzo et al., 1992; Weiner et al., 1993).

In this stud;, both the tumor cells and the treatment were given to nude mice via the i.p. route. All untreated nice mice died within 31 days. Therapy with K29-OKT3 heteroconjugate alone, or with Dal K29 plus OKT3 plus PBL (E/T ratio, 10 to 1), showed minimal effect on the growth of Nu-caki-1 tumor. The anti-tumor effect of the heteroconjugate was dependent on the number of effector cells that were coinjected. Therapy with K29-OKT3 heteroconjugate plus PBL (E/T ratio, 10 to 1) led to a significant anti-tumor effect. Two out of 4 mice survived tumor free over 150 days. The other two mice survived for 53 and 70 days, respectively. When an E/T ratio of 3 to 1 was used, the anti-tumor activity of the heteroconjugate was significantly lower than that when an E/T ratio of 10 to 1 was used. The treatment resulted only in prolongation of survive of one of 5 mice. In two recent reports in the therapy of human tumor xenografts in nude mice using bispecific antibodies and human effector cells, a E/T ratio of 1 to 1 (de Palazzo et al., 1992) or 5 to 1 (Weiner et al., 1993) was used. A significant tumor inhibitory effect was observed in both cases. However, in these studies, multiple injections (i.e., three times) of the effector cells, along with IL-2 were given to the mice. In my study, only one injection of effector cells was given to tumor inoculated nude mice. The antitumor effect of the K29-OKT3 heteroconjugate seems directly correlate with the number of effector cells used. Because of the small numbers of nude mice used in this study, confirmatory experiments using larger number of mice are needed to ascertain the superiority of the anti-tumor activity of the heteroconjugate.

SUMMARY

1. Two MoAbs directed against human B-cell chronic lymphocytic leukemia (CLL), i.e., Dal B01 (IgG2a) and Dal B02 (IgG1), were purified from the ascites fluid of BALb,c mice inoculated with appropriate hybridomas. F(ab)'2 fragments of these two MoAbs were produced by peptic digestion.

2. Both Dal B01, Dal B02 and their F(ab)'2 fragments had approximately the same number of binding sites on D10-1 cells (i.e., 10 to 12 million site per cell). The Ka of the intact MoAbs was higher than their respective F(ab)'2 fragments. Dal B02 preparation had the highest IRF (73.9 ± 3.9 %), followed by Dal B02 F(ab)'2 fragment (52.7 ± 3.6%), Dal B01 (28.3 ± 2.6%) and Dal B01 F(ab)'2 fragment (25.5 ± 4.1%).

3. Results obtained from protein iodination studies using chloramine T revealed that factors that determine the retention of the IRF of radiolabeled Dal B01, Dal B02 and their F(ab)'2 fragments include (i) the reaction conditions, i.e., the amount of chloramine T used and the reaction time; (ii) the level of incorporation of radioactive iodine; and (iii) the nature of antibody preparations.

4. There was no significant difference in the amount of Dal B01, Dal B02 and their F(ab)'2 fragments that bound to target D10-1 cells in vitro irrespective of whether the cells were incubated with the MoAbs at 4°C or 37°C. These results indicate that there was no significant endocytosis of cell surface bound Dal B01, Dal B02 and their F(ab)'2 fragments. Study using gold particle adsorbed Dal B01 or Dal B02 demonstrated that only about 15% of cell associated Dal B01-Au or Dal B02-Au complex were endocytosed by D10-1 cells after incubation at 37°C for 6 hr.

5. Both Dal B01, Dal B02 and their F(ab)'2 fragments selectively localized in s.c. xenografts of D10-1 cells in nude mice. The % ID / g tumor was much higher in mice given

intact Dal B01 or Dal B02 compared to the % ID / g tumor in mice given the respective F(ab)'2 fragments. The half-life of intact MoAbs in mice was about 5 to 6 times longer than that of the F(ab)'2 fragments. Excellent tumor images were obtained in mice given Dal B02, or Dal B02 F(ab)'2 fragment.

6. Three different protein iodination methods were compared using Dal B02 as the carrier antibody. Radioiodination method using N-succinimidyl para-iodobenzoate (PIB) as an intermediate yielded a protein that retained higher IRF, was more stable, and which after i.v. administration showed higher tumor localization and less nonspecific uptake of radioiodine by the thyroid, as compared to radiolabeled products obtained using the Bolton-Hunter reagent or the chloramine T. However, the low efficiency of radioiodine incorporation when the PIB was used for protein radioiodination rendered it less attractive for obtaining antitumor MoAbs with high specific activity for therapeutic use.

7. MTX has been linked to Dal B01 as well as Dal B02 via either the active ester or the hydrazide linkage. Both types of conjugates retained original antibody activity. In an in vitro DHFR inhibition assay, the IC50 values of these conjugates were approximately 5 to 6-fold higher than that of free MTX. The cytotoxicity of these conjugates towards target D10-1 cells was comparable to that of free MTX in a 6 hr pulse exposure assay. The selectivity ratio of these conjugate to D10-1 cells over non-target MOLT-3 cells reached as high as 40 to 50, indicating a very specific cytotoxicity. In vitro uptake studies showed that D10-1 cells took up much more Dal B01 or Dal B02 conjugated MTX than MOLT-3 cells did, although MOLT-3 cells took up more MTX when incubated with free MTX. The amount of uptake of MTX by D10-1 cells was also much higher when the cells were incubated with Dal B01 or Dal B02 conjugated MTX than the amount of uptake of MTX by the cells when the cells were incubated with free MTX.

8. Four different types of Dal B01-ADR or Dal B02-ADR conjugates were prepared and their in vitro cytotoxicity was evaluated. The conjugates prepared via the C13 moiety of ADR using a hydrazone bond was more potent than the conjugates prepared via the amino sugar group of the drug using an amide bond. The most potent conjugate was Dal B02-Dex-ADR (ss) conjugate. The IC_{50} for D10-1 cells of this conjugate was about 3-fold lower than that of free ADR. The selectivity ratio of this conjugate was about 20 to 30. Therapy in D10-1 xenograft bearing nude mice using this conjugate showed that at approximately equal toxic dose level, this conjugate yielded antitumor activity that was superior to the antitumor activity of free ADR, non-specific IgG1-Dex-ADR (ss) conjugate, Dex-ADR binary conjugate, or the mixture of Dex-ADR and Dal B02. The superior antitumor activity of the Dal B02-Dex-ADR (ss) conjugate was demonstrated in terms of both a inhibition of tumor growth and an increase in the proportion of mice that had complete cure.

9. Two reproducible human B-cell CLL models were established in SCID and irradiated nude mice by i.p. or i.v. inoculation of D10-1 cells into these mice. Hundred percent of tumor inoculated mice developed ascites or solid tumors with metastases in lymph nodes and a number of internal organs and died within 5 to 7 weeks after tumor inoculation. The tumor cells recovered from these mice retained their reactivity to Dal B01 and Dal B02, as well as the chemosensitivity to MTX or ADR. These results indicate that these xenograft models are suitable for evaluating new anti-human B-cell CLL agents.

10. Using these i.p., i.v. and s.c. models, the antitumor efficacy of Dal B02, either alone or labeled with ^{131}I, was investigated. Results demonstrated that, although Dal B02 alone had some antitumor activity, the ^{131}I labeled Dal B02 preparation was the most potent tumor inhibitor in these models. Injection of 50 μg of Dal B02 labeled with 300 μCi of ^{131}I resulted in significant tumor inhibition in all the three models. Again, the superior antitumor

activity of ^{131}I-Dal B02 was demonstrated in terms of both a inhibition of tumor growth and an increase in the proportion of mice that had complete cure.

11. The in vivo distribution of a Dal K29-OKT3 heteroconjugate in s.c. Nu-caki-1 xenograft tumor bearing nude mice was studied. Results showed that both parent Dal K29 and Dal K29-OKT3 heteroconjugate localized selectively in the xenografted tumors. However, the percentages of the injected dose of Dal K29 that localized in the tumors were higher than the percentage of the injected dose of the heteroconjugate that localized in the tumors. The therapeutic effectiveness of this heteroconjugate, along with human peripheral blood lymphocytes (PBL), was evaluated using an ascites model of human RCC, i.e., Nu-caki-1 ascites model. The Dal K29-OKT3 heteroconjugate plus PBL yielded a higher antitumor activity compared to heteroconjugate alone, or the mixture of Dal K29, OKT3 and PBL.

Human B cell CLL is the most common type of adult leukemia in Western countries. Although approximately 60% of patients respond to chlorambucil, the standard therapeutic agent for initial treatment, the response is usually partial and no therapeutic regimen has been demonstrated to be effective after the failure of initial therapy. Other currently used therapeutic regimens such as irradiation of lymph nodes, spleen, bone marrow and other tumor infiltrated tissues and splenectomy are mainly palliative and provide symptomatic relief to patients with bulky lymph nodes and/or enlarged spleen. In recent years, several new approaches have been attempted to improve the therapeutic outcome of human B cell CLL. Bone marrow transplantation along with the use of high dose chemotherapy and/or whole body irradiation has been employed to treat CLL patients. However, this approach only applies to less than 5% of cases of CLL because the majority of the CLL patients are usually too old and/or weak to fulfill the criteria for receiving this type of treatment. As regards immunotherapeutic approaches, recent studies have reported greater than 50%

response in patients with previously untreated low-risk CLL after the administration of low dose of recombinant α-IFN, but this treatment was not effective in patients with intermediate- and high-risk CLL. MoAbs directed against CD5 expressed on CLL B cells or anti-idiotypic MoAbs directed against malignant B cells have also been used to treat CLL and other lymphoid malignancies. However, the response is usually transient and CR is rare. There is thus a need to develop new therapeutic agents for the treatment of CLL. In this study, I have demonstrated that Dal B02 alone could effectively eradicate xenografted D10-1 cells in nude mice. Furthermore, when Dal B02 was conjugated to ADR or ^{131}I, the conjugates were more potent tumor inhibitors than unmodified Dal B02. Though Dal B02 reacts weakly with several subpopulations of normal human lymphocytes including approximately 20% of peripheral blood B lymphocytes, the target antigens of these MoAbs are expressed at a much higher level by human CLL B cells and several different histological types of human lymphomas including follicular large cell lymphomas, small cleaved cell lymphomas and diffuse mixed cell lymphomas. Thus Dal B02 may be useful clinically for the treatment of appropriate B cell lymphomas and CLL, either as a therapeutic agent by itself or as a tumor-specific carrier for cytotoxic agents or therapeutic amount radionuclides, especially after debulking of tumors to reduce tumor load. Further potentiation of these therapeutic modalities may be possible by (i) improvements in the methods of radioiodination of MoAbs, or the use of radionuclides that do not have the disadvantages of ^{131}I (e.g., its undesirable gamma radiation, low energy of its beta particles and the problem of dehalogenation in vivo); (ii) augmentation of antigen expression by target tumor cells using immunomodulators like IFN; and (iii) avoidance of bone marrow toxicity using dose fractionation, ABMT, and/or hematopoietic growth factors such as IL-1 and GM-CSF that do not stimulate neoplastic B cells. Before the clinical use of Dal B02, the reactivity of this MoAb with the neoplastic cells of different types of leukemias and lymphomas, especially B cell malignancies, should be investigated.

REFERENCES

Aboud-Pirak E, Hurwitz E, Bellot F, et al. Inhibition of human tumor growth in nude mice by a conjugate of doxorubicin with monoclonal antibodies to epidermal growth factor receptor. *Proc Natl Acad Sci USA* 86:3778-3781, 1989.

Adler S, Stutzman L, Sokal JE, et al. Splenectomy for hematology depression in lymphocytic lymphoma and leukemia. *Cancer* 35:521-528, 1975.

Albelda SM, Mette SP, Elder DE et al. Intergrins and other cell adhesion molecules. *FASEB J* 4:2868-2880, 1990.

Ali SA, Eary JF, Warren SD, et al. Synthesis and radioiodination of tyramine cellobiose for labeling monoclonal antibodies. *Nucl Med Biol* 15:557-561, 1988.

Ali SA, Warrenn SD, Richter KY, et al. Improving the tumor retention of radioiodinated antibody: Aryl carbohydrate adducts. *Cancer Res* 50:783s, 1990 (suppl).

Allegra CJ, Chabner BA, Drake JC, et al. Enhanced inhibition of thymidylate synthase by methotrexate polyglutamates. *J Biol Chem* 260:9720-9726, 1985.

Allegra CJ, Hoang K, Yeh GC, et al. Evidence for direct inhibition of de novo purine synthesis in human MCF-7 breast cells as a principal mode of metabolic inhibition by methotrexate. *J Biol Chem* 262:13520-13526, 1987.

Allegra CJ. Antifolates. In: *Cancer chemotherapy: Principles and Practice*. BA Chabner and JM Collins (eds), JB Lippincott Co., Philadelphia, 1990.

Alvarez FJ, Lopes AD, Lee C, et al. Site-specific modification of monoclonal antibodies. Study in indium-111-labeled antibodies using nude mouse xenograft systems. In: *Antibody-mediated Delivery Systems* (Rodwell JD, ed), New York: Marcel Dekker, p. 283-315, 1988.

Anthony AC, Kane MA, Portillo RM, et al. Studies of the role of a particular folate-binding protein in the uptake of 5-methyltetrahydrofolate by cultured human KB cells. *J Biol Chem* 260:14911-14917, 1985.

Appelbaumm FR. Radiolabeled monoclonal antibodies in the treatment of non-Hodgkin's lymphoma. *Hematol Oncol Clin North Am* 5:1013, 1991.

Arnon R and Sela M. In vitro and in vivo efficacy of conjugates of daunomycin with anti-tumor antibodies. *Immunol Rev* 62:5-27, 1982.

Aronsson EF, Gretarsdottir J, Jacobsson L, et al. Therapy with ^{125}I-labeled internalized and non-internalized monoclonal antibodies in nude mice with human colon carcinoma xenografts. *Nucl Med Biol* 20:134-144, 1993.

Astarita G. *Mass Transfer with Chemical Reactions*. Amsterdam: Elsevier, 1967.

Autio K, Turunen O, Penttil O, et al. Human chronic lymphocytic leukemia: karyotypes in different lymphocyte populations. *Cancer Genet Cytogenet* 1:147-155, 1979.

Awasthi S, Sharma R Awasthi YC, et al. The relationship of doxorubicin binding to membrane lipids with drug resistance. *Cancer Letters* 63:109-116, 1992.

Bachur NR, Gordon SL and Gee MV. A general mechanism for microsomal activation of quinone anticancer agents to free radicals. *Cancer Res* 38:1745-1752, 1977.

Badger CC and Bernstein ID. Prospects for monoclonal antibody therapy of leukemia and lymphoma. *Cancer* 58:584-589, 1986.

Baldwin RW and Byers VS. Monoclonal antibodies in drug targeting. In: *Tumor Immunology -- Mechanisms, Diagnosis, Therapy* (Otter WD and Ruitenberg EJ, ed.), Elsevier Science Publishers, p. 251-264, 1987.

Baldwin RW, Embleton MJ, Gallego J, et al. Monoclonal antibody drug conjugates for cancer therapy. In: *Monoclonal Antibodies in Cancer: Advances in Diagnosis and Treatment* (Roth JA, ed.), Futura Publishing, Mount Kisco, New York, P 215-, 1986.

Balinska M, Galivan J and Coward JK. Efflux of methotrexate and its polyglutamate derivatives from hepatic cells in vitro. *Cancer Res* 41:2751-2756, 1981.

Ball ED, Bernier GM, Cornwell, et al. Monoclonal antibodies to myeloid differentiation antigen: In vivo studies of three patients with acute myelogenous leukemia. *Blood* 62:1203, 1983.

Ballou B, Jaffe R, Persiani S, et al. Tissue localization of methotrexate-IgM immunoconjugates: anti-SSEA-1 and MOPC 104E in mouse teratocarcinomas and normal tissues. *Cancer Immunol Immunother* 35:251-256, 1992.

Bancroft GJ, Scheiber RD and Unanue ER. Natural immunity A T-cell-independent pathway of macrophage activation defined in the SCID mice. *Immunol Rev* 124:5-24, 1991.

Baram J, Allegra CJ, Fine RL et al. Effect of methotrexate on intracellular folate pools in purified myeloid precursor cells from normal human bone marrow. *J Clin Invest* 79:692-697, 1987.

Barnd DL, Lan M, Metzgar R and Finn OJ. Specific, MHC-unrestricted recognition of tumor-associated mucins by human cytotoxic T cells. *Proc Natl Acad Sci USA* 86:7159-7163. 1989.

Baserga R. The cell cycle. *N Engl J Med* 304:453-459, 1981.

Basu A, Murthy U, Rodeck U et al.. Presence of tumor-associated antigens in epidermal growth factor receptors from different human carcinomas. *Cancer Res* 47:2531-2536, 1987.

Batra JK, Chaudhary VK, FitzGerald D, et al. TGF-α-anti-Tac(Fv)-PE40: A bifunctioal toxin cytotoxic for cells with EGF or IL2 receptors. *Biochim Biophys Res Commun* 171:1-6, 1990a.

Batra JK, FitzGerald D, Chaudhary VK and Pastan I. Single-chain immunotoxin directed at the human transferrin receptor containing pseudomonas exotoxin A or diphtheria toxin: Anti-TRF(Fv)-PE40 and DT-388-Anti-TRF(Fv). *Mole Cell Biol* 11:2200-2205, 1991.

Batra JK, FitzGerald D, Gately M, et al. Anti-Tac(Fv)-PE40, a single chain antibody Pseudomonas fusion protein directed at interleukin 2 receptor bearing cells. *J Biol Chem* 265:15194-16202, 1990b.

Batra JK, Jinno Y, Chaudhary VK, et al. Antitumor activity in mice of an immunotoxin made with antitransferrin receptor and a recombinant form of Pseudomonas exotoxin. *Proc Natl Acad Sci USA* 86:8545-8549, 1989.

Baxter LT and Jain RK. Transport of fluid and macromolecules in tumors. I. Role of interstitial pressure and convection. *Microvasc Res* 37:77-104, 1989.

Beale D and Feinstein A. Structure and function of the constant regions of immunoglobulins. *Q Rev Biophys* 9:135-180, 1976.

Benchimol S, Fuks A, Jothy S, et al. Carcinoembryonic antigen, a human tumor marker, functions as an intercellular adhesion molecule. *Cell* 57:327-334, 1989.

Bennett JM. The use of " CHOP " in the treatment of CLL. *Br J Haematol* 74:546, 1990.

Bernstein ID, Eary JF, Badger CC, et al. High dose radiolabeled antibody therapy of lymphoma. *Cancer Res* 50:1017s-1021s, 1990 (suppl)

Binet JL, Auguier A, Dighiero G et al. A new prognostic classification of chronic lymphocytic leukemia derived from a multivariate survival analysis. *Cancer* 48:198-216, 1981.

Bird RE, Hardan KD, Jacobson JW, et al. Single-chain antigen binding proteins. *Science* 242:423, 1988.

Bizzozero OJ Jr, Johnson KG, Ciocco A, et al. Radiation-related leukemia in Hiroshima and Nagasaki 1946-1962. II. Observations on type-specific leukemia survivorship, and clinical behavior. *Ann Intern Med* 66:522-530, 1967.

Blair AH and Ghose T. Linkage of cytotoxic agents to immunoglobulins. *J Immunol Method* 59:129-143, 1983.

Blankenstein T, Rowley DA and Schreiber H. Cytokines and cancer: experimental systems. *Curr Opin Immunol* 3:594-598, 1991.

Boerman OC, Sharkey RM, Wong GY, et al. Influence of antibody protein dose on therapeutic efficacy of radioiodinated antibodies in nude mice bearing GW-39 human tumor. *Cancer Immunol Immunother* 35:127-134, 1992.

Bolhuis RLH, Gravekamp C and van de Griend RJ. Cell-cell interaction. *Clin Immuno Allergy* 6:29-90, 1986.

Bolton AE and Hunter WM. The labeling of proteins to a I-125 containing acylating agent. *Biochem J* 133:529-539, 1973.

Boon T. Antigenic tumor variants obtained with mutations. *Adv Cancer Res* 39:121-151, 1983.

Bosma MJ and Carroll AM. The SCID mouse mutant: definition, characterization and potential uses. *Annu Rev Immunol* 9:323-350, 1991.

Boulianne GL, Nobumichi H and Shulman MJ. Production of functional chimeric mouse/human antibody. *Nature* 312:643-646, 1984.

Bradwell AR, Fairweather DS, Dykes PW, et al. Limiting factors in the localization of tumor with radiolabeled antibodies. *Immunol Today* 6:163-170, 1985.

Braslawsky GR, Edson MA, Pearce W, et al. Antitumor activity of adriamycin (hydrazone-linked) immunoconjugates compared with free adriamyin and specificity of tumor cell killing. *Cancer Res* 50:6608-6614, 1990.

Braslawsky GR, Kadow K, Knipe J, et al. Adriamycin (hydrazone)-antibody conjugates require internalization and intracellular acid hydrolysis for antitumor activity. *Cancer Immunol Immunother* 33:367-374, 1991.

Braslawsky GR, Ran M and Witz IP. Tumor bound immunoglobulins: the relationship between the in vivo coating of tumor cells by potentially cytotoxic antitumor antibodies, and the expression of complex receptors in vivo. *Int J Cancer* 18:116-121, 1976.

Brissinck J, Demaner C, Moser M, et al. Treatment of mice bearing BCL1 lymphoma with bispecific antibodies. *J Immunol* 147:4019-4026, 1991.

Britton KE. Overview of radioimmunotherapy: A European perspective. *Anti Immunoconj Radiopharm* 4:133-150, 1991.

Brown PS Jr, Parenteau GL, Dirbas FM, et al. Anti-Tac-H, a humanized antibody to interleukin 2 receptor, prolongs primate cardiac allograft survival. *Proc Natl Acad Sci USA* 88:2663-2667, 1991.

Brown SL, Miller RA, Horning SJ, et al. Treatment of B-cell lymphomas with anti-idiotype antibodies alone and in combination with alpha interferon. *Blood* 73:651-661, 1989.

Buchegger F, Pfister C, Fourhier K, et al. Ablation of human colon carcinoma in nude mice by 131I-labeled monoclonal anti-carcinoembryonic antigen antibody F(ab)'2 fragments. *J Clin Invest* 83:1449-1456, 1989.

Buchsbaum DJ and Lawrence TS. New trends in the use of radioimmunoconjugates for the therapy of cancer. In: *Targeted Therapeutic Systems* (Tyle P and Ram BP, ed.), New York: Marcel Dekker, Inc., p.215-255, 1990.

Buchsbaum DJ, Sinkule JA, Susan Stites M, et al. Localization and imaging with radioiodine-labeled monoclonal antibodies in a xenogeneic tumor model for human B-cell lymphoma. *Cancer Res* 48:2475-2482, 1988.

Buchsbaum DJ, Wahl RL, Normolle DP and Kaminski MS. Therapy with unlabeled and 131I labeled pan-B-cell monoclonal antibodies in nude mice bearing Raji Burkitt's lymphoma xenografts. *Cancer Res* 52:6476-6481, 1992.

Bunn PA Jr, Foon KA, Ihde DC, et al. Recombinant leukocyte A interferon: an active agent in advanced cutaneous T-cell lymphoma. *Ann Intern Med* 101:484-487, 1984.

Burrows FJ, Watanable Y and Thorpe PE. A murine model for antibody-directed targeting of vascular endothelial cells in solid tumors. *Cancer Res* 52:5954-5962, 1992.

Burton JD, Weitz CH, Kay NE, et al. Malignant chronic lymphocytic leukemia B cells elaborate soluble factors that down-regulate T cell and NK function. *Am J Hematol* 30:61-67, 1989.

Cannon JB and Hui HW. Immunoconjugates in drug delivery systems. In: *Targeted Therapeutic Systems* (Tyle P and Ram BP, ed.), New York: Marcel Dekker, Inc., p.121-140, 1990.

Cannon MJ, Pisa P, Fox RI and Cooper NR. Epstein-Barr virus induced aggressive lymphoproliferative disorders of human B cell origin in SCID/hu chimeric mice. *J Clin Invest* 85:1333, 1990.

Carney PL, Rogers PE and Johnson DK. A dual isotope study of I-125 and In-111 labeled antibody in athymic mice. *J Nucl Med* 30:379-384, 1989.

Carrasquillo JA, Abrams PG, Schroff RW, et al. Effect of antibody dose on the imaging and biodistribution of indium-111 9.2.27 anti-melanoma monoclonal antibody. *J Nucl Med* 29:39-47, 1988.

Carter P, Presta L, Gorman CM, et al. Humanization of an anti-p185[HER2] antibody for human cancer therapy. *Proc Natl Acad Sci USA* 89:4285-4289, 1992.

Champlin R, Ho W, Gajewski J, et al. Selective depletion of CD8+ lymphocytes for prevention of graft-versus-host disease after allogeneic bone marrow transplantation. *Blood* 76:418, 1990.

Chan PC, Lisco E and Adelstein SJ. The radiotoxicity of iodine-125 in mammalian cells, II. A comparative study on cell survival and cytogenic responses to [125]IUdR, [131]IUdR and [3]HTdR. *Radit Res* 67:332-343, 1976.

Chang T, Dazord A and Neville Jr. DM. Artificial hybrid protein containing a toxin protein fragment and a cell membrane receptor-binding moiety in a disulfide conjugate. *J Biol Chem* 252:1515-1522, 1977.

Chapel HM and Bunch C. Mechanisms of infection in chronic lymphocytic leukemia. *Sem Hematol* 24:291-296, 1987.

Chaudhary VK, Batra JK, Gallo MR, et al. A rapid method of cloning functional variable-region antibody genes in *Escherichia coli* as single-chain immunotoxins. *Proc Natl Acad Sci USA* 87:1066-1070, 1990b.

Chaudhary VK, Gallo MG, FitzGerald D, et al. A recombinant single-chain immunotoxin composed of anti-Tac variable regions and a truncated diphtheria toxin. *Proc Natl Acad Sci USA* 87:9491-9494, 1990a.

Chaudhary VK, Queen C, Junghans RP, et al. A recombinant immunotoxin consisting of two antibody variable domains fused to Pseudomonas exotoxin *Nature* 339:394-397, 1988.

Chello PL, Sirotnak FM and Dorick DM. Alternations in the kinetics of methotrexate transport during growth of L1210 murine leukemia cells in culture. *Mol Pharmacol* 18:274-278, 1980.

Chervonsky AV, Faerman AI, Evdonina LV, et al. A simple metabolic system for selection of hybrid hybridomas (tetramas) producing bispecific monoclonal antibodies. *Mol Immunol* 25:913, 1988.

Cheson BD, Bennett JM, Rai KR, et al. Guideline for clinical protocols for chronic lymphocytic leukemia: recommendations of the National Cancer Institute-Sponsored Working Group. *Am J Hematol* 29:152-163, 1988.

Chiou RK, Vessella RL, Limas C, et al. Monoclonal antibody-targeted radiotherapy of renal cell carcinoma using a nude mice model. *Cancer* 61:1766-1775, 1988

Cobb LM. Intratumor factors influencing the access of antibody to tumor cells. *Cancer Immunol Immunother* 28:235-240, 1989.

Colapinto EV, Humphrey PA, Zalutsky MR, et al. Comparative localization of murine monoclonal antibody Mel-14 F(ab)'2 fragment and whole IgG2a in human glioma xenografts. *Cancer Res* 48:5701-5707, 1988.

Colapinto EV, Zalutsky MR, Archer GE, et al. Radioimmunotherapy of intracerebral human glioma xenografts with ^{131}I-labeled F(ab)'2 fragments of monoclonal antibody Mel-14. *Cancer Res* 150:1822-1827, 1990.

Colcher D, Bird R, Roselli M, et al. In vivo tumor targeting of a recombinant single-chain antigen-binding protein. *J Natl Cancer Inst* 82:1191-1197, 1990.

Cone L and Uhr JW. Immunc - deficiency disorders associated with chronic lymp : cytic leukemia and multiple myeloma. *J Clin Invest* 43:2241-2248, 1964.

Cope DA, Dewhirst MW, Friedman HS, et al. Enhanced delivery of a monoclonal antibody F(ab)'2 fragment to subcutaneous human glioma xenografts using local hyperthermia. *Cancer Res* 50:1803-1809, 1990.

Corvalan JRF and Smith W. Construction and characterization of a hybrid-hybrid monoclonal antibody recognizing both carcinoembryonic antigen (CEA) and vinca alkaloids. *Cancer Immunol Immunother* 24:127-132, 1987a.

Corvalan JRF, Smith W and Gore VA. Tumor therapy with vinca alkaloids targeted by a a hybrid-hybrid monoclonal antibody recognizing both CEA and vinca alkaloids. *Int J Cancer* 2:22, 1988 (suppl).

Corvalan JRF, Smith W, Gore VA and Brandon DR. Specific in vitro and in vivo drug localization to tumor cells using a hybrid-hybrid monoclonal antibody recognizing both carcinoembryonic antigen (CEA) and vinca alkaloids. *Cancer Immunol Immunother* 24:133-137, 1987b.

Cotton RGH and Milstein C. Fusion of two immunoglobulin-producing myeloma cells. *Nature* 244, 42, 1973.

Courtney-Luck NS, Epenetos AA, Moore R, et al. Development of primary and secondary immune responses to mouse monoclonal antibodies used in the diagnosis and therapy of malignant neoplasms. *Cancer Res* 46:6489-6493, 1986.

Cumber JA, Forrester JA, Foxwell BMJ, et al. Preparation of antibody-toxin conjugates. *Methods Emzymol* 112:207-225, 1985.

Cummings J, Neville W and Smyth JF. The molecular pharmacology of doxorubicin in vivo. *Eur J Cancer* 27:532, 1991.

Cunningham BA, Hemperly JJ, Murray BA et al. Neutral cell adhesion molecule: structure, immunoglobulin-like domains, cell surface modulation, and alternative RNA splicing. *Science* 236:799-806, 1987.

Czuczman MS, Straus DJ, Divgi CR, et al. A phase I dose escalation trial of ^{131}I-labeled monoclonal antibody OKB7 in patients with non-Hodgkin's lymphoma. *Blood* 76:345a (Abs.), 1990 (suppl 1).

Dalmark M and Strom HH. A fickian diffusion transport process with feature of transport catalysis. *J Gen Physiol* 78:349-364, 1981.

De Klein A, van Kessel AG, Grosveld G, et al. A cellular oncogene is translocated to the Philadelphia chromosome in chronic myelogenous leukemias. *Nature* 300:550-554, 1982.

De Lau WBM, van Loon AE, Heije K, et al. Production of hybrid hybridomas based on HAT^s-neomycin^r double mutants. *J Immunol Methods* 117:1, 1989.

De Meij JR. Colloidal gold probes in immunocytochemistry. In: *Immunochemistry: Practical Application in Pathology and Biology* (Polak JM and Van Noorden S, ed.), Bristol-London-Boston: John Wright and Sons, p. 82-112, 1983.

De Palazzo IG, Holmes M, Gercel-Taylor C and Weiner LM. Antitumor effects of a bispecific antibody targeting CA19-1 antigen and CD16. *Cancer Res* 52:5713-5719, 1992.

Dedrick RL and Flessner MF. Pharmacokinetic consideration of monoclonal antibodies. In: *Immunity to Cancer II* (Mitchell M, ed.), p. 429-438, 1989.

DeFreitas E, Suzuki H, Herlyn D, et al. Human antibody induction to the idiotypic and anti-idiotypic determinants of a monoclonal antibody against a gastrointestinal carcinoma antigen. *Curr Top Microl Immunol* 119:75-89, 1985.

Deleo AB, Jay G, Appelia E, et al. Detection of a transformation-related antigen in chemically induced sarcomas and other transformed cells of the mouse. *Proc Natl Acad Sci USA* 76:2420-2424, 1979.

Deleo AB, Shiku H, Takahashi T, et al. Cell surface antigens of chemically induced sarcomas of mouse. MuLV related antigens and alloantigens on cultured fibroblasts and sarcoma cells: description of a unique antigen on BALB/c meth A sarcoma. *J Exp Med* 146:1516-1530, 1977.

Demaner C, Brissinck J, VanMechelen M, et al. Treatment of murine B cell lymphoma with bispecific antibodies (anti-idiotype x anti-CD3). *J Immunol* 147:1091-1097. 1991.

Dembo M, Sirotnak FM and Moccio DM. Effects of metabolic deprivation on methotrexate transport in L1210 cells: further evidence for separate influx and efflux systems with different energetic requirement. *J Membrane Biol* 78:9-12, 1984.

DeNardo GL, DeNardo SJ, O'Grady LF, et al. Fractionated radioimmunotherapy of B-cell malignancies with ¹³¹I-Lym-1. *Cancer Res* 50:1014s-1016s, 1990 (suppl).

DeNardo GL, Young WC, DeNardo SJ, et al. Urinary metabolites after injection of monoclonal antibodies (Mab) or Fibrinogen (F) radioiodinated with a small and large number of iodine atoms. *J Nucl Med* 27:958 (Abs.), 1986.

DeVita VT, Hellman S and Rosenberg SA (eds): *Cancer: Principles and Practice of Oncology*. Second Edition. JB Lippincott Co., Philadelphia, 1985.

Dillman RO, Beauregard J, Shawler DL, et al. Continuous infusion of T101 monoclonal antibody in chronic lymphocytic leukemia. *J Biol Resp Mod* 5:394 , 1986a.

Dillman RO, Beauregard JC, Halpern SE and Clutter M. Toxicities and side effects associated with intravenous infusions of murine monoclonal antibodies. *J Biol Resp Mod* 5:73, 1986b.

Dillman RO, Johnson DE and Shawler DL. Immune interferon modulation of in vitro murine anti-human T cell monoclonal antibody-mediated cytotoxicity. *J Immunol* 136:728-731, 1986c.

Dillman RO, Johnson DE, Shawler DL and Koziol LA. Superiority of an acid-labile daunorubicin-monoclonal antibody immunoconjugate compared to free drug. *Cancer Res* 48:6097-6102, 1988.

Dillman RO, Mick R and McIntyre OR. Pentostatin in chronic lymphocytic leukemia: a phase II trial of cancer and leukemia group. *J Clin Oncol* 7:433-438, 1989a.

Dillman RO, Shawler DL, Dillman JB and Royston I. Therapy of chronic lymphocytic leukemia and cutaneous T-cell lymphoma with T101 monoclonal antibody. *J Clin Oncol* 2:881-891, 1984a.

Dillman RO, Shawler DL, Johnson DE, et al. Preclinical trials with combinations and conjugates of T101 monoclonal antibody and doxorubicin. *Cancer Res* 46:4886-4891, 1986d.

Dillman RO, Shawler DL, Sobol RE, et al. Murine monoclonal antibody therapy in two patients with chronic lymphocytic leukemia. *Blood* 59:1036-1045, 1982.

Dillman RO. Monoclonal antibodies in the treatment of cancer. *CRC Crit Rev Oncol Hematol* 1:357-386, 1984b.

Dillman RO. Monoclonal antibodies for treating cancer. *Ann of Intern Med* 111:592-603, 1989b.

DiMarco A. Adriamycin (NSC-123127): mode and mechanisms of action. *Cancer Chemother Rep* 6:91-106, 1975.

Donella-Deana A, Monti E and Pinna LA. Inhibition of tyrosine protein kinases by the antineoplastic agent adriamycin. *Biochem Biophys Res Commun* 160:1309-1315, 1989.

Dorshkind K, Pollack SB, Bosma MJ and Phillips RA. Natural killer (NK) cells are present in mice with severe combined immunodeficiency (scid). *J Immunol* 134:3798, 1985.

Douillard JY, Lehur PA, Aillet G, et al. Immunohistochemical antigenic expression and in vivo tumor uptake of monoclonal antibodies with specificity for tumors of gastrointestinal tract. *Cancer Res* 46:4221-4224, 1986.

Drebin JA, Link VC and Greene MI. Monoclonal antibodies reactive with distinct domains of the neu oncogene-encoded P185 molecule exert synergistic anti-tumor effects in vivo. *Oncogene* 2:273-277, 1988.

Drebin JA, Link VC, Weinberg RA and Greene MI. Inhibition of tumor growth by a monoclonal antibody reactive with an oncogene-encoded tumor antigen. *Proc Natl Acad Sci USA* 83:9129-9133. 1986.

Duijvestijin A and Hamann A. Mechanisms and regulation of lymphocyte migration. *Immunol Today* 10:23, 1989.

Dupou-Cezanne L, Sautereau AM and Tocanne JF. Localization of adriamycin in model and natural membrane: influence of lipid molecular packing. *Eur J Biochem* 181:695-702, 1989.

Dyers MJS, Hale G, Hayhoe FGJ and Waldmann H. Effects of CAMPATH-1 antibodies in vivo in patients with lymphoid malignancies: Influence of antibody isotype. *Blood* 73:1431-1439, 1989.

Dykes PW, Bradwell AR, Chapman CE and Vaughan ATM. Radioimmunotherapy of cancer: clinical studies and limiting factors. *Cancer Treat Rev* 14:87-117, 1987.

Eary JF, Krohn KA, Kishore R and Nelp WB. Radiochemistry of halogenated antibodies. In: *Antibodies in Radiodiagnosis and Therapy* (Zalutsky MR, ed.), Boca Raton: CRC Press Inc., p. 83-102, 1989.

Eary JF, Press OW, Badger CC, et al. Imaging and treatment of B-cell lymphoma. *J Nucl Med* 31:1257-1268, 1990.

Ehrlich P. A general review of the recent work in immunity. In: *Collected Papers of Paul Ehrlich, Vol. 2: Immunology and Cancer Research*, Pergamon Press, London, p. 442-447, 1956.

Elias DJ, Hirschowitz L, Kline LE, et al. Phase I clinical comparative study of monoclonal antibody KS1/4 - methotrexate immunoconjugate in patients with non-small cell lung carcinomas. *Cancer Res* 50:4154-4159, 1990.

Embleton MJ and Ho TH. Comparative effects of methotrexate and monoclonal antibody-targeted methotrexate against methotrexate resistance and sensitive human osteogenic sarcoma cells. *IRCS Med Sci* 14:1163, 1986.

Embleton MJ. Targeting of anti-cancer therapeutic agents by monoclonal antibodies. *Biochem Soc Trans* 14:393, 1986.

Endo N, Takeda Y, Kishida K, et al. Target-selective cytotoxicity of methotrexate conjugated with monoclonal anti-MM46 antibody. *Cancer Immunol Immunother* 25:1, 1987.

Epenetos PA, Snook D, Durbin, et al. Limitation of radiolabeled monoclonal antibodies for localization of human neoplasms. *Cancer Res* 46:3183-3191, 1986.

Epstein AL, Marder RJ, Winter JN, et al. Two new monoclonal antibodies. Lym-1 and Lym-2, reactive with human B-lymphocytes and derived tumors, with immunodiagnostic and immunotherapeutic potential. *Cancer Res* 47:830-840, 1987.

Epstein AL, Zimmer AM, Spies SM, et al. Radioimmunodetection of human B-cell lymphomas with a radiolabeled tumor-specific monoclonal antibody (Lym-1). In: *Malignant Lymphomas and Hodgkin's Disease: Experimental and Therapeutic Advances* (Cavalli F, Bonadonna G and Rozencweig M , ed.), Boston: Martinus Nijoff publishing Co., p. 569-577, 1985.

Esteban JM, Schlom J, Gansow OA, et al. New method for the chelatio... indium-111 to monoclonal antibodies: biodistribution and imaging of athymic mice bearing human colon carcinoma xenografts. *J Nucl Med* 26:861-870, 1987.

Fagnani R, Hagan MS and Bartholomew R. Reduction of immunogenicity by covalent modification of murine and rabbit immunoglobulins with oxidized dextrans of low molecular weight. *Cancer Res* 50:3638-3645, 1990.

Faguet GB, Agee JF, DiPiro JT. Blood kinetics, tissue distribution, and radioimaging of anti-common chronic lymphocytic leukemia antigen (cCLLa) monoclonal antibody CLL2 in mice transplanted with cCLLa-bearing human leukemic cells. *Blood* 75:1853-1861, 1990.

Fell HP, Gayle MA, Grosmaire I and Ledbetter JA. Genetic construction and characterization of a fusion protein consisting of a chimeric F(ab)'2 with specificity for carcinomas and human IL-2. *J Immunol* 146:2446-2452, 1991.

Fenwick JR, Philpott GW and Connett JM. Biodistribution and histological localization of anti-human colon cancer monoclonal antibody (MAB) 1A3: the influence of administered MAB dose on tumor uptake. *Int J Cancer* 44:1017, 1989.

Fidlerr IJ, Gerstein DM and Hart IR. The biology of cancer invasion and metastasis. *Adv Cancer Res* 28:149-250, 1978.

Finn OJ. T cell recognition of human epithelia tumor mucins: identification for active immunotherapy. *Proc Amer Assoc Cancer Res* 32:490-491, 1991.

Fishwild DM, Aberle S, Berhard SL and Kung AHC. Efficacy of an anti-CD7-ricin A chain immunoconjugate in a novel murine model of human T-cell leukemias. *Cancer Res* 52:3056-3062, 1992.

Flickinger RA and Trost SR. Cytotoxicity of antibody-phospholipase C conjugates on cultured Friend leukemia cells. *Eur J Cancer* 12:159-160, 1976.

Foley. Antigenic properties of methylcholanthrene-induced tumor in nude mice of the strain of origin. *Cancer Res* 13:835-837, 1953.

Folger WE, Sun LK, Klinger M, et al. Biological characterization of a chimeric mouse-human IgM antibody directed against the 17-1A antigen. *Cancer Immunol Immunother* 30:43-50, 1989.

Folkman J. Tumor angiogenesis. *Adv Cancer Res* 43:175-201, 1985.

Foon KA and Todd RF III. Immunological classification of leukemia and lymphoma. *Blood* 68:1-31, 1986a.

Foon KA, Maluish AE, Abrams PG, et al. Recombinant leukocyte A interferon therapy for advanced hairy cell leukemia: therapeutic and immunologic results. *Am J Med* 80:351-356, 1986b.

Foon, KA, Rai, KR and Gale, RP. Chronic lymphocytiv leukemia: new insight into biology and therapy. *Ann Intern Med* 113: 525-539, 1990.

Foon KA, Schroff RW, Bunn PA, et al. Effects of monoclonal antibody therapy in patients with chronic lymphocytic leukemia. *Blood* 64:1085 , 1984a.

Foon KA, Sherwin SA, Abrams PG, et al. Treatment of advanced non-Hodgkin's lymphoma with recombinant leukocyte A interferon. *N Engl J Med* 311:1148-1152, 1984b.

Ford CHJ, Newman CE, Johnson Jr, et al. Localization and toxicity study of a vindesine-anti-CEA conjugate in patients with advanced cancer. *Br J Cancer* 47:35-42, 1983.

Frank MM. Complement in the pathophysiology of human diseases. *N Engl J Med* 316:1525-1530, 1987.

Frankel AE, ed. *Immunotoxins*. Boston:Kluwer Acad., 1988.

Frankel ME and Gerhard W. The rapid determination of binding constants for antiviral antibodies by a radioimmunoassay. An analysis of the interaction between hybridoma proteins and influenza virus. *Mol Immunol* 16:101-106, 1979.

Freeman AS, Boyd AW, Bieber FR et al. Normal cellular counterparts of B cell chronic lymphocytic leukemia. *Blood* 70:418-427, 1987.

French Cooperation Group on Chronic Lymphocytic Leukemia. A randomized clinical trial of chlorambucil versus COP in stage B chronic lymphocytic leukemia. *Blood* 75:1422-1425, 1990b.

French Cooperation Group on Chronic Lymphocytic Leukemia. Effect of chlorambucil and therapeutic decision in initial forms of chronic lymphocytic leukemia (Stage A): results of a randomized clinical trial on 612 patients. *Blood* 75:1414-1421, 1990a.

French Cooperation Group on Chronic Lymphocytic Leukemia. Long-term results of the chop regimen in Stage C chronic lymphocytic leukemia. *Br J Haematol* 73:334-340, 1989.

Frens G. Controlled nucleation for the regulation of the particle s: .e in monodisperse gold suspensions. *Nature Physical Sci* 241:20-22, 1973.

Fujimori K, Covell DG, Fletcher JE and Weinstein JN. A modeling analysis of monoclonal antibody percolation through tumors: A binding site barrier. *J Nucl Med* 31:1191, 1990.

Fulop GM and Phillips RA. Full reconstitution of the immune deficiency in SCID mice with normal stem cells required low-dose irradiation of the recipients. *J Immunol* 136:4438, 1986.

Fung YK, Lewis WG, Crittenden LB and Kung HJ. Activation of the cellular oncogene *c-erb* B by LTR insertion: molecular basis for induction of erythroblastosis by avian leukosis virus. *Cell* 33:357-368, 1983.

Furukawa KS, Furukawa R, Real FX, et al. A unique antigenic epitope of human melanoma is carried on the common melanoma glycoprotein gp 95/97. *J Exp Med* 169:585-590, 1989.

Gadol N and Ault KA. Phenotypic and functional characterization of human Leu 1 (CD5) B ells. *Immunol Rev* 93:23-35, 1986.

Gale RP and Foon KA. Chronic lymphocytic leukemias. Recent advances in biology and treatment. *Ann Intern Med* 103:101-120, 1985.

Galivan J. Evidence for the cytotoxic activity of polyglutamate derivatives of methotrexate. *Mol Pharmacol* 17:105-109, 1980.

Gallego J, Price MR and Baldwin RW. Preparation of four daunomycin-monoclonal antibody 791T/36 conjugates with anti-tumor activity. *Int J Cancer* 33:737-744, 1984.

Gallo RC, Kalyanaraman VS, Sarngadharan MG et al. Association of the human type C retrovirus with a subset of adult T-cell cancers. *Cancer Res* 43:3892-2899, 1983.

Gannon JV, Greaves R, Iggo R and Lane DP. Activating mutations in p53 produce a common conformational effect. A monoclonal antibody specific for the mutant form. *EMBO J* 1595-1602, 1990.

Garnett MC and Baldwin RW. Endocytosis of a monoclonal antibody recognizing a cell surface glycoprotein antigen, visualised using immunoelectron microscopy. *Eur J Cell Biol* 41:214-221, 1986.

Garnett MC, Embleton MJ, Jacobs E and Baldwin RW. Preparation and properties of a drug-carrier-antibody conjugate showing selective antibody-directed cytotoxicity in vitro. *Int J Cancer* 31:661, 1983.

Garrido MA, Valdayo MJ, Winkler DF, et al. Targeting human T-lymphocytes with bispecific antibodies to react against human ovarian carcinoma cells growing in nu/nu mice. *Cancer Res* 50:4227-4232, 1990.

Geissler F, Anderson SK and Press OW. Intracellular catabolism of radiolabeled anti-CD3 antibodies by leukemia T cells. *Cellular Immunol* 137:96-110, 1991.

Gendler S, Taylor-Papadimitriou J, Duhlig T, et al. A highly immunogenic region of a human polymorphic epithelia mucin expressed by carcinomas is made up of tandem repeats. *J Biol Chem* 263:12820-12823, 1988.

Gerretsen M, Schrijvers AHGJ, van Walsum M, et al. Radioimmunotherapy of human head and neck squamous cell carcinoma xenografts with 131I-labeled monoclonal antibody E48 IgG. *Br J Cancer* 66:496-502., 1992.

Ghetie M, Richardson J, Tucker T, et al. Antitumor activity of Fab' and IgG-anti-CD22 immunotoxins in disseminated human B lymphoma grown in mice with severe combined immunodeficiency disease: effect on tumor cells in extranodal steps. *Cancer Res* 51:5876-5880, 1991.

Ghetie MA, Tucker T, Jones D, et al. Disseminated or localized growth of a human B-cell tumor (Daudi) in SCID mice. *Int J Cancer* 45:481-485, 1990.

Ghose T and Blair AH. Antibody-linked cytotoxic agents in the treatment of cancer: current status and future prospects. *J Natl Cancer Inst* 61:657-676, 1978.

Ghose T and Blair AH. The design of cytotoxic-agent-antibdy conjugates. *CRC Crit Rev of Ther Drug Carrier Syst* 3:263-361, 1987.

Ghose T and Cerini M. Radiosensitization of Ehrlich ascites tumor cells by a specific antibody. *Nature* 222:993-994, 1969.

Ghose T and Guclu A. Cure of a mouse lymphoma with radio-iodinated antibody. *Eur J Cancer* 10:787-792, 1974.

Ghose T and Nigam S. Antibody as carrier of chlorambucil. *Cancer* 29:1398-1400, 1972a.

Ghose T, Blair AH and Kulkarni P. Preparation of antibody-linked cytotoxic agents. *Methods Enzymol* 93:280-332, 1983b.

Ghose T, Blair AH, Kralovec J, et al. Synthesis and testing of antibody-antifolate conjugates for drug targeting. In: *Antibody-Mediated Delivery System* (Rodwell JD, ed.), Marcel Dekker Inc., New York, p 81-122, 1988a.

Ghose T, Blair AH, Kulkarni, et al. Targeting of radionuclides and drugs for the diagnosis and treatment of cancer. In: *Targeting of Drugs* (Gregoriadis G, ed.), Plenum Press, p. 55-82, 1982a.

Ghose T, Blair AH, Martin RH, et al. Tumor imaging by antitumor antibody linked radionuclides. In: *Tumor Imaging* (Burchiel S, ed.), New York: Masson, p. 167-178, 1982b.

Ghose T, Blair AH, Uadia P, et al. Antibodies as carriers of cancer chemotherapeutic agents. *Ann N Y Acad Sci* 446:213, 1985.

Ghose T, Blair AH, Vaughan K and Kulkarni P. Antibody-directed drug targeting in cancer. In: *Targeted Drugs* (Goldberg, EP, ed.), John Wiley & Sons, New York, Vol.2, p. 1-22, 1983a.

Ghose T, Cerini M, Carter M and Nairn RC. Immunoradioactive agent against cancer. *Br Med J* 1:90, 1967.

Ghose T, Lee CLY, Faulkner G, et al. Progression of a human B cell chronic lymphocytic leukemia line in nude mice. *Am J Hematol* 28:146-154, 1988b.

Ghose T, Lee CLY, Fernandez LA, et al. Role of 1q trisomy in tumorigenicity, growth, and metastasis of human leukemic B-cell clone in nude mice. *Cancer Res* 50:3337-3342, 1990.

Ghose T, Norvell ST, Guclu A, et al. Immunochemotherapy of cancer with chlorambucil-carrying antibody. *Br Med J* 1:495-499, 1972b.

Ghose T, Norvell ST, Guclu A, et al. Immunochemotherapy of malignant melanoma with chlorambucil-bound anti-melanoma globulins: Preliminary results in patients with disseminated disease. *J Natl Cancer Inst* 58:845-852, 1977.

Ghose T, Norvell ST, Guclu A, et al., Immunochemotherapy of human malignant melanoma with chlorambucil-carrying antibody. *Eur J Cancer* 11:321-326, 1975.

Ghose T, Ramakrishnan S, Kulkarni P, et al. Use of antibodies against tumor-associated antigens for cancer diagnosis and treatment. *Transp Proc* 13:1970-1972, 1981.

Ghose T, Singh M, Faulkner G, et al. Antibody-aimed liposomal drug delivery. In: *Liposomes as Drug Carriers* (Gregoriadis G, ed.), New York: John Wiley and Sons, p. 697-708, 1988c.

Ghose T, Tai J, Guclu A, et al. Antibodies as carriers of radionuclides and cytotoxic drugs in the treatment and diagnosis of cancer. *Ann NY Acad Sci* 277:671-689, 1976.

Gianni L, Corden B and Myers C. The biochemical basis of anthracycline toxicity and anti-tumor action. *Rev Biochem Toxicol* 5:1-82, 1983.

Gil J, Alvarez R, Juan E, et al. Inhibition of in vivo tumor growth by a monoclonal IgM antibody recognizing tumor cell surface carbohydrates. *Cancer Res* 50:7301-7306, 1990.

Gillies SD, Wesolowski JS and Lo KM. Targeting human cytotoxic T lymphocytes to kill heterologous epidermal growth factor-bearing tumor cells. *J Immunol* 146:1067-1071, 1991.

Girling A, Bartkova J, Burchell J, et al. A core protein epitope of the polymorphic epithelial mucin detected by the monoclonal antibody SM-3 is selectively exposed in a range of primary carcinomas. *Int J Cancer* 43:1072-1076, 1989.

Glennie MJ, Brennand DM, Bryden F, et al. Bispecific F(abγ)2 antibody for the delivery of saporin in the treatment of lymphoma. *J Immunol* 141:3662-3670, 1988.

Glennie MJ, McBride HM, Worth AT and Stevenson GT. Prepaiation and performance of bispecific F(ab'γ)'2 antibody containing thioether-linked fragments. *J Immunol* 139:2367-2375, 1987.

Gobuty A, DeNardo GL and DeNardo SJ. Lym-1 radioimmunotherapy: a case history of how we do it. *Anti Immunoconj Radiopharm* 5:13-22, 1992.

Godal A, Fodstad O and Pihl A. Antibody formation against the cytotoxic protein abrin and ricin in humans and mice. *Int J Cancer* 32:515-521, 1983.

Goedegebuure PS, Sea D, Braakman E, et al. Induction of lysis by T cell receptor γδ+/CD3+ T lymphocytes via CD2 requires triggen via the T11.1 epitope only. *J Immunol* 142:1797, 1989.

Goldenberg DM and Larson SM. Radioimmunodetection in cancer identification. *J Nucl Med* 33:803-814, 1992.

Goldenberg DM, Blumeathal RD, Sharkey RM, et al. Biological and clinical perspectives of cancer imaging and therapy with radiolabeled antibodies. *Semin Cancer Biol* 1:217-225, 1990.

Goldenberg DM, Horowitz JA, Sharkey RM, et al. Targeting, dosimetry, and radioimmunotherapy of B-cell lymphomas with iodine-131-labeled LL2 monoclonal antibody. *J Clin Oncol* 9:548-564, 1991c.

Goldenberg DM. Cancer imaging and therapy with radiolabeled antibodies. *Adv Exp Med Biol* 303:107-117, 1991b.

Goldenberg DM. Challenge to the therapy of cancer with monoclonal antibodies (editorial comment). *J Natl Cancer Inst* 83:78-79, 1991a.

Goldenberg DM. Radioimmunotherapy of cancer: arming the missiles (editorial comment). *J Nucl Med* 33:1110-1112, 1992.

Goldenberg DM. Targeting of cancer with radiolabeled antibodies: Prospects for imaging and therapy. *Arch Path Lab Med* 112:580-587, 1988.

Goldman ID, Lichtenstein NS and Oliverio VT. Carrier-mediated transport of the folic acid analogue, methotrexate, in the L1210 leukemia cells. *J Biol Chem* 243:5007-5010, 1968.

Goldman ID. A model system for the study of heteroexchange diffusion: methotrexate-folate interactions in L1210 leukemic and Ehrlich ascites tumor cells. *Biochem Biophys Acta* 233:624-634, 1971.

Goldstein B, Wofsy C and Echsavarria-Hersa H. Effect of membrane flow on the capture of receptor by coated pit. *J Biophys* 53:405-414, 1988.

Goodman GE, Hellstrom I, Yelton DE, et al. Phase I trials of chimeric (human-mouse) monoclonal antibody L6 inpatients with non-small-cell lung, colon, and breast cancer. *Cancer Immunol Immunother* 36:267-273, 1993.

Goormaghtigh E and Ruysschaert JM. Anthracycline gycoside-membrane interaction. *Biochim Biophys Acta* 779:271-288, 1984.

Goormaghtigh E, Chatelain P, Caspers J and Ruysschaert JM. Evidence of a specific complex between adriamycin and negatively charged phospholipids. *Biochim Biophys Acta* 597:1-14, 1980.

Gorman SC, Clark MR, Routledge EG and Cobbold SP. Reshaping a therapeutic CD4 antibody. *Proc Natl Acad Sci USA* 88:4181-4185.

Gosalvez M, Blanco M, hunter J, et al. Effects of anticancer agents on the respiration of isolated mitochondria and tumor cells. *Eur J Cancer* 10:567-573, 1974.

Gould BJ, Borowitz MJ, Groves ES, et al. Phase I study of an anti-breast cancer immunotoxin by continuous infusion. *J Natl Cancer Inst* 81:775-781, 1989.

Goustin AS, Leof EB, Shipley GD and Moses HL. Growth factors and cancer. *Cancer Res* 46:1015-1029, 1986.

Gravelle M and Ochia. The targeting of CD4+ lymphocytes to a B cell lymphoma. A comparison of anti-CD3-anti-idiotype antibody conjugate and antigen-anti-idiotype antibody conjugates. *J Immunol* 142:4079-4084, 1989.

Green R, Collins J, Jenkins J et al. Plasma pharmacokinetics of adriamycin and adriamycinol: implications for the design of in vitro experiments and treatment protocols. *Cancer Res* 43:3417-3422, 1983.

Greenfield RS, Kaneko T, Daues A, et al. Evaluation in vivo of adriamycin immunoconjugates synthesized using an acid-sensitive hydrazone linker. *Cancer Res* 50:6600-6607, 1990.

Greiner JW, Guadagni F, Noguchi P, et al. Recombinant interferon enhances monoclonal antibody-targeting of carcinoma lesions in vivo. *Science* 235:895-898, 1987.

Gribben JG, Freedman AS, Neuberg D, et al. Immunologic purging of marrow assessed by PCR before autologous bone marrow transplantation for B-cell lymphoma. *N Engl J Med* 325:1525, 1991.

G.)ssbard ML, Freedman AS, Ritz J, et al. Serotherapy of B-cell neoplasms with anti-B4-blocked ricin: A phase I trial of daily bolus infusion. *Blood* 79:576, 1992a.

Grossbard ML, Press OW, Appelbaum FR, et al. Monoclonal antibody-based therapies of leukemia and lymphoma. *Blood* 80:863-878, 1992b.

Guclu A, Tai J and Ghose T. Endocytosis of chlorambucil-bound antitumor globulin following capping in EL4 lymphoma cells. *Immunol Commun* 4:229, 1975.

Guha AK, Ghose T, Luner SJ, et al. Monoclonal antibodies against Epstein-Barr virus transformed B lymphocytes from a CLL patient. *Hybridoma* 9:119-131, 1990.

Guha AK, Ghose T, Singh M, et al. Tumor localization of monoclonal antibodies against human renal carcinoma in a xenograft model. *Cancer Lett* 61:35-43, 1991.

Gupta S and Good RA. Markers of human lymphocyte subpopulations in primary immunodeficiency and lympho: ioliferative disorders. *Semin Hematol* 17:1-29, 1980.

Hadziak RM, Lewis GD, Winget M, et al. P185^{HER2} monoclonal antibody has antiproliferative effects in vitro and sensitizes human breast tumor cells to tumor necrosis factor. *Mol Cell Biol* 9:1165-1172, 1989.

Hakomori S, Nudelman E, Levery SB and Kannagi R. Novel fucolipids accumulating in human adenocarcinoma. I. Glycolipids with di or trifucosylated type 2 chain. *J Biol Chem* 259:4672-4680, 1984.

Hakomori S. Aberrant glycosylation in tumors and tumor-associated carbohydrate antigens. *Adv Cancer Res* 52:257-331, 1989.

Hakomori S. Biochemical basis of tumor-associated carbohydrate antigens: current trends, future perspectives, and clinical applications. *Immunol Aller Clin N Am* 10:781-802, 1990.

Hakomori S. Possible functions of tumor-associated carbohydrate antigens. *Curr Opin Immunol* 3:646-653, 1991.

Hale G, Dyer MJS, Clark MR, et al. Remission induction in non-Hodgkin lymphoma with reshaped human monoclonal antibody CAMPATH-1H. *Lancet* 2:1394 , 1988.

Han T, Ezdinli EZ, Shimaoka KS et al. Chlorambucil vs. combined chlorambucil-corticosteroid therapy in chronic lymphocytic leukemia. *Cancer* 31:5021-5028, 1973.

Hariharan IK, Harris AW, Crawford M, Ábud H, Webb E, Cory S and Adams JM. The bcr-abl oncogene induces lymphomas in transgenic mice. *Mol Cell Biol* 9:2798-2805, 1989.

Hasmann M, Vale: GK, Tapiero H, et al. Membrane potential differences between adriamycin sensitive and resistant cells as measured by flow cytometry. *Biochem Pharmacol* 38:305-312, 1989.

Hellstrom I, Beaumier PL and Hellstrom KE Antitumor effects of L6, an IgG2a antibody that reacts with most human carcinomas *Proc Natl Acad Sci* 83:7059-7063, 1986.

Henderson GB and Zevely EM Transport routes utilized by L1210 cells for the influx and efflux of methotrexate *J Biol Chem* 259:1526-1531, 1984.

Henderson GB, Tsuji JM and Kumar H. Transport of folate compounds by leukemic cells: evidence for a single influx carrier for methotrexate, 5-methyltetrahydrofolate, and folate in CCRF-CEM human lymphoblasts. *Biochem Pharmacol* 36:3007-3010, 1987.

Henderson GB, Tsuji JM and Kurmar HP. Characterization of the individual transport routes that mediate the influx and efflux of methotrexate in CCRF-CEM human lymphoblastic cells. *Cancer Res* 46:16'3-1636, 1986.

Herlyn D, Ross AH, Iliopoulos D, Koprowski H. Induction of specific immunity to human colon carcinoma by anti-idiotypic antibodies to monoclonal antibody CO-17A *Eur J Immunol* 17:1649-1652, 1987.

Herlyn DM and Koprowski H. Monoclonal anticolon carcinoma antibodies in complement-dependent cytotoxicity. *Int J Cancer* 27:769-774, 1981.

Herlyn DM and Koprowski H. IgG2a monoclonal antibodies inhibit human tumor growth through interaction with effector cells. *Proc Natl Acad Sci* 79:4761-4765, 1982.

Herlyn DM, Steplewski Z, Herlyn MF and Koprowski H. Inhibition of growth of colorectal carcinoma in nude mice by monoclonal antibody. *Cancer Res* 40:717-721, 1980.

Herlyn M and Koprowski H. Melanoma antigens: immunological and biological characterization and clinical significance *Annu Rev Immunol* 6:283-308, 1988.

Herlyn M, Menrad A and Koprowski H. Structure, function and clinical significance of human tumor antigens. *J Natl Cancer Inst* 82:1883-1889, 1990.

Herlyn M, Rodeck U and Koprowski H. Shedding of tumor-associated antigens in vitro and in vivo. *Adv Cancer Res* 49 189-221, 1987

Hertler AA, Schlossman DM, Boiowitz MJ, et al. A phase I study of T101-ricin A chain immunotoxin in refractory chronic lymphocytic leukemia *J Biol Res Mod* 7 97-113, 1988.

Hill BT, Bailey BD, White JC, et al. Characteristic of transport of 4-amino antifolates and folate compounds by two lines of L5178Y lymphoblasts, one with impaired transport of methotrexate. *Cancer Res* 39:2440-2446, 1979

Hnatowich DJ, Chinol M, Siebecker DA, et al. Patient biodistribution of intraperitoneally administered yttrium-90-labeled antibody. *J Nucl Med* 29:1428-1434, 1988.

Hnatowich DJ, Gionet M, Rusckowski M, et al. Pharmacokinetics of In-111 labeled OC-125 antibody in cancer patients compared with the 19-9 antibody. *Cancer Res* 47:6111-6117, 1987.

Hnatowich DJ, Layne WW, Childs RL, et al. Radioactive labeling of antibody: a simple and efficient method. *Science* 220, 613-615, 1983.

Hnatowich DJ. Antibody radiolabeling, problems and promises. *Nucl Med Biol* 17:49-52, 1990.

Holland JF. Karnofsky memorial lecture: breaking the cure barrier. *J Clin Oncol* 1:75-90, 1983.

Holton OD, Black CDV and Parker RJ. Biodistribution of monoclonal IgG1, F(ab)'2 and Fab' in mice after intravenous injection: A comparison between anti-B cell (anti-LyB8.2) and irrelevant (MOPC-21) antibodies. *J Immunol* 139:3041, 1987.

Hopkins CR and Trowbridge IS. Internalization and processing of transferrin and the transferrin receptor in human carcinoma A431 cells. *J Cell Biol* 97:508-521, 1983.

Houghton A and Scheinberg D. Monoclonal antibodies in the treatment of hematopoietic malignancies. *Semin Hematol* 25:23-29, 1988.

Hsieh-Ma S, Eatn AM, Shi T and Ring DB. In vitro cytotoxic targetng by human mononuclear cells and bispecific antbody 2B1, recognizing c-erbB-2 protooncogene production and Fcγ receptor III. *Cancer Res* 52:6832-683, 1992.

Humphrey PA, Gangarosa LM, Wong AG, et al. Deletion-mutant epithelial growth factor receptor in human gliomas: effect of type-II mutation on receptor function. *Biochem Biophys Res Commun* 178:1413-1420, 1991.

Hurwitz E, Kashi R, Arnon R, et al. The covalent linking of two nucleotide analogies to antibodies. *J Med Chem* 28:137, 1985.

Hurwitz E, Levy R, Maron R, et al. The covalent binding of daunomycin and adriamycin to antibodies, with retention of both drug and antibody activities. *Cancer Res* 35:1175-1181, 1975.

Hurwitz E, Maron R, Bernstein A, et al. The effect in vivo of chemotherapeutic drug-antibody conjugates in two experimental tumor systems. *Int J Cancer* 21:747-755, 1978.

Hyams DM, Estaban JM, Lollo CP, et al. Therapy of peritoneal carcinomatosis of human colon cancer xenografts with yttrium 90-labeled anti-carcinoembryonic antigen antibody ZCE025. *Arch Surg* 122:1333-1337, 1987.

Iliopoulos D, Ernst C, Steplewski Z, et al. Inhibition of metastases of a human melanoma xenograft by monoclonal antibody to the GD2/GD3 gangliosides. *J Natl Cancer Inst* 81:440-444, 1989.

International Workshop on Chronic Lymphocytic Leukemia. Chronic lymphocytic leukemia: recommendations for diagnosis, staging, and response criteria. *Ann Intern Med* 110:236-238, 1989.

Ioannides CG and Den Otter W. Concepts in immunotherapy of cancer: Introduction. *In Vivo* 5:551-552, 1991.

Itzkowitz SH, Tuan M, Fukushi Y, et al. Lewis^x and sialylated Lewis^x-related antigen expression in human malignant and nonmalignant colonic tissues. *Cancer Res* 46:2627-2632, 1986.

Jain R. Tumor blood response to heat and pharmacological agents. In: *Radiation Research (Proceeding of the Eighth International Congress of Radiation Research,* Fielden EM, Fowler JF, Hendry JH and Scott D, ed.), Vol. 2, p. 813-818, London: Taylor and Francis, 1987.

Jain RK and Baxter LT. Mechanisms of heterogeneous distribution of monoclonal antibodies and other macromolecules in tumors: significance of elevated interstitial pressure. *Cancer Res* 48:7022-7032, 1988.

Jain RK, Weissbrod J and Wei J. Mass transfer in tumors: characterization and applications. *Adv Cancer Res* 33:251-310, 1980.

Jain RK. Determinants of tumor blood flow: a review. *Cancer Res* 48:2641-2658, 1988.

Jain RK. Physiological barriers to delivery of monoclonal antibodies and other macromolecules in tumors. *Cancer Res* 50:814s-819s, 1990 (suppl).

Jain RK. Transport of molecules across tumor vasculature. *Cancer Metastasis Rev* 6:559-594, 1987a.

Jain RK. Transport of molecules in tumor interstitium: a review. *Cancer Res* 47:3039-3051, 1987b.

Jansen B, Uckun FM, Jaszcz WB, Kersey JH. Establishment of a human t (4;11) leukemia in severe immunodeficient mice and successful treatment using anti-CD19 (B43)-pokeweed antiviral protein immunotoxin. *Cancer Res* 52:406-412, 1992.

Jansen CH, Tehrani M, Wigzell H, et al. Rational use of biological response modifiers in hematological malignancies - a review of treatment with interferon, cytotoxic cells and antibodies. *Leuk Res* 13:1039-1046, 1989.

Jennrich RI, McIlhinney R, Raghavan D and Neville AM. Application of stepwise regression to non-linear least squares estimation. *Technometrics* 10:63-72, 1968.

Jerne NK. Toward a network theory of the immune system [Abs.]. *Ann Immunol* 125C:373, 1974.

Johns DG and Bertino JR. Folate antagonists. In:*Cancer Medicine* (Holland JF and Frei E, eds.) Lea and Febiger, Philadelphia, p 775-790, 1982.

Johnson DA and Laguzza RC. Antitumor xenograft activity with a conjugate of a vinca derivative and the squamous carcinoma-reactive monoclonal antibody PF1/D. *Cancer Res* 47:3118, 1987.

Johnson JP, Stade BG, Holzmann B et al. De novo expression of intercellular-adhesion molecule 1 in melanoma correlates with increased risk of metastasis. *Proc Natl Acad Sci USA* 86:641-644, 1989.

Johnstone RW, Andrew SM, Hogarth MP, et al. The effect of temperature on the binding kinetics and equilibrium constants of monoclonal antibodies to cell surface antigens. *Mol Immunol* 27:327-333, 1990.

Joliver J, Fauchei F and Pinard MF. Influence of intracellular folates on methotrexate metabolism and cytotoxicity. *Biochem Pharmacol* 36:3310-3312, 1987.

Joliver J, Schilsky RL, Bailey BD et al. Synthesis, retention and biological activity of methotrexate polyglutamates in cultured human breast cancer cells. *J Clin Invest* 70:351-360, 1982.

Jones K and Bell GT. Human monoclonal antibody production: Current status and future prospects. *J Immunol Methods* 100:5, 1987.

Jones PL, Brown BA and Sands H. Uptake and metabolism of 111In-labeled monoclonal antibody B6.2 by the rat liver. *Cancer Res* 50:852s-856s, 1990 (suppl).

Jones PT, Dear PH, Foote J, et al. Replacing the complementarity-determining regions in a human antibody with those from a mouse *Nature* 321:522-525, 1986.

Juliusson G and Gahrton G. Chromosomi aberrations in B-cell chronic lymphocytic leukemia. Pathogenetic and clinical applications. *Cancer Genet Cytogenet* 45:143-160, 1990.

Jung G, Ledbetter JA and Muller-Eberhard HJ. Induction of cytotoxicity in rest human T lymphocytes bound to tumor cells by antibody heteroconjugates. *Proc Natl Acad Sci USA* 84:4611-4615, 1987.

Juranka PF, Zastawny RL and Ling V. P-glycoprotein: Multidrug-resisiance and a superfamily of membrane-associated transport proteins. *FASEB J* 3:2583-2592, 1989.

Kalofonos H, Rowlinson G and Epenetos AA. Enhancement of monoclonal antibody uptake in human colon tumor xenograft following irradiation. *Cancer Res* 50:159-163, 1990.

Kamel-Reid S, Letarte M, Sirari C, et al. A model of human acute lymphoblastic leukemia in immune deficient SCID mice. *Science* 246:1597-1600, 1989.

Kamen BA, Whyte-Bauer W and Bertino JR. A mechanism of resistance to methotrexate: NADPH but nor NADH stimulation of methotrexate binding to dihydrofolate reductase. *Biochem Pharmacol* 32:1837-1841, 1983.

Kaminski MS, Fig LM, Zasadny KR, et al. Imaging, dosimetry, and radioimmunotherapy with iodine-131-labeled anti-CD37 antibody in B-cell lymphoma. *J Clin Oncol* 10:1696-1711, 1992.

Kanellos J, Pietersz GA and McKenzie IFC. Studies of methotrexate-monoclonal antibody conjugates for immunotherapy. *J Natl Cancer Inst* 75:319-329, 1985.

Kaplan P and Meier EL. Nonparametric estimations from incomplete organizations. *J Am Stat Assoc* 53:457-481, 1958.

Karawajew L, Behrsing D, Kaiser G and Micheel B. Production and ELISA application of bispecific monoclonal antibodies against fluorescein isothiocyanate (FITC) and horseradish peroxidase (HRP). *J Immunl Methods* 111:95-99, 1988.

Karawajew L, Michell B, Behrsing O and Gaestel M. Bispecific antibody-producing hybrid hybridomas selected by a fluorescence activated cell sorter. *J Immunol Methods* 96:265, 1987.

Karpovsky B, Titus JA, Stephany DA and Segal DM. Production of target-specific effector cells using hetero-cross-linked aggregates containing anti-target cells and anti-Fc receptor antibodies. *J Exp Med* 160:1686-1701, 1984.

Kartner N, Riordan JR and Ling V. Cell surface P-glycoprotein associated with multidrug resistance in mammalian cell lines. *Science* 221:1285-1288, 1983.

Kasprzyk PG, Song SU, Fiore PPD and King CR. Therapy of an animal model of human gastric caner using a combination of anti-*erb*B-2 monoclonal antibodies. *Cancer Res* 2771-2776, 1992

Kassis AI, Adelstein SJ and Bloomer WD. Therapeutic implications of Auger emitting radionuclides. In: *Radionuclides in Therapy* (Spencer RP, Friedman A and Seevers RH, ed.), Boca Raton: CRC Press, p. 119-134, 1987.

Kaufman RJ, Bertino JR and Schimke RT. Quantitation of dyhydrafolate reductase in individual parental and methotrexate-resistant murine cells: use of a fluorescence activated cell sorter. *J Biol Chem* 253:5852-5860, 1978.

Kay NE. Abnormal T-cell subpopulation function in chronic lymphocytic leukemia: excessive suppressor (T) and deficient helper (T) activity with respect to B-cell proliferation. *Blood* 57:418-420, 1981.

Keating MJ, Kantarjian H, Talpaz M, et al. Fludarabine: a new agent with major activity against chronic lymphocytic leukemia. *Blood* 74:19-25, 1989.

Kennedy DG, Van den Berg HW, Clarke R, et al. The effect of the rate of cell proliferation on the synthesis of methotrexate poly-gamma-glutamates in two human breast cancer cell lines. *Biochem Pharmacol* 34:3087-3093, 1985.

Kerr L, Huntoon C, Donohue J, et al. Heteroconjugate antibody-directed killing of autologous human renal carcinoma cells by in vitro activated lymphocytes. *J Immunol* 44:4060-4067, 1990.

Kerzer HG, Pinedo HM, Schuvrhuis GJ and Joenje H. Doxorubicin (adriamycin). A critical review of free radical-dependent mechanisms. *Pharmacol Ther* 47:219, 1990.

Kessel D, Hall TC, Roberts D, et al. Uptake as a determinant of methotrexate response in mouse leukemia. *Science* 150:752-754, 1965.

Khawli LA, Chen FM, Alauddin MM and Epstein AL. Radioiodinated monoclonal antibody conjugate: Synthesis and comparative evaluation. *Antib Immunoconj Radiopharm* 4:163-182, 1991.

Kipps TJ, Fong S, Tomhave E, et al. Gigh-frequency expression of the conserved kappa light variable region gene in chronic lymphocytic leukemia. *Proc Natl Acad Sci USA* 84:2916-2920, 1987.

Knospe WH, Loeb V Jr and Hugiley CM Jr. Bi-weekly chlorambucil treatment of chronic lymphocytic leukemia. *Cancer* 33:555-562, 1974.

Kobayashi R, Picchio G, Kirven M, et al. Transfer of human chronic lymphocytic leukemia to mice with severe combined immune deficiency. *Leuk Res* 16:1013-1023, 1992.

Kohler G and Milstein C. Continuous cultures of fused cells secreting antibody of predefined specificity. *Nature* 256:455-457, 1975.

Kooiwijk P, Rozemuller E, Stad RK, et al. Enrichment and selection of hybrid hybridoma by percoll density gradient centrifugation and fluorescence activated cell sorting. *Hybridoma* 7:217, 1988.

Kralovec J, Singh M, Mammen M, et al. Synthesis of site-specific methotrexate-IgG conjugates. Comparison of stability and antitumor activity with active-ester-based conjugates. *Cancer Immunol Immunother* 29:293-302, 1989b.

Kralovec J, Spencer G, Blair AH, et al. Synthesis of methtrexate-antibody conjugates by regiospecific coupling and assessment of drug and antitumor activities. *J Med Chem* 32:2426-2431, 1989a.

Krizan Z, Murra JL, Hersh EM, et al. Increased labeling of human melanoma cells in vitro using combinations of monoclonal antibodies recognizing separate cell surface antigenic determinants. *Car...er Res* 45:4904-4909, 1985.

Krolick KA, Villemez C, Isakson P, et al. Selective killing of normal or neoplastic B-cells by antibodies coupled to the A-chain of toxin. *Proc Natl Acad Sci USA* 775419-5423. 1980.

Kulkarni PN, Blair AH and Ghose T. Covalent binding of methotrexate to immunoglobulins and the effect of antibody-linked drug on tumor growth in vivo. *Cancer Res* 41:2700-2706, 1981.

Kulkarni PN, Blair AH, Ghose T and Mammem M. Conjugation of methotrexate to IgG antibodies and their F(ab)'2 fragments and the effect of conjugated methotrexate on tumor growth in vivo. *Cancer Immunol Immunother* 19:211, 1985.

Kurkela R, Vuolas L and Vihko P. Preparation of F(ab)'2 fragments from mouse IgG1 subclass for use in radiolabeling. *J Immunol Methods* 110:229-236, 1988.

Kvaiheim G, Sorensen O, Fodstad O, et al. Immunomagnetic removal of B-lymphoma cells from human bone marrow: A procedure for clinical use. *Bone Marrow Transplant* 3:31, 1984.

Kyriakos RJ, Shih B, Ong CL, et al. The fate of antibodies bound to the surface of tumor cells in vitro. *Cancer Res* 52:835-842, 1992.

Lamoyi E and Nisonoff A. Preparation of F(ab)'2 fragment from mouse IgG of various subclasses. *J Immunol Methods* 56:235-243, 1983.

Landolfi NF. A chimeric IL-2/Ig molecule possesses the functional activity of both proteins. *J Immunol* 146:915-919, 1991.

Langmuir VK. Radioimmunotherapy: Clinical results and dosimetric considerations. *Nucl Med Biol* 19:213-225, 1992.

Lanzavecchia A and Scgeidegger D. The use of hybrid hybridomas to target human cytotoxic T lymphocytes. *Eur J Immunol* 17:105, 1987.

Larson SM. Radioimmunology: imaging and therapy. *Cancer* 67:1253-1260, 1991.

LeBerthon , Khawli LA, Alauddin M, et al. Enhanced tumor uptake of macromolecule induced by a novel vasoactive interleukin 2 immunoconjugate. *Cancer Res* 51:2694-2698, 1991.

Ledermann JA, Begent RHJ, Bagshawe KD, et al. Repeated antitumor antibody therapy in man with suppression of the host response by cyclosporin A. *Br J Cancer* 58:654-657, 1988.

Lee, CLY, Ghose T, Fernandez LA and Lee SHS. The emergence and establishment of a clonal subline with partial duplication of chromosome 1q from a tumorigenic human chronic lymphocytic leukemic B-cell line. *Cancer Genet Cytogenet* 33:139-143, 1988.

Lee CLY, Welch JP and Winsor EJT. Banding pattern in human chromosomes: Production by proteolytic enzymes. *J Hered* 63:206-197, 1972.

Lee CLY, Uniyal S, Fernandez LA, et al. Growth and spread in nude mice of Epstein-Barr virus transformed B cells from a chronic lymphocytic leukemia patient. *Cancer Res* 46:2497-2501, 1986.

Legha SS, Benjamin RS, Mackay B et al. Reduction of doxorubicin cardiotoxicity by prolonged continuous intravenous infusion. *Ann Intern Med* 96:133-139, 1982.

Lehmann JM, Riethmuller G and Johnson JP. MUC 18, a marker of tumor progression in human melanoma, shows sequence similarity to the neutral cell adhesion molecules of the immunoglcbulin superfamily. *Proc Natl Acad Sci USA* 86:9891-9895, 1989.

LeMaistre C, Rosen S, Frankel A, et al. Phase I trial of H65-RTA immunoconjugate in patients with cutaneous T-cell lymphoma. *Blood* 78:1173-1182, 1991.

LeMaistre F, Rosenblum M, Runben J, et al. Phase I study of genetically engineered DAB486IL-2 in LI-2 receptor expressing malignancies. *Blood* 76:360a (Abs.), 1990.

Lerner RA, Benkovic SJ and Schultz PG. At the crossroads of chemistry and immunology: catalytic antibodies. *Science* 252:659-667, 1991.

Letarte M, Vera S, Tran R, et al. Common acute lymphocytic leukemia antigen is identical to neutral endopeptidase. *J Exp Med* 168:1247-1253, 1988.

Levine AJ, Momand J and Finlay CA. The p53 tumor suppressor gene. *Nature* 351:453-456, 1991.

Levy R and Miller RA. Therapy of lymphoma directed at idiotypes. *J Natl Cancer Inst Monogr* 61-68, 1990.

Levy R, Hurwitz E, Maron R, et al. The specific cytotoxic effects of daunomycin conjugated to antitumor antibodies. *Cancer Res* 35: 1182-1186, 1975.

Lindmo T and Bunn PA Jr. Determination of the true immunoreactive fraction of monoclonal antibodies after radiolabeling. *Methods Enzymol* 121:687-691, 1986.

Lindmo T, Boven E, Cuttitta F, et al. Determination of the immunoreactive fraction of radiolabeled monoclonal antibodies by linear extrapolation to binding at infinite antigen excess. *J Immunol Methods* 72:77-89, 1984.

Lloyd KO. Molecular characteristic of tumor antigens. *Immunol Allergy Clinics N Am* 10:765-769, 1990.

LoBuglio AF, Wheeler RH, Trang J, et al. Mouse/human chimeric monoclonal antibody in man: kinetics and immune response. *Proc Natl Acad Sci USA* 86:4220-4224, 1989.

LoBuglio AF, Wheeler R, Lea ED, et al. Pharmacokinetics and immune response to chimeric mouse/human monoclonal antibody (Ch-17-1A) in man. *Proc Amer Soc Clin Oncol* 1:111, 1988.

Lowry OH, Rosebrough NJ, Farr AL and Randall RJ. Protein measurement with the Folin phenol reagent. *J Biol Chem* 193:265-275, 1951.

Lubeck MD, Steplewski Z, Baglia F, et al. The interaction of murine IgG subclass proteins with human monocyte Fc receptors. *J Immunol* 135:1299-1304, 1985.

Luner SJ, Ghose T, Chatterjee S, et al. Monoclonal antibodies to kidney and tumor-associated surface antigens of human renal cell carcinoma. *Cancer Res* 46:5816-5820, 1986.

Lurquin CA, Vanpel A, Mariame A, et al. Structure of the gene coding for Tum⁻ transplantation antigen P91A. A peptide encoded by the mutated exon is recognized with L^d cytolytic T cells. *Cell* 58:293-303, 1989.

Mach JP, Pelegrin A and Buchegger F. Imaging and therapy with monoclonal antibodies in non-hematopoietic tumors. *Curr Opin Immunol* 3:685-693, 1991.

Madshus IH, Stenmark H, Sandvig K and Olsnes S. Entry of diphtheria toxin-protein A chimeras into cells. *J Biol Chem* 266:17446-17453, 1991.

Mailer K and Petering DH. Inhibition of oxidative phosphorylation in tumor cells and mitochondria by daunomycin and adriamycin. *Biochem Pharmacol* 25:2085-2089, 1976.

Maki RG, Old LJ and Srivastava PK. Human homologue of murine tumor rejection antigen gp 96: 5' regulatory and coding regions and relationships t stress-induced proteins. *Proc Natl Acad Sci USA* 87:5658-5662, 1990.

Mariani G, Kassis AI and Adelstein SJ. Antibody internalization by tumor cells: implications for tumor diagnosis and therapy. *J Nucl Med Allied Sci* 34:51-54, 1990.

Martin JMC, Paques M, van der Velden-de Groot TAM and Beuvery EC. Characterization of antibody labeled colloidal gold particles and their applicability in a sol particle immuno assay (SPIA). *J Immunoassay* 11:31-47, 1990.

Mathe G, Log T and Bernard J. Effet sur la leucemie 1210 de la siuris d'un combinaison par diazotation d'A-methopterine et de γ- globulines de hamsters porteurs de cette leucemie par heterogreffe. *C R Acad Sci* 246:1626-1628, 1958.

Matthews DC, Smith FO and Bernstein ID. Monoclonal antibodies in the study and therapy of hematopoietic cancers. *Curr Opin Immunol* 4:641-646, 1992.

Matzku S, Brocker EB, Bruggen J, et al. Modes of binding and internalization of monoclonal antibodies to human melanoma cell lines. *Cancer Res* 46:3848, 1986.

Matzku S, Tilgen W, Kalthoff H, et al. Dynamics of antibody transport and internalization. *Int J Cancer* 2:11, 1988 (suppl).

May WS Jr and Cuatrecasas P. Transferrin receptor: its biological significance. *J Membrane* 88:205-216, 1985.

McDougall IR, Dunnick JK, McNamee MG ands Kriss JP. Distribution and fate of synthetic lipid vesicle in the mouse. A combined radionuclide and spin label study. *Proc Natl Acad Sci USA* 71:3487-3491, 1974.

Mckinney MM and Parkinson A. A simple, non-chromatographic procedure to purify immunoglobulins from serum and ascites fluid. *J Immunol Methods* 96:271-278, 1987.

Meeker T, Lowder J, Cleary ML, et al. Emergence of idiotype variants during treatment of B-cell lymphoma with anti-idiotype antibodies. *N Engl J Med* 312:1658-1665, 1985.

Melino G, Hobbs JR, Radford, et al. Drug targeting for 7 neuroblastoma patients using human polyclonal antibodies. *Protides Biol Fluids* 32:413-416, 1984.

Mellstedt H, Frodin JE, Masucci G, et al. The therapeutic use of monoclonal antibody in colorectal cancer. *Semin Oncol* 18:462-477, 1991.

Mellstedt H. Monoclonal antibodies in cancer therapy. *Curr Opin Immunol* 2:708-713, 1990.

Mezzanzanica D, Garrido MA, Neblock DS, et al. Humna T-lymphocytes targeted against an established human ovarian carcinoma with a bispecific F(ab)'2 antibody prolong host survival in a murine xenograft model. *Cancer Res* 51:5716-5721, 1991.

Miller R, Oseroff AR, Stratte PT and Levy R. Monoclonal antibody therapeutic trials in seven patients with T-cell lymphoma. *Blood* 62:988 , 1983.

Miller RA and Levy R. Response of cutaneous T cell lymphoma to therapy with hybridoma monoclonal antibody. *Lancet* 2:226-230, 1981.

Miller RA, Maloney DG, Warnke R and Levy R. Treatment of B-cell lymphoma with monoclonal anti-idiotypy antibody. *N Engl J Med* 306:517-522, 1981.

Milstein C and Cuello AC. Hybrid hybridomas and their use in immunohistochemistry. *Nature* 305:537, 1983.

Mitra AK and Ghosh MK. Drug immunoglobulin conjugates as targeted therapeutic systems. In: *Targeted Therapeutic Systems* (Tyle P and Ram BP, ed.), New York: Marcel Dekker, Inc., p.141-188, 1990.

Montserrat E, Alcala A, Parody R et al. Treatment of chronic lymphocytic leukemia in advanced stages: a randomized trail comparing chlorambucil plus prednisone versus cyclophosphamide, vincristine and prednisone. *Cancer* 56:2369-2375, 1985.

Moore SK, Rijli F and Appelia E. Characterization of the mouse 84 kD HSP gene family. *DNA and Cell Biology* 9:387-400, 1990.

Morrison S. In vitro antibodies. Strategies for production and application. *Annu Rev Immunol* 10:239-265, 1992.

Morrison SL, Johnson MJ, Herzenberg LA, et al. Chimeric human antibody molecules: mouse antigen-binding domains with human constant region domains. *Proc Natl Acad Sci USA* 81:6951-6855, 1984.

Moseley KR, Battaile RA, Knapp RC and Haisma HJ. Localization of radiolabeled F(ab)'2 fragments of monoclonal antibodies in nude mice bearing intraperitoneally growing human ovarian cancer xenografts. *Int J Cancer* 42:368, 1988.

Munz DL, Alavi A, Koprowski H and Herlyn D. Improved radioimmaging of human tumor xenografts by a mixture of monoclonal antibody F(ab)'2 fragments. *J Nucl Med* 27:1739-1745, 1986.

Murphree SA, Cunningham LS, Hwang KM and Sartorelli A. Effects of adriamycin on surface properties of sarcoma 180 ascites cells. *Biochem Pharmacol* 25:1227-1231, 1976.

Myers CE Jr and Chabner BA. Anthracyclines. In: *Cancer chemotherapy: Principles and Practice.* BA Chabner and JM Collins (eds), JB Lippincott Co., Philadelphia, 1990.

Nadler LM, Stashenko P, Hardy R, et al. Serotherapy of a patient with a monoclonal antibody directed against a human lymphoma-associated antigen. *Cancer Res* 40:3147-3154, 1980.

Naruki Y, Carrasquillo JA, Reynolds JC, et al. Differential cellular catabolism of ^{111}In, ^{90}Y and ^{125}I radiolabeled T101 anti-CD5 monoclonal antibody. *Nucl Med Biol* 17:201, 1990.

Neidle S. The molecular basis for the action of some DNA binding drugs. *Prog Med Chem* 16:156-221, 1979.

Nelson H, Ramsey PS, Kerr LA, et al. Regional and systemic distribution of anti-tumor x anti-CD3 heteroconjugate antibodies and cultured human peripheral blood lymphocytes in a human cocon cancer xenograft. *J Immunol* 145:3507-3515, 1990.

Neuwelt EA, Sprecht HD, Barnett RA, et al. Increased delivery of tumor specific monoclonal antibodies to brain after osmotic blood-brain barrier modification in patients with melanoma metastatic to central nervous system. *Neuosurgery* 20:885-895, 1987.

Nio Y, Shiraishi T, Imai S, et al. Binding and internalization of human immunoglobulin G conjugated with melphalan (K18) to human tumor cell lines. *Anticancer Res* 9:59-64, 1989.

Nisonoff A and Rivers MM. Recombination of a mixture of univalent antibody fragments of different specificity. *Arch Biochem Biophys* 93:460, 1961.

Nitta T, Yagita H, Azuma T, et al. Bispecific F(ab)'2 monomer prepared with anti-CD3 and antitumor monoclonal antibodies is most potent in induction of cytolysis of human T cells. *Eur J Immunol* 19:1437-1441, 1989.

Noguchi A, Takahashi T, Yamaguchi T, et al. Tumor localization and in vivo antitumor activity of the immunoconjugate composed of anti-human colon cancer monoclonal antibody and mitomycin C-dextran conjugate. *Jpn J Cancer Res* 82:219-226. 1991.

Nourigat C, Badger CC and Bernstein ID. Treatment of lymphoma with radiolabeled antibody: Elimination of tumor cells lacking target antigen. *J Natl Cancer Inst* 82:47, 1990.

Ohta s, Honda A, Tokutake Y, et al. Antitumor effects of a novel monoclonal antibody with high binding affinity to ganglioside GD3. *Cancer Immunol Immunother* 36:260-266,1993.

Okana M, Taguchi Y, Nakamine H, et al. Characterization of Epstein-Barr virus induced lymphoproliferation derived from human peripheral blood mononuclear cells transferred to severe combined immunodeficient mice. *Am J Pathol* 137:517, 1990.

Okubo M, Sato N, Wada Y, et al. Identification by monoclonal antibody of tumor antigen of a human autologous breast cancer cell that is involved in cytotoxicity by a cytotoxic T-cell clone. *Cancer Res* 49:3950-3954, 1989.

Olch PD, Eck RV and Smith RR. An experimental study on the effect of external irradiation on a "primary" tumor and its distant metastases. *Cancer* 12:23-26, 1959.

Oldham RK, Lewis M, Orr DW, et al. Adriamycin custom-tailored immunoconjugates in the treatment of human malignancies. *Mol Biother* 1:103-113, 1988.

Oldham RK, Lewis M, Orr Dw, et al. Individually specified immunoconjugates in cancer treatment. *Int J Biol Markers* 4:65-77, 1989.

Oldham RK. Monoclonal antibody in cancer therapy. *J Clin Oncol* 1:582-590, 1983.

Order SE, Klein Jl, Ettinger D, et al. Phase II study of radiolabeled antibody integrated in the treatment of primary hepatoma malignancies. *Int J Radiat Oncol Biol Phys* 6:703-710, 1980.

Orr D, Oldham R, Lewis M, et al. Phase I trial of mitomycin C immunoconjugates cocktails in human malignancies. *Mol Biother* 1:229-240, 1989.

Ortaldo JK, Woodhouse C, Morgan AC, et al. Analysis of effector cells in human antibody-dependent cellular cytotoxicity with murine monoclonal antibodies. *J Immunol* 138:3566-3572, 1987.

Osterman LA. Iodination with chloramine T. In: *Methods of Protein and Nucleic Acid Research*, New York: Springer-Verlag, p. 131-143, 1984.

Ostlund L,Einhorn S, Robert KH, et al. Chronic B-lymphocytic leukemia cells proliferate and differentiate following exposure to interferon in vitro. *Blood* 67:152-159, 1986.

Pai LH, Batra JK, FitzGerald D, et al. Antitumor activity of immunotoxins made of monoclonal antibody B3 and various forms of Pseudomonas exotoxin. *Proc Natl Acad Sci USA* 88:3358-3362, 1991.

Parham P. The fragmentation of monoclonal IgG1, IgG2a and IgG2b from BALB/c mice. *J Immunol* 131:2895-2902, 1983.

Parker BA, Vassos AB, Halpern SE, et al. Radioimmunotherapy of human B-cell lymphoma with ^{90}Y-conjugated antiidiotype monoclonal antibody. *Cancer Res* 50:1022s-1028s, 1990 (suppl).

Pastan I and Willingham MC. Receptor-mediated endocytosis: coated pits, receptosomes and the Golgi. *Trends Biochem Sci* 8:250-254, 1983.

Pastan I, Pai L, Bookman M, et al. OVB3-PE clinical trial. In: *Biology and Therapy of Ovarian Cancer*, Marble Island, Vt. (Abs.), p. 14-17, 1990.

Pawlak-Byczkowska EP, Hansen HJ, Dion.AS, Goldenberg DM. Two new monoclonal antibodies, EPB-1 and EPB-2, reactive with human lymphoma. *Cancer Res* 49:4568-4577, 1989.

Peterson DL, Gleisner JM and Blakely Rl. Bovine liver dihydrofolate reductase: purification and properties of the enzyme. *Biolchem* 14:5261-5267, 1975.

Pietersz GA and McKenzie IFC. Antibody conjugates for the treatment of cancer. *Immunol Rev* 129:57-80, 1992.

Pietersz GA,Smyth MJ and MaKenzie IFC. Immunochemotherapy of a murine thymoma with the use of idarubicin monoclonal antibody conjugates. *Cancer Res* 48:926-931, 1988.

Pimm MV, Clegg JA, Garnett MC and Baldwin RW. Biodistribution and tumor localization of a methotrexate-monoclonal antibody 791T/36 conjugate in nude mice with human tumor xenografts. *Int J Cancer* 41:886, 1988.

Pimm MV, Jones JA, Price MR, et al. Tumor localization of monoclonal antibody against a rat mammary carcinoma and suppression of tumor growth with adriamycin-antibody conjugates. *Cancer Immunol Immunother* 12:125-134, 1982..

Pimm MV. Drug-monoclonal antibody conjugates for cancer therapy: potentials and limitations. *CRC Crit Rev Ther Drug Carrier Syst* 5:189-227, 1988.

Piro LD, Carrera CJ, Beutler E and Carson DA. Chorodeoxyadenosine: an effective new agent for the treatment of chronic lymphocytic leukemia. *Blood* 72:1069-1073, 1988.

Pizzorno G, Mini E, Coronnello M et al. Impaired polyglutamation of methotrexate as a cause of resistance in CCRF-CEM cells after short-term, high-dose treatment with this drug. *Cancer Res* 48:2149-2155, 1988.

Powe J. Radiolabeling of monoclonal antibodies. *Hybridoma* 5:S39-S42, 1986 (suppl 1).

Preijers FW, de Witte ,Wessels JM, et al. Autologous transplantation of bone marrow purged in vitro with anti-CD7 (WT1)-ricin A chain immunotoxins in T-cell lymphoblastic leukemia and lymphoma. *Blood* 74:1151-1158, 1989.

Press O, Eary J, Badger C, et al. Radiolabeled antibody (Rab) therapy of relapsed B cell lymphomas. *Proc Am Soc Clin Oncol* 11:318, 1992.

Press OW, Appelbaum F, Ledbetter JA, et al. Monoclonal antibody IF5 (anti-CD20) serotherapy of human B cell lymphomas. *Blood* 69:584, 1987.

Press OW, Eary JF, Badger CC, et al. Treatment of refractory non-Hodgkin's lymphoma with radiolabeled MB-1 (anti-CD37) antibody. *J Clin Oncol* 7:1027-1038, 1989a.

Press OW, Farr AG, Borroz KI, et al. Endocytosis and degradation of monoclonal antibodies targeting human B-cell malignancies. *Cancer Res* 49:4906-4912, 1989b.

Press OW, Hansen JA, Farr A and Martin PJ. Endocytosis and degradation of murine anti-human CD3 monoclonal antibodies by normal and malignant T-lymphocytes. *Cancer Res* 48: 2249, 1988.

Press OW. Immunotoxins. *Biotherapy* 3:65-76, 1991.

Pupa SM, Canevari S, Fontanelli R, et al. Activation of mononuclear cells to be used for hybrid monoclonal antibody-induced lysis of human ovarian carcinoma cells. *Int J Cancer* 42455-459, 1988.

Queen C, Schneider WP, Selick HE, et al. A humanized antibody that binds to the interleukin 2 receptor. *Proc Natl Acad Sci USA* 86:10029-10033, 1989.

Raffeld M, Neckers L, Chapman PB, et al. Spontaneous alternation of idiotype in a monoclonal B-cell lymphoma. *N Engl J Med* 312:1653-1658, 1985.

Rai K. A critical analysis of staging in CLL. In: Gale RP, Rai K, eds. *Chronic Lymphocytic Leukemia: Recent Progress and Future Directions.* New York: Liss; 253-264, 1987.

Rai KR, Sawitsky A, Cronkite EP, et al. Clinical staging of chronic lymphocytic leukemia. *Blood* 46:219-234, 1975.

Ramakrishnan S, Fryxell D, Mohanraj D, et al. Cytotoxic conjugates containing translational inhibitory proteins. *Annu Rev Pharmacol Toxicol* 32:579-621, 1992.

Ramakrishnan S. Current status of antibody-toxin conjugates for cancer therapy. In: *Targeted Therapeutic Systems* (Tyle P and Ram BP, ed.), New York:Marcel Dekker, p. 189-214, 1990.

Raso V and Griffin T. Hybrid antibodies with dual specificity for the delivery of ricin to immunoglobulin-bearing target cells. *Cancer Res* 41:2073-2078, 1981.

Real FX, Mattes MJ, Houghton AN, et al. Class I (unique) tumor antigens of human melanoma: identification of a 90, 000 D cell surface glycoprotein by autologous antibody. *J Exp Med* 160:1219-1227, 1984.

Reddehase MJ, Rothbard JB and Koszinowski UH. A pentapeptide as minimal antigenic determinant for MHC class I-restricted T lymphocytes. *Nature* 337:651-653, 1989.

Regoeczi E. Methods of protein iodination. In: *Iodine-Labeled Plasma Proteins* (Regoeczi E, ed.), Vol. I, Boca Raton: CRC Press Inc., p. 35-102, 1984.

Reichman L, Clark M, Waldmann H and Winter G. Reshaping human antibodies for therapy. *Nature* 332:323-327, 1988.

Riethmuller G and Johnson JP. Monoclonal antibodies in the detection and therapy in micrometastatic epithelial cancers. *Curr Opin Immunol* 4:647-655, 1992.

Ritz J, Pesando JM, Sallan SE, et al. Serotherapy of acute lymphoblastic leukemia with monoclonal antibody. *Blood* 58:141, 1981.

Rodeck U, Herlyn M and Herlyn D, et al. Tumor growth modulation by a monoclonal antibody to the epithelial growth factor receptor: immunologically mediated and effector-independent effects. *Cancer res* 47:3692-3696, 1987.

Rodwell JD, Alvarez VL, Lee C, et al. Site-specific covalent modification of monoclonal antibodies: in vitro and in vivo evaluations. *Proc Natl Acad Sci* 83:2632-2636, 1986.

Rose TM, Plowman GD, Teplow DB et al. Primary structure of the human melanoma-associated antigen p97 (melanotransferrin) deduced from the mRNA sequence. *Proc Natl Acad Sci USA* 83:1261-1265, 1986.

Rosen ST, Zimmer AM, Goldman-Leikin R, et al. Progress in the treatment of cutaneous T-cell lymphomas with radiolabeled monoclonal antibodies. *Nucl Med Biol* 16:667, 1989.

Rosenblum LM, Lamki JL, Murray DJ, et al. Interferon induced changes in pharmacokinetics and tumor uptake of ^{111}In-labeled antimelanoma antibody 96.5 in melanoma patients. *J Natl Cancer Inst* 80:160-165, 1988.

Ross WA, Glaubiger DL and Kohn KW. Protein-associated DNA breaks in cells treated with adriamycin and ellipticine. *Biochem Biophys Acta* 519:23-30, 1978.

Roth J. The colloidal gold marker system for light and electron microscopic cytochemistry. In: *Techniques in Immunocytochemistry* (Bullock GR and Petrusz P, ed.), Vol. 2, London: Academic Press, p. 217-284, 1983.

Roth MS and Foon KA. Alpha interferon in the treatment of hematological malignancies. *Am J Med* 67:152-159, 1986.

Rowland GF, Axton CA, Baldwin RW, et al. Antitumor properties of vindesine-monoclonal antibody conjugates. *Cancer Immunol Immunother* 19:1-7, 1985.

Rowlinson G, Snook D, Busza A and Epenetos A. Antibody-guilded localization of intraperitoneal tumors following intraperitoneal or intravenous antibody administration. *Cancer Res* 46:6528-6531, 1987.

Rozman C, Montserrat E, Vinolas N, et al. Recombinant alpha-interferon in the treatment of B chronic lymphocytic leukemia in early stages. *Blood* 71:1295-1298, 1988.

Saha GB. Radioiodination of antibodies for tumor imaging. In: *Radioimmunoimaging and Radioimmunotheray* (Burchiell sw and Rhodes BA, ed.), New York: Elsevier Science Publishing, p.171-184, 1983.

Salzer JL, Holmes WP and Colman DR. The amino acid sequences of the myelin-associated glycoproteins: homology to the immunoglobulin gene superfamily. *J Cell Biol* 104:957-965, 1987.

Sands H and Jones PL. Physiology of monoclonal antibody accretion by tumors. In: *Cancer Imaging with Radiolabeled Antibodies* (Goldenberg DM, ed.), Norwell, MA: Martinus Nijhoff, 1990.

Sands H. Experimental studies of radioimmunodetection of cancer: an overview. *Cancer Res* 50:809s-813s, 1990 (suppl) .

Sauvage CA, Mendelsohn JC, Lesley JF and Trowbridge IS. Effects of monoclonal antibodies that block transferrin receptor function on the in vivo growth of a syngeneic murine leukemia. *Cancer Res* 47:747-753, 1987.

Schechter B, Pauzner R, Arnon R, et al Selective cytotoxicity against tumor cells by cisplatin complexed to antitumor antibodies via carboxymethyl dextran. *Cancer Immunol Immunother* 25:225, 1987.

Scheinberg DA, Lovett D, Divgi CR, et al. A phase I trail of monoclonal antibody M195 in acute myelogenous leukemia: specific bone marrow targeting and internalization of radionuclide. *J Clin Oncol* 9:478-490, 1991a.

Scheinberg DA, Straus DJ, Yeh SD, et al. A phase I toxicity, pharmacology, and dosimetry trial of monoclonal antibody OKB7 in patient with non-Hodgkin's lymphoma: Effects of tumor burden and antigen expression. *J Clin Oncol* 8:792, 1990.

Scheinberg DA. Current application of monoclonal antibodies for the therapy of hematopoietic cancers. *Curr Opin Immunol* 3:679-684, 1991b.

Schlom J, Eggensperger D, Colcher D, et al. Therapeutic advantage of high-affinity anticarcinoma radioimmunotherapy. *Cancer Res* 52:1067-1072, 1992.

Schlom J, Hand PH, Greiner JW, et al. Innovations that influence the pharmacology of monoclonal antibody guided tumor targeting. *Cancer Res* 50:820s-827s, 1990a (suppl).

Schlom J, Molinolo A, Simpson JF, et al. Advantage of dose fractionation in monoclonal antibody-targeted radioimmunotherapy. *J Natl Cancer Inst* 82:763-771, 1990b.

Schneck D, Butler F, Dugan W, et al. Phase I studies with a murine monoclonal antibody vinca conjugate (KS1.4-DAVLB) in patients with adenocarcinomas. *Antibody Immunoconj Radiopharm* 2:93-100, 1989.

Schroff RW, Foon KA, Beatty SM, et al. Human anti-murine immunoglobulin response in patients receiving monoclonal antibody therapy. *Cancer Res* 45:879-885, 1985.

Schroff RW, Morgan AC Jr, Woodhouse CS, et al. Monoclonal antibody therapy in malignant melanoma: factors affecting in vivo localization. *J Biol Resp Mod* 6:457-472, 1987.

Schuetz JD, Matherly LH, Westin EH et al..Evidence for a functional defect in the translocation of the methotrexate transport carrier in a methotrexate-resistant murine L1210 leukemia cell line. *J Biol Chem* 263:9840-9847, 1988.

Schwartz MK. Tumor markers in diagnosis and screening. In *Human Tumor Markers*. Edited by SW Ting, JS Chen, MK Schwartz. Elsevier Science Publishers, Amsterdam, 1989.

Schwartz MK. Tumor markers: what is their role ? *Cancer Invest* 8:439-440, 1990.

Scott CF Jr, Lambert JM, Kalish RS, et al. Human T cell can be directed to lyse tumor targets through the alternative activation / T11-E rosette receptor pathway. *J Immunol* 140:8-14, 1988.

Seeburg PH, Colby WW, Capon DJ, et al. Biological properties of human c-Ha-*ras* genes mutated at codon 12. *Nature* 312:71-75, 1984.

Sfakianakis GN, Garty II and Serafini AN. Radioantibodies for the diagnosis and treatment of cancer: radioimmunoimaging (RAI) and radioimmunotherapy (RAT). *Clin Invest* 8:381-405, 1990.

Shakib F, ed. *Basic and Clinical Aspects of IgG Subclasses*. New York:Karger, 1986.

Shawler DL, Bartholomew RM, Smith LM and Dillman RO. Human immune response to multiple injections of murine monoclonal immunoglobulin. *J Immunol* 135:1530-1535, 1985.

Shawler DL, Johnson DE, McCallister TJ, et al. Mechanisms of human CD5 modulation and capping induced by murine monoclonal antibody T101. *Clin Immunol Immunopathol* 47:219-229, 1988.

Shen WC and Ryser HJP. Cis-aconityl spacer between daunomycin and macromolecular carriers: A model of pH-sensitive linkage releasing drug from a liposomotrophic conjugate. *Biochem Biophys Res Comm* 102:1048-1054, 1981.

Shih LB and Goldenberg DM. Effects of methotrexate-carcinoembryoni immunoconjugates on GW-39 human tumors in nude mice. *Cancer Immunol Immunother* 31:197-201, 1990.

Shih LB, Goldenberg DM, Xuan H, et al. Anthracycline immunoconjugates prepared by a site-specific linkage via an amino dextran intermediate carrier. *Cancer Res* 51:4192-4198. 1991.

Shokat KM and Schultz PG. Catalytic antibodies. *Annu Rev Immunol* 8:335-363, 1990.

Siegall CB, Chaudhary VK, FitzGerald D and Pastan I. Cytotoxic activity of an interleukin 6-Pseudomonas extoxin fusion protein on human myeloma cells. *Proc Natl Acad Sci USA* 85:9738-9742, 1988.

Siegall CB, Xu Y, Chaudhary VK, et al. Cytotoxic activities of a fusion protein comprised of TGF-α and Pseudomonas extoxin. *FASEB* 3:2647-2652, 1988.

Sikora K, Alderson J, Ellis J, et al. Human hybridomas from patients with malignant diseases. *Br J Cancer* 47:135-145, 1983.

Sikorska HM. Therapeutic applications of antiidiotypic antibodies. *J Biol Resp Mod* 7:327-358, 1988.

Singh M, Ghose T, Mezei M and Belitsky P. Inhibition of human renal cancer by monoclonal antibody targeted methotrexate-containing liposomes in an ascites tumor model. *Cancer Lett* 56:97-102, 1991.

Singh M. Monoclonal antibody aided delivery of liposomal methotrexate. Ph.D. thesis, Dalhousie University, May 1989.

Singletary SE, Baker FL, Spitzer G, et al. Biological effect of epidermal growth factor on the in vitro growth of human tumors. *Cancer Res* 47:403-406, 1987.

Smyth MJ, Pietersz GA, Classon BJ and McKenzie IFC. Specific targeting of chlorambucil to tumors with the use of monoclonal antibodies, *J Natl Cancer Inst* 76:503-510, 1986.

Songsivilai S and Lachmann PJ. Bispecific antibody: A tool for diagnosis and treatment of disease. *Clin Exp Immunol* 79:315-321, 1990.

Songsivilai S, Clissold PM and Lachmann PJ. A novel strategy for producing chimeric bispecific antibodies by gene transfection. *Biochem Biophys Res Commun* 164:271, 1989.

Spitler LE, del Rio M, Khentigan A, et al. Therapy of patients with malignant melanoma using monoclonal antimelanoma antibody-ricin A chain immunotoxin. *Cancer Res* 47:1717-1723, 1987.

Srivastava PK and Maki RG. Stress-induced proteins in immune response to cancer. *Curr Top Mocrobiol Immunol* 167:109-123, 1991.

Srivastava PK and Old LJ. Individually distinct transplantation antigen of chemically induced mouse tumors. *Immunol Today* 9:78-83, 1988.

Srivastava PK, Chen YT and Old LJ. 5' structural analysis of genes encoding polymorphic antigens of chemically induced tumors. *Proc Natl Acad Sci USA* 84:3807-3811, 1987.

Srivastava PK and Das MR. The serologically unique cell surface antigen of zajdela ascitic hepatoma is also its tumor associated transplantation antigen. *Int J Cancer* 33:417-422, 1984.

Srivastava PK, Deleo AB and Old LJ. Tumor rejection antigens of chemically induced tumors of inbred mice. *Proc Nalt Acad Sci USA* 83:3407-3411, 1986.

Srivastava PK. Protein tumor antigens. *Curt Opin Immunol* 3:654-658, 1991.

Staerz UD and Baven MJ. Hybrid hybridoma producing a bispecific monoclonal antibody that can focus effector T-cell activity. *Proc Natl Acad Sci USA* 83:1453-1457, 1986.

Starling JJ, Maciak RS, Law KL, et al. In vivo activity of a monoclonal antibody-vinca alkaloid immunoconjugate directed against a solid tumor membrane antigen characterized by heterogeneous expression and noninternalization of antibody-antigen complexes. *Cancer Res* 51:2965-2972, 1991.

Steinman RM, Mellman IS, Muller WA and Cohen Z. Endocytosis and the recycling of plasma membrane. *J Cell Biol* 96:1-27, 1983.

Steplewski Z, Sun LK, Shearman CW, et al. Biological activity of human -mouse IgG1, IgG2, IgG3, and IgG4 chimeric monoclonal antibodies with antitumor specificity. *Proc Natl Acad Sci USA* 85:4852-4856, 1988.

Stewart JSW, Hird V, Snook B, et al. Intraperitoneal Yttrium-90-labeled monoclonal antibody in ovarian cancer. *J Clin Oncol* 8:1941-1950, 1990.

Stewart JSW, Hird V, Sullivan M, et al. Intraperitoneal radioimmunotherapy for ovarian cancer. *Br J Obstetric Gynaecol* 96:529-536, 1989.

Stickney DR, Slater JB and Frincke JM. Imaging and therapeutic potential of bifunctional antibody (BFA) in colon carcinoma. In: *Fourth International Conference n Monoclonal Antibody Immunoconjugates for Cancer (Abs.)*, UCSD, San Diego, p. 29, 189.

Sullivan DC, Silva JS, Cox CE, et al. Localization of I-131 labeled goat and primate anti-carcinoembryonic antigen (CEA) antibodies in patients with cancer. *Invest Radiol* 17:350-355, 1982.

Suresh MR, Cuello AC and Milstein C. Advantages of bispecific hybridomas in one-step immunochemistry and immunoassays. *Proc Natl Acad Sci USA* 83:7989, 1986b.

Suresh MR, Cuello AC and Milstein C. Bispecific monoclonal antibodies from hybrid hybridomas. *Methods Enzymol* 121:210, 1986a.

Swabb EA, Wei J and Gullino PM. Diffusion and convection in normal and neoplastic tissues. *Cancer Res* 34:2814-2822, 1974.

Swallow DM, Gendler S, Griffiths B, et al. The human tumor associated epithelial mucine are coded by an expressed hypervariable gene locus PUM. *Nature* 328: 82-84, 1987.

Tada H, Toyoda Y and Iwasa S. Bispecific antibody-producing hybrid hybridoma and its use in one-step immunoassay for human lymphotoxin. *Hybridoma* 8:73-83, 1989.

Tai J, Blair AH and Ghose T. Immunochemotherapy of mouse lymphoma with drug-antibody conjugate. *Proc Can Fed Biol Sci* 19: Abs. No. 502, 1976.

Takahashi M and Fuller SA. Production of murine hybrid hybridoma secreting bispecific monoclonal antibodies for use in urease-based immunoassays. *Clin Chem* 34:1693-1696, 1988.

Takahashi T, Yamaguchi T, Kitamura K, et al. Clinical application of monoclonal antibody-drug conjugates for immunotargeting chemotherapy of colorectal carcinoma. *Cancer* 61:881-888, 1988.

Takai N, Tanaka R, Yoshida S, et al. In vivo and in vitro effect of adoptive immunotherapy of experimental murine brain tumors using lymphokine-activated killer cells. *Cancer Res* 48:2407, 1988.

Taparowski E, Suard Y, Fasano O, et al. Activation of the T24 bladder carcinoma transforming gene is linked to a single amino acid change. *Nature* 300:762-765, 1982.

Terasaki T, Iga T, Sugiyama Y et al.. Experimental evidence of characteristic tissue distribution of adriamycin: tissue DNA concentration as a determinant. *Pharmacol Rev* 53:496-501, 1989.

Tewey KM, Chen GI, Nelson EM, et al. Intercalative anti-tumor drugs interfere with the breakage-reunion reaction of mammalian DNA topoisomerase. *J Biol Chem* 259:9182-9186, 1984.

Thomas GD, Chappell MJ, Dykes PW, et al. Effect of dose, molecular size, affinity, and protein binding on tumor uptake of antibody or ligand: A biomathematical model. *Cancer Res* 49:3290-3296, 1989.

Thurin J, Thurin M, Kimoto Y, et al. Monoclonal antibody-defined correlations in melanoma between levels of GD3 and GD3 antigens and antibody-mediated cytotoxicity. *Cancer Res* 47:1229-1233, 1987.

Thurin J. Characterization and molecular biology of tumor-associated antigens. *Curr Opinions Immunol* 2:702-707, 1990.

Tiebout RF, van Boxtel-Oosterhof E, et al. A human hybrid hybridoma. *J Immunol* 139:3402, 1987.

Tilgen W and Matzku S. Pitfalls in the clinical application of monoclonal antibodies in malignant melanoma: modulation by and impaired accessibility of antigens to monoclonal antibodies. *Cancer Treat Rev* 17:357-371.

Titus JA, Garrido MA, Hecht TT, et al. Human T cells targeted with anti-T3 cross-linked to antitumor antibody prevent tumor growth in nude mice. *J Immunol* 138:4018-4022, 1987.

Tjandra JJ, Pietersz GA, Smyth MJ, et al. Phase I clinical trial of drug-monoclonal antibody conjugates in patients with advanced colorectal carcinoma - preliminary report. *Surgery* 106:533-545, 1989.

Trail PA, Willner D, Lasch SJ, et al. Antigen-specific activity of carcinoma-reactive BR64-doxorubicin conjugates evaluated in vitro and in human tumor xenograft models. *Cancer Res* 52:5693-5700, 1992.

Tramontano A, Janda KD and Lerner RA. Catalytic antibodies. *Science* 234:1566-1570, 1986.

Tritton TR and Dorshow JH. Role of hydrogen peroxide and hydroxyl radical formation in the killing of Ehrlich tumor cells by anticancer quinones. *Proc Natl Acad Sci USA* 83:4514-4518, 1986.

Tritton TR and Yee G. The anticancer agent adriamycin can be actively cytotoxic without entering cells. *Science* (Washington DC) 217:248-250, 1982.

Tritton TR, Murphree SA and Sartorelli AC. Adriamycin: a proposal on the specificity of drug action. *Biochem Biophys Res Commun* 84:802-808, 1978.

Trouet A, Baurain R, Masomelier M and Deprez-De Campeneere D. Covalent and reversible linkage of daunorubicin to protein. Lysosomal hydrolysis and antitumoral activity of conjugates prepared with oligopeptidic spacer arms. *EORTC Symposium:*

"Promising New Anti-Cancer Agents in Clinical Trails" (Mathe G, Ed.), Masson, Paris, 1982.

Tsukada Y, Bischof WKD, Hibi N, et al. Effect of a conjugate of daunomycin and antibodies to rat a-fetoprotein on the growth of a-fetoprotein-producing tumor cells. *Proc Natl Acad Sci USA* 79:621-625, 1982.

Tyle P and Ram BP. Monoclonal antibodies, Immunoconjugates and liposomes as targeted therapeutic systems. In: *Targeted Therapeutic Systems* (Tyle P and Ram BP, ed.), New York: Marcel Dekker, Inc., p.3-24, 1990.

Uadia P. Blair AH, Ghose T and Ferrone S. Uptake of methotrexate linked to polyclonal and monoclonal anti-melanoma antibodies by a melanoma cell line. *J Natl Cancer Inst* 74:29, 1985.

Uadia P. Blair AH and Ghose T. Uptake of methotrexate linked to an anti-EL4-lymphoma antibody by EL4 cells. *Cancer Immunol Immunother* 16:127-129, 1983.

Uckun FM, Gajl-Peczalska K, Myers DE, et al. Temporal association of CD40 antigen expression with discrete stages of human B cell ontogeny and the efficacy of anti-CD40 immunotoxins against clonogenic B lineage acute lymphoblastic leukemia as well as B lineage non-Hodgkin's lymphoma cells. *Blood* 76:2449-2456, 1990.

Uckun FM, Manivel C, Arthur D, et al. In vivo efficacy of B43 (anti-CD19)-pokeweed antiviral protein immunotoxin against human pre-B cell acute lymphoblastic leukemia in mice with severe combined immunodeficiency *Blood* 79:2201-2214, 1992.

Ullrich SE, Robinson EA, Law LW, et al. A mouse tumor-specific transplantation antigen is a heat shock protein. *Proc Natl Acad Sci USA* 83:3121-3125, 1986.

Umemoto N, Kato Y, Endo N, et al., Preparation and in vitro cytotoxicity of a methotrexate-anti-MM46 monoclonal antibody conjugate via an oligopeptide spacer. *Int J Cancer* 43:677-684, 1989.

Urban JL and Scnreiber H. Tumor antigens. *Annu Rev Immunol* 10:617-644, 1992.

Urnovitz HB, Chang Y, Scott M, et al. IgA:IgM and IgA:IgA hybrid hybridomas secrete heteropolymeric immunoglobulins that are polyvalent and bispecific. *J Immunol* 140:558, 1988.

Vaidyanathan G and Zalutsky MR. Radioiodination of antibodies via N-succinimidyl-2, 4-dimethoxy-3-(trialkylstannyl) benzoates. *Bioconj Chem* 1:387-393, 1990.

Vallera DA, Quinones RR, Azemove SM and Soderling CC. Monoclonal antibody-toxin conjugates reactive against human T lymphocytes: A comparison of antibody linked to intact ricin toxin with antibody linked to ricin A chan. *Transplantation* 37:387-392, 1984.

Van den Eynde B, Lethe B, Van Pel A, et al. The gene coding for a major tumor-rejection antigen of tumor P815 is identical to the normal gene of syngeneic DBA/2 mice. *J Exp Med* 173:1373-1384, 1991.

Van der Bruggen P, Traverasri C, Chomez P, et al. A gene encoding an antigen recognized by cytolytic T lymphocytes on a human melanoma. *Science* 254:1643-1647, 1991.

Van Dijk J, Warnaar SO, van Eendenburg JD, et al. Induction of tumor-cell lysis by bi-specific monoclonal antibodies recognizing renal-cell carcinoma and CD3 antigen. *Int J Cancer* 43:344-349, 1989.

Van Dijk J, Zegveld ST, Fkeuren GJ and Warnaar SO. Localization of monoclonal antibody G250 and bispecific monoclonal antibody CD3/G250 in human renal cell carcinoma xenografts: relative effects of size and affinity. *Int J Cancer* 48:738-743, 1991.

Varga JM, Asato N, Lande S, et al. Melanotropin-daunomycin conjugate shows receptor-mediated cytotoxicity in culture murine melanoma cells. *Nature* 267:56-58, 1977.

Vitetta ES, Stone M, Amlot P, et al. Phase I immunotoxin trial in patients with B-cell lymphoma. *Cancer Res* 51:4052-4058, 1991.

Vriesendorp H, Herpst JM, Germack MA, et al. Phase I-II studies of yttrium-labeled antiferritin treatment for the end-stage Hodgkin's disease, including Radiation Therapy Oncology Group 87-01. *J Clin Oncol* 9:918, 1991.

Waldmann TA, Goldman CK, Bongiovanni KF, et al. Therapy of patients with human T-cell lymphotropic virus 1-induced adult T-cell leukemia with anti-Tac, a monoclonal antibody to the receptor for interleukin 2. *Blood* 72:1805-1816, 1988.

Waldmann TA, Pastan IH, Gansow OA and Junghans RP. The multichain interleukin-2 receptor: a target for immunotherapy. *Ann Intern Med* 116:148, 1992.

Waldmann TA. The structure, function, and expression of interleukin-2 receptors on normal and malignant lymphocytes. *Science* 232:727-732, 1986.

Waring MJ. DNA modification and cancer. *Annu Rev Biochem* 50:159-192, 1981.

Warren RD, Nichols AP and Bender RA. Membrane transport of methotrexate in human lymphoblastoid cells. *Cancer Res* 38:668-671, 1978.

Wawrzyneczak EJ, Watson GJ, Cumber AJ, et al. Blocked and non-blocked ricin immunotoxins against CD4 antigen exhibit higher cytotoxic potency than a ricin A chain immunotoxin potentiated with ricin B chain or with a ricin B chain immunotoxins. *Cancer Immunol Immunother* 32:289-295, 1991.

Webb KS, Ware JL, Parks SF, et al. Evidence for a novel hybrid immunotoxin recognizing ricin A-chain by one antigen-combining site and a prostate-restricted antigen by

the remaining antigen-combining site: potential for immunotherapy. *Cancer Treatment Rep* 69:663, 1985.

Weiner GJ, and Hillstrom JR. Bispecific anti-idiotype/anti-CD3 antibody therapy of murine B cell lymphoma. *J Immunol* 147:4035-4044, 1991.

Weiner LM, Holmes M, Adams GP, et al. A human tumor xenograft model of therapy with bispecific monoclonal antibody targeting c - *erb* B-2 and CD16. *Cancer Res* 53:94-100, 1993.

Weinstein Y, Ihle JN, Lavu S and Reddy EP. Truncation of the *c-myb* gene by a retroviral integration in an interleukin 3-dependent myeloid leukemia cell line. *Proc Natl Acad Sci USA* 83:5010-5014, 1986.

Wensel TG and Meares CF. Bifunctional chelating agents for binding metal ions to proteins. In: *Radioimmunoimaging and Radioimmunotheray* (Burchiell sw and Rhodes BA, ed.), New York: Elsevier Science Publishing, p.185-196, 1983.

Wessels BW. Current status of animal radioimmunotherapy. *Cancer Res* 50:970s-973s, 1990 (suppl).

Whitehead VM, Rosenblatt DS, Vuchich MJ, et al. Methotrexate polyglutamate synthesis in lymphoblasts from children with acute lymphoblastic leukemia. *Dev Pharmacol Ther* 10:443-447, 1987.

Whitehead VM. Synthesis of methotrexate polyglutamates in L1210 murine leukemia cells. *Cancer Res* 37:408-412, 1977.

Wilbur DS, Hadley SW, Grant LM and Hylavides MD. Radioiodinated iodobenzyl conjugates of a monoclonal antibody fragment. In vivo comparison with chloramine T labeled Fab. *Bioconj Chem* 2:111-116, 1991.

Wilbur DS, Hadley SW, Hylarides MD, et al. Development of a stable radioiodinating reagent to label monoclonal antibodies for radiotherapy of cancer. *J Nucl Med* 30:216-226. 1989,

Wilbur DS. Radiohalogenation of proteins: An overview of radionuclides, labeling methods, and reagents for conjugate labeling. *Bioconj Chem* 3:433-470, 1992.

Wilkinson I, Jackson CJ, Lang C, et al. Tolerogenic polythylene glycol derivatives of xenogeneic monoclonal immunolglobulins. *Immunol Lett* 15:17-22, 1987.

Williams JW, Duggleby RG Cutler R, et al.. The inhibition of dihydrofolate reductase by folate analogues: structural requirement for slow- and tight-binding inhibitors. *Biochem Pharmacol* 29:589-595, 1980.

Winer BJ. *Statistical Principles in Experimental Designs*. McGraw-Hill Bank Co., New York, p 514-539, 1971.

Winkler MA, Price JO, Foglesong PD and West WH. Biodistribution and plasma survival in mice of anti-melanoma monoclonal antibody cross-linked to OKT3. *Cancer Immunol Immunother* 31:278-284, 1990.

Witz IP. The biological significance of tumor-bound immunoglobulins. *Curr Top Microbiol Immunol* 61:157-171, 1973.

Wong JT and Colvin RB. Bi-specific monoclonal antibodies: selective binding and complement fixation to cells that express two different surface antigens. *J Immunol* 139:1369, 1987.

Wortzel RD, Philipps C and Schreiber H. Multiplicity of unique tumor-specific antigens expressed on a single malignant cell. *Nature* 304:165-167, 1983.

Wrobleski VJ. Mechanisms of deiodination of 125I-human growth hormone in vivo: Relevance to the study of protein disposition. *Biochem Pharmacol* 42:889-897, 1991.

Yamamoto K, Acton EM and Henry PW. Antitumor activity of some derivatives of daunomycin at the amino and methylketone functions. *J Med Chem* 15:872-875, 1972.

Yang HM and Reisfeld RA. Doxorubicin conjugated with a monoclonal antibody directed to a human melanoma-associated proteoglycan suppresses the growth of established tumor xenografts in nude mice. *Proc Natl Acad Sci USA* 85:1189-1193, 1988.

Zalutsky MR and Narula AS. A method for the radiohalogenation of proteins resulting in decreased thyroid uptake of radioiodine. *Appl Radiat Isot* 38:1051-1055, 1987.

Zalutsky MR and Narula AS. An improved method for the radiohalogenation of monoclonal antibodies. In: *Immunological Approaches to the Diagnosis and Therapy of Breast Cancer* (Ceriani RL, ed.), New Rork: Plenum Press, p. 187-203, 1987.

Zalutsky MR and Narula AS. Radiohalogenation of a monoclonal antibody using a N-succinimidyl 3-(tri-n-butylstannyl) benzoate intermediate. *Cancer Res* 48:1446-1450, 1988.

Zalutsky MR, Colcher D, Kaplan W and Kufe D. Radioiodinated B6.2 monoclonal antibody: further characterization of a potential radiopharmaceutical for the identification of breast cancer. *Int J Nucl Med Biol* 12:227-233, 1985.

Zhao FK, Chuang LF, Israel M and Chuang RY. Adriamycin interacts with diacylglycerol to inhibit human leukemia protein kinase-C. *Anticancer Res* 9:225-230, 1989.

Zimmer AM, Kaplan EH, Kazikiewicz JM, et al. Pharmacokinetics of I-131 T101 monoclonal antibody in patients with chronic lymphocytic leukemias. *Anti Immunoconj Radiopharm* 1:291, 1988.

Zutter MM, Martin PJ, Sale GE, et al. Epstein-Barr virus lymphoproliferation after bone marrow transplantation. *Blood* 72:520, 1988.